SEDIMENT DYNAMICS AND STABILITY OF TIDAL INLETS

By

Shu Gao (B.Sc., M.Sc.)

Submitted to the University of Southampton in fulfilment of the requirements for the degree of Doctor of Philosophy

DEPARTMENT OF OCEANOGRAPHY
FACULTY OF SCIENCE

February 1993

UNIVERSITY OF SOUTHAMPTON

ABSTRACT

FACULTY OF SCIENCE

OCEANOGRAPHY

Doctor of Philosophy

by Shu Gao

Sediment transport patterns and equilibrium conditions of three tidal inlet systems (i.e. Christchurch, Langstone and Yangpu Harbours) are investigated. Various approaches to the study are adopted: (1) sediment transport rates are calculated on the basis of the empirical equations of Madsen and Grant (1976), Gadd *et al.* (1978) and Vincent et al. (1981); (2) an original model for grain size trend analysis (McLaren and Bowles 1985) is modified for use in shallow marine environments, based upon identification of "transport vectors" and a "critical vector length"; (3) a mathematical model is developed to simulate movement of natural trace sediments, from the continental shelf to the tidal basin; and (4) an analytical approach to inlet equilibrium is developed, based upon mass conservation of water and sediment.

Data sets for the application of these methods are derived from geophysical surveys, analyses of sediment samples, tidal cycle observations, and long-term monitoring of water levels and suspended sediment concentrations.

In the entrance to Christchurch (Harbour), significant velocity asymmetry is present, which results in the seaward transport of sediment under the combined action of currents and waves (without considering longshore drift). Net sand transport is directed, however, to landward according to the trace sediment exchange model.

Significant grain size trends exist in Christchurch and Yangpu Harbours. In the entrance to Christchurch, net transport is landward, in agreement with the pattern defined by the trace sediment exchange model. Within the harbour, the trends show seaward and landward transport in the south and north, respectively. In yangpu Harbour, landward transport in the inner part of the tidal basin, seaward transport in the entrance, and clockwise circulation outside the harbour have been identified.

Equilibrium conditions of the three inlet systems indicate that Christchurch is wave-dominated and characterised by a small cross- sectional area, whilst Langstone and Yangpu show tidal dominance and larger cross-sectional areas. Thus, the degree of stability of Christchurch Harbour is lower than that of the other inlets.

It is concluded that: (i) application of the grain size trend analysis to marine environments requires sampling intervals large enough to reflect the real grain size trends resulting from sediment transport, but small compared with the dimensions of the sedimentary environment; (ii) the model for trace sediment exchange developed here can be used to identify net transport patterns in estuaries and tidal inlets, overcoming the difficulty of using the mere presence of the tracer as an indicator of net transport; and (iii) as a modification of the classical O'Brien (1969) and Bruun Methods, inlet equilibrium and stability conditions should be related to sediment transport patterns and other factors (in addition to the tidal prism and, in the Bruun's Method, the longshore sediment transport rate).

ACKNOWLEDGEMENTS

This study is supported financially by the British Council and the Chinese Government, through a grant from the TC (U.K.-China Technical Cooperation) scheme.

I am grateful to Professor M. B. Collins for his invaluable supervision and continuous encouragement. Discussions with him have been proved to be fruitful in terms of improvements in both the science and English. Further, his advice and guidance have been very beneficial to the field observations.

Discussions on grain size trends with Dr P. McLaren (GeoSea Consultant Ltd. (Canada)) and Dr C. L. Amos (Bedford Institute of Oceanography, Canada) have resulted in the development of the new approach to the grain size trend analysis.

Professor J. W. Murray (Department of Geology) and George Voulgaris are thanked for their critical and positive comments to the model for trace sediment exchange.

Adonis Velegrakis, without whose assistance the sediment sampling and tidal cycle observations would have been impossible, has accompanied me for many days and nights at the sea. Mr J. Davis and Mr J. Cross have spent many long days in the installation and maintenance of the tide gauge and siltmeter system. Mr J. Cross, Bruce Tomlinson and Huw Powell provided valuable help in the bathymetric survey at Mudeford. Xiankun Ke has assisted in the collection of short cores on the intertidal flat.

Assistance in the sediment sampling and grain size analysis of Yangpu Harbour has been provided by Mingzuo Fu, Yehua Xu (Nanjing University, China), and Xiankun Ke, under the supervision of Professors Ying Wang and Dakui Zhu (Nanjing University, China).

Dr S. R. Boxall and Dr J. Taylor are thanked for providing the tidal gauge for use at Mudeford. I am indebted to Dr P. Statham and Mr P. Goody for their help with the analysis of the concentration of suspended matter, and for the use of filtering equipment. Thanks are due also to Mr C. Hill (GeoData Institute and Unit, University of Southampton), who provided the levelling equipment and the Partech turbidity monitor, and Dr P. Tosswell (Civil Engineering Department), who provided his results of the 1978 investigation at Mudeford.

Logistic support is due to the technical and secretarial staff of the Department of Oceanography; in particular, I would like to thank Mr W. J. Gibbs, Mr N. W. Jenkinson and P. Riddy for preparing and repairing instruments, and Mr K. Padley for his help with the transport of equipment. Fieldwork has been supported also by George Voulgaris, Dr S. E. Poulos, Mike Wilkin and Caroline Hobson. Miss K. Saull has helped with drawing of some (4) of the figures.

The skippers and crew of *MVs "Wessex Explorer"*, *"Stella Barbara"*, *"Avon Valley"* and *"Satina"* are thanked for their work for the sediment sampling and geophysical surveys. The data of freshwater discharges (for 1991), for Christchurch Harbour, were provided by the National Water Authority (Wessex Region). Thanks are due to Mrs D. Foster and Mr B. Foster for their help with the field observations at Mudeford. Dr D. L. Blackman (Proudman Oceanographic Laboratory) is thanked for his help with the harmonic analysis of the tidal data. Mr M. Mannion and Mr F. Tyhurst (Christchurch Borough Council) are thanked for providing local information on topography and tides.

Finally, I would like to thank my wife Zhang Hongshia for her tremendous efforts to look after the family and her constant support for my "sediment indulgence".

TABLE OF CONTENTS

	Page
ABSTRACT	i
ACKNOWLEDGEMENTS	ii
TABLE OF CONTENTS	iii
FIGURE HEADINGS	vi
TABLE HEADINGS	xiii
NOTATIONS	xv
CHAPTER 1. INTRODUCTION	1
CHAPTER 2. LITERATURE REVIEW	4
2.1. Sediment Transport Rate	4
2.1.1. Transport Theories	4
2.1.2. Bed-load Transport Rate	9
2.1.3. Suspended Load Transport Rate	12
2.2. Net Transport Patterns	12
2.2.1. Transport Mechanisms	12
2.2.2. Qualitative Approaches to Transport Pathways	13
2.3. Criteria of Inlet Stability	15
2.3.1. Concept of Stability	15
2.3.2. Equilibrium of the Entrance Channel	16
2.3.3. Criteria for Overall Stability	17
CHAPTER 3. THE STUDY AREAS	18
3.1. Christchurch Harbour	18
3.1.1. Regional Geology	18
3.1.2. Geomorphology	19
3.1.3. Waves	21
3.1.4. Tides	23
3.1.5. The Estuarine Waters	24
3.2. Comparative Areas (U.K. and China)	24
3.2.1. Langstone Harbour	24
3.2.2. Yangpu Harbour	26
CHAPTER 4. METHODS	29
4.1. Data Collection	29
4.1.1. Geophysical Survey	29
4.1.2. Oceanographic Measurements	32
4.1.3. Sediment Sampling and Analysis	40
4.1.4. Bathymetric Survey	46
4.1.5. Collation of Available Data	47

4.2. Grain Size Trend Analysis 48
4.2.1. The Grain Size Trends Used in the Analysis 48
4.2.2. Analytical Procedure 50
4.3. Mathematical Model of Sediment Exchange 54
4.3.1. Background 54
4.3.2. Analysis of Components of Sediment Budget 54
4.3.3. Model Formulation 56
4.4. Computation of Sediment Transport Rate 59
4.4.1. Computation of Current Speeds in Entrance Channel 59
4.4.2. Bed-load Transport 60
4.4.3. Suspended Load Transport 64
4.5. Determination of Inlet Equilibrium 64
4.5.1. Definition of Equilibrium 64
4.5.2. Factors Affecting Equilibrium 65

CHAPTER 5. RESULTS 68
5.1. Characteristics of the Seabed 68
5.1.1. Morphology of Entrance Channel and Tidal Deltas 68
5.1.2. Seabed Sediments 70
5.2. Hydrodynamics 91
5.2.1. Tidal Characteristics 91
5.2.2. Currents in the Entrance Channel 94
5.2.3. Estuarine Processes 97
5.3. Sediment Budget 118
5.3.1. Bed-Load 118
5.3.2. Suspended Load 127
5.4. Transport Pathways Inferred from Grain Size Trends 130
5.4.1. Net Transport in Christchurch Harbour 130
5.4.2. Net Transport in Yangpu Harbour 133
5.5. Exchanges of Sediments 139
5.5.1. Conceptual Experiments 139
5.5.2. Experiments for Christchurch Harbour 144
5.6. Inlet Equilibrium 153
5.6.1. Equilibrium of Christchurch Harbour 153
5.6.2. Equilibrium of Langstone Harbour 159
5.6.3. Equilibrium of Yangpu Harbour 164
5.6.4. Comparison of Equilibrium Conditions 169

CHAPTER 6. DISCUSSION 171
6.1. The Use of Natural Trace Sediments 171
6.2. Interpretation of Grain Size Trends 172
6.2.1. The Need to Improve the "McLaren Method" 172
6.2.2. Changes in Response to Transport Processes 176
6.2.3. Time-Scales and Sampling Density 178
6.3. Stability of Tidal Inlets 180
6.3.1. P-A Relationships 180
6.3.2. Other Criteria 183

CHAPTER 7. SUMMARY 187

REFERENCES 191

APPENDICES A.1
Appendix A. Records of Tidal Cycle measurements A.1
Appendix B. Seabed Sediment Data A.24
Appendix C. Time-Series of Water Levels, Cross-sectional Mean Current Speeds and Suspended Sediment Concentrations (at Mudeford) A.39
Appendix D. Freshwater Discharges Data A.100
Appendix E. Publications A.105

FIGURE HEADINGS

Chapter 3.

Page

Figure 3-1. Geomorphological characteristics of the Christchurch Harbour area: (A) location of the Harbour (the scope of the drainage basin being denoted by the dashed line); and (B) the tidal inlet system (bathymetry in metres). 20

Figure 3-2. Wave height exceedence curves for: (A) offshore areas areas of Christchurch Bay, 1974-1989 (after Hydraulics Research 1989a); and (B) nearshore areas of Milford-on-Sea, between July 1987 and May 1989 (after Hydraulics Research 1989b). 22

Figure 3-3. Location map of Langstone Harbour, southern England (bathymetry in metres). 25

Figure 3-4. Location map of Yangpu Harbour, southern China (bathymetry in metres). 27

Chapter 4.

Figure 4-1. Course tracks of side-scan sonar survey. 30

Figure 4-2. Course tracks of sub-bottom profiler survey. 30

Figure 4-3. Location map showing stations for tidal cycle measurements. 34

Figure 4-4. Relationship between the SSC, determined from filters dried in the constant humidity tank for 46 hr (C_{HT}), and that determined from filters dried first in the constant humidity tank and then in oven at 50-70 °C for 2.5 hr (C_{OV}). 35

Figure 4-5. Calibration line for SSCs, for the Partech turbidity monitor readings. 35

Figure 4-6. Layout of instrumentation for long-term monitoring (schematic and not to scale). 37

Figure 4-7. Tidal water level and SSC data recovery (January 1991 - January 1992). 38

Figure 4-8. Calibration curve for water levels. 38

Figure 4-9. Relationship between the chart recorder readings and siltmeter readings, for various SSC data. 39

Figure 4-10. Calibration curve for SSCs, from the Operation Manual of ABP Siltmeter. 40

Figure 4-11. Relationship between the SSC determined from Equation [4-6] and that from the filtration of water samples. 41

Figure 4-12. Sites for seabed sediment sampling, in western Christchurch Bay and around Hengistbury Head. 42

Figure 4-13. Sites for seabed sediment sampling (○) within Christchurch Harbour and short cores (Δ) near Stanpit Marsh. 43

Figure 4-14. Positions of the transects for bathymetric survey, tide staff station and sediment sampling sites within the Run. 46

Figure 4-15. Sampling sites in the Yangpu Harbour area. 47

Figure 4-16. Procedures for grain size trend analysis: (A) definition of "trend vectors"; (B) summation of trend vectors for each site; (C) determination of "transport vectors"; and (D) formation of "residual" patterns. 51

Figure 4-17. Major components of the sediment balance for an inlet system. 55

Figure 4-18. Schematic diagram showing the change in the moving layer, between t (the dashed box) and $t+\Delta t$ (the solid box). 58

Chapter 5.

Figure 5-1. Bathymetry of 3 transects within the Run, surveyed during February and March, 1992. 68

Figure 5-2. Seabed sediments in Christchurch Harbour (the classification scheme based upon Folk (1980), modified slightly). 70

Figure 5-3. Seabed sediments outside the Harbour (the classification scheme based upon Folk (1980), modified slightly). 71

Figure 5-4. (A) Some representative grain size distributions of gravel fractions; and (B) sample locations (including those for Figures 5-6 and 5-7). 72

Figure 5-5. Sediments within the entrance channel (for notations, see Figure 5-2). 73

Figure 5-6. Some representative grain size distributions of sand 74 sub-samples collected from: (A) the Harbour and ebb tidal delta areas; and (B) the area to the south of Hengistbury Head. the sample locations are shown on Figure 5-4(B).

Figure 5-7. Some representative grain size distributions of mud sub-samples within the Harbour (A) and outside the Harbour (B). The sample locations are shown on Figure 5-4 (B). 76

Figure 5-8. Mean grain size of the surficial sediments (in ϕ units). 77

Figure 5-9. Sorting coefficient of the surficial sediments (in ϕ units). 77

Figure 5-10. Skewness of the surficial sediments (in ϕ units). 78

Figure 5-11. Locations for sub-bottom profiler and side-scan sonar data presented on Figures 5-12 to 5-20. A-A' to E-E' are the selected sub-bottom profiler lines and F to I are the areas covered by the selected side-scan sonar sonographs. 78

Figure 5-12. Christchurch Ledge, characterised by boulders and exposed Tertiary strata shown on the sub-bottom profiler image (Profile A-A', Figure 5-11). The vertical scale is in terms of TWT. 79

Figure 5-13. Interpretation of the sub-bottom profiler image of Profile B-B' (Figure 5-11), showing reflectors due to the underlying Tertiary strata. The vertical scale is in terms of TWT. 81

Figure 5-14. Interpretation of the sub-bottom profiler image of Profile C-C' (Figure 5-11), showing reflectors due to the underlying Tertiary strata. The vertical scale is in terms of TWT. 82

Figure 5-15. Interpretation of the sub-bottom profiler image of Profile D-D' (Figure 5-11), showing reflectors due to the underlying Tertiary strata and a channel-like feature. The vertical scale is in terms of TWT. 83

Figure 5-16. Interpretation of the sub-bottom profiler image of Profile E-E' (Figure 5-11), showing reflectors due to the underlying Tertiary strata and a channel-like feature. The vertical scale is in terms of TWT. 84

Figure 5-17. Side-scan sonar image of Area F (Figure 5-11), showing erosive seabed and exposed Tertiary strata. The vertical scale is in terms of the slant range. 85

Figure 5-18. Side-scan sonar image of Area G (Figure 5-11), showing erosive seabed and exposed Tertiary strata. The vertical 86 scale is in terms of the slant range.

Figure 5-19. Side-scan sonar image of Area H (Figure 5-11), showing erosive seabed and exposed Tertiary strata (with a hard layer protruding the seabed). The vertical scale is in terms of the slant range. 87

Figure 5-20. Side-scan sonar image of a seabed covered with sand and gravel, in Area I (Figure 5-11). The vertical scale is in terms of the slant range. 88

Figure 5-21. Holocene (marine/brackish) sedimentary sequence along the Stanpit Marsh profile. 89

Figure 5-22. Thickness of Holocene (marine/brackish) sediments (in metres). 89

Figure 5-23. Amplitudes of oscillations with different periods, as derived from the spectral analysis of the time-series of water levels. 92

Figure 5-24. Relationship between cross-sectional area and water level in the entrance channel of Christchurch Harbour (for Transect G2). 94

Figure 5-25. Hypsometric curve and characteristic water levels of Christchurch Harbour (after Tosswell, 1978). 95

Figure 5-26. Comparison between calculated cross-sectional mean current speeds (thick line) and measured surface current speeds (thin line) within the Run on: (A) 27 July 1991; and (B) 3 August 1991. 96

Figure 5-27. Oceanographic observations at Station 5, on 3-4 May 1992 (spring tide): (A) current speed (m s^{-1}, negative values are in down-estuary directions); (B) salinity (ppt); and (C) temperature (°C). 99

Figure 5-28. Stick diagram showing current vectors within (A) surface, (B) middle and (C) bottom layers, Station 5, spring tide. 100

Figure 5-29. Oceanographic observations at Station 5, on 10-11 May 1992 (neap tide): (A) current speed (m s^{-1}, negative values are in down-estuary directions); (B) salinity (ppt); and (C) temperature (°C). 101

Figure 5-30. Stick diagram showing current vectors within (A) the surface, (B) middle and (C) bottom layers, Station 5, neap tide. 102

Figure 5-31. Tidal cycle variations in SSCs (thin line with dots) and 103 current speeds (thick line) Station 5, on 3-4 and 10-11 May 1992: (A) middle layer (spring tide); (B) surface layer (neap tide); (C) middle layer (neap tide); and (D) bottom layer (neap tide).

Figure 5-32. Oceanographic observations at Station 3, on 1-2 October 1989 (spring tide): (A) current speed (cm s^{-1}, values with dashed contours are in up-estuary directions); (B) salinity (ppt); (C) temperature (°C); and (D) SSC (mg l^{-1}). 104

Figure 5-33. Oceanographic observations at Station 3, on 8-9 October 1989 (neap tide): (A) current speed (cm s^{-1}, values with dashed contours are in up-estuary directions); (B) salinity (ppt); (C) temperature (°C); and (D) SSC (mg l^{-1}). 105

Figure 5-34. Observations of water level, surface current speeds, SSC, salinity and temperature at Station 4, on 27 July 1991. 106

Figure 5-35. Observations of water level, surface current speeds, SSC, salinity and temperature at Station 4, on 3 August 1991. 107

Figure 5-36. Oceanographic observations at Station 1, on 15-16 May 1991 (spring tide): (A) current speed (m s^{-1}, negative values are in the ebb directions); (B) salinity (ppt); and (C) temperature (°C). 108

Figure 5-37. Stick diagram showing current vectors within (A) the surface, (B) middle and (C) bottom layers, Station 1, spring tide. 109

Figure 5-38. Oceanographic observations at Station 1, on 31 July - 1 August 1990 (neap tide): (A) current speed (m s^{-1}, negative values are in the ebb directions); (B) salinity (ppt); and (C) temperature (°C). 110

Figure 5-39. Stick diagram showing current vectors within (A) the surface, (B) middle and (C) bottom layers, Station 1, neap tide. 111

Figure 5-40. Oceanographic observations at Station 2, on 14-15 May 1991 (spring tide): (A) current speed (m s^{-1}, negative values are in the ebb directions); (B) salinity (ppt); and (C) temperature (°C). 112

Figure 5-41. Oceanographic observations at Station 2, on 1 August 1990 (neap tide): (A) current speed (m s^{-1}, negative values are in the ebb directions); (B) salinity (ppt); and (C) temperature (°C). 113

Figure 5-42. Stick diagram showing current vectors within (A) the surface, (B) middle and (C) bottom layers, Station 2, spring tide. 114

Figure 5-43. Stick diagram showing current vectors within (A) the surface, (B) middle and (C) bottom layers, Station 2, neap tide. 115

Figure 5-44. East-west components of current velocities observed at Station 2, on 14-15 May 1991. 116

Figure 5-45. A typical grain size distribution curve for seabed sediments within the Run, compared with material (shaded area) investigated by Thompson (1985). 119

Figure 5-46. Relationship between f_w and A_0/k_s on the basis of data from Sleath (1990). 120

Figure 5-47. Frequency distribution functions of current speeds during: (A) flood tides; (B) flood tides, with water level above 0.1 m OD; (C) flood tides, with water level below 0.1 m OD; (D) ebb tides; (E) ebb tides, with water level above 0.1 m OD; and (F) ebb tides, with water level below 0.1 m OD. 121

Figure 5-48. Distribution of U_{av}/U across the Run (A), which is derived from an assumed distribution pattern of u/u_{max} over the cross-section (based upon information presented in Chadwick and Morfett (1986)) (B). 123

Figure 5-49. Frequency distribution of U_w/U_b, on the basis of Equation [5-2]. 125

Figure 5-50. The identified grain size trends, over the Christchurch Harbour area. 131

Figure 5-51. Frequency distribution of the length of "characteristic" vectors, for randomly-arranged sample grids for Christchurch Harbour. 132

Figure 5-52. Seabed sediment distribution (the classification scheme based upon Folk (1980), modified slightly). 133

Figure 5-53. Mean grain size (in ϕ units) of the surficial sediments, Yangpu Harbour. 134

Figure 5-54. Sorting coefficients (in ϕ units) of the surficial sediments, Yangpu Harbour. 134

Figure 5-55. Skewness (in ϕ units) of the surficial sediments, Yangpu Harbour. 135

Figure 5-56. The identified grain size trends of Yangpu Harbour. 136

Figure 5-57. Frequency distribution of the length of "characteristic" vectors, for randomly-arranged sample grids for Yangpu Harbour. 137

Figure 5-58. Exchange of trace sediments, in the surficial sediments (for details of the various Cases, see text). 142

Figure 5-59. Exchange of trace sediments, in the sedimentary sequence. 143

Figure 5-60. Concentration of foraminiferal tests (in terms of mass) in Christchurch Harbour ($\times 10^{-3}$). 146

Figure 5-61. Percentages of exotic benthic foraminiferal tests in Christchurch Harbour, after Murray (1966) and Wang and Murray (1983). 147

Figure 5-62. Definition of flood or ebb durations, for a tidal cycle associated with double highs. 153

Figure 5-63. Relationship between water level and water volume in Christchurch Harbour, as derived from Figure 5-25. 154

Figure 5-64. Frequency distributions of flood tidal prisms (A) and ebb tidal prisms (B), for Christchurch Harbour. 155

Figure 5-65. Frequency distributions of flood tidal durations (A) and ebb tidal durations (B), for Christchurch Harbour. 156

Figure 5-66. Frequency distributions of water levels at Mudeford Quay. 157

Figure 5-67. Hypsometric curve and characteristic water levels for Langstone Harbour (after Portsmouth Polytechnic, 1976). 160

Figure 5-68. Relationship between water level and water volume for Langstone Harbour, as derived from Figure 5-67. 160

Figure 5-69. A comparison of the morphology of Langstone Harbour: (A) Sheet 86 of the first edition of the one-inch O.S. maps (published in 1810); and (B) Sheets 196 and 197 (published in 1989 and 1990, respectively) of 1:50000 O.S. Landranger Series. Solid lines denote MHWS and dashed lines represent MLWS. 163

Figure 5-70. Frequency distribution function of dimensionless current speeds, P(ß). 165

Figure 5-71. Hypsometric curve and characteristic water levels of Yangpu Harbour. 167

Figure 5-72. Relationship between water level and water volume in Yangpu Harbour, derived from Figure 5-71. 167

Chapter 6.

Figure 6-1. Three possible patterns represented by the x-y curves 174

($x = \mu_2 - \mu_1$, $y = S_{k1} - S_{k2}$): (A) $x_1 < 0$; (B) $x_1 = 0$; and (C) $x_1 > 0$.

Figure 6-2. Relationship between $Z/N^{1/2}$ and N_x/N for different numbers of samples and background probabilities. 175

Figure 6-3. Inlet cross-sectional area related to tidal prism, for tidal inlets in the U.K. (Evans and Collins 1975), the U.S.A. (Jarrett 1976), Japan (Shigemura 1980), and China (Zhang 1987; Gao 1988). 181

TABLE HEADINGS

Chapter 4.

Page

Table 4-1. Stations for tidal cycle measurements (observation were throughout the water column, except at Station 4). 33

Table 4-2. Observed changes in grain size parameters, in the direction of net sediment transport. 49

Table 4-3. Periods of water level data availability, for current speed calculations, between 3 January 1991 and 7 January 1992 (time in GMT). 61

Chapter 5.

Table 5-1. Exposure and inundation events associated with water levels recorded by the tide gauge in the Run (3 August, 1991). 69

Table 5-2. Sedimentary sequences of the short cores (SC1, SC2 and SC3 are located at 0, 50, and 100 m from the salt marsh cliff, respectively). 90

Table 5-3. Harmonic tidal constituents analysed using TIRA. 93

Table 5-4. Harmonic tidal current constituents analysed using TIRA. 98

Table 5-5. Residual current velocities (U_R) and water transport rates (q_w), derived from tidal cycle measurements at 3 stations (the directions in degrees, in terms of azimuth). 117

Table 5-6. Representative wave periods (T), wave heights (H) and associated frequency of occurrence in nearshore areas of Christchurch 124

Bay (based upon data from Hydraulics Research (1989b)). Also listed are A_0 and U_b, calculated on the basis of Equations [2-17] and [2-18].

Table 5-7. Mean bed-load transport rates, based upon the formulae of Madsen and Grant (1976) and Vincent *et al.* (1981). 126

Table 5-8. Average SSC (C_Q) related to water discharges (Q) (see text, for explanation). 128

Table 5-9. SSC and salinity of water samples collected from the Run, between January and March, 1991. 129

Table 5-10. Input parameters for the conceptual experiments. 141

Table 5-11. Equilibrium tracer concentrations ($C_{m,eq}$) for the 4 cases of the conceptual experiments. 144

Table 5-12(A). Contents of foraminiferal tests and organic matter in the sand fractions of seabed sediment samples in Christchurch Harbour (for sample locations, see Appendix B). 145

Table 5-12(B). Contents of foraminiferal tests and organic matter in the sand fractions of seabed sediment samples outside Christchurch Harbour (for sample locations, see Appendix B). 148

Table 5-13. Critical levels of content of exotic tracers, calculated for 23 cases ($A^b=1.91\times10^6$ m^2 ; $C_1=0.228\times10^{-3}$; $D_L=0.05$ m; and $a_r=0.9$). 152

Table 5-14. Equilibrium conditions of Christchurch, Langstone and Yangpu Harbours. 169

Chapter 6.

Table 6-1. Variations of *c* and *n* in the P-A relationship (the O'Brien Method), based upon data from various references (P in km^3, A in km^2). 182

Table 6-2. Stability conditions related to the ratio P/M, according to Bruun's stability concept (after Bruun, 1978). 184

NOTATIONS

$A, A_{<\eta>}$	Cross-sectional area of tidal inlets, below the mean sea level
A_b	Area of the tidal basin
A_{ba}	"Apparent" area of the tidal basin
A_D	Dispersion coefficient for sediments
A_E	Equilibrium cross-sectional area
A_0	Orbital amplitude of water particles, due to wave motion
a_r	Percentage of sediment input from the river which remains within an embayment
a_s	Percentage of sediment input from the sea which remains within an embayment
B	Width of entrance channel of a tidal inlet system
C	Suspended sediment concentration; concentration of trace sediments
C_b	Average tracer concentration in the estuarine deposits
C_m	Tracer concentration within the moving layer
C_Q	Suspended sediment concentration related to water discharge Q
c	Coefficient in O'Brien's formula
D	Grain size; horizontal distance; sampling depth
D_L	Thickness of the moving layer
D_R	Deposition rate of the estuarine basin
$f_a(f_c)$	Coefficient of friction (unidirectional currents)
f_w	Coefficient of friction (waves)
f_{cw}	Coefficient of friction (combined waves and currents)
g	Acceleration due to gravity
H	Wave height; water depth
H_s	Significant wave height
h	Water depth
K	Repletion coefficient
k	Parameter representing the difference between dynamic behaviour of foraminiferal tests and that of silica sands; ratio between the transport capacity by currents and the magnitude of longshore transport.
k_s	Turbulent roughness length
K_u	Kurtosis
k_1	Coefficient in the Gadd *et al.* (1978) equation
k_2	Coefficient in the Hardisty (1983) equation
M	Mass of the tracer passing through a cross-section during T_0; amount of annual gross littoral drift
M_n	Balance of "trace" material
M_s	Amount of moving sediments in the water column over a unit area
M_0	Transport of the tracer due to advection
N	Number of sediment samples along a line
N_x	Number of Case 1 or Case 2 trends along a line
P	Probability; cumulative probability; tidal prism
P_l	Wave energy flux parameter
Q	Water discharge
Q_F	Fresh water discharge
Q_l	Longshore sediment transport rate

Q_s	Sediment discharge
q_m	Part of sediments in the total output from the estuary to the open sea, which is from the estuarine deposit
q_n	Amount of sediments stored within the estuarine system over a unit time
q_o	Sediment output toward the open sea, over a unit time
q_s	Sediment transport rate
q_w	Water transport rate
q'	Net sediment transport rate through the entrance channel
R	Tidal range
R_D	Grain size distribution function of sediments within sampling depth
R_b	Tidal range within the tidal basin
R_o	Open sea tidal range
R_{in}	Rate of tracer injection
R_T	Grain size distribution function of the material in transit
S	Salinity
s	Grain size
S_k	Skewness
T	Tidal cycle period; wave period; temperature
T_n	Budget of trace sediments over a unit time
T_0	Time span for considering equilibrium
U	Cross-sectional mean current velocity
u	Instantaneous current velocity
U_a	Speed of unidirectional currents
U_{av}	Vertical mean current velocity
U_{max}	Maximum vertical or cross-sectional mean current speed
u_{max}	Maximum instantaneous current velocity
U_R	Residual current velocity
U_s	Mean velocity at which particles move
U_w	Near-bed wave oscillatory velocity
U_z	Current speed at a height of z above the bed
U_*	Friction velocity
V	Total volume of sediments in the estuarine system
V_m	Volume of "trace" material in V
w_s	Settling velocity of particles
Z	Z-score
z_0	Roughness length
γ	Bulk density of sediments
γ_s	Specific weight of sedimentary particles
ϵ	Phase lag between open sea tides and basin tides
η	Water level
η_b	Mean water level within the tidal basin
Θ_{cw}	Shields Parameter due to combined waves and currents
Θ_w	Shields Parameter due to waves
κ	von Kármán constant
l	Porosity of sediments
μ	Mean grain size
ρ	Water density
ρ_s	Sediment density
σ (σ^2)	Sorting coefficient

Subscripts and Abbreviations

cr	Critical
e	Ebb
eq	Equilibrium
f	Flood
init	Initial
MHWS	Mean High Water Spring (tides)
MLWS	Mean Low Water Spring (tides)
MHWN	Mean High Water Neap (tides)
MLWN	Mean Low Water Neap (tides)
POL	Vessel's lines of position
OD	Ordnance Datum (Newlyn)
SSC	Suspended Sediment Concentration
TWT	Two-Way Travelling time

CHAPTER 1. INTRODUCTION

Tidal inlets are distributed widely along tidally-influenced coast- lines; they are characterised by an entrance channel system, a tidal basin, and an ebb tidal delta area to seaward of the entrance (Hayes 1980).

The channel system is characterised by a relatively deep main channel, at the entrance to the tidal basin. During flood or ebb tides, tidal currents passing through the channel form a tidal jet. The channel becomes shallower, in both the seaward and landward directions, and is divided into a number of flood- or ebb-dominated channels over flood and ebb tidal deltas.

The tidal basin receives seawater during the flood tide and exports water through the entrance on the ebb. The water volume between the high and low water levels is defined as the "tidal prism"; this is controlled by the tidal range and the hypsometric characteristics of the basin. Rivers may discharge into the basin and, along its shorelines, intertidal flats and salt marshes are the typical geomorphic features present.

A flood tidal delta may develop in such a basin; this is due to the accumulation of sediments transported through the entrance channel by the flood tidal currents. Generally, the position of the flood tidal delta is close to the entrance of the system.

The ebb tidal delta is formed to seaward of the entrance; its position is controlled by interaction between ebb tidal currents and waves. A typical ebb tidal delta consists of a number of shoals, separated by tidal channels which link the entrance with the open sea. Because these coastal features are important to many human economical activities in coastal areas (sea transport, construction of tidal power stations, reclamation of intertidal land, entertainment, coastal defence, etc.), scientific research with regard to the geomorphology, hydrodynamics and sediment dynamics of tidal inlets has been undertaken since the beginning of this century.

In early times the emphasis of the investigations was focused upon an evaluation of the stability of tidal inlets, which were developed for navigation and the construction of sea ports. Brown (1928) was among the first to describe systematically the tidal inlet system. O'Brien (1931), Escoffier (1940), Price (1947, 1963), Keulegan (1951) and

Bruun and Gerritsen (1959) have also contributed greatly to the understanding of tidal inlet behaviour.

Most early investigations are characterised by their qualitative descriptions and statistical approaches. Such studies had inspired many coastal engineers in the 1970s, especially in the United States, to undertake further research into the hydrodynamics of tidal inlets. Thus, a project known as GITI (the General Investigation of Tidal Inlets) was carried out over a decade, undertaken by the Coastal Engineering Research Center of the U.S. Army Corps of Engineers (Sorensen 1980). A number of GITI reports were soon published, which investigated the hydrodynamics and stability of tidal inlets through field observations, historical data analysis, numerical and physical models, and remote sensing techniques. Other investigations during this period include those by Özsoy (1977) and Bruun (1978). Apart from the engineering efforts, geological aspects of tidal inlets (inlet off-set, tidal deltas, bedforms, sedimentary structures and depositional sequences) have been investigated by geologists and marine scientists (Hayes 1975; Boothroyd 1978).

Recent research into tidal inlets reflects not only the requirements of a solution to the problems encountered in early exploitation of inlet systems, but also the increasing concern of environmental problems associated with tidal inlets. For example, many process-orientated approaches have been developed in the 1980s. In particular, the importance of sediment dynamics has been realised: sediment transport patterns in inlet systems has been demonstrated to be associated with geological setting, hydrodynamics and stability (FitzGerald 1984; FitzGerald and Nummedal 1983; FitzGerald *et al.* 1984). This trend is shown also by the papers presented on the International Symposium on Hydrodynamics and Sediment Dynamics of Tidal Inlets, held at Woods Hole, in the United States, in 1986 (Aubrey and Weishar 1988).

From a purely scientific point of view, tidal inlets represent a challenge to the development and application of sediment dynamics theories. In such systems, the distribution patterns of waves, currents, bathymetry and sea-bed sediments are highly variable in both space and time. Consequently, large gradients in the parameters used in various sediment transport formulae may be present. As a result, a number of sediment transport mechanisms are introduced (e.g. Officer 1981); these increase significantly the difficulties in determining net sediment transport patterns.

The present study is an attempt to identify sediment transport patterns in tidal inlet systems, using three independent techniques. Firstly, sediment transport formulae are applied to the computation of material balance of bed-load and suspended load at the entrance channel, using long-term monitoring data of water levels and suspended sediment concentrations. Secondly, a mathematical model based upon the exchange of natural trace sediments between the tidal basin and the adjacent continental shelf is formulated to examine the sediment balance. Finally, a qualitative model on the basis of grain size trend analysis is developed to define net sediment transport pathways. Further, the sediment transport patterns are related to equilibrium cross-sectional area of the entrance channel, so that the inlet stability can be evaluated.

Christchurch Harbour, located on the southern coastline of England, is selected to be the major study area. In addition, Langstone Harbour (southern England) and Yangpu Harbour (Hainan Island, southern China) are included in this investigation as comparative inlet systems.

CHAPTER 2. LITERATURE REVIEW

2.1. Sediment Transport Rate

2.1.1. Transport Theories

The phenomenon of sediment transport can be investigated using a variety of methods (for reviews, see Chien (1956), Graf (1971), Yalin (1972), White *et al.* (1975), and Vanoni (1984)). In general, it has been analysed on the basis of the definition of the transport rate:

$$q_s = M_s \, U_s \qquad [2\text{-}1]$$

where M_s is the amount of all the moving sedimentary particles present in the water column over a unit area, and U_s is the mean velocity at which the particles move. The transport rate can be expressed in terms of mass, dry weight, immersed weight or volume, depending upon the quantity used to define M_s.

Most existing equations for sediment transport rate are derived according to the above definition, based upon various sets of assumptions (e.g. Bagnold 1956, 1966; Yalin, 1963; Ackers and White 1973; van Rijn 1984a, 1984b). The bed-load equation proposed by Einstein (1942, 1950) can be derived also from this definition directly, as demonstrated below.

In Einstein's analysis, only particles that move a distance of at least L during a period of T are included as bed-load in transport (thus, the threshold condition is expressed implicitly). Further, the thickness of the bed-load is of the order of the particle diameter. Thus, the total weight of the particles in transport over a unit area is:

$$M_s = \frac{\alpha \, \gamma_s \, D^3}{\alpha_1 \, D^2} \, P_1 \qquad [2\text{-}2]$$

where the term $\alpha \, \gamma_s \, D^3$ represents the average weight of a particle in motion (α is a coefficient, γ_s the specific weight and D the mean grain size of particles). Another term, $\alpha_1 \, D^2$, denotes the average projection area of a particle, and P_1 is the probability that a particle will move a distance of at least L during T. Let $n \times L$ be the average distance that the particles move during T. The mean velocity of the moving particles will then be:

$$U_s = \frac{n\,L}{T} \qquad [2\text{-}3]$$

Multiplying [2-2] by [2-3] and assuming that $n = 1/(1-P_1)$ yields:

$$q_s = \frac{\alpha\,\gamma_s\,D}{\alpha_1}\,\frac{L}{T}\,\frac{P_1}{1-P_1} \qquad [2\text{-}4]$$

This is precisely the form of the bed-load formula developed by Einstein (see Yalin 1972).

These mechanics-oriented formulae, which relate the transport rate to current speeds or near-bed shear stresses, contain two crucial parameters. One is associated with the physical properties of the sediments, such as grain size, sphericity, roundness, and their distributions. The other represents the threshold condition of the initiation of movement.

In addition to the semi-empirical approach, the sediment transport rate can be also determined by a "rating-curve" method. The relationship between the transport rate and any associated variable (such as depth mean current speed, or water discharge) is established through a statistical analysis (e.g. Collins 1970, 1981; Thompson 1985). This method expresses the threshold condition implicitly.

In early times, analyses and experiments were carried out to relate the threshold current speed or bottom shear stress to sediment and water properties, under unidirectional steady flow and uniform grain size conditions.

A relationship between the critical current speed (represented by a characteristic value, such as the depth mean speed) and grain size was proposed by Hjulström (1935, 1939), which was extended or modified subsequently by Menard (1950), Lane (1955), Sundborg (1956), Allen (1965), Postma (1967) and Miller *et al.* (1977) for use under various flow and sediment conditions.

Another threshold criterion used frequently, for non-cohesive particles, is the relationship between the dimensionless threshold shear stress ($\tau_{cr}/[(\rho_s-\rho)gD]$, known as the Shields Parameter) and the Grain Reynolds Number ($U_{*cr}D/\nu$) (Shields 1936). The curve has been extended for use with larger or smaller grain sizes and under unsteady flow conditions (Komar and Miller 1973; Miller *et al.* 1977; Dingler 1979; Bettess 1984;

Hammond *et al.* 1984; Diplas 1987; Wiberg and Smith 1989).

The threshold can be related also to particle settling velocities (Yang 1973; Collins and Rigler 1982; Komar and Clemens 1985). This relationship is useful because there have been many studies on settling velocities since those of Stokes (Gibbs *et al.* 1971; Baba and Komar 1981; McCave 1984; Lowe 1988).

A problem associated with the determination of threshold conditions is that the initial movement of a single particle is easy to define (White 1940; Tipper 1989), but the task becomes very difficult if sedimentary material with non-uniform grain sizes and various grain shapes are involved (Miller *et al.* 1977; Lavelle and Mofjeld 1987).

In any transport equation, it is only possible to use characteristic values to represent the conditions at threshold and sediment properties. However, the two parameters can vary even under the same flow and sediment conditions; this is due, for example, to bed armouring (Klingeman and Emmett 1982; Karim and Forrest 1986) and biological (Nowell *et al.* 1981; Grant *et al.* 1982; Line *et al.* 1989) effects. The threshold is obtained usually under some restricted conditions such as a narrow range of grain sizes and steady unidirectional flow (without these restrictions, a considerable amount of scatter will be introduced) (Miller *et al.* 1977). This implies that, for any environment, a specific transport equation is needed; a universally valid equation does not exist (Yalin 1972; Huntley and Bowen 1990).

Some transport equations are based upon Equation [2-1], but avoid use of the parameters described above. For example, transport rate can be determined using artificial tracer methods, or through the measurement of sandwave migration rates.

Methods of defining sediment transport rates using artificial tracers have been developed since the early 1960s (Crickmore and Leath 1962; Ingle 1966; Crickmore 1967). Three of these approaches are in common use i.e. SIM (Spatial Integration Method), TIM (Time Integration Method) and CIM (Continuous Injection Method) (for a review, see Madsen 1989).

In the SIM, the mass of particles in motion is $\rho_s(1-\lambda)D_L$ over a unit area (where D_L is thickness of the moving layer). The average velocity of the moving particles (U_s) is represented by the velocity of the centroid movement (u_0) which is a function of the quantity of the tracer introduced, average tracer concentration presented within the moving layer, and the time span during which the position of the centroid is moved. Hence, the transport rate in terms of mass becomes:

$$q_s = \rho_s (1-\lambda) D_L u_0 \qquad [2\text{-}5]$$

The TIM is based upon conservation of tracers. All of the tracer will pass through a cross-section some distance downstream, during a long time (T_0). Hence:

$$M_s = \int_0^{T_0} C B \rho_s (1-\lambda) D_L U_s \, dt \qquad [2\text{-}6]$$

where B is the width of the cross-section and C is the tracer concentration within the moving layer. Assuming that U_s and D_L are constant over the time (0, T_0), we have the mass transport rate:

$$q_s = \frac{M_s}{\int_0^{T_0} C B \, dt} \qquad [2\text{-}7]$$

Because the cross-section is involved in the computation, the transport rate defined by [2-7] is a cross-sectional averaged value.

The CIM is characterised by continuous injection of the tracer at a constant rate. After a steady state has been reached i.e. the rate of tracer injection is equal to that at which the tracer leaves a transect:

$$C_{eq} B \rho_s (1-\lambda) D_L U_s = R_{in} \qquad [2\text{-}8]$$

where C_{eq} is the equilibrium concentration of the tracer and R_{in} the rate of tracer injection. Thus:

$$q_s = \frac{R_{in}}{B C_{eq}} \qquad [2\text{-}9]$$

Similar to the TIM, steady and uniform U_s and D_L are assumed here, to obtain the cross-sectional mean transport rate.

To relate the bedform migration to sediment transport rate, a general equation can be derived in the following way. If the material above a certain level below the sandwave trough is considered as bed-load being transport, then the mass of moving sediments over a unit area can be written as:

$$M_s = \frac{1}{L} \rho_s (1-\lambda) \int_0^L \eta \, dx \qquad [2\text{-}10]$$

where L is the sandwave length and η is the height in relation to the base level. During the migration, the velocity of the gravity centre of moving sediment (U_g) is the mean velocity of the particles in transport. Hence:

$$q_s = \frac{1}{L} \rho_s (1-\lambda) U_g \int_0^L \eta \, dx \qquad [2\text{-}11]$$

Various simplified forms of [2-11] have been derived (for example, U_g can be replaced by the celerity of sandwave migration) (e.g. Harris 1991).

The transport rates obtained from the tracer and bedform migration methods have been used for the field testing of the mechanics-oriented transport equations (Heathershaw 1981; Pattiaratchi and Collins 1985; Huntley and Bowen 1990), although these two methods themselves need calibration. At the present stage, accurate direct measurements of the sediment transport rate is still a problem awaiting a solution. Recently, methods using horizontal sediment traps (Pickrill 1986) and underwater cameras (Thorne 1986; Drake *et al.* 1988) have been developed; this is likely to be a large step forward towards a solution of the problem.

An approach to the determination of the net transport rate may be developed on the basis of the law of conservation of sediment mass. Equations of sediment continuity have been derived to identify changes in sea-bed morphology caused by sediment movement (e.g. Kraus and Horikawa 1990), which have the following general form:

$$\frac{\partial q_x}{\partial x} + \frac{\partial q_y}{\partial y} + \gamma_s (D_R + S) = 0 \qquad [2\text{-}12]$$

where D_R is the deposition rate caused by sediment transport, γ_s is the bulk density of the sediment, S is a sink or source term, and q_x and q_y are components of the transport rate in terms of mass in the x and y directions, respectively. Equation [2-12] may be solved numerically if the spatial distributions of γ_s, D_R and S are known and proper boundary conditions are specified.

2.1.2. Bed-Load Transport Rate

Wave-Induced Transport

The longshore transport rate under wave action on the beach can be expressed by (Inman and Bagnold 1963; Komar and Inman 1970; Komar 1971):

$$Q_l = k_l \, P_l^m \qquad [2\text{-}13]$$

where Q_l is the volume transport rate, P_l is a variable associated with the wave energy flux, and k_l and m are parameters controlled by the sediment transport environment. For example, Komar and Inman (1970) have found that, for sand-size material:

$$Q_l = \frac{0.77}{\alpha \, (\rho_s - \rho) \, g} \, P_l \qquad [2\text{-}14]$$

where α is a correction factor for the pore space within the sediments, ρ the water density, and ρ_s the sediment density.

In offshore areas, wave-induced bed-load transport rate averaged over half wave period waves can be expressed as (Madsen and Grant 1976):

$$q_s = 12.5 \, w_s \, D \, \theta_w^3 \qquad [2\text{-}15]$$

where w_s is the particle settling velocity, D the grain size, and Θ_w the Shields Number due to waves. Θ_w is defined as:

$$\theta_w = \frac{0.5 \, f_w \, \rho}{(\rho_s - \rho) \, g \, D} \, U_w^2 \qquad [2\text{-}16]$$

The coefficient of friction due to waves, f_w, is a function of near-bed orbital amplitude of a water particle (A_0) and sea-bed roughness (z_0) (Sleath 1990). A_0 is controlled by water depth, wave height and wave period, according to Airy wave theory (Komar 1976). For example, in shallow water, we have:

$$A_0 = \frac{H\,T\sqrt{\frac{g}{h}}}{4\,\pi} \qquad [2\text{-}17]$$

where H is the wave height, T the wave period and h the water depth.

Under a steady flow with a immovable bed, z_0 ranges between 0.02 and 0.3 cm, depending upon sediment type (Soulsby 1983). In a time-varying flow associated with bedforms in motion, however, z_0 is not constant when measured using the von Kármám-Prandtl equation (Ludwick 1975). Under such conditions, the apparent roughness length is influenced highly by the near-bed shear velocity (being proportional to U_*^4) (Heathershaw and Hammond 1979; Dyer 1986).

In [2-16], U_w is the maximum wave-induced near-bed oscillatory velocity, which can be related to A_0 and T by:

$$U_w = \frac{2\,\pi\,A_0}{T} \qquad [2\text{-}18]$$

Equation [2-15] is valid when Θ_w exceeds a critical value; this is determined from an Shields diagram for waves.

Transport by Currents

Formulae of sediment transport rate frequently used for marine environments are an extension of the "Bagnold type" equations (Sternberg 1972; Gadd *et al.* 1978; Vincent *et al.* 1981, 1983; Hardisty 1983). These equations have the following forms:

$$q_s = k_1\,(\,U_{100} - U_{100cr}\,)^3 \qquad [2\text{-}19]$$

and $$q_s = k_2\,U_{100}\,(\,U_{100} - U_{100cr}\,)^2 \qquad [2\text{-}20]$$

where k_1 and k_2 are parameters relating to sediment property; U_{100} is the current speed, and U_{100cr} is the threshold current speed, both measured at 1 m above the bed.

Effect of Combined Waves and Currents

When both waves and currents are present, the resultant sediment transport rate can be much higher than that caused by the current alone (Owen and Thorn 1978; Hallermeier 1982; Kemp and Simons 1984). In the equations for transport rate, therefore, both the current speed and the near-bed wave oscillatory velocity should be taken into account. For example, an Einstein-type equation for bed-load transport (Brown 1950) has been modified to incorporate wave-induced flow (Madsen and Grant 1976) (the transport rate is expressed as a vector):

$$\vec{q}_s = 40\, w_s\, D\, \theta_{cw}^3 \frac{\vec{U}}{|\vec{U}|} \qquad [2\text{-}21]$$

where $\vec{U}$ is the vector sum of the wave induced oscillatory velocity, $\vec{U}_w$, and the current velocity, $\vec{U}_c$. Here, Θ_{cw} is the Shields Number due to combined waves and currents, defined by:

$$\theta_{cw} = \frac{0.5\, f_{cw}\, \rho}{(\rho_s - \rho)\, g\, D} (\vec{U}_w^2 + \vec{U}_c^2) \qquad [2\text{-}22]$$

where f_{cw} is the coefficient of friction due to currents and waves. In [2-21] the threshold condition is not expressed explicitly. The critical value of Θ_{cw} can be determined from an appropriate Shields diagram (Komar and Miller 1975; Madsen and Grant 1975). The coefficient f_{cw} can be calculated by (Madsen and Grant 1976):

$$f_{cw} = \frac{|\vec{U}_c|\, f_c + |\vec{U}_w|\, f_w}{|\vec{U}_c| + |\vec{U}_w|} \qquad [2\text{-}23]$$

where f_c is the coefficient of friction due to unidirectional currents alone. Equation [2-21] reduces to the original equation (Brown 1950) if wave-induced currents are not present and leads to Equation [2-16] if there are no advective currents. Equation [2-22] is averaged over half a wave period.

Vincent *et al.* (1981, 1983) have developed a Bagnold-type equation, which expresses the threshold condition in an explicit way:

$$\vec{q}_s = 0.09\, (\theta_{cw} - \theta_{cw,cr})\, \vec{U} \qquad [2\text{-}24]$$

2.1.3. Suspended Load Transport Rate

The transport rate of suspended sediments is defined by:

$$q_s = \int_0^h U_z\ C_z\ dz \qquad [2\text{-}25]$$

where U_z and C_z are current speed and SSC (Suspended Sediment Concentration) at a height z above the bed, respectively. An assumption in the use of [2-25] is that the suspended particles will move at the same speed as the water particles.

Suspended sediment transport rate is often calculated using observed U_z and C_z data. Alternatively, velocity and SSC profiles based upon some theories can be used (e.g. the von Kármán-Prandtl velocity profile equation and the Rouse (1937) equation for SSC profile) (Dyer 1986).

2.2. Net Transport Patterns

2.2.1. Transport Mechanisms

Estuaries and tidal inlets are characterised by the exchange of sediments between the tidal basin and the adjacent continental shelf, due to rectilinear material movement under the influences of tidal currents and gravitational circulations (Kirby 1987; O'Connor 1987).

Net transport is the integration of the sediment exchange. The time-series of q_s required for computation of the net sediment flux may be obtained from long-term monitoring of current speeds and seabed sediment characteristics (e.g. Harris and Collins 1988), or through a numerical model using transport formulae with appropriate threshold conditions and sediment properties (e.g. Black 1987; Falconer and Owens 1990).

It is difficult in many cases, however, to obtain long time-series of sediment transport rates; this causes uncertainty in estimating net transport directions at the river mouth or entrance to the tidal basin. One of possible solutions to this problem is to decompose the net transport rate into a series of components (each is controlled by a single transport mechanism), evaluate the relative importance of each component, then use the dominant components to account for the net transport pathways.

Officer (1981) has summarised 6 sediment transport mechanisms: (i) gravitational circulation; (ii) tidal variations in the SSC profiles; (iii) lag effects of erosion and deposition; (iv) time-velocity asymmetry; (v) tidal mixing; and (vi) near-bed residual circulation. As an example of the second mechanism, the vertical distribution of SSC, associated with a turbidity maximum and within unfilled estuaries, varies over a tidal cycle in such a pattern that suspended sediments are prevented from escaping to seaward (Schubel and Carter 1984). Erosion and deposition lags (the third mechanism) have been recognised as causes for landward sediment transport on intertidal flats (van Straaten and Kuenen 1957; van Straaten 1958; Postma 1961).

Quantitatively, Su and Wang (1986) have demonstrated that the mean flux of suspended sediment through an estuarine cross-section can be decomposed into 12 terms, among which 2 terms are due to advection, 3 are tidal dispersion terms and the remaining 8 terms are caused by dispersion due to circulation effects. In this particular study, the advection terms and one of the tidal dispersion terms are adequate to define net transport directions.

Results of the mechanism investigations imply that transport due to advection or mean flow may not be always dominant over other transport components caused by dispersion. Thus, in estuaries and tidal inlets, the net sediment transport direction can differ considerably from the direction of the residual flows; this phenomenon has been observed frequently (e.g. Gallivan and Davies 1981; Gao *et al.* 1990).

2.2.2. Qualitative Approaches to Transport Pathways

Qualitative methods have been developed to define net sediment transport directions. The methods use some characteristics of deposited sediments (bedforms, grain size trends and natural trace sediments) as indicators of transport paths.

Sandwaves show often a longitudinal asymmetry. In rivers, sandwaves have been observed to migrate in the direction faced by the steeper slope. This behaviour is assumed to be maintained in the marine environments (Johnson *et al.* 1982). Further, the patterns of sandwave asymmetry cannot change over a single flood (or ebb) period (Boothroyd 1985). The asymmetry is interpreted, therefore, as being indicative of net sediment transport directions.

In marine environments, sediment transport parallel to sandwave crests has been reported (Harris 1989). This observation appears to imply that the net transport is not associated strictly with a direction perpendicular to sandwave crests.

Grain size trends are indicative of net sediment transport (Russell 1939; Plumley 1948; Yeakel 1962; Pettijohn *et al.* 1972; McLaren 1981). This approach is based upon the concept that any grain size distribution of surficial sediments is the result of erosion, transport and accumulation — rather than the type of sedimentary environment (beaches, rivers, etc.) alone. A combination of changes in grain size parameters (mean, sorting coefficient and skewness) has been related to net transport paths, through an "one-dimensional" statistical procedure (McLaren and Bowles 1985).

The model proposed by McLaren and Bowles (1985) relates net sediment transport paths to spatial changes in the mean grain size (μ), the sorting coefficient (σ^2) and the skewness (S_k). For sampling sites d_1 and d_2, $d_1(s)$ is the grain size distribution of d_1 and $d_2(s)$ is that of d_2 (where s represents the grain size in ϕ units). If the net transport is from d_1 to d_2, the sediment at d_2 will be better sorted than that at d_1. Further, $d_2(s)$ can be related to $d_1(s)$ by means of a "transfer function" X(s), given by:

$$d_2(s) = k\ d_1(s)\ X(s) \qquad [2\text{-}26]$$

where k is a scaling coefficient. McLaren and Bowles (1985) have argued that if X(s) is positively skewed, sediments at d_2 will become coarser and more positively-skewed than the sediments at d_1. On the other hand, if X(s) is negatively-skewed, the sediments will become finer and more negatively skewed. Consequently, there are two cases associated with net transport from d_1 to d_2, defined as Case 1 and Case 2:

Case 1: $\sigma_2^2 < \sigma_1^2$, $\mu_2 > \mu_1$ and $S_{k2} < S_{k1}$

Case 2: $\sigma_2^2 < \sigma_1^2$, $\mu_2 < \mu_1$ and $S_{k2} > S_{k1}$

where the subscripts 1 and 2 represent sampling sites d_1 and d_2, respectively. Both Case 1 and Case 2 may occur even if there is no net transport (in the sense that the deposition sites involved have no relationship of material exchange with each other). In this situation, however, there are another six cases (in addition to Cases 1 and 2) which may also occur; the probability of Case 1 or Case 2 is assumed, therefore, to be 1/8. Thus, if there is transport along a line, the probability of a Case 1 or Case 2 condition, for one of the two directions associated with the line, will be considerably larger than 1/8.

To determine if the probability is high enough for such transport, a "significance test" method has been suggested. Using n samples along the survey line, $(n^2-n)/2$ possible sample pairs are formed. Then N_x (the observed occurrences of Case 1 or 2) for each direction is established. Finally, a Z-score for each case and each direction is calculated, using the formula:

$$Z = \frac{N_x - p\,N}{\sqrt{N\,p\,(1-p)}} \qquad [2\text{-}27]$$

where p is the background probability (p=1/8, according to McLaren and Bowles). A Z-score exceeding a certain level indicates highly probable transport in a preferred direction. Z is 1.645 and 2.330 at the 95% and 99% level of significance, respectively.

In extending this model to marine environments, two problems exist: (i) whether or not Cases 1 and 2 really represent grain size trends associated with net transport; and (ii) how to form the survey lines on the basis of a grid of sediment samples.

2.3. Criteria of Inlet Stability

2.3.1. Concept of Stability

There are two definitions of stability. According to Escoffier (1940), the stability refers to a dynamic equilibrium state of the inlet morphology in response to hydrodynamic forces. Examples of investigations which adopt this consideration include those of O'Brien (1931, 1969) and van de Kreeke (1985, 1990). Bruun (1978) defined stability, however, as the ability of a tidal inlet to maintain its geometric and geomorphic characteristics (i.e. location, planform, cross-sectional area, etc.) under the influences of both "normal" and "stormy" conditions. A stable inlet should be able to respond to a storm event with slow geomorphological changes and to restore its equilibrium state shortly after the storm. The degree of stability in Bruun's sense can be monitored through repeated field surveys and remote sensing (Machemehl *et al.* 1991). Alternatively, empirical criteria can be used to define the degree of stability (e.g. Bruun 1978; Gerritsen 1992).

Basically, the stability is determined by sediment transport patterns within the system; any change in the geomorphic features is due to sediment movement on the shorelines near the entrance and the tidal deltas. For example, the entrance position can migrate in either an updrift or downdrift direction, due to the accumulation/erosion of tidal deltas and storm-induced spit breaching (Aubrey and Speer 1984).

Hydrodynamical features, sediment transport patterns and the morphology form an interrelated system; this system evolves towards a dynamic equilibrium state. Many aspects of hydrodynamics (Boon and Byrne 1981; Aubrey and Speer 1985; Speer and Aubrey 1985; Joshi 1982; Özsoy and Ünlüata 1982), sediment dynamics (Bruun and Gerritsen 1959; Özsoy 1986; Jarvis and Riley 1987; Bale and Holley 1989; Fry and Aubrey 1990), and geomorphology (Oertel 1972; Finley 1978; Boothroyd 1985) have been studied extensively. Potentially, based upon these studies, various criteria for the inlet stability can be formulated.

2.3.2. Equilibrium of the Entrance Channel

For any entrance to the tidal basin, a "closure curve" i.e. the relationship between the maximum near-bed shear stress (τ_{max}) and the cross-sectional area (A) can be defined (Escoffier 1940). On this curve, an equilibrium point (τ_E, A_E) exists, due to the negative feedback between τ_{max} and A within the inlet system. Accumulation of sediment in the entrance will reduce A, which then enhances τ_{max}. An increase in τ_{max} will intensify sediment movement out of the entrance; this will enlarge A. Hence, there is a tendency for A to evolve toward an equilibrium level i.e. A_E. The concept of a closure curve has been developed further into "closure surface", to evaluate the relative stability of multiple entrances to a single tidal basin (van de Kreeke 1985).

The classic method of determining A_E is that proposed by O'Brien (1969). Earlier, O'Brien (1931) found a good linear relationship between $\log_{10}A$ and $\log_{10}P$ (where P is the tidal prism for spring tides), for a number of inlets along the Pacific coast of the United States. This P-A relationship has been believed to represent the equilibrium condition, which can be written in a general form (O'Brien 1969):

$$A_E = c\ P^n \qquad [2\text{-}28]$$

where c and n are constants. These two parameters are determined from linear regression analysis, using measured tidal prism and cross-sectional area data on a regional basis.

The application of the O'Brien method depends upon data from a number of inlet systems. For a single tidal inlet, equilibrium cannot be defined due to the statistical characteristics of the method.

2.3.3. Criteria for Overall Stability

The degree of overall stability of a tidal inlet can be related to other empirical criteria, without considering equilibrium. One of these criteria is the ratio P/M (where P is the spring tidal prism and M is the amount of annual gross littoral drift) (Bruun and Gerritsen 1959; Bruun 1978). P represents a factor for maintaining the entrance open, whilst M is a factor leading to closure of the inlet. The larger the ratio, the more stable is the inlet. A critical value of P/M, dividing stable and instable inlets, has been empirically determined to be around 100.

Battjes (1967) has argued that the flushing ability of an inlet depends not only on the tidal prism, but also on the cross-sectional area. These two factors could be expressed as the rate of sediment transport within the entrance channel. Consequently, he used the ratio of M/q_{max} (where q_{max} is maximum sediment transport rate through the entrance channel, in the absence of littoral drift) to evaluate the overall stability.

Another criterion concerns the maximum cross-sectional mean current speed (U_{max}) under stable conditions (Bruun, 1978). A stable inlet should have a U_{max} of around 1.0 m s^{-1}, so that the inlet has enough flushing momentum to prevent accumulation of sediments.

Equilibrium cross-sectional area (A_E) has been used also to evaluate stability conditions of an inlet (in Bruun's sense). For example, A_E (O'Brien and Dean 1972) and A_E/M (Bruun 1978) have been taken as the criteria for stability: the higher the value of A_E, the more stable is the inlet system against closure due to sediment accumulation. The lower limit of A_E for a stable inlet depends upon the intensity of sediment movement towards the entrance.

CHAPTER 3. STUDY AREAS

3.1. Christchurch Harbour

3.1.1. Regional Geology

The Christchurch Harbour area (Figure 3-1) is located within the southern part of the Hampshire Basin; the sedimentary history of the basin extends back into the Jurassic (Melville and Freshney 1982; Bristow *et al.* 1991). During most of the Jurassic and Cretaceous eras, the area was within a subtropical shallow sea environment and marine oolites, clays, Greensand and Chalk were deposited. Such deposits are not, however, exposed on the ground over the region. Between the late Cretaceous and the middle Palaeocene, the region was subjected to uplift and experienced, therefore, a short period of erosion.

At the beginning of the Tertiary, a large sedimentary basin known as Hampshire-Dieppe Basin was formed (Curry and Smith 1975). Thus, from the Middle Palaeocene to Lower Oligocene, alternating marine muds and sand interlayered with gravels were deposited. In the Miocene, the area was uplifted because of the Alpine mountain building movements.

The Pleistocene deposits are characterised by Plateau and Valley Gravels, which are either of river terrace (Burton 1933) or marine origin (Devoy 1982). The coastal area of southern England is believed to have been unglaciated during the Pleistocene (Nilsson 1983). The English Channel area might have been subjected to, however, one or more Quaternary glaciations (Kellaway *et al.* 1975). During interglacial periods in the early and middle Pleistocene, a "Solent Lake" was thought to exist (Kellaway *et al.* op.cit.) while, in the late Pleistocene, a river system known as "Solent River" developed (Reid 1902; Everard 1954; Dyer 1975). The lower Solent River valley was inundated during the Flandrian transgression. Consequently, the Holocene deposits of the Solent area occur in the forms of spits, beaches, salt marshes, intertidal flats, subtidal muds, and offshore sand or shingle banks.

The exposed Tertiary strata around Christchurch Harbour is the Barton Formation of the upper Eocene. The Hengistbury Beds, the lower part of the formation, are exposed

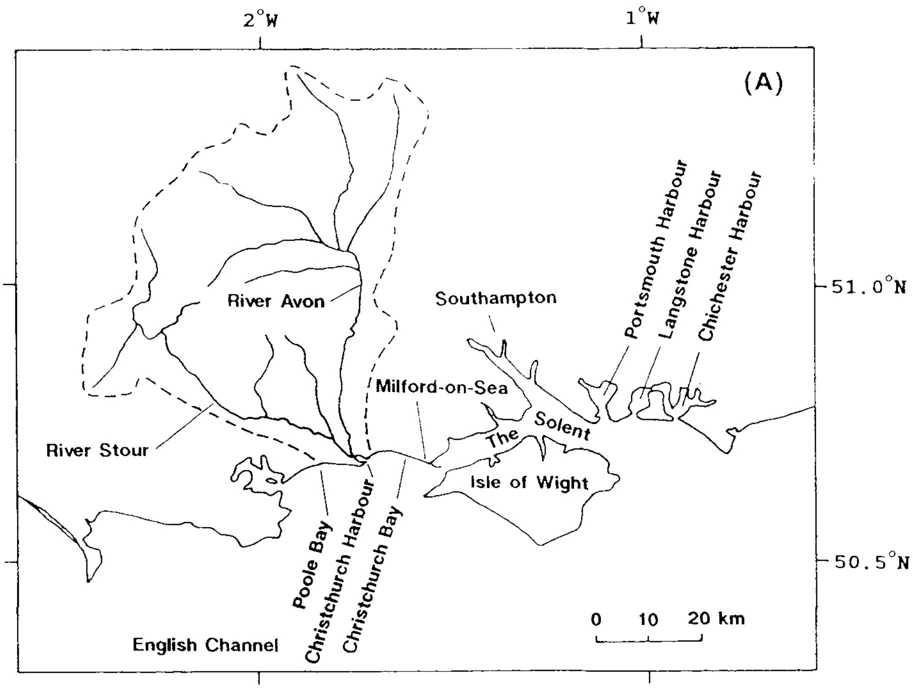

Figure 1(A).

at the cliff of Hengistbury Head (Curry 1976). The Barton Beds, the middle-upper Barton Formation, are seen at Highcliffe (Barton 1973).

3.1.2. Geomorphology

Poole and Christchurch Bays are characterised by cliffed coastlines. Intensive coastal erosion has taken place in Poole and Christchurch Bays since the final disappearance, during the Flandrian, of a Chalk ridge linking Purbeck and the Isle of Wight (Steers 1981). As a result, cliffs of 15 to 35 m in height have been formed in the two bays. The cliff is 5 to 30 m in height around Hengistbury Head and 30 to 37 m near Highcliffe.

Extending in a southeasterly direction from the eastern end of Hengistbury Head is Christchurch Ledge, an underwater ridge consisting of ironstones and bedrocks. The ridge forms a barrier to sediment exchange between Christchurch and Poole Bays, except on the beach and within the breaker zone. To the south of the ridge, the seabed is

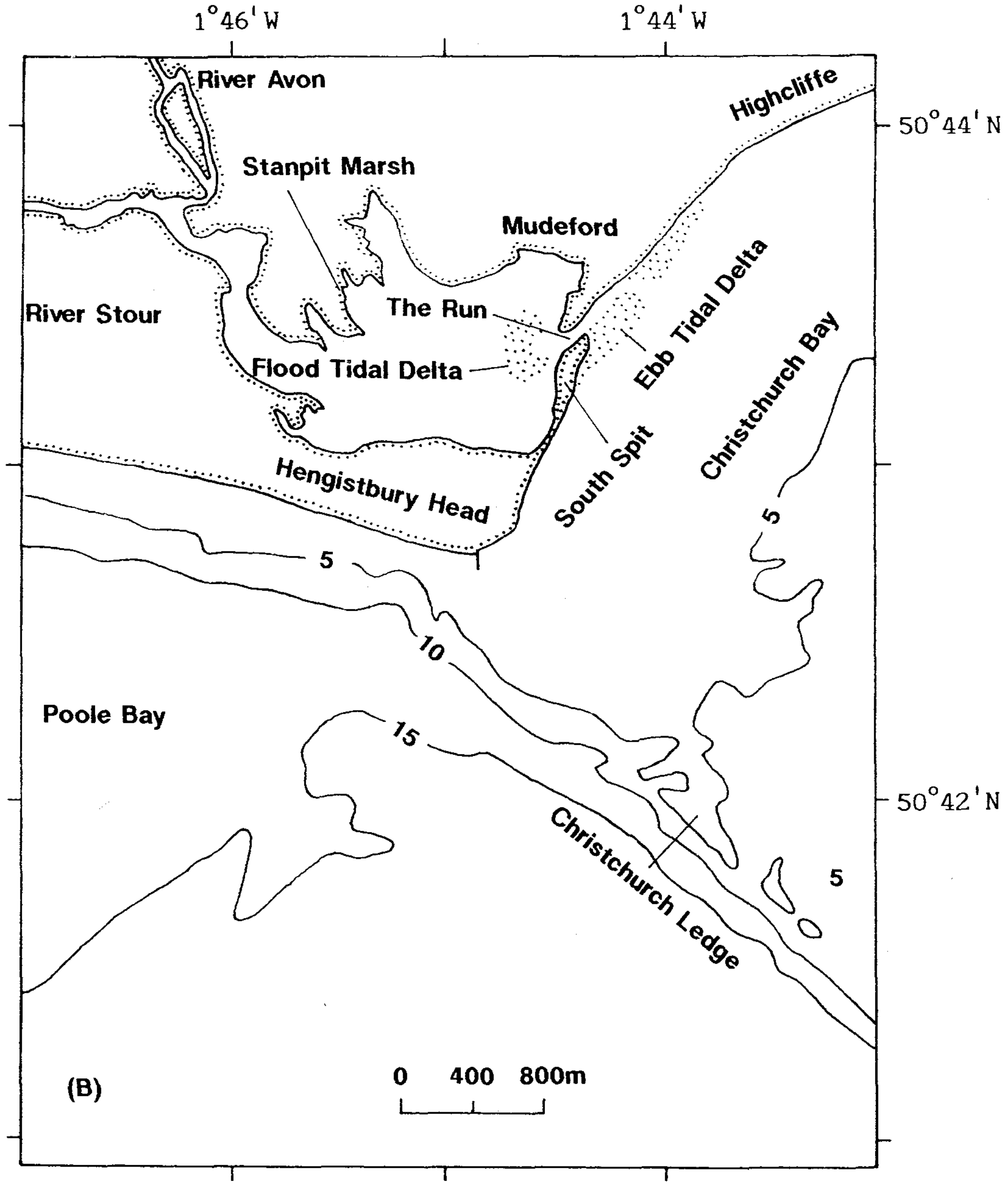

Figure 3-1. Geomorphological characteristics of the Christchurch Harbour area: (A) location of the Harbour (the scope of the drainage basin area being denoted by the dashed line); and (B) the tidal inlet system (bathymetry in metres).

covered with poorly sorted sediments. To the north, within Christchurch Bay, the sediment cover is thin, with the Tertiary rocks exposed in some places. Sediments around Hengistbury Head are mainly sands (mean grain size exceeding 2 ϕ), with an area to the south of the ridge covered with sandy gravel and gravelly sand (mean grain size between 0 and 2 ϕ) (Dyer 1969, 1970). The seabed sediments consist of less than 5 % of shells of mussel (*Mytilus edulis*), slipper limpets (*Crepidula fornicata*) and barnacles (*Balanus sp.*).

The longshore drift of sand and gravel eroded from the cliffs around Hengistbury Head and Highcliffe has led to the development of two spits (see Figure 3-1), which have semi-enclosed Christchurch Harbour to form an estuarine / tidal inlet system. This system can be categorized, according to Pritchard (1952), as a "bar-built" type. The tidal basin has an area of 1.9 km^2 at MHWS, with a tidal prism of 1.43×10^6 m^3 under mean spring tidal conditions (Tosswell 1978). Within the Harbour, the water is shallow, with extensive intertidal flats and salt marshes (Murray 1961, 1966). The salt marshes are bordered by a low "cliff", 0.4 to 0.7 m in height.

The entrance to Christchurch Harbour is through "the Run", a local name for the entrance channel. Flood and ebb tidal deltas are both present. The ebb tidal delta has been observed to be unstable (Burton 1931; Robinson 1955). The position of tidal channels over the ebb tidal delta and the height and shape of the delta have been changing continuously. Before 1939, when the large groyne et Hengistbury Head was built (Wise 1956), longshore sediment transport rate was higher than present; this resulted in periodic eastward extension of the ebb tidal delta and subsequent breaching during storms. Sediment supply to the delta was almost cut off after 1939. Consequently, the height and size of the delta has been reduced considerably.

3.1.3. Waves

In Christchurch Bay, southwesterly waves are the prevailing and dominant waves. This pattern results from a combination of the wind regime and the fetch available for wave generation. The area is dominated by westerly winds (between NW and SW) (Hydraulics Research 1989a). It is exposed to waves coming in directions ranging from SE to SSW, the greatest fetch being associated with the SW direction. The southwesterly waves are, therefore, the strongest. Near the entrance to Christchurch Harbour, however,

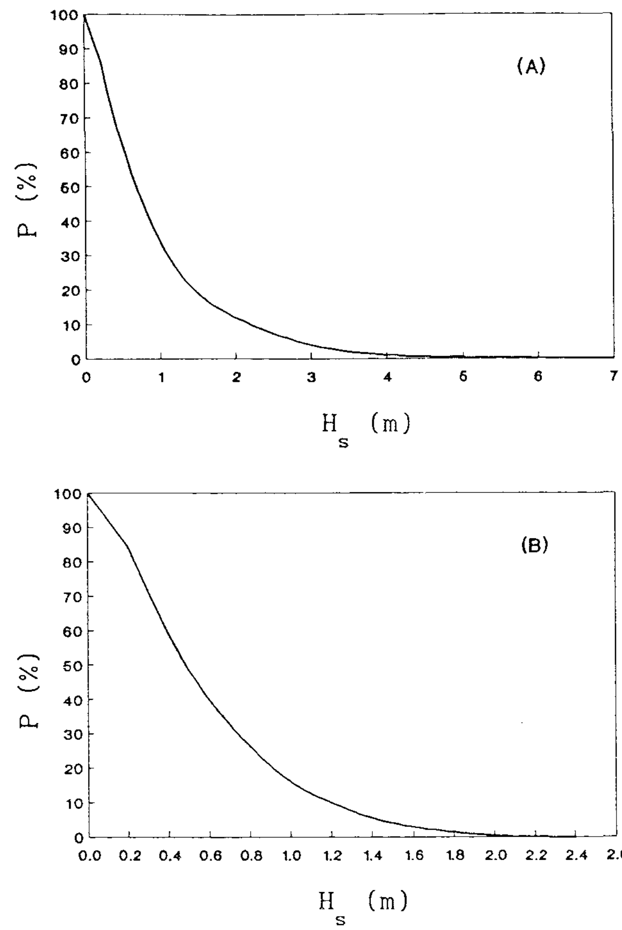

Figure 3-2. Wave height exceedence curves for: (A) offshore areas of Christchurch Bay, 1974-1989 (after Hydraulics Research 1989a); and (B) nearshore areas of Milford-on-Sea, between July 1987 and May 1989 (after Hydraulics Research 1989b). P is the cumulative probability of exceeding a particular height.

southeasterly waves may be the biggest because the height of southwesterly waves is reduced by the Hengistbury Head and Christchurch Ledge (Burton 1931).

The wave conditions in the offshore areas of Christchurch Bay have been hindcasted using the HINDWAVE model developed by Hydraulics Research (1989b). Wind data of a 15-year period (1974-1988), from Portland, were used as the model input. According to the results obtained from this model, the most frequently occurring wave heights are less than 0.6 m, but waves with a significant wave height (H_s) of up to 7 m can occur (Figure 3-2). All the waves with a hindcasted H_s over 6 m are from

SW-WSW directions.

The largest wave heights have been observed to be reduced considerably in the nearshore areas. For example, an analysis of the Waverider Buoy data obtained from a site 1.5 km to the south of Milford-on-Sea, between April 1987 and May 1989, shows that wave heights over 2.2 m are rare (Figure 3-2). This reduction in wave heights in the landward direction is largely the result of seabed friction.

3.1.4. Tides

Generally, the English Channel is characterised by semidiurnal tides, large tidal ranges and strong tidal currents (Le Provost and Fornerino 1985). The tides in the Christchurch area, however, show a different and unique pattern.

Firstly, the tidal water level has the "double high" feature, indicating a strong influence of the overtides, especially the M_4. Tide gauge data from western Poole Bay show that the high water occurs twice during a tidal cycle, except on neap tides (Tyhurst 1978). The first high water is higher than the second high water over spring tides and *vice versa* towards neaps. During two to three neap tidal cycles, this feature disappears, but a "stand" is present i.e. after the first phase of rising tides, the water level rises very slowly and the flood duration becomes considerably longer than that of the ebb. The tides of Christchurch Harbour are similar to those observed in Poole Bay; an important difference is, however, that the low water levels in Christchurch Harbour are much higher than those in Poole Harbour, although the high water levels are very close to each other in the two places.

Secondly, because this area is close to an amphidromic point, the tidal range in this area is the lowest within the English Channel (Doodson and Corkan 1931). At the mouth of Christchurch Harbour, the mean spring and neap tidal ranges are only 1.4 m and 0.8 m, respectively; these are "microtidal" according to Davies (1964). The mean spring tidal ranges increase towards the west and east (approximately 2 m at Portland and over 3 m at Southampton).

Finally, the tidal currents in Poole and Christchurch Bays are relatively weak, with spring tidal current speeds of less than 1.0 m s^{-1} (Blain 1980). Within the entrance (i.e. the Run) to Christchurch Harbour, however, tidal current speeds can reach more than 2.5 m s^{-1} (Burton 1931).

3.1.5. The Estuarine Waters

The drainage basin areas of the rivers Avon and Stour are 1725 km^2 and 1240 km^2, respectively (Codrington 1870); if a remaining 170 km^2 (which was not included in Codrington's calculation, including lower reaches of the rivers Avon and Stour and the Harbour itself) is added (as measured from the O.S. 1:50000 Landranger Sheets, 195 and 184), the total catchment area of Christchurch Harbour is approximately 3135 km^2.

Seasonal changes in the freshwater discharge are significant. The annually averaged highest and lowest of discharges occur in winter and summer, respectively. For example, in 1991, the maximum mean daily freshwater discharge for January reached 117 m^3 s^{-1}, whilst it was only 16 m^3 s^{-1} for August.

The interaction between the freshwater and sea water forms a distinct salt wedge. During summer and autumn, the upper limit of the wedge reaches the confluence of Avon and Stour (where salinity of over 30 ppt has been observed in the bottom layer); in winter, however, the wedge rarely penetrates into most of the harbour (with a salinity of below 6 ppt in the bottom layer over the bay head area) (Murray 1966). This seasonal change is associated with the pattern of freshwater discharges.

Seasonal changes in water temperature are also significant (with a maximum temperature over 20°C in summer and less than 5°C in winter) (Murray 1966); this is because the area is very shallow and water temperature is controlled by the air temperature.

3.2. Comparative Areas (U.K. and China)

3.2.1. Langstone Harbour

Langstone Harbour (Figures 3-3) is one of a number of tidal inlets located adjacent to the eastern Solent area, on the southern coast of England. It was formed by inundation of a small drainage basin, during the Flandrian transgression. The geology of the area is characterised by Tertiary muds and sands. The area of the tidal basin, at MHWS, is 19.4 km^2.

Within the entrance section and to seaward of it, the seabed is covered by sand and gravel. Along the eastern shoreline of the entrance, a shingle spit extends towards

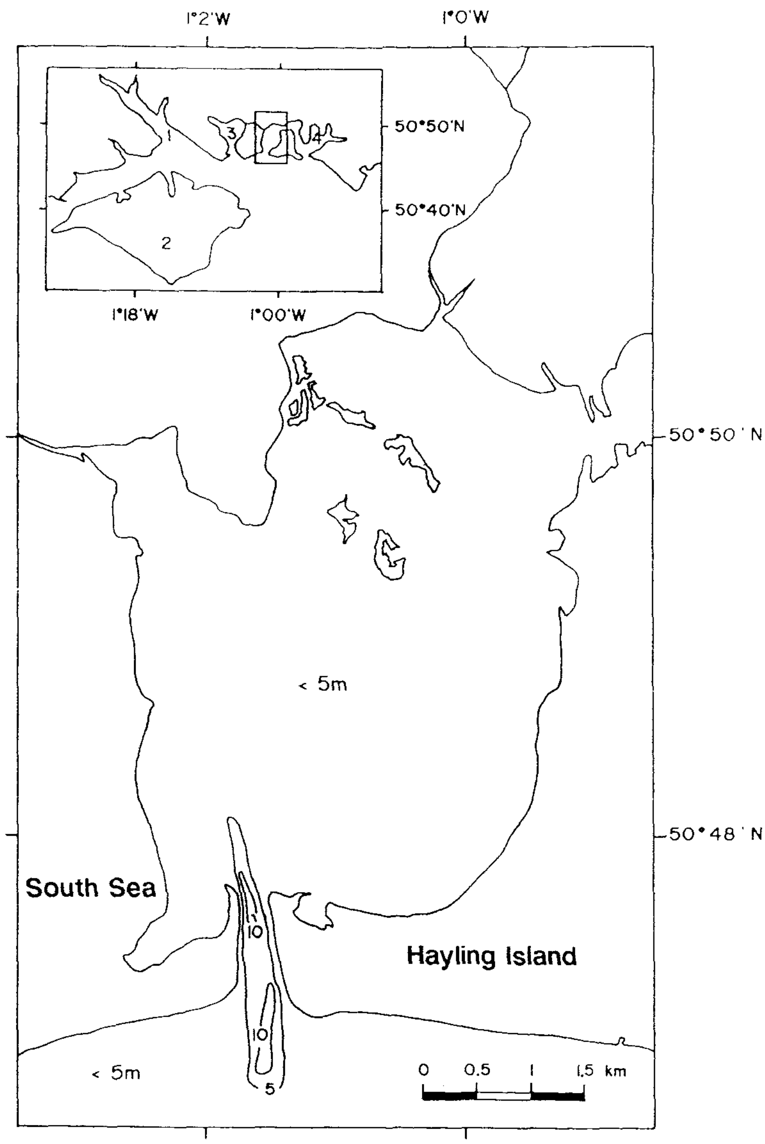

Inset key: 1. Southampton Water;

2. Isle of Wight;

3. Portsmouth Harbour; and

4. Chichester Harbour.

Figure 3-3. Location map of Langstone Harbour, southern England (bathymetry in metres).

the tidal basin. Most of the tidal basin is characterised, however, by muddy sediments; these consist of a mixture of clay, silt and sand. No flood delta has developed. Salt marshes (covered with *Spartina*) and mud flats are widely distributed within the tidal basin (Haynes and Coulson 1982). Sand is present around the harbour entrance (Dyer 1980), which seems to originate from a seaward source. An ebb delta is present, consisting of sand and gravel.

Tides in the Harbour are semidiurnal in character, with a flood duration of 7.1 hours and an ebb duration of 5.7 hours. Although the general tidal characteristics in the eastern Solent are notable for the combination of a week lunar semidiurnal (M_2) constituent and a strong shallow water (M_4) constituent, the effect of this combination is less pronounced in Langstone Harbour. The mean tidal range is 3.0 m, with mean spring and neap tidal ranges of 4.1 m and 2.0 m, respectively (mesotidal to macrotidal, according to Davies (1964)).

Freshwater discharge from the rivers is low, with a maximum daily inflow of 40.6×10^4 m^3 and a minimum of 10.3×10^3 m^3. In addition, there are two channels which connect Langstone Harbour with Portsmouth and Chichester Harbours, respectively. There is a net import of water from the large channelled connection with Chichester (3.50×10^6 m^3 on a spring tide and 0.97×10^6 m^3 on a neap) and a net export of water, through a small channel, towards Portsmouth (0.73×10^6 m^3 on springs; 0.20×10^6 m^3 on neaps) (Portsmouth Polytechnic 1976). Discharge from the freshwater and channel sources, other than the inlet entrance, is 45.0 m^3 s^{-1} .

3.2.2. Yangpu Harbour

Yangpu Harbour is a tidal inlet system, consisting of Yangpu and Xinying Bays, located in the northwestern part of Hainan Island (southern China) (Figure 3-4). During the Tertiary, the area lay within a depression zone (known as the Hainan - Leizhou Penisula Depression). Consequently, a thick layer (>3000 m) of shallow marine sequences, consisting of unconsolidated mud and sand with a small portion of gravel, were deposited. The sequences have been named as the Zhanjiang Formation. Since the beginning of the Quaternary, the region has experienced drastic geological movements associated with the formation of east-west trending deep faults and the eruption of volcanic lava; this occurred over a large area in northern Hainan. The tidal inlet was

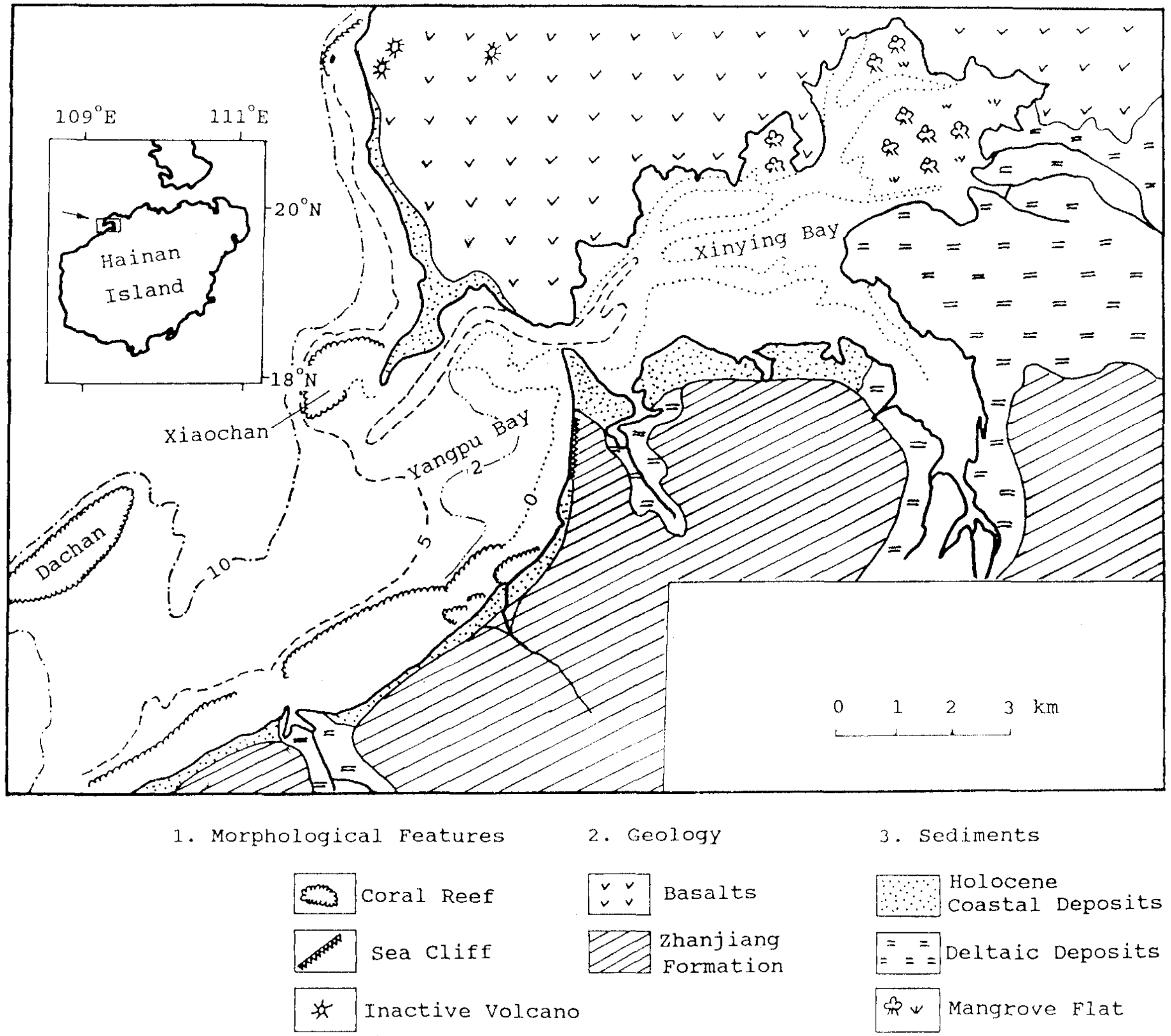

Figure 3-4. Location map of Yangpu Harbour, southern China (bathymetry in metres).

developed, therefore, within the fracture zone between the southerly Tertiary strata (the Zhanjiang Formation) and the northerly Quaternary volcanic strata (basalts).

Tides over the region are diurnal and highly regular. Time-asymmetry in the rising and falling phases of tide exists: the average duration of the flood is 13.2 hours, whilst that of the ebb is 11.6 hours. Outside the tidal basin, the mean spring and neap tidal ranges are 3.23 m and 0.52 m, respectively. Because Xinying Bay is relatively large in area (i.e. 50 km^2 at MHWS), the tidal prism is of the order of 10^8 m^3 for a spring tide (Wang *et al.* 1977). Tidal currents are active, therefore, in dispersing the seabed sediments.

The dominant waves over the region are from the southwest, with the frequency of occurrence of the significant wave height exceeding 0.5 m being approximately 3.3% (Zhu *et al.* 1984).

Sediment supply to Yangpu and Xinying Bays is mainly from coastal erosion and some small river inputs. Biogenic sediments, originating from coral reefs, constitute a secondary contribution.

Coastal erosion of the Zhanjiang Formation is caused by the southwesterly waves. This process results in the formation of a sea cliff, 5 to 15 m in height. The eroded material is transported to the north (Zhu *et al.* 1984). Some of the sediments are deposited as a bay-mouth bar, whilst other material is dispersed in an offshore direction by tidal currents; here, an ebb tidal delta is formed, known as the Yangpu Shoal.

The tidal inlet system has a freshwater drainage basin area of 1357 km^2 and some 6.2×10^4 m^3 of sediments are discharged into Xinying Bay annually (Wang *et al.* 1985). Most of the river-derived material accumulates over intertidal mudflats and mangrove flats within the bay-head area.

In the offshore area, coral reefs are present, of which the Dachan and Xiaochan Reefs are the largest (with areas of 4 km^2 and 2 km^2, respectively). Biogenic sediment supply produced by the reefs is of the order of 0.4×10^4 m^3 yr^{-1} (Wang *et al.* 1985); this is responsible for the relatively high carbonate contents in the seabed sediments (with the calcite content higher than 20 % over outer Yangpu Bay) (Zhu *et al.* 1984).

CHAPTER 4. METHODS

4.1. Data Collection

4.1.1. Geophysical Survey

Side-Scan Sonar Survey

The side-scan sonar survey was carried out on 26 August, 1989, using *MV Avon Valley*. A Waverley Electronics Model 3700 dual side-scan sonar system (100 KHz) was used to produce dual-channel sonographs. The range scale shown on the sonographs (the slant range) is 75 m. Position fixing was achieved on the basis of a Decca Main Chain Navigator System (SW British Chain, 1B), which has been described by Tetley and Calcutt (1986) and Sonnenberg (1988). The vessel's lines of position (LOP) were obtained from the red and purple decometers on the Mark 21 receiver. The positioning error is estimated to be of the order of 60 m over this region during the survey. Approximately 16 km of course tracks were completed (Figure 4-1).

Sub-Bottom Profiler Survey

On 29 May and 2 June, 1990, sub-bottom profiler surveys were undertaken on board *MV Wessex Explorer*. The system used was an EG&G Model 230-1 Uniboom system. Such a system provides high resolution (of around 0.5 m), coupled with moderate penetration (up to 50 m in the study area).

The vessel position was fixed using a Qubit Track IV-B, linked to the Decca system described previously. The Qubit printed out the fixed position and time, at 1 min intervals. A Del Norte Trisponder Navigation System (accuracy $\pm$3m) was also set up, with the transmitters installed at Hurst Point (Marine Cafe) and the Needles Coastguard Station on the Isle of Wight. Although the Trisponder readings were incomplete, they proved to be useful in calibrating the Decca records. Hence, the final course tracks (Figure 4-2), with a total length of 96 km, have been fixed on the basis of the Decca records, calibrated with some discontinuous Trisponder records.

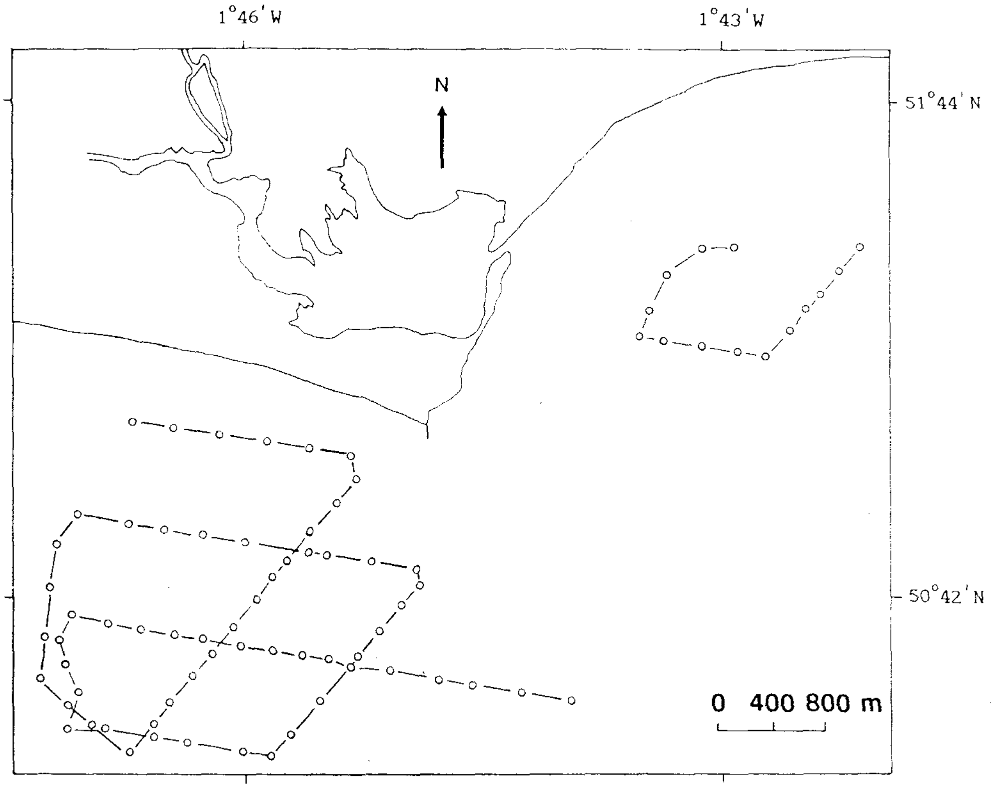

Figure 4-1. Course tracks of side-scan sonar survey.

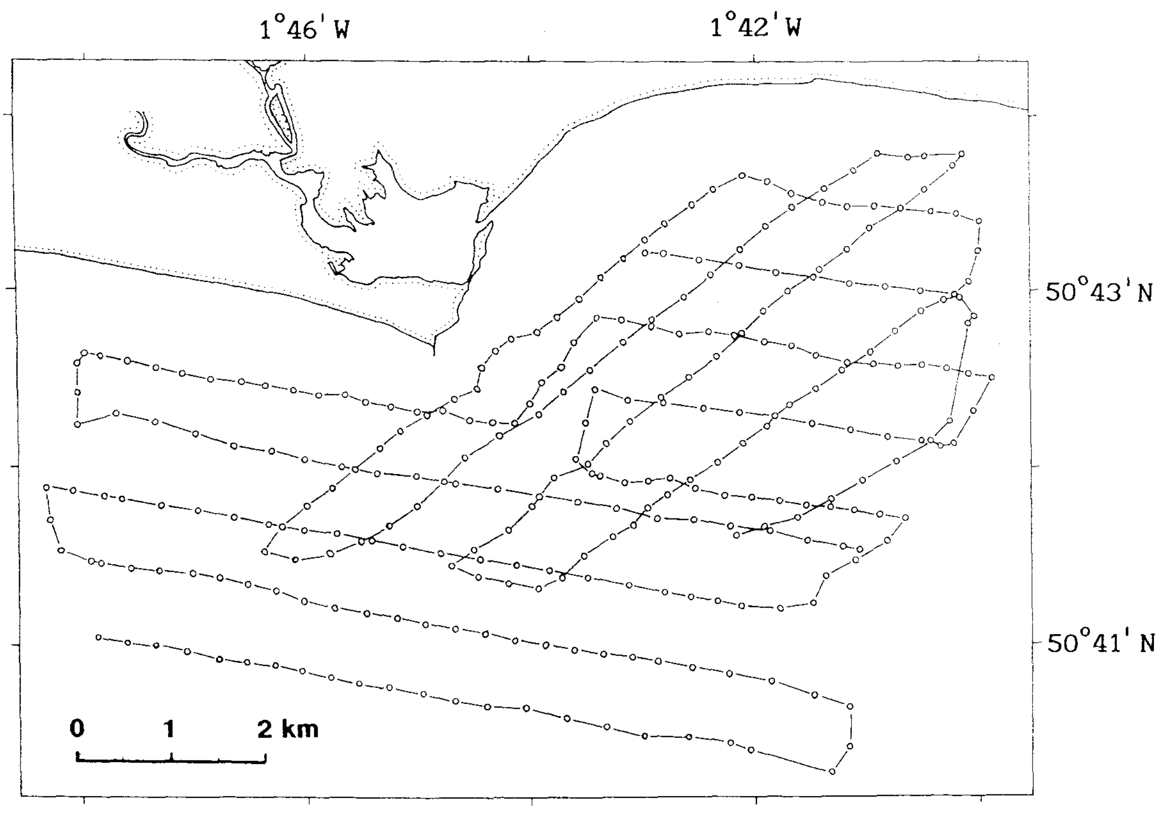

Figure 4-2. Course tracks of the sub-bottom profiler survey.

Analysis of Geophysical Data

Information on the surficial sediments, buried topography and bedrock characteristics was obtained on the basis of an interpretation of the geophysical data, in conjunction with seabed sediment sampling.

Water depth and the thickness of depositional units were calculated using the relationship (McQuillin and Ardus 1977):

$$H = 0.5\ v\ t \qquad [4\text{-}1]$$

where H is the water depth or deposit thickness, v is the velocity of sound in the medium (seawater or sub-bottom strata), and t is the two-way travel time (TWT). Over the Christchurch area, v was taken as 1500 m s^{-1} for seawater, 1600 m s^{-1} for loosely-consolidated Quaternary sediments and 2160 m s^{-1} for the underlying Tertiary strata (Dyer *et al.* 1969; Dyer 1975).

On the basis of tone intensity and line features on the side scan sonograph (D'Olier 1979; Russell-Cargill 1982), different types of sediments and bedrocks and associated bedforms were identified. The position of points on the boundaries dividing the various types were related then to the ship position by:

$$D = \sqrt{H^2 + D_a^2} \qquad [4\text{-}2]$$

where D is the horizontal distance from a point to the location beneath the ship, H the water depth, and D_a the apparent distance measured on the side-scan sonograph.

Surficial sediment thickness was interpreted based upon identification of sub-bottom reflectors (for a review, see Geyer (1983) and McQuillin *et al.* (1984)). The TWT was measured from the Uniboom record, with the distance from the seabed to the reflector then being calculated. Where the sub-bottom reflectors were obscured by multiples or located within the pulse length, only approximate values or ranges could be estimated.

4.1.2. Oceanographic Measurements

Tidal Cycle Observations

Spring and neap tidal cycle measurements of current speed, salinity, temperature and suspended sediment concentrations (SSCs) were carried out at 5 stations (their positions are listed in Table 4-1 and shown on Figure 4-3). Each data set covers a period of 12.5 to 13 hr (Appendix A).

At Stations 1 and 2, observations of current velocity, salinity, temperature and water depth were undertaken on board *MV Satina*. Current speed and direction were measured using a Valeport direct reading current meter, salinity and temperature by a direct reading salinometer, and water depth using an echo-sounder. Measurements of SSC were carried out during the 1990 observations, using an ABP siltmeter (transmissometer type). Because the sea water was very clear, this instrument was influenced seriously by ambient sunlight; consequently, the data were not satisfactory and this part of the field programme was finally abandoned.

At Station 3, because of busy boat traffic within the Run during late summer, it was impossible to anchor a boat in the central part of the channel. As a result, the vessel (*MV Stala Barbara*) was attached to the Quay wall during the measurements. The distance from the Quay wall to the measuring position was approximately 3 m.

Current speed and direction were measured using a NBA direct reading current meter (model DNC-3), salinity and temperature by a direct reading salinometer, and SSC using the Partech (Model 7000-3RP) turbidity monitor. The DNC-3 meter had a poor resolution in direction readings (10°) and sometimes malfunctioned; however, this did not affect the overall quality of the data substantially, since the current direction here was rectilinear and controlled by the orientation of the channel.

The turbidity data were calibrated by filtration. For this purpose, a number of water samples were collected in conjunction with the siltmeter readings. Filtration was carried out by suction, following the procedure described in McCave (1979). Around 2 litres of each water sample were filtered, using a pre-weighed Whatman GF/F Glass Microfibre filter (with the retention diameter of 0.7 μm). The filter was rinsed three times with distilled water, after the sea water was removed.

Two methods for drying the filters were investigated. The first method utilises a constant humidity tank. Filters retaining sediment were put into the tank, floored with saturated sodium nitrite ($NaNO_2$) solution for 46 hr. The filters were weighed then immediately after removal from the tank, using a R200D electronic semimicro balance (a product of Sartorius), which has a readability down to 10^{-5} g.

In the second method, the filters (after being removed from the tank) were placed into an oven for 2.5 hours, at a temperature of around 70°C. The filters were then weighed, and the amount retained was calculated.

Table 4-1. Stations for tidal cycle measurements (observations were throughout the water column, except at Station 4).

Station Number	Latitude	Longitude	Variables Measured	Date of Observations
1	50°42.55'N	1°43.66'W	H,U,S,T	31 July 1990 15 May 1991
2	50°43.54'N	1°42.83'W	H,U,S,T	1 August 1990 16 May 1991
3	50°43.39'N	1°44.38'W	H,U,S,T,C	1 October 1989 8 October 1989
4	50°43.37'N	1°44.42'W	η,U,S,T,C	27 July 1991 3 August 1991
5	50°43.27'N	1°45.56'W	H,U,S,T,C	3-4 May 1992 10-11 May 1992

Key: H, Water depth; U, Current Velocity; S, Salinity; T, Temperature; C, Suspended sediment concentration; and η, Water level.

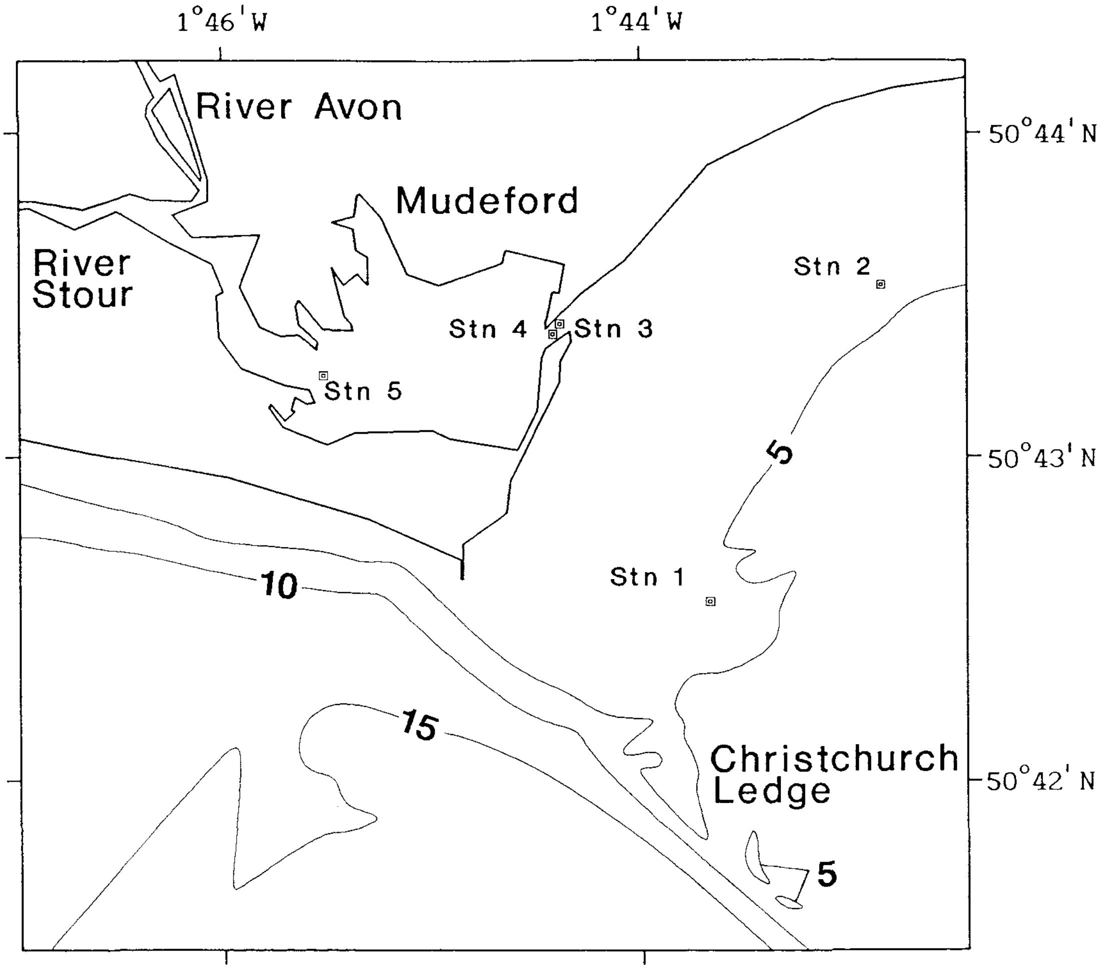

Figure 4-3. Location map showing stations for tidal cycle measurements.

The relationship between the amount retained (Figure 4-4), determined by the two methods, showed that the oven dry procedure introduced a further 3.5 % of weight loss. This result implies that both methods are applicable for high SSCs; for low SSCs, such as those encountered in Christchurch Bay, relatively large errors (exceeding 5 percent) may occur if no more than 2 liters of water sample is filtered. Consequently, the calibration curve (Figure 4-5) is based upon the oven dry method. The obtained regression line can be expressed as:

$$C_{FIL} = 4.75 \times 10^{-3} R_P - 0.047 \qquad (n{=}6,\ r{=}0.98) \qquad [4\text{-}3]$$

where C_{FIL} is SSC (in g l^{-1}) determined from filtration and R_P is the Partech turbidity monitor readings.

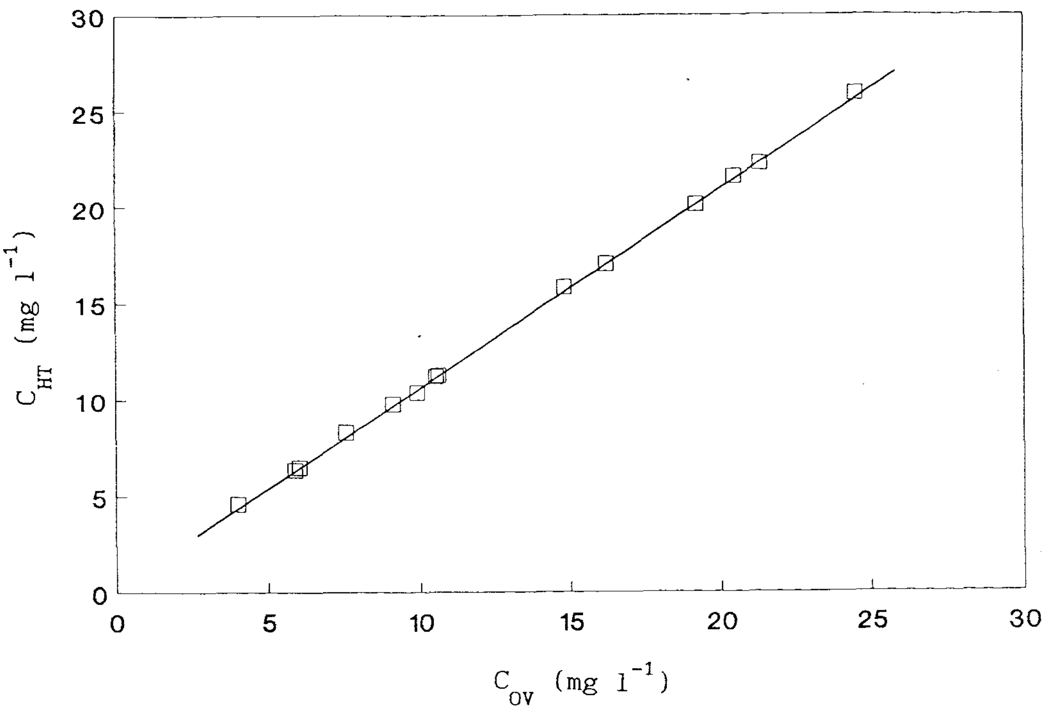

Figure 4-4. Relationship between the SSC, determined from filters dried in the constant humidity tank for 46 hr (C_{HT}), and that determined from filters dried first in the constant humidity tank and then in oven at 50-70°C for 2.5 hr (C_{OV}).

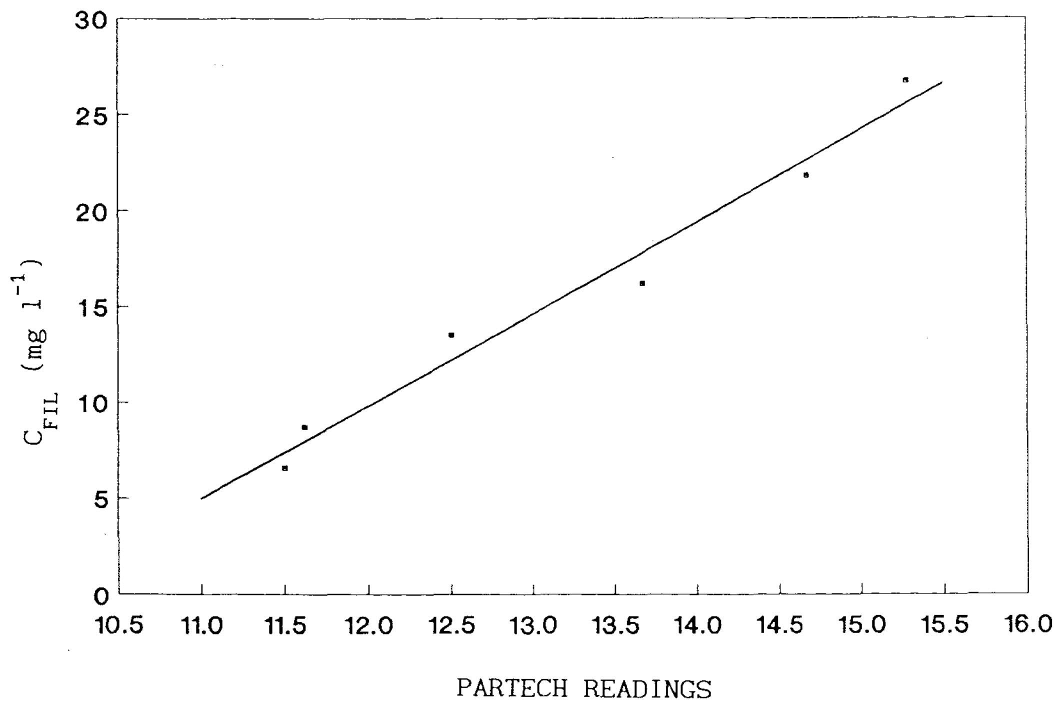

Figure 4-5. Calibration line for SSCs, from the Partech turbidity monitor readings.

The purpose of the measurements made at Station 4, over two tidal cycles, was mainly to calibrate the long-term tide gauge and siltmeter data obtained from the Run (see below). Hence, water samples were taken from the depth where the siltmeter sensor was installed, at half hourly intervals. The SSCs were determined then by the filtration method, described previously. The water level at the tide gauge station was determined, once again on a half-hour basis, by measuring the vertical distance from the water surface to a fixed point on the Quay wall, of known elevation.

At this station, salinity and temperature in the surface water layer were measured using the TC salinometer; surface current speed was determined by measuring the time period needed for a float, set in the central part of the channel, to travel a fixed distance using a stop watch. It was relatively calm during period of the observations; float movement was controlled, therefore, by the currents alone (i.e. with very limited wind influence).

In addition, for the purpose of calibrating the silt meter data, 10 water samples were collected at the tide gauge station, in the same depth as the siltmeter sensor, over the period of the long-term monitoring, between January and December, 1991.

Within Christchurch Harbour, tidal cycle observations were carried out at Station 5, on 3-4 May (spring tide) and 10-11 May (neap tide), 1992. Current velocity, salinity and temperature of the upper (0.2 m below the water surface), middle and lower (0.2 m above the bed) layers were measured, at half hourly intervals. For the spring tide measurements, water samples were collected from the middle of the water column and filtered to obtain the SSC. For the neap tide, a PT-1 turbidity meter (a product of Alec Electronics) was used to obtain SSC data.

Long-Term Monitoring

Long-term water levels and suspended sediment concentrations were monitored at a station within the Run. The layout of the monitoring system is shown on Figure 4-6. The tide gauge (a pressure sensor type) was made by the Department of Oceanography, University of Southampton. The system used for SSC monitoring was an ABP siltmeter (transmissometer type). Both the pressure and siltmeter sensors were connected, through underground cables, to a recording system installed in Mrs D. Foster's house (known as "Little Haven"). Signals from both sensors were recorded continuously using an

Electronic Polyrecorder (model EPR-121A, a product of TOA Electronics). Both sensors were mounted to a plate which was then fixed against the Quay wall on the northern side of the Run (the elevation of the sensors was -1.005 m OD). The period of data recovery is summarised on Figure 4-7.

The data on water levels were read from the chart recorder papers, on half hourly intervals. The readings were calibrated then using tidal staff readings obtained at Station 4 in July and August (as described previously). The two data sets show a marked linear relationship, with very low relative errors (Figure 4-8). The calibration line is expressed by:

$$\eta = 0.6036\ R_W - 3.1293 \qquad (n{=}58,\ r{=}0.9984) \qquad [4\text{-}4]$$

where η is water level (in m OD) and R_W is the chart recorder reading for the tide gauge.

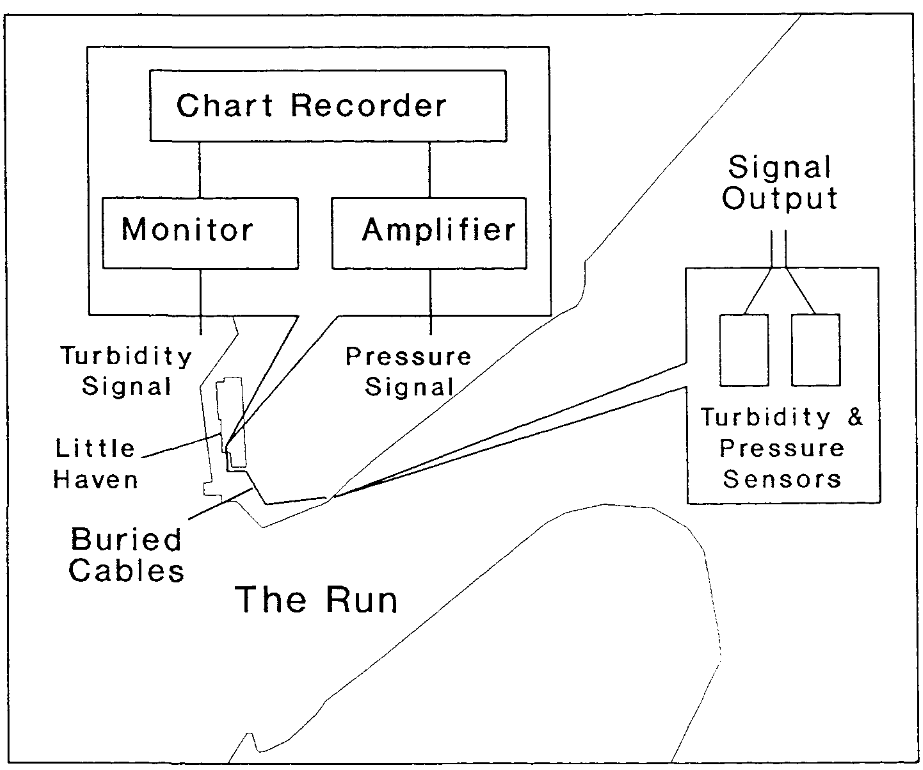

Figure 4-6. Layout of instrumentation for long-term monitoring (schematic and not to scale).

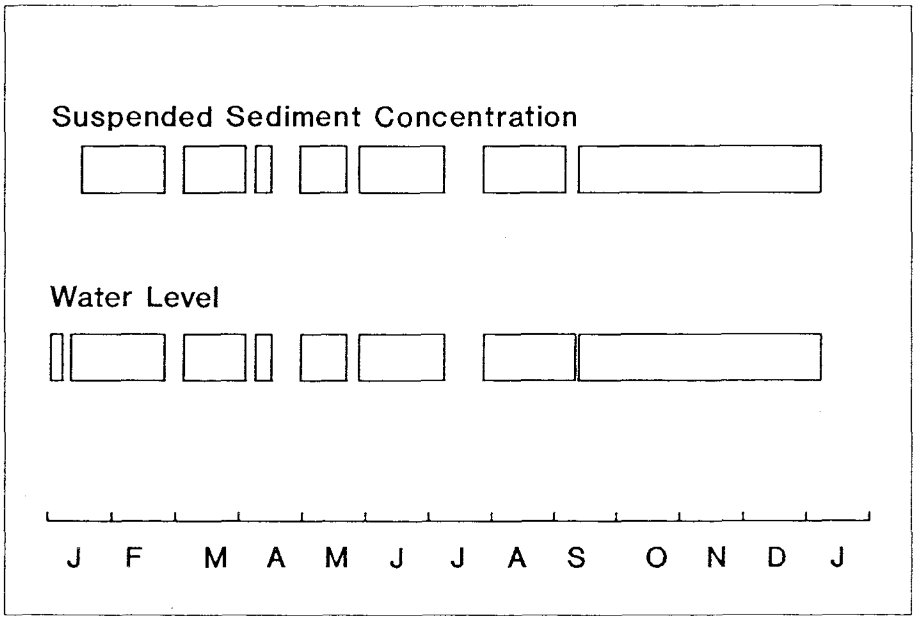

Figure 4-7. Tidal water level and SSC data recovery (January 1991 - January 1992).

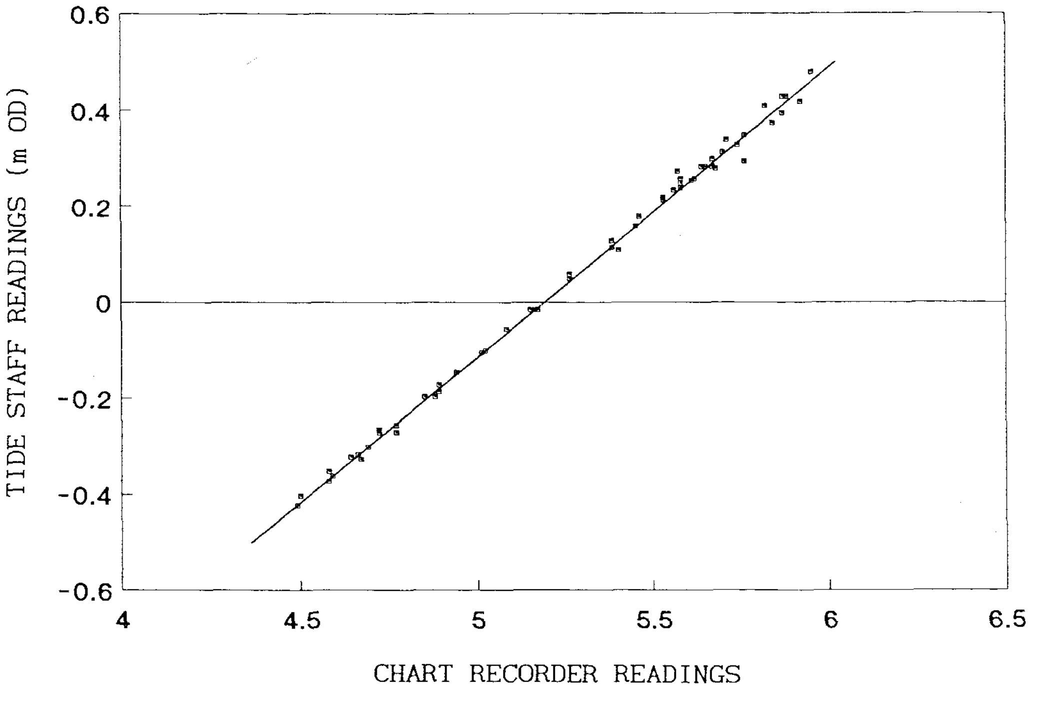

Figure 4-8. Calibration curve for water levels.

The siltmeter started to function on 17 January 1991, but the records were very sensitive to the effects of daylight. On 8 April 1991, the side of the sensor subject to direct sunlight was covered with a black plastic film. The data then became much better, but affected still by intensive sunlight. Further, starting in early summer, the records were disturbed by biological activities. Although the sensor was cleaned regularly (i.e. every two months), a large amount of the data were not reliable and had to be abandoned. Hence, the SSC data available are much fewer than those of water level.

The SSC records were read at hourly intervals; only the data not influenced by sunlight and biological activity were used. Altogether, around 4000 data points have been obtained, covering the different seasons. To obtained the concentration data, the chart recorder readings are transformed firstly into siltmeter readings, using a calibration line (Figure 4-9). The line is expressed in the following form:

$$R_S = 133.85 - 19.80\ R_C \qquad (n=18,\ r=0.996) \qquad [4\text{-}5]$$

where R_S and R_C are siltmeter and chart recorder readings, respectively. R_S data were transferred then into SSCs, using the calibration curve in the Operation Manual of the ABP Siltmeter provided by the manufacturer (Figure 4-10), which can be written as:

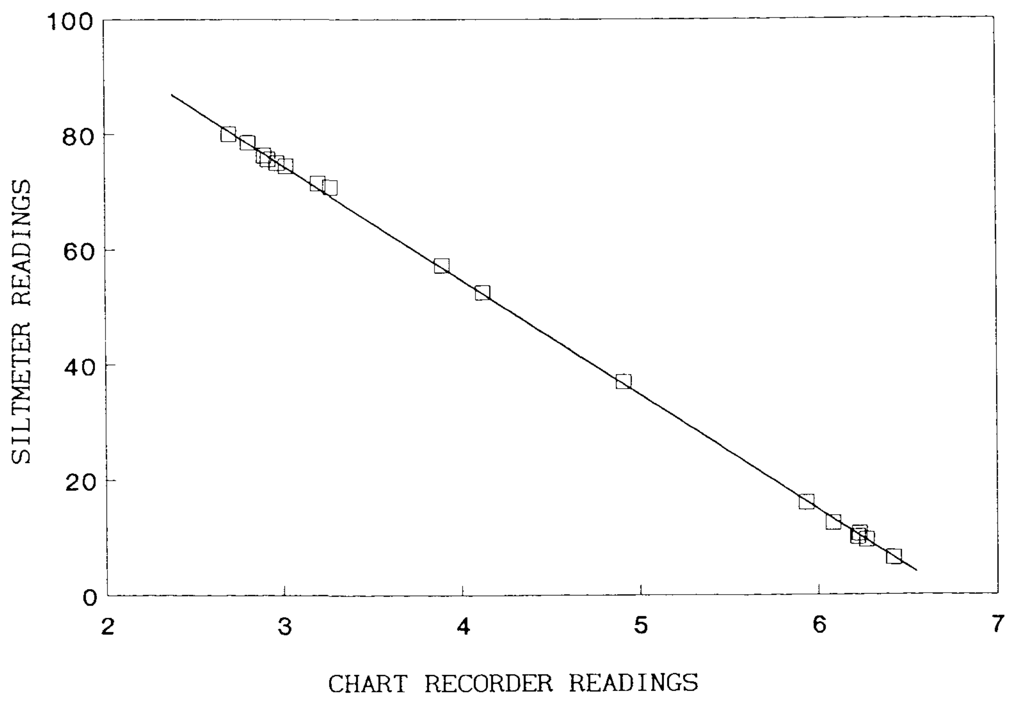

Figure 4-9. Relationship between the chart recorder readings and siltmeter readings, for various SSC data.

$$C_{ABP} = 941.0 - 29.675\ R_S + 0.365\ R_S^2 - 0.00169\ R_S^3 \qquad [4\text{-}6]$$

where C_{ABP} is in terms of mg l^{-1} .

It was found, however, that SSCs based upon Equation [4-6] differed significantly from those determined from the filtration of *in situ* water samples (Figure 4-11). Their relationship is:

$$C = 0.447\ C_{ABP} - 17.480 \qquad (n=29,\ r=0.6958) \qquad [4\text{-}7]$$

In this study, therefore, Equation [4-7] was used to derive SSCs.

4.1.3. Sediment Sampling and Analysis

Collection of Sediment Samples and Short Cores

During May and October of 1989, 450 seabed sediment samples were collected over the Christchurch area. The van Veen grab sampler was used for the subtidal sites, where direct access was impossible. A dory was used for sampling within the Harbour and *MV Stella Barbara* was chartered for sampling outside of the Harbour.

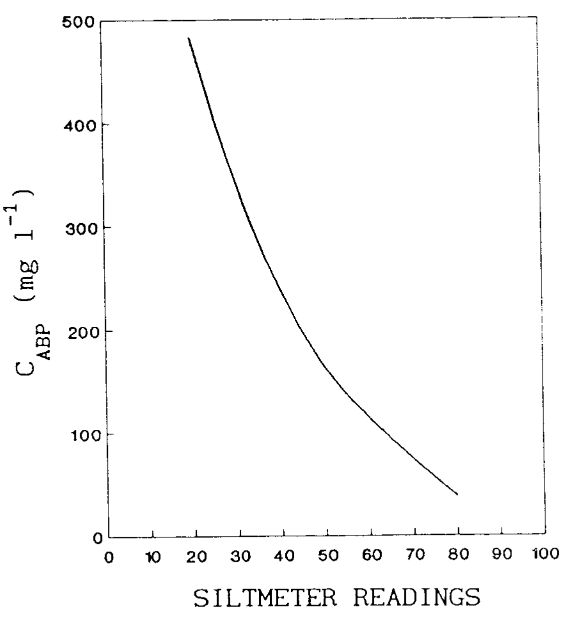

Figure 4-10. Calibration curve for SSCs, from the Operation Manual of ABP Siltmeter.

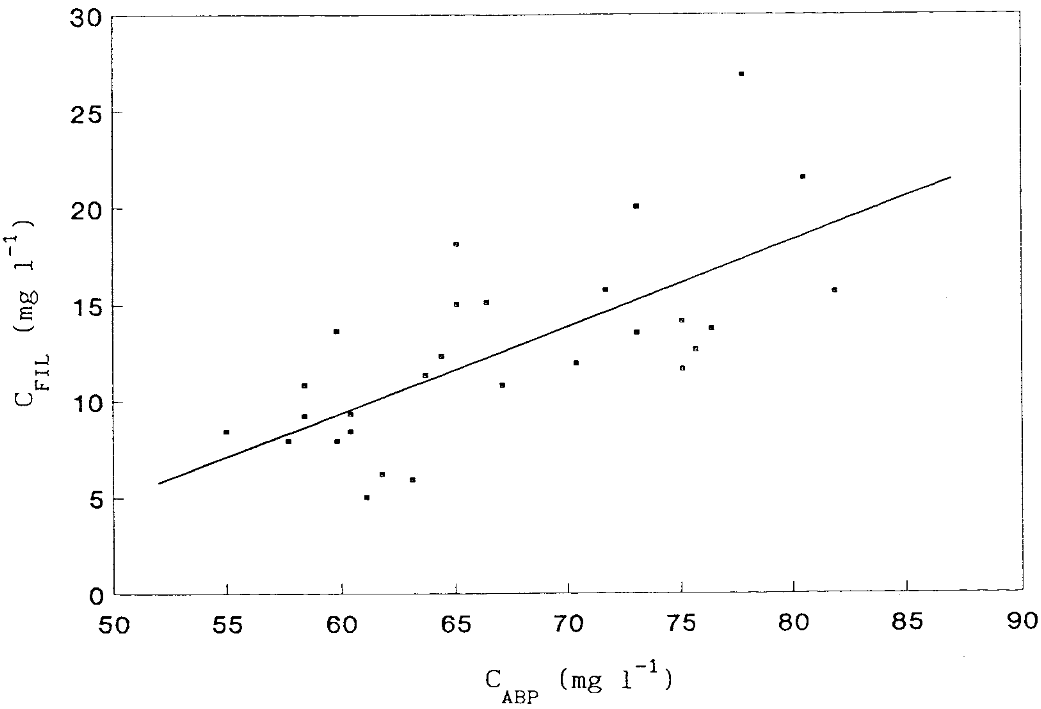

Figure 4-11. Relationship between the SSC determined from Equation [4-6] and that from the filtration of water samples.

Outside the Harbour, the Philips AP Navigator was used to determine the sampling positions (Figure 4-12), which were displayed in terms of longitude and latitude. The fixed positions were examined against known landmarks (for example, known sites at the Mudeford Quay) and errors were found to be less than 30 m during the sampling.

Within Christchurch Harbour, a series of sampling lines were prescribed, with their start and end points fixed using known landmarks. A number of bed samples were then collected along each line. Assuming that the sampling sites were evenly distributed along the line, all the sampling sites could be fixed. Because the sampling interval was relatively small (at around 70 m) and tidal currents were weak during the sampling operation, the error of position fixing is considered to be within 30 m. The sampling sites are shown on Figure 4-13.

Additional sampling work and mapping of the surficial sediments in the Run were carried out on 12 February, 1992, in order to determine the fabric of the surficial sediments within the Run. The types of sediments present were identified and 5 sediment samples representative of each type were collected. The positions of the sampling sites were fixed using a theodolite (Figure 4-14, Section 4.1.4.).

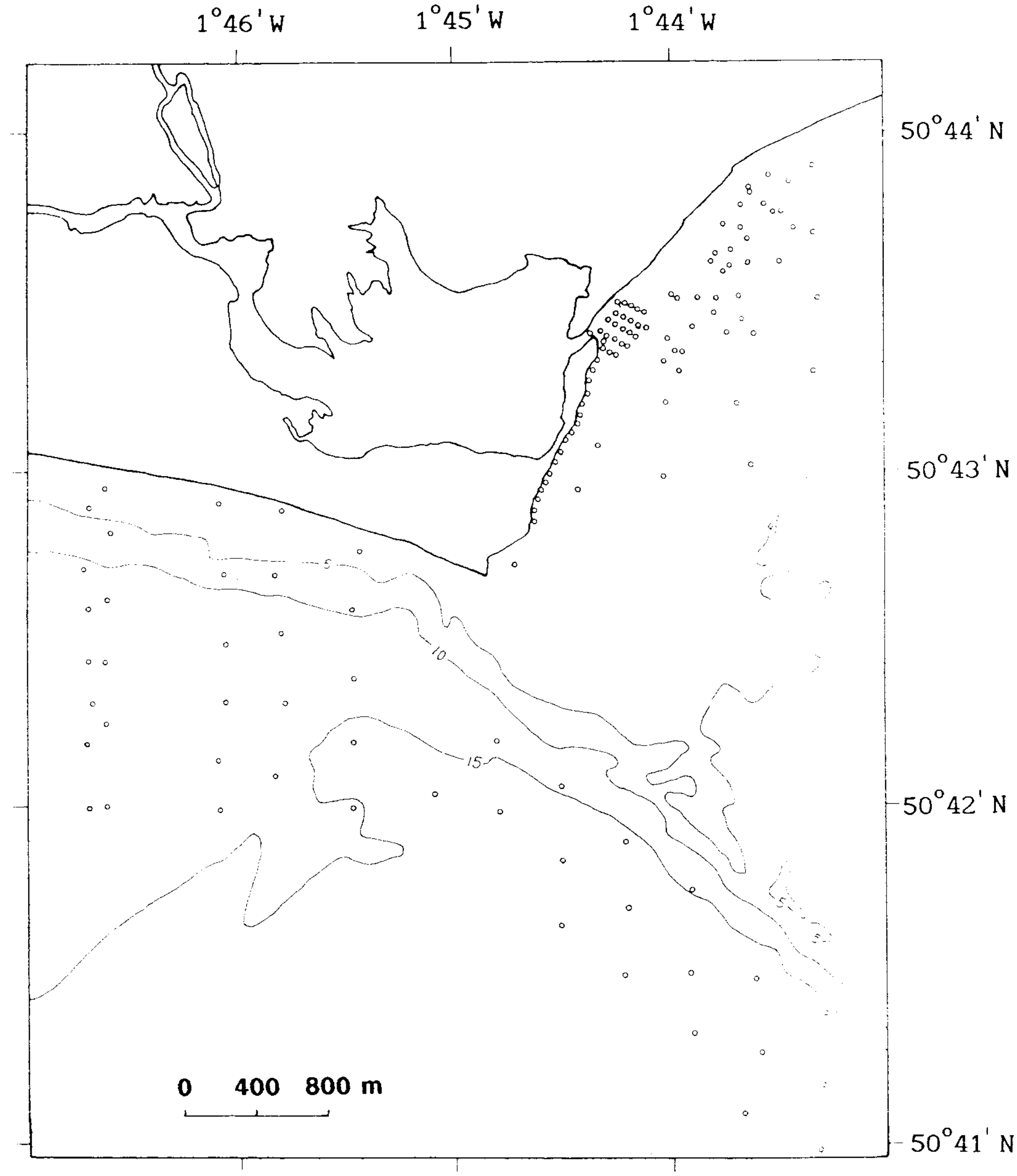

Figure 4-12. Sites for seabed sediment sampling, in western Christchurch Bay and around Hengistbury Head.

On 16 August, 1991, 3 short cores (0.56 m to 0.76 m in length) were collected along an intertidal flat profile at Stanpit Marsh (the profile topography was measured by levelling on 18 May, 1989) (Figure 4-13). The position of the western end and the orientation of the profile were determined using a DataScope digital compass (a product of KVH Industries, Inc.). The profile extended from the salt marsh cliff, towards 88°

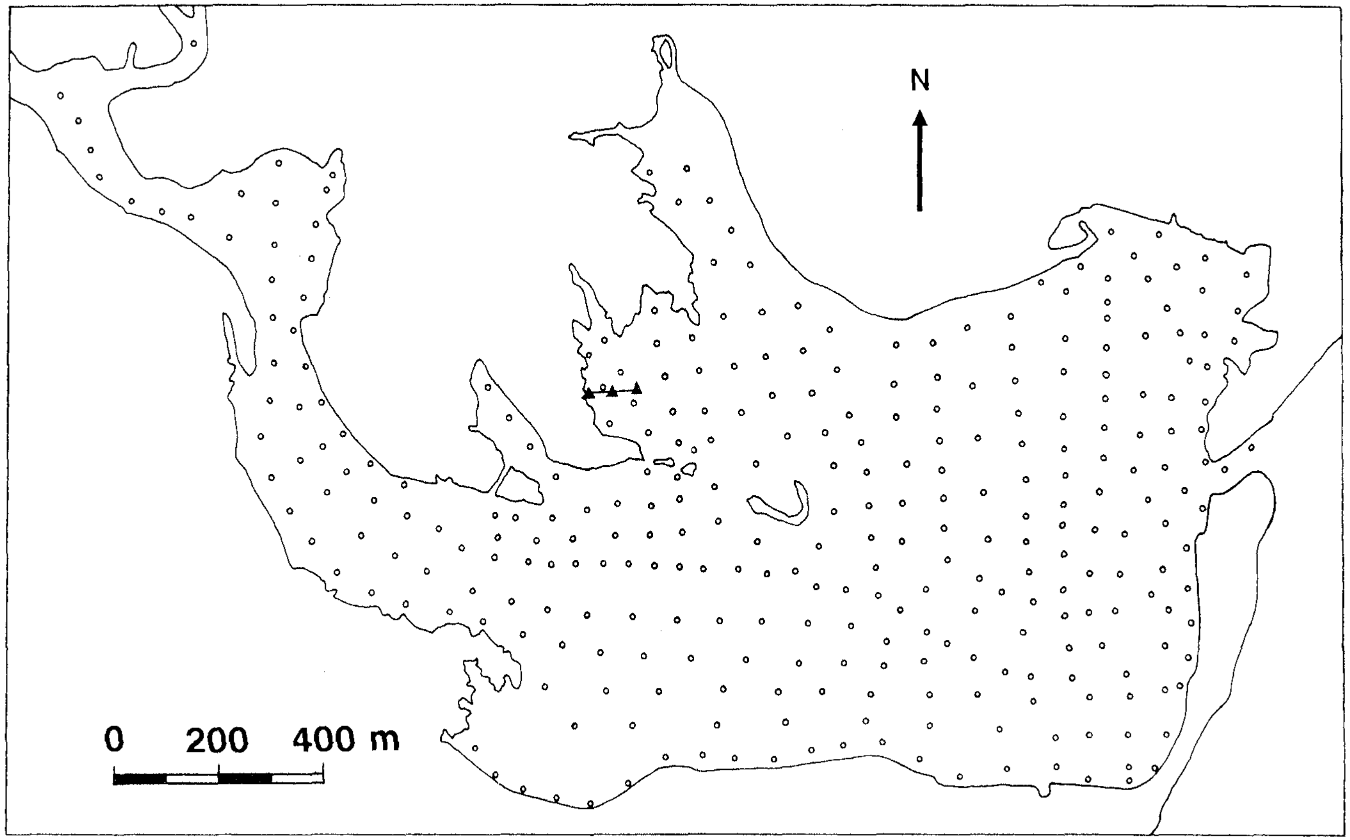

Figure 4-13. Sites for seabed sediment sampling (o) within Christchurch Harbour and short cores (▲) near Stanpit Marsh.

in azimuth. The sites of the short cores were 0 m, 50 m, and 100 m away from the western end, respectively. Further, 5 samples were collected from the salt marsh cliff face.

Grain Size Analysis

In order to analyse the samples for grain size, each was separated into three sub-samples, using wet and dry sieving methods, to obtain the percentages of the mud, sand and gravel fractions. For each sand sub-sample, 100-150 g were analysed using sieves with an interval of 0.5 ϕ, between -1 ϕ and 4 ϕ. The gravel sub-samples for use in the grain size trend analysis were also dry-sieved, at an interval of 0.5 ϕ.

Some 60 mud sub-samples were selected for analysis on a SediGraph 5100. The sub-samples were considered to be representative of the sampling area with a relatively large percentage of mud content. To prepare the suspension for the SediGraph operation, around 2 g of the mud sample were placed in a beaker and 80-100 ml of 0.05 % sodium hexametaphosphate ($NaPO_3$) solution was added. The beaker was then put into an ultrasonic bath (Decon FS400 frequency sweep, in this study) to let the mud disperse for 20-30 minutes. During the SediGraph analysis, the magnetic stirrer installed in the mixing chamber was kept on, to prevent the sediment from settling within the mixing chamber. The truncate point for the analysis was selected to be 10 ϕ.

Grain size distributions of mud fractions of other samples involved in the grain size trend analysis were determined, either on the basis of linear interpolation or by using the distribution curve of the closest adjacent sampling site (if the mud content of that sample was lower than 4 %).

The grain size data from the analyses of sub-samples were then merged together, to obtain complete grain size distributions. Based upon these distributions, grain size parameters (mean (μ), sorting coefficient (σ), skewness (S_k) and kurtosis (K_u)) were calculated using the moment formulae (McManus 1988):

$$\mu = \sum_{1}^{n} P_i \, s_i \qquad [4\text{-}8]$$

$$\sigma = [\sum_{1}^{n} P_i (s_i - \mu)^2]^{1/2} \qquad [4\text{-}9]$$

$$S_k = [\sum_{1}^{n} P_i (s_i - \mu)^3]^{1/3} \qquad [4\text{-}10]$$

$$K_u = [\sum_{1}^{n} P_i (s_i - \mu)^4]^{1/4} \qquad [4\text{-}11]$$

where P_i is the frequency of occurrence of the material represented by the grain size s_i and n is the total number of grain size fractions.

Analysis of Concentration of Foraminiferal Tests

For the study of the exchange of sediments between nearshore and offshore waters (and *vice versa*), benthic foraminiferal tests were selected as natural trace sediments. The content of foraminiferal tests of 53 sand sub-samples has been determined. Of these samples, 43 are from inside of Christchurch Harbour and 10 from outside the Harbour.

In the analysis, foraminiferal tests were concentrated using a heavy liquid (carbon tetrachloride, CCl_4) separation method (Murray 1991). The experiments were undertaken in a fume chamber. The heavy liquid and the pre-weighed sub-sample (with a volume ratio of 2.5:1) were put into a beaker. The content in the beaker was stirred with a rod, then the foraminiferal tests floating at the liquid surface were decanted gently into a pre-weighed Whatman 41 filter (with a retention size of 70 μm), together with some organic matter (wood debris, etc.). After being dried in the fume chamber, the filter containing foraminiferal tests and organic matter was re-weighed. Hydrochloric acid (HCl) was used then to dissolve the foraminiferal tests (this implies that only calcareous tests are taken into account in the analysis). The filter with the organic matter was rinsed with distilled water and dried in an oven, at a temperature of around 70 °C. Finally, the concentration of the tests (C_F) and that of organic matter contained in the sand fraction (C_{org}) were calculated using:

$$C_F = \frac{W_2 - W_3}{W_s} \quad [4\text{-}12]$$

$$C_{org} = \frac{W_3 - W_1}{W_s} \quad [4\text{-}13]$$

where W_1 is the filter mass, W_2 the mass of the filter after filtration and before removal of foraminiferal tests, W_3 the mass of the filter with organic matter, and W_s the mass of the sub-sample. The errors on the concentration analysis were estimated to be around $\pm 5\%$.

4.1.4. Bathymetric and Topographic Surveys

The bathymetry of the entrance section at Mudeford was surveyed, along 3 transects (Figure 4-14). Topographic details of an intertidal part of the transects (above -1.0 m OD), on the southern bank of the Run, were measured by levelling on 20 February, 1992. The underwater (sub-tidal) part was measured on 5 March, 1992, by echo-sounding and using a dinghy. The position of the dinghy was fixed using a theodolite. During the survey, a tide staff was established for water depth calibration against the OD elevations (Figure 4-14).

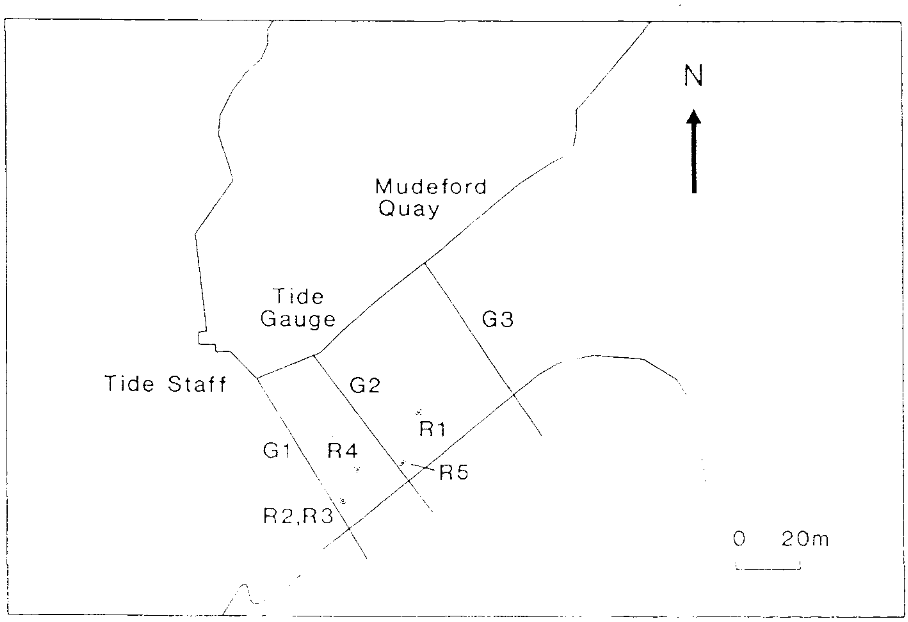

Figure 4-14. Position of the transects for bathymetric survey, tide staff station and sediment sampling sites within the Run.

4.1.5. Collation of Available Data

Freshwater Discharge

Information of freshwater discharges into Christchurch Harbour was provided by the National Rivers Authority (Wessex Region). The data consisted of daily mean flow from the Rivers Stour, Avon and Moors, for the year 1991, with the exception of data missing from May, July and August for the River Avon.

Regression analyses were carried out to relate the freshwater from Avon to that of Stour and Moors, using the data of April, June and September. A linear relationship and high correlation between Avon and Stour freshwater discharges was found, as follows:

$$Q_{F(Avon)} = 6.01 + 1.06\ Q_{F(Stour)} \qquad (n{=}90,\ r{=}0.90) \qquad [4\text{-}14]$$

Consequently, Equation [4-14] was used to fill the gap in data for the River Avon.

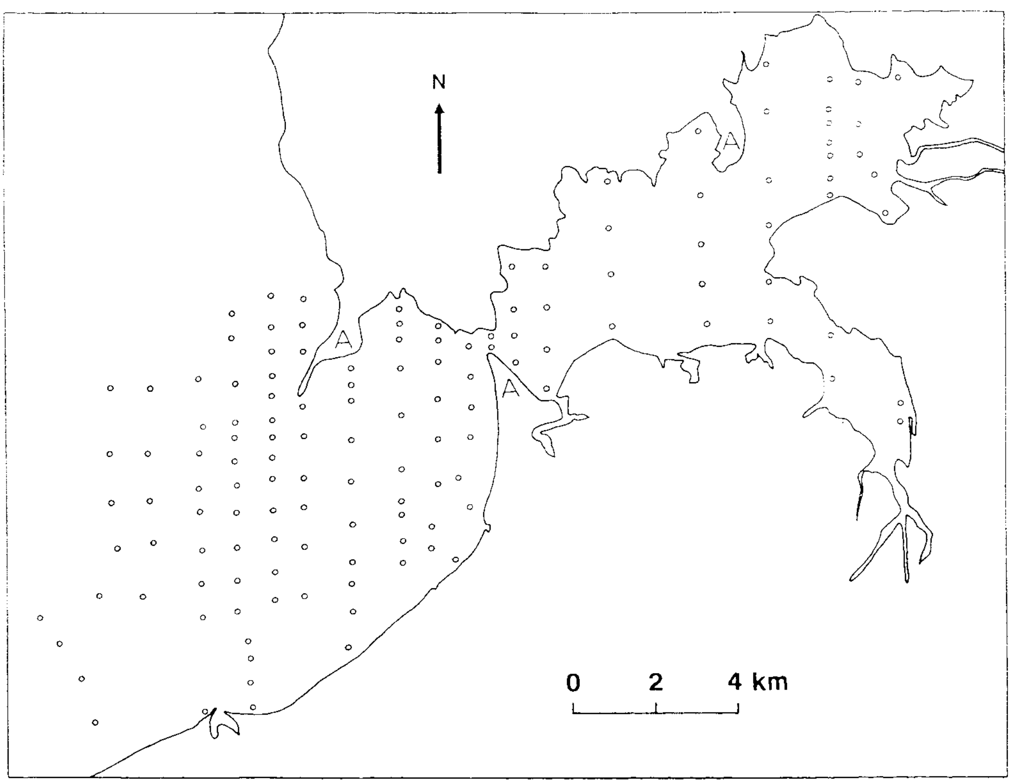

Figure 4-15. Sampling sites in the Yangpu Harbour area.

Grain Size Data

Grain size data from the Yangpu Harbour area were obtained by (and from) Nanjing University, China. From December 1983 to September 1984, a number of seabed sediment samples were collected, on a grid basis and using a van Veen grab (for sampling sites, see Figure 4-15). In analysing the grain sizes, material coarser than 4 ϕ was dry-sieved, whilst the fine-grained material (finer than 4 ϕ) was analysed using the pipette method. These data were then merged, to produce complete grain size distributions. For the present study, grain size parameters of 137 of these samples were determined using a graphic method (Folk and Ward 1957). The data were used then for grain size trend analysis.

4.2. Grain Size Trend Analysis

4.2.1. The Grain Size Trends Used in the Analysis

The major mechanisms which cause changes in grain size parameters during the course of transport include abrasion, selective transport and mixing. Such processes or combinations thereof, may result in a number of different grain size trends. For the purpose of the grain size trend analysis, it is important to determine which trends to utilise.

The two types of hypothetical trends used by McLaren and Bowles (1985) have been described previously (Section 2.2.2.). An empirical assessment of the hypothesis is presented here, through a statistical examination of the published information from previous investigations. On the basis of these data (Table 4-2), sorting may be seen to generally improve (decrease) in the direction of net transport; only in a few cases does sorting remain essentially unchanged, or worsen. Further, in most cases, sediments in the transport direction can be either finer (with an increase in μ, in ϕ units) with no increase in skewness or coarser with no decrease in skewness. Taking all three parameters (mean, sorting and skewness) into account, two grain size trends will dominate, if the net transport is from sampling site d_1 to that at d_2 :

Case 1: $\sigma_2 \leq \sigma_1$, $\mu_2 > \mu_1$ and $S_{k2} \leq S_{k1}$

Case 2: $\sigma_2 \leq \sigma_1$, $\mu_2 < \mu_1$ and $S_{k2} \geq S_{k1}$

where subscripts 1 and 2 denote the various sampling sites. These empirical observations differ only slightly from the hypothesis proposed by McLaren and Bowles (1985). In the present study, therefore, both Case 1 and Case 2 are used as trends associated with net sediment transport paths.

Table 4-2. Observed changes in grain size parameters, in the direction of net sediment transport.

Observed Changes			Associated Environment	Author(s)
μ	σ	S_k		
+	u	u	Alluvial Fan	Blissenbach, 1954
+	-	u	Beach	Pettijohn and Ridge, 1932
-	n	n	Beach	Schalk, 1938
+	-	n	Beach	Schalk, 1946
-	-	+	Beach	Carr, 1969
+	-	+	Beach	Self, 1977
-	u	u	Beach	McCave, 1978
-	-	u	Beach	Bryant, 1982
+	n	-	River	Plumley, 1948
+	u	u	River	Basumallick, 1966
-	-	+	River	McLaren and Bowles, 1985
-	-	+	Spit	McLaren and Bowles, 1985
-	-	u	Spit	Nordstrom, 1981
+	n	u	Spit	Nordstrom, 1989
+	-	-	Delta/Lake	McLaren and Bowles, 1985
+	u	u	Submarine Canyon	Hand and Emery, 1964
-	-	u	Flume	Bagnold, 1968

Key: +, increase in ϕ value; -, decrease in ϕ value; n, no significant change; u, unknown.

4.2.2. Analytical Procedure

In order to avoid the difficulty to form "survey lines" for grain size trend analysis (associated with the McLaren method), a new analytical procedure is developed here.

The trends summarised above (Case 1 and Case 2) are associated with net sediment transport; this does not imply, however, that the cases always define such a transport pathway. Such cases can occur under other circumstances. For example, they can be present even amongst sampling sites without any material exchange relationships. As a result, in the natural environment, Case 1 and Case 2 trends not caused by net transport may be superimposed on those which represent the true (net transport) pattern. Case 1 and Case 2 trends which are not consistent with net transport paths are defined here as "*noise*". As it is important to separate the trends associated with the net transport, from the noise, this is realised by a semi-quantitative filtering technique. The analytical procedure is shown on Figure 4-16 and is described below.

(i) Definition of "*Trend Vectors*"

The first step is to define "trend vectors" for a grid of sampling sites, by comparing each sample with its neighbour (Figure 4-16(A)). In order to identify a "neighbouring" site, a characteristic distance (D_{cr}), which is taken as the maximum spatial sampling interval, is specified. If the distance between any two sites is smaller than this characteristic distance, they are considered as neighboring sites and their grain size parameters are compared. If either a Case 1 or a Case 2 trend (described previously) is identified between the two sites, then a dimensionless "trend" vector is defined for the site with the higher sorting coefficient, the direction of such a vector running from the site with the higher sorting coefficient to that with the lower value. Because the mean, sorting and skewness all combine to form a trend, it is difficult to define the length of the vector on the basis of the parameters themselves, without any bias towards one of the parameters. Hence, for convenience, The length of the vector is assumed to be unity.

At each sampling site, there may be more than one unit-length vector. For such a site, vectors are summed to produce a single vector (Figure 4-16(B)), as follows:

$$\vec{R}(x,y) = \sum_{1}^{n} \vec{r}(x,y)_i \qquad [4\text{-}15]$$

where n is the number of trend vectors identified for the site, $\vec{r}(x,y)$ is a trend vector, and $\vec{R}(x,y)$ is the sum of the trend vectors. Both the "real" transport trend and "noise" trend are included in $\vec{R}(x,y)$, although some noise may have been reduced already due to the summing process.

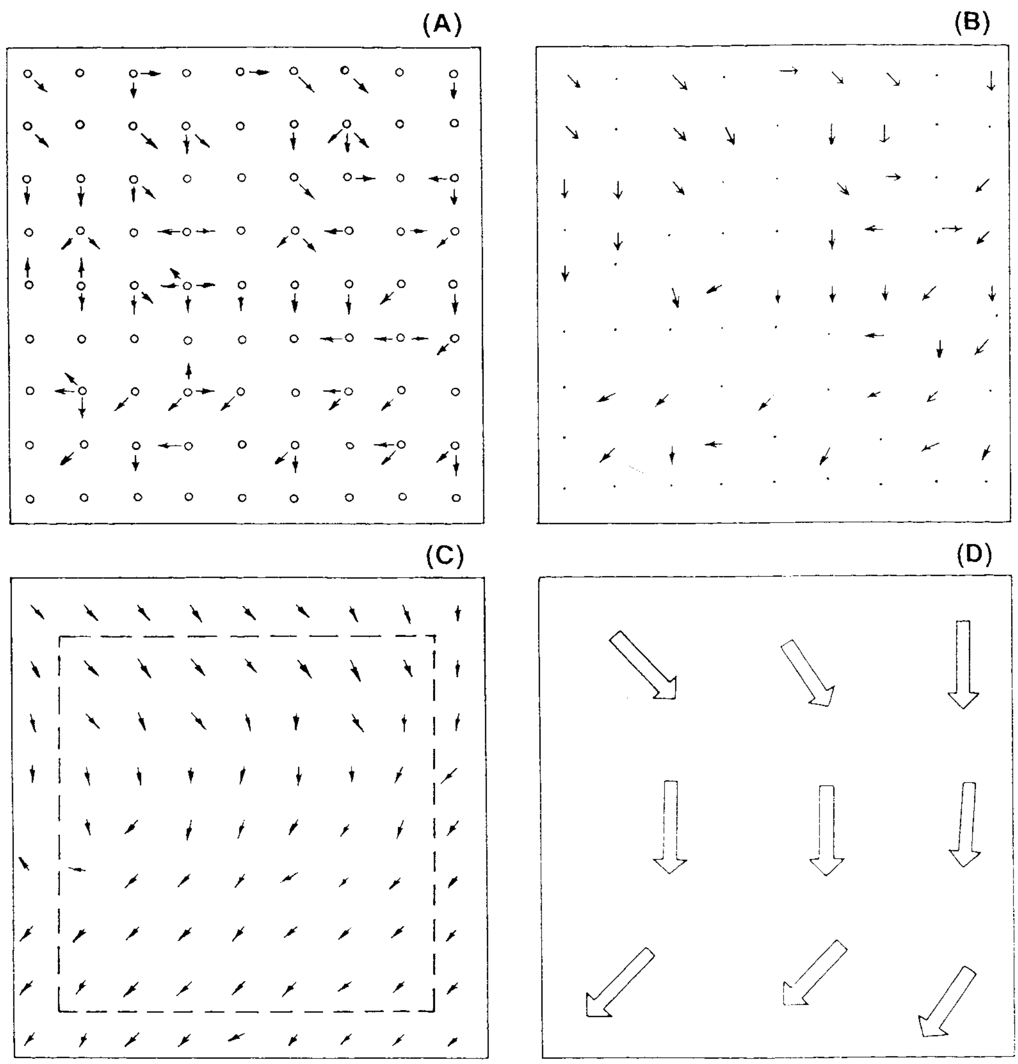

Figure 4-16. Procedures for grain size trend analysis: (A) definition of "trend vectors"; (B) summation of trend vectors for each site; (C) determination of "transport vectors"; and (D) formation of "residual" patterns.

(ii) Averaging and Definition of "Transport Vectors"

To remove the noise included in the vectors at each site, an averaging operation is applied (Figure 4-16(C)). Here, it is assumed that the various components of noise do not show any ordered pattern: when observed in a frequency domain, these components are present in the form of high frequency fluctuations. Thus, the noise is removed by averaging the vectors of a particular sampling site with those at adjoining sites. Once again, an adjoining site is assessed on the basis of a characteristic distance (D_{cr}), as defined previously. The averaging procedure is equivalent to the following mathematical transformation for the site at which $\vec{R}(x,y)$ is defined:

$$\vec{R}_{av}(x,y) = \frac{1}{k+1} \left[\vec{R}(x,y) + \sum_{1}^{k} \vec{R}_j \right] \qquad [4\text{-}16]$$

where $\vec{R}_j$ is a summed trend vector obtained on the basis of equation [4-15] at a neighbouring site, and k is the total number of such sites.

The vectors $\vec{R}_{av}(x,y)$ can be defined as "*transport vectors*"; they form a "residual" pattern (Figure 4-16(D)), with little influence from noise with high frequency (it may be noted that the transport vectors within the dashed box on Figure 4-16(C) are averaged over a larger number of sampling sites than those on the edge). If the residual trends have an ordered pattern in the arrangement of the transport vectors, then they should represent net transport paths.

(iii) Significance Test on the Transport Vectors

The extent of orderliness is examined on the basis of a significance test; in this, the assumption is made that the noise is of high frequency in character. As an example, it may be supposed that a grid of trend vectors consist of noise alone. At any site in the grid, therefore, there would be no difference in the probability of having a trend vector in any direction. After the averaging operation described previously, according to the assumption adopted, these vectors will cancel each other out; consequently, relatively short "transport" vectors are produced. Thus, the average length of the transport vectors (referred to as the length of a "*characteristic vector*" in the succeeding text) in any identified residual pattern can be used as a variable for the purpose of the significance test. The length of the characteristic vector is defined by:

$$L = \sum_{1}^{N} \mid \vec{R}_{av}(x,y)_i \mid \qquad [4\text{-}17]$$

where N is the total number of sampling sites. If there is a marked pattern in the residual trends, then L will be significantly larger than in the case without an ordered pattern; in the latter, trend vectors would partly cancel each other out, during the averaging procedure (see above).

To evaluate if the average length is "significant", a critical length, with a certain confidence level, is needed for the significance test. Such a length should be obtained from situations in which every trend vector belongs to noise. In the present study, a critical vector was determined on the basis of a number of experiments on randomly re-arranged samples. For each experiment, N (the same number as the seabed samples obtained) random numbers, ranging between 1 and N (including 1 and N), were generated using a FORTRAN programme modified from Press *et al.* (1986). Each random number has the same probability of being between 1 and N. The samples (and, therefore, the grain size parameters) are redistributed then according to the random numbers, to form a matrix. For example, if the first random number generated is 45, then Sample 45 is allocated to Site 1 (it is probable for a sample to be reallocated several times). It seems a reasonable assumption that the randomly-reallocated pattern should result in a grid which is representative of high frequency noise.

Trend vectors in the randomly-reallocated pattern were defined; this was followed by summing, averaging and calculation of the length of the characteristic vector (as demonstrated previously). The experiment was repeated a number of times, to obtain a series of characteristic vector lengths; these were sufficient to establish a frequency distribution for the vector lengths. From the frequency distribution curve, a critical value L_{cr}, with a certain level of confidence (such as 90 %, 95 % or 99 %), was defined. The significance of the original residual pattern was judged then, on the basis of the following considerations:

(1) $L > L_{cr}$, with the trends being significant; and

(2) $L \leq L_{cr}$, with the trends being not significant.

In the first situation, the trends identified should represent the net sediment transport pathways with a high level of confidence. The second situation, on the other hand, dictates that net transport patterns cannot be identified on the basis of the grain size trend analysis.

The technique described above is applied to the study of sediment transport in Christchurch and Yangpu Harbours.

4.3. Mathematical Model of Sediment Exchange

4.3.1. Background

Estuaries are sinks for sediments until basin infilling is completed, but it is necessary to establish: (i) the source of the deposited sediments; and (ii) whether or not there is a net sediment transport to landward, crossing the entrance to the estuarine system.

There have been many attempts to solve these problems by relating the source of sediment supply and the patterns of net sediment transport to tracer dynamics. Natural tracers have been used as indicators of sediment supply and of net transport. The tracers used often include benthic foraminiferal tests (Nigam 1986; Murray 1987), marine diatoms (Gessner and Simonsen 1967), trace metals (Merefield 1981; Brown 1987; Salomons and Mook 1987), and heavy and clay mineral suites (Trask 1952; Byrne and Kulm 1967; Eisma *et al.* 1978). Although studies of sediment supply based upon the tracer technique appear to have been successful, some doubts exist as to whether or not, and under what conditions, net transport pathways can be inferred from the flux of the trace material.

Here, a mathematical model for the exchange of natural trace sediments between an estuary and the open sea, under various sediment transport regimes (i.e. net transport to landward or seaward), is described. Based upon the model, an approach to relate the dispersal of natural trace sediments to net sediment transport is developed.

4.3.2. Analysis of Components of Sediment Budget

The major components of sediment input and output over a unit time, for a tidal estuary (Figure 4-17), are: (i) input from the sea through the entrance, q_s; (ii) output towards the sea, q_o; and (iii) input from the river, q_r. The sediment budget will then be:

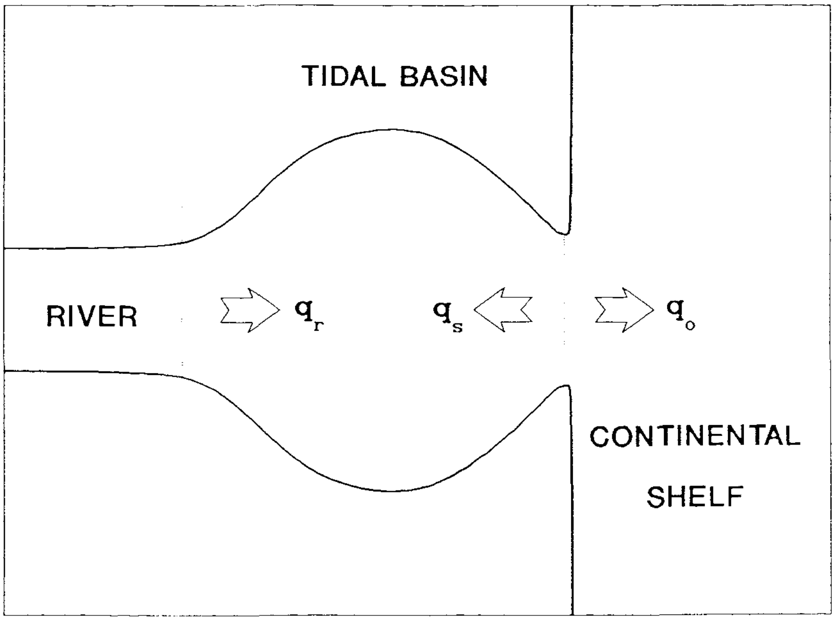

Figure 4-17. Major components of sediment balance for an inlet system.

$$q_n = q_s + q_r - q_o \qquad [4\text{-}18]$$

where q_n is the amount of sediments stored within the estuarine system, over unit time. In any sedimentary environment, there is mixing between the sediments in transit and the bed material, due to either the physical processes of exchange (Einstein 1950) or bioturbation at the bed (Clifton and Hunter 1973; Ludtke and Bender 1979; Robbins 1986). As a result, q_o cannot consist of sediments from q_s and q_r alone; rather, it contains some material from the deposit itself. Therefore, q_o can be written as

$$q_o = (1 - a_s)\, q_s + (1 - a_r)\, q_r + q_m \qquad [4\text{-}19]$$

where a_s and a_r are the fractions of the material from q_s and q_r, respectively; these remain in the basin, due to mixing between the input material and the bay sediments. q_m is part of q_o, which is derived from the moving layer (or the depth of disturbance i.e. the surficial layer which is subject to transport processes). Combining Equations [4-18] and [4-19] yields, for the amount stored:

$$q_n = a_s\, q_s + a_r\, q_r - q_m \qquad [4\text{-}20]$$

Assuming that the trace sediments under consideration are present only in the marine sediments (i.e. they are absent in the river sediments), the budget of the tracers over the unit time can be expressed as:

$$T_n = k\ C_1\ q_s - k\ C_2\ q_o \qquad [4\text{-}21]$$

where T_n is the amount of the tracers stored within the estuarine system; C_1 and C_2 are the concentrations of the trace material in q_s and q_o, respectively; and *k* is introduced to take into account the difference in transport character between the tracer and the bulk sediments. In a similar manner to Equation [4-19], $C_2\ q_o$ can be written as

$$C_2\ q_o = (1 - a_s)\ C_1\ q_s + C_m\ q_m \qquad [4\text{-}22]$$

where C_m is the concentration of the tracer within the moving layer. From Equations [4-21] and [4-22] we have

$$T_n = k\ a_s\ C_1\ q_s - k\ C_m\ q_m \qquad [4\text{-}23]$$

Equations [4-18] to [4-23] define the basic relationship between the major components of an overall sediment budget for an inlet system.

4.3.3. Model Formulation

The average tracer concentration of the loosely-consolidated sediments within the estuarine system can be defined as

$$C_b = \frac{V_m}{V} \qquad [4\text{-}24]$$

where V is the total volume of the loosely-consolidated sediments within the estuary and V_m is the volume of the tracer in V. The time change rate of C_b will be

$$\begin{aligned} \frac{dC_b}{dt} &= \frac{d(V_m/V)}{dt} \\ &= \frac{1}{V}\left(\frac{dV_m}{dt} - C_b \frac{dV}{dt} \right) \qquad [4\text{-}25] \\ &= \frac{1}{V}\left(T_n - C_b\ q_n \right) \end{aligned}$$

Inserting Equations [4-20] and [4-23] into [4-25],

$$\frac{dC_b}{dt} = \frac{1}{V} [\, k\, a_s\, C_1\, q_s - k\, C_m\, q_m - (a_s\, q_s + a_r\, q_r - q_m)\, C_b \,] \qquad [4\text{-}26]$$

In a finite differential form, Equation [4-26] can be rewritten as

$$C_{b,t+\Delta t} - C_{b,t} = \frac{1}{V_t} [\, k\, a_s\, C_1\, q_s - k\, C_{m,t}\, q_m - (a_s\, q_s + a_r\, q_r - q_m)\, C_{b,t} \,]\, \Delta t \qquad [4\text{-}27]$$

In Equation [4-27], V_t and $C_{m,t}$ also vary with time (with other parameters assumed to be constant). The total volume of the bay sediments (V) will change according to the following equation:

$$\begin{aligned} V_{t+\Delta t} &= V_t + q_n\, \Delta t \\ &= V_t + (\, a_s\, q_s + a_r\, q_r - q_m \,)\, \Delta t \end{aligned} \qquad [4\text{-}28]$$

The concentration of the tracer within the moving layer is controlled by accretionary processes within the estuary. If the thickness of the moving layer remains constant then, after a time Δt, the newly-deposited sediments and the upper part of the original moving layer will form a "new" moving layer (Figure 4-18). At the same time, the lower part of the original moving layer will become immobile. Let $C_{m,t}$ be the tracer concentration in the original moving layer. After unit time, the quantity of the tracer per unit area consists of two parts which combine together to form a "new" moving layer. One part is the amount of tracer contained in the influx, over the time Δt:

$$V_1 = \frac{T_n\, D_R\, \Delta t}{q_n} \qquad [4\text{-}29]$$

where D_R is the deposition rate ($D_R = q_n/A_b$, where A_b is the area of the embayment). The other part is the contribution made by the original moving layer:

$$V_2 = C_{m,t}\, (\, D_L - D_R\, \Delta t \,) \qquad [4\text{-}30]$$

where D_L is the thickness of the moving layer. Thus, the concentration within the "new" moving layer becomes:

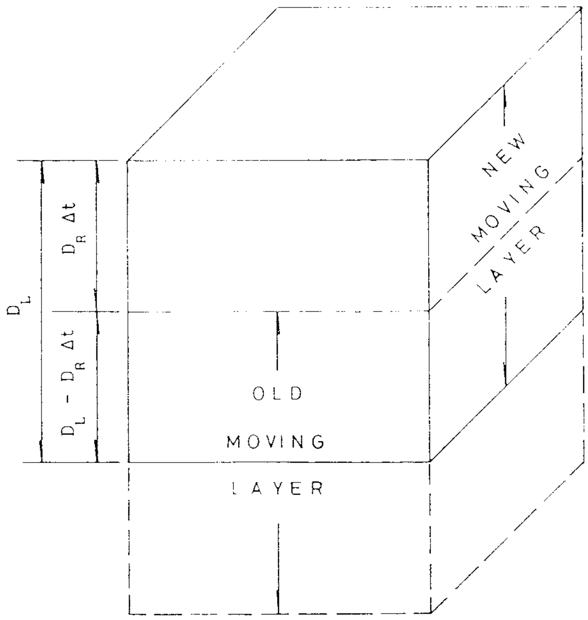

Figure 4-18. Schematic diagram showing the change in the moving layer, between t (the dashed box) and t+Δt (the solid box).

$$
\begin{aligned}
C_{m,t+\Delta t} &= \frac{V_1 + V_2}{D_L} \\
&= \frac{1}{D_L} \left[\frac{T_n \, \Delta t}{A_b} + C_{m,t} \left(D_L - D_R \, \Delta t \right) \right] \\
&= \frac{1}{D_L} \left[\frac{k \, a_s \, C_1 \, q_s \, \Delta t}{A_b} + \left(D_L - D_R \, \Delta t \right.\right. \\
&\quad \left.\left. - \frac{k \, q_m \, \Delta t}{A_b} \right) C_{m,t} \right] \qquad (\textit{assuming } D_L > D_R \, \Delta t)
\end{aligned}
\qquad [4\text{-}31]
$$

Equation [4-27], [4-28] and [4-31] form a basis for modelling changes in the concentration of the tracer, in the total estuarine sediments and within the moving layer. As described previously, the assumptions for the model include: (i) the tracers in consideration are derived from marine sediments; (ii) the components of the sediment budgets, the budgets of the total sediments and the tracers, and the tracer concentration of the marine sediments are constant (although these are represented as variables in the controlling equation); (iii) the concentrations of the tracers in the total estuarine sediments and the moving layer are space-averaged (i.e. they are functions of time only); (iv) the thickness of the moving layer is much greater than the thickness of the layer deposited over unit time; and (v) the deposition rate and thickness of the moving layer are uniform over all the basin area.

The model was used in this study to: (i) carry out a series of conceptional experiments; and (ii) determine the status of balance of sandy material for Christchurch Harbour.

4.4. Computation of Sediment Transport Rate

4.4.1. Computation of Current Speeds in Entrance Channel

The time-series of water level data were used to calculate the cross-sectional mean current speeds within the Run. This task can be realised using a numerical model. For example, Amein (1975) has developed such a model which requires the technique of solving non-linear equations. For the purpose of the present study, however, a much simpler method is used, as described below.

The relationship between the current speed and the water level of the tidal basin can be written as, according to the law of conservation of mass:

$$U\,A + Q_F = A_b \frac{d\eta_b}{dt} \qquad [4\text{-}32]$$

where U is mean current speed over the cross-section, A is cross- sectional area, Q_F is freshwater discharge, A_b is the tidal basin area, and η_b is mean water level within the tidal basin. Because both A_b and $d\eta_b/dt$ and their relationship with the water level measured within the entrance channel are not known, Equation [4-32] cannot be used directly to compute the current speed. If, however, an "apparent" basin area (instead of A_b) is used, then Equation [4-32] is changed into:

$$U\,A + Q_F = A_{ba} \frac{d\eta}{dt} \qquad [4\text{-}33]$$

where η is measured within the entrance channel; A_{ba} is the "apparent" basin area, which is related to A_b by:

$$A_{ba} = A_b \frac{d\eta_b / dt}{d\eta / dt} \tag{4-34}$$

Equation [4-33] was used to compute cross-sectional mean current speeds. Time-series of the water level data (η_i) were transformed into time series of the instantaneous cross-sectional area, the "apparent" basin area and the rate of water level change by using the following functions:

$$A_j = F_1(\eta_{i+1/2}) \tag{4-35}$$

$$A_{ba,j} = F_2\ (\eta_{i+1/2}) \tag{4-36}$$

$$\frac{d\eta}{dt}\bigg|_j = \frac{\eta_{i+1} - \eta_i}{1800} \tag{4-37}$$

where $\eta_{i+1/2} = 0.5\ (\eta_i + \eta_{i+1})$.

The functions F_1 and F_2 are determined based upon the observed bathymetric and hypsometric data.

The water level data for calculating current speeds cover 594 tidal cycles (including 21 spring-neap tidal cycles) (Table 4-3). These data form a basis for the calculation of sediment discharges through the Run and the determination of inlet equilibrium conditions, as described in the following sections.

4.4.2. Bed-load Transport

Transport of Sandy Sediments

The entrances to Langstone and Yangpu Harbours are characterised by sandy sediments, deep channel and low wave energy levels (see Chapter 3). Hence, the formulae of Gadd *et al.* (1978) (Equation [2-19]) has been used to estimate sediment flux through the entrances. U_{100}, which is required by this equation, is related to the vertical mean current speed, through the use of von Kármán-Prandtl velocity profile equation:

$$U_z = \frac{U_*}{\kappa} \ln \frac{z}{z_0} \qquad [4\text{-}38]$$

where U_z is the current speed measured at height z, U_* is the friction velocity and z_0 the roughness length. Thus, the vertical mean current speed becomes:

$$U_{av} = \frac{U_*}{\kappa} \ln \frac{H}{e\, z_0} \qquad [4\text{-}39]$$

where H is the water depth, U_{av} the vertical mean of current speed, and *e* is the base of natural logarithms (=2.718). The relationship between U_{100} and U_{av} will then be:

$$\frac{U_{100}}{U_{av}} = \frac{\ln\,(100\,/\,z_0)}{\ln\,[\,H\,/\,(e\,z_0)\,]} = \alpha_1 \qquad [4\text{-}40]$$

i.e. $$U_{100} = \alpha_1\, U_{av} \qquad [4\text{-}41]$$

Table 4-3. Periods of water level data availability, for current speed calculations, between 3 January 1991 and 7 January 1992 (time in GMT).

TSN[x]	Period of Observations	NOD[y]	NTC[z]
1	6.22, 3 January - 9.02, 7 January	212	8
2	13.41, 11 JAN - 12.50, 24 February	2109	85
3	19.15, 4 March - 6.50, 3 April	1434	57
4	11.06, 8 April - 16.48, 14 April	299	12
5	18.20, 30 April - 10.03, 20 May	944	38
6	4.01, 26 May - 11.38, 7 July	2031	82
7	16.42, 26 July - 15.58, 7 September	2062	83
8	7.05, 11 September - 18.25, 7 January	5708	229

[x] Time-series number;

[y] Number of data points;

[z] Number of tidal cycles covered.

If the cross-section was shallow compared with their width (i.e. $H \ll B$), then the vertical mean U_{av} was used to represent the cross-sectional mean of the current speed. Otherwise, the vertical mean current speed was related to the cross-sectional mean speed (U), using an assumed distribution of vertical mean current speed across the channel:

$$U_{av} = \alpha_2 \, U \qquad [4\text{-}42]$$

where α_2 is a distribution function of U_{av}/U across the channel.

The current speeds as a time-series have a time-averaged value $<U>$ and a frequency distribution function. U is related to $<U>$ by:

$$U = \alpha_3 <U> \qquad [4\text{-}43]$$

Combining Equation [2-20] with Equations [4-41], [4-42] and [4-43], we have:

$$q_s = k_1 \, (\alpha_1 \, \alpha_2 \, \alpha_3 <U> - U_{100cr})^3 \qquad [4\text{-}44]$$

when $\alpha_1 \alpha_2 \alpha_3 <U>$ exceeds U_{100cr}. Thus, the transport rate averaged across the transect with a width of B and over the time T_0 becomes:

$$\begin{aligned} <\overline{q_s}> &= \frac{1}{T\,B} \int_0^{T_0} \int_0^{B} q_s \, dy \, dt \\ &= \int_{\beta_0}^{\beta_{max}} k_1 \, (\alpha_1 \, \beta <U> - U_{100cr})^3 \, p(\beta) \, d\beta \end{aligned} \qquad [4\text{-}45]$$

where $\beta = \alpha_2 \alpha_3$ and $p(\beta)$ is the frequency distribution function of β. Because α_2 and α_3 are mutually independent (i.e. they represent the effects of spatial and temporal changes, respectively), the function $p(\beta)$ was determined from the frequency distribution functions of α_2 and α_3 (i.e. $p_1(\alpha_2)$ and $p_2(\alpha_3)$, respectively):

$$p(\beta) = \int_{-\infty}^{\infty} \frac{p_1(x) \, p_2(\beta/x)}{|x|} \, dx \qquad [4\text{-}46]$$

In Equation [4-45], β_0 and β_{max} are defined by the following equations:

$$\beta_0 = \frac{U_{100cr}}{\alpha_1 <U>} \qquad [4\text{-}47]$$

$$\beta_{max} = \frac{U_{max}}{<U>} \qquad [4\text{-}48]$$

where U_{max} is the maximum of the vertically-averaged current speeds in the entrance channel.

Transport of Gravelly Sediments

In the entrance to Christchurch Harbour, the sediments consist mainly of gravelly material (Chapter 3). Further, because the channel is shallow, the bed is influenced by waves. Thus, Equations [2-21] and [2-24] are used to estimate sediment transport rates. Due to the presence of the ebb delta, waves cannot propagate into the channel when the delta is exposed. Therefore, two situations must be taken into account: (i) if the water level was lower than the top part of the ebb tidal delta, then transport is related to currents alone; and (ii) if the water level was high, so that wave can propagate into the entrance (with some breaking over the delta), then the combined effects of waves and currents were considered.

The transport rate averaged across the transect and over time is controlled by four independent factors: (i) variations in the cross-sectional mean current speeds; (ii) lateral changes in the vertical mean current speeds; (iii) various wave conditions; and (iv) changes in the orbital velocity of an oscillatory flow during a wave period. Taking these factors into account, the mean transport rate for combined waves and currents becomes:

$$<\overline{q_s}> = \sum_{I,J,K,L} P_{1,i}\, P_{2,j}\, P_{3,k}\, P_{4,l}\, q_{s(i,j,k,l)} \qquad [4\text{-}49]$$

The mean transport rate for currents alone can be written as:

$$<\overline{q_s}> = \sum_{I,J} P_{1,i}\, P_{2,j}\, q_{s(i,j)} \qquad [4\text{-}50]$$

In Equations [4-49] and [4-50], P_1 is the frequency distribution of the cross-sectional mean current speeds, P_2 is the frequency distribution of the ratio of U_{av}/U (U_{av} and U being vertical and cross-sectional mean current speeds, respectively) along the transect, P_3 is the frequency distribution of waves associated with characteristic wave height and period, and P_4 is the distribution of of the ratio U_w/U_b (U_w and U_b being the instantaneous and maximum orbital velocities over a wave period, respectively). I, J, K, L are the numbers of P_1, P_2, P_3 and P_4 data sets, respectively.

4.4.3. Suspended Load Transport

The discharge of suspended sediment through the entrance channel can be defined as:

$$\begin{aligned} Q_s &= \int_0^{T_0} Q\ C\ dt \\ &= T_0 \int_0^{Q_{max}} Q\ C_Q\ P(Q)\ dQ \end{aligned} \qquad [4\text{-}51]$$

where Q is the water discharge, C_Q is the average SSC corresponding to Q, and P(Q) is the frequency distribution function of Q, which is determined from the time series of Q on the basis the time-series of A and U, defined by Equations [4-33] to [4-37]. C_Q is represented here by the SSCs obtained from the long-term monitoring station (as described previously).

4.5. Determination of Inlet Equilibrium

4.5.1. Definition of Equilibrium

The concept of an equilibrium cross-sectional area for an entrance implies that, for any tidal inlet, the cross-sectional area will evolve to such a stage that it fluctuates only around a mean value; this depends upon environmental conditions remaining constant. Several points concerning this concept of equilibrium should be clarified.

Firstly, the time-span for an inlet to reach equilibrium is controlled largely by sediment availability. If there is only a limited sediment supply, then the cross-sectional area will be mainly an inherited feature, rather than the result of dynamic equilibrium. Alternatively, an inlet with abundant sediment supply will reach its equilibrium within a relatively short time period. An equilibrium cross-section results, therefore, from a balance between the dynamic forces which are responsible for sediment transport and sedimentation within the inlet itself. Tidal inlets in their equilibrium state should have, therefore, a boundary which is covered (at least partly) by loosely-consolidated sediments.

Secondly, it is the time-averaged cross-sectional area which is in equilibrium with the environment. Statistically, environmental factors (wave climate, tidal currents and sediment supply) change only slowly; hence, the time-averaged cross-sectional area will also change slowly. On this basis, the equilibrium cross-sectional area can be written as:

$$A_E = \frac{1}{T_0} \int_0^{T_0} A \, dt \qquad [4\text{-}52]$$

where T_0 is the time-scale over which equilibrium is considered.

Thirdly, the equilibrium cross-sectional area exists only when A_E, determined from Equation [4-52], is larger than A_{cr}:

$$A_E > A_{cr} \qquad [4\text{-}53]$$

Based upon the points outlined above, equilibrium cross-sectional area can be defined as the time-averaged cross-sectional area of the entrance to a tidal inlet, which is larger than A_{cr} (defined by Escoffier's closure curve) and is formed under conditions of sufficient sediment supply.

4.5.2. Factors Affecting Equilibrium

The factors which control the equilibrium of the cross-sectional area can be analysed in terms of the equations of water mass and sediment continuity. For any tidal inlet, Equation [4-32] represents the water mass continuity. It can be integrated for flood tide durations over a period T_0, containing n flood tide durations, using Equation [4-32], to produce:

$$T_f <U_f> A_E + T_f <U_f' A'> + T_f <Q_F> = <P> \qquad [4\text{-}54]$$

where T_f is the mean flood tide duration, U_f' is the fluctuating component of $<U_f>$ ($U_f' = U_f - <U_f>$), A' is the fluctuating component of A_E ($A' = A - A_E$), and P is tidal prism. The diamond brackets denote cross-sectional mean, and the subscript *f* denotes "flood tide".

The same procedure can be applied to Equation [4-32] for ebb tide durations, yielding:

$$T_e <U_e> A_E + T_e <U_e^{\prime} A^{\prime}> + T_e <Q_F> = - <P> \qquad [4\text{-}55]$$

where the subscript *e* represents "ebb tide".

For the entrance channel, the sediment continuity is defined as:

$$\frac{\partial A}{\partial t} + \frac{\partial (B\, \overline{q_s})}{\partial x} = 0 \qquad [4\text{-}56]$$

where q_s is volume sediment transport rate (with B representing the channel width, and the over bar denoting the cross-sectional mean). Equation (4-56), when averaged over $n(T_f+T_e)$, becomes:

$$\frac{\partial A_E}{\partial t} + \frac{\partial <B\, \overline{q_s}>}{\partial x} = 0 \qquad [4\text{-}57]$$

Because the change of A_E with time is generally small, it is reasonable to assume that:

$$\frac{\partial <B\, \overline{q_s}>}{\partial x} = 0 \qquad [4\text{-}58]$$

which means that at any position in the inlet:

$$<B\, \overline{q_s}> = q^{\prime} \qquad [4\text{-}59]$$

The physical meaning of q' is the net sediment transport through the inlet during T_0. This quantity can be decomposed into 3 terms: (i) transport during the ebb phase of the tide; (ii) transport the flood phase of the tide; and (iii) transport into the entrance along the beach, in the form of longshore drift caused by waves. Equation [4-55] can be rewritten, therefore, as:

$$T_f <B\, \overline{q_{sf}}> + T_e <B\, \overline{q_{se}}> + (T_f + T_e)\, k\, q_l = q^{\prime} \qquad [4\text{-}60]$$

where q_{sf} is the sediment transport rate caused by the flood currents, q_{se} is the transport rate on the ebb, and k q_l is the rate of sediment supply into the channel by longshore currents (q_l being the magnitude of the longshore drift and the parameter k (between 0 and 1) representing the type of sediment bypassing).

Because the sediment transport rate can be expressed as a function of current speed, $<U_f>$ and $<U_e>$ are related to each other through Equation [4-60].

The analysis, described above, demonstrates that the equilibrium of any tidal inlet is determined by groups of environmental factors: (i) geomorphological features i.e. the area and hypsometric curve representing the tidal basin and the length and width of the inlet; (ii) hydraulic conditions, including the mean and any variability in the adjoining oceanic and basin tidal ranges, freshwater discharge, and the duration and speed of flood and ebb flows; and (iii) factors related to sediment transport, such as grain size characteristics of surficial sediments, tidally- and wave-induced current velocities and any superimposed wave action.

The method developed here were applied to examine the comparative equilibrium conditions of Langstone, Yangpu and Christchurch Harbours. The purpose of such a comparison study is to form a basis for evaluating some of the existing criteria for inlet stability, rather than to determine A_E for these inlets (although Equations [4-54]. [4-55] and [4-60] can be used to calculate A_E).

CHAPTER 5. RESULTS

5.1. Characteristics of the Seabed

5.1.1. Morphology of Entrance Channel and Tidal Deltas

The morphology of the entrance to Christchurch Harbour is represented by 3 transects (Figure 5-1). Generally, the entrance is shallow (the deepest part at around -4.0 m OD), with a relatively large width/depth ratio of between 12 and 16. The cross-sectional area has increased since 1978. For example, the area below mean sea level (0.15 m OD) is 135.7 m^2 at Transect G2, whilst it was 109.1 m^2 at a transect located 15 m to the east of G2 in 1978 (Tosswell 1978).

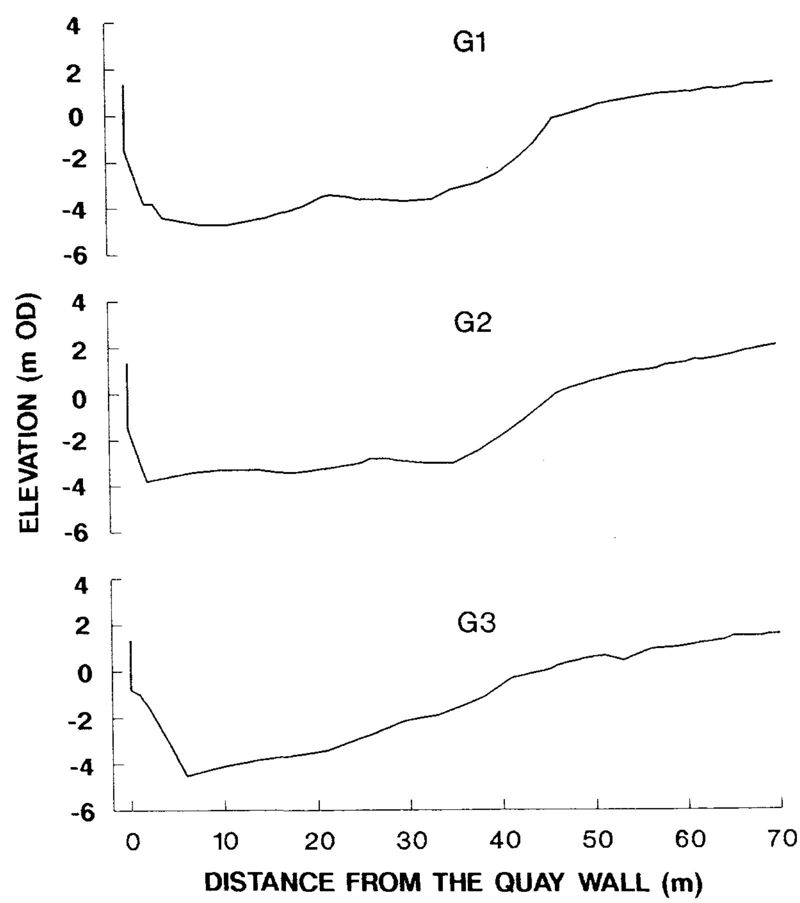

Figure 5-1. Bathymetry of 3 transects within the Run, surveyed during February and March, 1992 (for location of the transects, see Figure 4-14).

Table 5-1. Exposure and inundation events associated with water levels recorded by the tide gauge in the Run (3 August, 1991).

Location	Time (GMT)	Events	Water Level*
Ebb Delta	7.25	Completely inundated	-0.172
	7.35	Partly exposed	-0.202
	7.55	Most exposed	-0.244
	8.05	Completely exposed	-0.274
	9.35	Lower part inundated	-0.359
	9.45	Most inundated	-0.323
	9.55	Completely inundated	-0.304
Flood Delta	7.10	Highest part exposed	-0.135
	10.57	Highest part inundated	-0.105

* Elevation in m OD measured at the tide gauge station (250 m from the central part of the ebb delta and 350 m from the highest part of the flood delta).

Elevation of the upper part of the flood and ebb tidal deltas is estimated now, by relating tidal water levels to observed exposure and inundation events. On 3 August 1991, the process of exposure-inundation changes on the tidal deltas were recorded on the basis of tide gauge measurements (Table 5-1).

During the ebb tide, the flood delta was exposed initially when the water level in the Run was -0.135 m OD; during the subsequent flood phase of the tide, it became inundated when the water level reached -0.105 m OD. The difference in the water levels relating to exposure and inundation times is due to the water surface slope, which tilts towards the sea during the ebb and towards the land during the flood. Thus, the elevation of the top of the delta is approximately -0.12 m OD.

Water levels associated with the ebb delta exposure during the ebb and the inundation during the subsequent flood were -0.20 m OD and -0.30 OD, respectively. Consequently, the highest part of the ebb delta is approximately -0.20 m OD. Using the same method, the elevation of the main part of the ebb delta is estimated to be -0.28 m OD.

5.1.2. Seabed Sediments

Sediment Types

Christchurch Harbour and the ebb tidal delta is dominated by sandy sediments, whilst areas outside the harbour are covered by various combinations of sandy and gravelly material (Figures 5-2 and 5-3).

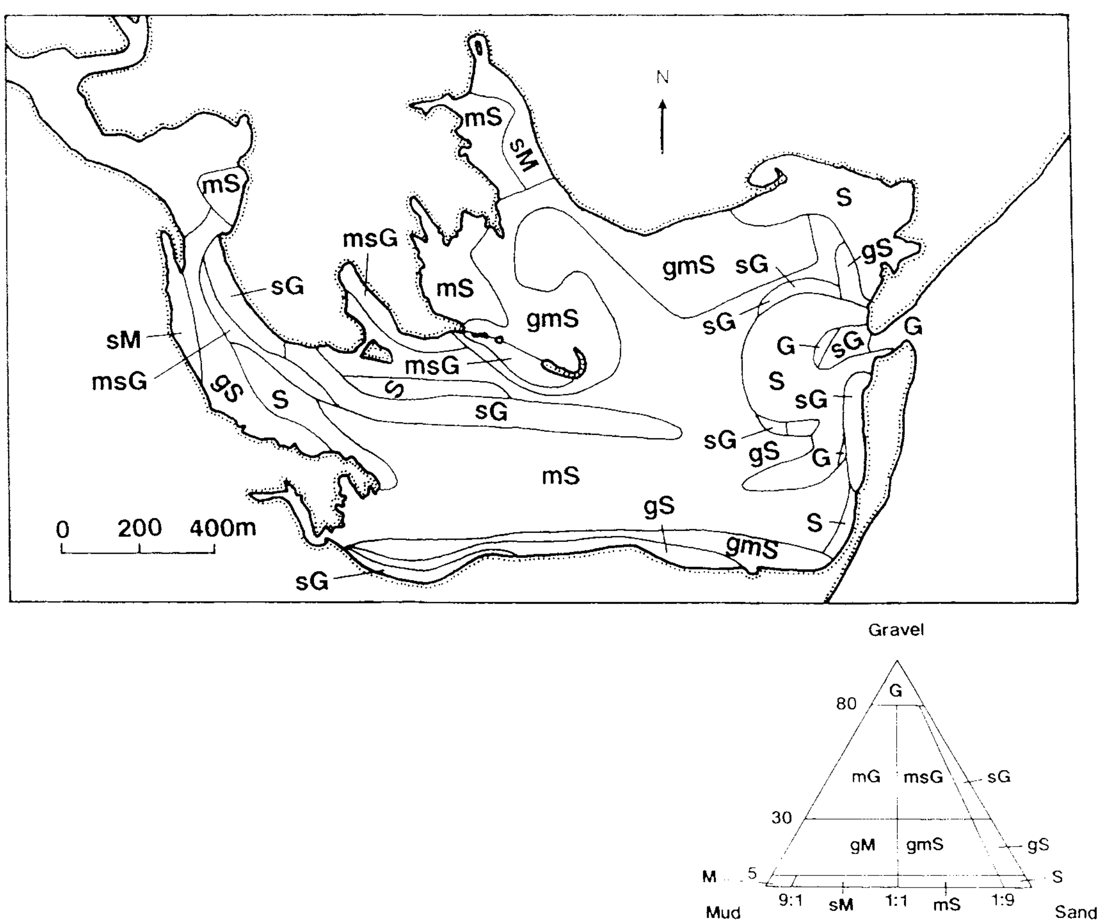

Figure 5-2. Seabed sediments in Christchurch Harbour (the classification scheme based upon Folk (1980), modified slightly).

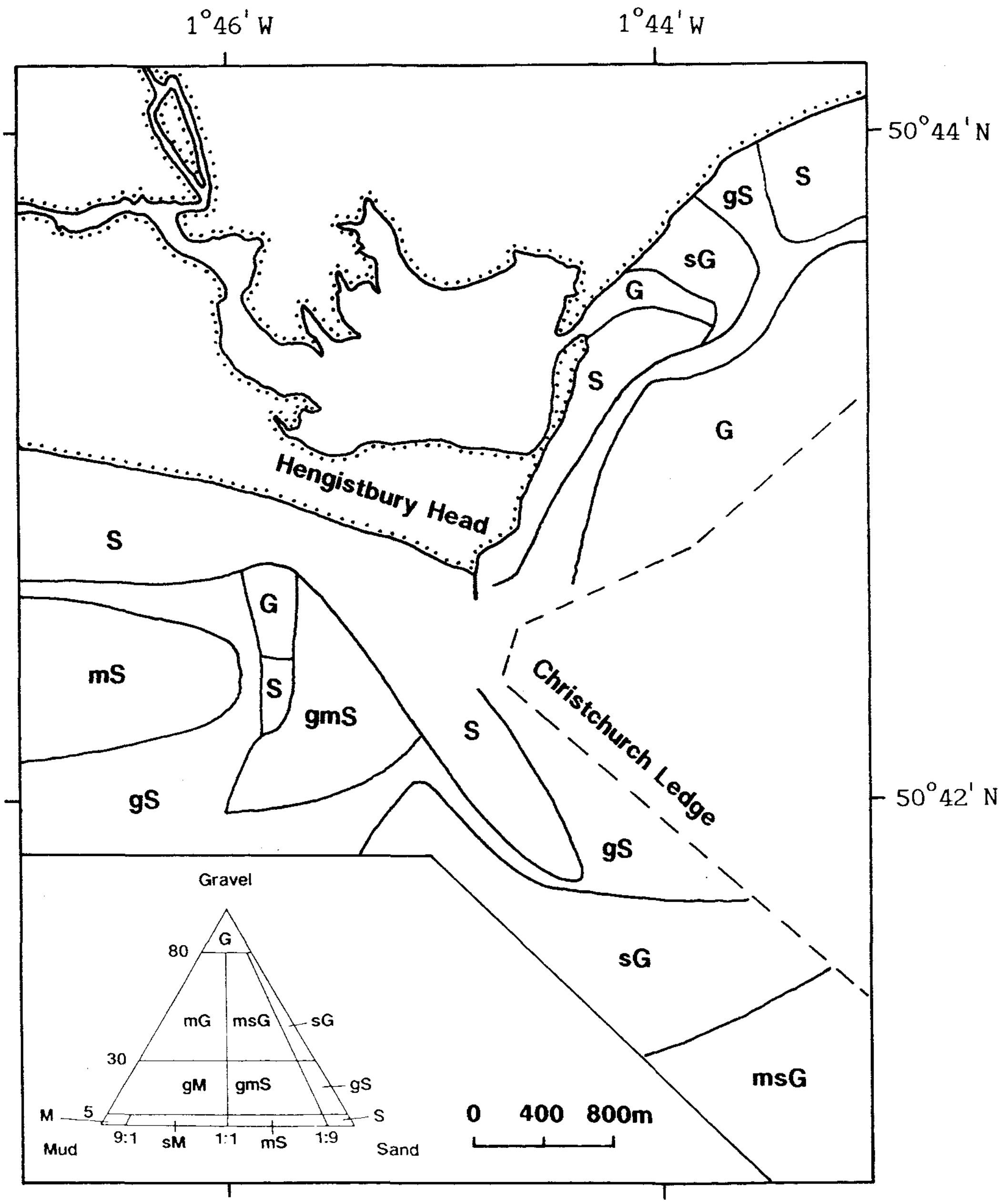

Figure 5-3. Seabed sediments outside the Harbour (the classification scheme based upon Folk (1980), modified slightly).

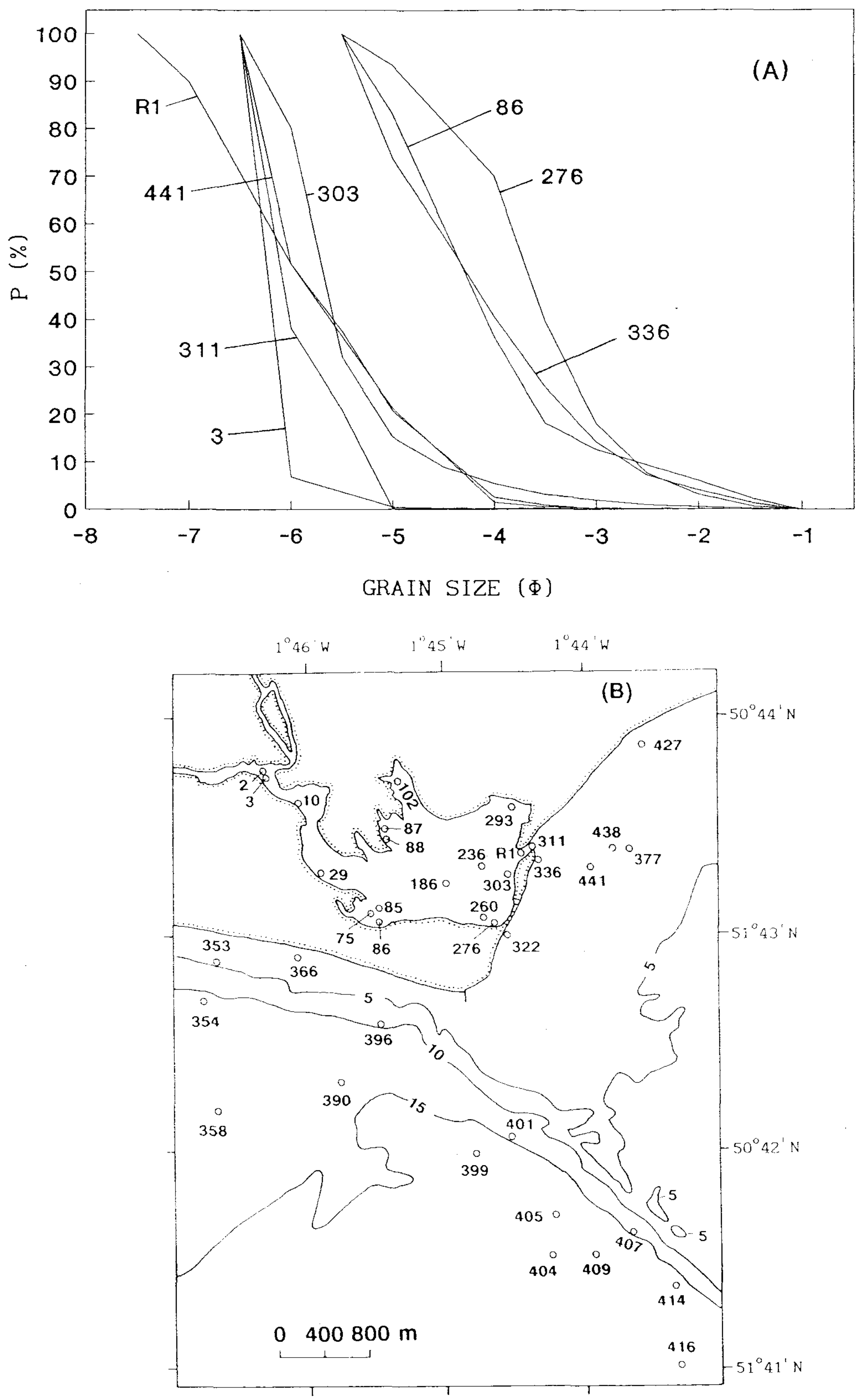

Figure 5-4. (A) Some representative grain size distributions of gravel fractions; and (B) sample locations (including those for Figures 5-6 and 5-7).

Gravels are distributed mainly over the ebb tidal delta, in the river channel, along the eroded coastline, on the South Spit, and in the offshore areas. The gravelly material near the entrance to the harbour is much coarser than around Stanpit Marsh (with mean grain sizes of 40 and 10-20 mm, respectively) (Figure 5-4).

Gravelly sediments within the Run are dominated by large pebbles (Figure 5-5). Sand and sandy gravel are confined within a narrow zone near High Water Mark on the southern side of the channel. Stones with a diameter over 0.2 m have been collected, each weighing 2 to 3 kg. This material acts as an armouring layer, which is not very mobile under calm weather conditions; this prevents erosion of the underlying sediments.

Sands are present mainly on the flood tidal delta and the linear sandbanks in the southern and southwestern parts of the harbour. The sandy material consists mainly of medium and fine sand (Figures 5-6).

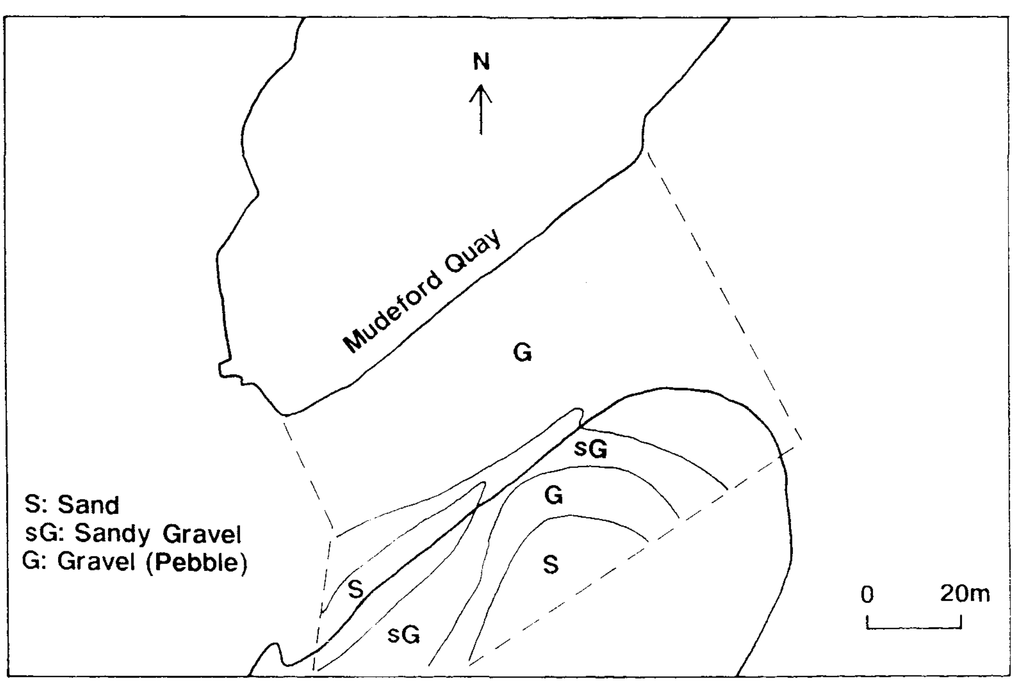

Figure 5-5. Sediments within the entrance channel (for notations, see Figure 5-2).

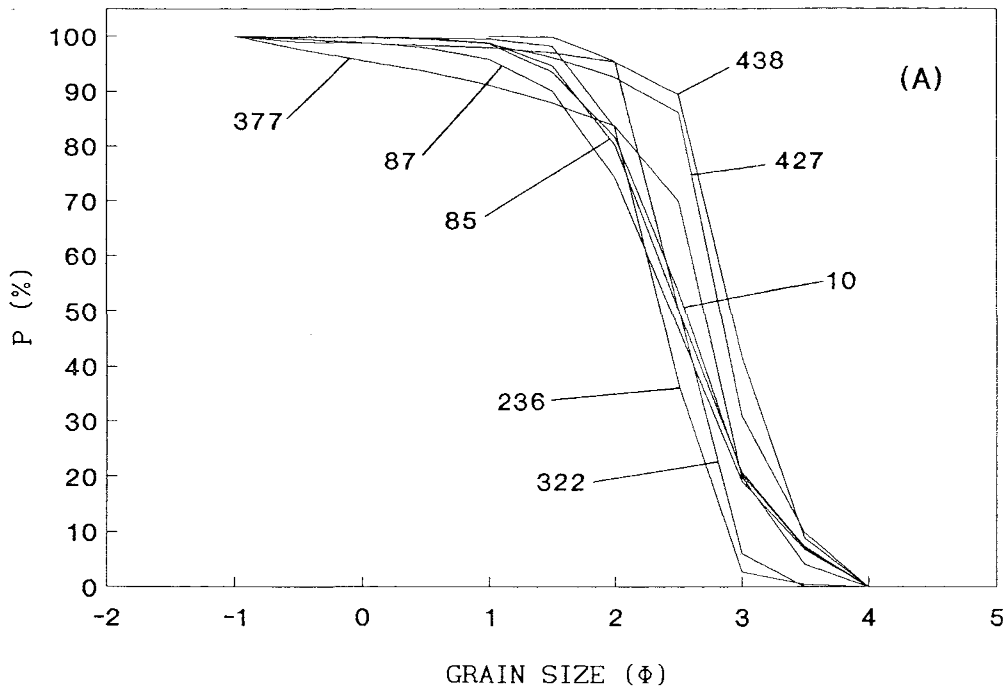

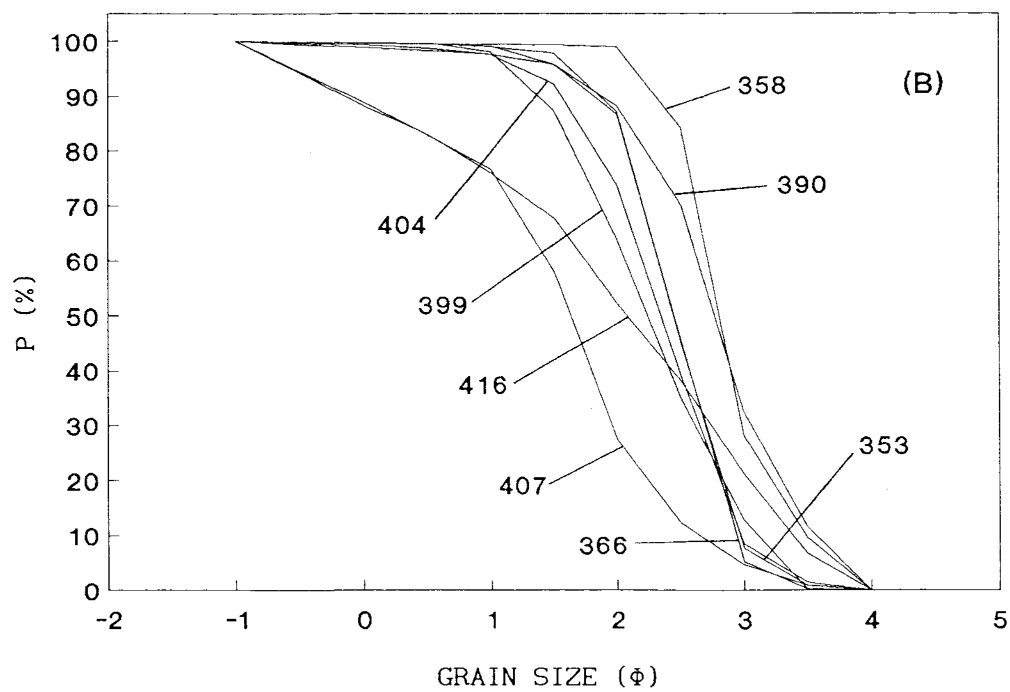

Figure 5-6. Some representative grain size distributions of sand sub-samples collected from: (A) the Harbour and ebb tidal delta areas; and (B) the area to the south of Hengistbury Head. The sample locations are shown on Figure 5-4 (B).

The mud content of the sediments is relatively low. Among the 455 samples, 242 have a mud content exceeding 5 %. In general, the mud content is less than 25 % over most of the area (10 to 15 % on average); only a very limited number of samples collected from the bay-head areas are highly muddy (with a mud content of over 50 %). Some locations denoted as "mud" on published maps (e.g. 1:10000 Ordnance Survey Sheet SZ19SE) are actually covered mainly with sandy material. Nevertheless, such a low mud content may influence the hydrodynamic behaviour (e.g. threshold of movement) of bulk sediment significantly.

Particles finer than 10 ϕ account for a relatively large percentage in the mud fractions of any sample (Figure 5-7). In the bay-head areas, the percentage of these particles in the mud sub-samples reaches 35 to 40%; elsewhere, it is around 20 to 25 %.

The distribution patterns of mean grain size, sorting coefficient and skewness are shown on Figures 5-8, 5-9 and 5-10 (these grain size parameters were determined from analyses of complete seabed samples). In general, sediments are much coarser within the entrance channel than at other locations. The distribution of mean grain size shows that sandy material dominates over majority of the area (Figure 5-8). The sediments from the tidal deltas are the best sorted. Relatively poor sorting is present for the sediments in the bay-head areas (within the Harbour) and offshore areas (outside the Harbour) (Figure 5-9). The sediments within the Harbour are mainly positively skewed; outside the Harbour, negative skewness tends to dominate (Figure 5-10). The correlation between mean grain size and skewness is not high.

The sample locations and the results of the analyses undertaken are listed in Appendix B.

Thickness of the Holocene Sediments

In western Christchurch Bay and the area around Hengistbury Head, the Holocene sediment cover is thin; this is shown by the sub-bottom profiler and side-scan sonar records (for locations of the sites of data collection, refer to Figure 5-11).

On Christchurch Ledge (Figure 5-12), there is no indication of sediment accumulation. The area is occupied by large boulders (iron stones), representing relict material eroded from the Eocene strata which contain the iron stones (Section 3.1.1.), or by exposed Eocene deposits.

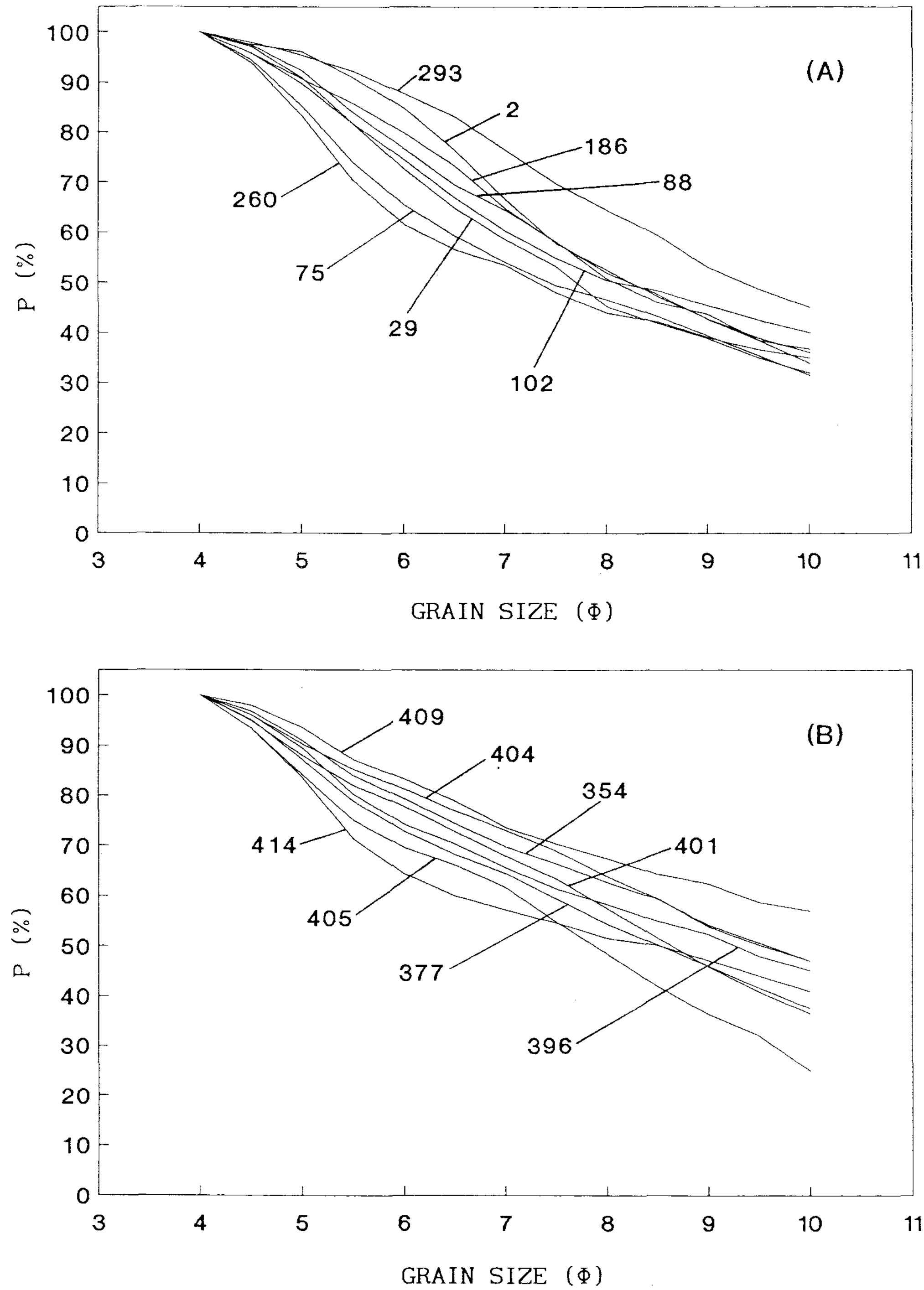

Figure 5-7. Some representative grain size distributions of mud sub-samples within the Harbour (A) and outside the Harbour (B). The sample locations are shown on Figure 5-4 (B).

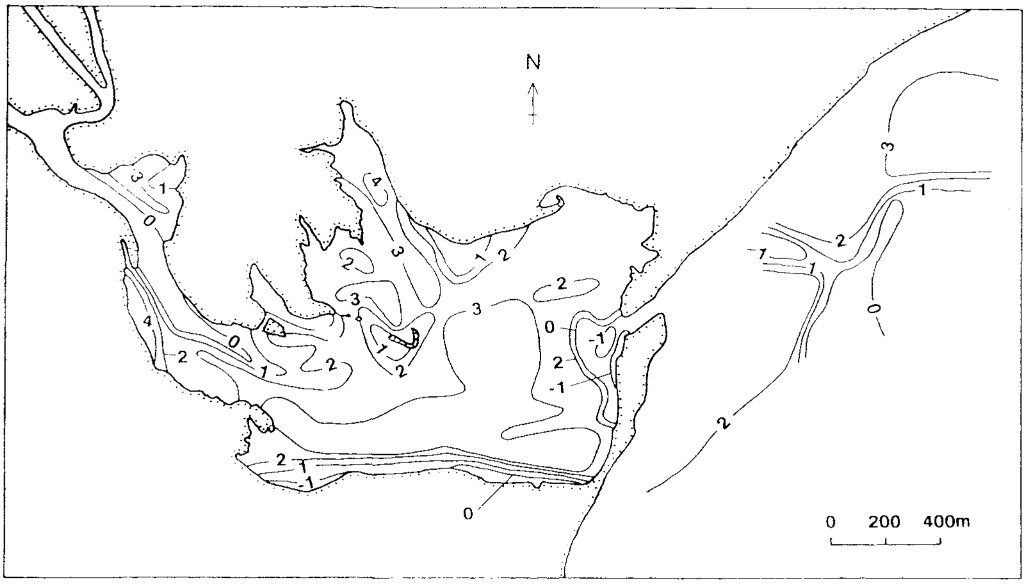

Figure 5-8. Mean grain size of the surficial sediments (in ϕ units).

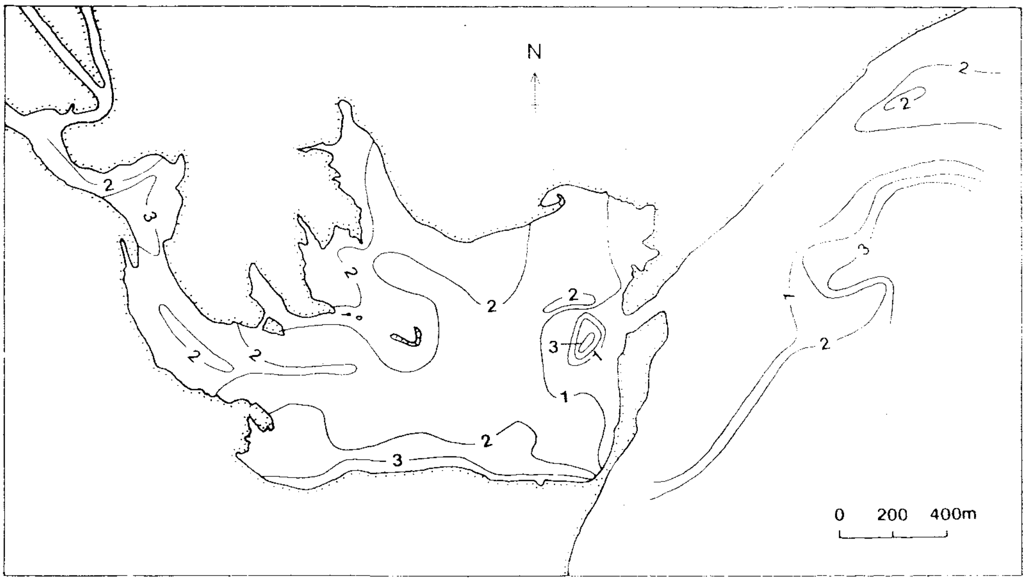

Figure 5-9. Sorting coefficient of the surficial sediments (in ϕ units).

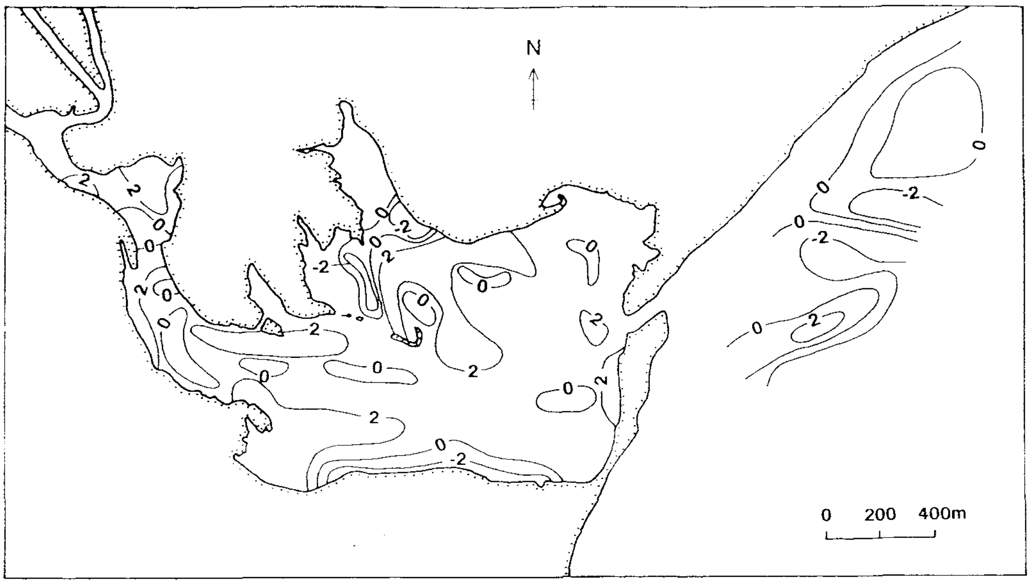

Figure 5-10. Skewness of the surficial sediments (in ϕ units).

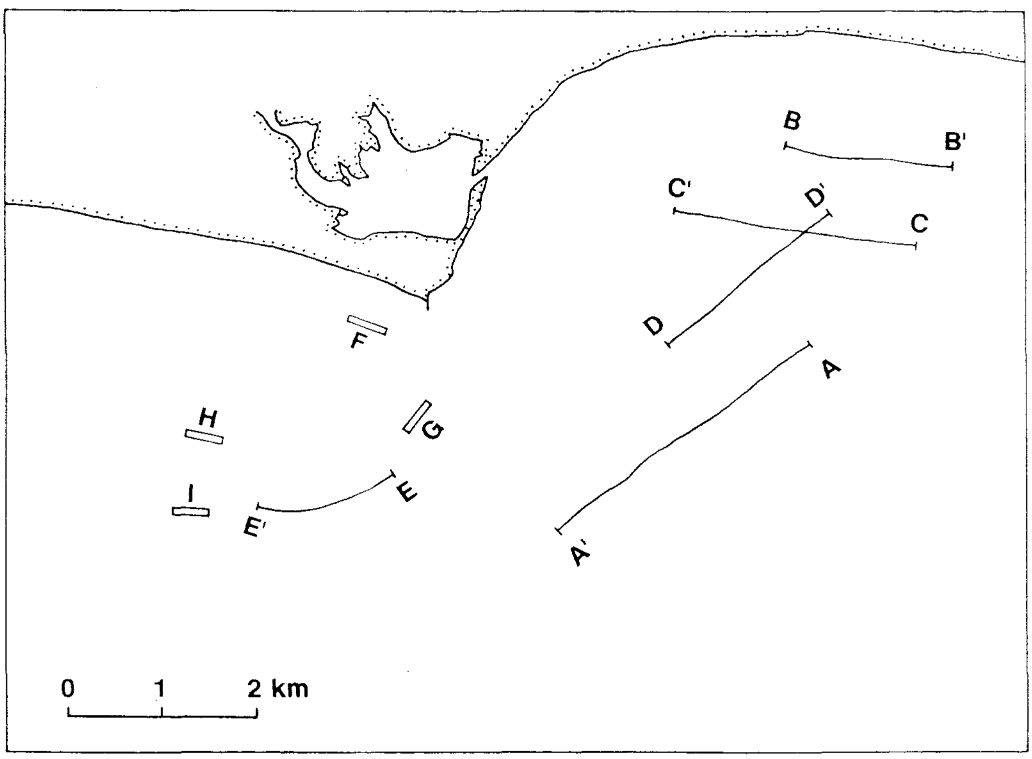

Figure 5-11. Locations for sub-bottom profiler and side-scan sonar data presented on Figures 5-12 to 5-20. A-A' to E-E' are the selected sub-bottom profiler lines and F to I are the areas covered by the selected side-scan sonographs.

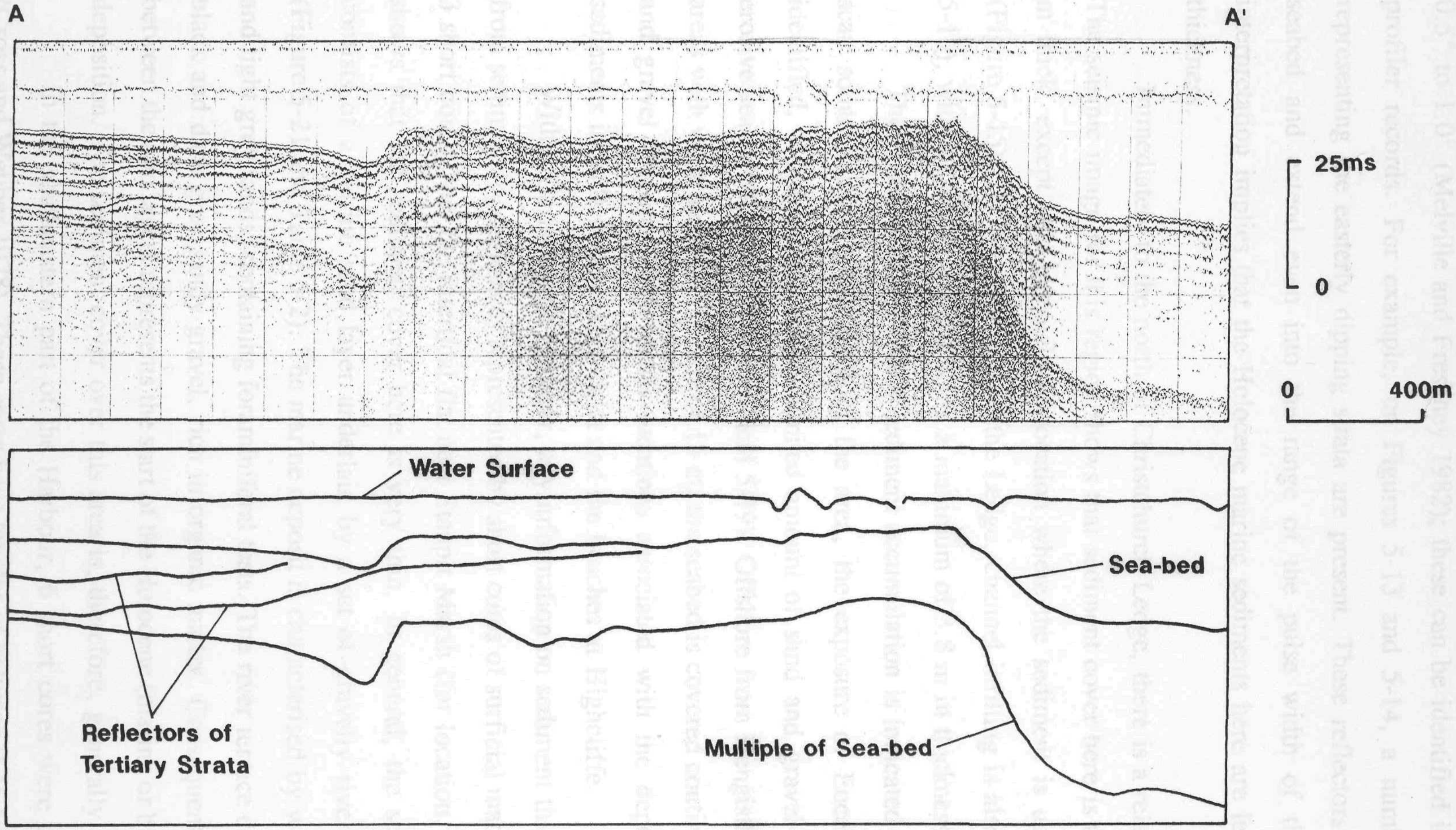

Figure 5-12. Christchurch Ledge, characterised by boulders and exposed Tertiary strata shown on the sub-bottom profiler image (Profile A-A', Figure 5-11). The vertical scale is terms of TWT.

In western Christchurch Bay, to the north of the Ledge, the sediment cover is very thin. Over this particular area, Eocene strata tilts towards the east with a dip of 0.5° to 1.0° (Melville and Freshney 1982); these can be identified in the sub-bottom profiler records. For example, on Figures 5-13 and 5-14, a number of reflectors representing the easterly dipping strata are present. These reflectors are close to the seabed and extend even into the range of the pulse width of the records. This interpretation implies that the Holocene marine sediments here are less than 1.5 m in thickness.

Immediately to the north of Christchurch Ledge, there is a relatively deep area. The seismic image for this region shows that sediment cover here is also less than 1.5 m thick, except at a channel-like location where the sediment is up to 3.2 m thick (Figure 5-15). To the southwest of the Ledge, channel infilling is also present (Figure 5-16), with the newer deposit being a maximum of 3.8 m in thickness.

The absence of any recent sediment accumulation is indicated also by the side-scan sonar images. Over most of the area, the exposure of Eocene strata can be identified, together with a very limited amount of sand and gravel scattered on the erosive seabed (Figures 5-17, 5-18 and 5-19). Offshore from Hengistbury Head and in areas with water depths in excess of 15 m, the seabed is covered continuously with sand and gravel (Figure 5-20). Other locations associated with the deposition of recent sediments include the ebb tidal delta and the beaches at Highcliffe.

Within Christchurch Harbour, any information on sediment thickness is derived from sedimentary sequences represented by short cores of surficial material. Analysis of 3 short cores from the intertidal flat near Stanpit Marsh (for location, see Figure 4-13) shows that the sediment cover here is very thin. In general, the sediment sequence consists of a marine sand layer underlain by a set of gravelly river terrace deposits (Figure 5-21 and Table 5-2). The marine deposit is characterised by white, light yellow and light grey sands, containing foraminiferal tests. The river terrace deposit consists of black and dark grey sandy gravel, rich in organic matter. Consequently, the boundary between the two layers represents the start of the Holocene (marine or brackish) sediment deposition. The sediment cover over this area is, therefore, generally less than 0.5 m.

In the southeastern part of the Harbour, 6 short cores were collected in 1978 (Cross and Webber 1978). These cores have lengths of between 0.46 and 0.82 m and are characterised by medium- and fine-grained sands. The sediment cover here is thicker

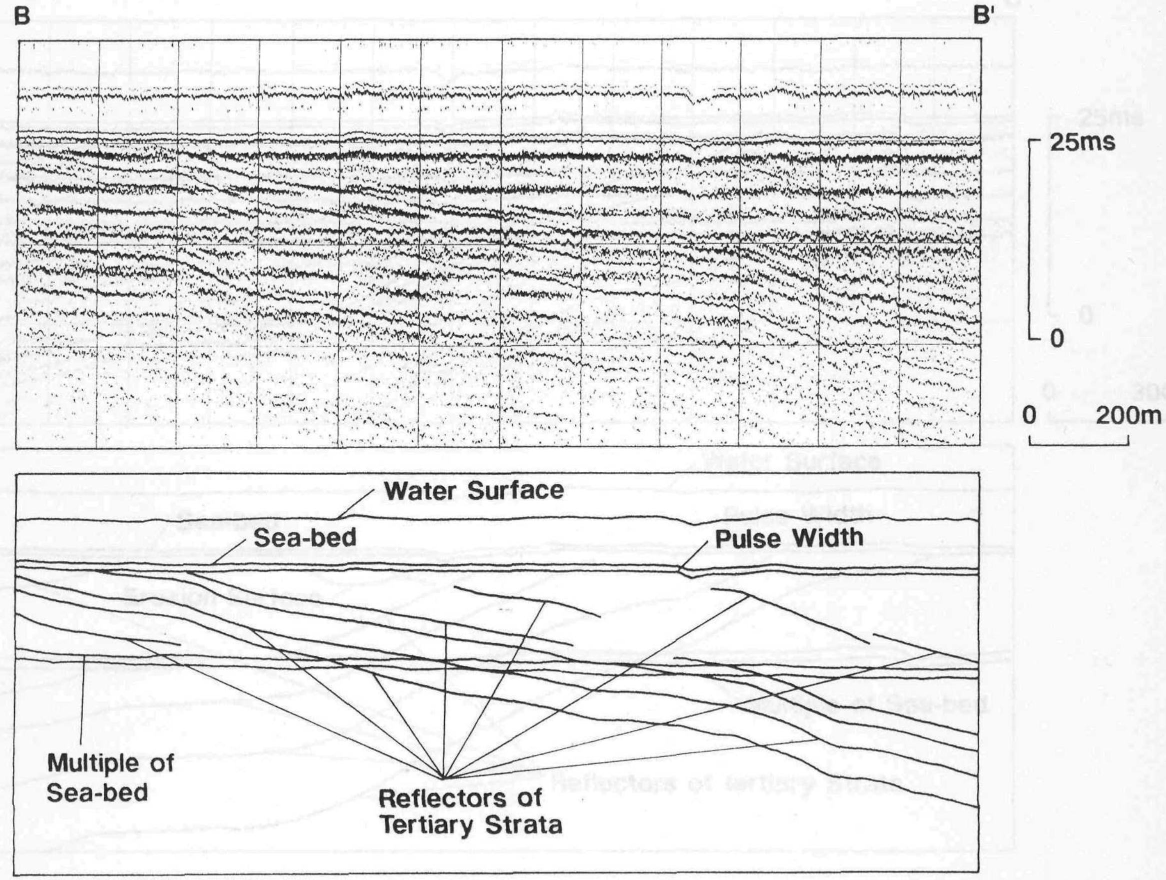

Figure 5-13. Interpretation of the sub-bottom profiler image of Profile B-B' (Figure 5-11), showing reflectors due to the underlying Tertiary strata. The vertical scale is terms of TWT.

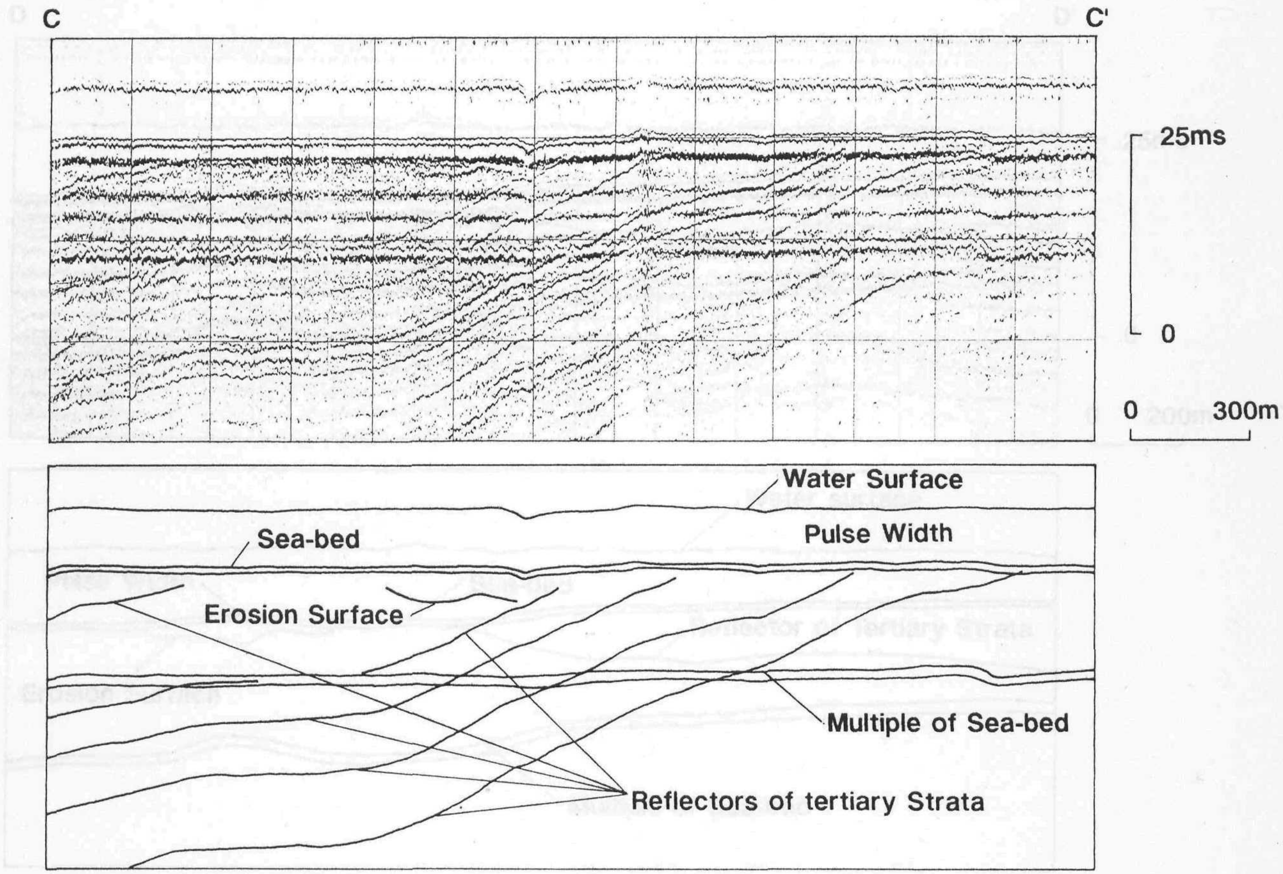

Figure 5-14. Interpretation of the sub-bottom profiler image of Profile C-C' (Figure 5-11), showing reflectors due to the underlying Tertiary strata. The vertical scale is terms of TWT.

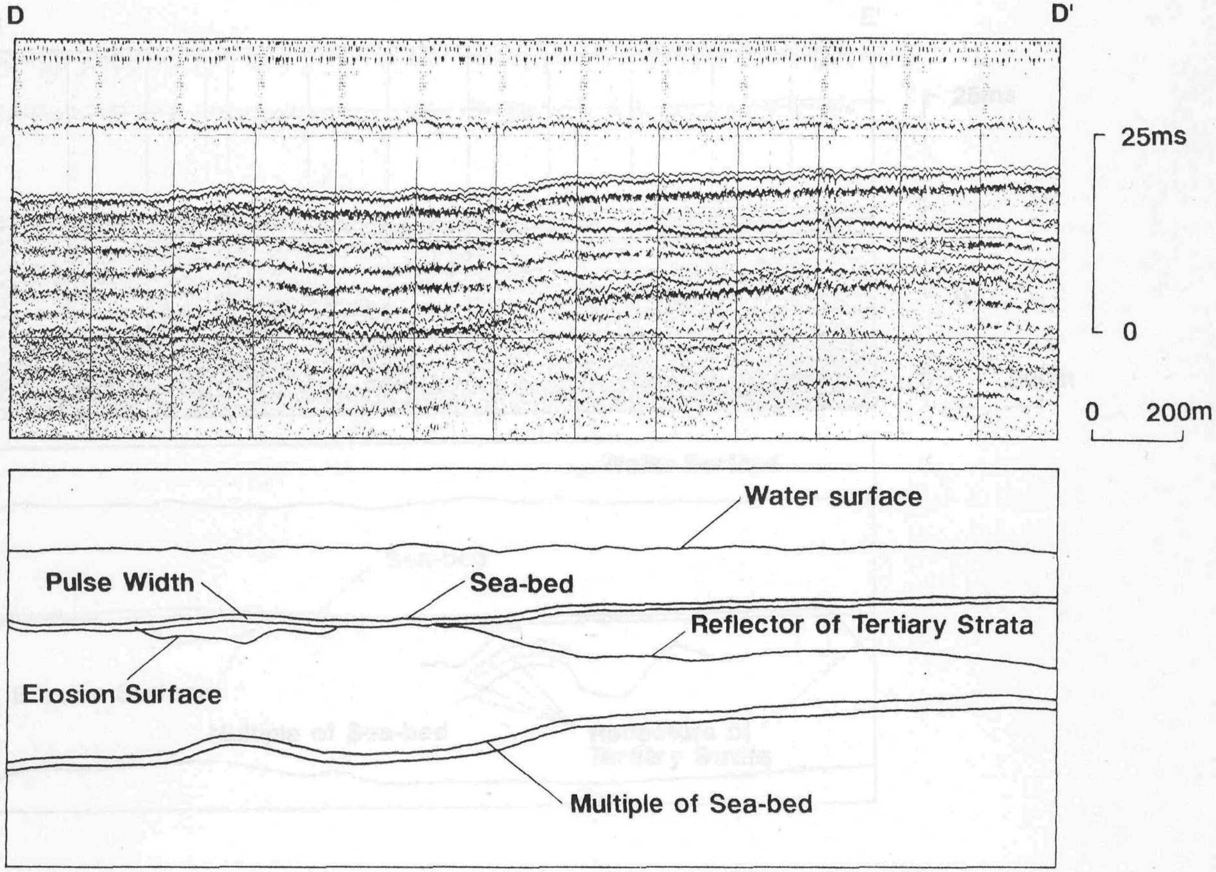

Figure 5-15. Interpretation of the sub-bottom profiler image of Profile D-D' (Figure 5-11), showing reflectors due to the underlying Tertiary strata and a channel-like feature. The vertical scale is in terms of TWT.

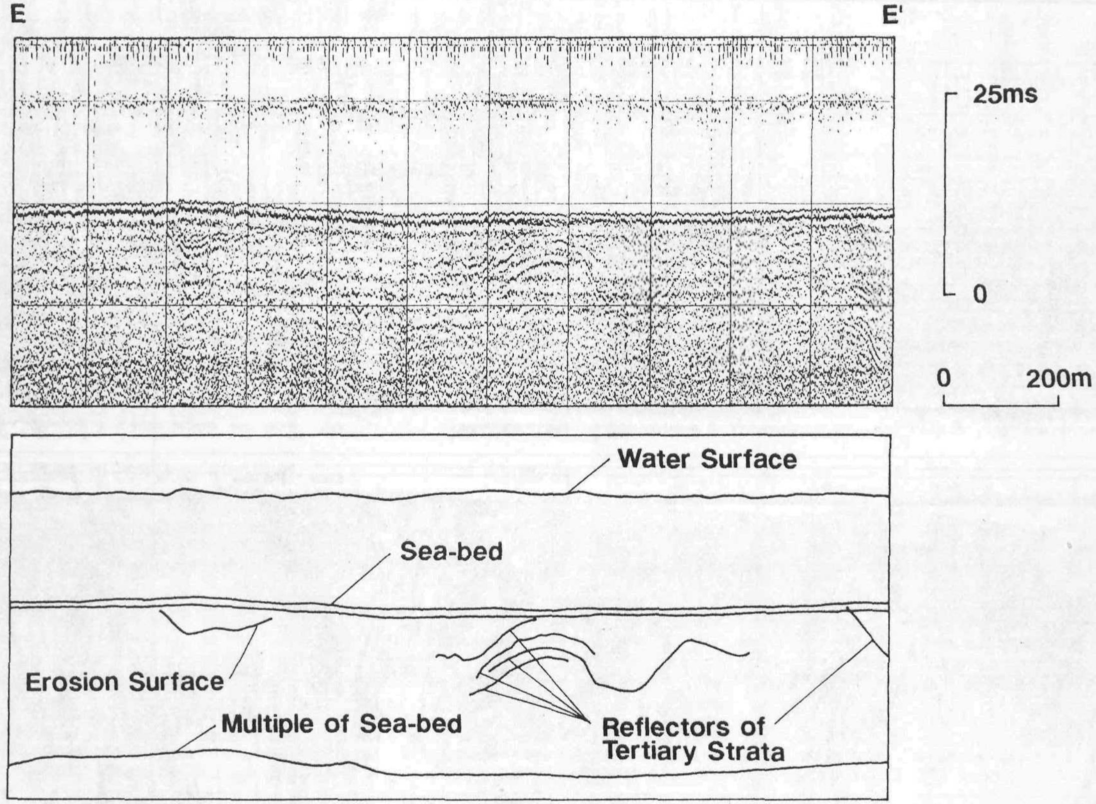

Figure 5-16. Interpretation of the sub-bottom profiler image of Profile E-E' (Figure 5-11), showing reflectors due to the underlying Tertiary strata and a channel-like feature. The vertical scale is in terms of TWT.

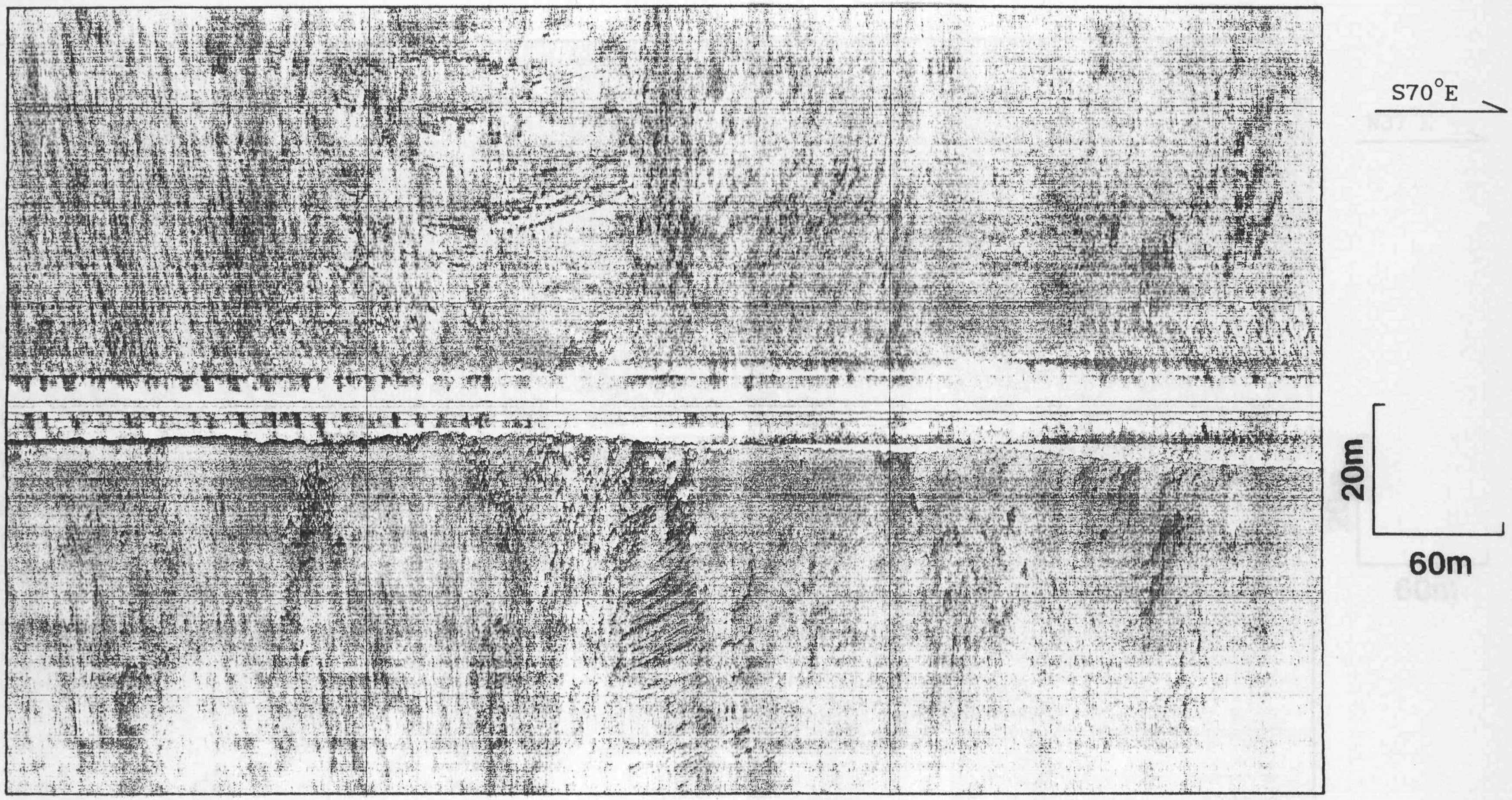

Figure 5-17. Side-scan sonar image of Area F (Figure 5-11), showing erosive seabed and exposed Tertiary strata. The vertical scale is in terms of the slant range.

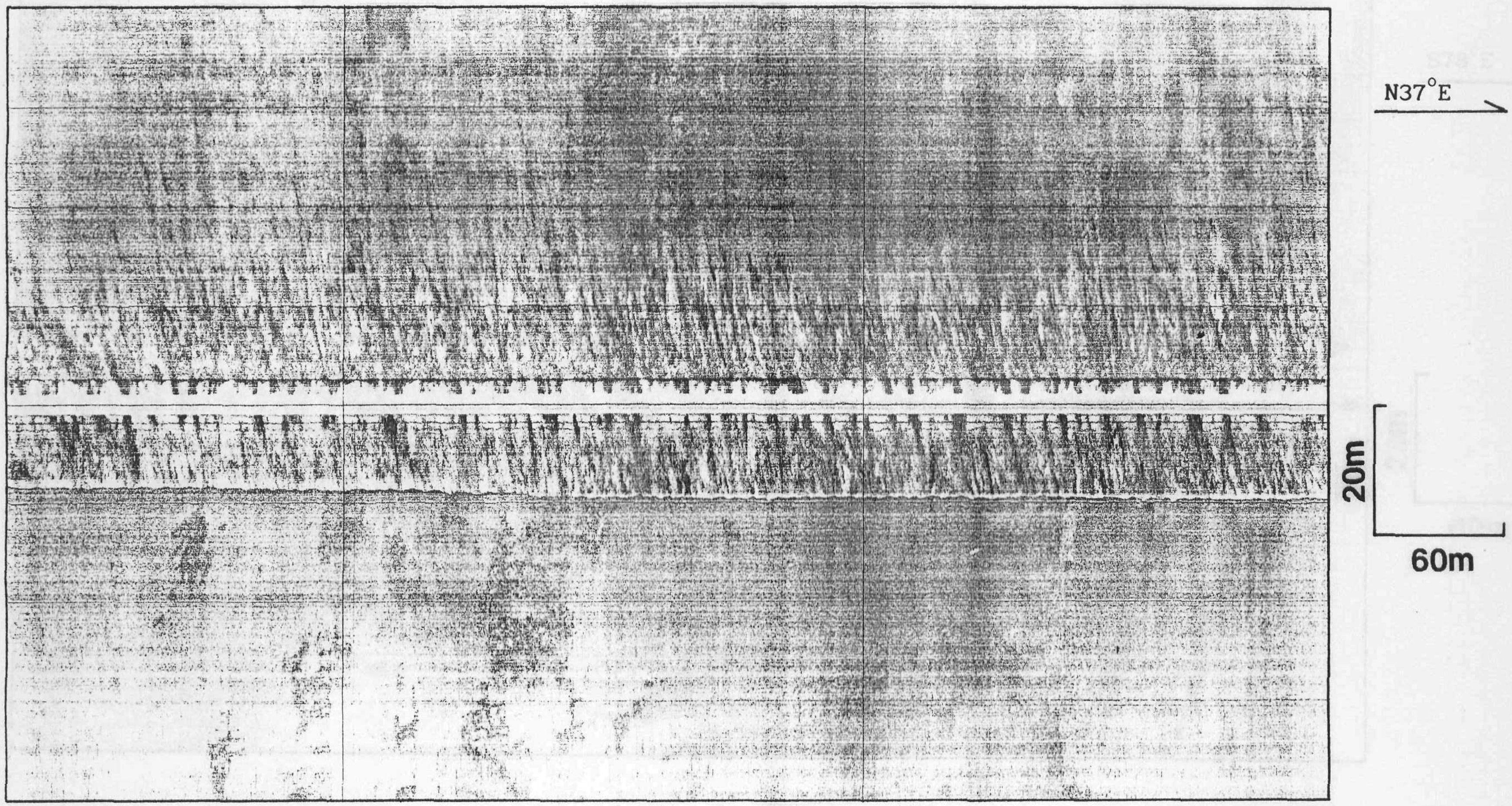

Figure 5-18. Side-scan sonar image of Area G (Figure 5-11), showing erosive seabed and exposed Tertiary strata. The vertical scale is in terms of the slant range.

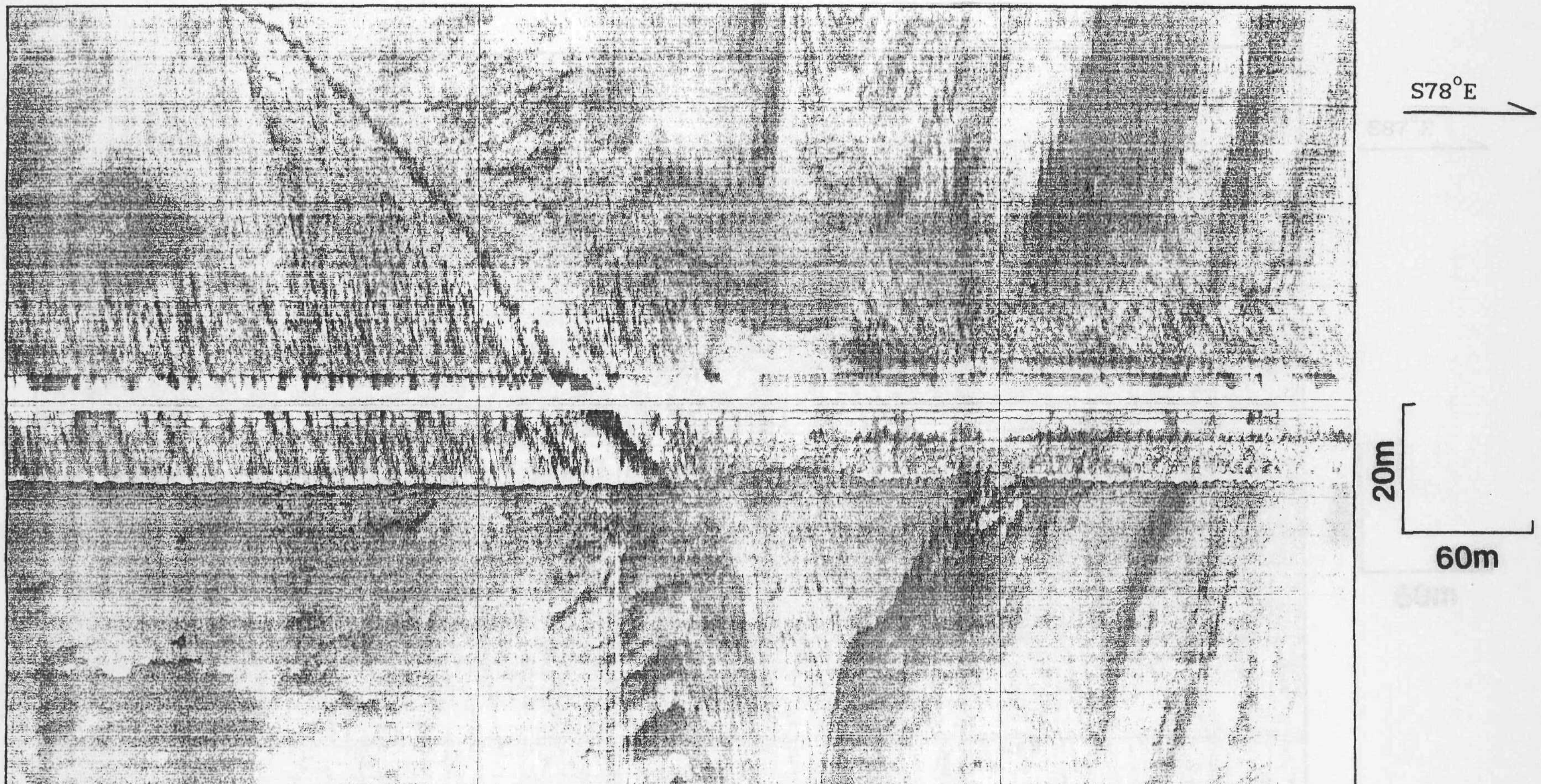

Figure 5-19. Side-scan sonar image of Area H (Figure 5-11), showing erosive seabed and exposed Tertiary strata (with a hard layer protruding the seabed). The vertical scale is in terms of the slant range.

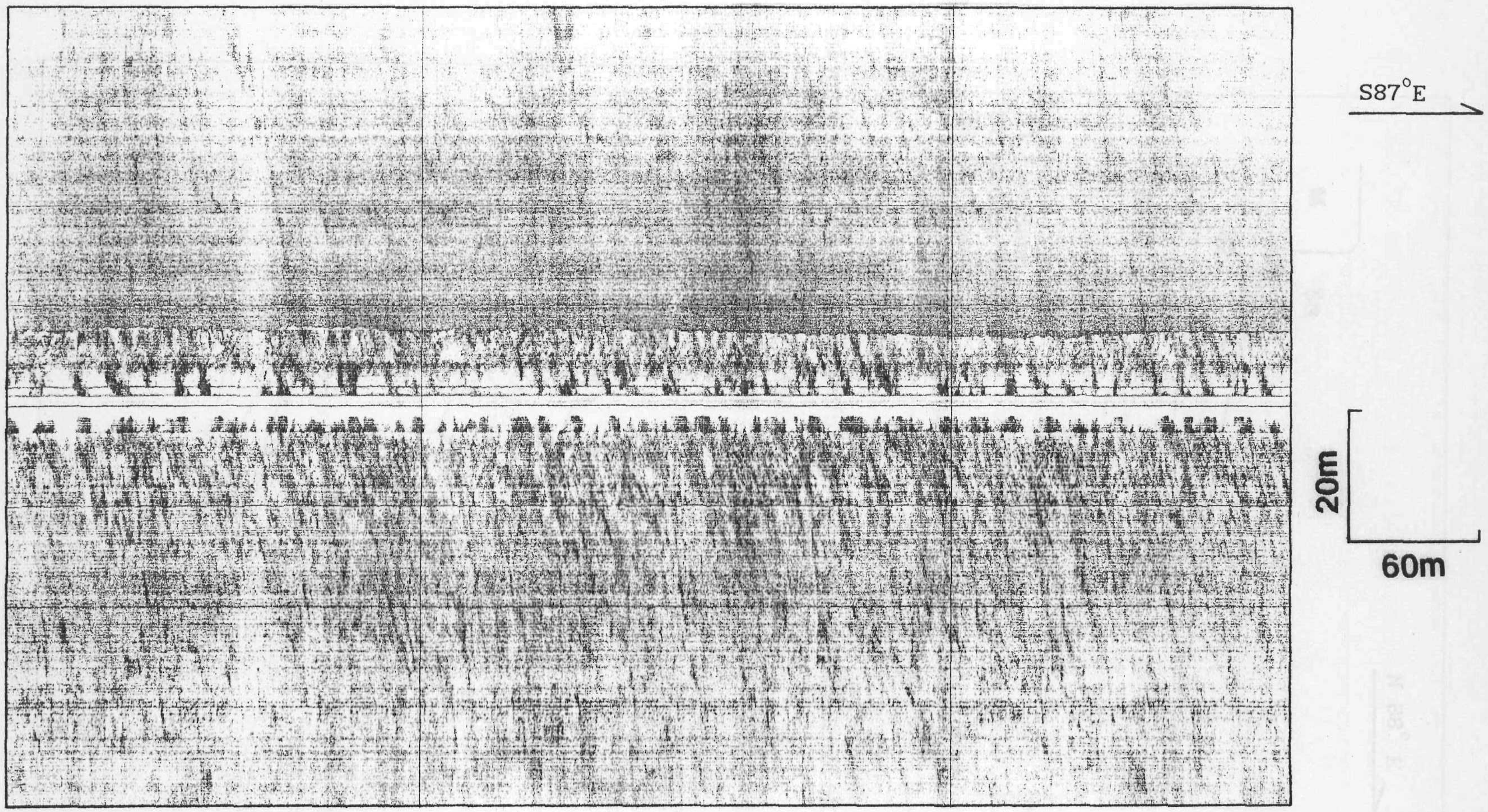

Figure 5-20. Side-scan sonar image of a seabed covered with sand and gravel, in Area I (Figure 5-11). The vertical scale is in terms of the slant range.

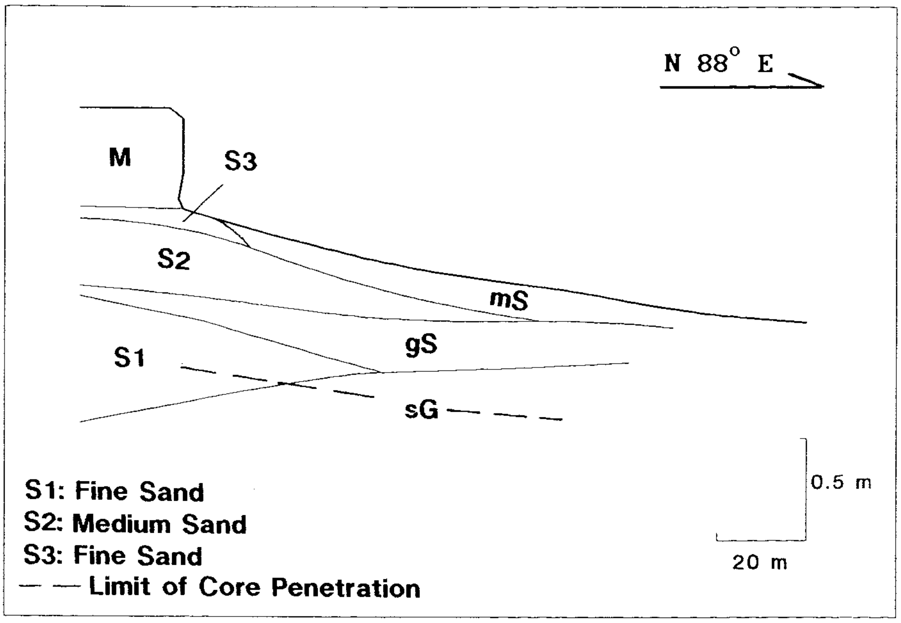

Figure 5-21. Holocene (marine/brackish) sedimentary sequence along the Stanpit Marsh profile (for notations, see Figure 5-2).

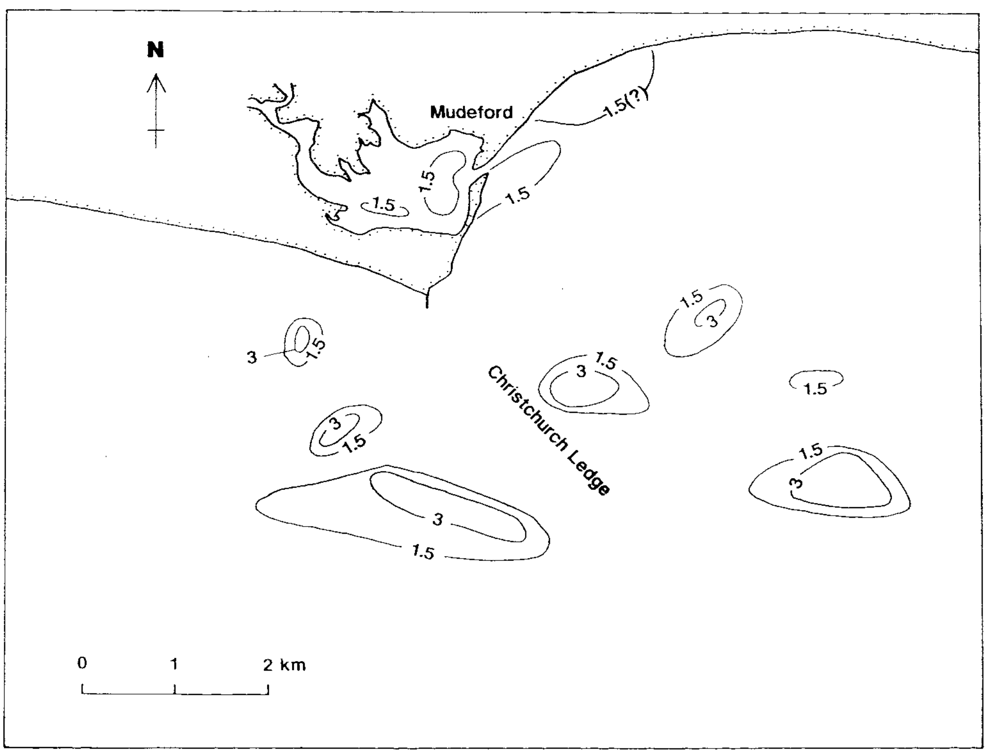

Figure 5-22. Thickness of Holocene (marine/brackish) sediments (in metres).

Table 5-2. Sedimentary sequence of the short cores (SC1, SC2 and SC3 are located at 0, 50, and 100 m from the salt marsh cliff, respectively).

Core	Layer	Depth (m)	Gravel (%)	Sand (%)	Mud (%)	Sediment Characteristics
SC1	1	0.00-0.07	0.0	86.6	13.4	Light yellow and grey sands
	2	0.07-0.41	0.0	96.2	3.8	White, clean sands
	3	0.41-0.50	5.4	88.6	6.0	White, clean sand and gravel
	4	0.50-0.76	0.0	94.3	5.7	Black sand
SC2	1	0.00-0.16	6.1	79.4	14.5	Grey muddy sand
	2	0.16-0.29	0.3	93.7	6.0	Light yellow sand
	3	0.29-0.46	0.5	92.9	6.6	White and light yellow sand
	4	0.46-0.50	0.7	91.3	8.0	Black sand
	5	0.50-0.68	54.8	40.9	4.3	Black sandy gravel
SC3	1	0.00-0.12	0.2	80.6	19.2	Muddy yellow and grey sand
	2	0.12-0.24	7.5	75.0	17.5	Grey gravelly muddy sand
	3	0.24-0.30	10.4	77.5	12.1	Yellow muddy sand and gravel
	4	0.30-0.47	54.6	43.0	2.4	Black sandy gravel
	5	0.47-0.56	53.4	43.0	3.6	Dark grey sandy gravel

than that on the intertidal flat near Stanpit Marsh. However, because the Run (which has a maximum water depth of less than 4 m (Section 5.1.1.)) has been found to be cut into Eocene strata (Burton 1931) (the entrance to Christchurch Harbour has not been in the same position, but the water depth in the past was presumably similar to that of today), the maximum newly-deposited sediment cover within the Harbour should not exceed 3 m. Thus, the average thickness is likely to range between 1 and 2 m over the whole area of the Harbour.

The interpreted thickness of Holocene sediments, based upon the analysis of seismic and short core information, is summarised on Figure 5-22. The derived pattern implies that the seabed here is dominated by erosion: small areas of accumulation are divided by Christchurch Ledge. Further, it may be inferred that sediment is transported from Poole Bay to Christchurch Bay, mainly through the surf zone around Hengistbury Head. Some easterly-moving material is prevented, by the Ledge, from entering Christchurch Bay; it is deposited to the south of the Ledge.

5.2. Hydrodynamics

5.2.1. Tidal Characteristics

Water level data obtained from the tide gauge are listed, as a time-series, in Table C-1 (Appendix C). In order to identify the tidal characteristics, spectral and harmonic analyses have been undertaken on the data set.

The spectral analysis defines the amplitude of water level oscillations associated with various periods, using the FFT (Fast Fourier Transformation) technique. Because the water level data are not continuous, the analysis is carried out separately for 6 time series; each of these has a length of more than 512 data points. Figure 5-23 shows the distribution of the amplitudes, averaged over the 6 time series. Due to the inadequate length of the various time series, the resolution is not high enough to distinguish between tidal components with periods which lie close to one another (e.g. the $\mathbf{M}_2$ and S_2 components). Nevertheless, it is shown clearly that semi-diurnal tides dominate over diurnal tides and that the fourth, sixth and eighth diurnal tidal harmonics also contribute significantly to the overall pattern of water movement.

An harmonic analysis has been carried out to determine the tidal components, using the FORTRAN program TIRA developed and made available by the Proudman Oceanographic Laboratory (Bidston). This program is based upon the least square procedure of analysis, which is capable of analysing a discontinuous time-series. For the time-series obtained from Mudeford, the amplitude and phase of 62 harmonic tidal constituents have been identified, as listed in Table 5-3.

The amplitudes of the major semidiurnal components are much higher than those of major diurnal tides. The $\mathbf{M}_2$ and S_2 amplitudes reach 33.53 cm and 10.36 cm, respectively. In comparison, the $\mathbf{K}_1$ and $\mathbf{O}_1$ tidal amplitudes are, however, only 6.65 cm and 1.97 cm, respectively. Hence, a Form Factor ($(H_{K1}+H_{O1})/(H_{M2}+H_{S2})$, where

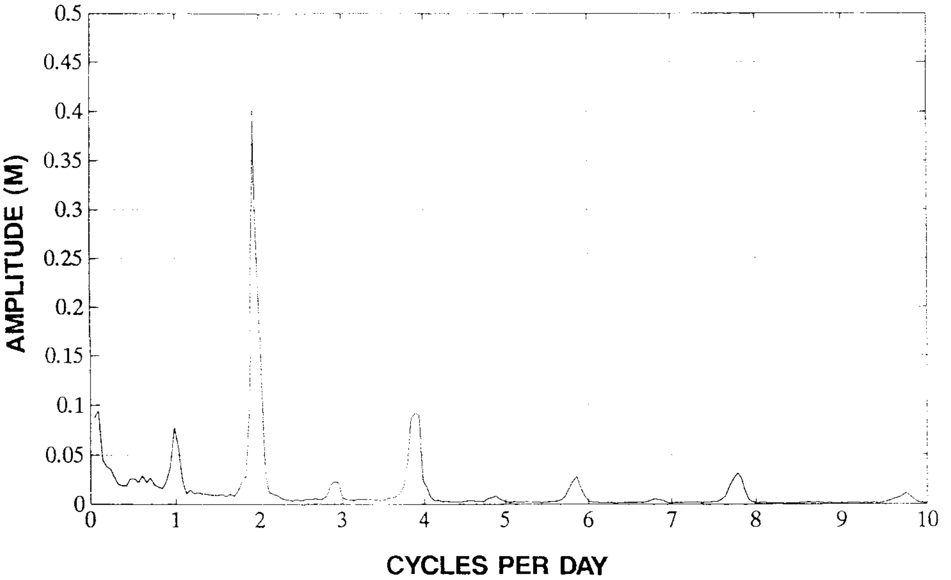

Figure 5-23. Amplitudes of oscillations with different periods, as derived from the spectral analysis of the time-series of water levels.

H_{K1}, H_{O1}, H_{M2} and H_{S2} represent the amplitudes of **K**1, **O**1, **M**2 and **S**2, respectively) of 0.20 has been determined for the area; this is indicative of predominantly semi-diurnal tides (Pugh 1987).

For such shallow water areas, however, the Form Factor is only a general description of the prevailing tidal characteristics. In this particular case, the overtides **M**4 and **MS**4 (with amplitudes of 8.07 cm and 6.61 cm, respectively) are more important than the diurnal constituents. In order to account for the double high waters present over the region, the phase difference $2g_{M2} - g_{M4}$ (where g_{M2} and g_{M4} are the phases of **M**2 and **M**4, respectively) can be used. Using the data in Table 5-3, the phase difference is 181.2 . On the basis of this analysis, the condition for the generation of the double high waters is, therefore, satisfied (Pugh 1987).

Overall, because the amplitudes of the major tidal constituents are relatively small, the tidal ranges fall into the microtidal category as defined by Davies (1964). During the period of the observations, the largest tidal range was around 1.4 m.

Table 5-3. Harmonic tidal constituents analysed using TIRA.

Tidal Species	Name	Amplitude (cm)	Phase (°)	Name	Amplitude (cm)	Phase (°)
Long-period	**SA**	10.94	206.9	**SSA**	7.39	18.2
	MM	1.00	324.6	**MSF**	4.75	58.4
	MF	0.42	171.1			
Diurnal	**2Q1**	0.46	285.7	$\sigma 1$	0.22	30.8
	Q1	0.49	5.4	$\rho 1$	0.65	273.8
	O1	1.97	353.4	**MP1**	1.78	179.1
	M1	0.44	257.1	$\chi 1$	0.08	352.2
	$\pi 1$	0.08	25.7	**P1**	2.66	129.1
	S1	0.83	64.7	**K1**	6.65	119.8
	$\psi 1$	0.16	71.0	$\phi 1$	0.38	302.0
	$\theta 1$	0.39	182.9	**J1**	0.31	203.8
	SO1	1.19	304.2	**OO1**	0.42	275.9
Semi-diurnal	**OQ2**	0.73	296.1	**MNS2**	1.12	107.8
	2N2	1.50	324.0	$\mu 2$	3.82	166.2
	N2	7.12	271.9	$\nu 2$	1.63	305.3
	OP2	0.68	38.5	**M2**	33.53	300.4
	MKS2	0.81	190.0	$\lambda 2$	0.79	25.7
	L2	1.37	13.1	**T2**	0.61	3.0
	S2	10.36	312.3	**R2**	0.70	97.7
	K2	3.16	310.4	**MSN2**	0.65	255.9
	KJ2	0.12	358.6	**2SM2**	0.44	283.5
	MA2	1.33	105.5	**MB2**	1.60	145.2
Third-diurnal	**MO3**	1.29	278.2	**M3**	0.42	220.9
	SO3	0.81	351.6	**MK3**	1.68	60.2
	SK3	0.25	124.2			
Fourth-diurnal	**MN4**	1.65	49.8	**M4**	8.07	58.6
	SN4	1.06	175.3	**MS4**	6.61	133.3
	MK4	1.67	120.8	**S4**	1.34	244.2
	SK4	0.94	260.3			
Sixth-diurnal	**2MN6**	0.98	12.2	**M6**	1.90	45.1
	MSN6	0.73	73.4	**2MS6**	2.22	93.3
	2MK6	0.67	103.1	**2SM6**	0.65	159.0
	MSK6	0.36	168.0			

5.2.2. Currents in the Entrance Channel

The relationship between A and η at Transect G2 has been obtained from bathymetric data from the Run (Figure 5-24). Based upon the least squares regression analysis, the A-η relationship (i.e. function F_1 in Equation [4-35]) can be written as:

$$A = 128.49 + 47.57\eta + 3.42\,\eta^2 \qquad [5\text{-}1]$$

where η is expressed in m OD and A in m^2.

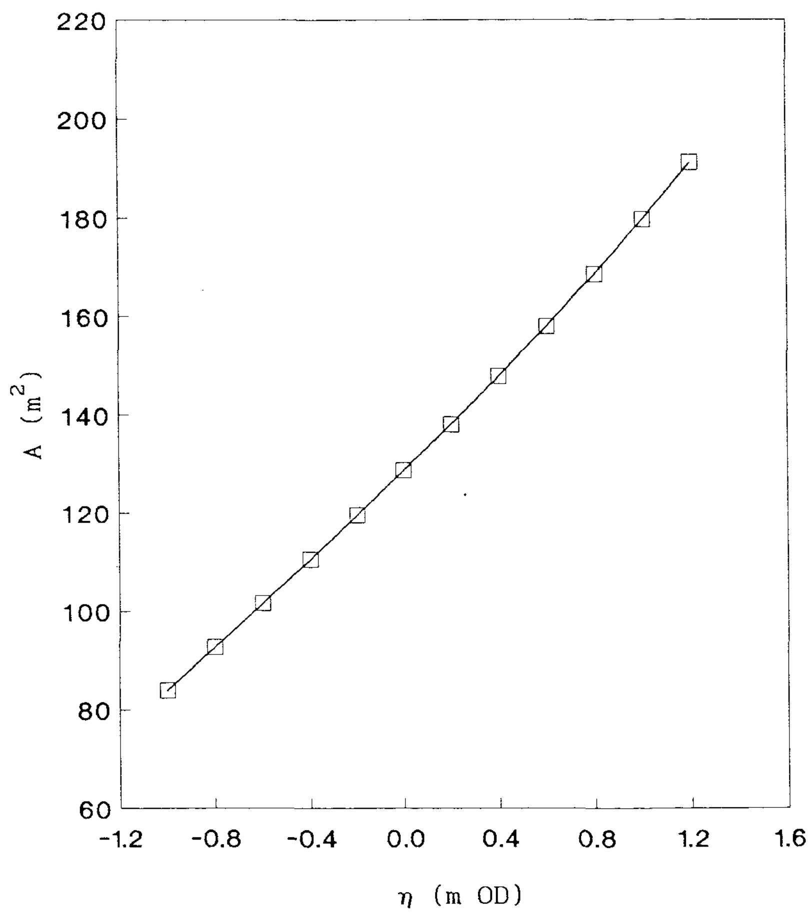

Figure 5-24. Relationship between cross-sectional area and water level in the entrance channel of Christchurch Harbour (for Transect G2).

The function F_2 in Equation [4-36] (i.e. the relationship between the apparent tidal basin area (A_{ba}) and the water level in the entrance (η)) has been determined empirically (Tosswell 1978); this relationship (Figure 5-25) is used in the present analysis.

Hence, a time-series of the cross-sectional mean current speeds is derived here on the basis of Equations [4-33], [4-35], [4-36] and [4-37]; these data are listed as Table C-2, in Appendix C (with the currents directed to seaward having a negative sign). Through the use of Equation [4-37], the current speeds have a 15 min lag behind the water level data. Thus, the water level records commence at 0.00 GMT on each day, whilst the records of the current speed start at 0.15 GMT. A comparison between the data and the measured <u>surface</u> current speeds, in the central part of the Run over two tidal cycles (Figure 5-26), shows that the two data sets are in good agreement. In the comparison, it should be taken into account that the cross-sectional mean value is approximately 0.7 times the vertical mean value measured in the central channel (Section 5.3.1.); likewise, the latter is around 0.85 times of the surface current speed, according to Equation [4-38], for a water depth of between 3 and 4 m and with the roughness length (z_0) taken as 6 mm.

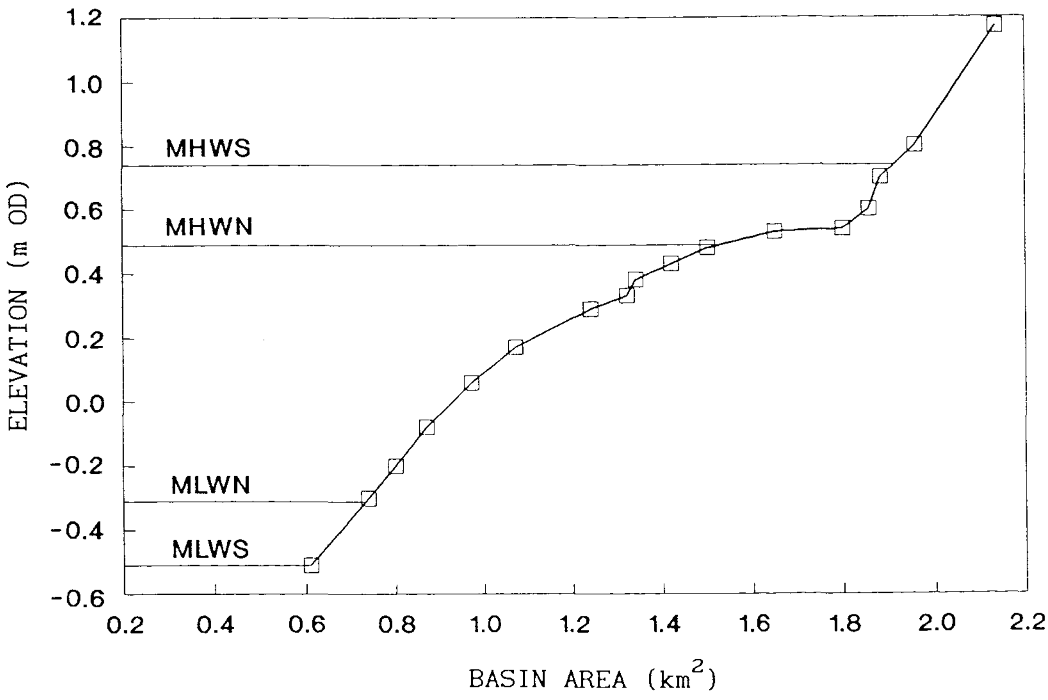

Figure 5-25. Hypsometric curve and characteristic water levels of Christchurch Harbour (after Tosswell, 1978).

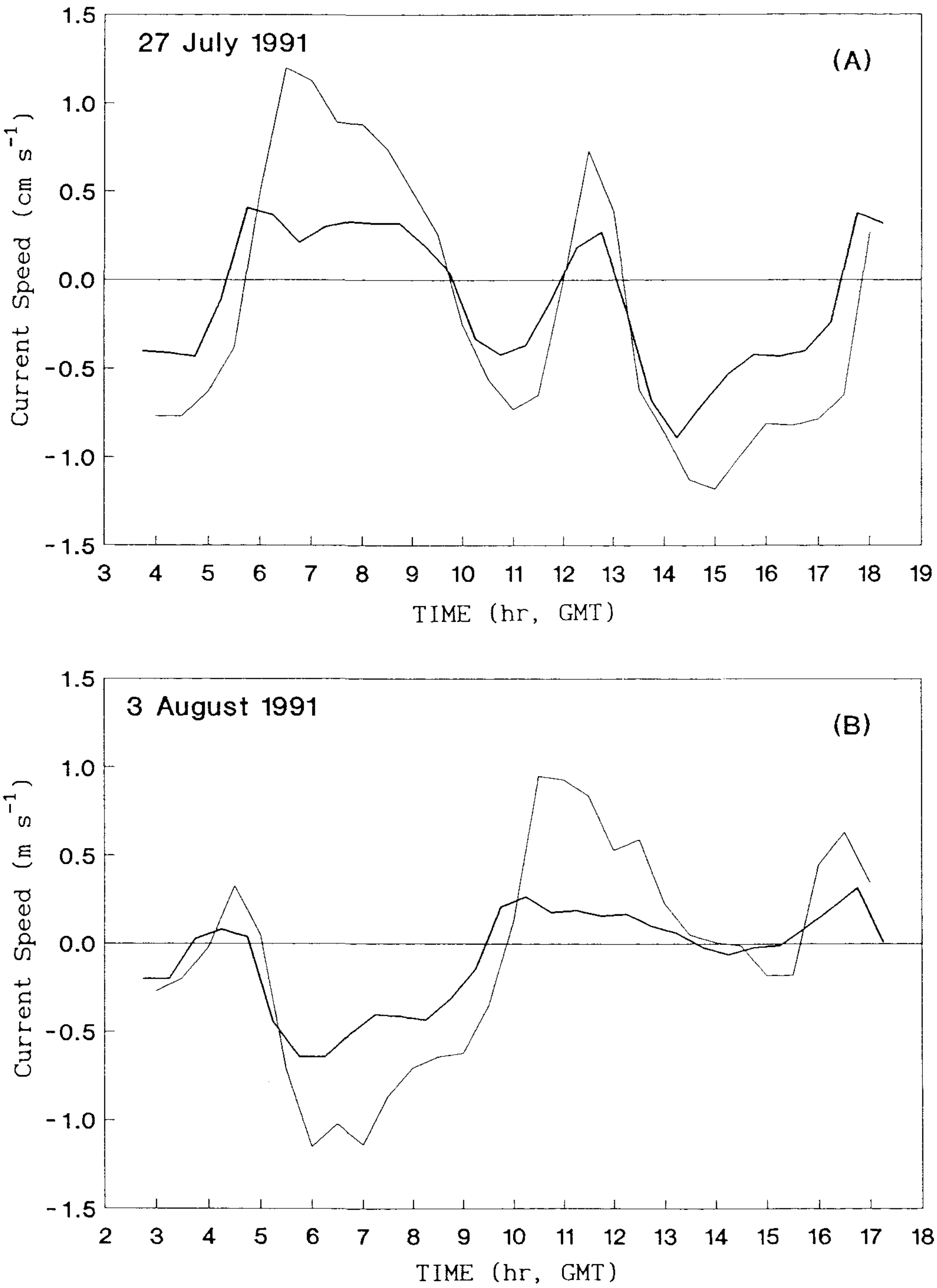

Figure 5-26. Comparison between calculated cross-sectional mean currents speeds (thick line) and measured surface current speeds (thin line) on: (A) 27 July 1991; and (B) 3 August 1991.

Compared with water levels, the calculated current speeds are influenced more strongly by local bathymetric features, as shown by the results of the harmonic analysis using TIRA (Table 5-4). The shallow water constituents, especially the M_4, MS_4, $2MS_6$ and M_6, are not small in comparison with the major semidiurnal components (M_2 and S_2). As a result, the entrance channel is characterised by significant quarter diurnal tidal currents on springs. Current speeds over 1 m s^{-1} can occur frequently between the double high waters.

This fourth-diurnal dominance can be related to the hypsometric features of the Harbour. During the period between the double high waters, although the rate of the water level change is small, the basin area is large. Hence, even a small change in the water level can result in strong currents, in accordance with Equation [4-33]. This observation implies that the shallow water constituents of the tidal currents are more sensitive to localised morphological features, whilst those of water level are controlled mainly by regional morphological features.

5.2.3. Estuarine Processes

Oceanographic data, collected at Stations 1 to 5 are used here to describe the estuarine processes. Because the observations at these stations were carried out between early summer and autumn, when the freshwater discharge is low, the results may be not representative of all seasons. For example, high freshwater discharges can prevent sea water from penetrating into the inner part of the harbour (Murray 1966). Nevertheless, the observed phenomena are considered to represent the majority of the year.

The Bay-Head Area

Significant stratification in the water column and gravitationally- induced circulation are present in the bay-head area; these are represented by the tidal cycle observations carried out at Station 5.

Table 5-4. Harmonic tidal current constituents analysed using TIRA.

Species of Tidal Currents	Name	Amplitude (cm s^{-1})	Phase (°)	Name	Amplitude (cm s^{-1})	Phase (°)
Long-period	**SA**	12.10	162.4	**SSA**	2.65	160.8
	MM	0.81	89.7	**MSF**	0.83	22.9
	MF	0.82	16.9			
Diurnal	**2Q**$_1$	0.27	187.3	σ_1	0.25	243.3
	Q$_1$	0.35	315.8	ρ_1	0.16	167.4
	O$_1$	0.83	260.3	**MP**$_1$	1.00	95.6
	M$_1$	0.24	186.0	χ_1	0.21	354.4
	π_1	0.10	157.7	**P**$_1$	1.84	43.1
	S$_1$	0.52	298.3	**K**$_1$	4.09	38.2
	ψ_1	0.10	334.6	ϕ_1	0.22	266.8
	Θ_1	0.25	110.2	**J**$_1$	0.20	147.3
	SO$_1$	0.63	208.1	**OO**$_1$	0.35	188.4
Semi-diurnal	**OQ**$_2$	0.82	212.8	**MNS**$_2$	1.24	38.9
	2N$_2$	1.57	245.5	μ_2	5.03	85.6
	N$_2$	8.17	183.3	ν_2	1.87	218.9
	OP$_2$	1.65	329.8	**M**$_2$	38.24	213.4
	MKS$_2$	0.67	155.8	λ_2	0.94	326.7
	L$_2$	1.43	298.5	**T**$_2$	1.32	280.3
	S$_2$	12.85	224.5	**R**$_2$	0.79	343.6
	K$_2$	4.01	225.4	**MSN**$_2$	0.77	161.2
	KJ$_2$	0.21	166.8	**2SM**$_2$	0.88	223.7
	MA$_2$	2.96	358.9	**MB**$_2$	2.64	53.0
Third-diurnal	**MO**$_3$	2.69	190.8	**M**$_3$	0.57	125.0
	SO$_3$	1.47	269.8	**MK**$_3$	3.90	334.7
	SK$_3$	0.64	30.2			
Fourth-diurnal	**MN**$_4$	3.06	337.4	**M**$_4$	16.07	333.8
	SN$_4$	3.05	89.5	**MS**$_4$	15.74	52.8
	MK$_4$	4.00	45.8	**S**$_4$	4.30	155.3
	SK$_4$	2.76	166.8			
Sixth-diurnal	**2MN**$_6$	4.19	283.8	**M**$_6$	8.35	310.1
	MSN$_6$	3.55	344.7	**2MS**$_6$	10.39	359.9
	2MK$_6$	3.67	7.5	**2SM**$_6$	3.45	62.4
	MSK$_6$	1.86	76.5			

The spring tidal data show that the maximum current speeds reach up to 0.5 m s^{-1} (Figures 5-27 and 5-28). During the ebb, the currents throughout the water column are directed to seaward and the associated salinity is low. Stratification and gravitational circulation occur during the flood tidal phase; saline water with a salinity up to 33.9 ppt is transported in an up-estuary direction, whilst the surface layer (0.3 m in thickness and with a salinity of around 5 ppt) continues to move to seaward.

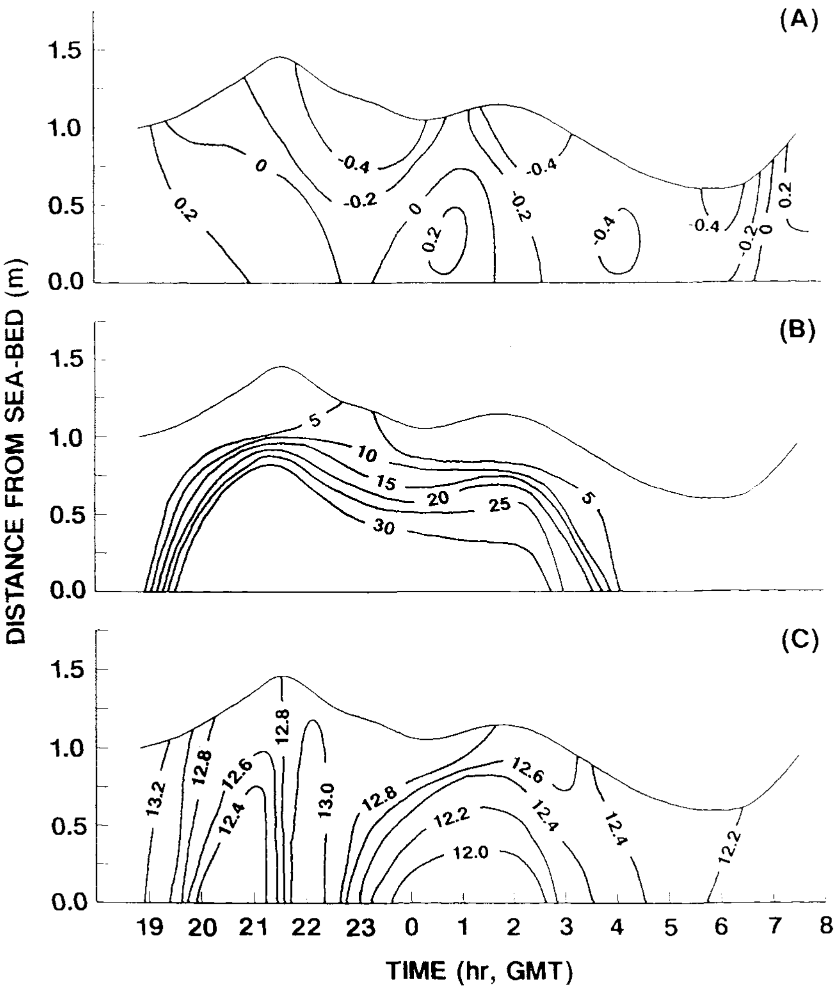

Figure 5-27. Oceanographic observations at Station 5, on 3-4 May 1992 (spring tide): (A) current speed (m s^{-1}, negative values are in down-estuary directions); (B) salinity (ppt); and (C) temperature (°C).

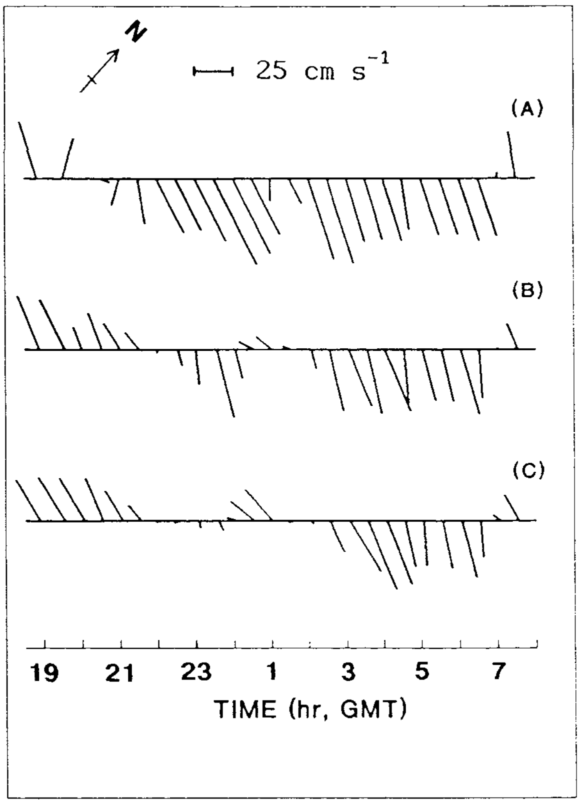

Figure 5-28. Stick diagram showing current vectors within (A) the surface, (B) middle and (C) bottom layers, Station 5, spring tide.

During neap tides, the phenomena are even more distinctive (Figures 5-29 and 5-30). The surface water moves to seaward at speeds close to values on spring tides, throughout almost the complete tidal cycle. In contrast, the bottom layer is characterised by landward currents with speeds of over 0.2 m s^{-1}. Even during the ebb phase, the bottom layer continues to move to landward or becomes essentially motionless. The salinity is maintained around 5 ppt in the surface, reaching up to 33.4 ppt in the bottom waters.

SSCs increase generally downwards in the water column, but vary only slightly throughout the tidal cycle (Figure 5-31). Resuspension due to tidal currents does not appear to be significant.

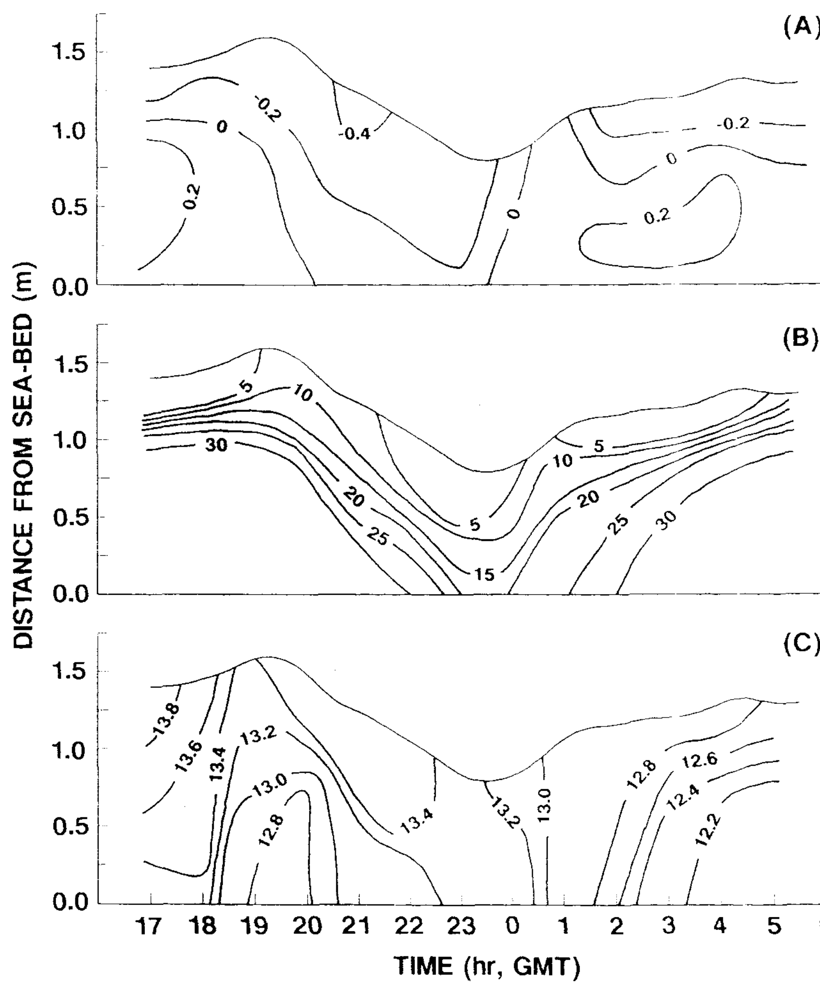

Figure 5-29. Oceanographic observations at Station 5, on 10-11 May 1992 (neap tide): (A) current speed (m s^{-1}, negative values are in down-estuary directions); (B) salinity (ppt); and (C) temperature (°C).

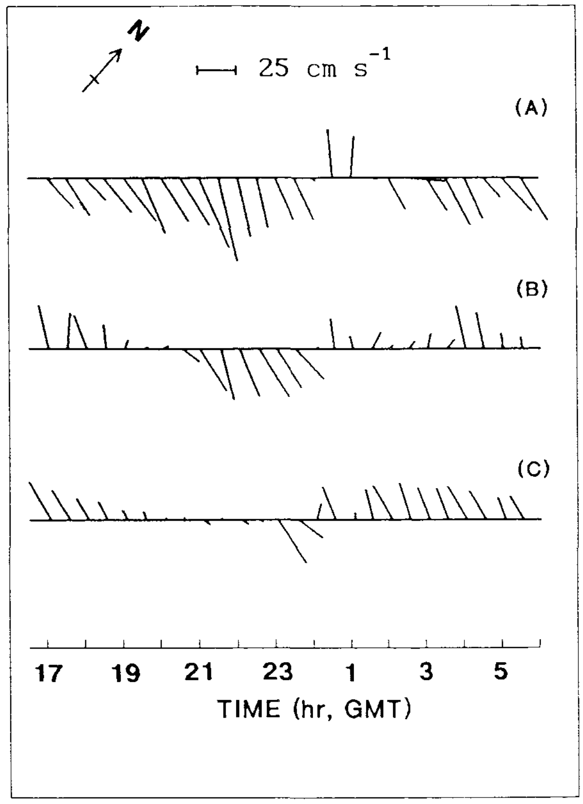

Figure 5-30. Stick diagram showing current vectors within (A) the surface, (B) middle and (C) bottom layers, Station 5, neap tide.

The Run

In the autumn of 1989, stratification and mixing of the estuarine waters at Station 3 varied from spring to neap tides. During the spring tide, a well-mixed pattern was present (Figure 5-32) associated with a maximum surface current speed in excess of 1.25 m s^{-1}. Salinities and temperatures were almost constant throughout the water column. Low (i.e. below 10 mg l^{-1}) and high (over 25 mg l^{-1}) SSCs occurred during high and low water periods, respectively.

During the neap, the estuarine waters were partially mixed (Figure 5-33). This pattern was associated with a maximum current speed of around 0.50 m s^{-1}. SSCs ranged between 4 and 18 mg l^{-1}, with low and high values associated with high and low salinity waters, respectively.

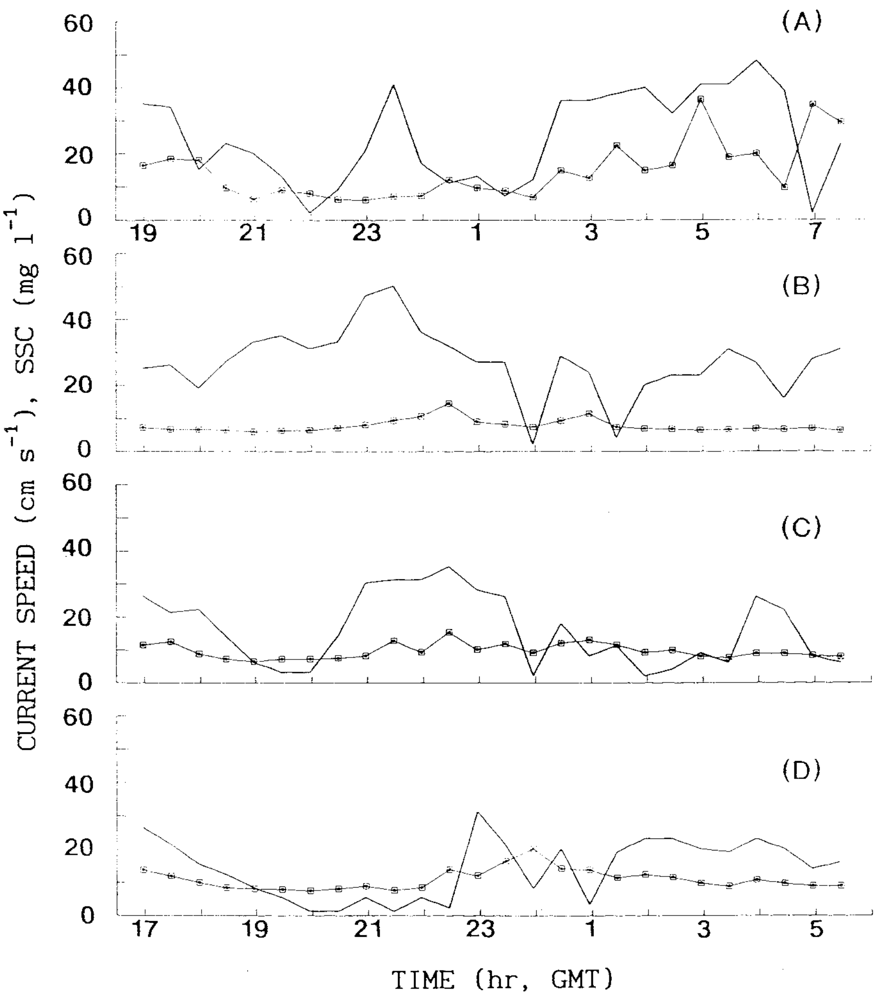

Figure 5-31. Tidal cycle variations in SSCs (thin line with dots) and current speeds (thick line), Station 5 on 3-4 and 10-11 May, 1992: (A) Middle layer, spring tide; (B) surface layer (neap tide); (C) middle layer (neap tide); and (D) bottom layer (neap tide).

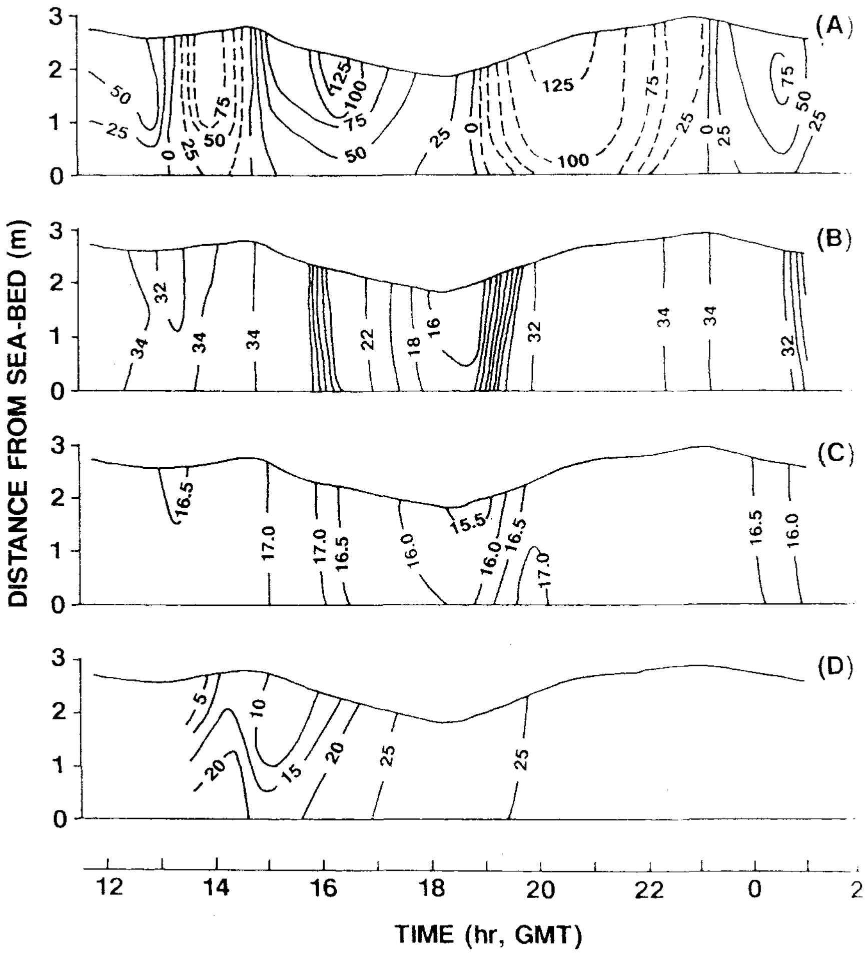

Figure 5-32. Oceanographic observations at Station 3, on 1-2 October 1989 (spring tide): (A) current speed (cm s^{-1}, values with dashed contours are in up-estuary directions); (B) salinity (ppt); (C) temperature (°C); and (D) SSC (mg l^{-1}).

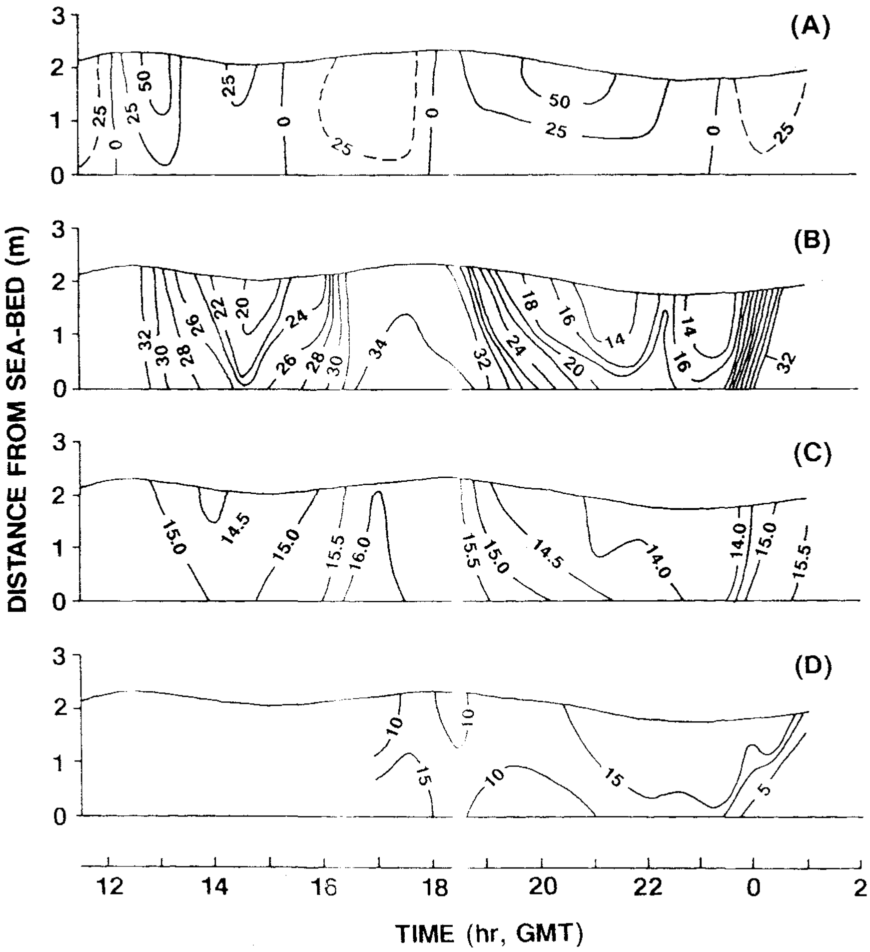

Figure 5-33. Oceanographic observations at Station 3, on 8-9 October 1989 (neap tide): (A) current speed (cm s^{-1}, values with dashed contours are in up-estuary directions); (B) salinity (ppt); (C) temperature (°C); and (D) SSC (mg l^{-1}).

At Station 4, only data within the surface layer have been obtained. The current speed, salinity, temperature and SSC time-series, over spring and neap tides, are similar (Figures 5-34 and 5-35). The salinity data are correlated highly to rising and falling water levels, indicating that the water is either well- or partially-mixed. Once again, SSCs are higher at low water than at high water; they are also higher during springs than on neaps.

In general, once the estuarine waters extend into the Run, they become well- or partially-mixed due to strong currents. Variations in SSCs, with time, is associated, therefore, with the longitudinal movement of the turbidity maximum; this reaches the entrance channel during low water. Resuspension by tidal currents is not considered to be significant over a single tidal cycle, but its importance is enhanced over the time scale of a spring-neap tidal cycle.

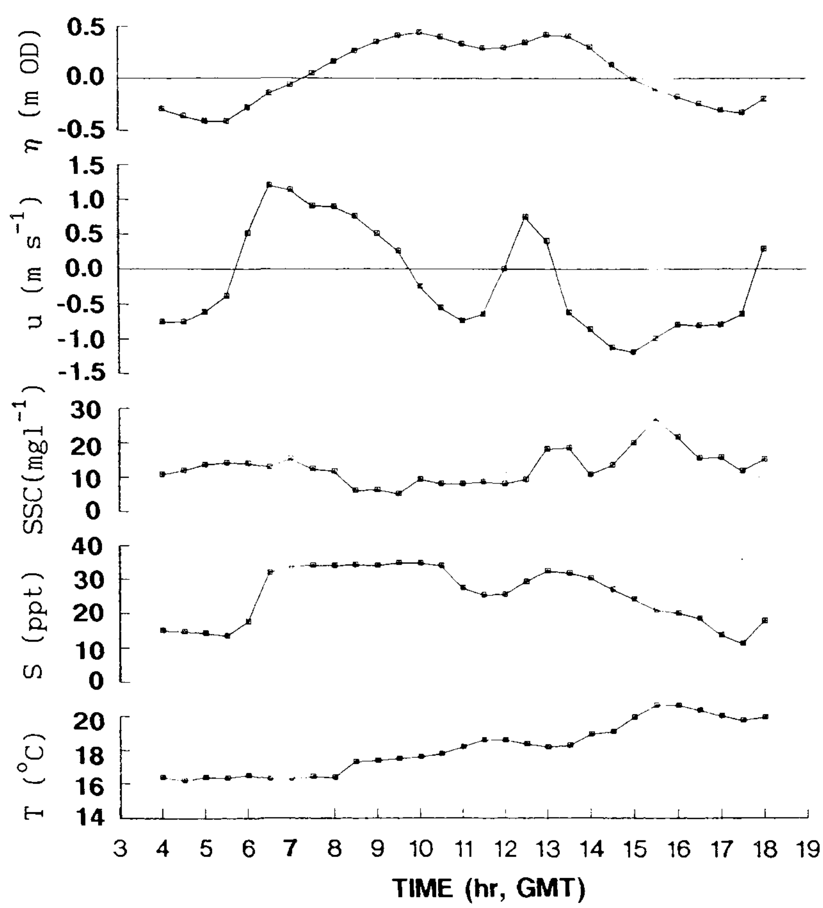

Figure 5-34. Observations of water level, surface current speeds, SSC, salinity, and temperature at Station 4, on 27 July 1991.

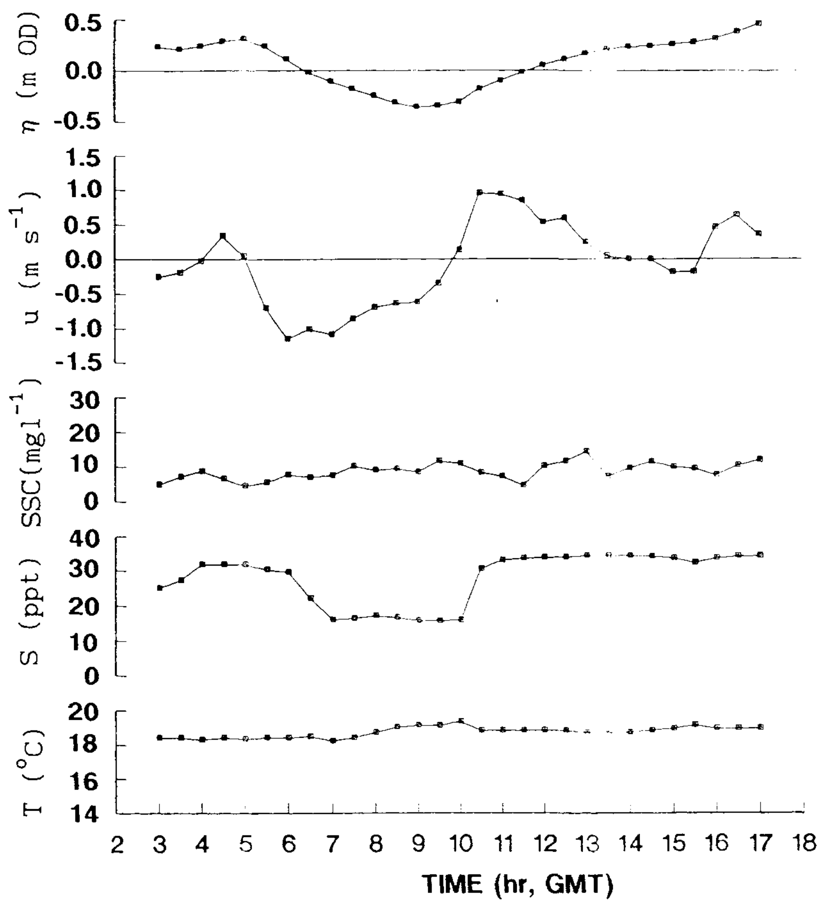

Figure 5-35. Observations of water level, surface current speeds, SSC, salinity, and temperature at Station 4, on 3 August 1991.

Western Christchurch Bay

Station 1 is located approximately 2 km to the south of the entrance. During a spring tide, current speeds up to 0.86 m s^{-1} have been observed (Figure 5-36). The water here is influenced only very little by the estuarine waters from Christchurch Harbour, as shown by the salinity and temperature data (Figure 5-36). Only during the final stage of the ebb tides do waters with a slightly low salinity (of around 33.5 ppt) reach the station. The currents are rectilinear in character, with the westerly-flowing currents being stronger (Figure 5-37).

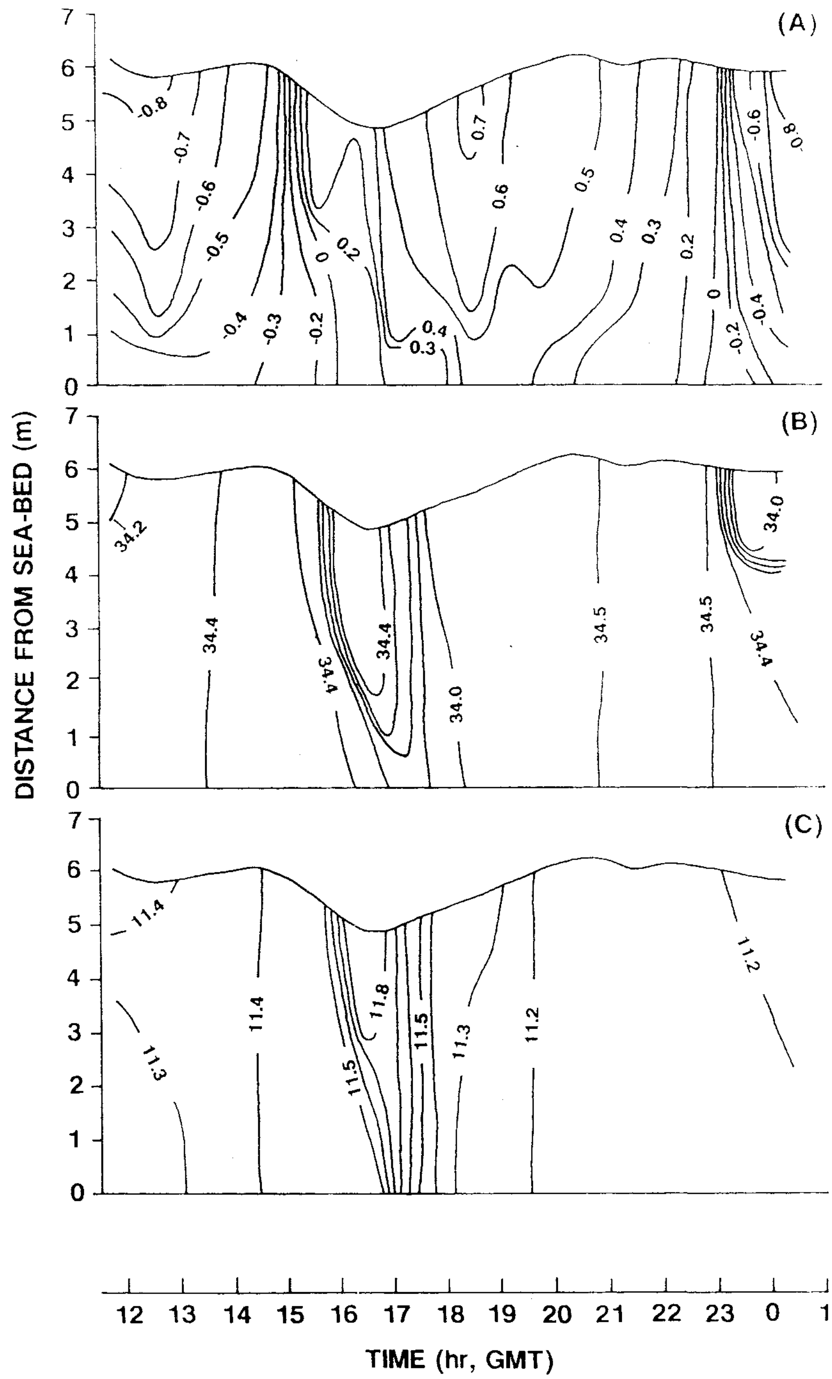

Figure 5-36. Oceanographic observations at Station 1, on 15-16 May, 1991 (spring tide): (A) current speed (m s^{-1}, negative values are in the ebb directions); (B) salinity (ppt); and (C) temperature (°C).

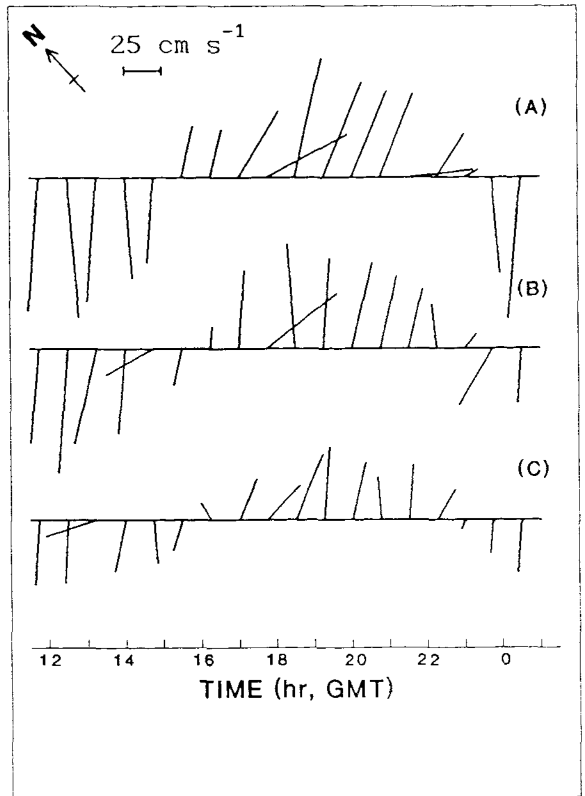

Figure 5-37. Stick diagram showing current vectors within (A) the surface, (B) middle and (C) bottom layers, Station 1, spring tide.

The influence of the estuarine waters is similar during a neap tide, except that the temperature stratification is slightly more significant than that during a spring tide (Figure 5-38). The different patterns between salinity and temperature distributions may be due to different mechanisms for the transport of salt and heat associated with the plume (for example, salt is conservative in character but heat is not). On the other hand, The currents are rectilinear and weak, with maximum current speeds of less than 0.2 m s^{-1} (Figure 5-39). Generally, the ebb currents are slightly stronger than those on the flood.

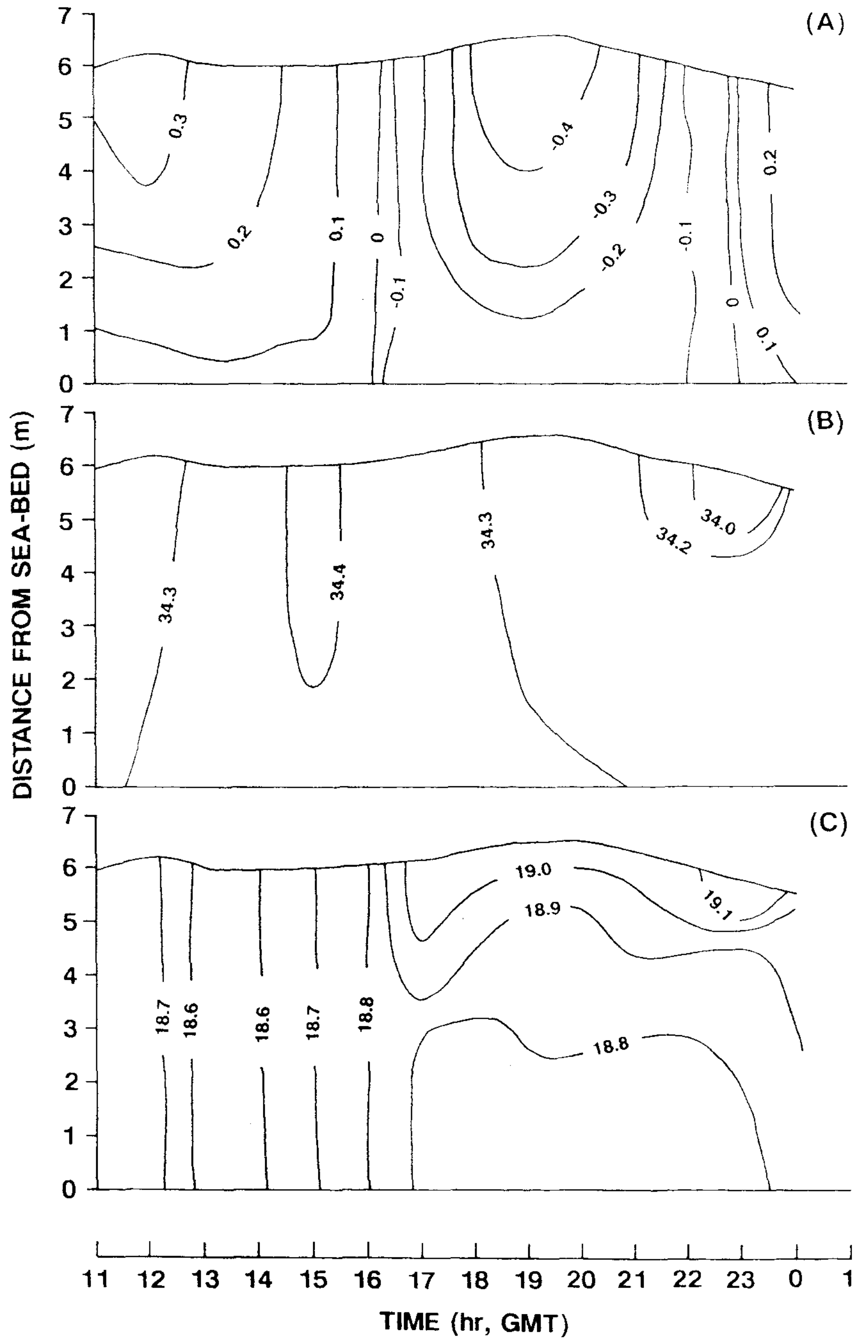

Figure 5-38. Oceanographic observations at Station 1, on 31 July - 1 August, 1990 (neap tide): (A) current speed (m s^{-1}, negative values are in the ebb directions); (B) salinity (ppt); and (C) temperature (°C).

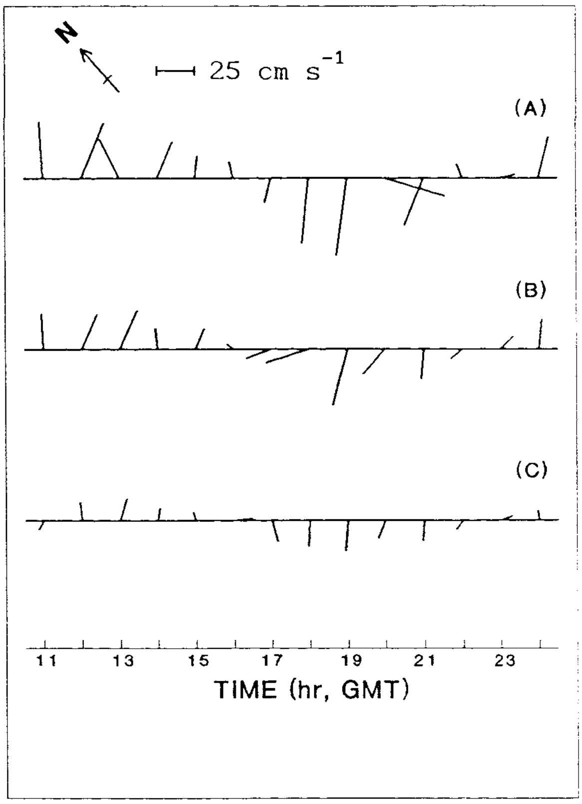

Figure 5-39. Stick diagram showing current vectors within (A) the surface, (B) middle and (C) bottom layers, Station 1, neap tide.

Station 2 is located approximately 2 km to the east of the entrance. At this station, the surface water layer (1 to 2 m in thickness) is occupied almost continuously by waters with relatively low salinity and high temperature, during both spring and neap tides (Figures 5-40 and 5-41). The surface waters are characterised by salinities of between 32.0 and 34.0 ppt, whilst the bottom waters have salinities of over 34.2 ppt. Spring tide current speeds are weaker than at Station 1, with a maximum of around 0.30 m s^{-1} (Figure 5-42). During neaps, the currents are of the same order of magnitude as at Station 1, with a maximum of 0.19 m s^{-1} (Figure 5-43).

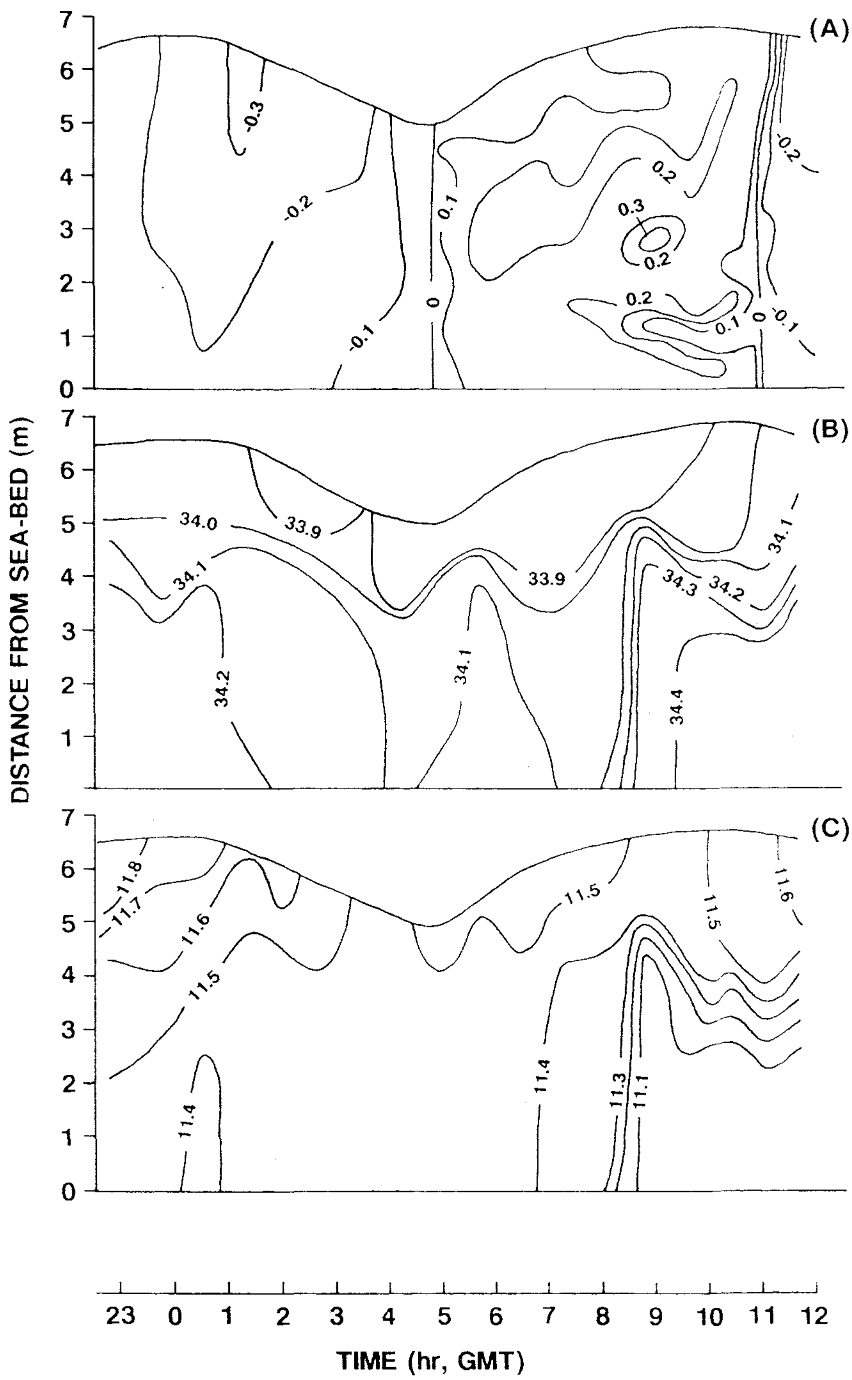

Figure 5-40. Oceanographic observations at Station 2, on 14-15 May, 1991 (spring tide): (A) current speed (m s^{-1}, negative values are in the ebb directions); (B) salinity (ppt); and (C) temperature (°C).

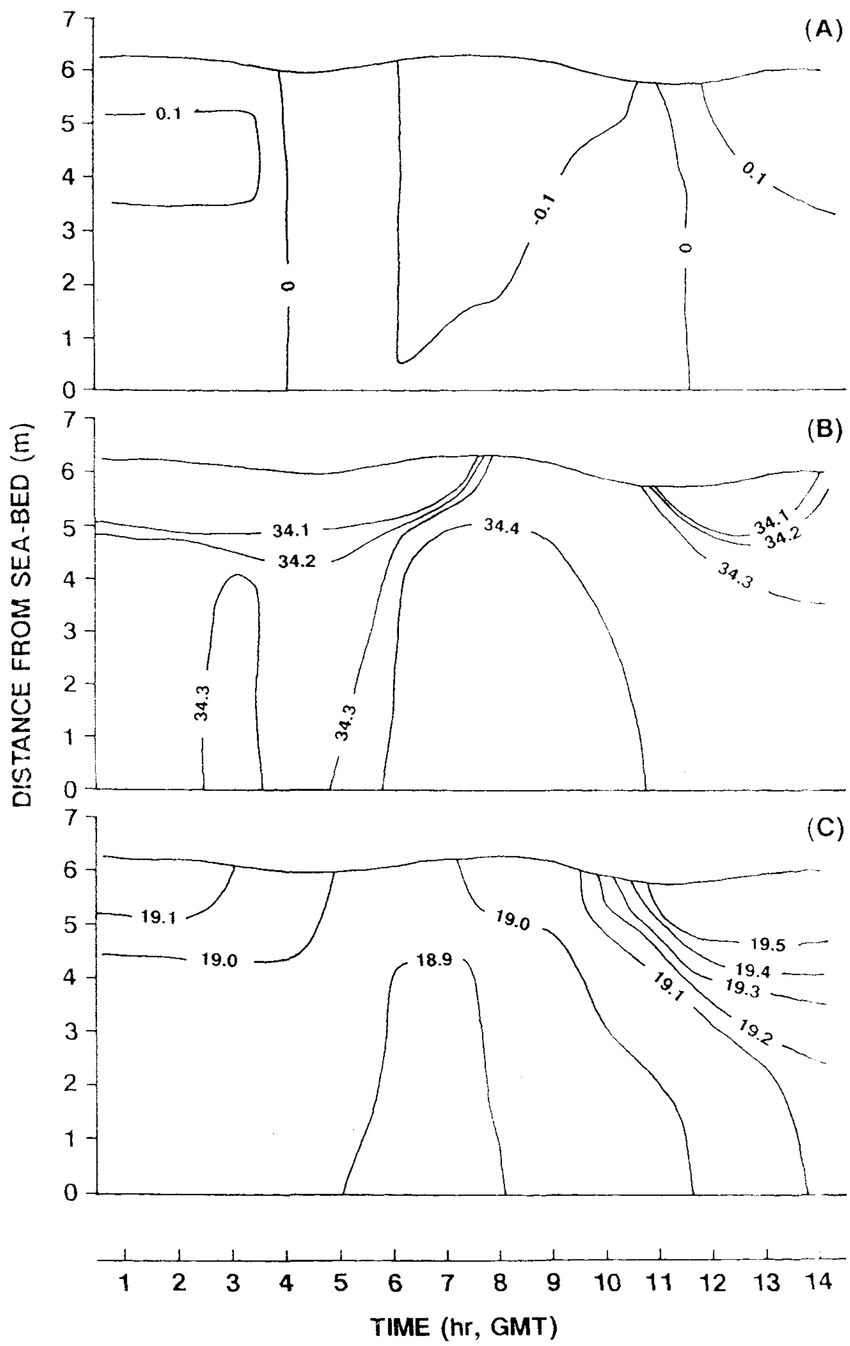

Figure 5-41. Oceanographic observations at Station 2, on 1 August, 1990 (neap tide): (A) current speed (m s^{-1}, negative values are in the ebb directions); (B) salinity (ppt); and (C) temperature (°C).

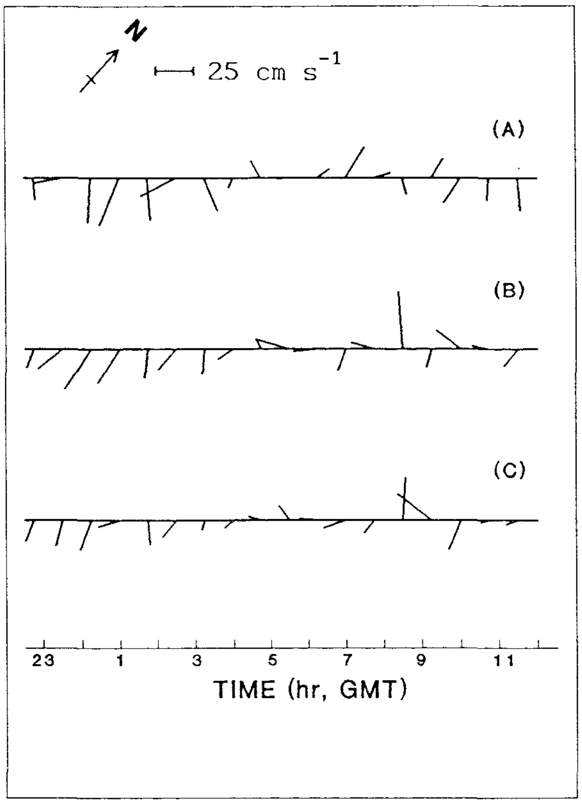

Figure 5-42. Stick diagram showing current vectors within (A) the surface, (B) middle and (C) bottom layers, Station 2, spring tide.

It may be noted that internal waves may be generated, due to the presence of stratification in the water column. The spring tide data shown for Station 2 provide a particular example. For example, on the basis of the salinity structures shown on Figure 5-40, a series of internal waves can be identified. Such waves have periods of between 2 and 4 hr and wave heights of the order of 1 to 2 m. The flow structure is disturbed significantly by the internal waves (i.e. quasi-steady flow patterns are replaced by oscillatory currents) (Figures 5-40 and 5-42) during the flood tide phase, between 4.00 and 11.00 GMT on that day. The destruction of normal flow patterns is demonstrated clearly when the east-west components of the current velocities are plotted (Figure 5-44). In the Figure and before 4.00 GMT, the flow structure is normal. Around 8.00 GMT, however, the easterly-directed and relatively large vectors are associated with much smaller or even reverse vectors: such a pattern occurs regularly throughout the water column.

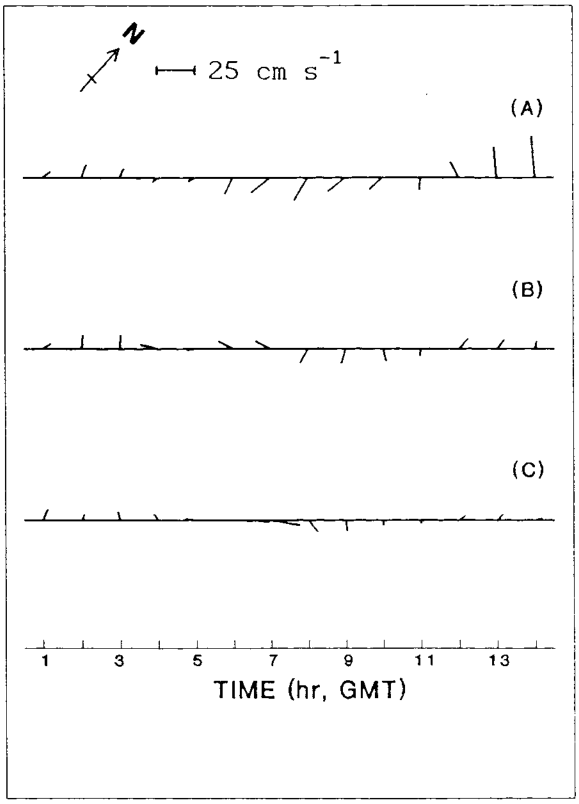

Figure 5-43. Stick diagram showing current vectors within (A) the surface, (B) middle and (C) bottom layers, Station 2, neap tide.

Summary of General Water Circulation Pattern

The general circulation pattern can be represented by residual current speeds: these are listed in Table 5-5 for Stations 1, 2 and 5. Station 5 is characterised by strong residual currents in association with vertical water circulation.

Station 2 is influenced frequently by the estuarine waters issuing from Christchurch Harbour. The residual current speeds vary, therefore, depending upon the intensity of the river plume output and tidal phase (i.e. spring-neap variations).

Station 1 is influenced less frequently by the estuarine waters. The residual currents here are strong over springs and weak over neaps, with a net southwesterly water transport.

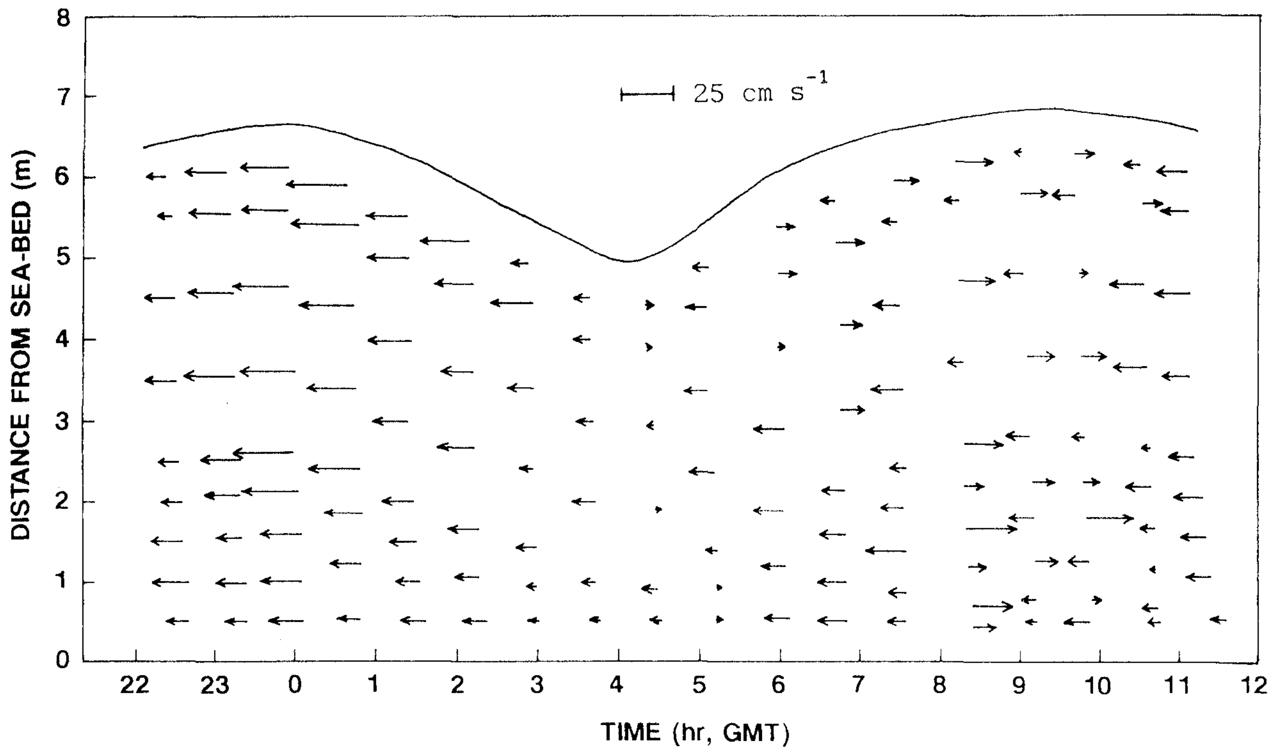

Figure 5-44. East-west components of current velocities observed at Station 2, on 14-15 May, 1991.

In general, the estuarine waters are stratified within the Harbour, becoming vertically mixed at the entrance; they form a plume outside the Harbour, with a lowered degree of stratification. The plume moves, in most cases, towards the east.

The turbidity maxima, characterised by SSCs of 35 mg l during springs and 20 mg l^{-1} during neaps, move with the tidal currents. The maxima reach the open sea at the end of the ebb. Hence, fine-grained sediments can escape to the sea because the tidal excursion is longer than the physical dimension of the harbour and the more turbid estuarine waters exchange with the clearer sea water during each tide cycle.

Table 5-5. Residual current velocities (U_R) and water transport rates (q_w) derived from tidal cycle measurements at 3 stations (the directions are in degrees, in terms of azimuth).

Station	Tide	U_R [cm s^{-1} (°)]			q_w
		Surface	Middle	Bottom	[$m^3m^{-1}s^{-1}$(°)]
1	Spring	8.7 (229)	9.9 (278)	8.8 (286)	0.499 (268)
	Neap	2.7 (133)	1.8 (271)	3.1 (211)	0.085 (204)
2	Spring	15.0 (152)	1.2 (85)	1.7 (60)	0.264 (153)
	Neap	4.2 (296)	2.7 (323)	1.1 (316)	0.154 (308)
5	Spring	24.5 (112)	9.3 (131)	4.5 (155)	0.100 (122)
	Neap	22.6 (96)	4.1 (19)	8.9 (285)	0.063 (76)

5.3. Sediment Budget

5.3.1. Bed-Load

Parameters Used in the Transport Equations

In using Equations [4-49] and [4-50] for estimating bed-load transport rate, a number of parameters must be determined: (i) the mean grain size of the sediments; (ii) the threshold velocity of sediment movement; (iii) current- and wave-induced friction factors (f_c and f_w); and (iv) the settling velocity (w_s).

As described previously, the Run is floored with gravelly material (Figure 5-5):

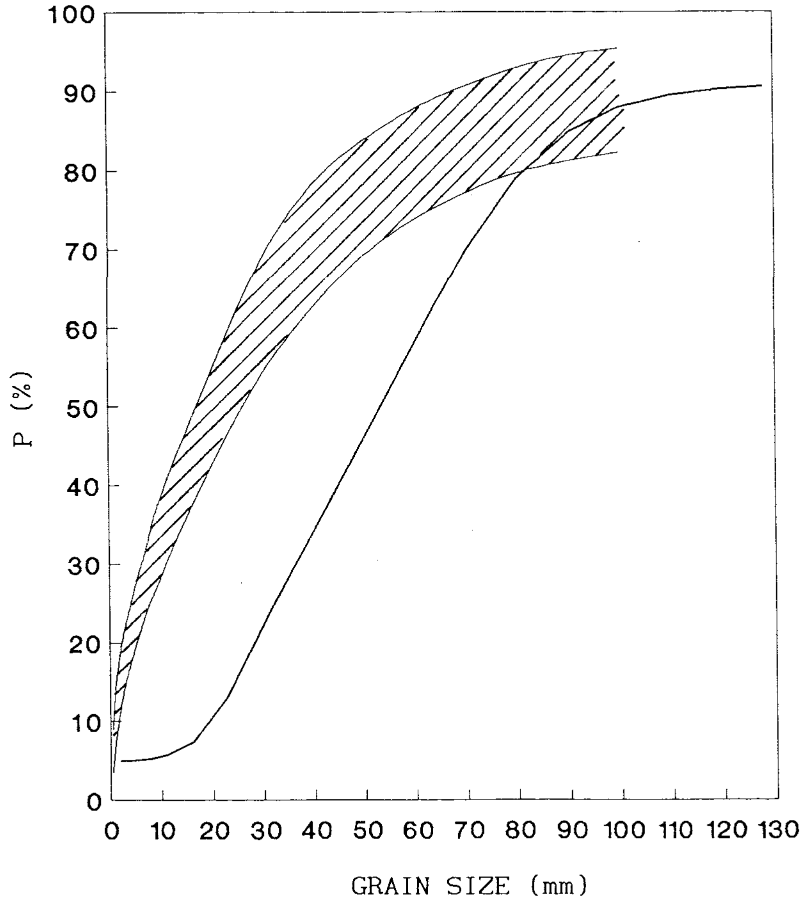

Figure 5-45. A typical grain size distribution curve for seabed sediments within the Run, compared with material (shaded area) investigated by Thompson (1985).

represented by Sample R1, the mean grain size (D) is 4.05 cm (Appendix B). On the southern side of the channel, sands and sandy gravels are present, but they are confined to a very narrow zone close to the high water level (Figure 5-5).

The threshold velocity for such gravels will be of the order of 3 m s^{-1}, on the basis of the equation $U_{cr} = 160.0\ D^{0.45}$ (Miller *et al.* 1977). However, natural sediments consist of various grain sizes and the threshold can be considerably lower. For example, Thompson (1985) has found a threshold (depth mean current speed) of 1.35 m s^{-1} for gravelly material with a mean size of 2 cm. This value would be 2.17 m s^{-1} if the above equation was used. Thorne *et al.* (1989) have found also a lower threshold value for gravels with a mode of around 1.5 cm. The sediments in the Run are coarser than those in Thompson's study area (Figure 5-45). Using the same rate of reduction, the threshold current speed should range between 1.70 and 1.90 m s^{-1}. Consequently, a number of transport rates have been derived, for U_{cr} of 1.70, 1.75, 1.80, 1.85 and 1.90 m s^{-1}, respectively.

The friction factor due to currents (f_c) in the entrance to a tidal basin ranges through four orders of magnitude, with a mean value of 6.5×10^{-3} (Ludwick 1975). Because the material is very coarse here, $f_c = 0.01$ is assumed.

The friction factor due to waves, under the rough turbulence conditions, is a function of the relative roughness (defined as A_0/k_s) (Figure 5-46). In calculating f_w on the basis of A_0/k_s, A_0 is determined using Equation [2-17] and the mean water depth on Transect G2 (2.90 m), and k_s is taken as 2 D (i.e. 81 mm for this particular entrance channel) for gravels according to observed data from Sleath (1990).

The settling velocity for gravels is influenced by turbulence and grain shape. Due to the presence of turbulence, substantial deviations from the Stokes Law can be introduced. The shape factor causes a wide scatter in settling velocity, for sediments coarser than -2 ϕ (4 mm). In the present study, the settling velocity curve for a shape factor of 0.5 (Komar and Reimers 1978) is used, yielding a settling velocity of the order of 0.75 m s^{-1} for the sediments under investigation.

Determination of the Frequency Distribution Functions

The four frequency distribution functions in Equations [4-49] and [4-50] are obtained on the basis of the following procedures.

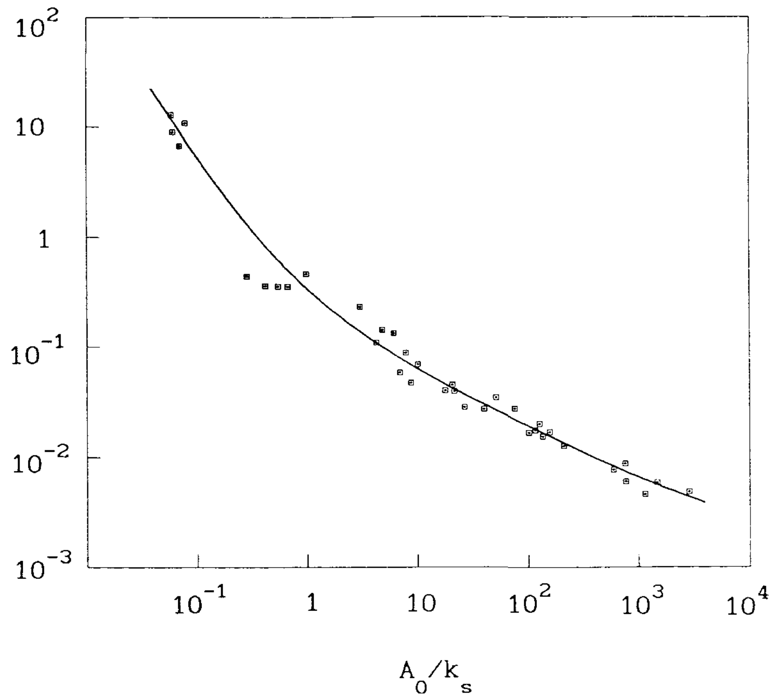

Figure 5-46. Relationship between f_w and A_0/k_s, on the basis of data from Sleath (1990).

The frequency distribution patterns of cross-sectional mean current speeds for flood and ebb tides are determined from statistical analyses of the time series of the current speed data. If any data point occurred within the rising water level phase, then it was taken as a flood current speed (hence, a flood current speed may be in the ebb direction). Otherwise it was considered as an ebb current speed. The flood and ebb current speeds were then grouped, at 0.05 m s^{-1} intervals, and the frequency of occurrence for each group calculated. Further, the same procedure is applied then to determine the frequency of each group for the cases of the water level being above 0.1 m OD and below that elevation, respectively. The elevation of 0.1 m was selected because the upper part of the ebb tidal delta lies at -0.20 m OD in height; this prevents relatively large waves from propagating into the channel when the water level is below 0.1 m OD. Altogether, 6 distribution patterns have been derived (Figure 5-47).

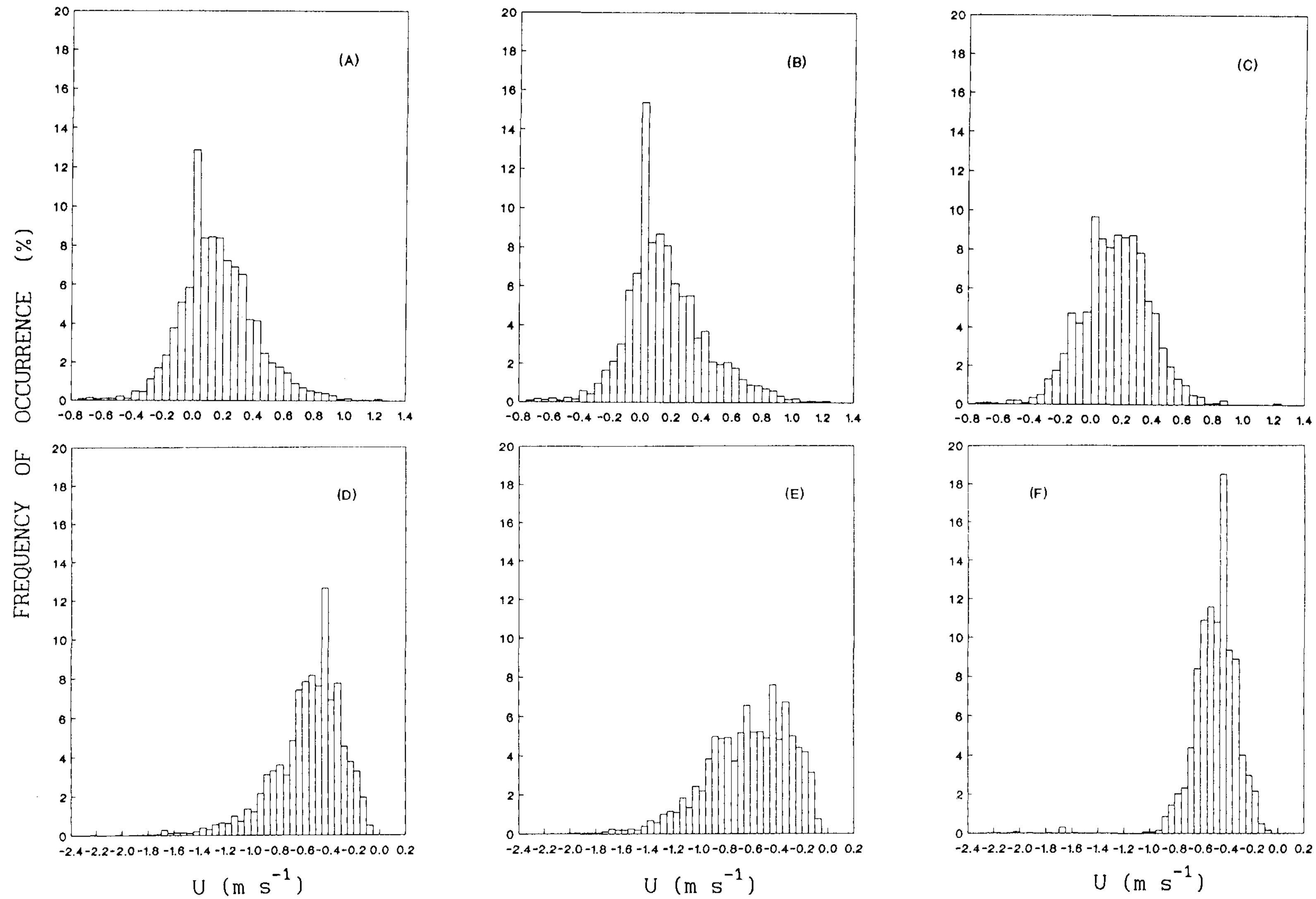

Figure 5-47. Frequency distribution functions of current speeds during: (A) flood tides; (B) flood tides, with water level above 0.1 m OD; (C) flood tides, with water level below 0.1 m OD; (D) ebb tides; (E) ebb tides, with water level above 0.1 m OD; and (F) ebb tides, with water level below 0.1 m OD.

Because the Run is narrow, the deviation of the vertical mean current speeds from the cross-sectional mean value cannot be neglected. Thus, U_{av}/U as a function of the distance from the Mudeford Quay wall has been calculated, based upon an assumed distribution pattern of the u/u_{max} ratio over the cross-section (u and u_{max} being the instantaneous current speed at a point and its maximum value, respectively) (Figure 5-48). From Figure 5-48(A) the frequency distribution function of U_{av}/U along the transect was determined.

The frequency distribution of waves has been derived from the statistics of significant wave height and zero crossing wave period data recorded in the nearshore area of Milford-on-Sea (Hydraulics Research 1989b). The wave climate is represented by 30 groups of waves, each of which is characterised by a particular wave height, wave period, amplitude of water particle oscillation, maximum orbital speed, and associated frequency of occurrence (Table 5-6).

The instantaneous orbital speed U_w can be related to the maximum orbital speed U_b by:

$$U_w = U_b \cos\left(\frac{2 \pi t}{T}\right) \qquad [5\text{-}2]$$

where T is the wave period. Based upon this relationship, the frequency of occurrence of U_w/U_b is obtained (Figure 5-49).

Calculated Mean Sediment Transport Rates

The estimated (temporally and cross-sectionally averaged) sediment transport rates are listed in Table 5-7. These results are now summarised.

Firstly, the bed-load transport rate is enhanced considerably under the combined action of waves and currents. During the flood tide, no transport occurs due to currents alone. The ebb currents are much stronger, but can cause only relatively low transport rates in the absence of waves. This pattern is consistent with field observations undertaken during calm conditions. For example, the bed within the Run was covered with seaweeds during the summer of 1991, indicating that the sediments were immobile. Hence, the transport of sediment (as bed-load) within the Run is associated mainly with waves, especially during storms.

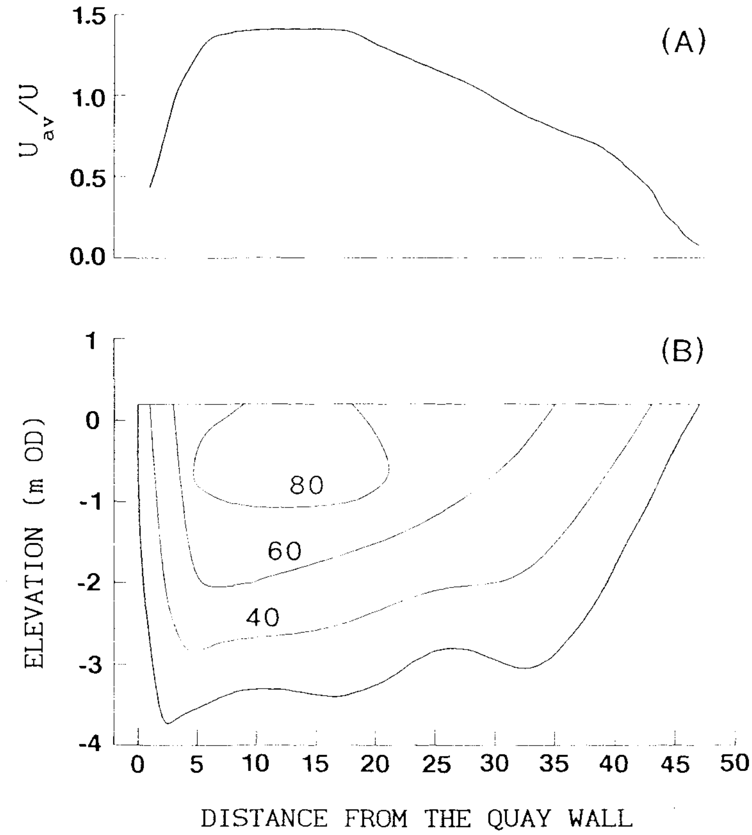

Figure 5-48. Distribution of U_{av}/U across the Run (A), which is derived from an assumed distribution pattern of u/u_{max} over the cross-section (based upon information presented in Chadwick and Morfett (1986) (B).

Secondly, a remarkable flood-ebb asymmetry, in terms of sediment transport, is present. Transport during the ebb is one to two orders of magnitude higher than during the flood.

Finally, transport rates estimated using the Vincent equation are one to two times larger than those derived on the basis of the Madsen-Grant equation (except for transport under currents alone, in which case the difference is even larger). Similar differences have been identified elsewhere, in a continental shelf environment (Vincent *et al.* 1983). In general, the results based upon both equations are in agreement in terms of their order of magnitude; they show a steady increase, with a decrease in the threshold current speed.

Table 5-6. Representative wave periods (T), wave heights (H) and associated frequency of occurrence in the nearshore areas of Christchurch Bay (based upon data from Hydraulics Research (1989b)). Also listed are A_0 and U_b, calculated on the basis of Equations [2-17] and [2-18].

T (s)	H (m)	Frequency (%)	A_0 (m)	U_b (m s^{-1})
1.5	0.25	14.34	0.055	0.23
	0.75	0.91	0.165	0.69
2.5	0.25	26.65	0.092	0.23
	0.75	13.93	0.275	0.69
	1.25	0.99	0.458	1.15
3.5	0.25	7.65	0.128	0.23
	0.75	12.29	0.383	0.69
	1.25	7.05	0.641	1.15
	1.75	1.14	0.897	1.61
4.5	0.25	2.14	0.165	0.23
	0.75	3.33	0.494	0.69
	1.25	3.33	0.824	1.15
	1.75	1.83	1.153	1.61
	2.25	0.13	1.482	2.07
5.5	0.25	0.86	0.201	0.23
	0.75	1.08	0.604	0.69
	1.25	0.44	1.007	1.15
	1.75	0.49	1.409	1.61
	2.25	0.18	1.812	2.07
6.5	0.25	0.35	0.238	0.23
	0.75	0.27	0.714	0.69
	1.25	0.08	1.190	1.15
	1.75	0.03	1.665	1.61
7.5	0.25	0.15	0.275	0.23
	0.75	0.13	0.824	0.69
	1.75	0.04	1.922	1.61
8.5	0.25	0.08	0.311	0.23
	0.75	0.04	0.933	0.69
	1.25	0.02	1.556	1.15
9.5	0.25	0.05	0.348	0.23

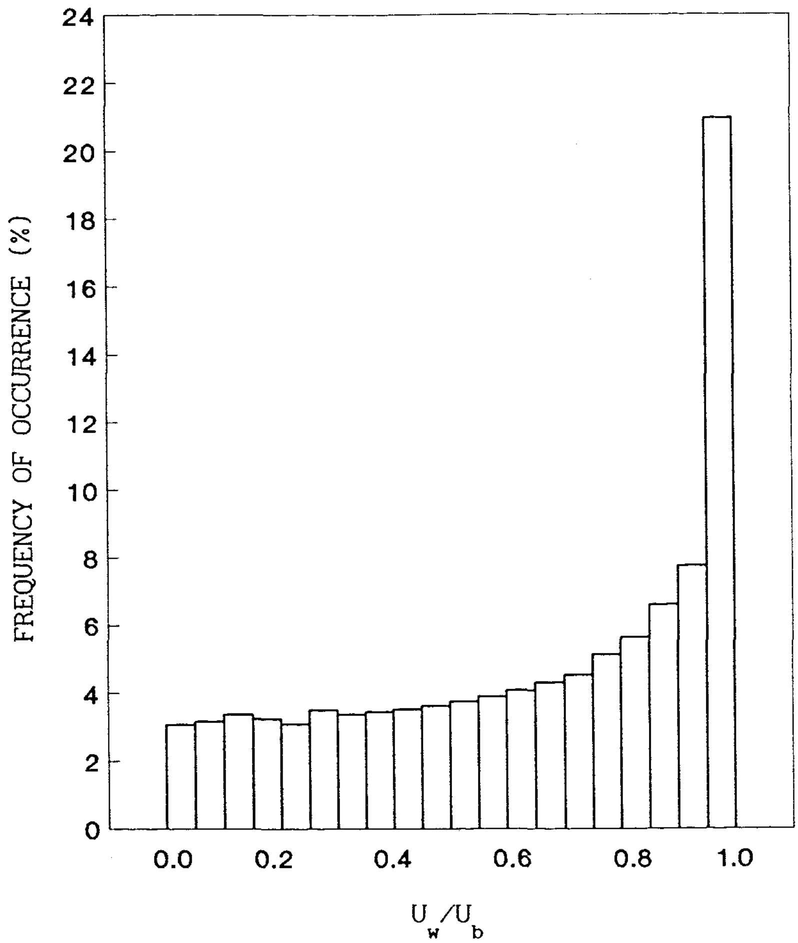

Figure 5-49. Frequency distribution of U_w/U_b, on the basis of Equation [5-2].

Estimates of Annual Bed-load Discharges

If a critical current speed of 1.80 m s^{-1} is used, then the annual transport through the Run caused by tidal currents and current-wave interaction is, based upon the Madsen-Grant equation, of the order of 11150 m^3yr^{-1} towards the sea (i.e. 650 m^3yr^{-1} during the flood phase of the tides and 11800 m^3yr^{-1} during the ebb).

The value derived by the Vincent equation is approximately 2.6 times that defined by the equation of Madsen and Grant, with a net seaward discharge of 29040 m^3yr^{-1} (860 m^3yr^{-1} on the flood and 29900 m^3yr^{-1} on the ebb).

Both values are lower than the quantity of longshore transport due to waves on the beach. As estimated by Lacey (1985) using wave data, the longshore transport around Hengistbury Head is of the order of 5.8×10^5 m^3yr^{-1}. Nicholls and Wright (1991) have obtained much lower values (5.8×10^3 to 4.9×10^4 m^3yr^{-1}), on the basis of artificial tracer (aluminum pebble) experiments, but the values are still much higher than the estimates of net discharge through the Run. Thus, the coefficient k in Equation [4-60] is small, the inlet is wave-dominated (in the sense of Hubbard *et al.* (1979)) and sediment bypassing is controlled mainly by wave action.

Table 5-7. Mean bed-load transport rates, based upon the formulae of Madsen and Grant (1976) and Vincent *et al.* (1981).

Transport Formula Used	U_{cr} (ms^{-1})	$<q_s>$ ($\times 10^{-8}$ $m^3m^{-1}s^{-1}$) q_f	$q_{f(cw)}$	$q_{f(c)}$	q_e	$q_{e(cw)}$	$q_{e(c)}$
MG[x]	1.70	97.11	173.16	0.00	2091.3	3697.6	0.75
	1.75	90.01	160.50	0.00	1871.9	3309.6	0.73
	1.80	84.89	151.37	0.00	1644.4	2907.3	0.72
	1.85	84.62	150.89	0.00	1562.0	2761.5	0.69
	1.90	13.84	24.68	0.00	1353.1	2392.2	0.64
VIN[y]	1.70	247.18	440.76	0.00	5788.7	10183.0	69.45
	1.75	178.51	318.31	0.00	4888.9	8595.6	64.67
	1.80	112.16	200.00	0.00	4164.9	7315.2	64.67
	1.85	47.98	85.56	0.00	3522.2	6184.1	57.63
	1.90	17.17	30.62	0.00	2984.0	5239.1	49.10

[x] Madsen and Grant (1976); [y] Vincent et al. (1981)

Key: q_f = transport rate during flood tides; $q_{f(cw)}$ = transport rate during flood tides, under the combined action of currents and waves; $q_{f(c)}$ = transport rate during flood tides, due to currents; q_e = transport rate during ebb tides; $q_{e(cw)}$ = transport rate during ebb tides, under the combined action of currents and waves; and $q_{e(c)}$ = transport rate during ebb tides, due to currents.

5.3.2. Suspended Load

A time series of water discharges through the Run (Q) has been obtained, based upon Equations [4-33], [4-36 and [4-37]. The data set covers 594 tidal cycles. The frequency distribution of Q is determined at 5 m^3s^{-1} intervals, as listed in Table 5-8. Each group of water discharges in the Table is represented by the middle point value of the group. For example, water discharges between 50 and 55 m^3s^{-1} are represented by 52.5 m^3s^{-1}. The positive and negative values denote landward and seaward water discharges, respectively.

The SSCs associated with each water discharge group are averaged to obtain C_Q, as defined in Equation [4-51]. The C_Q values are listed in Table 5-8. For low discharges (i.e. lower than 65 m^3s^{-1} for landward discharges and 125 m^3s^{-1} for seaward discharges), these numbers are large enough for the determination of the mean values. Since the probability of occurrence of higher water discharges is low, the numbers of the corresponding SSCs are small. From the point of view of the statistics, the mean values for the higher discharges might not be representative. The data listed in the Table show, however, that C_Q is relatively stable (at between 0.0137 g l^{-1} and 0.0087 g l^{-1}), although Q is highly variable. As mentioned previously (Section 5.2.3.), changes in the SSC through the tidal cycle are small. The SSCs of a number of water samples collected during winter (see Table 5-9, where the 2nd and 11th January samples are associated with storm conditions) show that even during storms, resuspension of fine-grained sediments cannot cause high concentrations. Hence, the SSC data for the higher discharges are considered to be acceptable.

Annual suspended sediment discharge through the Run has been calculated using the Q, C_Q and P(Q) data. For some of the higher water discharges without SSC data (see Table 5-8), a linear interpolation or extension was applied. Because the SSC data are stable and the frequency of occurrence of high discharges is low, this approximation should not result in large errors. According to Equation [4-51], the net suspended sediment discharge through the Run is estimated to be 7.75×10^6 kg yr^{-1} towards the open sea, with a landward movement of 4.51×10^6 kg yr^{-1} and a seaward discharge of 12.26×10^6 kg yr^{-1}.

Table 5-8. Average SSC (C_Q) related to water discharges (Q) (see text, for explanation).

Q (m^3s^{-1})	P (%)	C_Q ($g\ l^{-1}$)	N	Q (m^3s^{-1})	P (%)	C_Q ($g\ l^{-1}$)	N
2.5	2.89	0.0105	132	-52.5	4.06	0.0100	213
7.5	2.92	0.0103	135	-57.5	3.28	0.0100	148
12.5	3.41	0.0106	137	-62.5	3.54	0.0101	135
17.5	3.10	0.0107	133	-67.5	2.99	0.0099	123
22.5	3.31	0.0110	132	-72.5	2.37	0.0100	96
27.5	2.75	0.0110	121	-77.5	1.90	0.0096	89
32.5	2.84	0.0109	116	-82.5	1.77	0.0098	75
37.5	2.52	0.0109	99	-87.5	1.68	0.0099	63
42.5	2.14	0.0107	97	-92.5	1.42	0.0099	55
47.5	1.84	0.0109	66	-97.5	1.32	0.0100	52
52.5	1.65	0.0104	54	-102.5	1.22	0.0098	50
57.5	1.33	0.0106	46	-107.5	1.28	0.0098	45
62.5	1.05	0.0101	31	-112.5	0.89	0.0095	27
67.5	0.88	0.0096	20	-117.5	0.94	0.0096	36
72.5	0.65	0.0104	23	-122.5	0.76	0.0098	35
77.5	0.47	0.0115	17	-127.5	0.60	0.0094	22
82.5	0.50	0.0098	10	-132.5	0.60	0.0098	26
87.5	0.36	0.0106	10	-137.5	0.50	0.0093	14
92.5	0.36	0.0109	11	-142.5	0.42	0.0099	17
97.5	0.19	0.0102	8	-147.5	0.41	0.0093	8
102.5	0.21	0.0100	5	-152.5	0.41	0.0091	13
107.5	0.24	0.0115	3	-157.5	0.37	0.0100	13
112.5	0.17	0.0118	3	-162.5	0.28	0.0095	12
117.5	0.17	0.0114	3	-167.5	0.21	0.0108	7
122.5	0.19	0.0114	4	-172.5	0.15	0.0090	4
127.5	0.12	0.0111	1	-177.5	0.19	0.0097	10
132.5	0.06	-	0	-182.5	0.21	0.0097	10
137.5	0.09	0.0137	1	-187.5	0.15	0.0111	2
142.5	0.07	0.0087	1	-192.5	0.11	0.0087	4
147.5	0.05	-	0	-197.5	0.11	0.0094	4
152.5	0.05	-	0	-202.5	0.11	0.0093	4
157.5	0.01	-	0	-207.5	0.09	0.0102	1
162.5	0.03	-	0	-212.5	0.07	0.0098	3
167.5	0.03	-	0	-217.5	0.09	0.0105	1
172.5	0.01	0.0122	1	-222.5	0.07	0.0124	2
177.5	0.01	-	0	-227.5	0.05	0.0122	1
				-232.5	0.03	-	0
-2.5	2.89	0.0107	128	-237.5	0.07	0.0096	2
-7.5	2.53	0.0103	127	-242.5	0.03	0.0094	2
-12.5	2.60	0.0103	100	-247.5	0.01	-	0
-17.5	2.86	0.0104	123	-252.5	0.01	-	0
-22.5	2.67	0.0100	118	-257.5	0.04	0.0102	1
-27.5	2.43	0.0099	118	-262.5	0.03	0.0102	2
-32.5	2.42	0.0100	98	-267.5	0.02	-	0
-37.5	2.63	0.0099	101	-277.5	0.03	-	0
-42.5	3.09	0.0099	107	-312.5	0.02	-	0
-47.5	4.27	0.0105	172	-542.5	0.01	-	0

Table 5-9. SSC and salinity of water samples collected from the Run, between January and March, 1991.

Time (GMT)	Date	S (ppt)	SSC (mg l^{-1})
12.30	2 January	13.9	75.7
11.30	11 January	0.0	56.2
13.00	16 January	1.6	8.3
16.55	17 January	9.1	14.3
14.15	19 January	2.6	8.1
12.40	31 January	9.9	6.9
12.00	15 February	15.3	9.2
11.30	16 March	17.8	10.1

Because the SSCs are both low and stable, the suspended matter can be considered as consisting mainly of wash load. If a SSC of 0.01 kg m^{-3} is assumed for the freshwater from the drainage basin (SSCs of such an order of magnitude have been observed at Station 5 (*cf.* Figure 5-31)), then the mean freshwater discharge of 26.9 m^3s^{-1} will lead to a suspended sediment discharge of 8.48×10^6 kg yr^{-1}, for 1991. This figure is close to that derived for net discharge through the Run. Thus, it would appear that almost all the suspended material (consisting mainly of mud) supplied by the rivers escapes to the sea: only a small amount is trapped in the Harbour itself.

5.4. Transport Pathways Inferred From Grain Size Trends

5.4.1. Net Transport in Christchurch Harbour

A Rejected Pattern

Within the harbour, the sampling sites are distributed densely, at between 70 and 100 m intervals in general. At such sampling densities, any differences in derived grain size parameters between neighbouring sites tend to be small. This interpretation implies that errors in determining the grain size parameters, introduced by the procedure of grain size analysis, are likely to be so large that the representative transport trends become vague. The data sets provide, therefore, an opportunity to examine interaction between grain size trends and errors in grain size analysis.

Trend analysis has been carried out, using grain size parameters of 302 sediment samples within the harbour. The characteristic distance D_{cr} has been taken as 112 m. Following the procedure described in Chapter 4 (Section 4.2.2.), transport vectors are defined for all the sites. The pattern obtained has a characteristic vector length of 0.36.

For a significance test on the derived pattern, 150 experiments were undertaken, using randomly reallocated grain size data. Such analyses show that the average length of the 150 characteristic vectors is 0.32, with a maximum 5.55 and a minimum of 0.25. At the 90 % and 95 % significant levels, L_{cr} is 0.36 and 0.37, respectively. Because the observed length of the characteristic vector is even not above the 90 % level, the pattern is not considered as being significant; it has been, therefore, rejected.

A Pattern with Acceptable Significance

The grain size trend analysis has been applied also to a reduced number of sampling sites. Of the more than 300 sites available, around 100 are used. The sites were selected in such a way that they are distributed evenly over the whole area of the Harbour. In this case, the characteristic distance D_{cr} used was 225 m. In addition, because the sampling sites outside the Harbour and near the entrance have the same spatial scale of sampling interval, they are included also in the analysis; thus, 152 sampling site are involved.

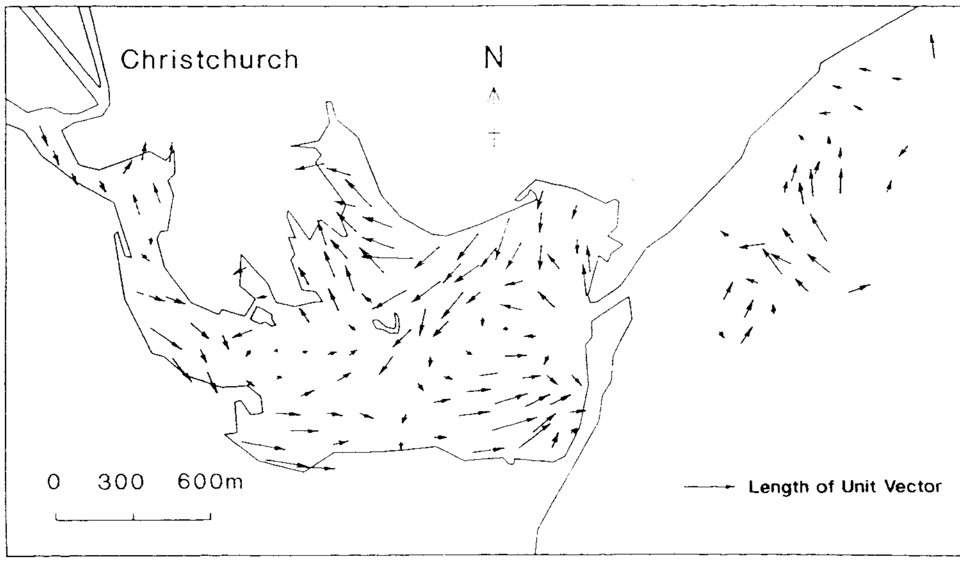

Figure 5-50. The identified grain size trends, over the Christchurch Harbour area.

The resultant transport vectors (Figure 5-50) have an orderly pattern, with the characteristic vector length of 0.41. For the 152 sampling sites, 150 experiments are carried out, in order to define the critical vector lengths. The average length of the 150 characteristic vectors is 0.35, with a maximum 0.45 and a minimum of 0.27 (Figure 5-51). At the 90 % and 95 % significance levels, L_{cr} is 0.39 and 0.42, respectively. Thus, the pattern is acceptable in terms of L_{90}, although it should be rejected in terms of L_{95}.

Trends within the Harbour are characterised by easterly transport along the river channel and westerly transport to the north of the area. Near the entrance, the transport vectors are directed to landward; this indicates that the net transport is from the sea, into the Harbour. Transport is flood dominated to the north of the flood tidal delta and is ebb dominated in the south, probably due to the river flows. Outside the Harbour, the transport vectors are directed generally towards the north and northwest.

The pattern shown on Figure 5-50 is supported by some sedimentological evidence. For example, transport towards the north and northwest outside the Harbour denoted by the transport vectors is consistent with a northwesterly longshore drift identified previously (Lacey 1985) and an offshore area incorporating erosive features

(Section 5.1.2.). The eastern part of the flood delta is characterised by a series of flood oriented sandwaves (with a spacing of around 10 m), as shown on an aerial photograph (supplied by Christchurch Borough Council) taken on 16 July, 1989. Such bedforms are indicative of landward transport, in agreement with the grain size trends at the same location.

The relatively low level of significance of the trend pattern can be caused by a number of factors. For example, the area is small but the sediments are supplied from a variety of sources (including river input, longshore transport and local seabed and coastal erosion). The mixing of material from these various sources would reduce the orderliness of the grain size trends.

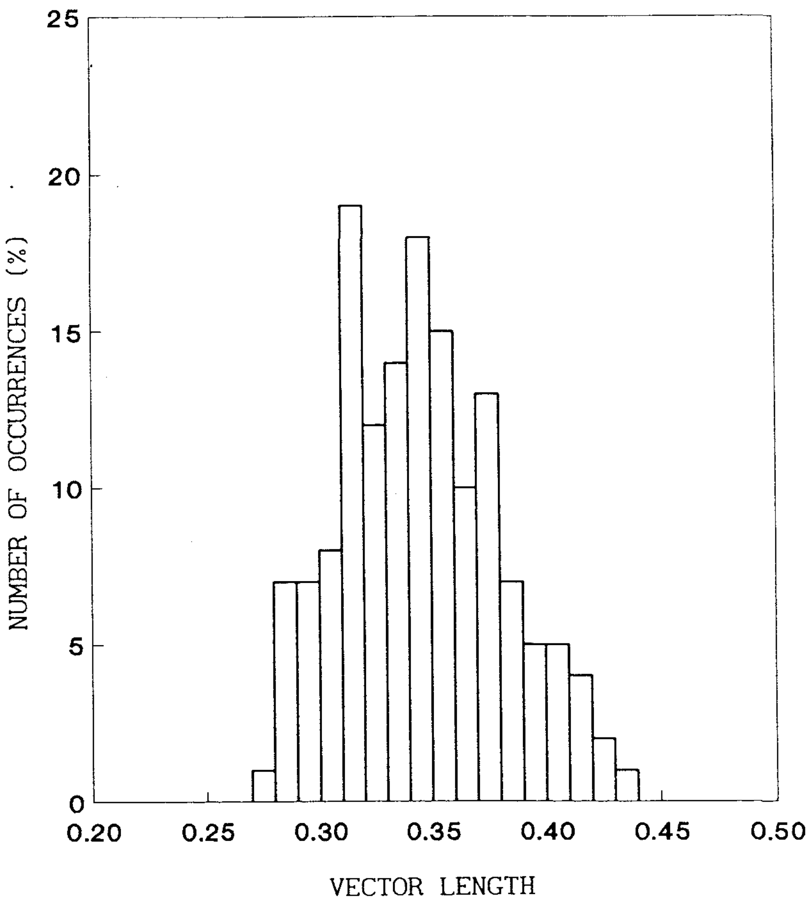

Figure 5-51. Frequency distribution of the length of "characteristic" vectors, for randomly-arranged sample grids for Christchurch Harbour.

5.4.2. Net Transport in Yangpu Harbour

Surficial Sediments

The surficial sediment distribution pattern for Yangpu Harbour area is shown as Figure 5-52. The distribution patterns of mean grain size, sorting coefficient and skewness are shown on Figures 5-53, 5-54 and 5-55, respectively.

Beach material and that in the shallow water areas is dominated by sandy and gravelly sediments, with a mean grain size of -1.5 ϕ to 3.0 ϕ (Figures 5-52 and 5-53). Muddy sediments, with a mean grain size of 5 ϕ to 7 ϕ, are present on the intertidal flats at the head of Xinying Bay and in the majority of the relatively deep tidal channels (*cf.* Figure 3-4). In the deepest part of the entrance channel, however, sandy material is the major component of the sediments.

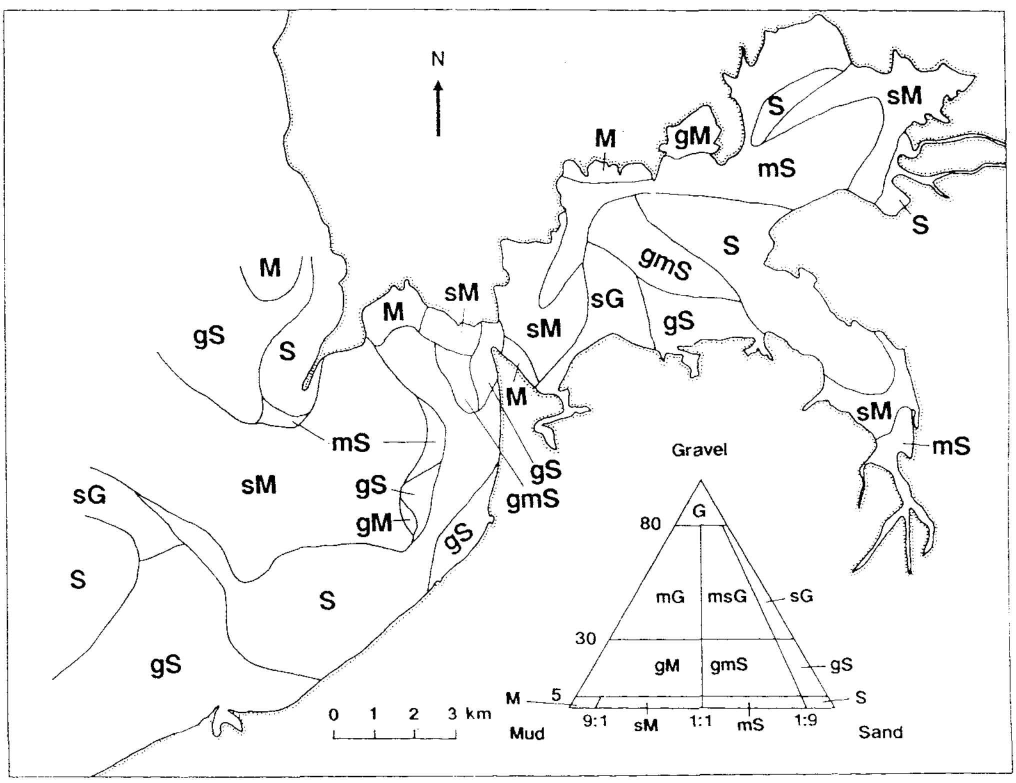

Figure 5-52. Seabed sediment distribution (the classification scheme based upon Folk (1980), modified slightly).

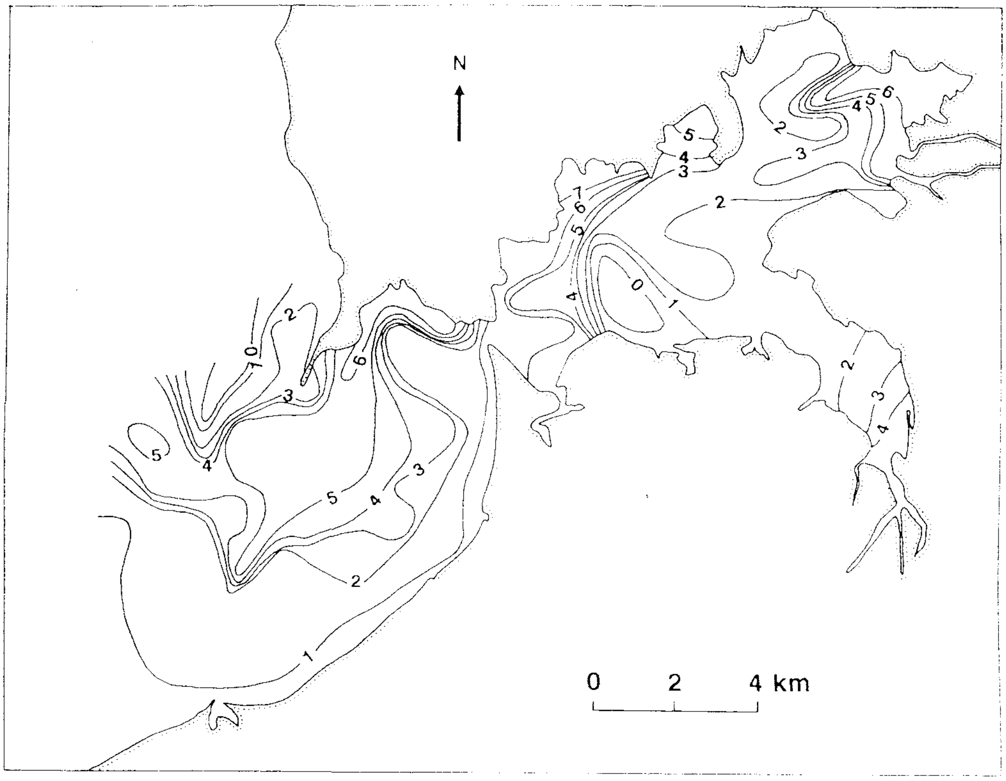

Figure 5-53. Mean grain size (in ϕ units) of the surficial sediments, Yangpu Harbour.

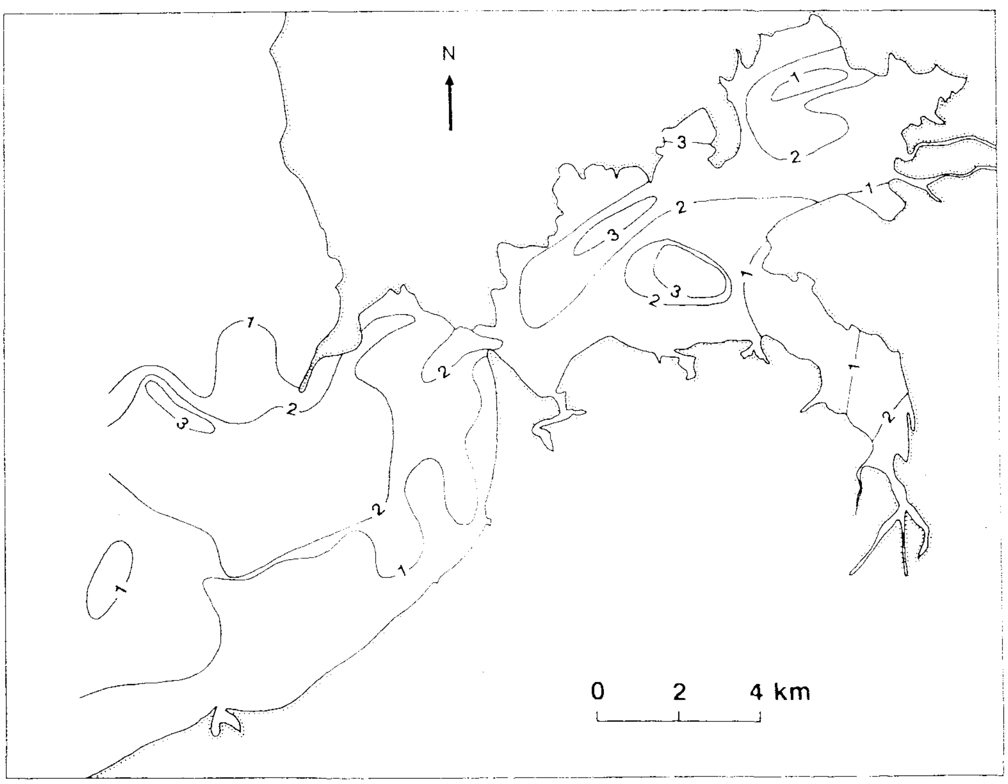

Figure 5-54. Sorting coefficients (in ϕ units) of the surficial sediments, Yangpu Harbour.

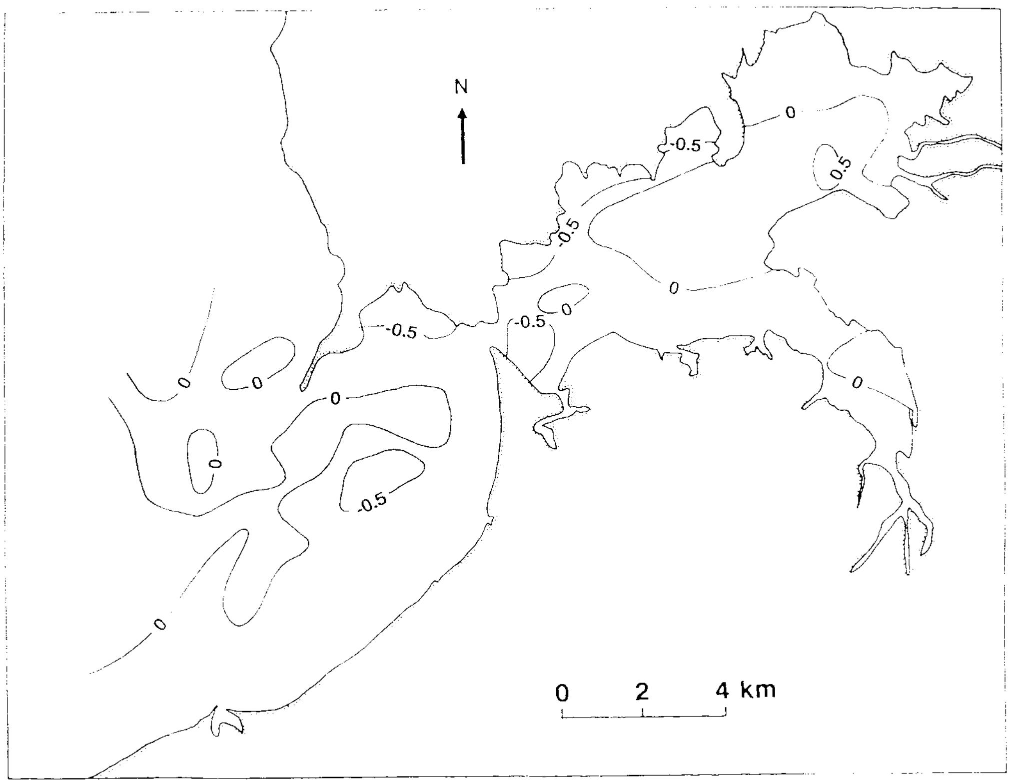

Figure 5-55. Skewness (in ϕ units) of the surficial sediments, Yangpu Harbour.

Towards the east, from the central part of Yangpu Bay to the land, the seabed sediments become generally coarser, better sorted and more negatively skewed (Figures 5-53, 5-54 and 5-55). Coarsening of sediments, accompanied by an improvement in the sorting and an increasing negative skewness, have been observed elsewhere; these have been related to variations in the dominance of the dynamic processes (Friedman 1961, 1967, 1979). Grain size parameter sensitivity to environmental setting appears, therefore, to be characteristic of this particular area.

Grain Size Trends

The same grain size parameters were used for the trend analysis. In order to define trend and transport vectors, the characteristic distance D_{cr} has been taken as the maximum sampling interval for this particular investigation (2.15 km). Any two samples with a distance of less than D_{cr} are compared, therefore, except where there is a morphological obstruction (as indicated by "A", for example, on Figure 4-15) between the sampling sites. Transport vectors are derived according to Equations [4-15] and [4-16]. The final "*residual*" grain size trends (Figure 5-56) show a highly ordered pattern, with a characteristic vector length (L) of 0.68.

The significance of the pattern shown on Figure 5-56 is evaluated on the basis of a comparison between L and L_{cr}, with the latter being determined on the basis of the procedure described previously. Altogether, some 151 analyses have been carried out; for each of these, 137 sampling sites are reallocated randomly and a characteristic vector length defined. The mean of the 151 vector lengths obtained is 0.44, with a maximum of 0.55 and a minimum of 0.29. The standard deviation is 0.0021. From the frequency distribution of the lengths obtained from the analyses (Figure 5-57), $L_{cr}=0.54$ at the 99% confidence level. Because it is valid that $L>L_{cr}$, the grain size trends of the Yangpu Harbour area are considered to be acceptable at the 99% significance level.

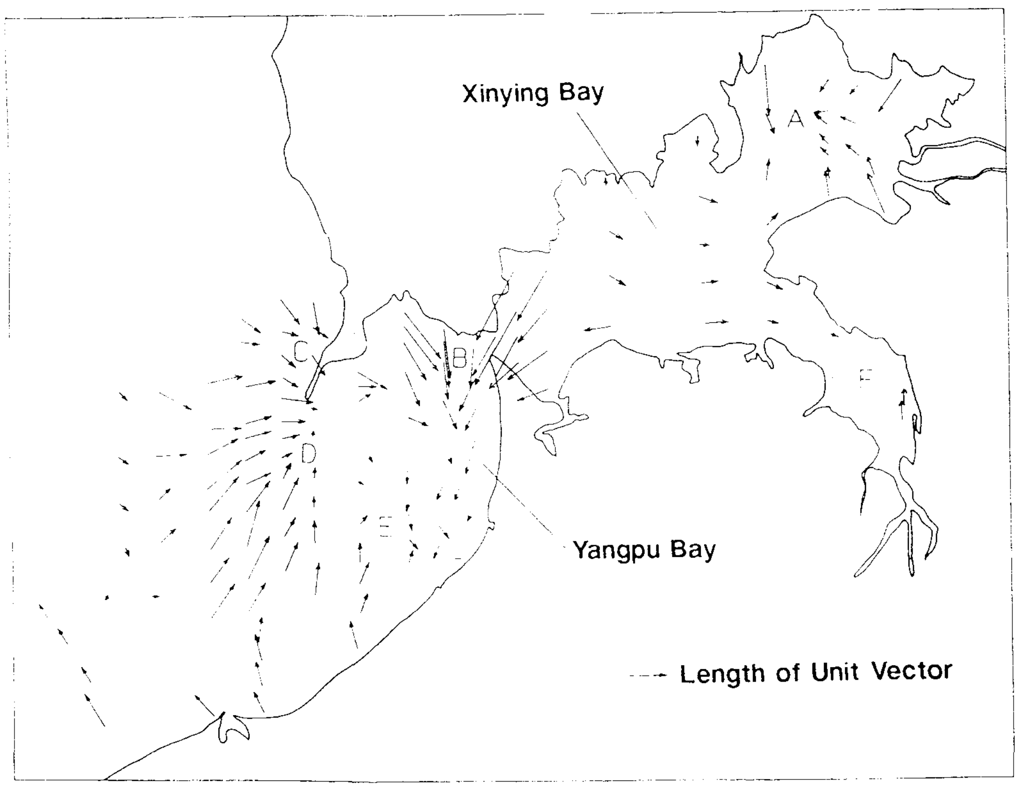

Figure 5-56. The identified grain size trends of Yangpu Harbour.

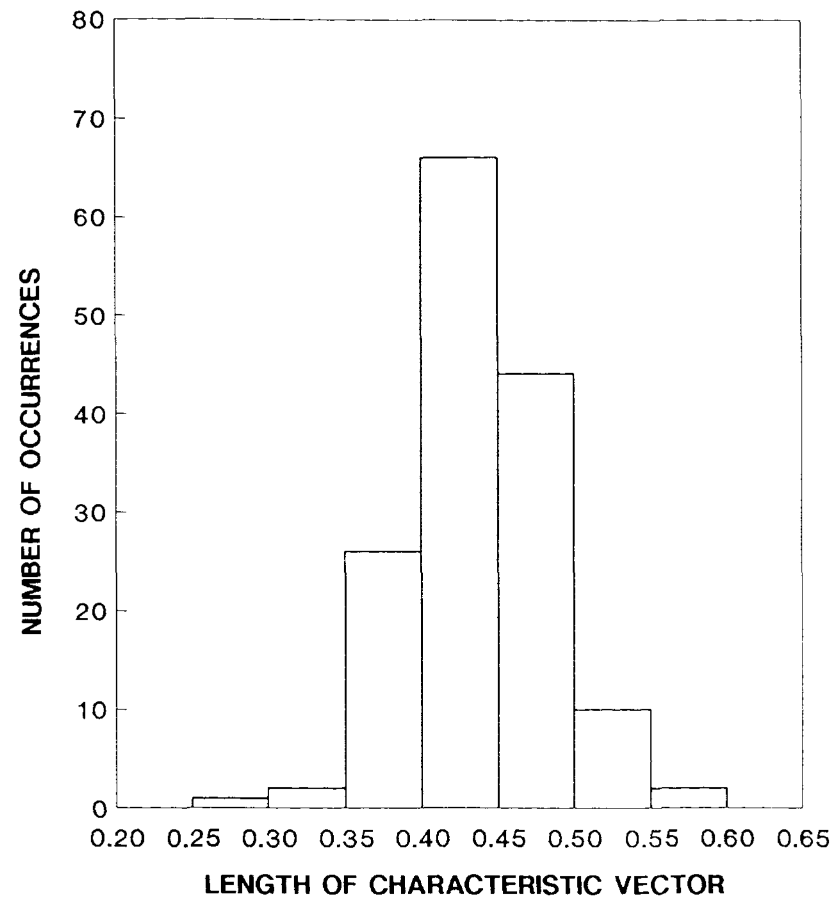

Figure 5-57. Frequency distribution of the length of "characteristic" vectors, for randomly-arranged sample grids for Yangpu Harbour.

The net sediment transport patterns, represented by the grain size trends, reveal several distinct characteristics.

The area between Dachan and Xiaochan Reefs (outside Yangpu Bay) is dominated by landward transport. Within Yangpu Bay, a clockwise sediment circulation pattern persists. In the southwestern part of the bay, the transport is mainly towards the northeast. For the nearshore area of eastern Yangpu Bay, however, there is dispersal of sediments towards the south.

Relatively complicated patterns of movements are present in Xinying Bay. Over the bay-mouth area, sediment transport is directed to seawards. The middle part of the bay is characterised by transport towards the bay-head areas, to the east and the south, where sediments appear to accumulate; this is shown by a convergence in the transport vectors over this region.

Geomorphological and Sedimentological Evidence

Few data sets are available to examine the predicted trend pattern in association with net transport pathways. Some of the geomorphological and sedimentological evidence appears, however, to be consistent with the predicted trends. As a demonstration of this correspondence, the observations relating to a number of locations shown on Figure 5-56 (indicated by *A*, *B*, *C*, *D*, *E* and *F*) are described.

There are extensive mud and mangrove flats at location *A* (Figure 5-56). On the intertidal flats, tidal creeks and channels are present which are floored with sandy material. The flats themselves are covered by muddy sediments. Accumulation of sediments takes place here, with the material being supplied mainly from small local river systems (Wang *et al.* 1985). Transport trends at this location are indicative also of a depositional environment, with convergence of the transport vectors.

Location *B* lies on the Yangpu Shoal, an ebb tidal delta. Immediately outside the mouth of Xinying Bay, the inlet channel divides. The main channel is directed towards the northwest, whilst a secondary channel passes through the delta towards the south (shown by the 5 m and 0 m isobaths, respectively, on Figure 3-4); these discharge 60% and 40% of the ebb flow, respectively (Wang *et al.* 1977). In both channels, the flow is ebb-dominated; hence, net sediment transport is likely to be controlled by the regional ebb tidal currents. Ebb dominance has been observed at the bay-mouth of Xinying Bay, on the basis of current meter observations (Wang *et al.* 1985); it is indicated also by the grain-size trends. It is worth noting, at this juncture, that longshore drift (on the beach) is directed towards the north (Zhu *et al.* 1984). Such northerly longshore drift and southerly offshore transport form an anti-clockwise sediment circulation pattern, which may be partly responsible for the ebb tidal delta formation.

Around Location *C*, the dominant southwesterly waves are sheltered by offshore coral reefs: waves from a northwesterly direction are the major influence on sediment movement. Hence, morphological features (such as the spits on Xiaochan Reef) are aligned towards the south, indicating transport in that direction. This pattern is consistent, once again, with the grain size trends described here.

At the seaward end of the main channel (Location *D*, Figure 5-56), net deposition is taking place, but at a low rate of accumulation (Zhu *et al.* 1984; Zhang and Zhu 1989). Some convergence patterns in the transport vectors (Figure 5-52) define such a zone of deposition. Landward transport outside Yangpu Bay may be caused by low energy wave approach (with a mean wave height of less than 0.6 m). For such an area with weak wave action, any seaward dispersal of fine-grained sediments would be at a relatively slow rate. This process may be compared with the factors which affect landward transport, which is enhanced by flood-dominant tidal currents over the area.

At Location *E*, the 2 m isobath extends to seaward (Figure 3-4); this is indicative probably of an accumulation of sediment, which coincides with the convergence of the southerly and northeasterly-trending transport vectors. Deposition here can be interpreted, therefore, as being the result of a decrease in tidal currents and an increase in wave energy, passing from north to south.

Finally, the area around Location *F* is characterised by accreting salt marshes and intertidal sand bodies.

5.5. Exchange of Sediments

5.5.1. Conceptual Experiments

Parameters for Model Input

In order to run the model used in the analyses (Section 4.3.3.), the unit time and initial conditions should be specified. For the initial conditions, because the trace material is assumed to be absent in the river sediments, it is assumed that

$$C_{b,init} = C_{m,init} = 0 \qquad [5\text{-}3]$$

For the total volume of bay sediments, the initial value is defined as the volume of the moving layer:

$$V_{init} = D_L \, A_b \qquad [5\text{-}4]$$

The input parameters required by the model include A_b (the area of the estuarine basin), D_R (the deposition rate), C_l (tracer concentration in the marine sediments), D_L (the thickness of the moving layer), q_s (sediment input from the sea), q_o (sediment output toward the open sea), q_r (sediment input from the river), q_m (part of sediment output derived from the estuarine sediments), a_s (fraction of the marine sediments remaining within the estuary) and a_r (fraction of the river sediments remaining within the estuary). In addition, the length of the unit time (Δt) and the parameter *k* in Equation [4-27] need to be specified. These parameters are now derived, on the basis of published information combined with some calculations.

Generally, the plan area of estuarine systems is of the order of 1-10^3 km^2. For the present study, A_b has been assumed to be 20 km^2. In modern estuaries, the average rates of sediment accumulation are 2×10^{-3} m yr^{-1} for estuaries located in regions with a predominantly humid climate and 1×10^{-3} m yr^{-1} for arid and semi-arid regions (Rusnak 1967). Thus, D_R in the model input has been taken to be within the same order of magnitude, except for the case of a "neutral" condition (i.e. without landward or seaward net transport at the entrance).

The concentration of the trace material varies with location, depending upon the type of tracer being considered. Some information is available in the literature, however, concerning the order of magnitude of such tracer concentrations. On continental shelves adjacent to an estuary, concentrations of heavy minerals can be as high as 10-30 % (Barrie *et al.* 1988) and those of foraminiferal tests can be up to 40 % (Milliman 1976). A value of C_l for the model input has been assumed, therefore, to be 10 %.

The depth of disturbance on coastal beaches is dependent upon wave height and type, together with grain size characteristics of the beach material. Under breaking wave heights of around 1 m, the depth of disturbance has been reported to be of the order of 30 mm (King 1951), or 0.2-0.4 m (Otvos 1965; Williams 1971). The thickness is assumed here, therefore, to be 0.1 m.

For the determination of q_s, q_o and q_r, 4 transport cases at the entrance are considered: (1) landward net sediment transport ($q_s>q_o$); (2) no net transport ($q_s=q_o$); (3) seaward net transport, with sediment accumulation within the tidal basin ($q_s<q_o$ and $q_r>q_o-q_s$); and (4) seaward net transport, with no accretion in the basin ($q_o=q_s+q_r$). Sediment discharge (q_r) from the river system is asssumed to be 4×10^4 m^3 yr^{-1}. Further, q_s, q_o, a_s and a_r are selected to satisfy each of the 4 possible transport cases. D_R and q_m are then calculated from these parameters. Input parameters for the 4 cases are listed in

Table 5-10.

For convenience, the parameter $k=1$ is assumed and Δt is taken as a year to satisfy the condition $D_L > D_R \Delta t$ in Equation [4-31].

Table 5-10. Input parameters for the conceptual experiments.

Case	A_b km^2	q_s m^3yr^{-1}	q_o m^3yr^{-1}	q_r m^3yr^{-1}	q_m^{x} m^3yr^{-1}	D_L m	D_R^{y} mm	a_s	a_r	C_1 %
1	20	80000	70000	40000	2000	0.1	2.5	0.3	0.7	10
2	20	70000	70000	40000	9000	0.1	2.0	0.3	0.7	10
3	20	50000	70000	40000	23000	0.1	1.0	0.3	0.7	10
4	20	30000	70000	40000	37000	0.1	0.0	0.3	0.7	10

[x] On the basis of Equation [4-19].

[y] Based upon $D_R = q_n / A_b = (q_s + q_r - q_o) / A_b$.

Model Output

The model for changes in the tracer concentrations is run for a period of 500 unit time spans (i.e. over 500 years). For each case, a time-series of C_b is obtained (Figure 5-58). A significant feature is that C_b increases progressively with time (i.e. there is, indeed, some transport from the source), no matter what the net sediment transport patterns are. In other words, there is some transport from the source, independent of the landward or seaward net transport at the entrance. Because net sediment transport consists of two components, advection and dispersion, the influx of the tracer must be influenced strongly by dispersion. This influence is particularly significant in Cases 3 and 4, in which the advection component is directed to seaward. That the dispersion component is not small compared with the advection component has been identified also for beach environments (Price 1969) and in shallow marine areas (Pizzuto 1987).

According to Fischer *et al.* (1979), the flux due to dispersion can be expressed as - A_D dC/dx (where C is the tracer concentration and A_D is the dispersion coefficient for the tracer). This, together with the flux due to advection (M_0), forms the total budget:

$$\frac{T_n}{B\ D_L} = -A_D \frac{\partial C}{\partial x} + \frac{M_0}{B\ D_L} \qquad [5\text{-}5]$$

From Equations [4-23] and [5-5] we have:

$$A_D \frac{\partial C}{\partial x} = \frac{1}{B\ D_L}(M_0 - k\ a_s\ C_1\ q_s + k\ C_m\ q_m) \qquad [5\text{-}6]$$

An estimate of A_D, on the basis of the parameters of the present experiments, is that it is of an order of magnitude between 10^{-4} and 10^{-2} m^2s^{-1}; this is equivalent to that found in high energy environments.

Figure 5-59 shows the distribution of the tracer concentration in the stratigraphic records, for the four cases. It reveals a number of characteristics.

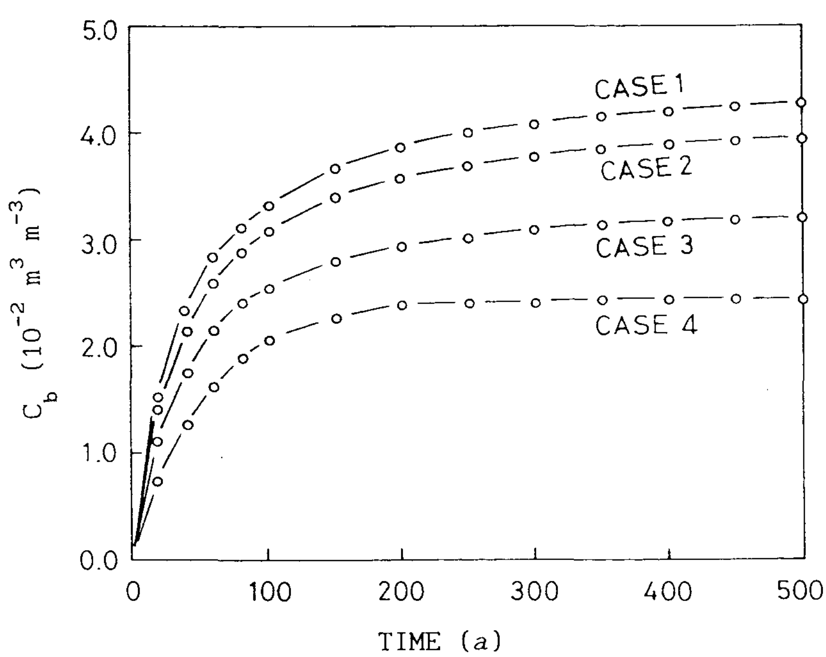

Figure 5-58. Exchange of trace sediments, in the surficial sediments (for details of the various Cases, see text).

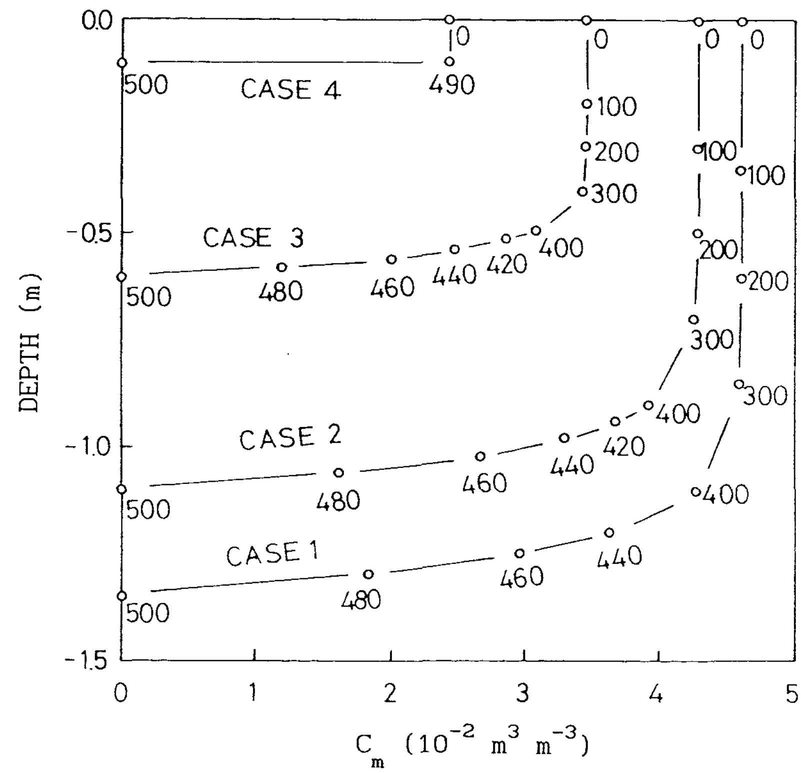

Figure 5-59. Exchange of trace sediments, in the sedimentary sequence.

Firstly, after a period of sediment exchange, an equilibrium state for C_m is attained eventually. The concentration becomes stable afterwards, throughout the record. The length of time for C_m to reach equilibrium (T_{eq}) is considerable (Table 5-11). For all cases, the amount of time for equilibrium to occur lies between 300 and 360 years. Thus, T_{eq} is another factor which influences the observed tracer concentration.

Secondly, the equilibrium tracer concentrations ($C_{m,eq}$), or the dimensionless ratio ($C_{m,eq}/C_1$) for the 4 cases vary considerably (Table 5-11). This equilibrium level should be controlled by the following 4 factors which form the basis of the model: (i) sediment discharge from the river; (ii) the concentration in the source area; (iii) landward-seaward net transport patterns; and (iv) the processes of dispersion. Because, for the 4 cases, only q_s among the input parameters is an independent variable, the derived equilibrium levels should represent the influence of net transport patterns.

As an example of this process, Wang and Murray (1983) noticed differences in the percentage of exotic benthic foraminiferal tests in estuaries with a variety of tidal ranges. Such differences were interpreted in terms of the magnitude of tidal energy and

Table 5-11. Equilibrium state for the 4 cases.

Case	T_{eq} (yr)	$C_{m,eq}$	$C_{m,eq}/C_1$
1	357	0.0462	0.462
2	351	0.0429	0.429
3	320	0.0349	0.349
4	311	0.0243	0.243

net sediment transport patterns. The concentration under "neutral" conditions (i.e. net transport through the entrance is zero) may be considered as a critical value. If any observed tracer concentration within an estuarine system exceeds this critical level, it should define the status of net landward sediment transport. In the case of the present investigation (Table 5-11), the critical level is $C_{m,eq}$=0.0429 or $C_{m,eq}/C_1$=0.429. Thus, Case 1 defines a net landward transport and Cases 3 and 4 represent net seaward transport.

5.5.2. Experiments for Christchurch Harbour

Foraminiferal Test Data

The model utilised in Section 5.5.1. is applied here to identify net sand transport direction through the entrance. Exotic (i.e. open sea derived) foraminiferal tests are used as natural trace sediments.

Concentrations of foraminiferal tests (including both exotic and estuarine species) have been determined using the procedure described in Chapter 4, for 53 sand sub-samples (Table 5-12). The distribution of the concentrations (Figure 5-60) shows them to be generally lower than 3.0×10^{-3}, but relatively high in an embayment to the north. Outside the Harbour and near the entrance, the values are lower 1.0×10^{-3}. Percentages of the exotic species (Figure 5-61) are higher, however, near the entrance than in the bay-head areas.

Table 5-12 (A). Contents of foraminiferal tests and organic matter in the sand fractions of seabed sediment samples in Christchurch Harbour (for sample locations, see Appendix B).

No.	W_s (g)	W_1 (g)	W_2 (g)	W_3 (g)	C_F ($\times 10^{-3}$)	C_{org} ($\times 10^{-3}$)
6	69.12	0.524	1.324	1.073	3.631	7.943
10	128.33	0.525	1.520	1.204	2.462	5.291
15	46.00	0.522	1.046	0.820	4.913	6.478
17	51.41	0.536	0.864	0.706	3.073	3.307
21	41.15	0.510	0.697	0.572	3.038	1.507
35	109.55	0.529	0.861	0.728	1.214	1.817
43	88.04	0.526	0.763	0.678	0.965	1.726
50	152.65	0.516	0.834	0.723	0.727	1.356
57	75.23	0.522	0.847	0.720	1.688	2.632
67	37.73	0.548	0.684	0.602	2.173	1.431
77	125.50	0.532	1.292	0.711	4.629	1.426
80	105.92	0.525	1.194	0.753	4.164	2.153
85	180.48	0.527	1.318	1.045	1.513	2.870
86	92.40	0.537	0.662	0.624	0.411	0.942
92	97.23	0.539	0.952	0.814	1.419	2.828
101	26.90	0.528	0.983	0.642	12.677	4.238
118	99.41	0.529	0.912	0.588	3.259	0.594
121	43.39	0.536	0.990	0.661	7.582	2.881
129	138.02	0.536	0.897	0.730	1.210	1.406
131	57.38	0.526	1.397	1.001	6.901	8.278
136	72.41	0.543	0.767	0.668	1.367	1.726
141	115.80	0.531	1.511	1.224	2.478	5.984
143	135.63	0.535	0.755	0.602	1.128	0.494
157	100.68	0.537	1.037	0.787	2.483	2.483
184	155.83	0.534	1.170	0.968	1.296	2.785
195	92.80	0.501	0.907	0.650	2.769	1.606
203	132.31	0.522	1.172	0.926	1.859	3.053
205	64.10	0.527	0.786	0.700	1.342	2.699
211	85.58	0.532	0.668	0.582	1.005	0.584
215	42.09	0.520	0.693	0.620	1.734	2.376
219	99.59	0.540	0.713	0.658	0.552	1.185
224	133.48	0.533	1.202	0.966	1.768	3.244
232	153.25	0.524	0.820	0.644	1.148	0.783
236	123.92	0.516	0.543	0.534	0.073	0.145
243	159.75	0.523	0.815	0.668	0.920	0.908
258	96.55	0.534	0.662	0.606	0.580	0.746
276	127.55	0.526	0.771	0.584	1.466	0.455
278	107.55	0.527	0.780	0.574	1.915	0.437
282	147.28	0.525	0.570	0.534	0.244	0.061
284	19.53	0.527	0.610	0.575	1.792	2.458
287	41.14	0.529	0.547	0.532	0.365	0.073
290	118.78	0.509	0.852	0.737	0.968	1.920
300	150.50	0.537	0.568	0.542	0.173	0.033

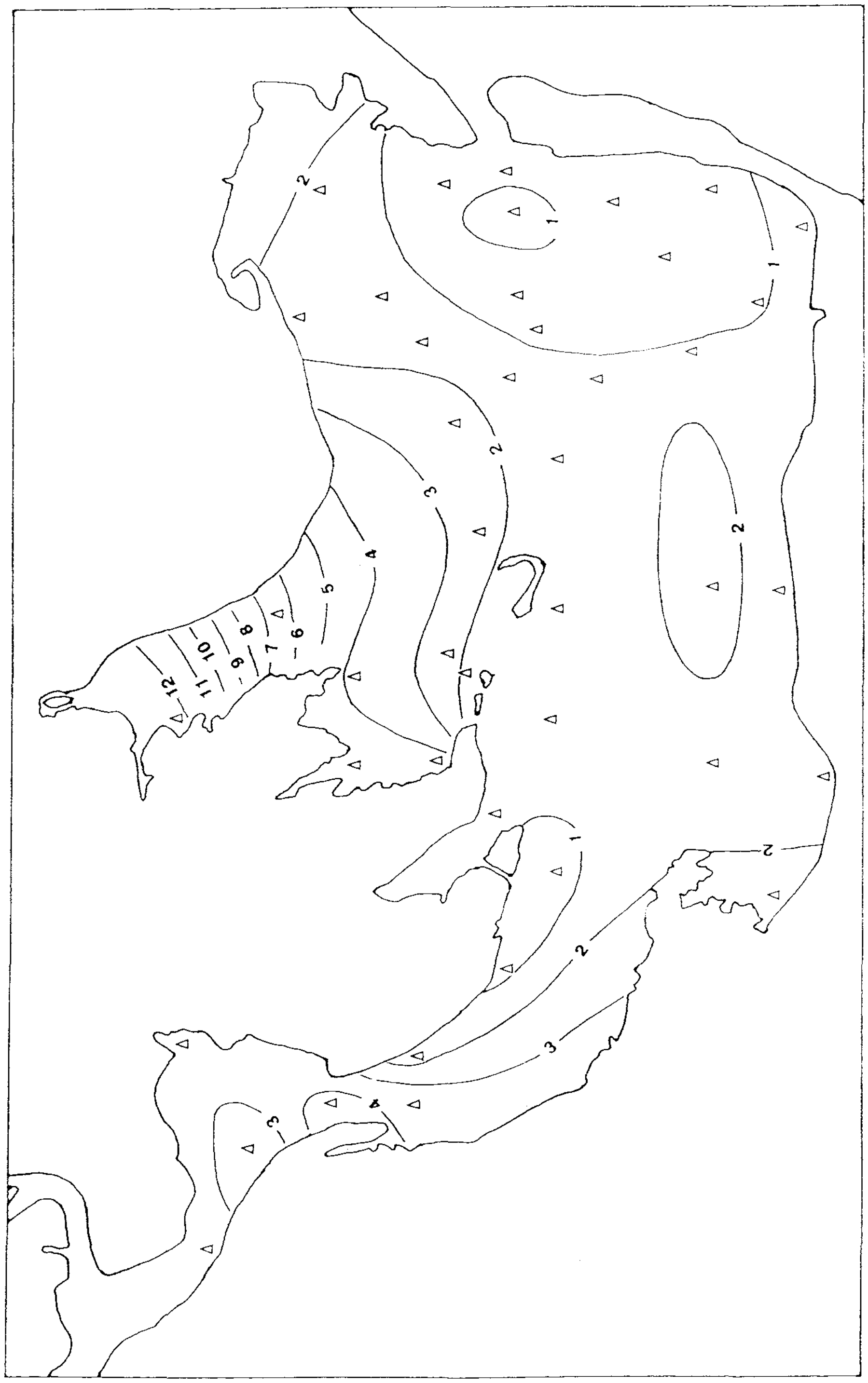

Figure 5-60. Concentration of foraminiferal tests (in terms of mass) in Christchurch Harbour (×10^{-3}).

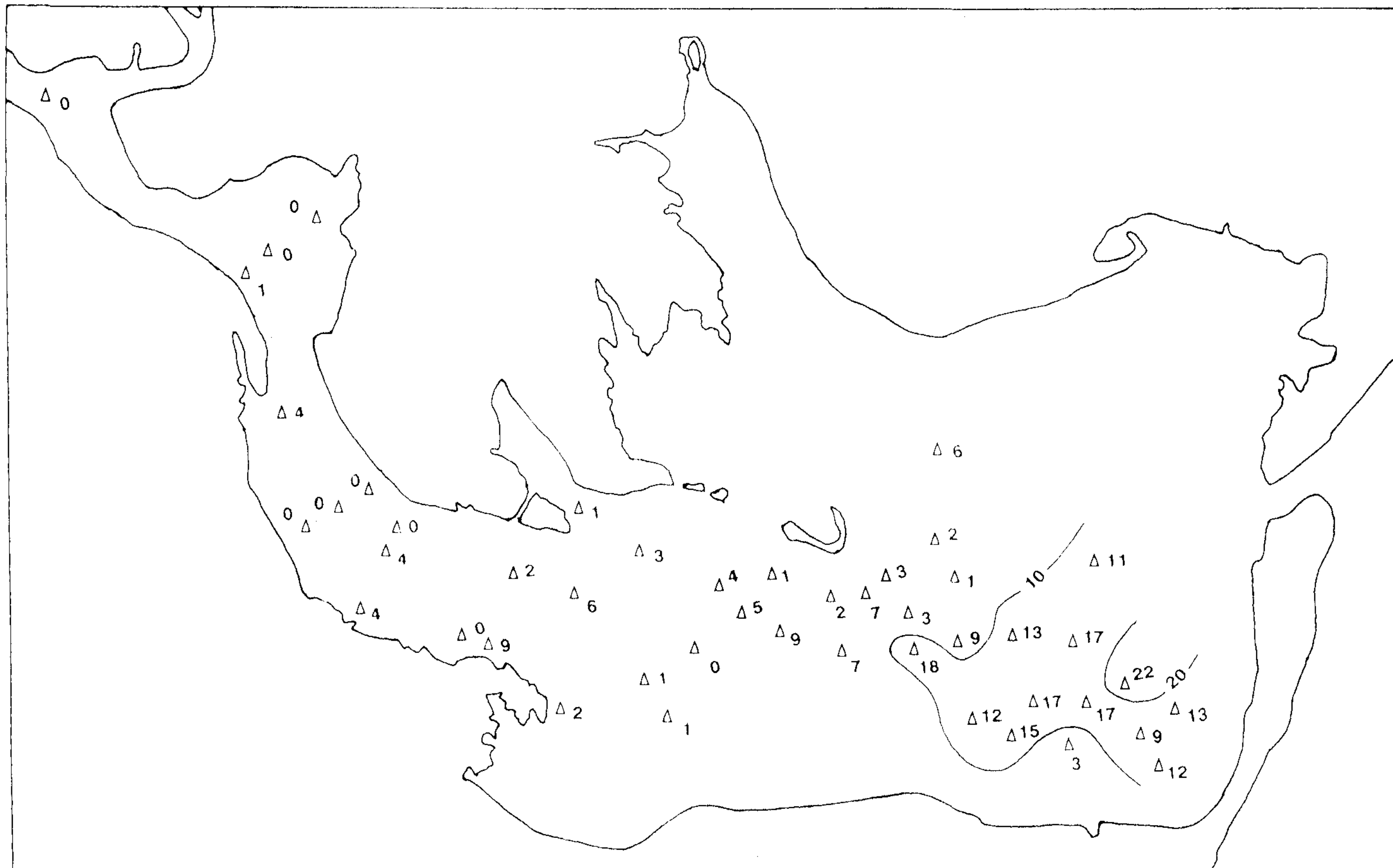

Figure 5-61. Percentages of exotic benthic foraminiferal tests in Christchurch Harbour, after Murray (1966) and Wang and Murray (1983).

Table 5-12(B). Contents of foraminiferal tests and organic matter in the sand fractions of seabed sediment samples outside Christchurch Harbour (for sample locations, see Appendix B).

No.	W_s (g)	W_1 (g)	W_2 (g)	W_3 (g)	C_F ($\times 10^{-3}$)	C_{org} ($\times 10^{-3}$)
423	125.78	0.535	0.554	0.535	0.151	0.000
424	116.69	0.544	0.558	0.544	0.120	0.000
425	106.85	0.535	0.555	0.535	0.187	0.000
430	137.75	0.530	0.546	0.530	0.116	0.000
431	84.20	0.529	0.542	0.529	0.154	0.000
436	125.04	0.523	0.555	0.523	0.256	0.000
437	48.85	0.534	0.549	0.534	0.307	0.000
442	114.77	0.527	0.546	0.527	0.166	0.000
444	78.09	0.528	0.554	0.528	0.333	0.000
447	52.72	0.512	0.546	0.512	0.645	0.000

Based upon the data listed in Table 5-12(A) and shown on Figure 5-61, the mass concentration of the exotic benthic foraminiferal tests averaged over the tidal basin (which is taken as representing the observed $C_{m,eq}$) were calculated, using the following equation:

$$C_{m,eq} = \frac{1}{n} \sum_{1}^{n} P_{Ei}\, C_{Fi} \qquad [5\text{-}7]$$

where n is the total number of number of the sampling sites shown on Figure 5-61, P_{Ei} is the percentage of exotic species in the total foraminiferal tests, and C_{Fi} is the concentration of the total foraminiferal tests defined for the sampling sites on Figure 5-61. C_{Fi} is calculated by interpolating the C_F data listed in Table 5-12(A). Thus, $C_{m,eq}$ is estimated to be 0.10×10^{-3}, which will be compared later with the simulated $C_{m,eq}$ data using Equations [4-27], [4-28] and [4-31].

Estimates of Critical Levels

The conceptual model developed earlier demonstrates that, for any tidal basin, a critical level of the content of exotic tracers exists. If the observed level exceeds the critical level, then the net transport is directed towards the basin. Otherwise, there is no landward net transport, even though the exotic tracers are present within the basin. Under the critical conditions (Section 5.5.1.), q_o must be equal to q_s. Hence, the model to define the critical level requires the following parameters as inputs: k (in Equations [4-27] and [4-31]), A_b, C_1, q_s, q_r, Δt, D_L, a_s and a_r. The method adopted here is to estimate, for some of the parameters which are difficult to determine accurately, a range of in which the parameters under consideration fall. Some representative values are selected then from the range and a number of combinations of the parameters are formed. For each of the combinations, a $C_{m,eq}$ value can be obtained. The basic foundation for this approach is that, from the results based upon every combinations (which is probably representative of the reality), a general pattern may be inferred. Such an approach incorporates also some sensitivity analysis.

Two situations exist with regard to the hydrodynamic behaviour of foraminiferal tests, in relation to silica sands. Firstly, the tests with the same grain size will have different threshold of movement from silica sands and differential transport between the tests and the silica sands is expected. Secondly, the mixture of foraminiferal tests and silica snads becomes well-sorted after significant hydraulic sorting, in which the tests and the silica sands have similar threshold of movement. The sands are generally well-sorted over the flood and ebb tidal delta areas; this implies that the foraminiferal tests contained in the sediments have been subjected to substantial hydraulic sorting. The dynamic behaviour of the tests is assumed, therefore, to be similar to that of the bulk sediment (i.e. $k=1$).

The water surface area of Christchurch Harbour is 1.91×10^6 m^2 at MHWS on the basis of the hypsometric curve (Figure 5-25), which is taken as A_b.

The mass concentration of exotic benthic foraminiferal tests is, on average, 0.228×10^{-3} for the 10 samples outside the Harbour (samples 423 to 447, Table 5-12(B); sample locations are listed in Appendix B). C_1 in Equations [4-27] and [4-31] is, however, volume concentration. Nevertheless, these equations are still valid when the volume concentration is replaced by the mass concentration, if a constant α is used to transfer the latter into the former (i.e. $C_{volume} = \alpha\, C_{mass}$). Hence, the mass concentration is taken to represent C_1.

The sediment discharged through the Run during the ebb phase of the tides are between 12000 and 29400 $m^3\ yr^{-1}$, on the basis of predictions using the Madsen-Grant and Vincent equations (Section 5.3.1.). Further, sediments within the Run contain between 5 and 10 % of sands. Hence, q_s values are taken at between 1200 and 3000 $m^3\ yr^{-1}$ and four values are used (i.e. 1200, 1800, 2400 and 3000 $m^3\ yr^{-1}$).

The mean thickness of Holocene marine sediments is of the order of 1 to 2 m (Section 5.1.2.). Under the critical condition (i.e. $q_s = q_o$), if the sediments have been deposited since 6000 yr B.P. when the sea level reached its present level, then the river input should be of the order of 320 to 640 m^3yr^{-1}. Thus, q_r values of 200, 450 and 700 m^3yr^{-1} are used here. These values imply that the deposition rate within the Harbour ranges between 0.1 and 0.4 mm yr^{-1}.

D_L is a function of current speed, grain size of sediments and the time scale under consideration. Most of Christchurch Harbour is sheltered from open sea waves (except the entrance). Hence, the thickness of the moving layer on the time scale of a tidal cycle should be, on average over the Harbour, smaller than that observed for beaches (Section 5.5.1.). However, because the deposition rate for the Harbour is low, the unit time used for the study can be longer than a tidal cycle. If Δt is taken as a year, then D_L is considered to have the order of 10 to 100 mm. For the present analysis, therefore, Δt and D_L are taken as 1 yr and 50 mm, respectively. These data satisfy the relationship $D_L > D_R\, \Delta t$, which is assumed in Equation [4-31].

Sedimentary material from the rivers is trapped within the Harbour, especially in the bay-head areas; hence, a_r is taken as 0.9 for the input. In estimating a range of magnitude for a_s, the following two factors are considered. Firstly, in Equation [4-19], q_m is positive (i.e. $q_m > 0$). Thus, according to [4-19] and the assumption that $q_s = q_o$, we have:

$$a_s > \frac{(1 - a_r)\, q_r}{q_s} \qquad [5\text{-}8]$$

Secondly, since the movement of the tracer is caused by dispersion alone (as implied by $q_s = q_o$), the flux of the tracer can be expressed as:

$$\frac{1}{B\ D_L}\ (\ k\ a_s\ C_1\ q_s\ -\ k\ C_m\ q_m\ )\ =\ -\ A_D\ \frac{\partial C}{\partial x} \qquad [5\text{-}9]$$

where C is the concentration of exotic tests. If A_D is assumed to be between 10^{-3} and 10^{-2} m^2s^{-1}, then two values of a_s (0.05 and 0.10) are considered to be suitable according to Equation [5-9]. Such values satisfy also Equation [5-8], except for one of the combinations (i.e. q_r=700 m^3yr^{-1}, q_s=1200 m^3yr^{-1} and a_s=0.05 (this combination is not used, therefore, in the analysis).

The same initial conditions as those defined in Equations [5-3] and [5-4] are used for this analysis.

All of the q_r, q_s and a_s combinations form 23 cases. The model was run for each of the cases, to determine the critical levels within the depth of disturbance and associated equilibrium times. In each case, the running of the model was ended and the results obtained when the increase in C_m was less than 0.001×10^{-3} over 100 yr; this implies that C_m has reached equilibrium. The results are listed in Table 5-13.

The time required for $C_{m,eq}$ to occur is of the order of 450 to 950 yr. Since the period are all considerably shorter than the post-glacial high sea level period (which started 6000 yr B.P.), the observed concentration of the tests represents the equilibrium level and can be compared with the values derived from calculations. Over such a period, however, the annual mean sediment discharge and concentration of the benthic exotic tests in the open sea sediments may have varied. In the analysis, C_1, q_s and q_r are taken as constants rather than variables; this is based upon the assumption that these parameters have also reached their equilibrium state or fluctuate only slightly around an average state.

From Table 5-13 it can be seen that $C_{m,eq}$ is sensitive to q_r, q_s and a_s: it increases in response to an increase in q_s or a_s, but decreases in response to an increase in q_r. Of the 23 cases, 3 (i.e. Cases 4, 6 and 8 in Table 5-13) result in $C_{m,eq}$ values which exceed the observed level (i.e. 0.10×10^{-3}). These high values are associated, however, with combinations of a low q_r and a high a_s, which may be less probable than the other cases. Furthermore, a q_r value of 200 m^3yr^{-1} is beyond the lower limit (i.e. 300 m^3yr^{-1}). The other 20 cases all have their calculated (critical) $C_{m,eq}$ levels below the observed $C_{m,eq}$ level. These results represent, consequently, the landward net sediment transport of sands within the entrance to the tidal basin.

Such results contradict the ebb dominated transport defined using the empirical

Table 5-13. Critical levels of content of exotic tracers, calculated for the 23 cases ($A_b=1.91\times10^6$ m^2; $C_1=0.228\times10^{-3}$; $D_L=0.05$ m; and $a_r=0.9$)

Case	$q_r(m^3yr^{-1})$	$q_s(m^3yr^{-1})$	a_s	$C_{m,eq}(\times10^{-3})$	$T_{eq}(yr)$
1	200	1200	0.05	0.052	930
2	200	1200	0.10	0.087	945
3	200	1800	0.05	0.072	995
4	200	1800	0.10	0.111	930
5	200	2400	0.05	0.087	945
6	200	2400	0.10	0.129	970
7	200	3000	0.05	0.100	830
8	200	3000	0.10	0.142	980
9	450	1200	0.05	0.029	710
10	450	1200	0.10	0.052	800
11	450	1800	0.05	0.041	725
12	450	1800	0.10	0.070	755
13	450	2400	0.05	0.052	800
14	450	2400	0.10	0.085	805
15	450	3000	0.05	0.061	735
16	450	3000	0.10	0.097	700
17	700	1200	0.10	0.037	460
18	700	1800	0.05	0.028	445
19	700	1800	0.10	0.051	660
20	700	2400	0.05	0.037	460
21	700	2400	0.10	0.063	550
22	700	3000	0.05	0.044	585
23	700	3000	0.10	0.074	700

formulae (Section 5.3.1). It may be pointed out that these formulae contain a constant mean grain size, which is used for both flood and ebb phases of the tide. Such a parameter implies that the availability of material for transport during the flood is the same as that during the ebb. However, the flood tidal delta adjacent to the entrance is characterised by flood- and ebb-dominated zones. Thus, part of sediments transported onto the delta during the flood may trapped there and not become available for ebb transport. If the material trapped on the flood delta is not compensated by additional sources, then the formation of the flood delta is result of landward net sediment transport. This may be the case in Christchurch Harbour.

The net landward transport, inferred from the present study, appears to suggest there to be a need to include in any empirical formula a factor which represents material availability.

5.6. Inlet Equilibrium

5.6.1. Equilibrium of Christchurch Harbour

Determination of $<P>$, T_f *and* T_e

The mean tidal prism and flood and ebb durations have been defined on a semi-diurnal time scale. High and low water level data, together with their associated times in terms of GMT, were read from the tide gauge records. The water level data were transferred then into elevations, in terms of OD, using Equation [4-4].

If the double high waters are present, then the first and the second flood (or ebb) phases are added together to form a unified flood (or ebb) duration. For example, Figure 5-62 is a tidal cycle record of the water level on 14 April 1991, which is typical of a double high water period. The curve can be divided into four phases (i.e. I, II, III and IV on Figure 5-62). Phases I and II are associated with a rise in the water level, whilst Phases II and IV are within the falling water level stage. Hence, the sum of the time durations of Phases I and III represents the flood duration of the tidal cycle. Likewise, the sum of Phases II and IV is defined as the ebb duration.

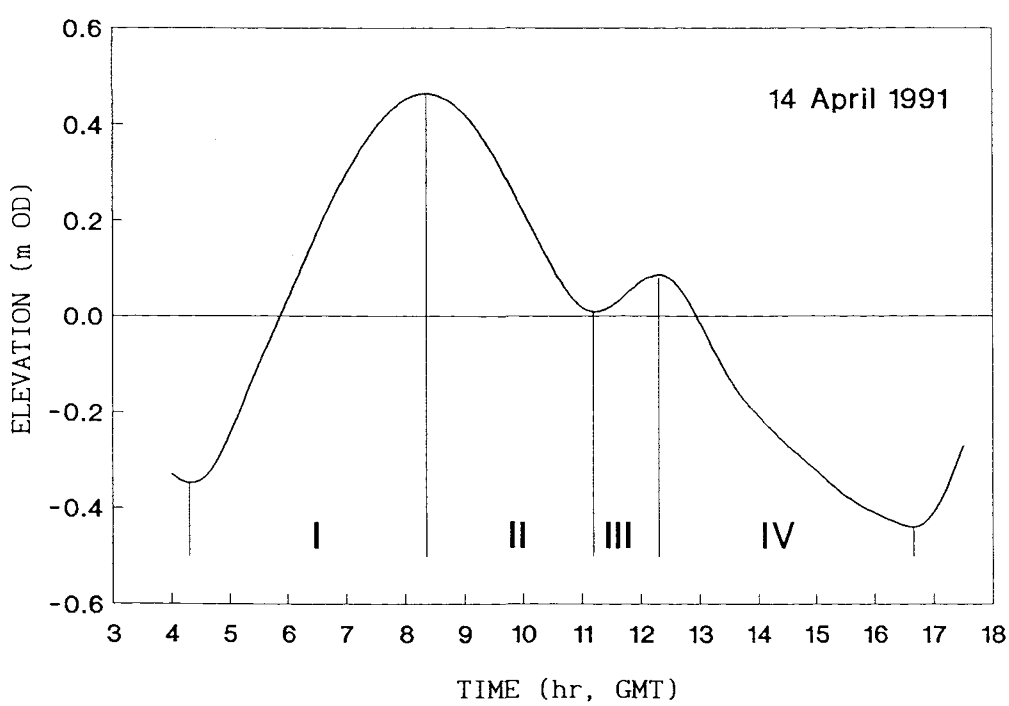

Figure 5-62. Definition of flood or ebb durations, for a tidal cycle associated with double highs.

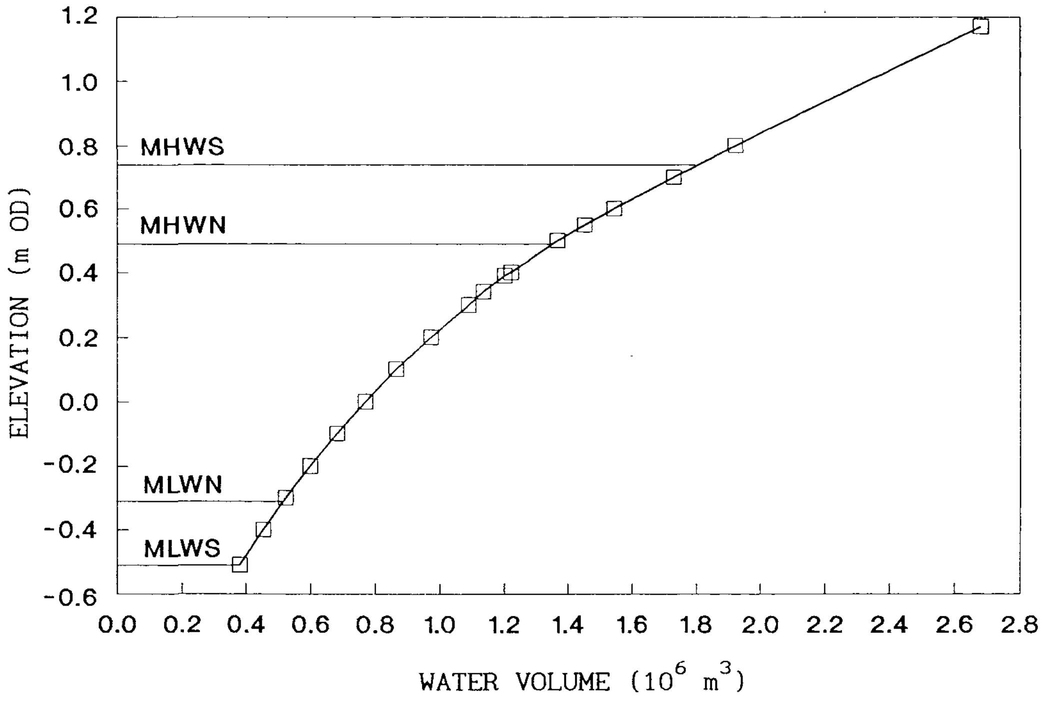

Figure 5-63. Relationship between water level and water volume in Christchurch Harbour, as derived from Figure 5-25.

Similarly, a unified flood or ebb tidal prism is defined for each tidal cycle. Based upon the hypsometric curve of Christchurch Harbour (Tosswell 1978) (Figure 5-25), the relationship between the water level and the volume of water stored within the basin has been derived (Figure 5-63). A series of tidal prisms are derived then from the high and low water levels, using the curve shown on Figure 5-63. For tidal cycles with double high waters (Figure 5-62), the flood tidal prism is defined as the sum of the tidal prisms of Phases I and III; the sum of the tidal prisms associated with Phases II and IV forms the ebb tidal prism.

From frequency distribution patterns of the tidal prism and duration data over the 594 tidal cycles (Figures 5-64 and 5-65), the mean tidal prism has been estimated to be 1.06×10^6 m^3. The mean flood and ebb durations are 6.40 and 6.01 hr, respectively.

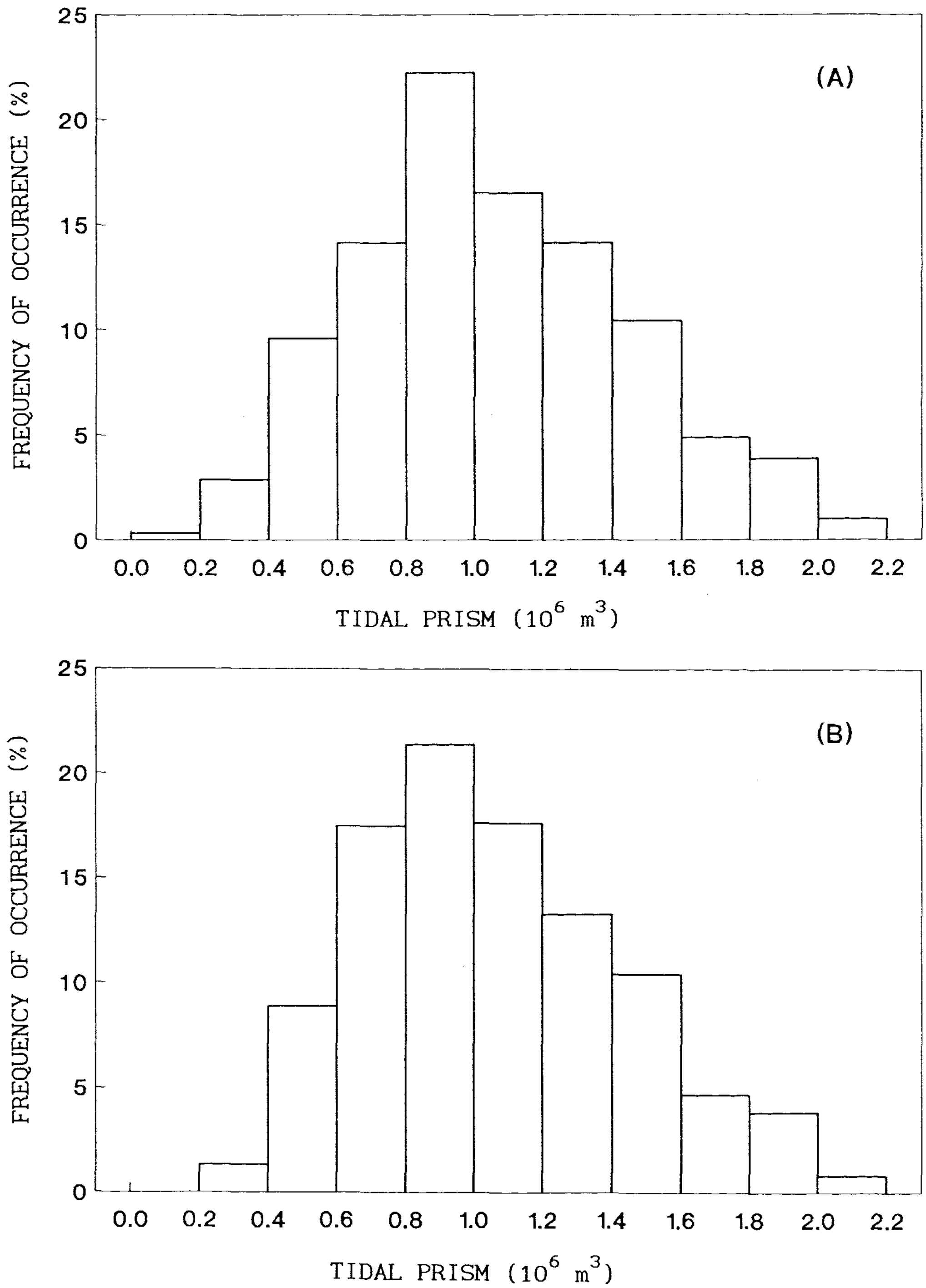

Figure 5-64. Frequency distributions of flood tidal prisms (A) and ebb tidal prisms (B), for Christchurch Harbour.

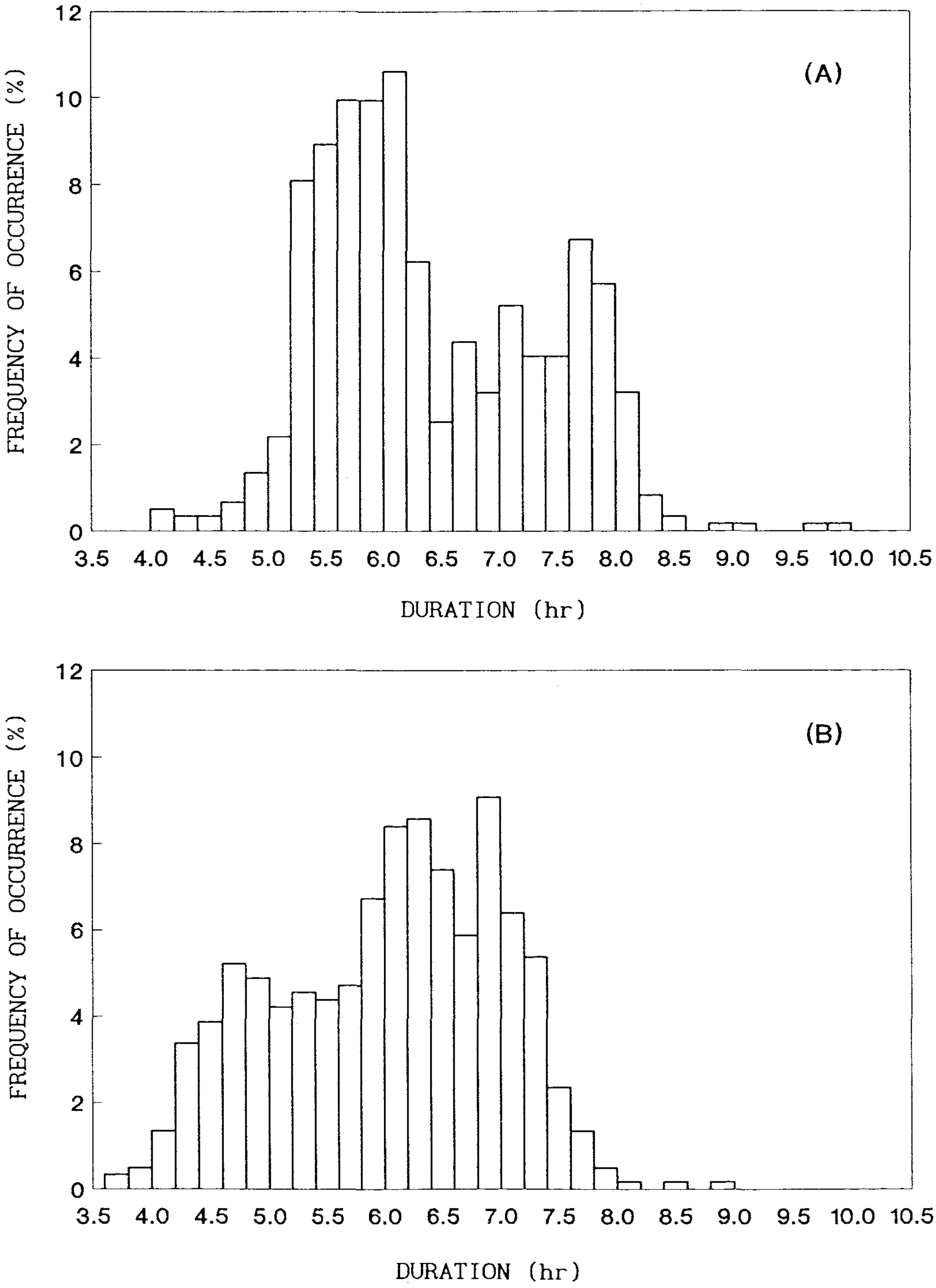

Figure 5-65. Frequency distributions of flood tidal durations (A) and ebb tidal durations (B), for Christchurch Harbour.

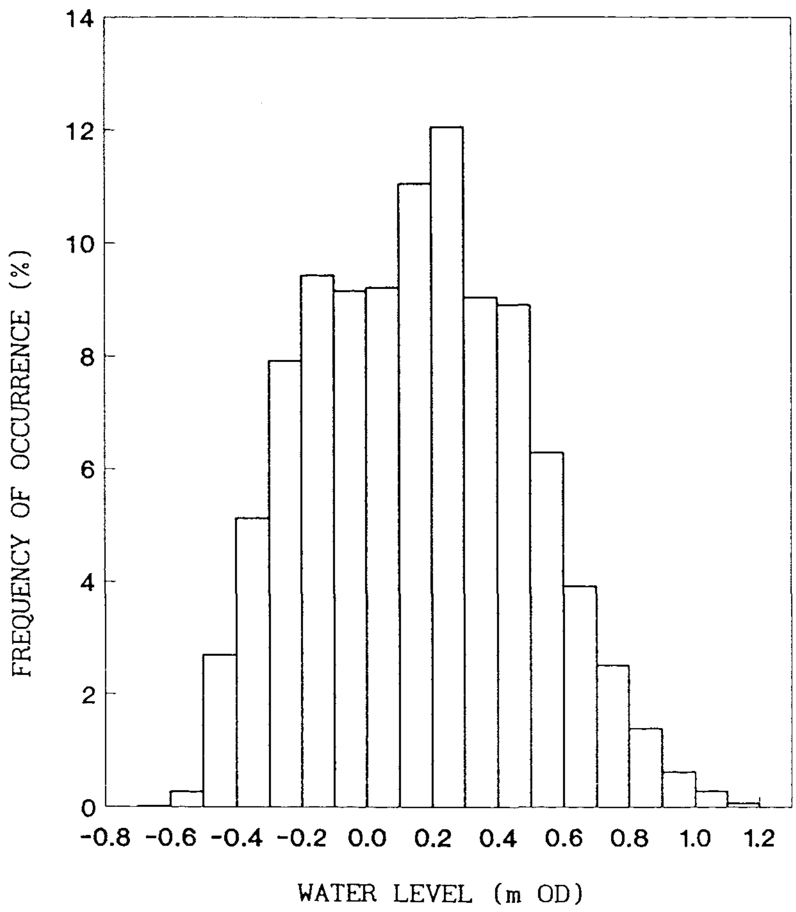

Figure 5-66. Frequency distributions of water levels at Mudeford Quay.

Equilibrium Cross-sectional Area

The equilibrium cross-sectional area (A_E) of Christchurch Harbour has been calculated according to Equation [4-52], averaged over 14799 cross-sectional area data, to be 136.0 m^2.

In early investigations (e.g. O'Brien 1969; Johnson 1973), the cross-sectional area below the mean sea level was used to represent the equilibrium value. The frequency distribution of water levels (Figure 5-66) results in the mean sea level of 0.15 m OD; the area below this level is 135.7 m^2. This value is very close to A_E, because of a nearly linear relationship between η and A (*cf.* Figure 5-24). In fact, if the η-A relationship is linear, then these two values must be the same. Let $A = a + b\ \eta$, then:

$$A_E = \int_{-\infty}^{\infty} P(\eta)\,(\,a + b\,\eta\,)\,d\eta$$
$$= a + b <\eta> = A_{<\eta>} \qquad [5\text{-}10]$$

where $P(\eta)$ is the frequency distribution function of the water levels and $A_{<\eta>}$ is the cross-sectional area below the mean sea level.

Hence, it is reasonable to replace A_E with $A_{<\eta>}$, because most entrance channels have a nearly constant width between high and low water levels.

Computation of $<U_f>$ *and* $<U_e>$

Based upon the frequency distribution of the currents during flood and ebb phases of the tides (Figure 5-47), mean flood current speed $<U_f>$ and mean ebb current speed $<U_e>$ are 0.165 and 0.556 m s^{-1}, respectively.

Using Equations [4-54] and [4-55], the relative importance of the fluctuating terms $<U_f'A'>$ and $<U_e'A'>$ can be examined. In this particular case, both terms are very small (3.4 and 1.1 % of $<U_f>$ A_E and $<U_e>$ A_E, respectively) and can be omitted. In many other cases they probably can be also neglected, due to their small magnitudes.

The significant current speed asymmetry is associated with only a weak time asymmetry. This feature should be attributable to relatively large freshwater discharges into the Harbour, due to the relationships shown in Equations [4-54] and [4-55]. Such an input has some effect of enhancing the ability of the inlet to maintain an equilibrium cross-section.

Because the equilibrium cross-sectional area is small, however, the inlet may be unstable in terms of Bruun's sense of stability; indeed this has been observed to be the case (Burton 1931; Steers 1946; Robinson 1955). The ebb tidal delta has been extended and breached periodically. During 1988 and 1992, the entrance channel on the ebb tidal delta changed its course on several occasions, between the eastern end of Mudeford Quay and a more easterly position. In the future, however, the stability is expected to improve because of a decrease in the amount of longshore transport around Hengistbury Head. A recent increase in the cross-sectional area (Section 5.1.1.) is indicative of a reduction of sediment supply.

5.6.2. Equilibrium of Langstone Harbour

Available Data

Between April 1973 and September 1974, an hydrographic survey was carried out to investigate the dispersion of sewage effluent within the inlet system (Portsmouth Polytechnic 1976). Information on tidal durations, freshwater discharges, surficial sediments and basin hypsometric features have been obtained from the results of the survey.

The tide in Langstone Harbour is quite regularly semi-diurnal. The double high waters, which is significant elsewhere over the Solent area, is less pronounced in Langstone Harbour. Average flood and ebb durations are 7.1 hr and 5.7 hr, respectively.

Freshwater discharge from the rivers is low, with a maximum daily inflow of 40.6×10^4 m^3 and a minimum of 10.3×10^3 m^3. In addition, there are two channels which connect Langstone Harbour with Portsmouth and Chichester Harbours, respectively (Figure 3-3). There is a net import of water from the large channelled connection with Chichester (3.50×10^6 m^3 on a spring tide and 0.97×10^6 m^3 on a neap) and a net export of water, through a small channel, to Portsmouth (0.73×10^6 m^3 on springs; 0.20×10^6 m^3 on neaps) (Portsmouth Polytechnic 1976). These water fluxes may be influenced also by weather conditions. On average, discharge from the freshwater and channel sources, other than the inlet entrance, is 45.0 m^3 s^{-1}. This input level is very small compared with volume flow through the inlet entrance.

Estimate of $<P>$

Figure 5-67 shows the hypsometric curve and characteristic tidal levels in Langstone Harbour, abstracted from the results of the survey. The cumulative curve of tidal basin water volume against water levels (derived from Figure 5-67) is shown on Figure 5-68.

In order to estimate the mean tidal prism, it is assumed that, during a spring-neap tidal cycle (taken as a nominal 15 days):

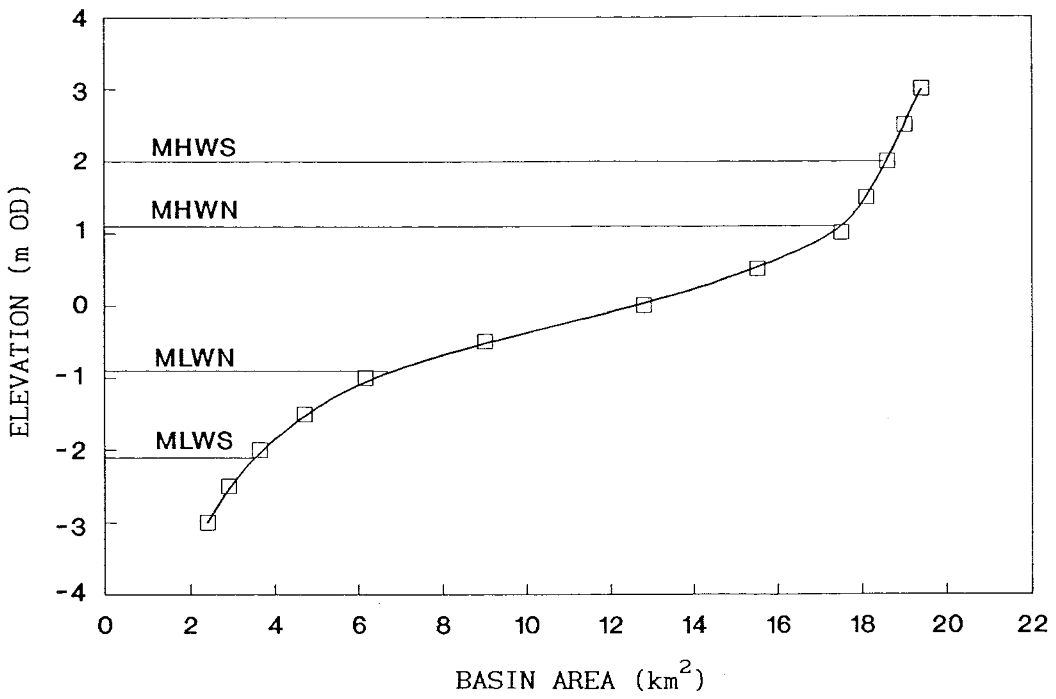

Figure 5-67. Hypsometric curve and characteristic water levels for Langstone Harbour (after Portsmouth Polytechnic, 1976).

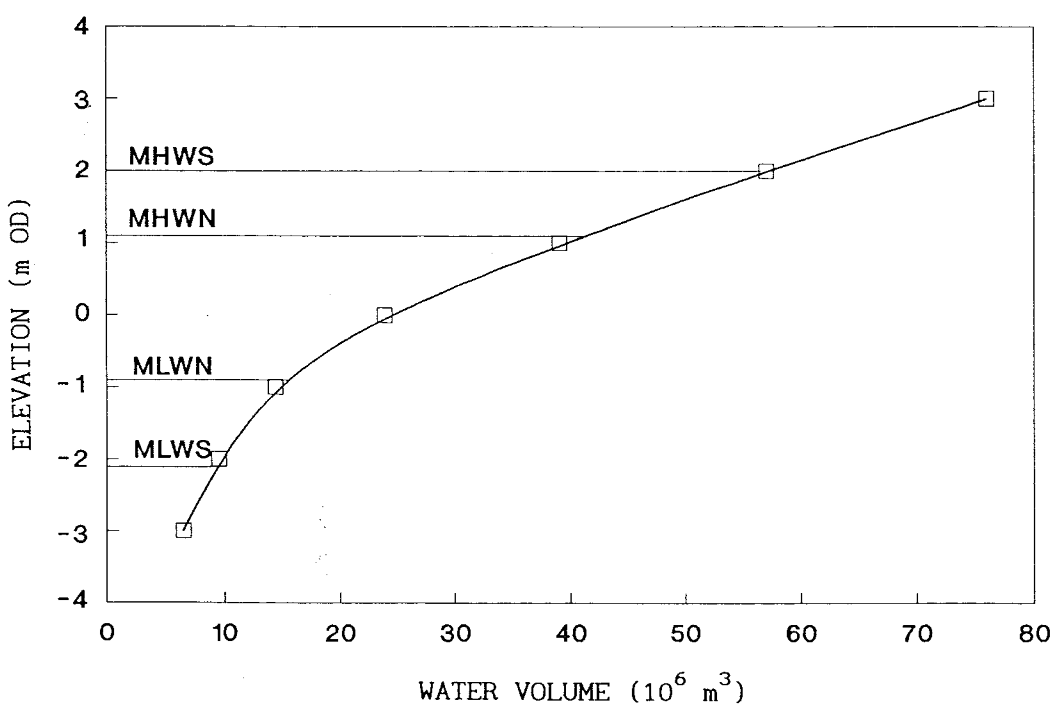

Figure 5-68. Relationship between water level and water volume for Langstone Harbour, as derived from Figure 5-67.

$$H_h = \frac{H_{h,s} + H_{h,n}}{2} + \frac{H_{h,s} - H_{h,n}}{2} \sin(\frac{2\pi}{15} t) \qquad [5\text{-}11]$$

$$H_l = \frac{H_{l,s} + H_{l,n}}{2} + \frac{H_{l,s} - H_{l,n}}{2} \sin(\frac{2\pi}{15} t) \qquad [5\text{-}12]$$

where H_h is high water level and H_l is low water level, with the subscripts *s* and *n* denoting spring and neap tides, respectively. Based upon these assumptions, a time series of tidal prisms were obtained from Figures 5-67 and 5-68. The mean tidal prism is estimated then to be 3.5×10^7 m^3.

Estimate of A_E, $<U_f>$ and $<U_e>$

A comparison between recent and old maps (charts) of the region (Figure 5-69) shows that the waterways within the harbour and the position of the harbour entrance has changed little since 1810; this indicates that the inlet is in equilibrium and stable within an historical time scale. In the present analysis, therefore, A_E is represented by $A_{<\eta>}$. As measured from Admiralty Chart No. 3418 published in 1974, the cross-sectional area of the entrance below the mean sea level is 3.20×10^3 m^2, with a width of 260 m and an average water depth of 12.3 m.

On the basis of Equations [4-54] and [4-55], $<U_f>$ and $<U_e>$ in the entrance of the harbour are estimated to be 0.44 m s^{-1} and 0.61 m s^{-1}, respectively.

Estimate of Sediment Discharges

Within the entrance section and to seaward of it, the sea bed is covered with sand and gravel. Along the eastern shoreline of the entrance, a shingle spit extends towards the tidal basin. Most of the tidal basin is characterised, however, by muddy sediments; these consist of a mixture of clay, silt and sand. No flood delta has developed and the major geomorphological features are the mud flats and salt marshes, especially in the inner (northern) part of the embayment. Some sand is present near to the harbour entrance (Dyer 1980), which seems to originate from a seaward source. The ebb delta consists of sand and gravel. The distribution patterns of surficial sediments show that net sediment transport rates through the entrance (q' in Equation [4-60]) should be low.

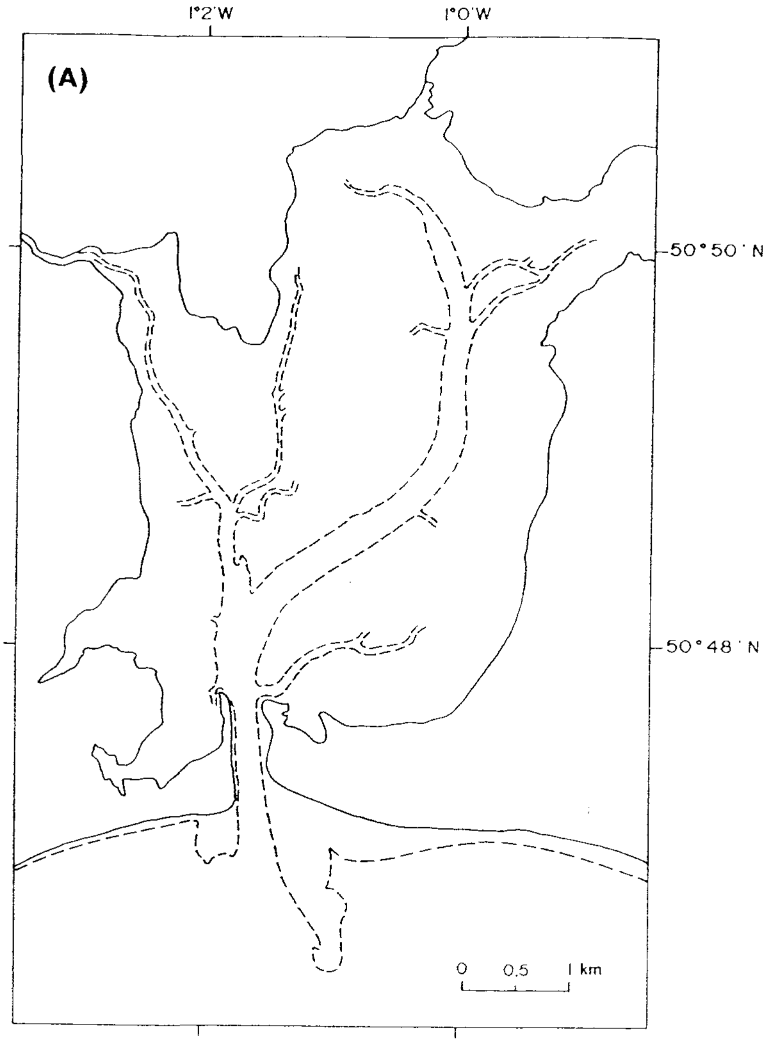

Figure 5-69 (A).

The term $k\ q_l$ in Equation [4-60] is now estimated, with $<q_{sf}>$ and $<q_{se}>$ derived on the basis of Equation [4-45]. For the use of Equation [4-45], k_l is taken as 4.48 kg $m^{-4}s^{-2}$, z_0 as 0.8 mm for the accelerating phase of the tide and 1.6 mm for the decelerating phase (Harris and Collins 1988), and C_{100cr} as 0.19 m s^{-1} (Dyer 1986) — because sediments in this channel entrance are dominantly "sandy" (Dyer 1980), although gravel is present on the beach. To determine the frequency distribution of the dimensionless current speeds, p(ß), a number of assumptions are made.

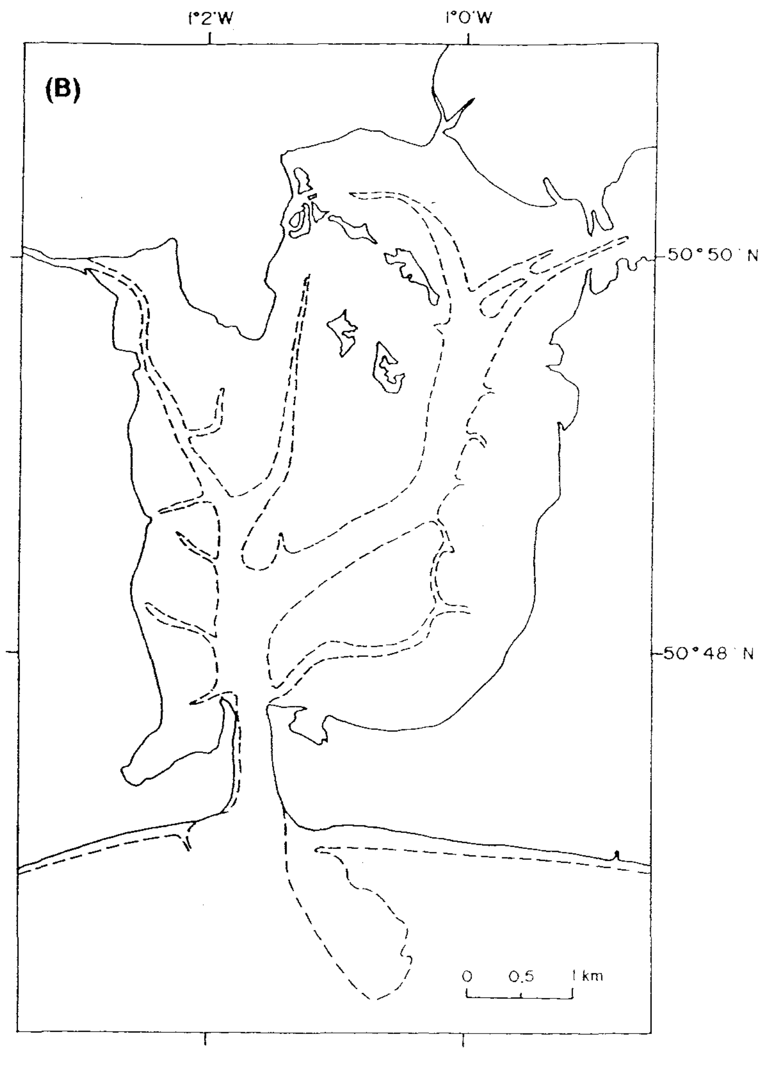

Figure 5-69. A comparison of the morphology of Langstone Harbour: (A) Sheet 86 of the first edition of the one-inch O.S. maps (published in 1810): and (B) Sheets 196 and 197 (published in 1989 and 1990, respectively) of 1:50000 O.S. Landranger Series. Solid lines denote MHWS and dashed lines represent MLWS.

Firstly, the channel width is considered to be much larger than the water depth, so that α_2 in Equation [4-42] equals unity.

Secondly, for both flood and ebb stages, the current speed varies periodically, according to:

$$U = \frac{U_0}{2} + \frac{U_0}{2} \sin t \qquad (0 \leq t \leq 2\pi) \qquad [5\text{-}13]$$

where U_0 is the peak speed during the flood or ebb.

Thirdly, U_0 also varies with spring-neap tidal cycles:

$$U_0 = \frac{U_{0,max} + U_{0,min}}{2} + \frac{U_{0,max} - U_{0,min}}{2} \sin(\frac{2\pi}{15} J) \qquad [5\text{-}14]$$

$$(J = 1, 2, ..., 15)$$

where $U_{0,max}$ and $U_{0,min}$ are U_0 values on spring and neap tides, respectively. Thus, a time-series of U is generated, from which $<U>$ and the frequency distribution of ß (= $U/<U>$) are determined. The resulting frequency distribution curve p(ß) is shown as Figure 5-70. Using this method, k q_l is estimated to be equivalent to a discharge of medium-sized sands of 2.2×10^9 kg yr^{-1} (i.e. approximately 1.38×10^6 m^3yr^{-1}, assuming a bulk sediment density of 1600 kg m^{-3}). This quantity should be understood as the transport capacity; if the sediments being transported involves coarser material, then the actual value will be considerably less.

No *in situ* measurements of the annual drift are available for comparison (Harlow (1979) has investigated into longshore transport over the area, but in terms of long-term averaged patterns only).

5.6.3. Equilibrium of Yangpu Harbour

Estimate of $<P>$

Data on tidal ranges within the tidal basin are not available, but this omission has been solved on the basis of the following relationship (O'Brien and Dean 1972):

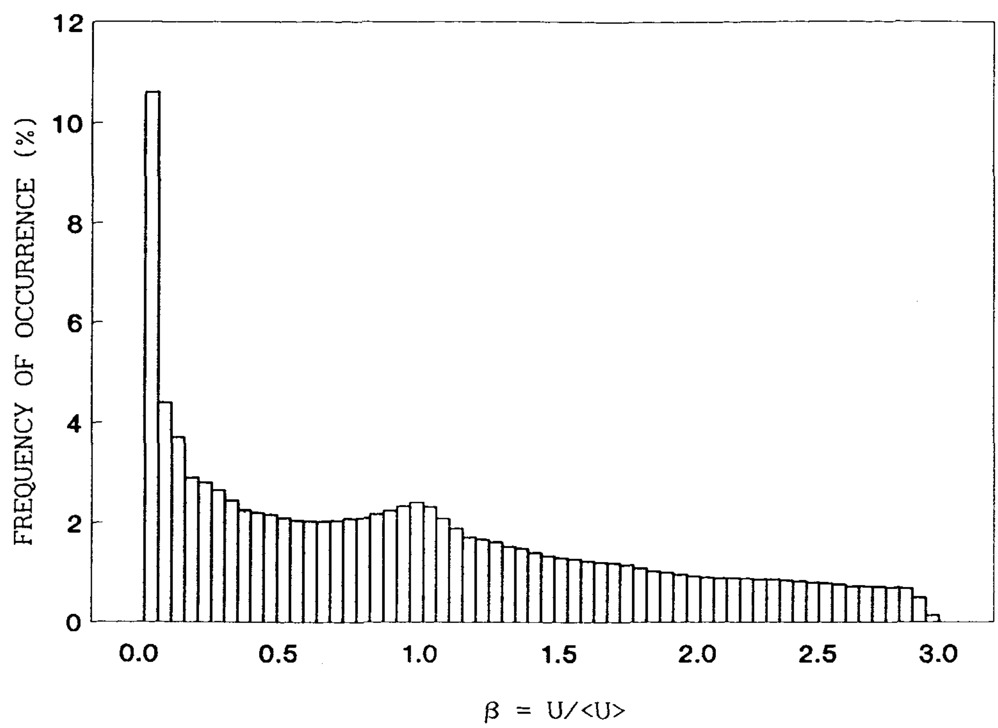

Figure 5-70. Frequency distribution function of dimensionless current speeds, p(ß).

$$\frac{R_b}{R_o} = f(\varepsilon) \qquad [5\text{-}15]$$

where R_b is the tidal range within the tidal basin, R_o is the open sea tidal range, and ϵ is the phase lag between R_b and R_o. The ratio R_b/R_o has been related to the phase lag (ϵ) through the use of a "repletion" coefficient (K) (O'Brien and Dean 1972). The method of defining K has been developed by Keulegan (1951).

If tides within the basin are characterised by standing tidal waves (i.e. the time of occurrence of high water corresponds to the slack water at the entrance), then ϵ is approximately the time lag of the slack water behind the time of high water measured at the entrance. According to tidal cycle measurements of water depths and current speeds at a number of stations and during different tides (i.e. spring, neap and intermediate tides) carried out between 1983 and 1985 (Zhu *et al.* 1984; Wang *et al.* 1985), slack water is on average 1.5 to 2 hr behind the high water time. Hence, ϵ is taken as 1.75 hr, which defines a R_b/R_o ratio of 0.97 on the basis of the $R_b/R_o \sim K$ and $K \sim \epsilon$ curves given by O'Brien and Dean (1972).

Outside Xinying Bay, the mean spring and neap tidal ranges are 3.23 and 0.52 m, respectively. Thus, the mean tidal ranges within the basin are 3.13 m over springs and 0.50 m over neaps.

The hypsometric curve of Xinying Bay has been obtained from measurements of plan areas below various elevations, on the 1:50000 charts for the region. The curve and resultant volume-elevation curve, together with characteristic water levels, are shown on Figures 5-71 and 5-72. Applying the same method used for Langstone Harbour to Yangpu Harbour, the average tidal prism here is 6.28×10^7 m^3, with a maximum value of 10^8 m^3.

Estimate of k q_l and q'

Within Xinying Bay and near the entrance, the surficial sediments are dominated by mud and there is no flood tidal delta. Outside of the entrance, sand and gravel are the main components of the surficial sediments. Consequently, the net bed-load discharge through the entrance (q') is considered to be very small.

Because Yangpu Bay is bordered with rocky shorelines to the north, the southern spit is the terminal of the northerly transport of sediments, by wave action on the beach. Further movement to the west is due largely to tidal currents; this implies that sediment movement near the entrance is mainly caused by tidal by-passing. The coefficient *k* in Equation [4-60] is, therefore, very close to unity.

The annual gross longshore drift (q_l) has been estimated using the CERC formula (Zhu *et al.* 1984). The results show a northerly transport of 5.9×10^4 m^{3}yr^{-1} and a southerly transport of 1.0×10^4 m^{3}yr^{-1}; q_l is, therefore, 6.9×10^4 m^{3}yr^{-1}.

Other Parameters

The tide at Yangpu is diurnal and highly regular. Time-asymmetry in the rising and falling phases of tide exists: the average durations of the flood and the ebb are 13.2 hr and 11.6 hr, respectively. The entrance is 480 m wide, with a mean depth of 12.1 m. Yangpu Harbour receives a limited amount of freshwater runoff (of around 25 m^{3}s^{-1}).

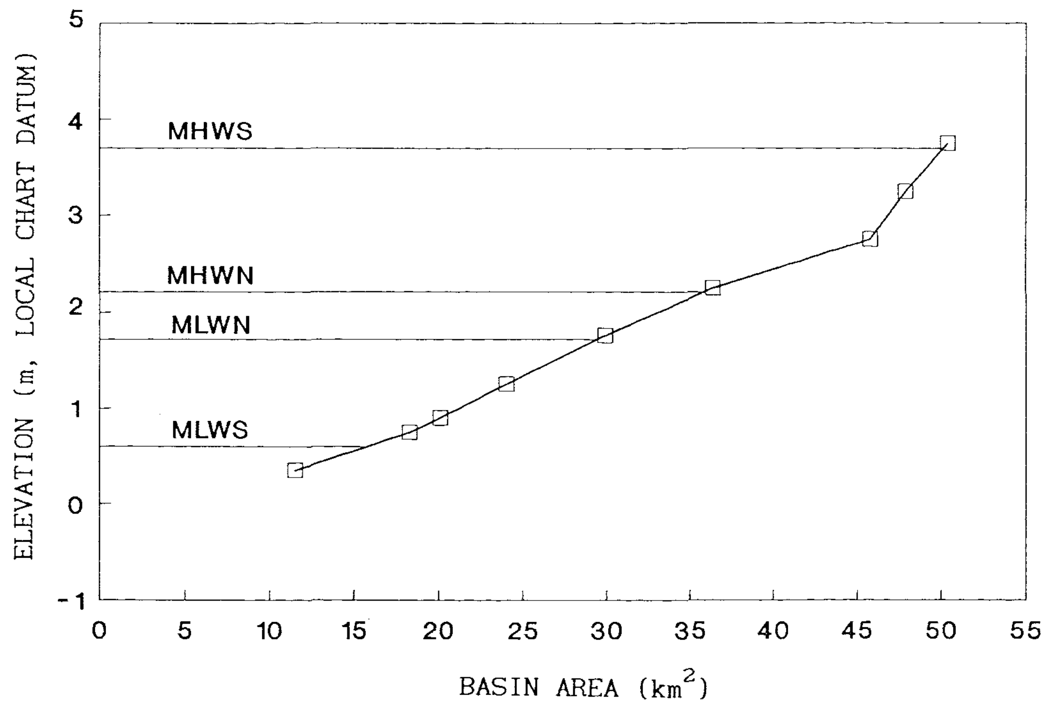

Figure 5-71. Hypsometric curve and characteristic water levels of Yangpu Harbour.

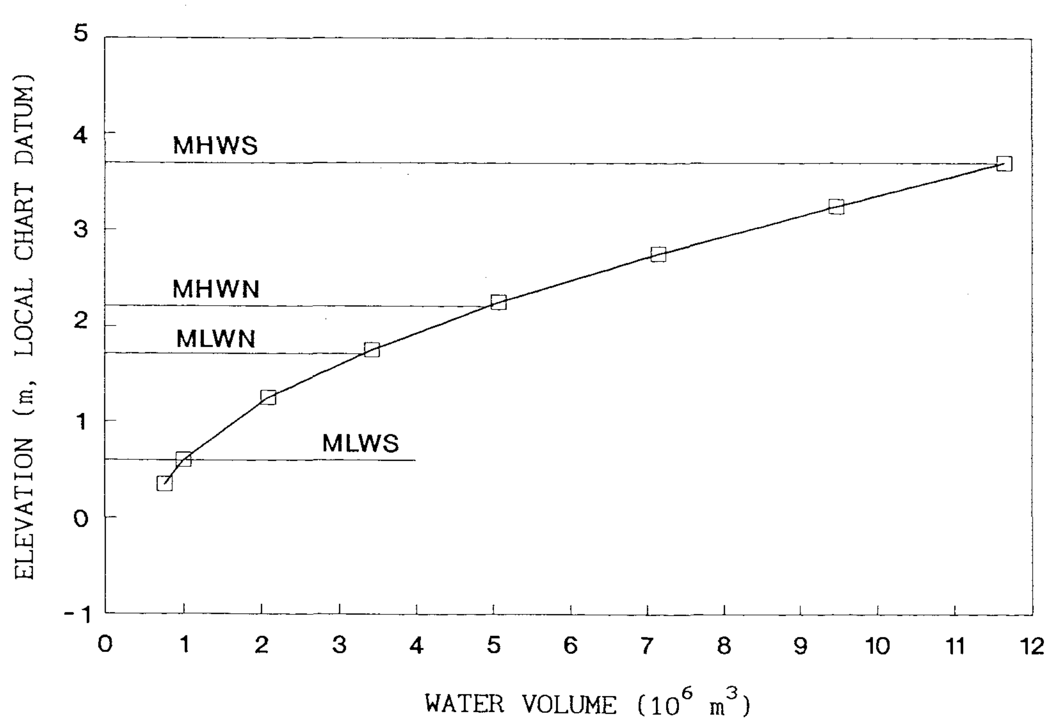

Figure 5-72. Relationship between water level and water volume in Yangpu Harbour, as derived from Figure 5-71.

Solutions for $<U_f>$, $<U_e>$ *and* A_E

Using the parameters derived above and adopting the same procedure of calculating sediment transport rates (with the same coefficient C and the function P(ß) appearing in Equation [4-45]) as applied to Langstone Harbour, the following equations are derived (based upon Equations [4-54], [4-55], [4-60] and [4-45]):

$$<U_f> A_E = 1.30 \times 10^3 \qquad [5\text{-}16]$$

$$<U_e> A_E = 1.53 \times 10^3 \qquad [5\text{-}17]$$

$$224.5 <q_e> - 255.5 <q_f> = \frac{\gamma \; 6.9\times10^4}{365 \times 86400} \qquad [5\text{-}18]$$

$$<\overline{q_e}> = 0.5 \int_{\beta_{0,e}}^{\beta_{max,e}} 4.48 \left[(0.83 \, \beta <U_e> - 0.19)^3 + (0.81 \, \beta <U_e> - 0.19)^3 \right] P(\beta) \, d\beta \qquad [5\text{-}19]$$

$$<\overline{q_f}> = 0.5 \int_{\beta_{0f}}^{\beta_{max,f}} 4.48 \left[(0.83 \, \beta <U_f> - 0.19)^3 + (0.81 \, \beta <U_f> - 0.19)^3 \right] P(\beta) \, d\beta \qquad [5\text{-}20]$$

where U_f and U_e are in m s^{-1}, A_E in m^2, and $<q_f>$ and $<q_e>$ in kg m^{-1} s^{-1}. The subscripts *e* and *f* represent ebb and flood, respectively. The parameter γ is the bulk density of the sediments (taken here as 1600 kg m^{-3}).

In Equations [5-13] to [5-17], $<U_f>$, $<U_e>$ and A_E are the unknowns. The solution of these values are $<U_f> = 0.216$ m s^{-1}, $<U_e> = 0.255$ m s^{-1} and $A_E = 6.0\times10^3$ m^2, respectively.

The current speed values can be compared with those estimated from current meter measurements. Averaged over a number of tidal cycle measurements, the mean flood and ebb tidal currents are 0.22 and 0.27 m s^{-1} , respectively (Zhang and Zhu 1989).

Based upon a study of the geomorphology and sedimentology of the area, the Yangpu inlet has been stable over the past 3000 yr, with only very small changes in the width and depth of the entrance channel (Zhang and Zhu 1989). At present, the cross-sectional area below the mean sea level is of the order of 5800 m^2, as measured from the 1:50000 chart of 1979. If this is taken as the equilibrium area, then the error of the value calculated in this study is small (3.5%).

5.6.4. Comparison of Equilibrium Conditions

The equilibrium conditions for Christchurch, Langstone and Yangpu Harbours are listed in Table 5-14. A comparison of the parameters relating to such tidal inlet equilibrium reveals the importance of other factors, apart from the tidal prism.

Firstly, equilibrium conditions differ with sediment transport patterns. If the current speeds in the entrance to Yangpu and Langstone Harbours were the same, then the equilibrium cross-sectional area of Yangpu would be smaller than that of Langstone (according to Equations [4-54] and [4-55]). This is not the case, however, due to the marked difference in the current speeds; in turn, this is due to differences in the intensity of the littoral drift (with the estimated annual gross longshore drift at Langstone being an order of magnitude greater than that at Yangpu).

Table 5-14. Equilibrium conditions of Christchurch, Langstone and Yangpu Harbours.

Inlet	T_e hr	T_f hr	$<P>$ 10^6m^3	$<Q_F>$ m^{3}s^{-1}	$<U_e>$ m s^{-1}	$<U_f>$ m s^{-1}	A_E m^2	$k\ q_l$ 10^4m^{3}yr^{-1}
Christchurch	6.0	6.4	1.1	27	0.56	0.17	136	2^x
Langstone	5.5	6.9	11.4	45	0.56	0.45	3200	138
Yangpu	11.6	13.2	34.1	25	0.26	0.22	5850	8

^{x} Averaged value for gravelly sediment transport rates, calculated using the Madsen-Grant (1976) and Vincent *et al.* (1981) equations.

This comparison demonstrates that, under the same conditions (of tidal prism, fresh water discharge and tide type), more intensive longshore transport of sediments leads to smaller cross-sectional area and stronger currents. In this analysis, the data from Christchurch Harbour are not comparable, because of the different transport equations which have been used.

Secondly, the type of tide is of some importance in influencing inlet stability. Tides are semi-diurnal in Langstone Harbour and diurnal in Yangpu Harbour. Hence, although the tidal prism of the latter is more than three times of that of the former, the cross-sectional area is only 0.8 times larger. If the intensity of sediment transport in Langstone Harbour were reduced to the same level as Yangpu Harbour, this effect would be even more significant.

Finally, freshwater discharge also influences inlet equilibrium conditions. In Langstone and Yangpu Harbours, the freshwater discharges are relatively low compared with the tidal prisms. As a result, the ratio $<U_f>/<U_e>$ is very close to T_e/T_f for both harbours. Christchurch Harbour, on the other hand, receives relatively large freshwater discharges and the velocity asymmetry is more significant in controlling sediment transport processes than the time asymmetry.

CHAPTER 6. DISCUSSION

6.1. The Use of Trace Sediments

The use of the mathematical model for tracer exchanges (Section 4.3.3.) provides examples which show that the mere presence of exotic tracers do not represent net transport directions. In fact, such a conclusion is indeed valid for all cases of trace sediment movement in tidally-influenced environments, as demonstrated below.

For Equation [4-25], if we let

$$C_b = C_b(t) \tag{6-1}$$

$$\frac{T_n}{V} = q(t) \tag{6-2}$$

$$-\frac{q_n}{V} = p(t) \tag{6-3}$$

then Equation [4-25] becomes a first order linear differential equation:

$$\frac{dC_b}{dt} = p(t)\ C_b(t) + q(t) \tag{6-4}$$

which has a general solution of

$$C_b(t) = e^{\int p(t)\,dt} \left(C_{b,0} + \int q(t)\ e^{-\int p(t)\,dt}\, dt \right) \tag{6-5}$$

Here, there will be no trace sediment present in the basin before sediment movement starts; $C_{b,0}$ should be zero. There are two possibilities for a instataneous value of T_n (defined by Equation [4-23]): (i) $T_n > 0$; and (ii) $T_n \leq 0$. A positive value of T_n implies that q(t) is a positive function; in this case, $C_b(t)$ will also have a positive value according to Equation [6-5]. Alternatively, if T_n is not a positive value, then C_m in Equation [4-23] must be positive so that $C_b(t)$ is also positive.

These observations demonstrate that as long as sediment transport is not always unidirectional, the exchange of sediments will result in net tracer transport but not necessarily net transport of the bulk sedimentary material.

The relationship between tracer movement and sediment transport is not important if artificial tracers are used for determination of the transport direction because, as described in Section 2.1.1., the net transport is represented by the centroid movement. In the case of natural tracers, however, the definition of the centroid movement is extremely difficult if not impossible; the observed concentration of the tracer within the tidal basin is indicative of the net transport direction only when it exceeds a certain critical level, as demonstrated previously (Section 5.5.1.). As shown in Section 5.5.2., in order to determine such a critical level accurately, the parameters (i.e. a_s, a_r and D_L) associated with dispersion must be known.

Due to a lack of knowledge of sediment dispersion processes, the analysis carried out in the present study is only preliminary. The parameters for the model input are estimated only in terms of magnitude. Further investigations are required to define quantitatively the three parameters for sedimentary environments, associated with various energy levels and dominant processes (i.e. tidally- or wave-dominated).

If the method is applied to an area associated with poorly-sorted material, the parameter k in Equation [4-23] must be defined to take into account of the differences in hydrodynamic behaviour between the tracer and the bulk sediments.

6.2. Interpretation of Grain Size Trends

6.2.1. The Need to Improve the "McLaren Method"

The model proposed by McLaren and Bowles (1985) for grain size trend analysis has been modified for use in the present study. Such a modification is essential to solve a number of problems associated with the original model, as analysed below.

Firstly, in their theory, McLaren and Bowles have argued that either Case 1 or Case 2 of grain size changes (Section 2.2.2.) will occur along a net transport path; on occasions, σ_2^2 might be larger than σ_1^2. This interpretation implies that $x=\mu_2-\mu_1$ and $y=S_{k1}-S_{k2}$ will always have the same signs. The relationship between x and y appears to be, however, more complicated than this (in the following analysis, the definitions for the mean, sorting coefficient and skewness in McLaren and Bowles (1985) are used). Because

$$x = \mu_2 - \mu_1 \qquad [6\text{-}6]$$

and

$$\sigma_2^2 = \int_{-\infty}^{\infty} (s - \mu_2)^2 \, d_2(s) \, ds \qquad [6\text{-}7]$$

we have:

$$\begin{aligned} y &= S_{k1} - S_{k2} \\ &= S_{k1} - (\sigma_2^2)^{-3/2} \int_{-\infty}^{\infty} (s - \mu_2)^3 \, d_2(s) \, ds \\ &= S_{k1} - (\sigma_2^2)^{-3/2} [\int_{-\infty}^{\infty} s^3 d_2(s) ds - 3 \, \sigma_2^2 (x+\mu_1) - (x+\mu_1)^3] \\ &= A \, x^3 + B \, x^2 + C \, x + D \end{aligned} \qquad [6\text{-}8]$$

where

$$A = (\sigma_2^2)^{-3/2} \qquad [6\text{-}9]$$

$$B = 3 \, \mu_1 \, A \qquad [6\text{-}10]$$

$$C = 3 \, (\sigma_2^2 + \mu_1^2) \, A \qquad [6\text{-}11]$$

$$D = S_{k1} - A \, [\int_{-\infty}^{\infty} s^3 \, d_2(s) \, ds - 3\sigma_2^2 \, \mu_1 - \mu_1^3] \qquad [6\text{-}12]$$

Equation [6-8] has only one real root, because

$$\begin{aligned} B^2 - 3AC &= 9\mu_1^2 A^2 - 3A \, 3(\sigma_2^2 + \mu_1^2)A \\ &= - 9\sigma_2^2 A^2 < 0 \end{aligned} \qquad [6\text{-}13]$$

Let the root be x_1. Corresponding to three possibilities (of $x_1 > 0$, $x_1 = 0$ and $x_1 < 0$) there are three patterns defined by the $x \sim y$ curves (Figure 6-1). For the situations when $x \neq 0$, there exists a gap with a width of $|x_1|$, in which x and y will have opposite signs. Because of this gap, whether x and y will always have the same sign remains a problem.

Secondly, the McLaren Method assumes that the probabilities of both Case 1 and Case 2 under "no transport" conditions are 1/8. To examine the validity of this assumption, let us consider the equations concerning the probabilities of Case 1 (P_b), and Case 2 (P_c). These are:

$$P_b = \underset{(P_1)}{P(\sigma_2^2<\sigma_1^2)}\ \underset{(P_2)}{P(\mu_2>\mu_1|\sigma_2^2<\sigma_1^2)}\ \underset{(P_4)}{P(S_{k1}>S_{k2}|\mu_2>\mu_1)} \qquad [6\text{-}14]$$

and

$$P_c = \underset{(P_1)}{P(\sigma_2^2<\sigma_1^2)}\ \underset{(P_3)}{P(\mu_2<\mu_1|\sigma_2^2<\sigma_1^2)}\ \underset{(P_5)}{P(S_{k1}<S_{k2}|\mu_2<\mu_1)} \qquad [6\text{-}15]$$

In the situation of "no transport", it can be proved that $P_1=1/2$. However, it is questionable that all the other probabilities (i.e. P_2, P_3, P_4 and P_5), are also 1/2. The reason for this is that P_2, P_3, P_4 and P_5 may be not completely independent of P_1. There are certain inherent relationships between mean grain size and sorting (Inman 1949; Griffiths 1967) and between the mean and the skewness (as shown in Equation [6-8]) within the grain size distributions of sediments from a particular environment. It may be not appropriate, therefore, to assume simply that both P_b and P_c, in any environment where there is no transport, are 1/8.

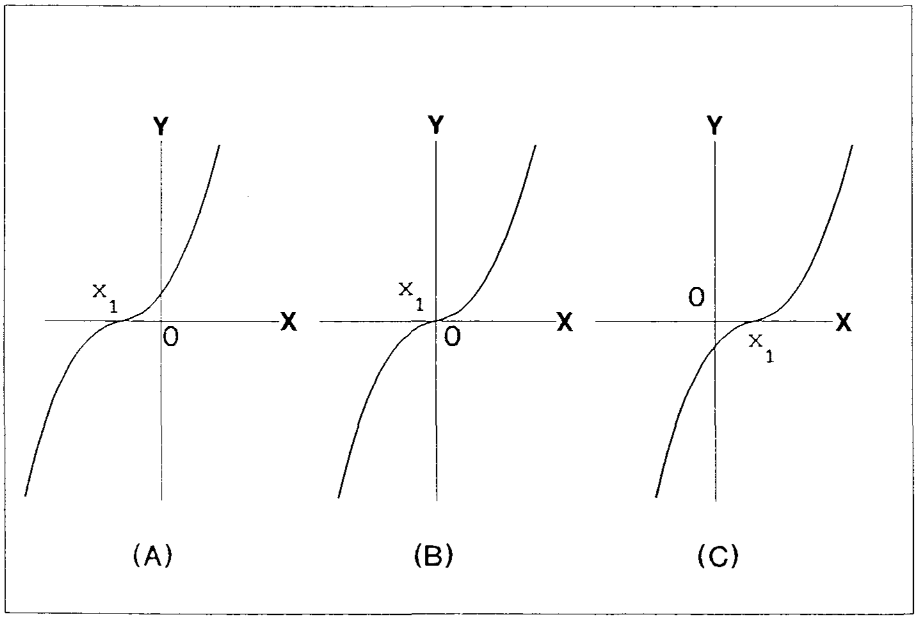

Figure 6-1. Three possible patterns represented by the x-y curves ($x=\mu_2-\mu_1$, $y=S_{k1}-S_{k2}$): (A) $x_1<0$; (B) $x_1=0$; and (C) $x_1>0$.

The result of the significance test designed by McLaren and Bowles (1985) are very sensitive to these two parameters. Equation [2-27] (for calculating the Z-score) can be rewritten as:

$$\frac{Z\sqrt{p(1-p)}}{\sqrt{N}} - \frac{N_x}{N} + p = 0 \qquad [6\text{-}16]$$

The relationship between $Z/N^{1/2}$ and N_x/N with various values of p is shown on Figure 6-2 by the solid lines, under the condition Z=2.330. The lower limit of N_x/N exceeding the significance level is defined by the intersection of a solid line (representing influence from p) and a dashed line (representing influence from N). For example, if 100 sediment samples are collected along a line and p=1/8 is used, then N_x/N must exceed 0.22 in order to define the transport direction. Figure 6-2 implies that the level of significance is related directly to the background probability used. If p is too low, then the Z-scores for both directions may be above the 99 % significance level, causing ambiguity in defining grain size trends.

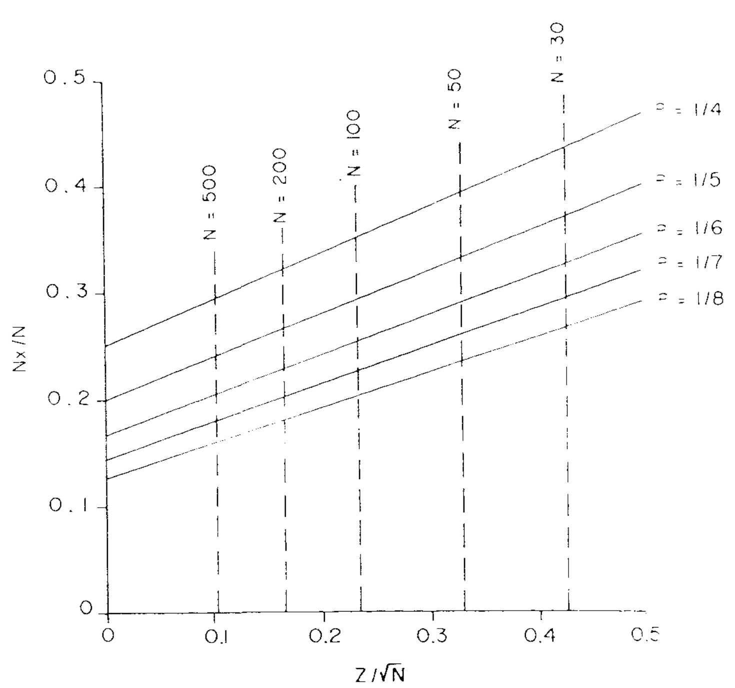

Figure 6-2. Relationship between $Z/N^{1/2}$ and N_x/N for different numbers of samples and background probabilities.

In the present study, the use of Z-scores has been avoided because of the difficulty of selecting an appropriate value. The new method for the significance test uses a critical level, which is based completely upon the grain size data themselves.

Finally, the McLaren Method considers all the possible n(n-1)/2 pairs, from n samples, along the survey line. The purpose of this approach is to satisfy the requirement of statistics, under the condition that there are only a limited number of samples available. However, the space scale is "confused" in this way. It does not mean the same to compare two neighbouring samples and two samples which are some distance apart. As a result of such a space scale confusion, the "noise" caused by samples with extreme grain size parameters or by additional sediment sources along the survey line, would be intensified.

6.2.2. Changes in Response to Transport Processes

In grain size trend analysis described previously, the trends used are based upon some empirical observations alone (i.e. the relationship between the trends and transport processes is unknown).

There are a number of mechanisms which cause changes in grain size parameters, in the course of transport. Some of the mechanisms have been reviewed by Russell (1939). The applicability of the grain size trend analysis depends largely upon which of the mechanisms dominates; these mechanisms are further discussed below.

Firstly, abrasion makes sedimentary particles finer along transport paths. For example and as early as 1875, a negative exponential decay function, which relates the weight of a particle to transport distance, was proposed by H. Sternberg (see Pettijohn *et al.* 1972). Such abrasion may be a significant control in relation to transport over long distances.

Secondly, selective transport results in changes in grain size parameters during transport, in response to a number of mechanisms.

Within the nearshore zone, grain size fining in the drift direction has been observed (Pettijohn and Ridge 1932; McMaster 1954; Self 1977); this has been attributed to the high erodibility of fine-grained particles, causing the rapid dispersal of material within the longshore currents. Using fluorescent sand tracers on beaches, however, very coarse sands have been found to move much faster than medium-grained sands (Komar

1977). Coarser grained particles tend to remain near the breaker zone and are transported, therefore, by the stronger longshore currents here. Finer grained sediments remain within the swash zone. Hence, sediments are likely to become coarser in the down-drift direction, under the influence of this differential movement.

Another coarsening trend in the direction of net wave-driven transport has been observed, for which a different mechanism has been suggested (McCave 1978). The winnowing effect of combined waves and strong tidal currents transfers fine-grained sediments progressively offshore, during longshore transport. Such a winnowing effect has been reported also by other investigators (Murray 1967; Nordstrom 1989).

For the transport of sediment by wind action, selective sorting relates to differences in transport modes and there is a general fining trend in the down-wind direction (Nickling 1983).

Selective transport can be caused also by differences in the particle densities; this has been reported, for example, for a beach environment (Komar and Wang 1984). This process leads to the enrichment of heavy minerals, resulting in the formation of a placer deposit. In flume experiments, grain sorting according to their density has been observed (Steidtmann 1982).

Finally, mixing of sediments, from different sources with different grain sizes and populations, can change significantly the grain-size characteristics. Along a beach, abrupt changes in grain size parameters are observed frequently; these are in response to the supply of new material, from a river or eroding cliff (e.g. Curray 1960; Self 1977; McManus *et al.* 1980). Likewise, in shallow marine environments, biogenic sediments (shell debris) act as additional sediment sources. Changes in grain size parameters, due to such mixing processes are somewhat unpredictable, destroying any ordered grain size patterns produced by the other mechanisms of transport; this makes the trends difficult to recognise.

Due to the various mechanisms, the grain size trend analysis is highly statistical in character i.e. an accepted pattern may be incorrect, although the probability of this is low, and rejection of a pattern does not necessarily mean that no net transport pattern exists.

On the basis of the analysis of such mechanisms (i.e. abrasion, selective sorting and mixing), further invstigations may be carried out to obtain an "theoretical" explanation of the grain size trends associated with transport pathways.

6.2.3. Time-Scales and Sampling Density

In interpreting the results of any grain size trend analysis, problems arise in defining the time-scale represented by the trends and the sampling density required by the analysis.

The observed grain size trends not only depend upon transport processes, but they are influenced also by sampling depth and density. To demonstrate this, a unidirectional sediment transport field is considered (i.e. with no lateral exchange of material), with a zero deposition rate. Further, deposited material and sediment in transport are assumed to have the same density and porosity.

For the analysis, let D be the sampling depth, R_D the grain size distribution function of thè sediments (within depth D), R_T the grain size distribution function of the material in transit, and q_s the volumetric sediment transport rate. For any grain-size, R is both time (t) and position (x, in the transport direction) dependent, in relation to sediment transport. $R_D(x,t+\Delta t)$ can be related to $R_D(x,t)$, by:

$$\begin{aligned} R_D(x,t+\Delta t) = \frac{1}{\Delta x\ \Delta y\ D} [\ & R_D(x,t)\ \Delta x\ \Delta y\ D \\ & + R_T(x,t)\ q_s(x,t)\ \Delta y\ \Delta t \\ & - R_T(x+\Delta x,t)\ q_s(x+\Delta x,t)\ \Delta y\ \Delta t\ ] \end{aligned} \qquad [6\text{-}17]$$

In the above equation, both $R_D(x,t+\Delta t)$ and $R_D(x,t)$ are defined over the area with a length of Δx and a width of Δy (Δx and Δy can be considered as the sampling intervals). Because a zero deposition rate is assumed ($\partial q_s/\partial x = 0$), we obtain from Equation [6-17]:

$$\frac{\partial R_D}{\partial t} = -\frac{q_s}{D}\frac{\partial R_T}{\partial x} \qquad [6\text{-}18]$$

The partial differential, with regard to the x-coordinate, of Equation [6-18] is:

$$\frac{\partial^2 R_D}{\partial x\ \partial t} = -\frac{q_s}{D}\frac{\partial^2 R_T}{\partial x^2} \qquad [6\text{-}19]$$

$$i.e. \quad \frac{\partial R_D}{\partial x} = - \frac{1}{D} \int_{t_1}^{t_2} q_s \frac{\partial^2 R_T}{\partial x^2} dt \qquad [6\text{-}20]$$

According to Equation [6-20] and if D is large, then the term on the left hand side will be small unless the time interval between t_1 and t_2 (in the integration on the right hand side) is sufficiently large. This relationship implies that, in order to obtain clearly-defined grain size trends, the sampling depth should not be too large. On the other hand, the sampling depth determines the time scale represented by the trend analysis. "Modern" net transport paths can be defined if the sampling depth is confined to the depth of disturbance which, in turn, depends upon the intensity of local hydrodynamic forces. In the present study of Christchurch and Yangpu Harbours, the actual sampling depth (5 to 10 cm) could be associated with a time-scale of the order of 1 to 10 years.

Equation [6-20] shows also that the sampling density, represented by Δx, is another crucial factor in the analysis. A small sampling interval can reduce greatly the magnitude of observed grain size trends between neighbouring sampling sites; thus, errors introduced by the grain size analysis may destroy the grain size trends. For example, excessive small sampling intervals for Christchurch Harbour have resulted in a rejected trend pattern (Section 5.4.1.). The sampling sites should not, therefore, be located too densely.

On the other hand, the sampling interval cannot be too large because, in addition to net transport processes, some grain size parameters are environmentally-sensitive (Friedman 1961, 1967, 1979; Allen 1971). Noise would be introduced, by comparisons between sampling sites in different environments as a result of excessively large sampling intervals. Consequently, although the sampling interval should be large to avoid noise introduced by grain size analysis, it must be small compared with the dimension of the sedimentary environment. The technique developed here may not be applicable, therefore, to areas where the types of sedimentary environment are highly variable over short distances (for example, a small area of intertidal flat associated with densely-distributed tidal creaks).

For the present investigation, the significance level of the grain size trends for Christchurch Harbour differs considerably from those for Yangpu Harbour. This characteristic is due probably to: (i) complicated transport processes introduced by superimposition of waves, tidal currents and river flows — combinations of all these are present over a small area at Christchurch, reducing the significance of any distinct trends; and (ii) the relatively small sampling intervals in the Christchurch area. In Yangpu Harbour, the environment is tidally- dominated and the sampling intervals are large compared with the dimension of the inlet system; the significance level of the grain size trends identified is, therefore, higher than those for Christchurch Harbour.

6.3. Stability of Tidal Inlets

6.3.1. P-A Relationships

The O'Brien method to determine a P-A relationship is applied widely because of its simplicity. Although there tends to be high correlation between $\log_{10}A$ and $\log_{10}P$, the two parameters (*c* and *n* in Equation [2-28]) vary for different regions of the world (Figure 6-3 and Table 6-1).

The wide range in *c* and *n* can be attributed to several causes. Firstly, some applications of the method appear to have distorted the original physical meaning of the O'Brien formula. For example, Shigemura (1980) classified the tidal inlets along the Japanese rocky coastlines into a number of groups, on the basis of the criterion A/A_b: *c* and *n* for each group were and then determined. In this way, the correlation between $\text{Log}_{10}A$ and $\text{Log}_{10}P$ was enhanced. However, because both variables (i.e. A and A_b) are associated with P and A themselves, the P-A relationship obtained cannot represent equilibrium conditions. In fact, the cross-sectional areas of these Japanese inlets are controlled mainly by geological structures, instead of modern hydrodynamic and sedimentary processes.

Secondly, a logical dilemma is associated with the O'Brien method itself. If all the inlets selected for analysis are already in equilibrium, then the derived P-A relationship will represent only an "average state" of equilibrium (i.e. all of the data points cannot be on the same regression line). Alternatively, if some of the inlets have not yet reached equilibrium, there will be some doubt as to whether or not the regression line actually represents equilibrium.

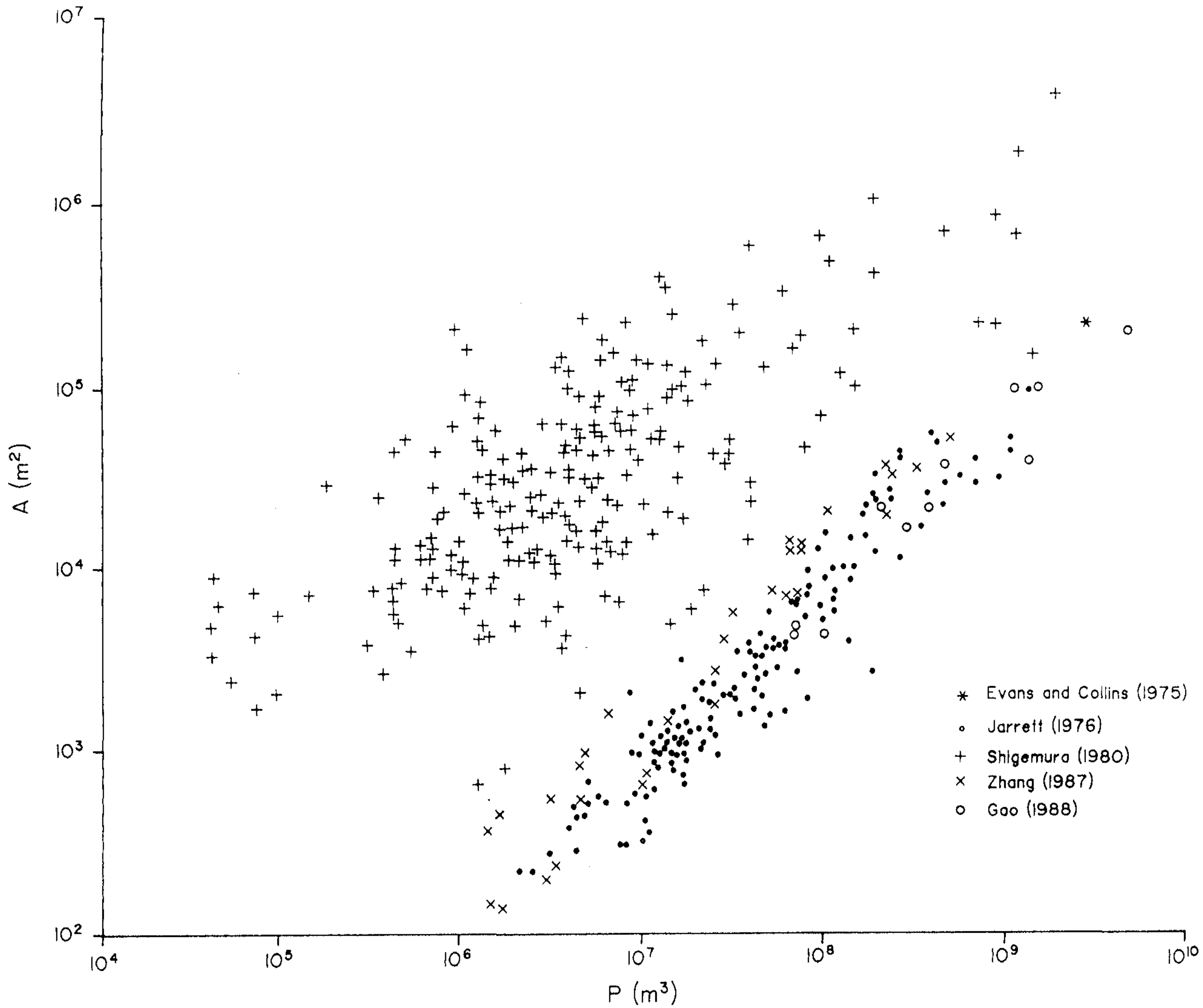

Figure 6-3. Inlet cross-sectional area related to tidal prism, for tidal inlets in the U.K. (Evans and Collins 1975), the U.S.A. (Jarrett 1976), Japan (Shigemura 1980), and China (Zhang 1987; Gao 1988).

Table 6-1. Variations of *c* and *n* in the A-P relationship (the O'Brien Method), based upon data from various references (P in km^3, A in km^2).

Location	Number of Inlets	c	n	R	Type of Inlets	References
PUSA	16	3.997×10^{-2}	0.85	-	N,S,T	O'Brien, 1931
PGAUSA	20	4.072×10^{-2}	0.85	-	S,T	O'Brien, 1969
PUSA	8	6.562×10^{-2}	1.00	-	N	O'Brien, 1969
PUSA	6	5.971×10^{-2}	1.00	-	N	Johnson, 1973
AUSA	79	8.564×10^{-2}	1.05	-	N,S,T	Jarrett, 1976
GUSA	36	3.381×10^{-2}	0.84	-	N,S,T	Jarrett, 1976
PUSA	47	4.387×10^{-2}	0.91	-	N,S,T	Jarrett, 1976
PJ	95	0.902	0.61	0.85	-	Shigemura, 1980
CJS	33	4.358	0.69	0.89	-	Shigemura, 1980
CKJ	71	0.235	0.45	0.74	-	Shigemura, 1980
ISCJ	32	0.337	0.68	0.66	-	Shigemura, 1980
CSCS	32	9.82×10^{-2}	0.96	-	N	Zhang, 1987
CECS	11	4.86×10^{-2}	0.92	0.97	N	Gao, 1988

Notes: R = Linear correlation coefficients, between $\log_{10}A$ and $\log_{10}P$; N = no jetty; S = single jetty; T = two jetties; PUSA = Pacific coast, U.S.A.; PGAUSA = Pacific, Gulf and Atlantic coasts, U.S.A.; AUSA = Atlantic coast, U.S.A.; GUSA = Gulf coast, U.S.A.; PJ = Pacific coast, Japan; CJS = Coast of Japan Sea; CKJ = West coast of Kyushu, Japan; ISCJ = Inland Sea coast, Japan; CSCS = Coast of South China Sea; and CECS = Coast of East China Sea.

Thirdly and probably most importantly, A_E is not controlled by the tidal prism alone, as indicated by the present study. Other factors, in addition to the tidal prism (i.e. the type of the tides, freshwater discharges, and the intensity of sediment transport within the inlet system), have an important influence on the control of equilibrium; this has been demonstrated (Section 5.6.4.) by comparing the equilibrium condition of Christchurch, Langstone and Yangpu Harbours.

In the analysis of equilibrium, therefore, sediment transport patterns should be emphasised particularly. For any inlet, in order to achieve equilibrium, there should be a balance between the transport capacity, provided by the currents through the entrance, and littoral transport (due to longshore currents). If the littoral drift is so large that the inlet system cannot provide currents (in terms of Equation [4-32]) strong enough to remove sediment from the entrance, then the equilibrium condition for the inlet does not exist. In this situation, Equation [4-53] in the previous definition is not valid. Such an inlet is not stable in terms of Escoffier's stability concept.

Also due to these reasons, A_E defined on the basis of the O'Brien method usually has a large error. For example, the P-A relationship for the inlets along the South China Sea coasts has been derived by Zhang (1987) (*cf.* Table 6-1) and the data from Yangpu Harbour are included. According to the derived line, A_E for Yangpu Harbour would be 11000 m^2, which implies a relative error of 90 %. For a more accurate evaluation of inlet stability, therefore, equilibrium conditions should be analysed individually for each inlet and by taking all the relevant factors into account.

6.3.2. Other Criteria

Escoffier's stability theory (1940) is based, as described previously, upon the equilibrium state of an inlet. Another theory (Bruun and Gerritsen 1960; Bruun 1978) relates the degree of stability to a number of empirical criteria, without considering equilibrium. One of these later criteria is the ratio P/M (Section 2.3.3.). The relationship between this criterion and the degree of stability, as determined empirically by Bruun (1978), is listed in Table 6-2.

Table 6-2 shows that the larger the ratio, the more stable is the inlet. This conclusion is consistent with the results of the present analysis, from the point of view of inlet equilibrium. If there is intensive littoral drift, a reduction in the cross-sectional area of the inlet will increase the current speed through the entrance, so as to maintain its equilibrium state. In this case, the equilibrium cross-sectional area is smaller than under conditions of weak littoral drift. Thus, on Escoffier's closure curve, A_E will move towards A_{cr} i.e. the inlet will become less stable.

Table 6-2. Stability conditions related to the ratio P/M, according to Bruun's stability concept (after Bruun, 1978).

P/M	Description of Stability Conditions
> 150[x]	Very good stability, with a small or no ebb tidal delta
100 ~ 150	Good stability, but an ebb tidal delta developed
50 ~ 100	Transitional stability condition, with a large ebb tidal delta which is close to the entrance but a channel through the delta still present
20 ~ 50[y]	Poor stability, with the entrance blocked by ebb tidal delta; remained open due to freshwater flows during storms
< 20	Very poor stability, with no permanent entrance channel

[x] Yangpu Harbour falls in this category.

[y] Christchurch Harbour falls in this category.

Another criterion is U_{max} (Section 2.3.3.). In Bruun's theory, U_{max} is close to 1.0 m s^{-1} for stable inlets. This view appears to be inconsistent, however, with the results of the present investigation. Equilibrium conditions for two examples of stable tidal inlets, from Langstone and Yangpu, show that it is not necessary for an inlet to be associated with a particular current speed to be stable. Instead, the current speed corresponding with stability can vary, depending upon sediment transport factors. In Langstone Harbour, U_{max} reaches 1.8 m s^{-1}; in Yangpu Harbour, however, it reaches only 0.67 m s^{-1}.

The criteria which have been defined appear, further, to contradict each other. For example, a statistical investigation carried out by Bruun and Gerritsen (1960) has shown that tidal inlets with a relatively high degree of stability have a high P/M ratio, but a low flushing force (represented by shear stresses applied to the bed). For any inlet in equilibrium, the current speed is controlled by the patterns of sediment transport. The current speed criterion cannot be used, therefore, as a reliable means to assess stability.

Rather, a complete understanding is required of longshore drift, tidal prism and freshwater discharge from land runoff; this was demonstrated in Section 5.6.4., with examples from Christchurch, Langstone and Yangpu Harbours.

Further, the criterion P/M does not include the influences of the type of tides and freshwater discharges. It may be more appropriate to replace P/M with a dimensionless parameter K_c:

$$K_c = \frac{T_{semi}}{T'} \frac{P + 0.5\, T\, Q_F}{T\, M} \qquad [6\text{-}21]$$

where T_{semi} is the period for semi-diurnal tides (i.e. 12.42 hr), T' is a unit time (taken as one second here), T is the tidal period, and Q_F is the freshwater discharge. If there is no freshwater input and the tide is semi-diurnal, then K_c reduces to P/M in terms of magnitude (i.e. the criterion P/M can be used under such conditions).

For applicability of K_c, Christchurch may be taken as an example. The spring tidal prism here is around 1.8×10^6 m^3 (as estimated from the data shown on Figure 5-64) and longshore transport rate has been estimated to be of the order of 5.3×10^4 m^3yr^{-1} (Nicholls and Wright 1991). Thus, P/M is around 34. Such an inlet would be blocked for majority of the time. The actual situation at Christchurch is that the entrance may be blocked only occasionally i.e. the inlet can be best described as being transitional between the description for the range $20<P/M<50$ and that for $50<P/M<100$.

On the other Hand, K_c is around 45 for Christchurch, using T=12.42 hr and Q_F=26.9 m^3 s^{-1}. Such a value is close to the boundary of the two situations (i.e $20<K_c<50$ and $50<K_c<100$) and appears to provide a better description of the stability conditions.

In essence, the stability is controlled by a combined effect of the flushing ability of the inlet and the amount of sediment input into the entrance channel. Thus, the dimensionless parameter k, defined in Equation [4-60], may be used as a criterion for stability. In Equation [4-60], if q' is assumed to be small, then we have:

$$k = -\frac{T_f <B\, \overline{q_{sf}}> + T_e <B\, \overline{q_{se}}>}{(T_f + T_e)\, q_l} \qquad [6\text{-}22]$$

It is clear that k represents a ratio between the transport capacity which is provided by currents within the entrance and the magnitude of longshore transport. If k is close to unity, then the inlet is stable (this is the case for Langstone and Yangpu Harbours); if it is close to zero, then the inlet is unstable. For Christchurch, k is estimated to be between 0.21 and 0.55, using the sediment transport data obtained from Section 5.3.1. and longshore transport rate of 5.3×10^4 m^3yr^{-1} (Nicholls and Wright 1991). Such a value of k may be indicative of a transitional state of stability.

CHAPTER 7. SUMMARY

Four aspects associated with sediment dynamics and stability of tidal inlets have been investigated: (i) sediment transport rates due to currents and the combined effects of currents and waves; (ii) the exchange of natural trace sediment between the estuarine basin and adjacent continental shelf areas; (iii) grain size trends representing net sediment pathways in shallow marine environments; and (iv) equilibrium conditions of tidal inlets. The results obtained and the conclusions reached are summarised below.

Hydrodynamics

(1) The tides observed at Mudeford are semi-diurnal in terms of their Form Factor, with significant influences of the shallow water constituents (especially M_4 and MS_4). The phase difference between the M_2 and M_4 tides is close to 180°; this results in distinctive double high waters over the area. With regard to tidal range, the tides belong to micro-tidal category. These characteristics are caused by interaction between the oceanic (Atlantic) tides and regional bathymetric features.

(2) Current speeds within the entrance to Christchurch Harbour are derived on the basis of the time-series of water levels recorded at the Mudeford Quay and empirically-determined "apparent" basin areas. This method provides satisfactory results, which compare with field measurements.

(3) The currents within the Christchurch entrance are characterised by dominance of the fourth-diurnal constituents i.e. the M_4 and MS_4 constituents for the currents are amplified significantly. Strong currents occur frequently between the double high waters. The enhancement of the shallow water constituents is due to local bathymetric conditions.

(4) At Christchurch, the estuarine waters are stratified within the Harbour; they become vertically mixed at the entrance (especially on spring tides), forming a secondary plume outside the Harbour with a lowered degree of stratification. The turbidity maxima, characterised by SSCs of 35 mg l^{-1} on springs and 20 mg l^{-1} on neaps, move with the tidal currents and reach the open sea towards the final phase of the ebb.

Sediment Dynamics

(1) Over the Christchurch region, the seabed is characterised by erosion, on the basis of the interpretation of seismic images. The Tertiary deposits are exposed extensively and the Holocene marine or brackish sediment cover is thin i.e. generally less than 1.5 m. Sediment exchange between Poole and Christchurch Bays takes place mainly through the surf zone, around Hengistbury Head. Within the Harbour, the surficial sediments are dominated by sandy material; outside, the seabed sediments contain large percentages of gravels.

(2) Sediment transport rates under annually averaged conditions can be estimated on the basis of empirical transport formulae and the definition of a number of frequency distribution functions relating to characteristics of currents and waves. In the study of Christchurch Harbour, 4 of such functions have been defined.

(3) The entrance to Christchurch Harbour is characterised by significant velocity asymmetry, with a mean ebb current speed of 0.556 m s^{-1} and a mean flood current speed of 0.165 m s^{-1}. The channel is floored with very coarse material with a mean grain size of around 40 mm. Hence, sediment transport occurs mainly during the ebb phase of the tides and in association with wave action. Using the Madsen-Grant equation, average annual sediment discharges are estimated to be 650 m^3 towards the Harbour and 11800 m^3 towards the sea; this results in a net seaward discharge of 11150 m^3. Use of the Vincent equation results in larger estimates, with a landward discharge of 860 m^3, a seaward discharge of 29900 m^3 and a net seaward discharge of 29040 m^3. Longshore transport by waves on the beach is not included in these computations.

(4) Suspended sediments at Christchurch consist mainly of mud; the SSCs range between 5 and 35 mg l^{-1}, but can reach 75 mg l^{-1} or higher during storms. Net suspended sediment discharge through the entrance to the Harbour has been estimated to be 7.75×10^6 kg yr^{-1}, towards the sea (with a landward discharge of 4.51×10^6 kg yr^{-1} and a seaward discharge of 12.26×10^6 kg yr^{-1}). The river input is of the order of 8.48×10^6 kg yr^{-1}. Thus, most of the suspended matter supplied from freshwater sources escapes to the sea; this is due mainly to active water exchange processes and the resuspension of fine-grained sediments, which is intensified by the dominant westerly winds in combination with the shallow water environment of the Harbour.

(5) A mathematical model is established to simulate natural trace sediment

exchanges. Both conceptual experiments and theoretical analysis indicate that the mere presence of exotic trace material is not indicative of net sediment transport. In order to define the net transport direction, the observed level of trace concentration should be compared with a critical value, which results from a zero net transport. Further investigations are required, however, to identify the magnitude of the parameters associated with the sediment dispersion processes.

(6) Exchange processes for sand-sized material have been simulated for Christchurch Harbour, using exotic benthic foraminiferal tests as the tracer. Using the most probable quantities of sediment discharges and assumed parameters representing sediment dispersion processes, the critical values for zero net transport have been estimated for 23 cases; 20 of these estimated values are below the observed tracer concentration. Thus, the net sediment transport appears to be directed to landward.

(7) Grain size trend analyses, based upon the McLaren method are associated with a number of limitations: (i) the assumption that an increase (decrease) in the mean grain size is related always to a decrease (increase) in skewness in the transport direction; (ii) the significance test, in terms of a critical level and with some degree of uncertainty; and (iii) the difficulty in forming survey lines without introducing enhanced "noise" (or bias).

(8) Modification to the McLaren model has been proposed, on the basis of definition of the "transport vectors". This approach avoids the difficulty of forming survey lines. Further, a new procedure for the significance test has been established, which determines the critical significance level from the frequency distribution of the characteristic vector lengths; these, in turn, represent patterns of background noise.

(9) The procedure for grain size trend analysis, developed here, can be applied to marine environments in general. For such an analysis, the area under investigation should be sampled at an interval large enough to reflect the real grain size trends resulting from net sediment transport, but small when compared with the dimensions of the sedimentary environment under investigation. The time-scale of the results depends upon the sampling depth. Application of the technique is likely to be somewhat limited, therefore, where the environment is highly variable over short distances. Further, due to its statistical character, the analysis may fail to identify net transport patterns.

(10) Grain size trends have been identified for Christchurch and Yangpu Harbours, at the 90 % and 99 % significance levels, respectively. At Christchurch, the trends show landward transport in the entrance (which is consistent with the result

derived from the simulation of exchange of trace sediments *cf.* (6)), on the flood tidal delta and to the north of the delta. Seaward transport is associated with the river channel in the southern part of the Harbour. At Yangpu, the trends show that dominant transport directions within the tidal basin are towards the bay-head areas, with seaward transport near the entrance. Outside the embayment, there is a clockwise circulation of sediments. These trends are supported by some geomorphological and sedimentological evidence.

Morphodynamics

(1) Equilibrium conditions of tidal inlets can be determined analytically, based upon the conservation of water and sediment masses. Sediment transport patterns, freshwater discharges, and flood and ebb tidal durations are other factors which affect the equilibrium, in addition to the tidal prism. Thus, the use of the P-A relationship (the "O'Brien Method") or the U_{max} criterion (the "Bruun Method") is inadequate to define the equilibrium.

(2) An analytical approach to inlet equilibrium has been developed so that equilibrium cross-sectional area for individual inlet systems can be defined. Further, the factors affecting equilibrium are used to form two criteria (i.e. K_c and k), to evaluate the degree of stability according to Bruun's concept.

(3) Equilibrium of the three inlets has been examined. In Langstone and Yangpu, the equilibrium cross-sectional areas are relatively large, with longshore sediment rates on the beach being of the same order of the net transport rates in the channel. Hence, the inlets are highly stable. In Christchurch Harbour, however, the cross-sectional area is small and the transport rate in the channel is much smaller than that due to waves on the beach. Consequently, the inlet has been shown to be unstable. Nevertheless, the degree of stability of the inlet is much higher than would be according to Bruun's P/M criterion, due to relatively large freshwater discharges into the Harbour.

REFERENCES

Ackers, P. and White, W. R. 1973 Sediment transport: new approach and analysis. *Journal of Hydraulics Division*, ASCE, 99, 2041-2060.

Allen, G. P. 1971 Relationships between grain size parameter distribution and current patterns in the Gironde Estuary (France). *Journal of Sedimentary Petrology*, 41, 74-88.

Allen, J. R. L. 1965 A review of the origin and characteristics of recent alluvial sediments. *Sedimentology*, 5, 89-191.

Amein, M. 1975 Computation of flow through Masonboro Inlet. *Journal of the Waterways, Harbors and Coastal Engineering Division*, ASCE, 101(WW1), 93-108.

Aubrey, D. G. and Speer, P. E. 1984 Updrift migration of tidal inlets. *Journal of Geology*, 92, 531-545.

Aubrey, D. G. and Speer, P. E. 1985 A study of non-linear tidal propagation in shallow inlet/estuarine systems, Part I: Observations. *Estuarine, Coastal and Shelf Science*, 21, 185-205.

Aubrey, D. G. and Weishar, L. (editors) 1988 *Hydrodynamics and Sediment Dynamics of Tidal Inlets*. Springer-Verlag, New York. 456pp.

Baba, J. and Komar, P. D. 1981 Settling velocities of irregular grains at low Reynolds Numbers. *Journal of Sedimentary Petrology*, 51, 121-127.

Bagnold, R. A. 1956 The flow of cohesionless grains in fluids. *Philosophical Transactions of the Royal Society of London*, A249, 235- 297.

Bagnold, R. A. 1966 An approach to the sediment transport problem from general physics. *U.S. Geological Survey Professional Paper 422-I*, 37pp.

Bagnold, R. A. 1968 Deposition in the process of hydraulic transport. *Sedimentology*, 10, 45-56.

Bale, J. D. and Holley, E. R. 1989 Sand transport in Texas tidal inlets. *Journal of the Waterways, Port, Coastal and Ocean Division*, ASCE, 115, 427-443.

Barton, M. E. 1973 The degradation of the Barton Clay cliffs of Hampshire. *Quarterly Journal of Engineering Geology*, 6, 423-440.

Barrie, J. V., Emory-Moore, M., Luternauer, J. L. and Bornhold, B. D. 1988

Origin of modern heavy mineral deposits, north British Columbia continental shelf. *Marine Geology*, 84, 43-51.

Basumallick, S. 1966 Size differentiation in a cross-stratified unit. *Sedimentology*, 6, 35-68.

Battjes, J. A. 1967 Quantitative research on littoral drift and tidal inlets. In: **Lauff, G. H.** (Editor), *Estuaries*. American Association of Advancement of Science, Washington, D.C. p.185-190.

Bettess, P. 1984 Initiation of sediment transport in gravel streams. *Proceedings of the Institution of Civil Engineers*, 77, Part 2, 79-88.

Black, K. 1987 A numerical sediment transport model for application to natural estuaries, harbours and rivers. In: **Noye, J.** (editor), *Numerical Modelling: Application to Marine Systems*. Elsevier, Amsterdam. p.77-105.

Blain, W. R. 1980 *Tidal Hydraulics of the West Solent (Vol.1)*. Unpublished Ph.D. Thesis, Department of Civil Engineering, University of Southampton, 326pp.

Blissenbach, E. 1954 Geology of alluvial fans in semiarid regions. *Bulletin of the Geological Society of America*, 65, 175-200.

Boon, J. D. III and Byrne, R. J. 1981 On basin hypsometry and the morphodynamic response of coastal inlet systems. *Marine Geology*, 40, 27-48.

Boothroyd, J. C. 1978 Estuaries. In: **Davis, R. A. Jr.** (editor), *Coastal Sedimentary Environments*. Springer-Verlag, New York. p.445-532.

Boothroyd, J. C. 1985 Tidal inlets and tidal deltas. In: **Davis, R. A. Jr** (editor), *Coastal Sedimentary Environments (second edition)*. Springer-Verlag, New York. p.445-532.

Bristow, C. R., Freshney, E. C. and Penn, I. E. *1991 Geology of the Country Around Bournemouth*. Her Majesty's Stationery Office, London, 116pp.

Brown, C. B. 1950 Sediment transportation. In: **Rouse, H.** (editor), *Engineering Hydraulics*. John Wiley, New York. p.769-857.

Brown, E. I. 1928 Inlets on sandy coasts. *Proceedings of the American Society of Civil Engineers*, 54, 505-553.

Brown, L. 1987 ^{10}Be as a tracer of erosion and sediment transport. *Chemical Geology*, 65, 189-196.

Bruun, P. 1978 *Stability of Tidal Inlets*. Elsevier, Amsterdam, 506pp.

Bruun, P. and Gerritsen, F. 1959 Natural bypassing of sand at coastal inlets. *Journal* *of Waterways and Harbors Division*, ASCE, 85, 75-107.

Bruun, P. and Gerritsen, F. 1960 *Stability of Coastal Inlets*. North-Holland, Amsterdam, 123pp.

Bryant, E. 1982 Behaviour of grain size characteristics on reflective and dissipative foreshores, Broken Bay, Australia. *Journal of Sedimentary Petrology*, 52, 431-450.

Burton, E. St. J. 1931 Periodic changes in the position of the Run at Mudeford. *Proceedings of the Geologists' Association*, 42, 157-174.

Burton, H. 1933 The Plateau Gravels of the Bournemouth area. *Proceedings of the Geologists' Association*, 44, 314-335.

Byrne, J. V. and Kulm, L. D. 1967 Natural indicators of estuarine sediment movement. *Journal of the Waterways and Harbors Division*, ASCE, 93(WW2), 181-194.

Carr, A. P. 1969 Size grading along a pebble beach: Chesil Beach, England. *Journal of Sedimentary Petrology*, 39, 297-311.

Chadwick, A. and Morfett, J. 1986 *Hydraulics in Civil Engineering*. Harper Collins Academic, London, 492pp.

Chien, N. 1956 The present status of research on sediment transport. *Transactions of the American Society of Civil Engineers*, 121, 833- 868.

Clifton, H. E. and Hunter, R. E. 1973 Bioturbation rates and effects in carbonate sand, St. John, U.S. Virgin Islands. *Journal of Geology*, 81, 253-268.

Collins, M. B. 1970 Discussion of design curves for suspended load estimation. *Proceedings of Civil Engineers*, 46, 85-88.

Collins, M. B. 1981 Sediment yield studies of headwater catchments in Sussex, SE England. *Earth Surface Processes and Landforms*, 6, 517-539.

Collins, M. B. and Rigler, J. K. 1982 The use of settling velocity in defining the initiation of motion heavy mineral grains, under unidirectional flow. *Sedimentology*, 29, 419-426.

Codrington, T. 1870 On the superficial deposits of the south of Hampshire and the Isle of Wight. *Quarterly Journal of the Geological Society of London*, 26, 528-551.

Crickmore, M. J. and Lean, G. H. 1962 The measurement of sand transport by means of radioactive tracers. *Proceedings of the Royal Society of London*, A266, 402-421.

Crickmore, M. J. 1967 Measurements of sand transport in rivers with special reference to tracer methods. *Sedimentology*, 8, 175-228.

Cross, J. and Webber, N. B. 1978 *Christchurch Harbour - Surveying and Sediment Sampling*. Report to Christchurch Borough Council, Department of Civil Engineering, University of Southampton, 3pp (plus figures).

Curray, J. R. 1960 Tracing sediment masses by grain-size modes. *Proceedings of the 21st Geological Congress*, p.119-130.

Curry, D. 1976 The age of the Hengistbury Beds (Eocene) and its significance for the structure of the area around Christchurch, Dorset. *Proceedings of the Geologists' Association*, 76, Part 2, 151-173.

Curry, D. and Smith, A. J. 1975 New discoveries concerning the geology of the central and eastern part of the English Channel. *Philosophical Transaction of the Royal Society of London*, A279, 155-167.

Davies, J. L. 1964 A morphogenic approach to world shorelines. *Zeitschrift für Geomorphologie*, 8, 27-42.

Devoy, R. J. 1982 Analysis of the geological evidence for Holocene sea- level movements in southeast England. *Proceedings of the Geologists' Association*, 93, 65-90.

Dingler, J. R. 1979 The threshold of grain motion under oscillatory flow in a laboratory wave channel. *Journal of Sedimentary Petrology*, 49, 287-294.

Diplas, P. 1987 Bedload transport in gravel-bed streams. *Journal of Hydraulic Engineering*, ASCE, 113, 277-292.

D'Olier, B. 1979 Side-scan sonar and reflection seismic profiling. In: **Dyer, K. R.** (editor), *Estuarine Hydrography and Sedimentation*. Cambridge University Press, Cambridge. p.57-86.

Doodson, A. T. and Corkan, R. H. 1931 The principal constituent of the tides in the English and Irish Channels. *Philosophical Transaction of the Royal Society of London*, A231, 29-53.

Drake, T. G., Shreve, R. L., Dietrich, W. E., Whiting, P. J. and Leopold, L. B. 1988 Bedload transport of fine gravel observed by motion-picture photography. *Journal of Fluid Mechanics*, 192, 193-217.

Dyer, K. R. 1969 *Some Aspects of Coastal and Estuarine Sedimentation*. Unpublished Ph.D. Thesis, University of Southampton, 102pp (plus figures).

Dyer, K. R. 1970 Sediment distribution in Christchurch Bay, S. England. *Journal of Marine Biological Association of U.K.*, 50, 673-682.

Dyer, K. R. 1975 The buried channels of the "Solent River", southern England. *Proceedings of the Geologists' Association*, 86, 239-245.

Dyer, K. R. 1980 Sedimentation and sediment transport. In: *The Solent Estuarine System*. The National Environment Research Council Publications, Series C, No.222, 20-24.

Dyer, K. R. 1986 *Coastal and Estuarine Sediment Dynamics*. John Wiley, Chichester, 342pp.

Dyer, K. R., Hamilton, N. and Pingree, R. D. 1969 A seismic refraction line across the Solent. *Geological Magazine*, 106, 92-95.

Einstein, H. A. 1942 Formulae for the transportation of bedload. *Transaction of the American Society of Civil Engineering*, 107, 561- 577.

Einstein, H. A. 1950 *The bed-load function for sediment transportation in open channel flows*. Technical Bulletin No.1026, U.S. Department of Agriculture, Washington D.C., 78pp.

Eisma, D., Gaast, van der S. T., Martin, J. M. and Thomas, A. T. 1978 Suspended matter and bottom deposits of the Orinoco delta: turbidity mineralogy and elementary composition. *Netherlands Journal of Sea Research*, 12, 224-251.

Escoffier, F. F. 1940 The stability of tidal inlets. *Shore and Beach*, 8, 114-115.

Evans, G. and Collins, M. B. 1975 The transportation and deposition of suspended sediment over the intertidal flats of the wash. In: **Hails, H. and Carr, A.** (editors), *Nearshore Sediment Dynamics and Sedimentation*. John Wiley, London, p. 273-306.

Everard, C. E. 1954 The Solent River: a geomorphological study. *Transaction of Institution of British Geographers*, 20, 41-58.

Falconer, R. A. and Owens, P. H. 1990 Numerical modelling of suspended sediment fluxes in estuarine waters. *Estuarine, Coastal and Shelf Science*, 31, 745-762.

Finley, R. J. 1978 Ebb-tidal delta morphology and sediment supply in relation to seasonal wave energy flux, North Inlet, South Carolina. *Journal of Sedimentary Petrology*, 48, 227-238.

Fischer, H. B., List, E. J., Koh, R. C. Y., Imberger, J. and Brooks, N. Y. 1979 *Mixing in Inland and Coastal Waters*. Academic Press, New York, 483pp.

FitzGerald, D. M. 1984 Interactions between the ebb-tidal delta and landward shoreline: Price Inlet, SC. *Journal of Sedimentary Petrology*, 54, 1303-1318.

FitzGerald, D. M. and Nummedal, D. 1983 response characteristics of an ebb dominated tidal inlet channel. *Journal of Sedimentary Petrology*, 53, 833-845.

FitzGerald, D. M., Penland, S. and Nummedal, D. 1984 Control of barrier island shape by inlet sediment bypassing: East Friesian Islands, West Germany. *Marine Geology*, 60, 355-367.

Folk, R. L. 1980 *Petrology of Sedimentary Rocks*. Hemphill Publishing Company, Austin (Texas), 184pp.

Folk, R. L. and Ward, W. C. 1957 Brazos River bar: a study in the significance of grain size parameters. *Journal of Sedimentary Petrology*, 27, 3-26.

Friedman, G. M. 1961 Distinction between dune, beach and river sands from their textural characteristics. *Journal of Sedimentary Petrology*, 31, 514-529.

Friedman, G. M. 1967 Dynamic processes and statistical parameters for size frequency distribution of beach and river sands. *Journal of Sedimentary Petrology*, 37, 327-354.

Friedman, G. M. 1979 Address of the retiring President of the International Association of Sedimentology: differences in size distributions of populations of particles among sands from various origins. *Sedimentology*, 26, 3-32.

Fry, V. A. and Aubrey, D. G. 1990 Tidal velocity asymmetries and bedload transport in shallow embayments. *Estuarine, Coastal and Shelf Science*, 30, 453-473.

Gadd, P. E., Lavelle, J. W. and Swift, D. J. P. 1978 Estimate of sand transport on the New York shelf using near-bottom current meter observations. *Journal of Sedimentary Petrology*, 48, 239-252.

Gallivan, L. B. and Davis, R. A. Jr. 1981 Sediment transport in a microtidal estuary: Matanzas River, Florida (U.S.A.). *Marine Geology*, 40, 69-83.

Gao, S. 1988 P-A relationships of tidal inlets along the East China Sea coast (in Chinese, with English abstract). *Marine Science*, No.1, 15-19.

Gao, S. and Collins, M. 1991 A critique of the "McLaren Method" for defining sediment transport paths. *Journal of Sedimentary Petrology*, 61, 143-146.

Gao, S., Xie, Q. -C. and Feng, Y. -J. 1990 Fine-grained sediment transport and sorting by tidal exchange in Xiangshan Bay, Zhejiang, China. *Estuarine, Coastal and Shelf Science*, 31, 397-409.

Gerritsen, F. 1992 Morphological stability of inlets and tidal channels in the western Wadden Sea. *Netherlands Institute for Sea Research Publication Series*, No.20, 151-160.

Gessner, F. and Simonsen, R. 1967 Marine diatoms in the Amazon? *Limnology and Oceanography*, 12, 709-711.

Geyer, R. A. 1983 *Handbook of Geophysical Exploration at Sea*. CRC Press, Boca Raton (Florida), 445pp.

Gibbs, R. J., Matthews, M. D. and Link, D. A. 1971 The relationship between sphere size and settling velocity. *Journal of Sedimentary Petrology*, 41, 7-18.

Graf, W. H. 1971 *Hydraulics of Sediment Transport*. McGraw-Hill, New York, 513pp.

Grant, W. D. and Madsen, O. S. 1979 Combined wave and current interaction with a rough bottom. *Journal of Geophysical Research*, 84, 1799-1808.

Grant, W. D., Boyer, L. and Sanford, L. P. 1982 The effect of bioturbation on the initiation of motion of intertidal sand. *Journal of Marine Research*, 40, 659-677.

Griffiths, J. C. 1967 *Scientific Method in Analysis of Sediments*. McGraw- Hill, New York, 508pp.

Hallermeier, R. J. 1982 Oscillatory bedload transport: data review and simple formulation. *Continental Shelf Research*, 1, 159-190.

Hammond, F. D. C., Heathershaw, A. D. and Langhorne, D. N. 1984 A comparison between Shields threshold criterion and the movement of loosely packed gravel in a tidal channel. *Sedimentology*, 31, 51-62.

Hand, B. M. and Emery, K. O. 1964 Turbidites and topography of north end of San Diego Trough, California. *Journal of Geology*, 72, 526-542.

Harris, P. T. 1989 Sandwave movement under tidal and wind-driven currents in a shallow marine environment: Adolphus Channel, north- eastern Australia. *Continental Shelf Research*, 9, 981-1003.

Harris, P. T. 1991 Reversal of subtidal dune asymmetries caused by seasonally reversing wind-driven currents in Torres Strait, north- eastern Australia. *Continental Shelf Research*, 11, 655-662.

Harris, P. T. and Collins, M. 1988 Estimation of annual bedload flux in a macrotidal estuary: Bristol Channel, U.K. *Marine Geology*, 83, 237- 252.

Hardisty, J. 1983 An assessment and calibration of formulations for Bagnold's bedload equation. *Journal of Sedimentary Petrology*, 53, 1007-1010.

Harlow, D. A. 1979 The littoral sediment budget between Selsey Bill and Gilkicker Point, and its relevance to coast protection works on Hayling Island. *Quarterly Journal of Engineering Geology*, 12 257-265.

Hayes, M. O. 1975 Morphology of sand accumulations in estuaries. In: **Cronin, L. E.** (editor), *Estuarine Research (Vol.2: Geology and Engineering)*. Academic Press, New York. p.3-22.

Hayes, M. O. 1980 General morphology and sediment patterns in tidal inlets. *Sedimentary Geology*, 26, 139-156.

Haynes, F. N. and Coulson, M. G. 1982 The decline of Spartina in Langstone Harbour, Hampshire. *Proceedings of the Hampshire Field Club and Archaeological Society*, 38, 5-18.

Heathershaw, A. D. 1981 Comparisons of measured and predicted sediment transport rates in tidal currents. *Marine Geology*, 42, 75-104.

Heathershaw, A. D. and Hammond, F. D. C. 1979 *Offshore sediment movement and its relation to observed tidal current and wave data*. Swansea Bay (Sker) Project Topic Report 6, Institute of Oceanographic Sciences Report No.93.

Hjulström, F. 1935 Studies in the morphological activity of rivers as illustrated by the River Fyris. *Bulletin of the Geological Institute of University of Uppsala*, 25, 221-528.

Hjulström, F. 1939 Transportation of Detritus by moving water. In: **Trask, P. D.** (editor), *Recent Marine Sediments*. The Society of Economic Paleontologists and Mineralogists, Tulsa (Oklahoma). p.5-31.

Hubbard, D. K., Oertel, G. and Nummedal, D. 1979 The role of waves and tidal currents in the development of tidal-inlet sedimentary structures and sand body geometry: examples from North Carolina, South Carolina and Georgia. *Journal of Sedimentary Petrology*, 49, 1073-1092.

Huntley, D. A. and Bowen, A. J. 1990 Modelling sand transport on continental shelves. In: **Davies, A. M.** (editor), *Modelling Marine Systems (Vol. 1)*. CRC Press, Florida. p.221-254.

Hydraulics Research 1989a *Christchurch Bay - Offshore Wave Climate and Extremes*. Hydraulics Research Limited Report No.EX1934, Wallingford, 9pp (plus Tables and Figures).

Hydraulics Research 1989b *Wind-Wave Data Collection and Analysis for Milford-on-*

Sea. Hydraulics Research Limited Report No.EX1979, Wallingford, 20pp (plus Tables and Figures).

Ingle, J. C. Jr. 1966 *The Movement of Beach Sand: An Analysis Using Fluorescent Grains*. Elsevier, Amsterdam, 221pp.

Inman, D. L. 1949 Sorting of sediments in the light of fluid mechanics. *Journal of Sedimentary Petrology*, 19, 51-70.

Inman, D. L. and Bagnold, R. A. 1963 Littoral processes. In: **Hill, M. N.** (editor), *The Sea (Vol.3)*. Interscience, New York. p.529-553.

Jarrett, J. T. 1976 *Tidal Prism - Inlet Area Relationships*. GITI Report No.3, the U.S. Army Corps of Engineers, Waterways Experiment Station, 32pp.

Jarvis, J. and Riley, C. 1987 Sediment transport in the mouth of the Eden estuary. *Estuarine, Coastal and Shelf Science*, 24, 463-481.

Johnson, J. W. 1973 Characteristics and behaviour of Pacific coast tidal inlets. *Journal of the Waterways, Harbors and Coastal Engineering Division*, ASCE, 99(WW3), 325-339.

Johnson, M. A., Kenyon, N. H., Belderson, R. H. and Stride, A. H. 1982 Sand transport. In: **Sride, A. H.** (editor), *Offshore Tidal Sands*. Chapman and Hall, London. p.58-94.

Joshi, P. B. 1982 Hydromechanics of tidal inlets. *Journal of the Waterway, Port, Coastal and Ocean Division*, ASCE, 108(WW3), 239-253.

Karim, M. F. and Forrest, M. H. Jr. 1986 Armouring and sorting simulation in alluvial rivers. *Journal of Hydraulic Engineering*, ASCE, 112, 705- 715

Kellaway, G. A., Redding, J. H., Shephard-Thorn, E. R. and Destombes, J. -P. 1975 The Quaternary history of the English Channel. *Philosophical Transaction of the Royal Society of London*, A279, 189-218.

Kemp, P. H. and Simons, R. R. 1984 Sediment transport due to waves and tidal currents. In: **Denness, B.** (editor), *Seabed Mechanics*. Graham and Trotman, London. p.197-206.

Keulegan, G. H. 1951 *Tidal Flows in Entrances: Water Level Fluctuations of Basins in communication with seas*. Third Progress Report, National Bureau of Standards Report, No.1146.

King, C. A. M. 1951 Depth of disturbance of sand on sea beaches by waves. *Journal of Sedimentary Petrology*, 21, 131-140.

Kirby, R. 1987 Sediment exchanges across the coastal margins of NW Europe. *Journal of the Geological Society (London)*, 144, 121-126.

Klingeman, P. C. and Emmett, W. W. 1982 Gravel bedload transport processes. In: **Hey, R. D., Bathurst, J. C. and Thorne, C. R.** (editors), *Gravel-Bed Rivers*. John Wiley, Chichester, p.141-179.

Komar, P. D. 1971 The mechanics of sand transport on beaches. *Journal of Geophysical Research*, 76, 713-721.

Komar, P. D. 1976 *Beach Processes and Sedimentation*. Prentice-Hall, Englewood-Cliffs (New Jersey), 429pp.

Komar, P. D. 1977 Selective longshore transport rates of different grain-size fractions within a beach. *Journal of Sedimentary Petrology*, 47, 1444-1453.

Komar, P. D. and Clemens, K. E. 1985 The relationship between a grain's settling velocity and threshold of motion under unidirectional currents. *Journal of Sedimentary Petrology*, 56, 258-266.

Komar, P. D. and Inman, D. L. 1970 Longshore sand transport on beaches. *Journal of Geophysical Research*, 75, 5914-5927.

Komar, P. D. and Miller, M. C. 1973 The threshold of sediment movement under oscillatory water waves. *Journal of Sedimentary Petrology*, 43, 1101-1110.

Komar, P. D. and Miller, M. C. 1975 On the comparison between the threshold of sediment motion under waves and unidirectional currents with a discussion of the practical evaluation of the threshold. *Journal of Sedimentary Petrology*, 45, 362-367.

Komar, P. D. and Reimers, C. E. 1978 Grain shape effects on settling rates. *Journal of Geology*, 86, 193-209.

Komar, P. D. and Wang, C. 1984 Processes of selective grain transport and the formation of placers on beaches. *Journal of Geology*, 92, 637- 655.

Lacey, S. L. 1985 *Coastal Processes in Poole and Christchurch Bays and the Effects of Coastal Protection Works*. Unpublished Ph.D. Thesis, Department of Civil Engineering, University of Southampton, 394pp.

Lane, E. 1955 Design of stable channels. *Transaction of the American Society of Civil Engineers*, 120, 1234-1260.

Lavelle, J. W. and Mofjeld, H. O. 1987 Do critical stresses for incipient motion and erosion really exist? *Journal of Hydraulic Engineering*, ASCE, 113, 370-388.

Le Provost, C. and Forneriono, M. 1985 Tidal spectroscopy of the English Channel with a numerical method. *Journal of Physical Oceanography*, 15, 1009-1031.

Lowe, D. R. 1988 Suspended-load fallout rate as an independent variable in the analysis of current structures. *Sedimentology*, 35, 765-776.

Ludtke, N. A. and Bender, M. L. 1979 Tracer study of sediment-water interactions in estuaries. *Estuarine and Coastal Marine Science*, 9, 643-651.

Ludwick, J. C. 1975 Variations in the boundary-drag coefficient in the tidal entrance to Chesapeake Bay, Virginia. *Marine Geology*, 19, 19-28.

Machemehl, J. L., Herbich, J, B. and Jo, C. H. 1991 Study of tidal-inlet stability. *Journal of the Waterway, Port, Coastal and Ocean Engineering*, ASCE, 117, 588-598.

Madsen, O. S. 1989 Transport determinations by tracers. A: Tracer theory. In: **Seymour, R. J.** (editor), *Nearshore Sediment Transport*. Plenum Press, New York. p.103-114.

Madsen, O. S. and Grant, W. D. 1975 The threshold of sediment movement under oscillatory waves: a discussion. *Journal of Sedimentary Petrology*, 45, 360-361.

Madsen, O. S. and Grant, W. D. 1976 Quantitative description of sediment transport by waves. *Proceedings of the 15th Coastal Engineering Conference*, p.1093-1112.

McCave, I. N. 1978 Grain-size trends and transport along beaches: an example from eastern England. *Marine Geology*, 28, M43-M51.

McCave, I. N. 1979 Suspended sediment. In: **Dyer, K. R.** (editor), *Estuarine Hydrography and Sedimentation*. Cambridge University Press, Cambridge. p.131-185.

McCave, I. N. 1984 Size spectra and aggregation of suspended particles in the deep ocean. *Deep-Sea Research*, 31, 329-352.

McLaren, P. 1981 An interpretation of trends in grain-size measurements. *Journal of Sedimentary Petrology*, 51, 611-624.

McLaren, P. and Bowles, D. 1985 The effects of sediment transport on grain-size distributions. *Journal of Sedimentary Petrology*, 55, 457- 470.

McManus, J. 1988 Grain size determination and interpretation. In: **Tucker, M.** (editor), *Techniques in Sedimentology*. Blackwell, Oxford. p.63-85.

McManus, J., Buller, A. T. and Green, C. D. 1980 Sediments of the Tay Estuary, VI: Sediments of lower and outer reaches. *Proceedings of the Royal Society of*

Edinbrough, B78, 133-154.

McQuillin, R. and Ardus, D. A. 1977 *Exploring the Geology of Shelf Seas*. Graham and Trotman, London, 234pp.

McQuillin, R., Bacon, M. and Barclay, W. 1984 *An Introduction to Seismic Interpretation*. Graham and Trotman, London, 287pp.

Melville, R. V. and Freshney, E. C. 1982 *The Hampshire Basin and Adjoining Areas (4th edition)*. Her Majesty's Stationery Office, London, 146pp.

Menard, H. 1950 Sediment movement in relation to current velocity. *Journal of Sedimentary Petrology*, 20, 280-292.

Merefield, J. R. 1981 Caesium in the up-estuary transport of sediments. *Marine Geology*, 39, M45-M55.

Miller, M. C., McCave, I. N. and Komar, P. D. 1977 Threshold of sediment motion under unidirectional currents. *Sedimentology*, 24, 507-528.

Milliman, J. D. 1976 Miniacina minacea: modern foraminiferal sands on the outer Moroccan shelf. *Sedimentology*, 23, 415-419.

Murray, J. W. 1961 *The Ecology and Systematics of the Benthic Foraminifera of Christchurch Harbour, Hampshire*. Unpublished Ph.D. Thesis, University of London, 538pp.

Murray, J. W. 1966 A study of the seasonal changes of the water mass of Christchurch Harbour, England. *Journal of Marine Biological Association of the United Kingdom*, 46, 561-578.

Murray, J. W. 1968 The living Foraminiferida of Christchurch Harbour, England. *Micropaleontology*, 14, 83-96.

Murray, J. W. 1987 Biogenic indicators of suspended sediment transport in marginal marine environments: quantitative examples from SW Britain. *Journal of the Geological Society (London)*, 144, 127-133.

Murray, J. W. 1991 *Ecology and Palaeoecology of Benthic Foraminifera*. Longman, New York, 397pp.

Murray, S. P. 1967 Control of grain dispersion by particle size and wave state. *Journal of Geology*, 75, 612-634.

Nicholls, R. J. and Wright, P. 1991 Longshore transport of pebbles: experimental estimates of K. In: **Kraus, N. C., Gingerich, K. J. and Krieebel, D. L.** (editors), *Coastal Sediment '91 (Vol. 1)*, ASCE, New York. p.920-933.

Nigam, R. 1986 Foraminiferal assemblages and their use as indicators of sediment movement: a study in the shelf region off Navapur, India. *Continental Shelf Research*, 5, 421-430.

Nilsson, T. 1983 *The Pleistocene: Geology and Life in the Quaternary Ice Age*. D. Reidel Publishing Company, London, 651pp.

Nordstrom, K. F. 1981 Differences in grain size distribution with shoreline position in a spit environment. *Northeastern Geology*, 3, 252-258.

Nordstrom, K.F. 1989 Downdrift coarsening of beach foreshore sediments at tidal inlets: an example from the coast of New Jersey. *Earth Surface Processes and Landforms*, 14, 691-701.

Nowell, A. R. M., Jumars, P. A. and Eckman, J. E. 1981 Effects of biological activity on the entrainment of marine sediments. *Marine Geology*, 42, 133-153.

O'Brien, M. P. 1931 Estuarine tidal prism related to entrance areas. *Civil Engineering*, 1, 738-739.

O'Brien, M. P. 1969 Equilibrium flow areas of inlets on sandy coasts. *Journal of Waterways and Harbour Division*, ASCE, 95(WW1), 43-52.

O'Brien, M. P. and Dean, R. G. 1972 Hydraulics and sedimentary stability of tidal inlets. *Proceedings of the 13th Coastal Engineering Conference*, p.761-780.

O'Connor, B. A. 1987 Short and long term changes in estuary capacity. *Journal of the Geological Society (London)*, 144, 187-195.

Oertel, G. F. 1972 Sediment transport of estuary entrance shoals and the formation of swash platforms. *Journal of Sedimentary Petrology*, 42, 857-863.

Officer, C. B. 1981 Physical dynamics of estuarine suspended sediments. *Marine Geology*, 40, 1-14.

Otvos, E. G. 1965 Sedimentation-erosion cycles of single tidal period on Long Island Sound beaches. *Journal of Sedimentary Petrology*, 35, 604-609.

Owen, M. W. and Thorn, M. F. C. 1978 Effect of waves on sand transport by currents. *Proceedings of 16th Coastal Engineering Conference*, p.1675-1687.

Özsoy, E. 1977 *Flow and Mass Transport in the Vicinity of Tidal Inlets*. Technical Report TR-036, Coastal and Oceanographic Engineering Laboratory, University of Florida, 196pp.

Özsoy, E. and Ünlüata, E. 1982 Ebb-tidal flow characteristics near inlets. *Estuarine, Coastal and Shelf Science*, 14, 251-263.

Özsoy, E. 1986 Ebb-tidal jets: a model of suspended sediment and mass transport at tidal inlets. *Estuarine, Coastal and Shelf Science*, 22, 45-62.

Pattiaratchi, C. B. and Collins, M. B. 1985 Sand transport under the combined influence of waves and tidal currents: an assessment of available formulae. *Marine Geology*, 67, 83-100.

Pettijohn, F. G. and Ridge, J. D. 1932 A textural variation series of beach sands from Cedar Point, Ohio. *Journal of Sedimentary Petrology*, 2, 76-88.

Pettijohn, F. G., Potter, P.D. and Siever, R. 1972 *Sand and Sandstone*. Springer-Verlag, New York, 618pp.

Pickrill, R. A. 1986 Sediment pathways and transport rates through a tide-dominated entrance, Rangaunu Harbour, New Zealand. *Sedimentology*, 33, 887-898.

Pizzuto, J. E. 1987 Dispersion of dyed sand tracers in an oscillatory flow field. *Journal of Geophysical Research*, 92(C2), 1923-1933.

Plumley, W. J. 1948 Black Hills terrace gravels: a study in sediment transport. *Journal of Geology*, 55, 526-577.

Portsmouth Polytechnic 1976 *Langstone Harbour Study: the Effect of Sewage effluent on the Ecology of the Harbour*. Report to the Southern Water Authority, 356pp.

Postma, H. 1961 Transport and accumulation of suspended matter in the Dutch Wadden Sea. *Netherlands Journal of Sea Research*, 1, 149-190.

Postma, H. 1967 Sediment transport and sedimentation in the marine environment. In: **Lauff, G. H.** (editor), *Estuaries*. American Association for Advancement of Science Publication, No. 83, 158-179.

Postma, H. 1981 Exchange of materials between the North Sea and the Wadden Sea. *Marine Geology*, 40, 199-215.

Press, W. H., Flannery, B. P., Teukolsky, S. A. and Vetterling, W. T. 1986 *Numerical Recipes*. Cambridge University Press, Cambridge, 818pp.

Price, W. A. 1947 Equilibrium of form and forces in tidal basins of coasts of Texas and Louisiana. *Bulletin of the American Association of Petroleum Geologists*, 31, 1619-1663.

Price, W. A. 1963 Patterns of flow and channelling in tidal inlets. *Journal of Sedimentary Petrology*, 33, 279-290.

Price, W. A. 1969 Variable dispersion and its effects on the movements of tracers on beaches. *Proceedings of 11th Conference on Coastal Engineering*, p.329-334.

Pritchard, D. W. 1952 Estuarine hydrography. *Advances in Geophysics*, 1, 243-280.

Pugh, D. T. 1987 *Tides, Surges and Mean Sea-Level: A Handbook for Engineers and Scientists*. John Wiley, Chichester, 472pp.

Reid, C. 1902 *The Geology of the Country Around Ringwood*. Memoirs of the Geological Survey of the United Kingdom, 62pp.

Rigler, J. K. and Collins, M. B. 1983 Initial grain movement under oscillatory flow: a comparison of some threshold criteria. *Geo-Marine Letters*, 3, 43-48.

Robbins, J. A. 1986 A model for particle-selective transport of tracers in sediments with conveyer belt deposit feeders. *Journal of Geophysical Research*, 91, 8542-8558.

Robinson, A. W. H. 1955 The harbour entrances of Poole, Christchurch and Pagham. *Geographical Journal*, 121, 33-50.

Rouse, H. 1937 Modern conceptions of the mechanisms of fluid turbulence. *Transactions of the American Society of Civil Engineers*, 102, 463-543.

Rusnak, G. A. 1967 Rates of sediment accumulation in modern estuaries. In: **Lauff, G. H.** (editor), *Estuaries*. American Association for the Advancement of Science, Washington, D.C. p.180-184.

Russell, R. D. 1939 Effects of transportation on sedimentary particles. In: **Trask, P. D.** (editor), *Recent Marine Sediments*. The Society of Economic Paleontologists and Mineralogists, Tulsa (Oklahoma). p.32-47.

Russell-Cargill, W. G. A. (editor) 1982 *Recent Developments in Side Scan Sonar Techniques*. ABC Press, Cape Town, 141pp.

Salomons, W. and Mook, W. G. 1987 Natural tracers for sediment transport studies. *Continental Shelf Research*, 7, 1333-1343.

Schalk, M. 1938 A textural study of the outer beach of Cape Cod, Massachussetts. *Journal of Sedimentary Petrology*, 8, 41-54.

Schalk, M. 1946 A study of textural changes in a beach by repeated sampling. *Journal of Sedimentary Petrology*, 16, 43-51.

Schubel, J. R. and Carter, H. H. 1984 The estuary as a filter for fine-grained suspended sediment. In: **Kennedy, V. S.** (editor), *The Estuary as a Filter*. Academic Press, New York. p.81-105.

Self, R. P. 1977 Longshore variation in beach sands, Nautla area, Veracruz, Mexico. *Journal of Sedimentary Petrology*, 47, 1437-1443.

Shields, A. 1936 *Application of Similarity Principles and Turbulence Research to*

Bedload Movement (in German). Mitteilungen Press, Berlin, No.26.

Shigemura, T. 1980 Tidal prism - throat area relationship of the bays of Japan. *Shore and Beach*, 48, 30-35.

Sleath, J. F. A. 1990 Seabed boundary layers. In: **le Méhauté, B. and Hanes, D. M.** (editors), *The Sea (Vol.9)*. John Wiley, New York. p.693-727.

Sonnenberg, G. J. 1988 *Radar and Electronic Navigation (sixth edition)*. Butterworths, London, 368pp.

Sorensen, R. M. 1980 The Corps of Engineers' general investigation of tidal inlets. *Proceedings of the 17th Coastal Engineering Conference*, p.2565-2580.

Soulsby, R. L. 1983 The bottom boundary layer of shelf seas. In: **Johns, B.** (editor), *Physical Oceanography of Coastal and Shelf Seas*. Elsevier, Amsterdam. p.189-266.

Speer, P. E. and Aubrey, D. G. 1985 A study of nonlinear tidal propagation in shallow inlet/estuarine systems, Part II: Theory. *Estuarine, Coastal and Shelf Science*, 21, 207-224.

Steers, J. A. 1946 *The Coastline of England and Wales*. Cambridge University Press, Cambridge, 644pp.

Steers, J. A. 1981 *Coastal Features of England and Wales*. Oleander, Cambridge, 206pp.

Steidtman, J. R. 1982 Size-density sorting of sand-size spheres during deposition from bedload transport and implication concerning hydraulic equivalence. *Sedimentology*, 29, 877-883.

Sternberg, R. W. 1971 Measurements of incipient motion of sediment particles in the marine environment. *Marine Geology*, 10, 113-119.

Sternberg, R. W. 1972 Predicting initial motion and bedload transport of sediment particles in the shallow marine environment. In: **Swift, D. J. P., Duane, D. B. and Pilkey, O. H.** (editors), *Shelf Sediment Transport: Processes and Pattern*. Dowden, Stroudsberg. p.61-82.

Sundborg, Å. 1956 The river Klarälven, a study of fluvial processes. *Geographic Annual*, 38, 127-316.

Su, J. -L. and Wang, K. -S. 1986 The suspended sediment balance in Changjiang Estuary. *Estuarine, Coastal and Shelf Science*, 23, 81-98.

Tetley, L. and Calcutt, D. 1986 *Electronic Aids to Navigation*. Edward Arnold, London, 357pp.

Thompson, S. M. 1985 Transport of gravel by flows up to 500 m /s, Ohau River, Otago, New Zealand. *Journal of Hydraulic Research*, 23, 285- 304.

Thorne, P. D. 1986 An intercomparison between visual and acoustic detection of seabed gravel movement. *Marine Geology*, 72, 11-31.

Thorne, P. D., Williams, J. J. and Heathershaw, A. D. 1989 In situ measurements of marine gravel threshold and transport. *Sedimentology*, 36, 61-74.

Tipper, J. C. 1989 The equilibrium and entrainment of a sediment grain. *Sedimentary Geology*, 64, 167-174.

Tosswell, P. 1978 *An Hydraulic Investigation of Christchurch Harbour with Particular Reference to the Entrance Channel.* Unpublished B.Sc. Dissertation, University of Southampton, 141pp.

Trask, P. D. 1952 *Source of beach sand at Santa Barbara, California, as indicated by mineral grain studies.* U.S. Army Corps Engineers, Beach Erosion Board Technical Memorandum No.28, 24pp.

Tyhurst, M. F. 1978 Tidal conditions in Poole Bay. *Journal of the Society of Civil Engineering Technicians*, 5(6), 6-11.

Vanoni, V. A. 1984 Fifty years of sedimentation. *Journal of Hydraulic Engineering*, 110, 1022-1057.

van de Kreeke, J. 1985 Stability of tidal inlets - Pas Cavallo, Texas. *Estuarine, Coastal and Shelf Science*, 21, 33-43.

van de Kreeke, J. 1990 Can multiple tidal inlets be stable? *Estuarine, Coastal and Shelf Science*, 30, 261-273.

van Rijn, L. C. 1984a Sediment transport, Part I: Bedload transport. *Journal of Hydraulics Division*, ASCE, 110, 1613-1641.

van Rijn, L. C. 1984b Sediment transport, Part II: suspended load transport. *Journal of Hydraulics Division*, ASCE, 110, 1613-1641.

van Straaten, L. M. J. U. 1958 Tidal action as a cause of clay accumulation. *Journal of Sedimentary Petrology*, 28, 406-413.

van Straaten, L. M. J. U. and Kuenen, Ph. H. 1957 Accumulation of fine grained sediments in the Dutch Wadden Sea. *Geologie en Mijnbouw*, 329-354.

Vincent, C. E., Young, R. A. and Swift, D. J. P. 1981 Bedload transport under waves and currents. *Marine Geology*, 39, M71-M80.

Vincent, C. E., Young, R. A. and Swift, D. J. P. 1983 Sediment transport on the Long Island shoreface, North American Atlantic Shelf: role of waves and currents in shoreface maintenance. *Continental Shelf Research*, 2, 163-183.

Wang, P. -X. and Murray, J. W. 1983 The use of foraminifera as indicators of tidal effects in estuarine deposits. *Marine Geology*, 51, 239-250.

Wang, W. -J., Li, C. -C. and Yang, G. -R. 1977 Formation and development of the estuarine geomorphology of Yangpu Harbour. In: **Institute of the South China Sea Oceanography (Chinese Academy of Science)** (editor), *Papers on Marine Geomorphology of the South Chine Sea*, No.3, p.80-100.

Wang, Y., Zhu, D. -K., Luo, Z. -W., Yang, J. -H., Ma, Z. -Q., He, H. -M., Zhou, L. -F., Wang, X. -Y., Cao, Q. -Y. and Zhang, H. -X. 1985 *Report on Sediment Supply and Siltation of Yangpu Harbour*. Nanjing University, Nanjing, 104pp.

White, C. M. 1940 Equilibrium of grains on bed of stream. *Proceedings of the Royal Society of London*, A174, 322-334.

White, W. R., Milli, H. and Crabbe, A. D. 1975 Sediment transport theories: a review. *Proceedings of Institution of Civil Engineers*, 59, Part 2, 265-292.

Whittaker, J. E. 1981 The living ostracoda of Christchurch Harbour, Dorset. In: **Neale, J. W. and Brasier, M. D.** (editors), *Microfossils from Recent and Fossil Shelf Seas*. Ellis Horwood, Chichester. p.293-303.

Wilberg, P. L. and Smith, J. D. 1989 Model for calculating bed load transport of sediment. *Journal of Hydraulic Engineering*, ASCE, 115, 101-123.

Williams, A. T. 1971 An analysis of some factors involved in the depth of disturbance of beach sand by waves. *Marine Geology*, 11, 145-158.

Wise, E. 1956 Sea defence work, Christchurch, Mudeford. *Journal of the Institution of Municipal Engineers*, 83, 19-29.

Yalin, M. S. 1963 An expression for bed-load transportation. *Proceedings of the American Society of Civil Engineering*, 89(HY3), 221-250.

Yalin, M. S. 1972 *Mechanics of Sediment Transport*. Pergamon Press, Oxford, 290pp.

Yang, C. T. 1973 Incipient motion and sediment transport. *Journal of Hydraulics Division*, ASCE, 99, 1679-1704.

Yeakel, L. S. Jr. 1962 Tuscarora, Juniata and Bald Eagle paleocurrents and paleogeograhpy in the central Appalachians. *Bulletin of the Geological Society of*

America, 73, 1515-1540.

Zhang, H. -X. and Zhu, D. -K. 1989 The stability of Yangpu Harbour, a tidal inlet on the west coast of Hainan Island, China (in Chinese, with English abstract). *Chinese Coastal Engineering*, 8(3), 31-38.

Zhang, Q. -M. 1987 Analysis of P-A correlationship of tidal inlets along the coasts of south China. *1987 Proceedings of Coastal and Port Engineering in Developing Countries (Vol. 1)*, p.412-422.

Zhu, D. -K., Ke, X. -K., Zhang, H. -X., Fu, M. -Z. and Gao, S. 1984 *A Report on Geomorphology of Yangpu Harbour, Hainan Island.* Nanjing University, Nanjing, 67pp.

APPENDICES

APPENDIX A. RECORDS OF TIDAL CYCLE MEASUREMENTS

Key to Tables A-1 to A-8:

GMT:	Greenwich Mean Time;
h:	Water depth (m);
h_m:	Water depth for measurements (m);
S:	Salinity (ppt);
T:	Temperature (°C);
U:	Current speed (m s^{-1});
D:	Current direction (degree in terms of azimuth, without declination corrections); and
C:	Suspended sediment concentration (mg l^{-1}).

Key to Tables A-9 and A-10:

GMT:	Greenwich Mean Time;
η:	Water level (m OD);
U:	Current speed measured at the surface —— positive values for the flood direction and negative values for the ebb direction (m s^{-1});
S:	Salinity (ppt), at 1.0 m below the surface;
T:	Temperature (°C), at 1.0 m below the surface; and
C:	Suspended sediment concentration, measured at the same elevation where the siltmeter sensor was installed (mg l^{-1}).

Table A-1. Station 3: tidal cycle measurements, 1-2 October 1989 (spring tide).

GMT	h	h_m	S	T	U	D
11.45	2.70	0.5	34.1	16.7	0.53	55
11.50		1.5	34.2	16.4	0.46	48
11.55		2.5	34.3	16.7	0.15	76
12.15		0.5	34.1	16.8	0.70	55
12.20	2.64	1.0	34.1	16.8	0.58	50
12.25		2.0	34.1	16.7	0.30	42
12.32		2.3	33.9	16.8	0.15	80
12.45	2.57	0.5	33.8	16.8	0.55	52
12.50		1.0	34.0	16.8	0.70	52
12.55		1.5	33.9	16.8	0.55	50
13.00		2.2	33.0	16.7	0.20	38
13.15	2.58	0.5	30.4	16.4	0.07	90
13.18		1.0	30.7	16.5	0.03	80
13.22		1.5	32.0	16.6	0.10	-
13.25		2.2	32.5	16.8	0.10	-
13.28		0.5	30.8	16.5	0.46	-
13.45	2.65	0.5	33.2	16.8	0.80	-
13.48		1.0	34.0	16.9	0.94	-
13.51		1.5	34.0	16.9	0.87	-
13.54		2.2	34.0	16.9	0.38	-
14.15	2.72	0.5	34.0	16.9	0.74	-
14.17		1.0	34.1	16.9	0.69	-
14.19		1.5	34.1	16.9	0.67	-
14.22		2.2	34.1	16.9	0.42	-
14.44	2.78	0.5	34.1	16.9	0.08	-
14.46		1.0	34.1	16.9	0.03	-
14.47		1.5	34.0	16.9	0.13	-
14.50		2.3	34.0	16.9	0.04	-
14.52		0.5	33.9	16.9	0.33	108
15.15	2.61	0.5	33.6	17.1	0.77	105
15.18		1.0	33.6	17.1	0.75	90
15.21		1.5	33.6	17.1	0.64	85
15.23		2.1	33.6	17.1	0.35	60
15.40		0.5	-	-	1.02	95
15.45	2.40	0.5	32.4	17.1	0.88	95
15.50		1.0	32.4	17.1	0.75	85
15.52		1.5	32.3	17.2	0.65	75
15.55		1.9	32.2	17.2	0.35	75
15.58		0.5	32.1	17.3	1.20	80
16.15	2.34	0.5	22.9	16.6	1.35	95
16.19		1.0	23.3	16.5	1.20	80
16.21		1.5	23.6	16.5	0.70	75
16.24		1.8	23.8	16.5	0.55	65
16.45	2.25	0.5	22.7	16.3	0.90	89

16.50		1.0	22.8	16.6	0.75	85
16.53		1.5	22.7	16.3	0.45	75
16.57		1.8	23.2	16.6	0.35	75
17.15	2.05	0.5	20.1	16.1	0.70	85
17.18		1.0	19.9	16.1	0.50	85
17.21		1.5	20.4	16.1	0.35	65
17.43	1.93	0.5	17.7	15.8	0.45	85
17.49		1.0	17.6	15.8	0.30	75
17.53		1.5	17.9	16.0	0.25	60
18.15	1.85	0.5	14.7	15.6	0.35	80
18.17		1.0	15.5	15.7	0.30	72
18.20		1.3	17.5	15.8	0.20	48
18.45	1.90	0.5	14.5	15.5	0.10	50
18.48		1.0	15.1	15.6	0.00	-
18.50		1.4	16.0	15.6	0.00	-
19.15	2.15	0.5	21.4	15.9	0.75	-
19.18		1.0	24.4	16.2	0.75	-
19.20		1.5	28.6	16.5	0.78	-
19.23		1.8	29.2	16.5	0.50	-
19.45	2.34	0.5	30.6	16.6	1.33	-
19.49		1.0	31.4	16.7	1.25	-
19.51		1.5	31.9	17.0	1.08	-
19.53		1.9	32.0	17.0	1.13	-
20.13		0.5	33.2	16.8	1.25	-
20.15	2.47	1.5	33.4	16.8	1.00	-
20.17		2.0	33.1	16.8	1.20	-
20.45	2.65	0.5	33.9	16.8	1.40	-
20.48		1.5	33.7	17.0	1.20	-
20.51		2.0	33.8	16.8	1.20	-
21.15	2.70	0.5	33.6	16.6	1.10	-
21.20		1.0	33.7	16.8	1.15	-
21.22		1.5	33.9	16.9	1.00	-
21.24		2.2	33.9	16.8	1.00	-
21.57	2.81	0.5	33.9	16.8	0.90	-
21.59		1.5	33.9	16.8	0.80	-
22.00		2.3	33.9	16.8	0.70	-
22.31	2.89	0.5	34.0	16.8	0.30	-
22.34		1.0	34.0	16.8	0.35	-
22.36		1.5	34.0	16.8	0.35	-
22.37		2.0	33.8	16.8	0.25	-
22.39		2.2	34.0	16.8	0.18	-
23.05	2.91	0.5	34.0	16.7	0.22	100
23.07		1.0	34.1	16.7	0.25	80
23.08		1.5	34.1	16.7	0.15	80
23.10		2.2	34.1	16.7	0.12	70
23.30	2.86	0.5	33.5	17.0	0.45	90
23.31		1.0	33.4	16.6	0.40	90
23.32		1.5	33.6	16.9	0.40	85
23.33		2.0	33.8	16.8	0.30	80
00.00	2.75	0.5	33.9	16.3	0.60	90

00.01		1.0	33.8	16.6	0.60	80
00.02		1.5	33.8	16.6	0.50	70
00.03		2.0	33.8	16.5	0.30	80
00.05		2.3	33.9	16.6	0.28	70
00.30	2.65	0.5	33.8	16.3	0.60	90
00.31		1.0	33.6	16.3	0.90	80
00.32		1.5	32.8	16.2	0.70	80
00.34		2.0	32.6	16.1	0.70	90
00.35		2.2	31.5	16.1	0.50	90
01.00	2.54	0.5	25.0	15.6	0.50	110
01.01		1.0	25.3	15.6	0.50	100
01.02		1.5	26.2	15.6	0.35	90
01.04		2.0	27.0	15.6	0.25	70
01.05		2.1	28.2	15.8	0.20	70

Table A-2. Station 3: tidal cycle measurements, 8-9 October 1989 (neap tide).

GMT	h	h_m	S	T	U	D
11.27	2.15	0.5	31.7	15.0	0.38	-
11.40		0.5	32.6	15.3	0.45	-
11.43		1.0	32.7	15.3	0.40	-
11.45		1.2	32.8	15.2	0.38	-
12.10		0.5	33.2	15.3	0.03	120
12.12		1.0	33.2	15.3	0.08	120
12.15		1.5	33.3	15.3	0.10	100
12.18		1.7	33.1	15.3	0.10	100
12.34	2.15	0.5	32.5	15.3	0.40	105
12.37		1.0	32.2	15.3	0.35	100
12.40		1.5	32.3	15.2	0.25	105
12.42		1.7	32.0	15.2	0.17	80
13.04	2.21	0.5	28.8	15.0	0.63	88
13.06		1.0	29.1	15.0	0.55	95
13.07		1.5	29.0	15.0	0.35	85
13.08		1.7	28.4	14.9	0.28	95
13.32	2.20	0.5	25.4	14.7	0.03	180
13.35		1.0	25.5	14.7	0.02	110
13.36		1.5	27.4	15.0	0.00	-
14.02	2.22	0.5	22.2	14.5	0.12	115
14.05		1.0	24.4	14.7	0.13	100
14.06		1.5	26.1	14.9	0.05	100
14.33	2.16	0.5	20.7	14.6	0.34	100
14.35		1.0	19.9	14.5	0.20	90
14.36		1.5	20.3	14.6	0.20	100
14.38		1.7	21.0	14.8	0.10	70
15.03	2.16	0.5	19.6	14.7	0.15	120
15.06		1.0	20.7	14.8	0.13	95

15.08		1.5	24.7	15.1	0.10	90
15.11		1.7	25.0	15.1	0.07	85
15.34	2.21	0.5	23.2	14.7	0.05	250
15.37		1.0	25.6	15.1	0.10	-
15.40		1.5	26.7	15.2	0.06	-
15.43		2.0	26.9	15.1	0.04	-
16.02	2.20	0.5	22.6	15.1	0.20	-
16.04		1.0	26.1	15.3	0.30	-
16.05		1.5	28.3	15.2	0.20	-
16.07		2.0	29.0	15.5	0.14	-
16.31	2.20	0.5	32.2	15.8	0.32	-
16.33		1.0	32.5	15.9	0.33	-
16.34		1.5	32.7	16.0	0.32	-
16.35		2.0	32.9	16.0	0.23	-
16.59	2.25	0.5	33.3	16.0	0.25	-
17.00		1.0	33.6	16.0	0.30	-
17.02		1.5	34.0	16.0	0.32	-
17.04		2.0	33.9	16.0	0.20	-
17.31	2.28	0.5	33.9	15.9	0.32	240
17.32		1.0	33.9	15.9	0.37	240
17.33		1.5	34.0	15.9	0.35	240
17.35		2.0	33.9	15.9	0.25	240
18.03	2.30	0.5	33.9	15.9	0.02	-
18.04		1.0	33.9	15.8	0.00	-
18.07		1.5	33.9	15.8	0.10	100
18.10		2.0	33.9	15.8	0.08	75
18.13		0.5	33.9	15.8	0.17	110
18.30	2.30	0.5	33.9	15.8	0.20	110
18.31		1.0	33.9	15.8	0.20	90
18.32		1.5	33.9	15.8	0.15	95
18.33		2.0	34.0	15.8	0.05	90
19.01	2.26	0.5	25.4	14.9	0.40	105
19.02		1.0	25.9	14.9	0.28	90
19.04		1.5	27.6	15.0	0.17	80
19.05		2.0	30.6	15.4	0.02	60
19.30		0.5	19.3	14.2	0.40	95
19.32		1.0	20.6	14.6	0.22	110
19.35		1.5	23.3	14.8	0.12	88
19.37		2.0	27.4	15.1	0.03	70
20.01	2.10	0.5	17.4	14.4	0.54	100
20.02		1.0	17.7	14.4	0.40	95
20.03		1.5	22.2	14.9	0.05	70
20.05		1.6	23.9	14.9	0.05	70
20.31	1.99	0.5	14.9	14.2	0.55	110
20.32		1.0	16.2	14.2	0.30	110
20.34		1.5	21.4	14.6	0.08	70
21.04	1.91	0.5	13.4	14.0	0.55	105
21.05		1.0	13.6	14.0	0.33	100
21.06		1.5	18.4	14.4	0.10	78
21.32	1.81	0.5	13.8	13.9	0.38	105

21.34		1.0	13.8	14.1	0.30	85
21.36		1.5	14.5	14.0	0.02	70
22.01	1.83	0.5	14.3	13.9	0.38	98
22.05		1.0	14.0	14.6	0.28	92
22.11		1.4	18.1	14.2	0.03	70
22.30	1.74	1.3	18.2	14.0	0.03	88
22.31		0.5	15.4	13.9	0.18	110
22.33		1.0	17.8	13.9	0.12	95
23.00	1.71	0.5	13.2	13.7	0.16	90
23.01		1.0	13.3	13.7	0.10	98
23.03		1.4	15.9	13.7	0.02	42
23.32	1.78	0.5	12.7	13.6	0.02	245
23.33		1.0	13.5	13.6	0.15	305
23.35		1.5	16.6	13.7	0.12	315
23.59	1.81	0.5	18.8	14.0	0.14	312
00.01		1.0	27.7	14.7	0.32	300
00.03		1.5	29.3	15.1	0.25	-
00.30	1.88	0.5	31.9	15.4	0.35	315
00.31		1.0	32.7	15.4	0.35	312
00.32		1.5	32.9	15.1	0.02	-
01.04	1.92	0.5	33.9	15.5	0.25	302
01.05		1.0	33.8	15.5	0.23	307
01.07		1.5	33.8	15.6	0.10	265

Table A-3. Station 2: tidal cycle measurements, 31 July - 1 August 1990 (neap tide).

GMT	h	h_m	S	T	U	D
11.05	6.0	5.5	34.2	18.7	0.05	260
11.08		5.0	34.2	18.7	0.10	60
11.11		4.5	34.2	18.7	0.12	50
11.13		4.0	34.2	18.7	0.14	50
11.15		3.5	34.2	18.7	0.20	40
11.17		2.5	34.2	18.7	0.27	50
11.19		1.5	34.2	18.7	0.30	50
11.22		0.5	34.2	18.7	0.32	40
12.00	6.2	0.5	34.2	18.7	0.33	70
12.02		1.5	34.2	18.7	0.30	70
12.04		2.5	34.2	18.7	0.30	70
12.06		3.5	34.2	18.7	0.24	70
12.08		4.0	34.3	18.7	0.17	50
12.10		4.5	34.3	18.7	0.13	50
12.12		5.0	34.3	18.7	0.13	30
12.14		5.5	34.3	18.7	0.09	40

13.00	6.0	0.5	34.3	18.5	0.28	30
13.01		1.5	34.3	18.5	0.27	70
13.02		2.5	34.3	18.5	0.24	70
13.03		3.5	34.3	18.5	0.25	70
13.05		4.0	34.3	18.5	0.17	50
13.06		4.5	34.3	18.5	0.16	80
13.07		5.0	34.3	18.5	0.14	80
13.09		5.5	34.3	18.5	0.13	60
14.00	6.1	0.5	34.3	18.6	0.24	70
14.01		1.5	34.3	18.6	0.19	30
14.03		2.5	34.3	18.6	0.20	90
14.04		3.5	34.3	18.6	0.15	40
14.06		4.0	34.3	18.6	0.16	80
14.08		4.5	34.3	18.6	0.20	40
14.09		5.0	34.3	18.6	0.17	50
14.10		5.5	34.3	18.6	0.06	50
15.00	6.0	0.5	34.4	18.7	0.13	50
15.02		1.5	34.3	18.7	0.16	40
15.04		2.5	34.4	18.7	0.11	20
15.05		3.5	34.4	18.7	0.12	70
15.06		4.0	34.4	18.7	0.11	50
15.07		4.5	34.3	18.7	0.09	70
15.09		5.0	34.3	18.7	0.11	50
15.10		5.5	34.3	18.7	0.05	30
16.08	6.0	0.5	34.3	18.9	0.09	30
16.10		1.5	34.3	18.8	0.05	330
16.13		2.5	34.3	18.8	0.05	340
16.14		3.5	34.3	18.8	0.04	350
16.15		4.0	34.3	18.8	0.09	270
16.17		4.5	34.3	18.8	0.09	250
16 18		5.0	34.3	18.8	0.07	230
16.20		5.5	34.3	18.8	0.11	130
17.00	6.2	0.5	34.3	19.0	0.17	240
17.01		1.5	34.3	19.0	0.20	200
17.03		2.5	34.3	18.9	0.21	220
17.04		3.5	34.3	18.7	0.19	300
17.06		4.0	34.3	18.7	0.17	230
17.08		4.5	34.3	18.7	0.13	280
17.10		5.0	34.3	18.7	0.12	210
17.58	6.4	0.5	34.3	19.0	0.40	230
18.00		1.5	34.3	18.9	0.40	240
18.02		2.5	34.3	18.8	0.36	250
18.04		3.5	34.3	18.7	0.32	260
18.05		4.0	34.3	18.7	0.32	300
18.07		4.5	34.3	18.7	0.24	260
18.09		5.0	34.3	18.7	0.22	240
18.10		5.5	34.3	18.7	0.14	230
19.07	6.5	0.5	34.2	18.9	0.47	230
19.09		1.5	34.2	18.8	0.40	230
19.11		2.5	34.2	18.8	0.40	260

19.12		3.5	34.2	18.8	0.37	240
19.14		4.0	34.3	18.8	0.35	240
19.16		4.5	34.2	18.7	0.25	240
19.18		5.0	34.2	18.8	0.21	240
19.20		5.5	34.3	18.7	0.18	230
19 58	6.5	0.5	34.2	19.0	0.42	150
20.00		1.5	34.2	18.8	0.37	300
20.01		2.5	34.2	18.8	0.35	250
20.03		3.5	34.2	18.8	0.30	220
20.04		4.0	34.2	18.7	0.21	0
20.06		4.5	34.2	18.7	0.20	230
20.08		5.0	34.2	18.8	0.19	300
20.09		5.5	34.2	18.8	0.12	250
21.00	6.2	0.5	34.2	19.0	0.31	250
21.01		1.5	34.1	19.0	0.31	310
21.03		2.5	34.2	18.8	0.25	230
21.04		3.5	34.2	18.7	0.17	230
21.05		4.0	34.2	18.7	0.16	220
21.07		4.5	34.2	18.7	0.14	220
21.08		5.0	34.2	18.7	0.12	230
21.10		5.5	34.2	18.7	0.11	230
22.00	5.6	0.5	34.1	18.9	0.08	20
22.01		1.5	34.2	18.9	0.14	200
22.03		2.5	34.2	18.8	0.05	200
22.04		3.5	34.2	18.7	0.10	280
22.07		4.0	34.2	18.7	0.09	210
22.09		4.5	34.2	18.7	0.10	320
22.10		5.0	34.2	18.7	0.06	260
22.57	5.8	0.5	32.4	19.5	0.10	130
22.59		1.5	34.1	18.8	0.11	80
23.01		2.5	34.2	18.8	0.12	70
23.03		3.5	34.2	18.8	0.10	100
23.05		4.0	34.2	18.7	0.10	70
23.06		4.5	34.2	18.7	0.05	110
23.08		5.0	34.2	18.7	0.06	120
23.10		0.5	32.7	19.4	0.14	90
23.59	5.5	0.5	34.2	18.9	0.27	60
00.01		1.5	34.2	18.8	0.30	50
00.03		2.5	34.2	18.9	0.25	50
00.04		3.5	34.2	18.8	0.19	50
00.05		4.0	34.2	18.9	0.21	70
00.07		4.5	34.2	18.8	0.12	50
00.08		5.0	34.2	18.9	0.11	40

Table A-4. Station 2: tidal cycle measurements, 1 August 1990 (neap tide).

GMT	h	h_m	S	T	U	D
00.50	6.2	0.5	30.9	19.8	0.07	100
00.52		1.5	34.2	19.0	0.12	50
00.53		2.5	34.2	18.9	0.11	60
00.55		3.5	34.2	18.9	0.05	100
01.02		4.0	34.2	18.9	0.09	50
01.04		4.5	34.2	18.9	0.08	60
01.05		5.0	34.2	18.9	0.07	60
01.07		5.5	34.2	18.9	0.07	70
02.00	6.2	0.5	32.5	19.5	0.08	70
02.02		1.5	34.2	19.0	0.13	60
02.03		2.5	34.2	18.9	0.10	60
02.05		3.5	34.2	18.9	0.08	50
02.07		4.0	34.2	18.9	0.08	30
02.09		4.5	34.2	18.9	0.08	50
02.11		5.0	34.2	18.9	0.04	50
02.13		5.5	34.2	18.9	0.04	60
02.58	6.2	0.5	32.5	19.1	0.06	70
03.00		1.5	34.1	19.0	0.14	130
03.02		2.5	34.3	18.9	0.11	50
03.03		3.5	34.3	18.9	0.08	50
03.05		4.0	34.3	18.9	0.05	50
03.06		4.5	34.3	18.9	0.05	40
03.07		5.0	34.3	18.9	0.06	10
03.09		5.5	34.3	18.9	0.05	30
04.01	6.0	0.5	33.9	19.0	0.05	280
04.03		1.5	34.1	19.0	0.06	40
04.04		2.5	34.2	18.9	0.06	0
04.05		3.5	34.2	18.9	0.12	330
04.07		4.0	34.2	18.9	0.08	330
04.09		4.5	34.2	18.9	0.05	10
04.11		5.0	34.2	18.9	0.04	10
04.12		5.5	34.2	18.9	0.05	0
05.17	6.0	0.5	33.5	18.8	0.06	290
05.19		1.5	34.2	18.9	0.04	320
05.20		2.5	34.2	18.9	0.04	330
05.22		3.5	34.2	18.9	0.06	310
05.24		4.0	34.3	18.9	0.07	310
05.26		4.5	34.3	18.8	0.08	310
05.27		5.0	34.3	18.8	0.08	320
05.29		5.5	34.3	18.8	0.07	320
06.08	6.2	5.5	34.4	18.8	0.15	300
06.10		5.0	34.4	18.8	0.10	310
06.12		4.5	34.4	18.8	0.11	290
06.14		4.0	34.4	18.8	0.11	340
06.15		3.5	34.4	18.8	0.10	340

06.17		2.5	34.4	18.8	0.08	290
06.18		1.5	34.3	18.9	0.10	270
06.20		0.5	33.8	18.9	0.10	260
06.58	6.3	0.5	33.9	18.9	0.15	280
07.00		1.5	34.4	18.9	0.12	280
07.02		2.5	34.4	18.8	0.11	280
07.04		3.5	34.4	18.8	0.11	270
07.05		4.0	34.4	18.8	0.10	340
07.07		4.5	34.4	18.8	0.11	270
07.08		5.0	34.4	18.8	0.07	280
07.10		5.5	34.4	18.8	0.07	290
07.58		5.5	34.4	18.8	0.09	180
08.00	6.2	5.0	34.4	18.8	0.09	260
08.02		4.5	34.4	18.9	0.10	260
08.04		4.0	34.4	18.9	0.08	200
08.06		3.5	34.4	18.9	0.10	260
08.07		2.5	34.4	18.9	0.11	200
08.09		1.5	34.4	18.9	0.13	250
08.10		0.5	34.3	19.1	0.17	260
08.56	6.2	0.5	34.3	19.0	0.14	280
08.58		1.5	34.4	18.9	0.11	280
09.00		2.5	34.4	18.9	0.10	260
09.02		3.5	34.4	18.9	0.09	250
09.03		4.0	34.4	18.9	0.09	240
09.04		4.5	34.4	18.9	0.07	230
09.06		5.0	34.4	18.9	0.05	230
09.07		5.5	34.4	18.9	0.06	220
09.58	5.9	5.5	34.4	18.9	0.03	220
10.00		5.0	34.4	18.9	0.07	190
10.02		4.5	34.4	18.9	0.07	180
10.03		4.0	34.4	18.9	0.07	190
10.05		3.5	34.4	18.9	0.07	210
10.07		2.5	34.3	19.0	0.07	210
10.08		1.5	34.3	19.0	0.05	230
10.10		0.5	34.3	19.2	0.12	280
10.58	5.8	0.5	34.3	19.5	0.06	230
11.00		1.5	34.3	19.1	0.02	320
11.02		2.5	34.3	19.0	0.04	340
11.04		3.5	34.3	19.0	0.03	230
11.05		4.0	34.3	18.9	0.06	220
11.07		4.5	34.3	18.9	0.07	170
11.08		5.0	34.3	18.9	0.06	210
11.10		5.4	34.3	18.9	0.02	220
11.15		0.5	34.4	-	-	-
11.16		0.5	31.7	-	-	-
11.17		0.5	30.7	-	-	-
11.18		0.5	26.6	-	-	-
11.19		0.5	26.2	-	0.08	90
11.20		0.5	25.7	-	-	-
11.21		1.0	32.5	-	-	-

11.22		1.5	34.2	-	0.04	220
11.24		1.5	34.2	-	-	-
11.25		1.5	34.2	19.4	-	-
11.30		0.5	28.9	20.3	-	-
11.31		0.5	27.0	20.7	-	-
11.32		0.5	27.5	20.6	-	-
11.34		0.5	27.5	20.4	-	-
11.36		0.5	27.0	20.6	-	-
11.38		0.5	28.2	20.6	-	-
11.45		0.5	28.3	20.5	-	-
11.50		0.5	28.0	20.7	-	-
11.55		0.5	30.1	20.4	-	-
11.56		0.5	30.6	20.4	0.10	20
11.58		1.5	34.3	19.4	0.06	40
12.00	5.8	2.5	34.3	19.2	0.06	70
12.01		3.5	34.3	19.0	0.08	90
12.02		4.0	34.3	19.0	0.06	90
12.04		4.5	34.3	19.0	0.07	100
12.05		5.0	34.3	19.0	0.06	100
12.07		5.4	34.3	19.0	0.05	100
12.56		0.5	30.3	20.9	0.18	40
12.58		1.5	34.2	19.4	0.12	30
13.00	6.0	2.5	34.3	19.2	0.08	70
13.01		3.5	34.3	19.1	0.07	80
13.03		4.0	34.3	19.0	0.06	80
13.04		4.5	34.3	19.0	0.06	90
13.05		5.0	34.3	19.0	0.07	80
13.07		5.5	34.3	19.0	0.05	90
13.10		1.0	33.9	19.6	-	-
13.10		0.8	33.8	19.7	-	-
13.11		0.5	31.2	20.6	-	-
13.11		0.2	31.1	20.7	-	-
14.00	6.0	0.5	34.2	19.8	0.19	40
14.01		1.5	34.2	19.5	0.13	50
14.03		2.5	34.3	19.3	0.10	70
14.04		3.5	34.3	19.2	0.05	60
14.05		4.0	34.3	19.1	0.06	60
14.07		4.5	34.3	19.1	0.03	60
14.08		5.0	34.3	19.1	0.04	80
14.10		5.5	34.3	19.1	0.04	120

Table A-5. Station 2: tidal cycle measurements, 14-15 May 1991 (spring tide).

GMT	h	h_m	S	T	U	D
22.25	6.5	0.5	34.0	11.8	0.13	220
22.28		1.0	33.9	11.8	0.08	210
22.30		2.0	34.1	11.6	0.17	300
22.32		3.0	34.2	11.5	0.14	280
22.34		4.0	34.2	11.5	0.12	250
22.36		4.5	34.2	11.4	0.11	300
22.38		5.0	34.2	11.4	0.19	240
22.39		5.5	34.2	11.4	0.18	250
22.41		6.0	34.2	11.4	0.13	250
22.44		6.2	34.2	11.4	0.14	300
23.10		0.5	33.9	11.7	0.19	260
23.12		1.0	33.9	11.6	0.20	270
23.15		2.0	34.0	11.6	0.22	290
23.18		3.0	34.0	11.5	0.24	280
23.20		4.0	34.2	11.4	0.20	280
23.21		4.5	34.2	11.4	0.17	280
23.22		5.0	34.2	11.4	0.15	240
23.24		5.5	34.2	11.4	0.16	240
23.26	6.6	6.0	34.2	11.4	0.16	240
23.55		1.0	33.9	11.6	0.29	250
23.56		0.5	33.9	11.7	0.27	230
23.58		2.0	34.0	11.5	0.27	270
00.00		3.0	34.2	11.4	0.26	270
00.01		4.0	34.2	11.3	0.29	260
00.03		4.5	34.2	11.3	0.28	260
00.05		5.0	34.2	11.3	0.21	290
00.07		5.5	34.2	11.3	0.22	260
00.09		6.0	34.2	11.3	0.19	250
00.10	6.6	6.2	34.2	11.3	0.15	280
00.40		0.5	33.9	11.5	0.31	250
00.42		1.0	33.9	11.5	0.31	250
00.43		2.0	34.1	11.4	0.30	250
00.45		3.0	34.1	11.4	0.25	260
00.47		4.0	34.1	11.4	0.24	260
00.49		4.5	34.1	11.4	0.18	230
00.50		5.0	34.1	11.4	0.14	250
00.51	6.0	5.5	34.2	11.4	0.15	300
01.25		0.5	33.4	11.6	0.25	220
01.27		1.0	33.9	11.5	0.22	290
01.28		2.0	34.1	11.4	0.21	290
01.29		3.0	34.1	11.4	0.20	230
01.30		4.0	34.1	11.4	0.17	230
01.31		4.5	34.1	11.4	0.15	230
01.32		5.0	34.1	11.4	0.14	290
01.33	6.0	5.5	34.1	11.4	0.14	220

02.10		0.5	33.1	11.5	0.25	290
02.12		1.0	33.9	11.5	0.24	320
02.13		2.0	34.1	11.4	0.18	220
02.14		3.0	34.1	11.4	0.19	220
02.15		4.0	34.1	11.4	0.16	270
02.16		4.5	34.1	11.4	0.14	270
02.17	5.7	5.0	34.1	11.4	0.13	270
02.55		0.5	33.9	11.4	0.21	200
02.56		1.0	33.9	11.4	0.22	250
02.58		2.0	34.0	11.4	0.14	290
02.59		3.0	34.1	11.4	0.11	230
03.00		4.0	34.1	11.4	0.11	230
03.01		4.5	34.1	11.4	0.09	210
03.02	5.4	4.9	34.1	11.4	0.08	250
03.40		0.5	32.0	11.4	0.07	250
03.41		1.0	32.4	11.4	0.10	300
03.42		2.0	34.0	11.4	0.10	300
03.44		3.0	34.0	11.4	0.11	280
03.45		4.0	34.0	11.4	0.06	290
03.46	5.0	4.5	34.0	11.4	0.06	280
04.25		0.5	31.7	11.5	0.12	10
04 26		1.0	34.0	11.4	0.06	20
04.28		2.0	34.0	11.4	0.10	350
04.29		3.0	34.0	11.4	0.07	20
04.30		4.0	34.0	11.4	0.10	310
04.31	5.0	4.5	34.1	11.4	0.08	330
05.10		0.5	32.8	11.4	0.08	310
05.11		1.0	34.0	11.4	0.16	320
05.12		2.0	34.1	11.4	0.20	320
05.13		3.0	34.1	11.4	0.22	330
05.14		4.0	34.1	11.4	0.17	340
05.16		4.5	34.1	11.4	0.10	20
05.17		5.0	34.1	11.4	0.10	10
05.19	5.6	5.2	34.1	11.4	0.10	310
05.58	6.0	0.5	30.3	11.5	0.09	100
06.00		1.0	31.8	11.5	0.09	50
06.02		2.0	33.9	11.4	0.30	10
06.04		3.0	34.0	11.4	0.22	310
06.05		4.0	34.0	11.4	0.16	310
06.07		4.5	34.1	11.4	0.15	310
06.08		5.0	34.1	11.4	0.13	300
06.10		5.5	34.1	11.4	0.12	320
06.25		0.5	32.8	11.4	0.10	120
06.30		0.5	29.8	11.5	0.09	130
06.41	6.3	0.5	30.6	11.5	0.08	230
06.43		1.0	32.5	11.4	0.15	80
06.45		2.0	33.8	11.3	0.10	60
06.46		3.0	34.0	11.3	0.29	30
06.48		4.0	34.0	11.3	0.13	250
06.50		4.5	34.0	11.3	0.20	320

06.51		5.0	34.0	11.3	0.14	270
06.53		5.5	34.0	11.3	0.15	300
06.55		6.0	34.0	11.3	0.16	320
06.59		0.5	30.2	11.6	0.22	80
07.26	6.5	0.5	31.8	11.5	0.10	90
07.27		1.0	33.4	11.4	0.08	230
07.29		2.0	34.0	11.3	0.26	320
07.30		3.0	34.0	11.3	0.16	270
07.32		4.0	34.0	11.3	0.16	330
07.33		4.5	34.0	11.3	0.16	290
07.35		5.0	34.0	11.3	0.20	250
07.36		5.5	34.0	11.3	0.22	340
07.38		6.0	34.1	11.2	0.10	270
07.41		0.5	32.9	11.3	0.12	120
08.15	6.7	0.5	33.6	11.4	0.17	80
08.17		1.0	33.6	11.4	0.07	230
08.19		2.0	34.2	11.0	0.22	60
08.20		3.0	34.3	11.0	0.07	280
08.22		4.0	34.3	11.0	0.34	40
08.24		4.5	34.3	11.0	0.07	80
08.25		5.0	34.3	11.0	0.31	50
08.26		5.5	34.3	11.0	0.09	50
08.28		6.0	34.3	11.0	0.25	50
08.29		6.3	34.3	11.0	0.17	50
08.41		0.5	33.7	11.4	0.10	210
09.00	6.8	0.5	33.8	11.4	0.06	220
09.02		1.0	33.9	11.4	0.13	110
09.03		2.0	33.9	11.4	0.11	230
09.05		3.0	34.3	11.1	0.24	40
09.06		4.0	34.4	11.0	0.11	240
09.08		4.5	34.4	11.0	0.16	50
09.09		5.0	34.4	11.0	0.14	260
09.10		5.5	34.4	11.0	0.20	40
09.12		6.0	34.4	11.0	0.08	260
09.13		6.3	34.4	11.0	0.26	350
09.18		0.5	33.8	11.4	0.14	80
09.23		0.5	33.9	11.5	0.12	310
09.41		0.5	33.9	11.5	0.10	270
09.45	6.8	0.5	33.9	11.5	0.10	70
09.46		1.0	33.9	11.4	0.20	210
09.48		2.0	33.9	11.5	0.07	40
09.50		3.0	34.2	11.2	0.11	90
09.51		4.0	34.4	11.0	0.18	350
09.53		4.5	34.4	11.0	0.07	80
09.54		5.0	34.4	11.0	0.27	60
09.55		5.5	34.4	11.0	0.08	250
09.57		6.0	34.4	11.0	0.08	40
09.58		6.3	34.4	11.0	0.17	250
10.00		0.5	33.9	11.4	0.19	260
10.29	6.7	0.5	34.0	11.5	0.13	230

10.31		1.0	34.0	11.5	0.14	120
10.32		2.0	34.0	11.5	0.19	250
10.34		3.0	34.1	11.4	0.18	250
10.35		4.0	34.4	11.1	0.08	330
10.37		4.5	34.4	11.0	0.13	250
10.38		5.0	34.4	11.0	0.09	240
10.40		5.5	34.4	11.0	0.08	340
10.41		6.0	34.4	11.0	0.11	240
10.43		6.2	34.4	11.0	0.05	300
11.06	6.6	0.5	34.0	11.6	0.28	220
11.08		1.0	34.1	11.6	0.25	220
11.09		2.0	34.1	11.4	0.21	300
11.11		3.0	34.4	11.2	0.16	240
11.12		4.0	34.4	11.0	0.13	270
11.14		4.5	34.4	11.0	0.17	270
11.15		5.0	34.4	11.0	0.13	250
11.17		5.5	34.4	11.0	0.12	280
11.18		6.0	34.4	11.0	0.08	300

Table A-6. Station 1: tidal cycle measurements, 15-16 May 1991 (spring tide).

GMT	h	h_m	S	T	U	D
11.47	6.0	0.5	34.2	11.4	0.80	230
11.48		1.0	34.3	11.4	0.76	230
11.50		2.0	34.3	11.3	0.72	230
11.51		3.0	34.3	11.2	0.61	290
11.53		4.0	34.3	11.2	0.55	230
11.54		4.5	34.3	11.2	0.43	220
11.56		5.0	34.3	11.2	0.40	240
11.57		5.5	34.3	11.2	0.38	230
12.00		0.5	34.3	11.3	0.76	220
12.30	5.8	0.5	34.2	11.4	0.82	220
12.32		1.0	34.3	11.3	0.78	240
12.33		2.0	34.3	11.3	0.76	240
12.35		3.0	34.3	11.3	0.73	230
12.37		4.0	34.3	11.2	0.60	230
12.38		4.5	34.3	11.2	0.62	240
12.40		5.0	34.3	11.2	0.50	220
12.41		5.4	34.3	11.2	0.37	230
13.15		0.5	34.3	11.3	0.72	230
13.16		1.0	34.3	11.3	0.68	240
13.17		2.0	34.3	11.3	0.64	230
13.19		3.0	34.3	11.3	0.58	240
13.20		4.0	34.3	11.3	0.56	230
13.21		4.5	34.3	11.3	0.48	240
13.23		5.0	34.3	11.3	0.49	250
13.24	5.9	5.5	34.3	11.3	0.35	300

14.00		0.5	34.4	11.3	0.58	220
14.02		1.0	34.4	11.3	0.59	220
14.03		2.0	34.4	11.3	0.55	230
14.05		3.0	34.4	11.3	0.45	230
14.06		4.0	34.4	11.3	0.49	230
14.07		4.5	34.4	11.3	0.51	240
14.08		5.0	34.4	11.3	0.37	230
14.10	6.0	5.5	34.4	11.3	0.32	240
14.45		0.5	34.4	11.4	0.49	230
14.46		1.0	34.4	11.4	0.46	220
14.47		2.0	34.4	11.4	0.44	220
14.49		3.0	34.4	11.4	0.39	230
14.51		4.0	34.4	11.4	0.37	290
14.52		4.5	34.4	11.4	0.26	290
14.54		5.0	34.4	11.4	0.26	230
14.55	6.0	5.5	34.4	11.4	0.25	220
15.30		0.5	34.3	11.4	0.32	60
15.31		1.0	34.3	11.4	0.33	190
15.33		2.0	34.3	11.4	0.34	100
15.34		3.0	34.4	11.4	0.22	240
15.36		4.0	34.4	11.4	0.20	250
15.37	5.0	4.5	34.4	11.4	0.19	240
16.16		0.5	33.4	11.9	0.29	60
16.18		1.0	33.5	11.8	0.19	160
16.20		2.0	33.7	11.8	0.24	60
16.22		3.0	34.3	11.5	0.13	50
16.23		4.0	34.3	11.4	0.19	50
16.24	4.9	4.5	34.3	11.4	0.12	10
17.00		0.5	34.1	11.7	0.48	80
17.02		1.0	34.1	11.7	0.53	70
17.03		2.0	34.1	11.7	0.49	60
17.04		3.0	34.1	11.7	0.46	50
17.05		4.0	34.1	11.7	0.41	100
17.06	4.9	4.5	34.2	11.7	0.27	70
17.45	5.2	0.5	34.4	11.3	0.60	110
17.48		1.0	34.4	11.3	0.64	120
17.49		2.0	34.3	11.3	0.58	40
17.51		3.0	34.3	11.3	0.57	100
17.53		4.0	34.3	11.3	0.33	120
17.54		4.5	34.3	11.3	0.29	90
17.55		1.0	34.4	11.3	0.68	60
18.30	5.5	0.5	34.4	11.3	0.71	60
18.31		1.0	34.4	11.3	0.67	70
18.33		2.0	34.4	11.2	0.63	60
18.34		3.0	34.4	11.2	0.61	40
18.36		4.0	34.4	11.2	0.57	50
18.37		4.5	34.4	11.2	0.47	50
18.38		5.0	34.4	11.2	0.43	70
19.10	5.8	0.5	34.4	11.2	0.61	70
19.12		1.0	34.4	11.2	0.59	60

19.13		2.0	34.4	11.2	0.61	60
19.15		3.0	34.4	11.2	0.53	50
19.16		4.0	34.4	11.2	0.47	60
19.17		4.5	34.4	11.2	0.46	60
19.19		5.0	34.4	11.2	0.50	60
19.20		5.3	34.4	11.2	0.42	50
19.50	6.0	0.5	34.4	11.1	0.56	70
19.51		1.0	34.4	11.1	0.54	60
19.53		2.0	34.4	11.1	0.51	60
19.54		3.0	34.4	11.1	0.52	60
19.55		4.0	34.4	11.1	0.52	60
19.56		4.5	34.4	11.1	0.47	60
19.57		5.0	34.4	11.1	0.41	40
19.59		5.5	34.4	11.1	0.35	60
20.30	6.2	0.5	34.4	11.1	0.54	70
20.31		1.0	34.4	11.1	0.53	60
20.32		2.0	34.4	11.1	0.53	50
20.34		3.0	34.4	11.1	0.47	60
20.35		4.0	34.4	11.1	0.44	60
20.36		4.5	34.4	11.1	0.47	40
20.37		5.0	34.4	11.1	0.40	60
20.39		5.5	34.4	11.1	0.33	40
20.40		5.8	34.4	11.1	0.25	40
21.15	6.0	0.5	34.5	11.1	0.43	130
21.16		1.0	34.5	11.1	0.43	70
21.17		2.0	34.5	11.1	0.47	50
21.19		3.0	34.5	11.1	0.39	60
21.20		4.0	34.5	11.1	0.37	60
21.22		4.5	34.5	11.1	0.31	50
21.23		5.0	34.5	11.1	0.28	60
21.24		5.5	34.5	11.1	0.32	50
21 59	6.1	0.5	34.5	11.1	0.31	80
22.00		1.0	34.5	11.1	0.35	80
22.01		2.0	34.5	11.1	0.36	60
22.02		3.0	34.5	11.1	0.29	60
22.03		4.0	34.5	11.1	0.26	40
22.04		4.5	34.5	11.1	0.28	70
22.06		5.0	34.5	11.1	0.26	50
22.07		5.5	34.5	11.1	0.21	80
22.40	6.0	0.5	34.5	11.1	0.10	110
22.41		1.0	34.5	11.1	0.08	60
22.43		2.0	34.5	11.1	0.12	70
22.44		3.0	34.5	11.1	0.08	40
22.45		4.0	34.5	11.1	0.11	90
22.47		4.5	34.5	11.1	0.10	40
22.48		5.0	34.5	11.1	0.10	70
22.49		5.5	34.5	11.1	0.06	250
23.25	5.9	0.5	33.6	11.2	0.56	220
23.25		1.0	33.8	11.2	0.48	220
23.28		2.0	34.4	11.1	0.39	210

23.29		3.0	34.4	11.1	0.40	220
23.30		4.0	34.4	11.1	0.39	260
23.31		4.5	34.4	11.1	0.32	220
23.33		5.0	34.4	11.1	0.31	220
23.34		5.5	34.4	11.1	0.20	230
00.10		0.5	34.0	11.2	0.86	230
00.11		1.0	34.0	11.2	0.77	230
00.12		2.0	34.3	11.2	0.75	230
00.14		3.0	34.3	11.2	0.72	230
00.15		4.0	34.3	11.1	0.57	230
00.16		4.5	34.4	11.1	0.52	220
00.17		5.0	34.4	11.1	0.43	230
00.18	5.9	5.5	34.4	11.1	0.32	230

Table A-7. Station 5: tidal cycle measurements, 3-4 May 1992 (spring tide).

GMT	h	h_m	S	T	U	D	C
18.50	1.00	0.20	0.3	13.3	0.36	290	-
18.55		0.50	0.3	13.2	0.35	290	16.2
18.57		0.80	0.4	13.2	0.30	280	-
19.30	1.05	0.20	4.0	13.2	0.24	350	-
19.32		0.55	15.0	13.2	0.34	280	18.2
19.34		0.85	23.7	13.0	0.31	280	-
20.00	1.15	0.20	1.5	12.8	0.00	-	-
20.02		0.60	15.8	12.7	0.15	290	17.9
20.04		0.95	31.4	12.4	0.30	280	-
20.30	1.25	0.20	2.0	12.5	0.07	70	-
20.32		0.65	27.8	12.5	0.23	290	9.4
20.34		1.05	33.2	12.3	0.26	290	-
21.00	1.35	0.20	1.7	12.7	0.16	160	-
21.02		0.70	33.0	12.2	0.20	280	5.9
21.04		1.15	33.6	12.4	0.19	280	-
21.30	1.50	0.20	2.6	13.0	0.26	130	-
21.32		0.75	33.8	12.8	0.13	270	8.8
21.34		1.30	33.9	12.8	0.12	270	-
22.00	1.40	0.20	2.0	13.0	0.36	110	-
22.03		0.70	31.8	13.0	0.02	160	7.7
22.06		1.20	33.9	13.2	0.03	220	-
22.30	1.25	0.20	4.4	12.9	0.34	110	-
22.33		0.65	26.5	12.7	0.09	120	5.9
22.36		1.05	33.4	12.2	0.04	210	-
23.00	1.20	0.20	6.8	12.8	0.46	110	-
23.02		0.60	19.8	12.4	0.21	130	5.8
23.05		1.00	32.3	11.9	0.04	120	-
23.33	1.15	0.20	4.9	12.8	0.56	120	-
23.35		0.60	9.8	12.8	0.41	120	6.9

23.38		0.95	28.0	12.2	0.06	110	-
00.00	1.05	0.20	3.8	12.9	0.50	120	-
00.03		0.55	14.9	12.4	0.17	120	7.0
00.05		0.85	33.9	11.9	0.06	240	-
00.30	1.05	0.20	5.0	12.8	0.37	110	-
00.32		0.55	29.2	12.3	0.11	250	11.9
00.34		0.85	33.5	12.1	0.20	260	-
01.00	1.10	0.20	2.5	12.8	0.12	140	-
01.02		0.55	21.8	12.2	0.13	260	9.5
01.04		0.90	33.4	12.0	0.25	270	-
01.30	1.15	0.20	5.1	12.8	0.16	120	-
01.33		0.60	27.5	12.4	0.07	240	8.7
01.35		0.95	32.9	12.0	0.03	220	-
02.00	1.15	0.20	4.0	12.6	0.50	110	-
02.03		0.60	27.8	12.2	0.12	120	6.6
02.05		0.90	32.6	12.0	0.02	110	-
02.30	1.10	0.20	4.8	12.6	0.51	120	-
02.33		0.55	14.8	12.4	0.36	120	14.8
02.35		0.80	32.5	12.0	0.20	110	-
03.00	1.00	0.20	5.0	12.7	0.39	120	-
03.03		0.50	5.2	12.5	0.36	110	12.5
03.05		0.70	21.2	12.3	0.37	100	-
03.30	0.90	0.20	3.2	12.6	0.37	120	-
03.33		0.45	3.5	12.5	0.38	120	22.3
03.35		0.70	11.5	12.6	0.45	110	-
04.00	0.80	0.20	2.2	12.3	0.38	120	-
04.02		0.40	2.9	12.4	0.40	110	14.9
04.04		0.60	3.0	12.5	0.41	110	-
04.30	0.70	0.20	2.3	12.2	0.30	130	-
04.33		0.35	2.8	12.2	0.32	130	16.3
04.35		0.50	2.8	12.3	0.28	120	-
05.00	0.65	0.20	2.5	12.3	0.35	120	-
05.02		0.35	2.9	12.3	0.31	120	36.3
05.04		0.45	3.2	12.2	0.27	130	-
05.30	0.60	0.20	2.6	12.2	0.35	120	-
05.32		0.30	2.6	12.2	0.31	120	19.0
05.34		0.40	2.7	12.3	0.29	120	-
06.00	0.60	0.20	2.3	12.3	0.41	120	-
06.02		0.30	2.2	12.3	0.38	120	20.4
06.04		0.40	2.3	12.2	0.35	120	-
06.30	0.60	0.20	1.8	12.3	0.36	120	-
06.32		0.30	1.9	12.2	0.29	130	19.6
06.34		0.40	1.9	12.2	0.21	130	-
07.00	0.75	0.20	1.8	12.2	0.02	320	-
07.02		0.40	1.8	12.2	0.02	250	34.8
07.04		0.55	1.6	12.2	0.06	260	-
07.30	0.95	0.20	1.8	12.2	0.27	300	-
07.32		0.50	1.5	12.2	0.23	290	29.5
07.34		0.75	1.5	12.2	0.17	280	-

Table A-8. Station 5: tidal cycle measurements, 10-11 May 1992 (neap tide).

GMT	h	h_m	S	T	U	D	C
17.00	1.40	0.20	3.0	13.9	0.25	90	6.9
17.03		0.70	32.4	13.7	0.26	300	11.0
17.05		1.20	33.1	13.4	0.26	280	13.3
17.30	1.40	0.20	3.6	13.8	0.26	100	6.4
17.32		0.70	32.7	13.4	0.21	320	12.2
17.34		1.20	33.1	13.4	0.21	280	11.5
18.00	1.45	0.20	4.8	13.7	0.19	90	6.4
18.02		0.75	32.6	13.5	0.22	290	8.4
18.04		1.25	33.6	13.5	0.15	280	9.4
18.30	1.50	0.20	6.6	13.5	0.27	100	6.3
18.32		0.75	32.9	13.0	0.14	310	6.9
18.34		1.30	33.7	12.9	0.12	280	8.0
19.00	1.60	0.20	4.1	13.3	0.33	100	5.7
19.02		0.80	33.4	13.1	0.06	330	6.2
19.04		1.40	33.8	12.8	0.08	280	7.6
19.30	1.60	0.20	6.7	13.2	0.35	110	6.1
19.32		0.80	33.9	12.8	0.03	30	7.0
19.34		1.40	34.0	12.8	0.05	290	7.5
20.00	1.50	0.20	11.8	13.4	0.31	100	6.2
20.02		0.75	33.3	12.8	0.03	20	6.9
20.04		1.30	33.9	12.8	0.00	-	7.1
20.30	1.30	0.20	11.3	13.6	0.33	100	6.9
20.32		0.65	26.0	13.7	0.14	80	7.2
20.34		1.10	33.8	12.9	0.00	-	7.6
21.00	1.25	0.20	6.2	13.5	0.47	110	7.9
21.02		0.65	15.0	13.6	0.30	100	7.9
21.04		1.05	33.2	13.1	0.05	80	8.5
21.30	1.15	0.20	4.9	13.4	0.50	120	9.2
21.32		0.60	8.0	13.4	0.31	120	12.5
21.34		0.95	32.8	12.9	0.00	-	7.3
22.00	1.05	0.20	4.7	13.5	0.36	120	10.5
22.03		0.55	19.6	13.5	0.31	110	9.0
22.05		0.85	28.8	13.2	0.05	80	8.1
22.30	0.95	0.20	4.3	13.4	0.32	120	14.4
22.32		0.50	16.1	13.5	0.35	100	15.1
22.34		0.75	28.6	13.2	0.02	80	13.5
23.00	0.82	0.20	3.1	13.3	0.27	110	8.8
23.02		0.40	4.0	13.3	0.28	100	9.8
23.04		0.60	14.8	13.4	0.31	100	11.7
23.30	0.78	0.20	3.2	13.2	0.27	110	8.2
23.32		0.40	5.6	13.3	0.26	90	11.6
23.34		0.60	9.8	13.5	0.21	80	16.1
00.03	0.82	0.20	2.7	13.1	0.02	90	7.3
00.05		0.40	5.5	13.3	0.02	20	8.9
00.07		0.60	12.4	13.3	0.08	320	19.8

00.30	0.92	0.20	4.8	13.2	0.29	310	9.2
00.32		0.45	17.0	13.1	0.18	300	11.9
00.34		0.70	25.8	13.0	0.20	290	13.9
01.00	1.08	0.20	14.0	12.9	0.24	320	11.3
01.02		0.55	20.2	12.9	0.08	300	12.8
01.04		0.90	24.8	12.9	0.03	310	13.5
01.30	1.15	0.20	5.0	12.8	0.04	50	7.4
01.32		0.60	15.4	12.9	0.11	350	11.3
01.34		0.95	17.9	12.9	0.19	290	11.2
02.00	1.15	0.20	3.2	12.9	0.20	100	6.8
02.02		0.60	15.8	12.8	0.02	10	9.0
02.04		0.95	24.9	12.8	0.23	280	12.2
02.35	1.20	0.20	2.8	12.9	0.23	50	6.6
02.37		0.60	23.8	12.4	0.04	10	9.7
02.39		1.00	30.3	12.3	0.23	290	11.3
03.00	1.20	0.20	2.6	12.8	0.23	100	6.4
03.02		0.60	28.2	12.4	0.09	330	7.9
03.04		1.00	32.6	12.4	0.20	290	9.6
03.34	1.22	0.20	3.4	12.8	0.31	110	6.5
03.36		0.60	32.5	12.4	0.06	350	7.5
03.38		1.00	33.4	12.2	0.19	290	8.6
04.00	1.30	0.20	5.0	12.8	0.27	110	6.8
04.02		0.65	33.2	12.2	0.26	300	8.8
04.04		1.10	33.4	12.2	0.23	280	10.5
04.30	1.35	0.20	5.1	12.6	0.16	90	6.5
04.32		0.70	32.2	12.3	0.22	300	8.7
04.34		1.15	32.9	12.2	0.20	280	9.4
05.00	1.28	0.20	5.9	12.6	0.28	90	6.9
05.02		0.65	32.7	12.1	0.08	330	8.2
05.04		1.10	33.0	12.1	0.14	290	8.7
05.30	1.30	0.20	6.1	12.6	0.31	100	6.3
05.32		0.65	32.7	12.2	0.06	330	7.8
05.34		1.10	33.0	12.1	0.16	280	8.8

Table A-9. Station 4: tidal cycle measurements, 27 July 1991 (spring tide).

GMT	η	U	S	T	C
04.00	-0.30	-0.77	15.2	16.4	10.8
04.30	-0.37	-0.77	14.3	16.2	11.9
05.00	-0.42	-0.63	14.2	16.4	13.5
05.30	-0.40	-0.38	13.5	16.3	14.1
06.00	-0.27	0.51	17.6	16.5	13.7
06.30	-0.15	1.20	32.0	16.3	12.6
07.00	-0.06	1.13	33.6	16.3	15.0
07.30	0.05	0.89	33.9	16.4	12.3
08.00	0.16	0.88	34.0	16.4	11.3
08.30	0.26	0.74	34.1	17.3	5.9
09.00	0.35	0.50	34.1	17.4	6.2
09.30	0.43	0.26	34.7	17.5	5.0
10.00	0.42	-0.25	34.6	17.6	9.2
10.30	0.37	-0.56	33.9	17.8	7.9
11.00	0.33	-0.73	27.4	18.2	7.9
11.30	0.28	-0.65	25.7	18.6	8.4
12.00	0.30	0.00	25.9	18.6	7.9
12.30	0.35	0.73	29.3	18.4	9.3
13.00	0.43	0.39	32.4	18.2	18.1
13.30	0.39	-0.62	32.1	18.3	8.4
14.00	0.28	-0.86	30.3	19.0	10.8
14.30	0.11	-1.13	27.1	19.1	13.6
15.00	-0.02	-1.18	24.3	20.0	20.0
15.30	-0.11	-0.99	21.2	20.7	26.9
16.00	-0.20	-0.81	20.4	20.7	21.5
16.30	-0.27	-0.82	18.8	20.6	15.6
17.00	-0.33	-0.79	13.9	20.1	15.7
17.30	-0.32	-0.65	11.5	19.8	11.6
18.00	-0.20	0.27	17.9	20.0	15.1

Table A-10. Station 4: tidal cycle measurements, 3 August 1991 (neap tide).

GMT	η	U	S	T	C
03.00	0.27	-0.27	25.1	18.4	4.8
03.30	0.22	-0.20	27.5	18.4	6.9
04.00	0.24	-0.02	31.8	18.3	8.5
04.30	0.28	0.33	31.7	18.4	6.4
05.00	0.31	0.05	31.7	18.3	4.4
05.30	0.26	-0.71	30.2	18.4	5.4
06.00	0.11	-1.15	29.4	18.4	7.3
06.30	-0.02	-1.02	22.1	18.5	6.8
07.00	-0.11	-1.14	16.2	18.2	7.5
07.30	-0.19	-0.86	16.5	18.4	10.0
08.00	-0.26	-0.70	17.1	18.7	8.9
08.30	-0.32	-0.64	16.4	19.0	9.2
09.00	-0.36	-0.62	15.6	19.1	8.3
09.30	-0.35	-0.35	15.7	19.1	11.4
10.00	-0.27	0.13	15.7	19.3	10.9
10.30	-0.17	0.95	30.4	18.8	8.2
11.00	-0.10	0.93	32.7	18.8	7.2
11.30	-0.02	0.84	33.4	18.8	4.5
12.00	0.06	0.53	33.6	18.8	10.1
12.30	0.13	0.59	33.7	18.8	11.5
13.00	0.18	0.23	34.3	18.7	14.4
13.30	0.21	0.05	34.3	18.7	7.0
14.00	0.23	0.00	34.2	18.7	9.5
14.30	0.25	0.00	34.0	18.8	11.3
15.00	0.25	-0.18	33.5	18.9	9.6
15.30	0.28	-0.18	32.2	19.1	9.2
16.00	0.34	0.45	33.8	18.9	7.5
16.30	0.41	0.63	34.0	18.9	10.2
17.00	0.48	0.35	34.0	18.9	11.6

APPENDIX B. SEABED SEDIMENT DATA

Table B-1. Positions and percentages of gravel, sand and mud in seabed sediment samples. Other analyses carried out are also listed (A and B - grain size analysis for gravel and sand sub-samples by dry sieving, respectively; C - grain size analysis for mud fractions using SediGraph; and D - analysis of the content of foraminiferal tests).

Sample Number	Latitude	Longitude	Sample Amount (g)	Gravel %	Sand %	Mud %	Analysis Carried Out
1	50°43.81'N	1°46.09'W	174.2	0.3	96.2	3.5	A,B
2	50°43.76'N	1°46.31'W	111.4	0.1	51.1	48.8	A,B,C
3	50°43.74'N	1°46.27'W	510.1	99.6	0.3	0.1	A,B
4	50°43.71'N	1°46.26'W	167.6	96.9	2.7	0.4	A,B
5	50°43.68'N	1°46.25'W	83.3	0.0	33.8	66.2	B
6	50°43.66'N	1°46.19'W	118.8	1.8	60.0	38.2	A,B,D
7	50°43.65'N	1°46.15'W	229.7	91.3	8.4	0.3	A,B
8	50°43.65'N	1°46.10'W	232.6	0.5	98.7	0.8	A,B
9	50°43.67'N	1°46.02'W	165.8	0.1	75.7	24.2	A,B
10	50°43.62'N	1°46.04'W	265.6	42.8	50.4	6.8	A,B,D
11	50°43.69'N	1°45.96'W	200.4	1.8	80.7	17.5	A,B
12	50°43.65'N	1°45.96'W	176.4	35.2	50.2	14.6	A,B
13	50°43.62'N	1°45.96'W	140.6	0.6	80.0	19.4	A,B
14	50°43.57'N	1°45.96'W	198.7	30.9	55.4	13.7	A,B,C
15	50°43.53'N	1°45.96'W	100.0	12.8	51.5	35.7	A,B,D
16	50°43.48'N	1°45.96'W	269.3	85.9	12.5	1.6	A,B
17	50°43.45'N	1°45.97'W	169.3	66.8	30.6	2.6	A,B,D
18	50°43.41'N	1°45.98'W	81.4	0.2	30.8	69.0	A,B,C
19	50°43.37'N	1°45.97'W	146.7	0.1	60.1	39.8	A,B
20	50°43.34'N	1°45.94'W	149.5	0.1	47.0	52.9	A,B
21	50°43.68'N	1°45.87'W	198.7	78.1	20.7	1.2	A,B,D
22	50°43.67'N	1°45.88'W	225.8	37.4	57.8	4.8	A,B
23	50°43.63'N	1°45.90'W	138.2	10.4	64.2	25.4	A,B
24	50°43.60'N	1°45.90'W	109.3	1.9	66.9	31.2	A,B,C
25	50°43.56'N	1°45.92'W	234.7	11.3	77.2	11.5	A,B
26	50°43.52'N	1°45.94'W	283.7	58.2	40.2	1.6	A,B
27	50°43.45'N	1°45.93'W	227.6	68.7	26.7	4.6	A,B,C
28	50°43.38'N	1°45.93'W	152.7	8.7	89.1	2.2	A,B
29	50°43.31'N	1°45.90'W	174.1	29.2	58.3	12.5	A,B,C
30	50°43.48'N	1°45.92'W	167.1	34.8	64.9	0.3	A,B
31	50°43.45'N	1°45.88'W	136.8	39.4	58.1	2.5	A,B
32	50°43.40'N	1°45.88'W	140.1	52.6	45.9	1.5	A,B
33	50°43.36'N	1°45.87'W	72.6	38.9	59.8	1.3	A,B
34	50°43.28'N	1°45.86'W	169.9	23.1	69.3	7.6	A,B
35	50°43.42'N	1°45.85'W	169.5	31.6	64.8	3.6	A,B,D
36	50°43.38'N	1°45.81'W	146.1	35.3	61.5	3.2	A,B
37	50°43.37'N	1°45.85'W	64.3	6.6	92.0	1.4	A,B

38	50°43.32'N	1°45.83'W	305.8	0.2	96.1	3.7	A,B
39	50°43.25'N	1°45.81'W	72.5	21.0	76.0	3.0	A,B
40	50°43.35'N	1°45.80'W	124.5	53.8	44.5	1.7	A,B
41	50°43.29'N	1°45.76'W	306.1	0.3	95.9	3.8	A,B
42	50°43.24'N	1°45.75'W	309.8	22.6	71.1	6.3	A,B,C
43	50°43.36'N	1°45.76'W	133.9	29.3	65.7	5.0	A,B,D
44	50°43.33'N	1°45.75'W	160.3	53.5	42.1	4.4	A,B,C
45	50°43.27'N	1°45.72'W	218.7	0.3	93.8	5.9	A,B
46	50°43.32'N	1°45.70'W	225.8	77.1	20.3	2.6	A,B,C
47	50°43.30'N	1°45.66'W	111.4	28.8	68.8	2.4	A,B
48	50°43.23'N	1°45.68'W	272.5	3.6	82.2	14.2	A,B
49	50°43.34'N	1°45.60'W	150.2	0.7	90.1	9.2	A,B,C
50	50°43.31'N	1°45.60'W	169.3	1.2	91.0	7.8	A,B,D
51	50°43.28'N	1°45.61'W	164.0	10.9	84.5	4.6	A,B,C
52	50°43.25'N	1°45.64'W	230.2	0.2	77.6	22.2	A,B
53	50°43.22'N	1°45.63'W	135.5	0.3	91.6	8.1	A,B
54	50°43.46'N	1°45.63'W	191.8	46.3	48.3	5.4	A,B
55	50°43.43'N	1°45.59'W	205.9	44.3	48.4	7.3	A,B
56	50°43.40'N	1°45.55'W	153.1	12.4	79.0	8.6	A,B
57	50°43.37'N	1°45.51'W	153.5	40.9	49.1	10.0	A,B,D
58	50°43.33'N	1°45.57'W	125.9	0.7	92.1	7.2	A,B
59	50°43.33'N	1°45.51'W	120.3	0.2	89.2	10.6	A,B,C
60	50°43.31'N	1°45.54'W	156.7	1.2	93.9	4.9	A,B
61	50°43.28'N	1°45.55'W	157.0	22.9	76.1	1.0	A,B
62	50°43.24'N	1°45.58'W	249.9	0.2	83.7	16.1	A,B
63	50°43.21'N	1°45.56'W	127.5	0.1	38.0	61.9	A,B,C
64	50°43.27'N	1°45.51'W	160.5	4.8	91.5	3.7	A,B
65	50°43.23'N	1°45.52'W	234.0	0.5	86.5	13.0	A,B,C
66	50°43.15'N	1°45.53'W	223.6	2.7	74.8	22.5	A,B
67	50°43.10'N	1°45.64'W	148.9	2.5	88.3	9.2	A,B,D
68	50°43.07'N	1°45.61'W	325.6	75.6	21.9	2.5	A,B
69	50°43.05'N	1°45.57'W	269.1	59.6	35.2	5.2	A,B
70	50°43.34'N	1°45.46'W	131.5	1.0	89.2	9.8	A,B
71	50°43.31'N	1°45.48'W	150.1	0.7	92.4	7.0	A,B
72	50°43.27'N	1°45.47'W	88.6	3.5	62.9	33.6	A,B
73	50°43.23'N	1°45.46'W	98.5	0.1	88.5	11.4	A,B
74	50°43.20'N	1°45.50'W	179.2	1.4	69.6	29.0	A,B
75	50°43.12'N	1°45.48'W	126.7	1.3	52.7	46.0	A,B,C
76	50°43.04'N	1°45.51'W	363.8	68.5	27.2	4.3	A,B
77	50°43.51'N	1°45.43'W	149.2	1.8	84.9	13.3	A,B,D
78	50°43.49'N	1°45.45'W	143.9	0.6	85.9	13.5	A,B
79	50°43.46'N	1°45.43'W	145.0	1.2	84.9	13.9	A,B
80	50°43.43'N	1°45.42'W	127.9	2.2	83.6	14.2	A,B,D
81	50°43.34'N	1°45.41'W	157.3	1.1	83.8	15.1	A,B
82	50°43.32'N	1°45.41'W	191.6	0.6	86.8	12.6	A,B
83	50°43.27'N	1°45.42'W	186.0	4.4	87.6	8.0	A,B
84	50°43.18'N	1°45.44'W	210.3	0.3	85.0	14.7	A,B
85	50°43.15'N	1°45.43'W	241.3	0.1	75.4	24.5	A,B,C,D
86	50°43.04'N	1°45.45'W	256.5	63.6	34.8	1.6	A,B,D
87	50°43.47'N	1°45.40'W	149.0	2.0	83.9	14.1	A,B

88	50°43.44'N	1°45.38'W	151.6	1.7	79.5	18.8	A,B,C
89	50°43.42'N	1°45.36'W	148.2	0.3	81.3	18.4	A,B
90	50°43.37'N	1°45.36'W	199.4	35.0	59.9	5.1	A,B
91	50°43.34'N	1°45.36'W	132.9	0.8	82.8	16.4	A,B,C
92	50°43.31'N	1°45.35'W	130.3	0.3	82.1	17.6	A,B,D
93	50°43.27'N	1°45.39'W	70.3	37.4	58.9	3.7	A,B,C
94	50°43.27'N	1°45.35'W	224.7	8.9	81.6	9.5	A,B
95	50°43.23'N	1°45.38'W	235.1	0.3	84.8	14.9	A,B
96	50°43.18'N	1°45.36'W	220.5	0.1	85.0	14.9	A,B
97	50°43.15'N	1°45.34'W	177.2	0.1	78.7	21.2	A,B
98	50°43.12'N	1°45.38'W	215.8	4.6	69.3	26.1	A,B
99	50°43.18'N	1°45.34'W	215.7	30.2	68.8	1.0	A,B,C
100	50°43.06'N	1°45.39'W	248.4	45.9	52.4	1.7	A,B
101	50°43.68'N	1°45.35'W	53.1	0.6	69.0	30.4	A,B,D
102	50°43.68'N	1°45.29'W	126.1	0.1	68.9	31.0	A,B,C
103	50°43.65'N	1°45.30'W	100.2	0.7	84.4	14.9	A,B
104	50°43.54'N	1°45.35'W	119.6	2.5	87.5	10.0	A,B
105	50°43.50'N	1°45.35'W	163.7	25.0	63.9	11.1	A,B
106	50°43.47'N	1°45.33'W	114.1	4.0	82.0	14.0	A,B
107	50°43.47'N	1°45.32'W	89.6	0.6	77.5	21.9	A,B
108	50°43.40'N	1°45.31'W	100.1	1.4	90.8	7.8	A,B
109	50°43.37'N	1°45.31'W	147.1	5.9	82.4	11.7	A,B
110	50°43.35'N	1°45.30'W	98.8	0.2	81.5	18.3	A,B
111	50°43.32'N	1°45.30'W	156.8	2.4	84.3	13.3	A,B
112	50°43.27'N	1°45.30'W	127.6	3.8	85.7	10.5	A,B
113	50°43.23'N	1°45.31'W	209.8	0.5	87.4	12.1	A,B
114	50°43.18'N	1°45.29'W	246.6	0.1	84.9	15.0	A,B
115	50°43.08'N	1°45.27'W	138.3	10.3	86.9	2.8	A,B
116	50°43.65'N	1°45.26'W	71.0	0.5	49.4	50.1	A,B
117	50°43.59'N	1°45.25'W	118.2	2.0	83.9	14.1	A,B
118	50°43.51'N	1°45.28'W	117.3	11.6	80.6	7.8	A,B,D
119	50°43.48'N	1°45.28'W	130.3	15.9	70.1	14.0	A,B,C
120	50°43.44'N	1°45.27'W	74.1	3.1	71.3	25.6	A,B
121	50°43.41'N	1°45.26'W	76.9	7.1	71.0	21.9	A,B,D
122	50°43.36'N	1°45.25'W	151.6	36.7	55.5	7.8	A,B
123	50°43.33'N	1°45.24'W	142.1	23.9	65.4	10.7	A,B
124	50°43.27'N	1°45.26'W	239.8	1.1	86.1	12.8	A,B
125	50°43.23'N	1°45.24'W	224.7	8.9	81.6	9.5	A,B,C
126	50°43.16'N	1°45.24'W	201.2	0.8	78.7	20.5	A,B
127	50°43.12'N	1°45.25'W	196.0	3.4	71.2	25.4	A,B,C
128	50°43.08'N	1°45.22'W	183.6	43.9	53.5	2.6	A,B
129	50°43.40'N	1°45.28'W	106.0	13.0	85.1	1.9	A,B,D
130	50°43.63'N	1°45.22'W	86.1	2.9	45.0	52.1	A,B
131	50°43.59'N	1°45.19'W	96.0	5.7	60.0	34.3	A,B,D
132	50°43.54'N	1°45.24'W	149.2	7.0	80.7	12.3	A,B
133	50°43.48'N	1°45.22'W	120.7	1.3	80.6	18.1	A,B
134	50°43.44'N	1°45.21'W	163.5	2.1	61.9	36.0	A,B
135	50°43.38'N	1°45.19'W	135.1	2.9	68.2	28.9	A,B
136	50°43.31'N	1°45.18'W	149.6	44.7	48.5	6.8	A,B,D
137	50°43.27'N	1°45.21'W	193.1	5.9	84.4	9.7	A,B,C

138	50°43.27'N	1°45.17'W	176.3	12.0	78.3	9.7	A,B
139	50°43.22'N	1°45.18'W	167.8	4.2	83.8	12.0	A,B
140	50°43.18'N	1°45.20'W	216.8	0.1	78.7	21.2	A,B,C
141	50°43.15'N	1°45.15'W	159.5	4.0	73.0	23.0	A,B,D
142	50°43.12'N	1°45.14'W	160.0	5.4	73.4	21.2	A,B
143	50°43.08'N	1°45.16'W	184.4	22.6	73.2	4.2	A,B,D
144	50°43.54'N	1°45.17'W	106.2	3.9	65.0	31.1	A,B,C
145	50°43.49'N	1°45.17'W	177.4	0.3	83.9	15.8	A,B
146	50°43.45'N	1°45.16'W	188.3	0.3	82.9	16.8	A,B
147	50°43.41'N	1°45.14'W	178.1	10.6	69.2	20.2	A,B,C
148	50°43.27'N	1°45.12'W	226.1	2.5	88.2	9.2	A,B
149	50°43.22'N	1°45.10'W	138.2	0.7	76.1	23.2	A,B
150	50°43.18'N	1°45.12'W	252.8	0.3	80.0	19.7	A,B
151	50°43.15'N	1°45.08'W	132.5	2.4	82.9	14.7	A,B
152	50°43.09'N	1°45.10'W	150.5	26.9	70.8	2.3	A,B
153	50°43.54'N	1°45.12'W	137.0	15.3	61.5	23.2	A,B
154	50°43.50'N	1°45.11'W	198.4	2.7	65.1	32.2	A,B
155	50°43.46'N	1°45.10'W	116.3	1.3	75.3	23.4	A,B
156	50°43.42'N	1°45.07'W	148.0	1.9	64.4	33.7	A,B
157	50°43.38'N	1°45.06'W	153.9	20.4	65.6	13.9	A,B,D
158	50°43.34'N	1°45.06'W	151.9	2.5	78.6	18.9	A,B,C
159	50°43.30'N	1°45.08'W	148.2	5.7	73.0	21.3	A,B
160	50°43.26'N	1°45.09'W	291.1	0.4	89.2	10.4	A,B
161	50°43.25'N	1°45.04'W	93.0	3.5	85.9	10.6	A,B
162	50°43.21'N	1°45.03'W	115.6	0.8	82.1	17.1	A,B
163	50°43.17'N	1°45.04'W	224.3	3.5	86.5	10.0	A,B,C
164	50°43.15'N	1°45.00'W	160.0	0.4	73.1	26.5	A,B
165	50°43.12'N	1°45.01'W	226.3	7.1	71.2	21.7	A,B
166	50°43.10'N	1°45.05'W	240.6	37.0	60.4	2.6	A,B
167	50°43.10'N	1°44.98'W	175.5	20.6	75.3	4.1	A,B
168	50°43.52'N	1°45.07'W	200.2	1.3	80.6	18.1	A,B
169	50°43.48'N	1°45.05'W	112.5	0.3	71.6	28.1	A,B
170	50°43.43'N	1°45.03'W	149.8	0.9	68.3	30.8	A,B,C
171	50°43.40'N	1°45.01'W	168.1	1.2	83.3	15.5	A,B
172	50°43.37'N	1°45.00'W	267.6	0.9	75.8	23.3	A,B
173	50°43.34'N	1°45.00'W	193.1	4.5	75.5	20.0	A,B
174	50°43.31'N	1°45.00'W	174.8	0.2	77.7	22.1	A,B
175	50°43.27'N	1°44.99'W	180.2	0.1	80.7	19.2	A,B
176	50°43.24'N	1°44.98'W	213.3	4.5	85.4	10.2	A,B
177	50°43.20'N	1°44.97'W	132.2	0.4	86.0	13.6	A,B
178	50°43.17'N	1°44.97'W	171.6	0.5	64.6	34.9	A,B
179	50°43.50'N	1°44.95'W	223.2	26.7	61.9	11.4	A,B,C
180	50°43.46'N	1°44.95'W	182.8	22.0	66.8	11.2	A,B
181	50°43.43'N	1°44.95'W	193.5	3.6	80.5	15.8	A,B
182	50°43 38'N	1°44.94'W	140.8	1.6	78.7	19.7	A,B
183	50°43.34'N	1°44.94'W	108.2	0.6	77.6	21.8	A,B
184	50°43.30'N	1°44.94'W	186.9	0.5	83.6	15.9	A,B,C,D
185	50°43.25'N	1°44.91'W	133.2	1.5	81.6	16.9	A,B
186	50°43.23'N	1°44.95'W	248.7	0.3	85.6	14.1	A,B,C
187	50°43.21'N	1°44.90'W	120.6	3.6	83.2	13.2	A,B

188	50°43.18'N	1°44.91'W	112.1	2.7	81.2	16.1	A,B
189	50°43.15'N	1°44.90'W	162.6	0.7	80.0	19.3	A,B,C
190	50°43.12'N	1°44.90'W	173.9	2.2	54.7	43.1	A,B
191	50°43.08'N	1°44.92'W	207.1	29.7	65.3	5.0	A,B
192	50°43.50'N	1°44.89'W	186.0	29.0	58.1	12.9	A,B
193	50°43.47'N	1°44.89'W	147.8	5.7	77.0	17.3	A,B
194	50°43.44'N	1°44.88'W	166.8	33.0	56.1	10.9	A,B
195	50°43.41'N	1°44.88'W	173.8	7.7	70.1	22.2	A,B,D
196	50°43.37'N	1°44.88'W	207.0	2.3	73.9	23.8	A,B
197	50°43.35'N	1°44.87'W	185.6	3.3	76.5	20.2	A,B
198	50°43.32'N	1°44.87'W	172.5	1.0	69.7	29.3	A,B
199	50°43.29'N	1°44.87'W	188.2	0.5	78.2	21.3	A,B
200	50°43.52'N	1°44.84'W	121.6	10.5	75.1	14.4	A,B
201	50°43.46'N	1°44.83'W	161.4	8.7	79.3	11.9	A,B
202	50°43.41'N	1°44.82'W	219.8	2.3	68.6	29.1	A,B,C
203	50°43.36'N	1°44.81'W	164.4	1.4	80.7	17.9	A,B,C,D
204	50°43.31'N	1°44.81'W	43.4	1.5	81.8	16.7	A,B
205	50°43.27'N	1°44.82'W	188.9	1.9	78.5	19.5	A,B,D
206	50°43.23'N	1°44.83'W	180.6	3.5	78.4	18.1	A,B
207	50°43.20'N	1°44.88'W	226.9	0.3	73.7	26.0	A,B
208	50°43.18'N	1°44.83'W	148.5	1.3	66.7	32.0	A,B,C
209	50°43.14'N	1°44.82'W	51.9	17.1	76.3	6.6	A,B
210	50°43.06'N	1°44.86'W	163.0	40.0	58.0	2.0	A,B
211	50°43.57'N	1°44.72'W	94.6	0.2	92.8	7.0	A,B,D
212	50°43.53'N	1°44.77'W	181.5	9.7	76.8	13.5	A,B,C
213	50°43.50'N	1°44.77'W	166.5	4.1	82.3	13.6	A,B
214	50°43.46'N	1°44.76'W	246.0	4.9	78.4	16.7	A,B
215	50°43.43'N	1°44.76'W	225.0	2.9	82.0	15.1	A,B,D
216	50°43.40'N	1°44.75'W	150.3	1.6	77.4	21.0	A,B
217	50°43.36'N	1°44.75'W	158.9	0.8	73.0	26.2	A,B
218	50°43.33'N	1°44.75'W	128.8	0.0	88.7	11.3	B
219	50°43.30'N	1°44.74'W	194.3	0.0	90.8	9.2	B,C,D
220	50°43.27'N	1°44.74'W	89.3	0.8	83.2	16.0	A,B
221	50°43.25'N	1°44.78'W	153.6	6.6	76.8	16.6	A,B,C
222	50°43.24'N	1°44.74'W	192.3	4.9	83.7	11.4	A,B
223	50°43.21'N	1°44.75'W	168.6	1.1	79.4	19.5	A,B
224	50°43.17'N	1°44.78'W	106.1	1.3	71.4	27.3	A,B,D
225	50°43.16'N	1°44.74'W	133.1	0.0	92.0	8.0	B
226	50°43.14'N	1°44.74'W	112.4	0.4	50.0	49.6	A,B
227	50°43.11'N	1°44.79'W	174.5	4.1	53.6	42.3	A,B,C
228	50°43.07'N	1°44.78'W	387.1	10.2	77.7	12.1	A,B
229	50°43.58'N	1°44.66'W	118.7	1.1	89.9	9.0	A,B
230	50°43.56'N	1°44.68'W	100.4	4.1	84.7	11.3	A,B
231	50°43.51'N	1°44.68'W	85.9	4.4	85.0	10.5	A,B
232	50°43.47'N	1°44.68'W	250.1	3.9	82.2	13.9	A,B,C,D
233	50°43.43'N	1°44.68'W	75.8	65.5	32.1	2.5	A,B
234	50°43.40'N	1°44.68'W	152.4	0.0	97.4	2.6	B,C
235	50°43.37'N	1°44.68'W	144.5	0.1	97.8	2.1	A,B
236	50°43.34'N	1°44.68'W	126.9	0.6	97.7	1.7	A,B,D
237	50°43.31'N	1°44.68'W	115.0	7.7	90.2	2.1	A,B

238	50°43.28'N	1°44.68'W	137.1	0.2	97.2	2.6	A,B
239	50°43.25'N	1°44.68'W	119.7	0.5	97.5	2.0	A,B
240	50°43.22'N	1°44.68'W	70.3	31.5	65.3	3.2	A,B
241	50°43.19'N	1°44.67'W	82.5	0.4	84.7	14.9	A,B
242	50°43.16'N	1°44.67'W	144.6	1.2	92.9	5.9	A,B
243	50°43.11'N	1°44.70'W	402.4	0.2	80.5	19.3	A,B,D
244	50°43.07'N	1°44.70'W	648.1	20.1	70.6	9.3	A,B
245	50°43.63'N	1°44.60'W	92.8	0.1	93.3	6.6	A,B
246	50°43.57'N	1°44.61'W	93.7	2.9	90.4	6.7	A,B
247	50°43.55'N	1°44.61'W	129.5	1.9	81.4	16.7	A,B
248	50°43.53'N	1°44.61'W	134.7	7.2	79.6	13.1	A,B,C
249	50°43.50'N	1°44.61'W	191.6	1.1	82.5	16.4	A,B
250	50°43.47'N	1°44.61'W	118.4	2.1	89.3	8.6	A,B
251	50°43.45'N	1°44.62'W	84.8	57.9	40.5	1.6	A,B
252	50°43.42'N	1°44.62'W	135.6	0.0	96.6	3.4	B
253	50°43.39'N	1°44.62'W	130.9	0.0	97.4	2.6	B
254	50°43.36'N	1°44.63'W	159.9	0.1	99.1	0.8	A,B
255	50°43.32'N	1°44.64'W	132.8	0.1	98.5	1.4	A,B
256	50°43.27'N	1°44.64'W	130.2	0.6	98.1	1.4	A,B
257	50°43.23'N	1°44.65'W	230.4	0.1	98.9	1.0	A,B
258	50°43.20'N	1°44.63'W	118.0	13.1	81.9	5.0	A,B,D
259	50°43.15'N	1°44.64'W	170.6	1.9	81.2	16.9	A,B,C
260	50°43.10'N	1°44.65'W	313.0	0.3	75.2	24.5	A,B,C
261	50°43.06'N	1°44.65'W	693.4	43.1	47.7	9.2	A,B
262	50°43.62'N	1°44.53'W	89.6	5.1	91.3	3.6	A,B
263	50°43.60'N	1°44.57'W	109.0	2.7	89.9	7.4	A,B
264	50°43.57'N	1°44.55'W	93.8	0.6	93.1	6.3	A,B
265	50°43.51'N	1°44.56'W	109.3	6.4	87.9	5.7	A,B
266	50°43.45'N	1°44.56'W	43.4	16.8	79.1	4.1	A,B
267	50°43.41'N	1°44.56'W	174.0	0.0	98.8	1.2	B
268	50°43.37'N	1°44.57'W	36.0	82.9	16.1	1.0	A,B
269	50°43.31'N	1°44.59'W	76.2	53.1	43.7	3.2	A,B
270	50°43.27'N	1°44.60'W	173.2	0.0	98.5	1.5	B
271	50°43.23'N	1°44.60'W	135.2	3.1	94.0	2.9	A,B
272	50°43.17'N	1°44.59'W	182.7	0.4	90.9	8.8	A,B
273	50°43.15'N	1°44.58'W	215.6	0.5	81.9	17.6	A,B
274	50°43.11'N	1°44.58'W	269.6	0.8	74.0	25.2	A,B
275	50°43.07'N	1°44.58'W	275.3	1.7	55.4	42.9	A,B
276	50°43.05'N	1°44.58'W	801.0	52.9	40.8	6.3	A,B,D
277	50°43.58'N	1°44.51'W	118.3	0.2	96.1	3.7	A,B
278	50°43.54'N	1°44.52'W	114.3	1.4	95.6	3.0	A,B,C,D
279	50°43.52'N	1°44.50'W	153.9	0.6	95.1	4.3	A,B
280	50°43.48'N	1°44.48'W	97.6	0.7	95.8	3.5	A,B
281	50°43.45'N	1°44.51'W	102.5	0.1	86.2	13.6	A,B
282	50°43.41'N	1°44.51'W	148.7	0.1	99.2	0.7	A,B,D
283	50°43.37'N	1°44.53'W	205.9	0.0	99.2	0.7	B
284	50°43.34'N	1°44.55'W	58.6	63.7	33.2	3.1	A,B,D
285	50°43.32'N	1°44.53'W	36.2	0.9	98.1	1.0	A,B
286	50°43.27'N	1°44.53'W	86.1	62.5	37.1	0.4	A,B
287	50°43.25'N	1°44.55'W	184.5	0.0	98.7	1.3	B,D

288	50°43.23'N	1°44.52'W	189.1	1.3	97.5	1.2	A,B
289	50°43.20'N	1°44.53'W	61.0	82.4	16.5	1.1	A,B
290	50°43.15'N	1°44.53'W	303.8	0.8	77.3	21.9	A,B,C,D
291	50°43.11'N	1°44.52'W	335.6	0.0	97.0	3.0	B
292	50°43.07'N	1°44.54'W	245.6	0.8	91.4	7.8	A,B
293	50°43.59'N	1°44.45'W	120.4	0.0	97.5	2.5	B,C
294	50°43.56'N	1°44.46'W	103.5	0.1	98.2	1.7	A,B
295	50°43.51'N	1°44.46'W	102.9	0.0	97.3	2.7	B
296	50°43.47'N	1°44.46'W	118.5	0.0	96.4	3.6	B
297	50°43.44'N	1°44.46'W	164.4	0.5	90.2	9.3	A,B
298	50°43.42'N	1°44.47'W	92.9	0.0	98.9	1.1	B
299	50°43.38'N	1°44.46'W	163.8	66.6	29.0	4.4	A,B
300	50°43.35'N	1°44.49'W	154.4	1.5	97.6	0.9	A,B,D
301	50°43.34'N	1°44.47'W	7514.1	82.3	17.6	0.1	A,B
302	50°43.30'N	1°44.49'W	8759.4	95.6	4.2	0.2	A,B
303	50°43.26'N	1°44.49'W	7302.2	96.9	3.0	0.1	A,B
304	50°43.22'N	1°44.49'W	528.8	70.5	28.2	1.3	A,B
305	50°43.18'N	1°44.49'W	551.1	52.5	44.5	3.0	A,B
306	50°43.15'N	1°44.51'W	257.6	0.1	98.9	1.0	A,B
307	50°43.58'N	1°44.39'W	124.3	0.5	98.1	1.4	A,B
308	50°43.54'N	1°44.41'W	130.0	0.2	94.0	5.7	A,B
309	50°43.50'N	1°44.41'W	101.2	0.7	96.8	2.5	A,B
310	50°43.37'N	1°44.43'W	91.2	99.8	0.0	0.2	A
311	50°43.40'N	1°44.29'W	745.6	99.9	0.0	0.1	A
312	50°43.34'N	1°44.34'W	178.5	11.6	87.2	1.2	
313	50°43.30'N	1°44.34'W	374.4	24.2	75.8	0.0	
314	50°43.27'N	1°44.36'W	67.1	0.0	99.0	1.0	B
315	50°43.24'N	1°44.36'W	71.1	0.0	99.2	0.8	B
316	50°43.20'N	1°44.39'W	54.7	0.0	99.1	0.9	B
317	50°43.17'N	1°44.40'W	180.1	0.9	99.1	0.0	A,B
318	50°43.15'N	1°44.42'W	66.4	0.0	99.4	0.6	B
319	50°43.13'N	1°44.44'W	77.7	0.0	99.3	0.7	B
320	50°43.10'N	1°44.47'W	73.3	0.0	99.1	0.9	B
321	50°43.06'N	1°44.50'W	76.4	0.0	99.2	0.8	B
322	50°43.03'N	1°44.52'W	75.1	0.0	99.0	1.0	B
323	50°43.00'N	1°44.54'W	81.2	0.0	99.0	1.0	B
324	50°42.96'N	1°44.57'W	98.2	0.0	99.1	0.9	B
325	50°42.93'N	1°44.58'W	101.7	0.0	99.0	1.0	B
326	50°42.90'N	1°44.60'W	100.6	0.0	99.3	0.7	B
327	50°42.86'N	1°44.62'W	95.4	0.0	99.3	0.6	B
328	50°42.83'N	1°44.62'W	96.4	0.0	99.0	0.9	B
329	50°43.37'N	1°44.34'W	150.5	0.0	100.0	0.0	
330	50°43.35'N	1°44.31'W	141.9	0.0	100.0	0.0	
331	50°43.33'N	1°44.29'W	193.7	0.0	100.0	0.0	
332	50°43.32'N	1°44.27'W	172.3	0.0	100.0	0.0	
333	50°43.34'N	1°44.23'W	163.7	0.0	100.0	0.0	
334	50°43.35'N	1°44.24'W	155.6	0.0	100.0	0.0	
335	50°43.37'N	1°44.27'W	218.7	49.0	51.0	0.0	
336	50°43.39'N	1°44.28'W	682.3	93.1	6.9	0.0	A,B
337	50°43.39'N	1°44.30'W	519.9	79.7	20.3	0.0	

338	50°43.41'N	1°44.33'W	451.2	88.0	12.0	0.0	
339	50°43.44'N	1°44.28'W	442.5	75.4	24.6	0.0	
340	50°43.43'N	1°44.26'W	186.8	0.0	100.0	0.0	
341	50°43.41'N	1°44.23'W	194.4	0.0	100.0	0.0	
342	50°43.39'N	1°44.20'W	188.6	0.0	100.0	0.0	
343	50°43.37'N	1°44.19'W	170.5	0.0	100.0	0.0	
344	50°43.41'N	1°44.13'W	271.8	0.6	99.4	0.0	
345	50°43.42'N	1°44.16'W	338.0	1.1	98.9	0.0	
346	50°43.44'N	1°44.20'W	123.8	0.0	100.0	0.0	
347	50°43.46'N	1°44.23'W	418.6	66.8	33.2	0.0	
348	50°43.47'N	1°44.25'W	634.9	84.6	15.4	0.0	
349	50°43.49'N	1°44.21'W	439.2	63.2	36.8	0.0	
350	50°43.48'N	1°44.18'W	278.5	2.4	97.6	0.0	
351	50°43.47'N	1°44.15'W	269.7	2.2	97.8	0.0	
352	50°43.46'N	1°44.12'W	242.9	0.2	99.8	0.0	
353	50°42.89'N	1°46.71'W	323.3	0.9	97.2	1.9	
354	50°42.72'N	1°46.75'W	531.2	0.9	98.2	0.9	B,C
355	50°42.60'N	1°46.73'W	203.4	1.8	89.0	9.2	B
356	50°42.43'N	1°46.74'W	252.1	2.0	80.3	17.7	B
357	50°42.32'N	1°46.70'W	369.6	1.8	82.4	15.8	B
358	50°42.18'N	1°46.73'W	271.5	0.7	88.1	11.2	B
359	50°41.99'N	1°46.73'W	147.9	3.7	91.8	4.5	B
360	50°41.99'N	1°46.64'W	568.3	12.4	81.5	6.1	B
361	50°42.24'N	1°46.64'W	256.8	0.9	70.8	28.3	B
362	50°42.43'N	1°46.64'W	243.6	0.8	76.4	22.8	B
363	50°42.62'N	1°46.63'W	166.4	2.1	91.5	6.4	B
364	50°42.81'N	1°46.61'W	238.5	0.2	98.1	1.7	B
365	50°42.95'N	1°46.64'W	607.9	0.7	99.3	0.0	B
366	50°42.91'N	1°46.12'W	651.5	1.8	98.2	0.0	B
367	50°42.69'N	1°46.08'W	915.0	0.3	96.8	2.9	B
368	50°42.49'N	1°46.08'W	314.1	2.7	71.8	25.5	B
369	50°42.32'N	1°46.08'W	311.3	3.8	68.9	27.3	B
370	50°42.14'N	1°46.12'W	973.3	2.2	90.4	7.4	B
371	50°43.89'N	1°43.33'W	172.2	0.0	92.9	7.1	B
372	50°43.69'N	1°43.33'W	309.6	0.0	100.0	0.0	B
373	50°43.50'N	1°43.31'W	918.2	100.0	0.0	0.0	
374	50°43.29'N	1°43.34'W	803.4	100.0	0.0	0.0	
375	50°43.02'N	1°43.64'W	717.9	100.0	0.0	0.0	
376	50°43.19'N	1°43.69'W	598.9	100.0	0.0	0.0	
377	50°43.40'N	1°43.62'W	1450.7	10.5	88.8	0.7	A,B,C
378	50°43.40'N	1°43.64'W	122.5	100.0	0.0	0.0	
379	50°43.60'N	1°43.65'W	593.7	42.2	54.6	3.2	A,B
380	50°43.81'N	1°43.63'W	393.1	13.1	86.9	0.0	A,B
381	50°43.38'N	1°44.01'W	280.1	0.0	100.0	0.0	B
382	50°43.20'N	1°44.02'W	300.4	100.0	0.0	0.0	
383	50°42.97'N	1°44.03'W	419.0	100.0	0.0	0.0	
384	50°43.07'N	1°44.33'W	409.3	0.0	100.0	0.0	B
385	50°42.95'N	1°44.42'W	159.4	26.8	73.2	0.0	A,B
386	50°42.72'N	1°44.73'W	355.8	0.2	99.8	0.0	A,B
387	50°42.90'N	1°45.80'W	465.7	0.3	99.7	0.0	B

388	50°42.69'N	1°45.83'W	823.4	99.1	0.7	0.2	B
389	50°42.50'N	1°45.81'W	2340.0	100.0	0.0	0.0	
390	50°42.31'N	1°45.79'W	344.5	1.0	92.9	6.1	B
391	50°42.09'N	1°45.82'W	360.3	3.4	84.8	11.8	B
392	50°41.98'N	1°46.09'W	653.0	3.1	91.7	5.2	B
393	50°42.99'N	1°45.51'W	747.6	12.0	81.4	6.6	B
394	50°42.20'N	1°45.49'W	703.9	5.7	84.5	9.8	B
395	50°42.39'N	1°45.50'W	768.4	4.0	79.9	16.1	B
396	50°42.59'N	1°45.51'W	461.5	0.2	98.6	1.2	B,C
397	50°42.77'N	1°45.47'W	431.3	0.2	99.8	0.0	B
398	50°42.04'N	1°45.11'W	1117.2	75.5	22.2	2.3	B
399	50°41.99'N	1°44.78'W	200.2	1.0	92.3	6.7	B
400	50°42.19'N	1°44.80'W	332.8	2.1	97.9	0.0	B
401	50°42.07'N	1°44.51'W	828.1	17.4	80.7	1.9	B,C
402	50°41.84'N	1°44.50'W	148.3	2.2	93.0	4.8	B
403	50°41.64'N	1°44.51'W	339.6	58.6	38.6	2.8	B
404	50°41.50'N	1°44.20'W	1177.0	76.8	21.6	1.6	B,C
405	50°41.70'N	1°44.21'W	719.6	69.6	28.0	2.3	B,C
406	50°41.90'N	1°44.21'W	721.6	5.6	94.4	0.0	B
407	50°41.75'N	1°43.91'W	1010.3	23.4	75.9	0.7	B
408	50°41.51'N	1°43.93'W	153.3	45.8	53.2	1.0	B
409	50°41.51'N	1°43.90'W	331.4	77.2	22.4	0.4	B,C
410	50°41.33'N	1°43.89'W	1472.3	70.1	28.4	1.5	B
411	50°41.09'N	1°43.67'W	1810.3	50.6	43.6	5.8	B
412	50°41.27'N	1°43.59'W	600.4	47.4	46.8	5.8	B
413	50°41.49'N	1°43.61'W	726.7	76.9	21.1	2.0	B
414	50°41.38'N	1°43.28'W	1875.9	63.8	32.5	3.7	B,C
415	50°41.17'N	1°43.30'W	1727.1	40.3	47.8	11.9	B
416	50°40.96'N	1°43.31'W	1685.3	61.9	33.4	5.6	B
417	50°43.51'N	1°43.99'W	3147.8	99.7	0.3	0.0	A,B
418	50°43.50'N	1°44.23'W	114.6	100.0	0.0	0.0	A
419	50°43.41'N	1°44.39'W	515.6	100.0	0.0	0.0	A
420	50°43.53'N	1°43.79'W	1609.1	13.6	84.6	1.8	A,B
421	50°43.61'N	1°43 76'W	788.4	2.7	89.3	8.0	A,B
422	50°43.64'N	1°43.82'W	1438.0	2.3	97.5	0.2	A,B
423	50°43 66'N	1°43.80'W	945.7	1.2	98.0	0.8	A,B,D
424	50°43.75'N	1°43.76'W	956.3	0.3	96.6	3.1	A,B,D
425	50°43.81'N	1°43.68'W	939.1	5.2	93.4	1.4	A,B,D
426	50°43.86'N	1°43.64'W	654.9	0.1	91.3	8.6	A,B
427	50°43.90'N	1°43.55'W	913.1	4.0	89.1	6.9	A,B
428	50°43.88'N	1°43.46'W	760.4	0.2	90.8	9.0	A,B
429	50°43.81'N	1°43.58'W	630.9	0.3	88.6	11.1	A,B
430	50°43.74'N	1°43.68'W	1038.0	1.8	97.1	1.1	A,B,D
431	50°43.63'N	1°43.73'W	606.1	5.7	90.9	3.4	A,B,D
432	50°43.67'N	1°43.73'W	233.4	3.5	94.3	2.2	A,B
433	50°43.71'N	1°43.65'W	749.3	0.0	92.5	7.5	A,B
434	50°43.79'N	1°43.50'W	171.2	100.0	0.0	0.0	
435	50°43.79'N	1°43.53'W	184.3	92.9	6.0	1.1	
436	50°43.74'N	1°43.44'W	986.5	0.2	91.6	8.2	A,B,D
437	50°43.64'N	1°43.50'W	489.8	28.9	66.9	4.2	A,B,D

438	50°43.55'N	1°43.64'W	930.7	42.9	48.8	8.3	A,B
439	50°43.47'N	1°43.67'W	823.2	0.3	98.9	0.9	A,B
440	50°43.43'N	1°43.74'W	502.8	97.8	2.2	0.0	A,B
441	50°43.39'N	1°43.84'W	1188.2	96.8	2.2	1.0	A,B
442	50°43.32'N	1°43.97'W	708.9	8.7	88.6	2.7	A,B,D
443	50°43.35'N	1°44.04'W	667.8	0.1	95.6	4.3	A,B
444	50°43.38'N	1°43.98'W	968.8	2.0	93.7	4.3	A,B,D
445	50°43.38'N	1°43.95'W	839.5	0.1	97.4	2.5	A,B
446	50°43.45'N	1°43.91'W	1024.9	4.4	91.1	4.5	A,B
447	50°43.51'N	1°43.79'W	368.1	38.0	61.2	0.8	A,B,D
448	50°43.49'N	1°43.80'W	1036.8	7.0	91.0	2.0	A,B
449	50°43.53'N	1°43.88'W	1302.0	19.7	77.9	2.4	A,B
450	50°43.52'N	1°43.98'W	2305.0	100.0	0.0	0.0	
R1	50°43.52'N	1°43.98'W	10419.8	95.0	5.0	0.0	A,B
R2	50°43.52'N	1°43.98'W	183.7	0.0	100.0	0.0	B
R3	50°43.52'N	1°43.98'W	126.0	0.0	100.0	0.0	B
R4	50°43.52'N	1°43.98'W	173.9	0.0	100.0	0.0	B
R5	50°43.52'N	1°43.98'W	174.7	0.0	100.0	0.0	B

Table B-2. Grain size parameters, based upon moment analysis (McManus 1988).

No.	M_d	μ	σ	S_k	K_u	No.	M_d	μ	σ	S_k	K_u
(For whole sample)											
1	1.87	1.98	1.00	1.50	2.18	2	3.34	4.23	2.44	2.09	2.96
3	-5.23	-5.20	0.37	1.09	1.97	4	-4.70	-4.57	0.84	1.66	2.70
5	5.31	5.18	2.46	1.16	2.85	6	1.92	3.17	2.78	2.62	3.49
7	-4.65	-4.13	1.85	2.58	3.31	8	1.26	1.25	0.69	1.07	1.78
9	2.89	3.44	1.86	2.18	2.81	10	1.76	-0.54	4.13	0.67	4.63
11	2.48	2.79	1.94	2.11	2.99	12	1.62	0.54	3.59	1.97	4.41
13	2.61	3.08	1.83	2.15	2.87	14	2.37	0.81	3.92	-2.40	4.71
15	2.72	2.98	3.29	-1.51	4.23	16	-3.86	-3.14	2.33	3.03	3.89
17	-2.66	-1.42	2.76	2.73	3.65	18	5.20	4.95	2.67	0.68	3.10
19	2.64	3.47	2.48	2.40	3.20	20	2.88	3.96	2.69	2.11	3.21
21	-3.35	-2.45	2.49	2.78	3.56	22	1.08	0.06	2.93	1.03	3.68
23	2.47	2.54	2.89	-0.66	3.97	24	2.73	3.32	2.18	2.19	3.09
25	2.48	2.16	2.35	-1.64	3.51	26	-2.65	-1.59	3.20	2.29	3.71
27	-2.72	-1.56	2.86	3.06	4.06	28	1.80	1.48	1.80	-1.82	2.88
29	1.56	0.74	3.14	1.20	4.02	30	0.72	-0.33	2.22	-1.79	2.63
31	1.01	-0.25	2.80	-1.32	3.44	32	-1.41	-0.73	2.49	1.79	3.09
33	1.04	-0.06	2.64	-1.35	3.06	34	1.75	1.02	2.70	-1.67	3.60
35	1.11	0.39	2.33	1.21	3.17	36	1.04	0.15	2.50	1.04	3.26
37	1.56	1.37	1.56	-1.50	2.59	38	1.89	1.97	1.25	1.48	2.27
39	1.64	1.01	2.32	-1.93	3.18	40	-1.74	-0.86	2.68	2.05	3.27
41	1.87	1.98	1.28	1.51	2.30	42	1.69	0.96	2.70	-1.86	3.62
43	1.57	0.57	2.73	-1.46	3.56	44	-1.65	-0.78	2.89	2.54	3.79
45	1.88	2.04	1.40	1.72	2.49	46	-2.96	-2.04	2.39	2.78	3.66
47	1.08	0.25	2.48	-1.76	3.21	48	1.96	2.25	1.95	2.15	3.06
49	1.57	1.87	1.64	2.18	2.92	50	1.32	1.60	1.55	2.09	2.84
51	1.66	1.33	1.97	-1.61	3.10	52	1.99	2.58	2.10	2.41	3.15
53	1.98	2.18	1.52	1.87	2.64	54	0.59	-0.43	3.25	1.72	3.84
55	0.56	-0.32	3.17	2.12	3.86	56	1.90	1.60	2.05	1.08	3.09
57	1.43	-0.18	3.53	1.72	4.21	58	1.80	2.01	1.53	2.00	2.76
59	1.85	2.17	1.78	2.29	3.02	60	1.29	1.49	1.39	1.92	2.68
61	1.54	0.39	2.58	-2.47	3.35	62	1.90	2.30	1.79	2.13	2.85
63	3.88	4.51	2.81	1.69	3.23	64	1.56	1.64	1.42	1.45	2.47
65	1.90	2.21	1.63	1.82	2.54	66	2.45	2.86	2.05	2.17	3.08
67	2.10	2.29	1.58	1.77	2.65	68	-3.31	-2.38	2.73	2.91	3.88
69	-2.61	-1.63	2.99	2.83	4.08	70	2.08	2.29	1.69	2.06	2.85
71	1.54	1.77	1.48	2.03	2.77	72	2.34	3.09	2.57	2.44	3.44
73	2.44	2.65	1.35	1.68	2.33	74	2.75	3.30	2.10	2.20	3.03
75	3.60	4.07	2.22	1.98	3.00	76	-3.54	-2.27	2.91	3.07	4.14
77	2.64	2.80	1.53	1.63	2.54	78	2.26	2.56	1.52	1.87	2.58
79	2.32	2.59	1.63	1.98	2.75	80	2.40	2.62	1.68	1.91	2.79
81	1.83	2.48	1.86	2.23	2.98	82	2.29	2.59	1.68	2.07	2.81
83	2.33	2.38	1.59	1.59	2.71	84	2.51	2.81	1.54	1.96	2.64

85	2.67	3.25	1.87	2.27	2.89	86	-3.60	-2.22	2.75	2.44	3.49
87	2.52	2.73	1.62	1.78	2.67	88	2.42	2.82	1.81	2.08	2.88
89	2.52	2.99	1.73	2.02	2.68	90	1.72	0.03	3.37	-2.16	3.95
91	2.50	2.88	1.65	2.01	2.73	92	2.44	2.93	1.71	2.16	2.81
93	1.74	0.09	3.33	-2.18	3.91	94	2.33	2.08	2.43	-2.38	3.85
95	2.48	2.81	1.49	1.87	2.52	96	2.49	2.85	1.55	1.99	2.63
97	2.57	3.08	1.80	2.20	2.84	98	3.00	3.35	2.16	1.84	3.13
99	1.03	-0.24	2.54	-2.19	3.17	100	0.04	-1.20	2.90	0.91	3.40
101	3.38	3.80	1.67	1.87	2.59	102	3.19	3.71	1.71	1.99	2.60
103	2.54	2.86	1.51	1.89	2.60	104	2.29	2.43	1.59	1.72	2.68
105	2.14	1.16	3.13	-2.16	4.00	106	2.73	2.87	1.75	1.64	2.82
107	3.10	3.44	1.71	1.87	2.61	108	2.12	2.26	1.41	1.71	2.51
109	2.18	2.22	2.00	0.54	3.26	110	2.56	2.98	1.67	2.09	2.73
111	2.39	2.68	1.65	1.92	2.81	112	2.37	2.55	1.64	1.76	2.81
113	2.42	2.71	1.41	1.82	2.50	114	2.44	2.80	1.48	1.93	2.55
115	1.44	0.99	1.79	-1.55	2.89	116	3.59	4.33	2.09	1.89	2.77
117	2.35	2.67	1.63	1.95	2.76	118	2.22	1.86	2.18	-1.59	3.28
119	2.21	1.79	2.90	-2.06	4.02	120	2.95	3.39	2.06	1.86	3.01
121	2.75	2.86	2.49	-1.96	3.73	122	1.65	0.32	3.21	1.28	3.93
123	1.80	1.06	2.91	-1.54	3.82	124	2.39	2.72	1.56	2.01	2.75
125	2.30	2.24	1.82	1.02	2.96	126	2.63	3.08	1.80	2.10	2.83
127	2.71	3.19	2.10	2.06	3.11	128	0.59	-0.81	2.97	0.97	3.55
129	1.74	1.25	1.98	-2.07	2.97	130	3.78	4.26	2.42	1.29	3.21
131	2.99	3.33	2.72	-2.04	3.99	132	2.24	2.23	2.25	-1.63	3.57
133	2.43	2.91	1.85	2.17	2.91	134	2.91	3.74	2.34	2.16	3.12
135	3.02	3.52	2.22	2.00	3.12	136	0.47	-0.20	3.06	2.19	3.81
137	2.25	2.16	1.98	-0.97	3.25	138	2.25	1.93	2.29	-1.65	3.44
139	2.40	2.56	1.65	1.54	2.76	140	2.55	3.01	1.66	2.02	2.63
141	2.70	3.04	2.05	1.88	3.08	142	2.94	3.11	2.08	1.52	3.12
143	1.48	0.42	2.76	-2.39	3.70	144	3.25	3.62	2.22	1.56	3.19
145	2.28	2.74	1.74	2.19	2.85	146	2.41	2.90	1.77	2.19	2.85
147	2.57	2.51	2.90	-2.11	4.12	148	2.38	2.53	1.50	1.63	2.63
149	2.60	3.10	1.78	2.06	2.75	150	2.64	3.01	1.60	1.93	2.58
151	2.67	2.84	1.67	1.74	2.75	152	1.51	0.16	2.86	-2.53	3.59
153	2.50	2.17	3.30	-2.47	4.43	154	2.78	3.43	2.23	2.04	3.11
155	2.84	3.30	1.91	2.03	2.86	156	3.06	3.73	2.16	2.02	3.01
157	2.02	1.51	2.82	-0.96	3.80	158	2.40	2.77	1.86	2.05	2.94
159	2.53	2.70	2.29	1.18	3.49	160	2.45	2.71	1.38	1.80	2.50
161	2.48	2.64	1.55	1.39	2.61	162	2.63	2.97	1.57	1.84	2.57
163	2.65	2.70	1.51	1.11	2.54	164	2.98	3.39	1.83	2.05	2.76
165	2.73	2.79	2.47	-1.86	3.75	166	1.37	-0.39	3.17	-2.13	3.68
167	1.74	0.83	2.54	-2.28	3.47	168	2.44	2.94	1.90	2.20	2.97
169	2.80	3.47	2.08	2.29	2.99	170	2.94	3.58	1.91	2.03	2.80
171	2.46	2.83	1.61	1.93	2.68	172	2.62	3.12	1.86	2.11	2.84
173	2.77	3.00	1.93	1.63	3.00	174	2.76	3.23	1.67	2.03	2.64
175	2.63	3.08	1.60	1.97	2.58	176	2.54	2.66	1.64	1.35	2.74
177	2.70	2.98	1.50	1.87	2.57	178	3.12	3.61	2.01	2.09	2.85
179	1.51	0.92	2.99	2.11	4.05	180	1.71	0.99	3.18	-2.03	4.24
181	2.59	2.77	1.90	1.83	2.96	182	2.79	3.18	1.68	1.87	2.69
183	2.74	3.20	1.69	1.99	2.68	184	2.52	2.90	1.54	1.91	2.58

185	2.70	3.01	1.74	1.97	2.81	186	2.70	3.03	1.57	1.97	2.66
187	2.75	2.86	1.72	1.57	2.78	188	2.91	3.01	1.71	1.54	2.75
189	3.13	3.26	1.54	1.70	2.50	190	3.62	4.01	2.20	1.74	3.01
191	1.74	0.50	2.76	-1.96	3.52	192	1.66	0.80	3.35	1.53	4.34
193	1.98	2.30	2.31	2.15	3.49	194	1.59	0.24	3.71	-1.83	4.55
195	2.56	2.68	2.45	1.50	3.51	196	2.82	3.18	1.94	1.95	2.91
197	2.86	3.17	1.84	1.69	2.91	198	3.08	3.58	1.92	2.05	2.85
199	2.80	3.26	1.71	2.06	2.74	200	1.82	1.89	2.42	2.01	3.59
201	2.23	2.15	2.28	-1.02	3.44	202	3.16	3.59	1.97	1.82	2.86
203	2.98	3.27	1.60	1.90	2.71	204	2.71	3.03	1.63	1.97	2.76
205	2.65	3.03	1.84	2.05	2.90	206	3.01	3.16	1.79	1.63	2.89
207	3.11	3.46	1.75	1.97	2.67	208	3.29	3.63	1.79	1.77	2.69
209	2.90	2.05	2.65	-2.79	3.72	210	1.61	0.01	2.82	-1.83	3.27
211	2.18	2.35	1.23	1.79	2.47	212	1.92	1.90	2.33	1.70	3.52
213	1.88	2.14	1.90	2.13	3.08	214	2.05	2.33	2.03	2.07	3.11
215	2.43	2.59	1.83	1.83	2.87	216	3.05	3.40	1.69	1.84	2.74
217	3.26	3.66	1.74	1.99	2.75	218	2.79	3.05	1.22	1.78	2.39
219	2.73	2.95	1.12	1.71	2.31	220	2.81	3.18	1.53	1.94	2.67
221	2.64	2.75	2.17	0.59	3.39	222	2.71	2.76	1.70	1.23	2.87
223	2.86	3.31	1.61	1.90	2.67	224	2.59	3.08	1.99	2.07	2.92
225	1.87	2.07	1.32	1.82	2.54	226	3.63	4.37	2.03	1.93	2.73
227	3.60	3.83	2.34	0.96	3.28	228	2.24	2.02	2.19	-1.65	3.39
229	2.07	2.33	1.42	1.94	2.67	230	2.20	2.37	1.73	1.86	2.94
231	2.15	2.30	1.69	1.74	2.87	232	1.97	2.15	1.81	1.90	2.94
233	-2.81	-1.29	2.66	2.62	3.43	234	2.32	2.39	0.72	1.22	1.83
235	2.40	2.47	0.66	1.11	1.73	236	2.36	2.38	0.67	0.98	1.70
237	2.28	1.85	1.90	-2.47	3.31	238	2.33	2.37	0.82	1.21	1.87
239	2.32	2.34	0.72	1.05	1.79	240	2.38	0.79	2.93	-2.37	3.48
241	2.96	3.30	1.36	1.78	2.45	242	2.78	2.89	1.00	1.28	2.14
243	2.94	3.38	1.35	1.79	2.37	244	2.14	1.13	2.95	-2.67	3.97
245	2.17	2.32	1.19	1.77	2.45	246	2.14	2.22	1.37	1.60	2.57
247	2.23	2.63	1.81	2.19	2.96	248	2.33	2.32	2.25	-1.54	3.53
249	2.32	2.73	1.75	2.12	2.87	250	2.19	2.30	1.48	1.68	2.56
251	-2.62	-1.11	2.88	2.25	3.35	252	2.48	2.55	0.80	1.31	1.90
253	2.42	2.45	0.73	1.19	1.80	254	2.28	2.28	0.54	0.78	1.39
255	2.32	2.36	0.61	0.95	1.57	256	2.39	2.42	0.63	0.82	1.60
257	2.31	2.33	0.57	0.88	1.49	258	2.69	2.05	2.24	-2.46	3.39
259	2.85	3.18	1.56	1.72	2.64	260	2.73	3.12	1.73	1.92	2.63
261	1.18	-0.33	3.45	1.58	4.04	262	2.11	2.00	1.33	0.80	2.46
263	2.07	2.19	1.42	1.73	2.66	264	2.38	2.49	1.17	1.63	2.37
265	2.10	1.96	1.75	-0.98	2.92	266	2.12	1.48	2.20	-2.01	3.15
267	2.26	2.25	0.65	0.95	1.57	268	-4.11	-2.92	2.58	3.15	3.84
269	-2.39	-1.17	3.61	1.95	4.00	270	2.53	2.54	0.53	0.92	1.47
271	2.54	2.44	1.04	-0.92	2.09	272	2.75	2.90	1.05	1.48	2.14
273	2.79	3.15	1.40	1.79	2.43	274	2.75	3.21	1.66	1.90	2.62
275	2.95	3.57	2.06	1.82	2.83	276	-2.49	-0.92	3.20	2.39	3.82
277	2.16	2.25	0.99	1.45	2.14	278	2.09	2.12	1.13	1.34	2.20
279	2.23	2.30	1.12	1.49	2.24	280	2.53	2.50	0.97	1.19	2.02
281	2.73	3.03	1.38	1.90	2.51	282	2.37	2.36	0.56	0.73	1.35
283	2.24	2.23	0.53	0.80	1.36	284	-3.73	-1.79	3.31	3.03	4.02

285	2.20	2.17	0.67	0.73	1.62	286	-3.79	-1.77	3.28	2.64	3.56
287	2.30	2.31	0.60	0.88	1.45	288	2.35	2.31	0.71	-0.52	1.58
289	-3.55	-2.55	2.47	2.93	3.59	290	2.71	3.10	1.46	1.75	2.42
291	2.22	2.28	0.66	1.13	1.67	292	2.13	2.26	1.08	1.53	2.21
293	2.22	2.29	0.79	1.28	1.92	294	2.17	2.16	0.76	1.09	1.80
295	2.26	2.31	0.81	1.30	1.96	296	2.17	2.25	0.86	1.42	2.04
297	2.13	2.36	1.29	1.90	2.57	298	2.23	2.24	0.54	0.96	1.52
299	-3.51	-1.87	3.17	3.14	4.16	300	1.74	1.71	0.69	0.76	1.65
301	-5.13	-3.84	2.76	3.13	3.77	302	-5.25	-4.82	1.61	2.39	3.12
303	-5.30	-4.99	1.39	2.22	2.97	304	-5.13	-3.03	3.45	3.43	4.17
305	-5.01	-1.62	3.89	2.33	4.11	306	2.27	2.27	0.59	0.68	1.34
307	2.22	2.19	0.75	0.94	1.74	308	2.25	2.37	1.07	1.66	2.34
309	2.20	2.20	0.87	1.21	2.00	310	-5.25	-5.22	0.46	1.35	2.37
311	-5.24	-5.22	0.36	1.10	2.00	314	2.41	2.45	0.45	0.83	1.36
315	2.32	2.32	0.53	0.77	1.34	316	2.34	2.37	0.49	0.82	1.36
317	2.34	2.36	0.34	-0.12	0.47	318	2.34	2.38	0.41	0.73	1.25
319	2.44	2.47	0.44	0.73	1.24	320	2.36	2.40	0.47	0.82	1.35
321	2.42	2.45	0.50	0.78	1.30	322	2.50	2.53	0.47	0.82	1.34
323	2.45	2.47	0.49	0.82	1.36	324	2.47	2.51	0.46	0.81	1.33
325	2.35	2.39	0.50	0.84	1.38	326	2.36	2.40	0.45	0.75	1.25
327	2.33	2.37	0.45	0.74	1.25	328	1.81	1.85	0.69	0.90	1.51
336	-4.17	-3.71	1.81	2.27	2.92	371	3.23	2.78	2.15	-2.83	3.82
372	3.24	3.15	0.56	-0.59	0.84	377	2.36	0.22	3.41	-3.00	3.91
379	1.74	-0.34	3.78	-2.15	4.12	380	2.72	1.86	2.49	-3.18	3.85
381	2.29	2.30	0.44	-0.33	0.70	384	2.61	2.55	0.45	-0.55	0.86
385	2.22	0.51	3.18	-3.24	3.89	386	2.27	2.27	0.46	-0.86	1.48
417	-5.24	-5.21	0.33	0.84	1.38	420	2.79	1.92	2.40	-2.89	3.64
421	2.60	2.60	1.30	1.24	2.47	422	2.32	2.20	0.84	-1.13	1.67
423	2.47	2.41	0.75	-0.67	1.57	424	2.65	2.65	0.73	1.09	1.80
425	2.54	2.20	1.67	-2.44	3.26	426	2.88	3.07	0.97	1.52	2.12
427	2.83	2.78	1.34	-0.74	2.46	428	3.08	3.19	1.06	1.44	2.14
429	2.94	3.19	1.12	1.57	2.25	430	2.49	2.43	0.82	-0.76	1.71
431	2.78	2.40	1.72	-2.16	3.06	432	2.46	2.39	1.01	-0.99	2.06
433	2.91	3.11	0.92	1.44	2.03	436	3.11	3.24	0.97	1.40	2.05
437	2.77	1.01	3.38	-3.07	4.04	438	2.50	-0.23	4.00	-1.76	4.44
439	2.83	2.88	0.52	0.53	1.38	440	-5.17	-4.89	1.11	1.90	2.60
441	-5.20	-4.85	1.45	2.54	3.56	442	2.78	2.19	2.25	-3.01	3.85
443	2.75	2.81	0.79	1.24	1.87	444	2.76	2.75	1.00	0.81	2.10
445	2.57	2.61	0.69	1.07	1.69	446	2.64	2.56	1.21	-0.94	2.33
447	2.60	-0.01	3.80	-2.95	4.09	448	2.76	2.33	1.82	-2.44	3.24
449	1.59	0.63	2.55	-2.59	3.51	R1	-5.85	-5.34	1.90	2.71	3.53
R2	2.26	2.25	0.30	-0.16	0.43	R3	2.16	2.12	0.37	-0.37	0.62
R4	2.22	2.20	0.31	-0.22	0.44	R5	2.20	2.17	0.35	-0.26	0.50

(For sand fractions only)

354	2.38	2.39	0.50	-0.55	0.89	355	2.52	2.48	0.57	-0.60	0.96
356	2.79	2.80	0.59	-0.59	0.97	357	2.94	2.98	0.53	-0.61	0.99
358	2.81	2.85	0.47	-0.45	0.85	359	2.75	2.73	0.48	-0.57	0.89
360	2.70	2.51	0.85	-1.04	1.39	361	2.79	2.78	0.38	-0.57	0.87
362	2.95	2.97	0.60	-0.66	1.02	363	2.47	2.46	0.57	-0.57	0.96
364	2.50	2.43	0.56	-0.53	0.84	365	2.57	2.53	0.40	-0.43	0.70

366	2.45	2.39	0.55	-0.72	1.03	367	2.13	2.12	0.61	-0.35	0.81
368	2.98	2.97	0.63	-0.76	1.12	369	3.05	3.01	0.63	-0.75	1.10
370	2.74	2.69	0.60	-0.73	1.08	387	2.21	2.17	0.49	-0.45	0.74
388	1.87	1.70	0.84	-0.80	1.14	390	2.77	2.73	0.65	-0.57	0.93
391	2.69	2.63	0.58	-0.66	1.01	392	2.62	2.44	0.80	-0.89	1.24
393	2.53	2.37	0.75	-0.75	1.12	394	2.68	2.67	0.58	-0.53	0.93
395	2.77	2.69	0.73	-0.67	1.03	396	2.38	2.33	0.56	-0.44	0.79
397	2.34	2.34	0.42	-0.38	0.67	398	2.64	2.55	0.68	-0.73	1.10
399	2.24	2.25	0.68	0.15	0.90	400	2.17	2.13	0.69	-0.51	0.96
401	2.15	2.11	0.60	-0.47	0.88	402	2.51	2.45	0.70	-0.69	1.08
403	1.65	1.62	1.37	-0.74	1.59	404	2.34	2.30	0.62	-0.59	0.96
405	1.39	1.50	1.29	0.53	1.53	406	2.22	2.24	0.60	0.19	0.86
407	1.63	1.49	0.98	-0.79	1.31	408	2.02	1.86	0.77	-0.78	1.15
409	2.10	1.89	0.82	-0.87	1.21	410	1.87	1.91	1.08	-0.83	1.42
411	1.98	1.98	1.15	-0.92	1.49	412	2.20	2.03	1.22	-1.02	1.53
413	2.10	1.87	1.29	-1.10	1.60	414	3.60	3.44	0.51	-0.64	0.83
415	2.16	2.03	1.22	-1.01	1.54	416	2.08	1.89	1.26	-1.03	1.56

APPENDIX C. TIME-SERIES OF WATER LEVELS, CROSS-SECTIONAL MEAN CURRENT SPEEDS AND SUSPENDED SEDIMENT CONCENTRATIONS (AT MUDEFORD)

Table C-1. Time-series of water levels (in m OD), at 30 minute intervals (starting at 0.00 GMT, daily).

January 1991

3	-	-	0.62	0.75	0.92	1.00	0.55	0.34	0.21	0.10	0.02	-0.08
	-0.15	-0.19	0.04	0.21	0.55	0.62	0.71	0.81	0.91	0.97	1.04	0.98
	0.87	0.71	0.63	0.68	0.76	0.81	0.66	0.40	0.21	0.08	0.02	-0.06
	-0.16	-0.21	-0.27	-0.11	0.08	0.24	0.43	0.53	0.66	0.78	0.92	0.95
4	0.94	0.85	0.71	0.65	0.72	0.82	0.85	0.69	0.49	0.23	0.11	0.02
	-0.06	-0.15	-0.16	0.02	0.21	0.39	0.62	0.75	0.81	0.87	0.95	1.02
	1.02	0.92	0.71	0.56	0.56	0.58	0.56	0.50	0.34	0.13	0.02	-0.08
	-0.16	-0.24	-0.29	-0.32	-0.34	-0.15	0.04	0.15	0.24	0.36	0.43	0.55
5	0.65	0.71	0.66	0.62	0.58	0.65	0.69	0.85	0.94	0.79	0.50	0.30
	0.15	0.05	-0.02	0.02	0.15	0.29	0.47	0.59	0.68	0.81	0.91	1.01
	1.01	0.97	1.01	0.87	0.73	0.62	0.60	0.58	0.46	0.36	0.17	0.05
	-0.06	-0.16	-0.24	-0.25	-0.32	-0.22	-0.05	0.11	0.24	0.29	0.39	0.50
6	0.59	0.65	0.65	0.66	0.60	0.49	0.46	0.47	0.43	0.36	0.31	0.14
	-0.03	-0.14	-0.22	-0.27	-0.34	-0.31	-0.24	-0.06	0.08	0.20	0.29	0.37
	0.49	0.58	0.66	0.75	0.73	0.72	0.71	0.73	0.84	0.92	0.91	0.69
	0.49	0.27	0.14	0.04	-0.03	-0.09	-0.09	0.05	0.20	0.36	0.50	0.53
7	0.59	0.65	0.71	0.78	0.82	0.85	0.81	0.82	0.92	1.00	1.04	1.04
	0.87	0.62	0.39	0.23	0.11	0.00	-0.03	0.02	0.11	0.24	0.37	0.46
	0.43	0.44	0.46	0.47	0.58	0.65	0.62	0.60	0.46	0.20	-	-
11	0.24	0.17	0.14	0.11	0.11	0.10	0.13	0.15	0.18	0.15	0.18	0.20
	0.24	0.26	0.30	0.37	0.37	0.36	0.37	0.43	0.37	0.36	0.27	0.24
12	0.17	0.13	0.08	0.07	0.07	0.13	0.18	0.24	0.30	0.34	0.39	0.43
	0.49	0.55	0.60	0.60	0.63	0.63	0.68	0.71	0.66	0.63	0.56	0.42
	0.30	0.21	0.14	0.08	0.04	0.01	-0.03	-0.02	0.00	0.02	0.04	0.04
	0.04	0.07	0.10	0.17	0.20	0.23	0.27	0.34	0.39	0.44	0.46	0.39
13	0.29	0.18	0.11	0.04	0.00	-0.06	-0.08	-0.05	0.10	0.21	0.29	0.29
	0.31	0.31	0.31	0.30	0.30	0.30	0.29	0.29	0.29	0.30	0.33	0.29
	0.21	0.10	0.01	-0.06	-0.14	-0.16	-0.21	-0.24	-0.27	-0.22	-0.12	-0.05
	0.01	0.05	0.10	0.13	0.14	0.17	0.17	0.18	0.18	0.23	0.34	0.36
14	0.33	0.27	0.15	0.04	-0.02	-0.11	-0.15	-0.19	-0.21	-0.15	0.01	0.14
	0.23	0.27	0.31	0.33	0.36	0.36	0.34	0.33	0.29	0.27	0.29	0.31
	0.30	0.23	0.11	0.00	-0.11	-0.16	-0.22	-0.27	-0.29	-0.32	-0.28	-0.15
	-0.03	0.05	0.10	0.15	0.20	0.21	0.21	0.21	0.21	0.20	0.21	0.24
15	0.33	0.36	0.27	0.14	0.02	-0.06	-0.15	-0.21	-0.27	-0.29	-0.18	-0.03
	0.10	0.21	0.33	0.37	0.46	0.49	0.50	0.49	0.43	0.36	0.33	0.36
	0.40	0.46	0.37	0.20	0.08	-0.03	-0.15	-0.19	-0.25	-0.29	-0.31	-0.24
	-0.09	0.04	0.14	0.20	0.24	0.33	0.36	0.37	0.39	0.36	0.34	0.31
16	0.36	0.37	0.46	0.33	0.17	0.04	-0.03	-0.15	-0.19	-0.27	-0.29	-0.22
	-0.06	0.08	0.23	0.34	0.40	0.49	0.52	0.55	0.52	0.46	0.40	0.31
	0.30	0.31	0.36	0.29	0.14	0.02	-0.06	-0.15	-0.22	-0.28	-0.32	-0.34

	-0.19	-0.03	0.08	0.23	0.36	0.46	0.53	0.60	0.65	0.65	0.62	0.62
17	0.62	0.65	0.79	0.84	0.79	0.56	0.31	0.17	0.10	0.00	-0.06	-0.19
	0.08	0.23	0.39	0.57	0.75	0.81	0.87	0.89	0.91	0.85	0.79	0.65
	0.55	0.50	0.50	0.50	0.40	0.24	0.10	0.00	-0.10	-0.20	-0.35	-0.41
	-0.46	-0.41	-0.26	-0.14	-0.06	0.04	0.11	0.19	0.25	0.31	0.28	0.21
18	0.16	0.11	0.15	0.24	0.33	0.27	0.09	-0.07	-0.16	-0.23	-0.31	-0.36
	-0.39	-0.23	-0.08	0.08	0.26	0.44	0.56	0.64	0.73	0.76	0.72	0.66
	0.52	0.50	0.48	0.57	0.64	0.61	0.46	0.23	0.06	-0.04	-0.12	-0.18
	-0.26	-0.28	-0.18	0.03	0.20	0.38	0.40	0.42	0.46	0.50	0.51	0.48
19	0.40	0.30	0.21	0.21	0.28	0.32	0.23	0.08	-0.06	-0.14	-0.20	-0.26
	-0.31	-0.35	-0.35	-0.25	-0.12	0.02	0.15	0.24	0.31	0.35	0.40	0.40
	0.35	0.27	0.17	0.15	0.21	0.28	0.28	0.16	-0.01	-0.11	-0.17	-0.24
	-0.28	-0.33	-0.35	-0.31	-0.14	-0.03	0.17	0.28	0.32	0.39	0.45	0.47
20	0.45	0.39	0.29	0.24	0.29	0.41	0.50	0.46	0.24	0.06	-0.04	-0.11
	-0.17	-0.22	-0.27	-0.29	-0.21	-0.08	0.09	0.18	0.23	0.29	0.37	0.37
	0.35	0.29	0.20	0.11	0.06	0.06	0.10	0.11	0.02	-0.09	-0.17	-0.22
	-0.26	-0.30	-0.32	-0.35	-0.36	-0.28	-0.15	-0.01	0.08	0.13	0.20	0.26
21	0.28	0.26	0.23	0.17	0.14	0.19	0.29	0.41	0.40	0.25	0.05	-0.06
	-0.14	-0.21	-0.27	-0.32	-0.34	-0.24	-0.09	0.07	0.21	0.29	0.36	0.40
	0.41	0.40	0.37	0.31	0.23	0.22	0.27	0.37	0.39	0.29	0.11	-0.04
	-0.12	-0.18	-0.25	-0.32	-0.36	-0.38	-0.31	-0.17	-0.04	0.05	0.10	0.12
22	0.16	0.16	0.15	0.11	0.06	0.03	0.02	0.10	0.23	0.29	0.15	0.00
	-0.11	-0.19	-0.27	-0.32	-0.38	-0.41	-0.42	-0.31	-0.19	-0.08	-0.01	0.05
	0.09	0.12	0.11	0.09	0.05	-0.01	-0.07	-0.09	-0.03	0.02	-0.01	-0.09
	-0.19	-0.27	-0.32	-0.37	-0.43	-0.46	-0.49	-0.50	-0.41	-0.31	-0.24	-0.20
23	-0.14	-0.08	-0.08	-0.06	-0.03	-0.04	-0.03	-0.01	0.09	0.19	0.27	0.24
	0.11	-0.04	-0.14	-0.22	-0.29	-0.35	-0.39	-0.41	-0.34	-0.24	-0.13	-0.07
	-0.03	0.00	0.04	0.05	0.05	0.05	0.05	0.05	0.05	0.10	0.15	0.15
	0.09	-0.05	-0.14	-0.22	-0.29	-0.35	-0.40	-0.44	-0.46	-0.41	-0.30	-0.22
24	-0.19	-0.16	-0.14	-0.08	-0.06	-0.01	0.03	0.06	0.11	0.16	0.25	0.34
	0.34	0.27	0.11	-0.04	-0.14	-0.22	-0.28	-0.35	-0.41	-0.39	-0.32	-0.23
	-0.15	-0.11	-0.09	-0.08	-0.08	-0.08	-0.04	-0.02	0.00	0.03	0.08	0.11
	0.11	0.11	0.05	-0.06	-0.16	-0.24	-0.31	-0.36	-0.42	-0.45	-0.44	-0.38
25	-0.30	-0.24	-0.20	-0.17	-0.14	-0.11	-0.08	-0.02	0.05	0.11	0.20	0.29
	0.37	0.41	0.40	0.32	0.17	0.02	-0.09	-0.18	-0.26	-0.32	-0.36	-0.38
	-0.35	-0.28	-0.23	-0.21	-0.20	-0.20	-0.17	-0.14	-0.09	-0.04	0.02	0.07
	0.10	0.14	0.17	0.16	0.11	0.03	-0.08	-0.16	-0.24	-0.30	-0.36	-0.40
26	-0.41	-0.39	-0.31	-0.24	-0.18	-0.14	-0.13	-0.09	-0.06	-0.01	0.07	0.11
	0.17	0.23	0.28	0.29	0.29	0.26	0.17	0.03	-0.09	-0.20	-0.26	-0.34
	-0.40	-0.43	-0.46	-0.43	-0.34	-0.28	-0.25	-0.21	-0.18	-0.14	-0.08	-0.01
	0.07	0.12	0.15	0.19	0.24	0.26	0.25	0.21	0.13	-0.01	-0.13	-0.22
27	-0.29	-0.35	-0.40	-0.41	-0.35	-0.25	-0.15	-0.08	-0.02	0.01	0.05	0.10
	0.14	0.20	0.24	0.26	0.28	0.30	0.32	0.30	0.26	0.14	-0.01	-0.13
	-0.22	-0.29	-0.37	-0.43	-0.47	-0.49	-0.44	-0.33	-0.26	-0.20	-0.14	-0.08
	-0.02	0.05	0.11	0.15	0.16	0.16	0.19	0.23	0.26	0.25	0.18	0.03
28	-0.10	-0.19	-0.28	-0.34	-0.39	-0.43	-0.39	-0.26	-0.12	-0.08	0.09	0.17
	0.24	0.31	0.37	0.38	0.37	0.35	0.32	0.28	0.31	0.30	0.27	0.15
	-0.01	-0.13	-0.22	-0.30	-0.36	-0.43	-0.48	-0.51	-0.44	-0.28	-0.17	-0.08
	0.02	0.11	0.22	0.28	0.34	0.35	0.33	0.29	0.28	0.28	0.33	0.34
29	0.27	0.09	-0.06	-0.16	-0.24	-0.32	-0.38	-0.43	-0.39	-0.21	-0.08	0.05

0.21 0.32 0.43 0.52 0.56 0.58 0.53 0.44 0.37 0.31 0.34 0.34
0.29 0.15 -0.02 -0.13 -0.20 -0.29 -0.36 -0.43 -0.49 -0.51 -0.36 -0.20
-0.08 0.04 0.16 0.28 0.40 0.50 0.55 0.53 0.44 0.36 0.32 0.37
30 0.43 0.44 0.31 0.10 -0.05 -0.14 -0.22 -0.30 -0.37 -0.44 -0.33 -0.15
-0.02 0.14 0.24 0.42 0.53 0.61 0.66 0.61 0.50 0.35 0.23 0.18
0.20 0.21 0.14 -0.01 -0.15 -0.24 -0.30 -0.38 -0.44 -0.49 -0.55 -0.57
-0.38 -0.20 -0.09 0.03 0.15 0.28 0.40 0.50 0.51 0.41 0.28 0.16
31 0.13 0.19 0.27 0.23 0.12 -0.07 -0.17 -0.25 -0.32 -0.39 -0.46 -0.48
-0.26 -0.10 0.05 0.23 0.41 0.56 0.69 0.78 0.77 0.69 0.53 0.37
0.23 0.22 0.28 0.28 0.17 -0.01 -0.13 -0.21 -0.29 -0.37 -0.43 -0.49
-0.55 -0.38 -0.17 -0.04 0.13 0.31 0.47 0.59 0.71 0.76 0.69 0.55
February 1991
1 0.41 0.29 0.34 0.41 0.49 0.35 0.15 -0.01 -0.12 -0.20 -0.28 -0.35
-0.41 -0.33 -0.13 0.02 0.20 0.41 0.57 0.72 0.82 0.87 0.82 0.70
0.52 0.34 0.23 0.26 0.29 0.28 0.12 -0.05 -0.14 -0.22 -0.30 -0.37
-0.44 -0.49 -0.47 -0.22 -0.07 0.07 0.23 0.38 0.52 0.64 0.70 0.68
2 0.56 0.40 0.28 0.23 0.29 0.39 0.40 0.21 0.02 -0.09 -0.17 -0.26
-0.33 -0.40 -0.43 -0.24 -0.07 0.08 0.23 0.39 0.51 0.63 0.70 0.65
0.55 0.40 0.23 0.10 0.11 0.17 0.19 0.09 -0.08 -0.18 -0.26 -0.33
-0.39 -0.46 -0.51 -0.55 -0.36 -0.20 -0.08 0.05 0.17 0.35 0.41 0.50
3 0.46 0.35 0.23 0.13 0.07 0.15 0.24 0.32 0.19 0.00 -0.11 -0.20
-0.27 -0.34 -0.41 -0.47 -0.35 -0.16 -0.03 0.09 0.23 0.37 0.48 0.55
0.54 0.46 0.34 0.21 0.09 0.05 0.10 0.16 0.11 -0.03 -0.16 -0.24
-0.32 -0.39 -0.45 -0.51 -0.55 -0.43 -0.26 -0.14 -0.03 0.09 0.20 0.29
4 0.37 0.38 0.34 0.27 0.17 0.13 0.20 0.27 0.34 0.23 0.05 -0.09
-0.18 -0.26 -0.33 -0.40 -0.46 -0.35 -0.26 -0.14 -0.03 0.08 0.18 0.25
0.31 0.32 0.28 0.22 0.15 0.08 0.05 0.11 0.17 0.14 0.01 -0.14
-0.23 -0.30 -0.38 -0.45 -0.50 -0.55 -0.52 -0.35 -0.22 -0.14 -0.07 0.01
5 0.07 0.10 0.12 0.10 0.07 0.04 0.03 0.08 0.16 0.25 0.21 0.08
-0.08 -0.19 -0.27 -0.35 -0.41 -0.47 -0.46 -0.32 -0.20 -0.10 -0.01 0.05
0.11 0.15 0.15 0.12 0.09 0.05 -0.01 -0.02 0.02 0.07 0.08 0.00
-0.12 -0.23 -0.31 -0.38 -0.44 -0.50 -0.53 -0.49 -0.39 -0.30 -0.21 -0.14
6 -0.08 -0.04 -0.01 0.01 0.02 0.03 0.04 0.06 0.12 0.20 0.28 0.28
0.19 0.05 -0.09 -0.19 -0.27 -0.34 -0.39 -0.40 -0.32 -0.23 -0.12 -0.05
0.00 0.03 0.07 0.07 0.03 0.01 0.01 -0.02 -0.01 0.05 0.11 0.15
0.10 -0.01 -0.11 -0.21 -0.29 -0.38 -0.43 -0.47 -0.49 -0.45 -0.35 -0.28
7 -0.25 -0.21 -0.20 -0.20 -0.18 -0.15 -0.13 -0.08 -0.02 0.06 0.13 0.19
0.20 0.16 0.06 -0.05 -0.15 -0.24 -0.30 -0.34 -0.36 -0.35 -0.32 -0.26
-0.20 -0.18 -0.18 -0.16 -0.15 -0.14 -0.09 -0.05 0.00 0.06 0.12 0.20
0.26 0.28 0.22 0.14 0.03 -0.08 -0.15 -0.21 -0.24 -0.24 -0.20 -0.14
8 -0.08 -0.02 -0.03 -0.02 -0.01 0.02 0.05 0.10 0.16 0.22 0.28 0.34
0.38 0.36 0.34 0.28 0.14 0.03 -0.07 -0.14 -0.21 -0.26 -0.28 -0.29
-0.28 -0.27 -0.27 -0.28 -0.29 -0.29 -0.28 -0.26 -0.20 -0.12 -0.03 0.04
0.12 0.18 0.19 0.16 0.11 0.09 0.00 -0.06 -0.12 -0.16 -0.19 -0.20
9 -0.20 -0.19 -0.15 -0.14 -0.11 -0.11 -0.08 -0.05 -0.01 0.03 0.09 0.14
0.21 0.26 0.28 0.28 0.26 0.22 0.17 0.12 0.05 -0.01 -0.08 -0.12
-0.14 -0.15 -0.16 -0.14 -0.11 -0.09 -0.08 -0.06 -0.04 -0.02 0.03 0.09
0.15 0.23 0.28 0.29 0.31 0.34 0.34 0.32 0.28 0.21 0.11 0.03
10 -0.05 -0.11 -0.14 -0.14 -0.14 -0.09 -0.04 -0.02 -0.02 -0.02 -0.01 0.02
0.05 0.10 0.15 0.16 0.17 0.16 0.16 0.17 0.15 0.10 0.03 -0.08

	-0.14	-0.22	-0.27	-0.32	-0.33	-0.33	-0.28	-0.20	-0.14	-0.10	-0.08	-0.06
	-0.02	0.02	0.07	0.10	0.12	0.16	0.19	0.22	0.23	0.23	0.20	0.11
11	0.00	-0.10	-0.19	-0.25	-0.30	-0.32	-0.28	-0.20	-0.10	-0.03	0.01	0.04
	0.08	0.09	0.11	0.14	0.14	0.14	0.16	0.18	0.19	0.18	0.17	0.10
	-0.01	-0.12	-0.21	-0.29	-0.36	-0.43	-0.44	-0.41	-0.31	-0.20	-0.13	-0.04
	0.02	0.08	0.13	0.18	0.22	0.24	0.29	0.34	0.40	0.44	0.46	0.41
12	0.32	0.17	0.03	-0.09	-0.20	-0.27	-0.32	-0.34	-0.27	-0.15	-0.06	0.04
	0.11	0.17	0.22	0.23	0.26	0.26	0.23	0.21	0.19	0.21	0.21	0.22
	0.17	0.08	-0.07	-0.18	-0.26	-0.33	-0.41	-0.47	-0.46	-0.33	-0.20	-0.09
	0.01	0.11	0.17	0.23	0.28	0.28	0.28	0.28	0.28	0.28	0.33	0.37
13	0.40	0.29	0.15	-0.02	-0.14	-0.23	-0.31	-0.39	-0.43	-0.36	-0.20	-0.08
	0.02	0.12	0.18	0.21	0.20	0.19	0.17	0.14	0.07	0.03	0.00	0.03
	0.05	0.01	-0.09	-0.20	-0.29	-0.38	-0.44	-0.50	-0.56	-0.60	-0.52	-0.35
	-0.21	-0.13	-0.02	0.07	0.14	0.21	0.23	0.22	0.16	0.12	0.09	0.12
14	0.19	0.25	0.21	0.08	-0.08	-0.20	-0.26	-0.35	-0.43	-0.49	-0.46	-0.26
	-0.12	0.00	0.14	0.28	0.36	0.44	0.46	0.44	0.37	0.27	0.17	0.11
	0.12	0.16	0.15	0.05	-0.11	-0.21	-0.30	-0.37	-0.44	-0.51	-0.56	-0.51
	-0.32	-0.16	-0.06	0.07	0.17	0.28	0.37	0.41	0.41	0.36	0.29	0.23
15	0.26	0.34	0.41	0.40	0.23	0.05	-0.08	-0.18	-0.26	-0.33	-0.38	-0.26
	-0.12	0.03	0.20	0.38	0.55	0.64	0.73	0.75	0.70	0.63	0.49	0.37
	0.28	0.24	0.24	0.21	0.11	-0.07	-0.15	-0.26	-0.33	-0.39	-0.46	-0.50
	-0.32	-0.15	-0.02	0.14	0.32	0.49	0.60	0.72	0.80	0.78	0.72	0.62
16	0.55	0.58	0.64	0.73	0.69	0.47	0.21	0.05	-0.06	-0.15	-0.24	-0.31
	-0.30	-0.11	0.03	0.23	0.44	0.58	0.70	0.78	0.82	0.78	0.70	0.52
	0.41	0.31	0.33	0.40	0.43	0.27	0.06	-0.08	-0.15	-0.25	-0.32	-0.39
	-0.44	-0.46	-0.26	-0.11	0.02	0.16	0.28	0.40	0.46	0.46	0.41	0.33
17	0.21	0.10	0.05	0.13	0.22	0.26	0.12	-0.05	-0.15	-0.24	-0.32	-0.38
	-0.44	-0.47	-0.27	-0.11	0.04	0.20	0.37	0.52	0.63	0.67	0.64	0.54
	0.41	0.28	0.11	0.15	0.20	0.23	0.15	-0.03	-0.14	-0.23	-0.31	-0.38
	-0.44	-0.49	-0.49	-0.32	-0.11	0.01	0.15	0.28	0.41	0.52	0.56	0.54
18	0.50	0.32	0.21	0.17	0.24	0.37	0.43	0.25	0.04	-0.08	-0.18	-0.26
	-0.33	-0.40	-0.43	-0.31	-0.08	0.07	0.24	0.40	0.52	0.63	0.67	0.64
	0.58	0.44	0.29	0.17	0.15	0.20	0.22	0.11	-0.04	-0.15	-0.24	-0.32
	-0.39	-0.45	-0.50	-0.52	-0.32	-0.17	-0.06	0.06	0.18	0.29	0.38	0.44
19	0.42	0.36	0.28	0.18	0.15	0.22	0.32	0.37	0.27	0.06	-0.08	-0.17
	-0.25	-0.32	-0.39	-0.44	-0.30	-0.14	0.00	0.15	0.29	0.41	0.53	0.59
	0.58	0.53	0.46	0.33	0.21	0.18	0.23	0.29	0.23	0.09	-0.07	-0.18
	-0.25	-0.32	-0.39	-0.46	-0.47	-0.30	-0.14	-0.02	0.11	0.23	0.34	0.42
20	0.49	0.52	0.46	0.40	0.34	0.34	0.41	0.53	0.58	0.49	0.25	0.05
	-0.06	-0.15	-0.23	-0.31	-0.36	-0.26	-0.11	0.02	0.17	0.29	0.41	0.50
	0.57	0.59	0.56	0.52	0.43	0.36	0.37	0.43	0.50	0.49	0.34	0.13
	-0.02	-0.14	-0.21	-0.28	-0.35	-0.38	-0.27	-0.14	-0.03	0.09	0.20	0.27
21	0.34	0.37	0.39	0.38	0.35	0.31	0.31	0.37	0.47	0.53	0.50	0.32
	0.13	-0.02	-0.12	-0.20	-0.27	-0.33	-0.33	-0.22	-0.09	0.03	0.15	0.24
	0.31	0.38	0.44	0.48	0.49	0.49	0.52	0.56	0.58	0.63	0.70	0.63
	0.37	0.16	0.04	-0.08	-0.16	-0.21	-0.24	-0.17	-0.08	0.02	0.09	0.18
22	0.23	0.26	0.28	0.28	0.29	0.32	0.37	0.37	0.37	0.42	0.46	0.48
	0.41	0.17	0.04	-0.08	-0.16	-0.25	-0.31	-0.34	-0.32	-0.27	-0.20	-0.11
	-0.04	0.01	0.05	0.11	0.19	0.25	0.34	0.41	0.49	0.56	0.64	0.68
	0.72	0.67	0.52	0.37	0.23	0.10	0.00	-0.05	-0.08	-0.04	0.02	0.09

23	0.14	0.14	0.14	0.13	0.14	0.16	0.21	0.26	0.30	0.32	0.34	0.34
	0.31	0.28	0.24	0.12	0.06	-0.03	-0.11	-0.17	-0.21	-0.26	-0.26	-0.25
	-0.22	-0.20	-0.14	-0.12	-0.09	-0.06	-0.04	0.06	0.14	0.20	0.24	0.29
	0.32	0.31	0.30	0.28	0.22	0.15	0.10	0.02	-0.07	-0.09	-0.14	-0.13
24	-0.10	-0.06	0.00	0.05	0.07	0.09	0.11	0.14	0.21	0.29	0.37	0.41
	0.46	0.49	0.49	0.48	0.46	0.43	0.29	0.16	0.05	-0.06	-0.13	-0.18
	-0.23	-0.27	-0.29	-0.27	-0.24	-0.21	-0.19	-0.15	-0.11	-0.06	-0.01	-
March 1991												
4	-	-	-	-	-	-	-	-	-	-	-	0.82
	0.75	0.60	0.46	0.35	0.34	0.41	0.51	0.49	0.30	0.07	-0.04	-0.13
	-0.21	-0.27	-0.33	-0.29	-0.12	0.00	0.14	0.31	0.46	0.59	0.67	0.72
5	0.67	0.61	0.52	0.37	0.38	0.40	0.49	0.51	0.47	0.15	0.00	-0.09
	-0.17	-0.19	-0.30	-0.34	-0.26	-0.12	-0.02	0.11	0.25	0.35	0.43	0.49
	0.51	0.44	0.37	0.27	0.20	0.20	0.25	0.29	0.28	0.13	-0.04	-0.13
	-0.21	-0.27	-0.33	-0.39	-0.36	-0.24	-0.09	0.04	0.15	0.28	0.37	0.46
6	0.49	0.49	0.49	0.44	0.43	0.46	0.54	0.63	0.66	0.53	0.34	0.12
	-0.01	-0.10	-0.17	-0.24	-0.24	-0.14	-0.01	0.15	0.31	0.40	0.46	0.47
	0.50	0.49	0.47	0.41	0.41	0.38	0.44	0.55	0.67	0.61	0.43	0.27
	0.08	-0.03	-0.11	-0.17	-0.21	-0.11	0.00	0.12	0.29	0.41	0.49	0.54
7	0.57	0.56	0.55	0.56	0.55	0.55	0.60	0.67	0.74	0.76	0.67	0.49
	0.28	0.11	0.00	-0.07	-0.13	-0.14	-0.09	-0.01	0.12	0.23	0.25	0.27
	0.26	0.26	0.26	0.26	0.27	0.31	0.36	0.46	0.52	0.58	0.60	0.52
	0.35	0.20	0.09	-0.01	-0.06	-0.08	-0.07	0.02	0.12	0.24	0.31	0.34
8	0.31	0.32	0.35	0.40	0.31	0.32	0.39	0.48	0.50	0.50	0.55	0.55
	0.46	0.28	0.14	0.07	0.05	0.03	0.03	0.10	0.15	0.22	0.31	0.37
	0.41	0.41	0.42	0.44	0.53	0.53	0.53	0.61	0.72	0.81	0.79	0.79
	0.78	0.65	0.52	0.44	0.36	0.28	0.23	0.24	0.26	0.31	0.34	0.37
9	0.36	0.34	0.31	0.31	0.34	0.38	0.44	0.48	0.55	0.59	0.61	0.61
	0.58	0.51	0.46	0.35	0.26	0.21	0.15	0.15	0.13	0.12	0.12	0.14
	0.15	0.16	0.16	0.16	0.16	0.17	0.23	0.28	0.31	0.37	0.43	0.47
	0.47	0.45	0.40	0.35	0.29	0.24	0.21	0.15	0.11	0.09	0.09	0.10
10	0.10	0.10	0.09	0.09	0.07	0.09	0.11	0.16	0.23	0.28	0.32	0.35
	0.37	0.37	0.35	0.34	0.34	0.31	0.29	0.28	0.23	0.21	0.18	0.13
	0.11	0.13	0.13	0.11	0.11	0.11	0.12	0.14	0.16	0.22	0.29	0.34
	0.35	0.40	0.44	0.43	0.43	0.40	0.37	0.34	0.29	0.22	0.17	0.14
11	0.11	0.09	0.09	0.09	0.08	0.09	0.09	0.11	0.11	0.12	0.15	0.17
	0.20	0.21	0.23	0.23	0.23	0.21	0.21	0.18	0.14	0.10	0.03	-0.02
	-0.07	-0.09	-0.12	-0.13	-0.11	-0.08	-0.04	-0.01	0.03	0.04	0.09	0.13
	0.16	0.22	0.26	0.31	0.34	0.38	0.41	0.44	0.43	0.41	0.28	0.20
12	0.09	0.02	-0.03	-0.07	-0.08	-0.05	0.04	0.10	0.12	0.15	0.18	0.21
	0.22	0.24	0.28	0.29	0.31	0.31	0.29	0.28	0.28	0.26	0.18	0.09
	-0.01	-0.09	-0.15	-0.20	-0.21	-0.24	-0.21	-0.12	-0.02	0.05	0.10	0.14
	0.17	0.21	0.26	0.31	0.33	0.36	0.38	0.40	0.43	0.43	0.42	0.34
13	0.21	0.09	-0.03	-0.11	-0.15	-0.19	-0.20	-0.11	0.01	0.11	0.20	0.24
	0.28	0.30	0.32	0.34	0.35	0.34	0.32	0.30	0.28	0.27	0.25	0.21
	0.09	-0.04	-0.12	-0.19	-0.24	-0.27	-0.30	-0.31	-0.22	-0.11	0.02	0.12
	0.19	0.24	0.27	0.32	0.34	0.37	0.34	0.31	0.32	0.37	0.38	0.40
14	0.34	0.17	0.03	-0.07	-0.15	-0.21	-0.27	-0.29	-0.22	-0.11	0.04	0.17
	0.28	0.32	0.39	0.44	0.46	0.43	0.38	0.34	0.28	0.25	0.27	0.28
	0.22	0.10	-0.03	-0.12	-0.19	-0.25	-0.30	-0.33	-0.36	-0.28	-0.14	0.01

	0.12	0.23	0.31	0.38	0.43	0.46	0.45	0.40	0.35	0.31	0.34	0.40
15	0.43	0.37	0.19	0.03	-0.07	-0.14	-0.21	-0.27	-0.31	-0.27	-0.12	0.04
	0.20	0.35	0.47	0.56	0.64	0.64	0.64	0.58	0.48	0.38	0.31	0.34
	0.37	0.35	0.23	0.05	-0.07	-0.15	-0.21	-0.27	-0.32	-0.35	-0.26	-0.11
	0.05	0.20	0.35	0.48	0.58	0.66	0.67	0.66	0.58	0.47	0.46	0.39
16	0.44	0.51	0.47	0.28	0.09	-0.03	-0.12	-0.18	-0.25	-0.30	-0.29	-0.12
	0.04	0.23	0.42	0.57	0.70	0.80	0.84	0.83	0.76	0.63	0.49	0.40
	0.41	0.43	0.41	0.29	0.10	-0.03	-0.12	-0.18	-0.24	-0.29	-0.33	-0.24
	-0.06	0.11	0.29	0.45	0.58	0.69	0.79	0.85	0.82	0.73	0.59	0.52
17	0.54	0.61	0.67	0.63	0.43	0.19	0.05	-0.04	-0.11	-0.17	-0.21	-0.21
	-0.05	0.14	0.37	0.56	0.72	0.85	0.93	0.98	0.95	0.85	0.70	0.55
	0.43	0.43	0.47	0.45	0.33	0.12	-0.01	-0.09	-0.14	-0.20	-0.24	-0.27
	-0.28	-0.11	0.07	0.22	0.38	0.51	0.60	0.69	0.71	0.69	0.59	0.45
18	0.30	0.28	0.35	0.43	0.40	0.24	0.06	-0.03	-0.09	-0.14	-0.19	-0.22
	-0.25	-0.17	0.01	0.21	0.38	0.55	0.66	0.76	0.82	0.81	0.74	0.61
	0.44	0.30	0.29	0.40	0.43	0.37	0.18	0.03	-0.04	-0.09	-0.15	-0.20
	-0.23	-0.21	-0.01	0.20	0.42	0.58	0.68	0.79	0.87	0.91	0.88	0.80
19	0.61	0.47	0.40	0.46	0.53	0.49	0.37	0.15	0.04	-0.03	-0.09	-0.15
	-0.19	-0.21	-0.18	-0.01	0.17	0.32	0.44	0.55	0.64	0.71	0.72	0.67
	0.55	0.40	0.26	0.25	0.29	0.31	0.26	0.11	-0.03	-0.09	-0.16	-0.21
	-0.24	-0.26	-0.26	-0.11	0.05	0.23	0.38	0.46	0.53	0.62	0.68	0.67
20	0.63	0.52	0.42	0.37	0.49	0.58	0.56	0.44	0.21	0.08	-0.01	-0.08
	-0.12	-0.15	-0.20	-0.19	-0.01	0.17	0.35	0.47	0.55	0.66	0.74	0.78
	0.75	0.69	0.55	0.46	0.42	0.53	0.63	0.60	0.46	0.23	0.09	0.00
	-0.06	-0.12	-0.15	-0.17	-0.05	0.11	0.29	0.43	0.51	0.58	0.62	0.65
21	0.64	0.60	0.52	0.43	0.34	0.37	0.45	0.50	0.41	0.21	0.05	-0.03
	-0.10	-0.15	-0.20	-0.24	-0.26	-0.19	-0.04	0.11	0.23	0.29	0.36	0.44
	0.51	0.54	0.50	0.46	0.40	0.40	0.49	0.56	0.58	0.52	0.30	0.11
	0.01	-0.07	-0.13	-0.18	-0.21	-0.15	-0.03	0.14	0.29	0.37	0.42	0.46
22	0.49	0.49	0.48	0.45	0.43	0.40	0.44	0.54	0.61	0.56	0.41	0.20
	0.05	-0.03	-0.10	-0.15	-0.21	-0.25	-0.26	-0.19	-0.08	0.03	0.09	0.14
	0.20	0.22	0.25	0.28	0.29	0.28	0.28	0.32	0.44	0.52	0.51	0.43
	0.23	0.08	-0.03	-0.09	-0.16	-0.20	-0.22	-0.18	-0.07	0.06	0.15	0.16
23	0.20	0.21	0.22	0.22	0.23	0.25	0.27	0.30	0.37	0.44	0.47	0.42
	0.28	0.11	-0.01	-0.09	-0.15	-0.21	-0.26	-0.30	-0.31	-0.26	-0.20	-0.14
	-0.12	-0.09	-0.08	-0.05	-0.01	0.05	0.10	0.13	0.20	0.28	0.35	0.40
	0.37	0.32	0.17	0.03	-0.06	-0.13	-0.19	-0.24	-0.26	-0.27	-0.21	-0.15
24	-0.11	-0.08	-0.08	-0.07	-0.06	-0.03	0.02	0.07	0.11	0.16	0.23	0.28
	0.28	0.26	0.19	0.06	-0.04	-0.12	-0.20	-0.26	-0.30	-0.33	-0.36	-0.35
	-0.32	-0.27	-0.26	-0.25	-0.23	-0.20	-0.15	-0.08	-0.03	0.04	0.13	0.21
	0.28	0.33	0.31	0.29	0.24	0.12	0.03	-0.08	-0.15	-0.21	-0.26	-0.29
25	-0.30	-0.27	-0.21	-0.19	-0.20	-0.20	-0.20	-0.19	-0.17	-0.14	-0.10	-0.08
	-0.04	-0.01	0.02	0.04	0.04	-0.01	-0.10	-0.18	-0.26	-0.30	-0.36	-0.40
	-0.44	-0.46	-0.45	-0.42	-0.36	-0.31	-0.28	-0.25	-0.20	-0.15	-0.11	-0.04
	0.03	0.09	0.10	0.11	0.17	0.22	0.22	0.21	0.09	-0.03	-0.12	-0.20
26	-0.25	-0.30	-0.33	-0.33	-0.27	-0.17	-0.09	-0.06	-0.04	-0.03	-0.01	0.01
	0.04	0.06	0.06	0.07	0.07	0.08	0.09	0.09	0.05	-0.04	-0.14	-0.21
	-0.27	-0.32	-0.37	-0.40	-0.44	-0.41	-0.30	-0.20	-0.11	-0.04	0.01	0.06
	0.11	0.16	0.20	0.21	0.21	0.22	0.22	0.25	0.28	0.24	0.15	-0.01
27	-0.10	-0.19	-0.25	-0.30	-0.34	-0.36	-0.32	-0.20	-0.09	0.02	0.08	0.13

	0.17	0.21	0.25	0.26	0.25	0.23	0.20	0.18	0.17	0.16	0.11	-0.03
	-0.14	-0.20	-0.27	-0.32	-0.37	-0.40	-0.44	-0.42	-0.28	-0.14	-0.03	0.06
	0.14	0.22	0.28	0.33	0.34	0.23	0.18	0.21	0.21	0.26	0.29	0.26
28	0.11	-0.03	-0.13	-0.20	-0.26	-0.32	-0.36	-0.39	-0.32	-0.18	-0.06	0.07
	0.14	0.21	0.26	0.28	0.27	0.22	0.16	0.08	0.01	0.00	0.03	0.04
	-0.02	-0.15	-0.23	-0.29	-0.33	-0.38	-0.41	-0.45	-0.49	-0.43	-0.24	-0.12
	-0.01	0.11	0.20	0.28	0.35	0.35	0.28	0.21	0.10	0.04	0.08	0.15
29	0.18	0.09	-0.07	-0.15	-0.23	-0.30	-0.34	-0.39	-0.43	-0.44	-0.30	-0.15
	-0.04	0.08	0.19	0.26	0.32	0.34	0.28	0.19	0.08	-0.03	-0.09	-0.08
	-0.04	-0.08	-0.18	-0.26	-0.32	-0.38	-0.41	-0.44	-0.49	-0.51	-0.50	-0.30
	-0.15	-0.04	0.08	0.19	0.29	0.39	0.41	0.35	0.23	0.12	0.02	-0.01
30	0.05	0.11	0.07	-0.07	-0.16	-0.24	-0.30	-0.36	-0.40	-0.45	-0.47	-0.32
	-0.17	-0.04	0.09	0.21	0.32	0.43	0.50	0.46	0.34	0.20	0.09	-0.01
	0.02	0.09	0.09	-0.03	-0.14	-0.21	-0.28	-0.34	-0.39	-0.44	-0.47	-0.46
	-0.26	-0.08	0.04	0.18	0.31	0.42	0.52	0.53	0.47	0.35	0.23	0.09
31	0.06	0.15	0.22	0.17	0.03	-0.09	-0.20	-0.26	-0.32	-0.38	-0.43	-0.45
	-0.32	-0.15	-0.02	0.11	0.26	0.38	0.47	0.54	0.51	0.41	0.27	0.14
	0.01	0.01	0.08	0.10	0.03	-0.10	-0.20	-0.26	-0.32	-0.38	-0.43	-0.46
	-0.46	-0.27	-0.12	0.05	0.15	0.28	0.40	0.47	0.52	0.46	0.37	0.23

April 1991

1	0.11	0.08	0.14	0.22	0.21	0.07	-0.08	-0.15	-0.24	-0.31	-0.36	-0.40
	-0.44	-0.30	-0.13	0.01	0.16	0.30	0.41	0.50	0.57	0.58	0.50	0.38
	0.21	0.10	0.10	0.18	0.22	0.16	-0.01	-0.14	-0.20	-0.26	-0.32	-0.38
	-0.42	-0.40	-0.21	-0.08	0.07	0.19	0.32	0.41	0.51	0.57	0.54	0.46
2	0.34	0.22	0.20	0.25	0.32	0.36	0.22	0.03	-0.09	-0.16	-0.24	-0.30
	-0.35	-0.37	-0.20	-0.04	0.11	0.27	0.41	0.50	0.60	0.68	0.71	0.67
	0.59	0.48	0.41	0.45	0.54	0.61	0.55	0.37	0.14	0.02	-0.08	-0.15
	-0.21	-0.26	-0.14	0.01	0.16	0.31	0.45	0.53	0.58	0.64	0.67	0.64
3	0.59	0.49	0.40	0.39	0.44	0.53	0.50	0.34	0.13	0.00	-0.09	-0.15
	-0.22	-0.29	-0.32	-0.20	-0.06	0.09	0.24	0.32	0.38	0.43	0.49	0.50
	0.49	0.46	0.38	0.34	0.39	0.50	0.56	0.52	0.38	-	-	-
8	-	-	-	-	-	-	-	-0.12	-0.15	-0.19	-0.20	-0.20
	-0.18	-0.15	-0.14	-0.13	-0.11	-0.09	-0.08	-0.02	0.05	0.12	0.20	0.23
	0.29	0.33	0.34	0.34	0.30	0.23	0.14	0.05	-0.01	-0.08	-0.12	-0.15
9	-0.18	-0.17	-0.15	-0.14	-0.13	-0.13	-0.12	-0.10	-0.08	-0.06	-0.02	0.01
	0.04	0.09	0.11	0.10	0.10	0.09	0.04	-0.04	-0.10	-0.16	-0.20	-0.25
	-0.27	-0.29	-0.29	-0.27	-0.25	-0.21	-0.20	-0.18	-0.17	-0.15	-0.11	-0.06
	0.00	0.01	0.05	0.10	0.13	0.13	0.14	0.12	0.07	-0.01	-0.09	-0.14
10	-0.19	-0.23	-0.25	-0.24	-0.20	-0.15	-0.11	-0.08	-0.07	-0.05	-0.03	0.01
	0.04	0.08	0.10	0.13	0.14	0.16	0.16	0.15	0.10	0.01	-0.08	-0.15
	-0.20	-0.25	-0.29	-0.30	-0.29	-0.23	-0.15	-0.08	-0.01	0.04	0.07	0.11
	0.15	0.21	0.24	0.26	0.29	0.32	0.36	0.37	0.37	0.27	0.19	0.05
11	-0.05	-0.12	-0.18	-0.22	-0.26	-0.27	-0.20	-0.13	-0.03	0.00	0.04	0.08
	0.09	0.12	0.14	0.17	0.16	0.14	0.10	0.09	0.09	0.06	-0.01	-0.09
	-0.17	-0.24	-0.28	-0.32	-0.35	-0.38	-0.35	-0.26	-0.15	-0.06	0.04	0.10
	0.15	0.20	0.24	0.28	0.29	0.29	0.28	0.29	0.33	0.34	0.31	0.23
12	0.08	-0.03	-0.11	-0.17	-0.22	-0.27	-0.29	-0.20	-0.08	0.04	0.14	0.23
	0.28	0.34	0.38	0.42	0.43	0.40	0.34	0.34	0.34	0.36	0.36	0.30
	0.15	0.00	-0.09	-0.15	-0.21	-0.27	-0.32	-0.31	-0.20	-0.06	0.09	0.23
	0.34	0.41	0.49	0.52	0.53	0.49	0.46	0.43	0.40	0.47	0.53	0.53

13	0.43	0.22	0.05	-0.04	-0.12	-0.20	-0.26	-0.30	-0.30	-0.16	-0.03	0.10
	0.23	0.31	0.40	0.46	0.47	0.43	0.35	0.25	0.15	0.10	0.11	0.14
	0.11	0.00	-0.13	-0.19	-0.26	-0.30	-0.34	-0.39	-0.41	-0.37	-0.21	-0.08
	0.04	0.17	0.28	0.37	0.43	0.46	0.40	0.35	0.28	0.21	0.24	0.31
14	0.40	0.29	0.11	-0.02	-0.11	-0.19	-0.25	-0.30	-0.33	-0.38	-0.25	-0.10
	0.03	0.18	0.30	0.40	0.46	0.47	0.43	0.34	0.22	0.10	0.00	0.01
	0.08	0.10	-0.01	-0.14	-0.21	-0.27	-0.32	-0.38	-0.41	-0.44	-0.45	-0.27
	-0.12	0.00	0.14	0.28	0.40	0.49	0.50	0.44	0.33	0.21	0.09	0.09
15	0.13	0.22	0.24	0.22	-	-	-	-	-	-	-	-
30	-	-	-	-	-	-	-	-0.01	-0.11	-0.19	-0.26	-0.32
	-0.35	-0.29	-0.14	0.02	0.20	0.35	0.44	0.46	0.48	0.46	0.41	0.36
May 1991												
1	0.27	0.15	0.15	0.27	0.37	0.31	0.17	-0.01	-0.12	-0.20	-0.25	-0.30
	-0.33	-0.37	-0.38	-0.26	-0.14	-0.02	0.05	0.10	0.16	0.19	0.20	0.17
	0.11	0.05	-0.01	0.05	0.15	0.27	0.25	0.11	-0.06	-0.14	-0.20	-0.26
	-0.30	-0.33	-0.35	-0.26	-0.11	0.04	0.16	0.26	0.32	0.34	0.34	0.28
2	0.21	0.12	0.05	0.01	0.06	0.16	0.20	0.10	-0.07	-0.15	-0.23	-0.30
	-0.35	-0.39	-0.44	-0.45	-0.38	-0.26	-0.14	-0.08	0.01	0.09	0.13	0.11
	0.09	0.06	-0.01	-0.05	-0.02	0.09	0.21	0.22	0.12	-0.05	-0.15	-0.23
	-0.30	-0.36	-0.41	-0.43	-0.33	-0.19	-0.08	0.07	0.16	0.22	0.25	0.25
3	0.20	0.18	0.11	0.09	0.07	0.13	0.20	0.21	0.12	-0.02	-0.15	-0.22
	-0.30	-0.36	-0.41	-0.46	-0.47	-0.38	-0.26	-0.14	-0.05	0.01	0.05	0.10
	0.10	0.11	0.08	0.07	0.07	0.13	0.22	0.34	0.37	0.27	0.09	-0.06
	-0.15	-0.23	-0.30	-0.35	-0.38	-0.29	-0.15	-0.04	0.08	0.13	0.15	0.16
4	0.15	0.12	0.09	0.08	0.05	0.05	0.10	0.15	0.17	0.11	-0.01	-0.14
	-0.22	-0.29	-0.35	-0.40	-0.46	-0.47	-0.43	-0.32	-0.22	-0.14	-0.10	-0.08
	-0.02	-0.01	-0.01	-0.01	0.01	0.07	0.13	0.23	0.34	0.35	0.28	0.13
	-0.03	-0.14	-0.22	-0.28	-0.34	-0.37	-0.33	-0.24	-0.13	-0.03	0.03	0.03
5	0.03	0.05	0.03	0.03	0.04	0.03	0.05	0.11	0.16	0.17	0.14	0.04
	-0.10	-0.19	-0.26	-0.33	-0.39	-0.44	-0.46	-0.44	-0.35	-0.27	-0.20	-0.18
	-0.17	-0.15	-0.14	-0.14	-0.10	-0.06	-0.01	0.09	0.18	0.29	0.38	0.37
	0.28	0.14	0.02	-0.10	-0.17	-0.24	-0.27	-0.27	-0.20	-0.10	-0.01	0.06
6	0.06	0.07	0.05	0.05	0.05	0.06	0.09	0.12	0.17	0.22	0.22	0.19
	0.12	-0.01	-0.12	-0.21	-0.27	-0.33	-0.38	-0.43	-0.43	-0.38	-0.31	-0.24
	-0.22	-0.18	-0.17	-0.16	-0.14	-0.11	-0.06	0.02	0.09	0.16	0.27	0.35
	0.35	0.31	0.21	0.16	-0.01	-0.11	-0.19	-0.24	-0.26	-0.26	-0.20	-0.15
7	-0.11	-0.11	-0.11	-0.11	-0.12	-0.11	-0.09	-0.06	-0.01	0.04	0.10	0.11
	0.09	0.09	0.03	-0.07	-0.15	-0.21	-0.27	-0.33	-0.36	-0.38	-0.38	-0.33
	-0.29	-0.24	-0.20	-0.18	-0.15	-0.13	-0.09	-0.03	0.04	0.11	0.19	0.28
	0.35	0.40	0.38	0.32	0.23	0.11	-0.01	-0.11	-0.18	-0.23	-0.27	-0.29
8	-0.29	-0.26	-0.23	-0.22	-0.22	-0.21	-0.21	-0.19	-0.15	-0.11	-0.08	-0.02
	0.02	0.03	0.02	0.00	-0.01	-0.08	-0.15	-0.21	-0.27	-0.32	-0.37	-0.39
	-0.41	-0.39	-0.32	-0.25	-0.20	-0.16	-0.14	-0.11	-0.08	-0.01	0.05	0.11
	0.17	0.26	0.32	0.34	0.35	0.32	0.28	0.17	0.05	-0.06	-0.15	-0.21
9	-0.27	-0.29	-0.29	-0.26	-0.21	-0.18	-0.17	-0.16	-0.15	-0.11	-0.09	-0.08
	-0.08	-0.06	-0.04	-0.05	-0.05	-0.06	-0.08	-0.12	-0.20	-0.27	-0.32	-0.38
	-0.43	-0.47	-0.48	-0.47	-0.38	-0.29	-0.21	-0.14	-0.08	-0.02	0.02	0.06
	0.11	0.16	0.21	0.25	0.29	0.34	0.36	0.32	0.26	0.12	0.01	-0.11
10	-0.23	-0.27	-0.32	-0.33	-0.33	-0.27	-0.15	-0.11	-0.03	-0.01	0.02	0.05
	0.08	0.07	0.07	0.06	0.07	0.07	0.06	0.04	-0.06	-0.15	-0.24	-0.31

	-0.38	-0.43	-0.46	-0.49	-0.42	-0.29	-0.20	-0.09	-0.03	0.04	0.09	0.11
	0.15	0.17	0.17	0.21	0.22	0.26	0.29	0.29	0.23	0.09	-0.06	-0.15
11	-0.23	-0.29	-0.35	-0.41	-0.43	-0.36	-0.25	-0.15	-0.08	-0.02	0.04	0.09
	0.11	0.12	0.13	0.09	0.09	0.07	0.08	0.09	0.07	0.03	-0.11	-0.20
	-0.27	-0.33	-0.39	-0.46	-0.50	-0.49	-0.36	-0.23	-0.14	-0.02	0.08	0.16
	0.22	0.28	0.31	0.31	0.29	0.28	0.29	0.34	0.37	0.34	0.22	0.04
12	-0.10	-0.17	-0.25	-0.32	-0.38	-0.44	-0.43	-0.30	-0.18	-0.08	0.02	0.09
	0.16	0.20	0.23	0.24	0.23	0.19	0.12	0.06	0.04	0.08	0.09	0.04
	-0.09	-0.19	-0.26	-0.32	-0.38	-0.45	-0.50	-0.53	-0.43	-0.26	-0.15	-0.03
	0.09	0.19	0.28	0.35	0.38	0.34	0.27	0.20	0.15	0.19	0.24	0.25
13	0.15	-0.02	-0.14	-0.21	-0.27	-0.34	-0.40	-0.46	-0.50	-0.39	-0.25	-0.14
	-0.03	0.08	0.17	0.27	0.34	0.34	0.29	0.21	0.13	0.09	0.11	0.17
	0.18	0.06	-0.09	-0.17	-0.25	-0.32	-0.37	-0.45	-0.49	-0.46	-0.27	-0.14
	-0.02	0.12	0.25	0.36	0.46	0.49	0.47	0.40	0.29	0.18	0.15	0.18
14	0.23	0.21	0.08	-0.08	-0.17	-0.24	-0.31	-0.37	-0.43	-0.48	-0.47	-0.26
	-0.14	-0.03	0.11	0.26	0.40	0.52	0.59	0.59	0.50	0.37	0.25	0.23
	0.28	0.35	0.29	0.11	-0.05	-0.14	-0.21	-0.27	-0.34	-0.39	-0.45	-0.33
	-0.19	-0.06	0.09	0.24	0.37	0.49	0.56	0.58	0.50	0.35	0.24	0.13
15	0.16	0.22	0.28	0.17	0.00	-0.11	-0.20	-0.26	-0.33	-0.38	-0.44	-0.50
	-0.40	-0.22	-0.12	-0.01	0.12	0.25	0.38	0.47	0.46	0.40	0.28	0.14
	0.05	0.09	0.15	0.18	0.08	-0.08	-0.17	-0.26	-0.31	-0.38	-0.44	-0.50
	-0.47	-0.26	-0.13	-0.01	0.15	0.29	0.44	0.55	0.61	0.58	0.47	0.34
16	0.23	0.21	0.28	0.37	0.34	0.17	-0.02	-0.12	-0.20	-0.27	-0.33	-0.39
	-0.45	-0.48	-0.27	-0.15	-0.03	0.10	0.22	0.34	0.46	0.52	0.49	0.40
	0.27	0.09	0.13	0.20	0.29	0.30	0.14	-0.03	-0.14	-0.21	-0.27	-0.33
	-0.40	-0.46	-0.37	-0.20	-0.08	0.07	0.22	0.34	0.46	0.52	0.53	0.46
17	0.35	0.23	0.15	0.16	0.23	0.29	0.21	0.03	-0.09	-0.19	-0.26	-0.33
	-0.40	-0.46	-0.51	-0.51	-0.33	-0.20	-0.11	0.01	0.12	0.24	0.34	0.40
	0.37	0.29	0.19	0.11	0.17	0.24	0.33	0.28	0.10	-0.06	-0.15	-0.23
	-0.30	-0.36	-0.43	-0.44	-0.29	-0.15	-0.03	0.11	0.23	0.34	0.42	0.46
18	0.44	0.37	0.28	0.17	0.12	0.17	0.22	0.23	0.11	-0.06	-0.17	-0.24
	-0.31	-0.38	-0.44	-0.50	-0.55	-0.51	-0.35	-0.24	-0.16	-0.07	0.04	0.13
	0.21	0.28	0.23	0.17	0.13	0.13	0.19	0.28	0.34	0.24	0.05	-0.07
	-0.15	-0.24	-0.31	-0.37	-0.42	-0.41	-0.27	-0.15	-0.05	0.06	0.15	0.21
19	0.28	0.29	0.29	0.23	0.18	0.12	0.11	0.15	0.18	0.17	0.03	-0.11
	-0.20	-0.27	-0.33	-0.39	-0.46	-0.52	-0.56	-0.49	-0.35	-0.26	-0.20	-0.12
	-0.04	0.05	0.12	0.18	0.19	0.18	0.17	0.22	0.31	0.40	0.40	0.29
	0.11	-0.04	-0.14	-0.21	-0.27	-0.33	-0.38	-0.38	-0.27	-0.17	-0.09	-0.01
20	0.05	0.10	0.12	0.13	0.15	0.13	0.11	0.09	0.10	0.13	0.16	0.11
	-0.01	-0.13	-0.21	-0.29	-0.35	-0.41	-0.47	-0.52	-0.56	-0.48	-0.36	-0.28
	-0.33	-	-	-	-	-	-	-	-	-	-	-
26	-	-	-	-	-0.26	-0.25	-0.28	-0.32	-0.33	-0.28	-0.11	-0.03
	-0.03	0.03	0.08	0.11	0.11	0.09	0.05	0.02	-0.01	-0.06	-0.04	-0.02
	-0.01	-0.11	-0.20	-0.27	-0.35	-0.40	-0.46	-0.49	-0.43	-0.28	-0.15	-0.05
	0.06	0.15	0.23	0.29	0.29	0.29	0.23	0.21	0.15	0.15	0.19	0.22
27	0.17	0.02	-0.09	-0.19	-0.26	-0.32	-0.38	-0.45	-0.50	-0.49	-0.35	-0.23
	-0.15	-0.08	0.00	0.09	0.13	0.16	0.15	0.10	0.05	0.01	0.05	0.11
	0.16	0.10	-0.03	-0.14	-0.21	-0.29	-0.34	-0.41	-0.47	-0.45	-0.32	-0.18
	-0.08	0.05	0.16	0.26	0.34	0.37	0.28	0.31	0.24	0.17	0.17	0.22
28	0.28	0.28	0.15	-0.01	-0.13	-0.22	-0.27	-0.33	-0.39	-0.45	-0.46	-0.35

	-0.24	-0.15	-0.08	0.01	0.09	0.15	0.17	0.16	0.11	0.06	0.02	0.03
	0.09	0.16	0.16	0.05	-0.09	-0.19	-0.26	-0.32	-0.38	-0.43	-0.44	-0.30
	-0.17	-0.06	0.08	0.20	0.31	0.38	0.41	0.37	0.31	0.22	0.15	0.10
29	0.13	0.18	0.20	0.10	-0.05	-0.15	-0.24	-0.30	-0.37	-0.44	-0.49	-0.50
	-0.41	-0.27	-0.19	-0.11	-0.01	0.09	0.16	0.19	0.17	0.14	0.09	0.04
	0.05	0.11	0.21	0.26	0.16	0.00	-0.11	-0.20	-0.27	-0.33	-0.39	-0.41
	-0.28	-0.15	-0.03	0.10	0.23	0.34	0.42	0.44	0.40	0.34	0.28	0.20
30	0.14	0.16	0.21	0.27	0.17	0.09	-0.10	-0.19	-0.26	-0.33	-0.39	-0.45
	-0.48	-0.41	-0.27	-0.17	-0.09	0.00	0.10	0.16	0.20	0.18	0.17	0.11
	0.09	0.09	0.14	0.24	0.31	0.23	0.08	-0.08	-0.15	-0.24	-0.30	-0.36
	-0.39	-0.30	-0.15	-0.04	0.09	0.22	0.32	0.40	0.43	0.40	0.35	0.29
31	0.21	0.17	0.19	0.23	0.28	0.23	0.05	-0.07	-0.15	-0.24	-0.30	-0.36
	-0.42	-0.45	-0.38	-0.26	-0.15	-0.08	0.01	0.10	0.17	0.20	0.21	0.19
	0.15	0.11	0.13	0.19	0.28	0.35	0.29	0.13	-0.01	-0.13	-0.19	-0.27
	-0.33	-0.30	-0.28	-0.15	-0.03	0.09	0.22	0.31	0.37	0.40	0.40	0.35
June 1991												
1	0.30	0.25	0.20	0.22	0.28	0.31	0.25	0.11	-0.04	-0.14	-0.22	-0.28
	-0.34	-0.41	-0.44	-0.40	-0.26	-0.15	-0.08	0.04	0.11	0.18	0.22	0.23
	0.21	0.17	0.17	0.20	0.26	0.35	0.44	0.38	0.23	0.05	-0.07	-0.15
	-0.22	-0.28	-0.33	-0.30	-0.17	-0.07	0.05	0.17	0.26	0.32	0.34	0.31
2	0.28	0.24	0.17	0.14	0.13	0.17	0.20	0.19	0.09	-0.04	-0.14	-0.22
	-0.28	-0.34	-0.41	-0.44	-0.43	-0.30	-0.20	-0.14	-0.05	0.02	0.08	0.11
	0.13	0.16	0.14	0.16	0.17	0.23	0.33	0.40	0.40	0.28	0.11	0.04
	-0.11	-0.18	-0.24	-0.27	-0.23	-0.13	-0.03	0.09	0.17	0.23	0.28	0.29
3	0.29	0.28	0.28	0.27	0.23	0.23	0.24	0.26	0.21	0.12	-0.02	-0.12
	-0.20	-0.26	-0.32	-0.38	-0.41	-0.37	-0.26	-0.16	-0.08	0.01	0.08	0.14
	0.18	0.23	0.28	0.31	0.34	0.40	0.47	0.55	0.61	0.55	0.46	0.28
	0.12	0.00	-0.09	-0.17	-0.21	-0.21	-0.15	-0.05	0.05	0.15	0.19	0.22
4	0.24	0.25	0.25	0.26	0.25	0.23	0.25	0.28	0.31	0.28	0.22	0.10
	-0.03	-0.13	-0.20	-0.27	-0.32	-0.37	-0.38	-0.32	-0.21	-0.14	-0.07	-0.01
	0.05	0.09	0.12	0.16	0.19	0.23	0.28	0.35	0.44	0.53	0.55	0.50
	0.35	0.19	0.05	-0.04	-0.13	-0.19	-0.21	-0.19	-0.11	-0.03	0.06	0.13
5	0.16	0.17	0.18	0.18	0.19	0.21	0.21	0.22	0.24	0.27	0.28	0.24
	0.17	0.05	-0.05	-0.14	-0.21	-0.27	-0.32	-0.33	-0.31	-0.23	-0.14	-0.08
	0.00	0.07	0.11	0.14	0.19	0.25	0.31	0.37	0.44	0.57	0.61	0.67
	0.69	0.61	0.46	0.34	0.17	0.07	-0.02	-0.08	-0.08	-0.06	0.01	0.09
6	0.14	0.15	0.16	0.16	0.17	0.19	0.21	0.25	0.28	0.29	0.30	0.28
	0.28	0.22	0.13	0.03	-0.08	-0.15	-0.22	-0.27	-0.31	-0.33	-0.29	-0.21
	-0.14	-0.08	-0.02	0.02	0.05	0.08	0.13	0.19	0.25	0.31	0.38	0.45
	0.52	0.55	0.53	0.43	0.29	0.17	0.06	-0.03	-0.12	-0.15	-0.16	-0.14
7	-0.07	0.01	0.09	0.11	0.11	0.21	0.19	0.22	0.26	0.29	0.33	0.35
	0.37	0.37	0.37	0.34	0.23	0.12	0.02	-0.08	-0.14	-0.21	-0.30	-0.30
	-0.19	-0.10	-0.01	0.09	0.16	0.21	0.24	0.28	0.34	0.40	0.46	0.49
	0.53	0.59	0.65	0.67	0.64	0.53	0.38	0.21	0.07	-0.03	-0.12	-0.18
8	-0.20	-0.19	-0.11	-0.03	0.04	0.10	0.10	0.15	0.18	0.22	0.23	0.25
	0.25	0.27	0.27	0.28	0.29	0.26	0.18	0.05	-0.04	-0.14	-0.21	-0.26
	-0.31	-0.33	-0.32	-0.23	-0.12	-0.03	0.06	0.13	0.20	0.27	0.32	0.36
	0.41	0.45	0.49	0.52	0.56	0.62	0.59	0.55	0.38	0.20	0.04	-0.06
9	-0.14	-0.21	-0.25	-0.26	-0.17	-0.09	-0.01	0.06	0.12	0.18	0.21	0.25
	0.28	0.29	0.28	0.28	0.26	0.25	0.21	0.19	0.15	0.03	-0.08	-0.15

	-0.23	-0.29	-0.33	-0.33	-0.27	-0.15	-0.04	0.06	0.16	0.25	0.35	0.44
	0.50	0.56	0.62	0.63	0.64	0.66	0.70	0.69	0.66	0.53	0.34	0.14
10	0.01	-0.08	-0.15	-0.23	-0.27	-0.23	-0.13	-0.05	0.05	0.14	0.21	0.26
	0.32	0.39	0.46	0.49	0.43	0.38	0.33	0.32	0.32	0.29	0.21	0.07
	-0.07	-0.15	-0.22	-0.27	-0.33	-0.37	-0.33	-0.22	-0.11	-0.01	0.10	0.20
	0.29	0.38	0.46	0.51	0.55	0.51	0.49	0.50	0.52	0.54	0.49	0.34
11	0.14	-0.01	-0.10	-0.18	-0.25	-0.32	-0.37	-0.38	-0.26	-0.14	-0.06	0.05
	0.16	0.25	0.34	0.43	0.46	0.45	0.38	0.32	0.31	0.34	0.40	0.40
	0.29	0.10	-0.04	-0.14	-0.21	-0.27	-0.33	-0.33	-0.32	-0.17	-0.06	0.09
	0.25	0.38	0.50	0.59	0.67	0.68	0.64	0.56	0.50	0.49	0.53	0.53
12	0.48	0.29	0.10	-0.03	-0.14	-0.20	-0.27	-0.33	-0.38	-0.34	-0.19	-0.08
	0.03	0.17	0.28	0.38	0.48	0.55	0.58	0.52	0.42	0.32	0.32	0.37
	0.38	0.34	0.21	0.02	-0.09	-0.18	-0.25	-0.30	-0.37	-0.37	-0.22	-0.06
	0.07	0.21	0.37	0.50	0.64	0.75	0.81	0.79	0.69	0.55	0.49	0.49
13	0.50	0.49	0.38	0.16	-0.02	-0.11	-0.20	-0.26	-0.32	-0.37	-0.43	-0.34
	-0.19	-0.06	0.04	0.16	0.31	0.41	0.59	0.64	0.67	0.59	0.47	0.37
	0.39	0.44	0.49	0.41	0.20	0.00	-0.09	-0.17	-0.25	-0.31	-0.37	-0.38
	-0.21	-0.08	0.05	0.20	0.36	0.49	0.61	0.69	0.73	0.68	0.56	0.44
14	0.37	0.38	0.43	0.43	0.28	0.08	-0.08	-0.15	-0.23	-0.29	-0.35	-0.42
	-0.45	-0.35	-0.20	-0.08	0.06	0.19	0.32	0.44	0.58	0.64	0.59	0.49
	0.36	0.29	0.35	0.43	0.48	0.35	0.13	-0.02	-0.13	-0.20	-0.27	-0.32
	-0.38	-0.33	-0.17	-0.04	0.10	0.26	0.43	0.57	0.67	0.76	0.80	0.71
15	0.56	0.44	0.37	0.43	0.47	0.47	0.28	0.05	-0.07	-0.15	-0.24	-0.30
	-0.36	-0.42	-0.44	-0.26	-0.11	0.00	0.14	0.28	0.43	0.54	0.64	0.70
	0.64	0.52	0.40	0.38	0.45	0.53	0.50	0.34	0.09	-0.04	-0.14	-0.21
	-0.27	-0.34	-0.38	-0.28	-0.14	-0.03	0.14	0.29	0.42	0.52	0.61	0.65
16	0.64	0.53	0.41	0.31	0.28	0.33	0.38	0.34	0.13	-0.03	-0.14	-0.21
	-0.27	-0.33	-0.39	-0.46	-0.46	-0.27	-0.14	-0.05	0.09	0.21	0.34	0.46
	0.52	0.52	0.45	0.34	0.27	0.30	0.39	0.49	0.47	0.29	0.07	-0.11
	-0.14	-0.21	-0.27	-0.33	-0.36	-0.24	-0.11	0.01	0.16	0.35	0.40	0.47
17	0.52	0.51	0.45	0.34	0.23	0.16	0.16	0.20	0.23	0.14	-0.03	-0.14
	-0.23	-0.29	-0.35	-0.40	-0.47	-0.52	-0.50	-0.33	-0.23	-0.16	-0.04	0.05
	0.15	0.23	0.29	0.29	0.23	0.17	0.16	0.20	0.30	0.38	0.34	0.16
	-0.03	-0.14	-0.20	-0.27	-0.34	-0.39	-0.40	-0.27	-0.15	-0.05	0.07	0.17
18	0.24	0.31	0.33	0.32	0.29	0.21	0.14	0.11	0.13	0.16	0.16	0.08
	-0.08	-0.19	-0.26	-0.32	-0.38	-0.44	-0.50	-0.53	-0.44	-0.31	-0.21	-0.14
	-0.06	0.02	0.11	0.16	0.22	0.23	0.19	0.19	0.22	0.30	0.40	0.43
	0.34	0.15	-0.02	-0.12	-0.20	-0.26	-0.33	-0.37	-0.35	-0.23	-0.12	-0.02
19	0.09	0.16	0.19	0.22	0.23	0.25	0.22	0.17	0.13	0.13	0.15	0.16
	0.15	0.04	-0.09	-0.19	-0.26	-0.33	-0.39	-0.44	-0.49	-0.50	-0.38	-0.26
	-0.19	-0.11	-0.03	0.04	0.11	0.18	0.23	0.28	0.28	0.34	0.41	0.50
	0.56	0.56	0.45	0.25	0.11	-0.03	-0.13	-0.20	-0.26	-0.27	-0.20	-0.11
20	-0.01	0.09	0.13	0.16	0.16	0.18	0.18	0.20	0.22	0.23	0.24	0.28
	0.28	0.31	0.28	0.17	0.03	-0.09	-0.19	-0.26	-0.32	-0.38	-0.39	-0.36
	-0.26	-0.15	-0.08	0.01	0.07	0.14	0.17	0.22	0.28	0.31	0.35	0.41
	0.50	0.58	0.58	0.55	0.46	0.28	0.11	-0.02	-0.12	-0.20	-0.26	-0.27
21	-0.25	-0.18	-0.09	-0.02	0.03	0.04	0.07	0.10	0.12	0.16	0.18	0.21
	0.24	0.27	0.30	0.31	0.31	0.21	0.08	-0.05	-0.14	-0.21	-0.27	-0.33
	-0.34	-0.31	-0.20	-0.12	-0.04	0.04	0.10	0.15	0.17	0.22	0.28	0.31
	0.35	0.40	0.46	0.49	0.49	0.46	0.37	0.22	0.08	-0.04	-0.14	-0.20

22 -0.26 -0.29 -0.28 -0.21 -0.14 -0.08 -0.05 -0.02 -0.02 0.01 0.04 0.09
0.14 0.16 0.19 0.21 0.24 0.26 0.25 0.20 0.06 -0.04 -0.14 -0.21
-0.28 -0.33 -0.35 -0.29 -0.21 -0.14 -0.06 0.03 0.09 0.15 0.20 0.25
0.31 0.35 0.41 0.44 0.49 0.49 0.50 0.44 0.35 0.21 0.04 -0.07
23 -0.15 -0.23 -0.28 -0.32 -0.33 -0.26 -0.20 -0.14 -0.08 -0.05 -0.03 -0.01
0.03 0.08 0.09 0.11 0.14 0.17 0.22 0.25 0.26 0.23 0.11 -0.01
-0.11 -0.20 -0.23 -0.24 -0.20 -0.11 -0.01 0.09 0.19 0.28 0.32 0.37
0.39 0.43 0.47 0.47 0.46 0.46 0.49 0.49 0.47 0.43 0.28 0.11
24 -0.02 -0.12 -0.19 -0.25 -0.30 -0.33 -0.36 -0.30 -0.20 -0.14 -0.08 -0.08
-0.01 0.04 0.11 0.16 0.21 0.23 0.24 0.29 0.32 0.35 0.34 0.28
0.12 -0.01 -0.09 -0.15 -0.21 -0.27 -0.28 -0.21 -0.11 0.02 0.13 0.21
0.25 0.28 0.30 0.33 0.34 0.34 0.33 0.30 0.29 0.31 0.32 0.29
25 0.17 0.03 -0.09 -0.15 -0.23 -0.27 -0.33 -0.37 -0.34 -0.24 -0.14 -0.03
0.05 0.10 0.16 0.20 0.23 0.26 0.25 0.24 0.23 0.27 0.30 0.33
0.28 0.17 0.04 -0.08 -0.16 -0.23 -0.27 -0.32 -0.27 -0.16 -0.04 0.09
0.20 0.27 0.34 0.39 0.42 0.43 0.40 0.40 0.35 0.34 0.33 0.31
26 0.30 0.21 0.05 -0.08 -0.15 -0.21 -0.27 -0.32 -0.38 -0.38 -0.26 -0.14
-0.06 0.04 0.11 0.18 0.24 0.29 0.33 0.34 0.31 0.31 0.33 0.38
0.43 0.42 0.33 0.15 0.00 -0.09 -0.16 -0.23 -0.27 -0.27 -0.18 -0.06
0.08 0.21 0.31 0.40 0.45 0.49 0.50 0.51 0.46 0.41 0.40 0.43
27 0.41 0.28 0.29 0.17 0.01 -0.09 -0.17 -0.24 -0.30 -0.33 -0.36 -0.26
-0.15 -0.04 0.08 0.17 0.21 0.26 0.33 0.39 0.39 0.32 0.29 0.31
0.40 0.48 0.47 0.37 0.19 0.03 -0.08 -0.15 -0.21 -0.28 -0.32 -0.25
-0.12 0.01 0.15 0.27 0.37 0.44 0.48 0.51 0.47 0.43 0.37 0.29
28 0.28 0.31 0.34 0.29 0.16 -0.01 -0.11 -0.19 -0.25 -0.31 -0.36 -0.39
-0.35 -0.21 -0.09 0.00 0.11 0.21 0.28 0.34 0.37 0.35 0.32 0.28
0.26 0.29 0.36 0.43 0.38 0.22 0.05 -0.07 -0.15 -0.21 -0.27 -0.32
-0.31 -0.15 -0.05 0.09 0.23 0.34 0.43 0.49 0.47 0.43 0.37 0.28
29 0.21 0.17 0.20 0.23 0.22 0.11 -0.03 -0.14 -0.21 -0.27 -0.33 -0.39
-0.44 -0.38 -0.31 -0.17 -0.08 0.04 0.13 0.22 0.28 0.31 0.28 0.25
0.21 0.19 0.22 0.31 0.39 0.38 0.23 0.05 -0.08 -0.15 -0.21 -0.27
-0.33 -0.33 -0.20 -0.08 0.04 0.17 0.28 0.35 0.41 0.43 0.40 0.34
30 0.27 0.17 0.14 0.16 0.18 0.19 0.10 -0.05 -0.15 -0.21 -0.27 -0.33
-0.39 -0.44 -0.44 -0.29 -0.17 -0.09 0.00 0.10 0.16 0.23 0.28 0.29
0.25 0.18 0.16 0.17 0.23 0.33 0.34 0.21 0.03 -0.09 -0.17 -0.24
-0.30 -0.35 -0.37 -0.25 -0.13 -0.01 0.11 0.22 0.31 0.37 0.40 0.40
July 1991
1 0.35 0.28 0.21 0.16 0.17 0.23 0.23 0.15 -0.01 -0.12 -0.20 -0.26
-0.32 -0.38 -0.44 -0.43 -0.34 -0.19 -0.11 -0.02 0.09 0.16 0.23 0.28
0.28 0.23 0.20 0.16 0.18 0.26 0.34 0.39 0.28 0.11 -0.04 -0.13
-0.21 -0.27 -0.32 -0.35 -0.26 -0.13 -0.04 0.09 0.20 0.28 0.34 0.37
2 0.34 0.29 0.25 0.20 0.12 0.14 0.17 0.17 0.11 -0.03 -0.14 -0.21
-0.27 -0.33 -0.39 -0.45 -0.49 -0.38 -0.26 -0.17 -0.09 0.00 0.09 0.15
0.19 0.20 0.19 0.16 0.14 0.16 0.22 0.31 0.36 0.28 0.12 -0.01
-0.12 -0.20 -0.26 -0.32 -0.34 -0.27 -0.17 -0.07 0.05 0.16 0.23 0.29
3 0.34 0.34 0.31 0.26 0.21 0.16 0.16 0.18 0.21 0.17 0.05 -0.09
-0.19 -0.26 -0.32 -0.38 -0.44 -0.46 -0.40 -0.27 -0.19 -0.11 -0.02 0.05
0.10 0.15 0.15 0.16 0.14 0.14 0.16 0.22 0.29 0.37 0.33 0.17
0.03 -0.09 -0.17 -0.23 -0.29 -0.33 -0.33 -0.23 -0.13 -0.03 0.07 0.14
4 0.19 0.23 0.23 0.22 0.21 0.16 0.12 0.11 0.15 0.15 0.12 0.05

	-0.08	-0.19	-0.25	-0.32	-0.38	-0.44	-0.49	-0.46	-0.34	-0.24	-0.16	-0.09
	-0.02	0.05	0.10	0.13	0.15	0.17	0.18	0.22	0.29	0.35	0.43	0.46
	0.35	0.21	0.04	-0.08	-0.16	-0.22	-0.27	-0.30	-0.24	-0.14	-0.05	0.04
5	0.11	0.16	0.18	0.21	0.21	0.21	0.19	0.17	0.17	0.20	0.22	0.21
	0.17	0.05	-0.08	-0.15	-0.25	-0.31	-0.37	-0.39	-0.39	-0.32	-0.21	-0.12
	-0.04	0.04	0.11	0.17	0.20	0.23	0.28	0.34	0.34	0.37	0.46	0.55
	0.61	0.52	0.43	0.25	0.10	-0.01	-0.11	-0.16	-0.20	-0.22	-0.14	-0.05
6	0.04	0.16	0.15	0.19	0.18	0.22	0.23	0.23	0.26	0.25	0.28	0.29
	0.29	0.29	0.21	0.10	-0.02	-0.10	-0.20	-0.25	-0.29	-0.32	-0.29	-0.21
	-0.13	-0.04	0.03	0.09	0.12	0.15	0.19	0.22	0.27	0.31	0.37	0.44
	0.49	0.55	0.55	0.50	0.35	0.20	0.08	-0.04	-0.13	-0.19	-0.22	-0.23
7	-0.16	-0.09	-0.02	0.03	0.06	0.09	0.10	0.13	0.16	0.19	0.22	0.25
	0.28	0.28	0.28	0.24	0.20	0.11	-0.01	-0.10	-0.15	-0.23	-0.27	-0.30
	-0.29	-0.22	-0.14	-0.05	0.04	0.11	0.18	0.22	0.26	0.29	0.38	0.44
	0.47	0.52	0.58	0.61	-	-	-	-	-	-	-	-
26	-	-	-	-	-	-	-	-	0.27	0.23	0.28	0.25
	0.32	0.38	0.35	0.23	0.07	-0.07	-0.15	-0.23	-0.29	-0.33	-0.33	-0.18
	-0.07	0.06	0.21	0.33	0.43	0.49	0.52	0.51	0.46	0.38	0.31	0.24
27	0.25	0.28	0.27	0.19	0.04	-0.09	-0.16	-0.24	-0.30	-0.36	-0.42	-0.41
	-0.28	-0.15	-0.06	0.05	0.16	0.26	0.35	0.41	0.44	0.40	0.34	0.29
	0.29	0.35	0.42	0.41	0.30	0.13	-0.01	-0.11	-0.18	-0.25	-0.31	-0.33
	-0.20	-0.08	0.04	0.20	0.32	0.43	0.51	0.54	0.53	0.48	0.39	0.29
28	0.21	0.20	0.21	0.23	0.16	0.01	-0.11	-0.20	-0.26	-0.33	-0.39	-0.45
	-0.45	-0.32	-0.17	-0.07	0.04	0.16	0.27	0.37	0.41	0.41	0.37	0.29
	0.23	0.23	0.28	0.37	0.38	0.26	0.08	-0.05	-0.14	-0.22	-0.29	-0.35
	-0.38	-0.23	-0.09	0.04	0.21	0.35	0.49	0.59	0.64	0.61	0.55	0.46
29	0.35	0.27	0.26	0.29	0.32	0.30	0.07	-0.06	-0.15	-0.24	-0.30	-0.38
	-0.43	-0.44	-0.27	-0.14	-0.04	0.10	0.24	0.34	0.44	0.50	0.49	0.43
	0.35	0.28	0.28	0.31	0.41	0.44	0.32	0.13	-0.01	-0.11	-0.18	-0.25
	-0.31	-0.33	-0.18	-0.05	0.10	0.27	0.43	0.57	0.67	0.73	0.70	0.65
30	0.53	0.44	0.31	0.34	0.36	0.39	0.29	0.12	-0.02	-0.12	-0.14	-0.27
	-0.33	-0.39	-0.41	-0.27	-0.14	-0.03	0.09	0.22	0.32	0.41	0.49	0.49
	0.46	0.41	0.35	0.28	0.34	0.43	0.47	0.37	0.17	0.03	-0.09	-0.16
	-0.24	-0.30	-0.33	-0.20	-0.07	0.07	0.23	0.38	0.50	0.59	0.64	0.64
31	0.59	0.47	0.40	0.32	0.31	0.34	0.34	0.28	0.12	-0.01	-0.12	-0.20
	-0.27	-0.33	-0.39	-0.41	-0.27	-0.14	-0.03	0.09	0.21	0.32	0.41	0.49
	0.52	0.47	0.41	0.34	0.33	0.37	0.43	0.52	0.45	0.24	0.08	-0.04
	-0.12	-0.19	-0.26	-0.36	-0.22	-0.10	0.02	0.16	0.31	0.43	0.51	0.57
August 1991												
1	0.57	0.54	0.49	0.39	0.31	0.29	0.32	0.37	0.31	0.18	0.01	-0.11
	-0.18	-0.25	-0.32	-0.38	-0.41	-0.30	-0.16	-0.06	0.05	0.17	0.28	0.36
	0.43	0.47	0.46	0.40	0.34	0.33	0.40	0.50	0.55	0.50	0.31	0.14
	0.00	-0.09	-0.18	-0.24	-0.29	-0.27	-0.14	-0.04	0.07	0.20	0.29	0.37
2	0.41	0.41	0.40	0.35	0.31	0.24	0.21	0.22	0.26	0.26	0.18	0.01
	-0.09	-0.18	-0.25	-0.31	-0.38	-0.43	-0.38	-0.24	-0.14	-0.04	0.07	0.16
	0.23	0.28	0.31	0.31	0.29	0.28	0.28	0.31	0.39	0.47	0.46	0.32
	0.13	0.00	-0.09	-0.18	-0.24	-0.30	-0.31	-0.23	-0.13	-0.03	0.06	0.15
3	0.21	0.26	0.29	0.28	0.28	0.25	0.23	0.21	0.24	0.28	0.31	0.24
	0.12	-0.01	-0.11	-0.18	-0.25	-0.32	-0.36	-0.36	-0.28	-0.18	-0.10	-0.02
	0.05	0.12	0.17	0.21	0.23	0.24	0.26	0.28	0.32	0.38	0.46	0.48

	0.39	0.23	0.08	-0.04	-0.12	-0.20	-0.26	-0.30	-0.31	-0.25	-0.17	-0.11
4	-0.04	0.00	0.05	0.08	0.09	0.11	0.13	0.11	0.14	0.17	0.21	0.23
	0.23	0.15	0.06	-0.07	-0.15	-0.21	-0.27	-0.33	-0.35	-0.33	-0.25	-0.15
	-0.09	-0.02	0.05	0.10	0.13	0.16	0.19	0.22	0.25	0.32	0.37	0.44
	0.50	0.49	0.40	0.24	0.11	0.00	-0.10	-0.17	-0.24	-0.28	-0.30	-0.27
5	-0.21	-0.15	-0.10	-0.05	-0.03	-0.01	0.03	0.07	0.12	0.15	0.18	0.22
	0.27	0.28	0.27	0.24	0.15	0.05	-0.07	-0.14	-0.21	-0.26	-0.30	-0.29
	-0.25	-0.17	-0.08	-0.01	0.02	0.05	0.08	0.12	0.17	0.22	0.28	0.34
	0.40	0.44	0.47	0.46	0.42	0.28	0.15	0.03	-0.06	-0.14	-0.20	-0.26
6	-0.30	-0.30	-0.23	-0.17	-0.11	-0.04	0.00	0.05	0.11	0.17	0.23	0.31
	0.38	0.43	0.47	0.52	0.55	0.52	0.47	0.31	0.18	0.08	-0.04	-0.12
	-0.17	-0.21	-0.19	-0.13	-0.03	0.04	0.11	0.14	0.19	0.22	0.26	0.31
	0.35	0.40	0.43	0.46	0.47	0.48	0.46	0.40	0.27	0.13	0.00	-0.08
7	-0.15	-0.21	-0.27	-0.30	-0.29	-0.21	-0.13	-0.06	0.03	0.10	0.15	0.20
	0.28	0.34	0.37	0.41	0.46	0.49	0.44	0.46	0.46	0.39	0.21	0.09
	-0.04	-0.12	-0.18	-0.24	-0.26	-0.20	-0.11	0.00	0.11	0.23	0.32	0.38
	0.42	0.46	0.50	0.53	0.51	0.46	0.47	0.48	0.47	0.40	0.27	0.12
8	-0.01	-0.11	-0.18	-0.25	-0.30	-0.37	-0.40	-0.35	-0.21	-0.13	-0.05	0.04
	0.13	0.22	0.30	0.37	0.39	0.35	0.32	0.29	0.33	0.37	0.40	0.31
	0.15	0.01	-0.09	-0.17	-0.24	-0.30	-0.36	-0.38	-0.24	-0.10	-0.01	0.13
	0.26	0.36	0.46	0.50	0.52	0.48	0.40	0.31	0.24	0.23	0.26	0.24
9	0.15	-0.01	-0.10	-0.18	-0.25	-0.31	-0.38	-0.44	-0.49	-0.44	-0.28	-0.17
	-0.08	0.03	0.15	0.28	0.38	0.46	0.43	0.34	0.25	0.20	0.20	0.25
	0.28	0.18	0.04	-0.08	-0.15	-0.23	-0.30	-0.37	-0.43	-0.43	-0.26	-0.11
	-0.01	0.11	0.26	0.41	0.53	0.59	0.60	0.52	0.40	0.27	0.21	0.21
10	0.23	0.22	0.09	-0.04	-0.14	-0.21	-0.27	-0.33	-0.39	-0.46	-0.50	-0.32
	-0.15	-0.05	0.06	0.20	0.35	0.51	0.61	0.67	0.59	0.46	0.34	0.30
	0.34	0.41	0.43	0.28	0.09	-0.03	-0.11	-0.19	-0.25	-0.33	-0.39	-0.27
	-0.10	0.03	0.18	0.34	0.52	0.65	0.77	0.82	0.75	0.59	0.41	0.25
11	0.21	0.23	0.25	0.17	0.01	-0.09	-0.16	-0.24	-0.30	-0.37	-0.43	-0.49
	-0.44	-0.22	-0.09	0.03	0.16	0.32	0.49	0.63	0.73	0.73	0.59	0.43
	0.31	0.32	0.37	0.44	0.40	0.19	0.03	-0.08	-0.15	-0.23	-0.30	-0.37
	-0.36	-0.15	-0.02	0.14	0.34	0.53	0.70	0.83	0.91	0.90	0.79	0.59
12	0.40	0.29	0.30	0.34	0.43	0.20	0.03	-0.08	-0.15	-0.21	-0.27	-0.33
	-0.41	-0.45	-0.26	-0.09	0.02	0.16	0.34	0.51	0.64	0.77	0.82	0.70
	0.53	0.40	0.34	0.40	0.49	0.55	0.40	0.15	0.03	-0.07	-0.15	-0.22
	-0.29	-0.35	-0.39	-0.10	0.10	0.28	0.46	0.64	0.76	0.87	0.89	0.82
13	0.64	0.42	0.24	0.22	0.27	0.31	0.24	0.06	-0.06	-0.14	-0.21	-0.28
	-0.35	-0.41	-0.47	-0.36	-0.17	-0.06	0.06	0.21	0.37	0.52	0.64	0.70
	0.66	0.52	0.36	0.28	0.31	0.40	0.47	0.40	0.19	0.04	-0.06	-0.14
	-0.21	-0.28	-0.35	-0.30	-0.12	0.01	0.15	0.31	0.49	0.61	0.72	0.78
14	0.72	0.60	0.46	0.29	0.23	0.27	0.32	0.35	0.18	0.02	-0.09	-0.15
	-0.23	-0.30	-0.36	-0.43	-0.38	-0.20	-0.08	0.03	0.15	0.29	0.41	0.52
	0.58	0.55	0.46	0.33	0.23	0.27	0.34	0.44	0.47	0.28	0.09	-0.03
	-0.13	-0.20	-0.27	-0.33	-0.35	-0.19	-0.06	0.06	0.20	0.34	0.47	0.55
15	0.60	0.59	0.53	0.40	0.29	0.22	0.25	0.31	0.37	0.35	0.17	-0.01
	-0.11	-0.19	-0.25	-0.32	-0.39	-0.39	-0.25	-0.12	-0.02	0.09	0.21	0.31
	0.40	0.45	0.46	0.41	0.34	0.29	0.29	0.35	0.44	0.49	0.36	0.16
	0.03	-0.08	-0.15	-0.22	-0.29	-0.33	-0.26	-0.12	-0.02	0.07	0.17	0.25
16	0.32	0.37	0.38	0.35	0.32	0.27	0.23	0.26	0.34	0.40	0.39	0.23

	0.06	-0.05	-0.14	-0.21	-0.28	-0.33	-0.33	-0.23	-0.11	-0.01	0.08	0.17
	0.25	0.31	0.35	0.36	0.37	0.35	0.35	0.40	0.49	0.58	0.63	0.53
	0.34	0.15	0.03	-0.08	-0.15	-0.21	-0.25	-0.23	-0.13	-0.03	0.05	0.11
17	0.16	0.19	0.21	0.20	0.19	0.21	0.20	0.19	0.23	0.29	0.34	0.35
	0.26	0.13	-0.01	-0.09	-0.18	-0.24	-0.29	-0.29	-0.24	-0.17	-0.09	-0.01
	0.04	0.09	0.13	0.16	0.18	0.21	0.24	0.29	0.35	0.46	0.53	0.58
	0.53	0.43	0.24	0.11	-0.01	-0.09	-0.15	-0.20	-0.20	-0.15	-0.09	-0.03
18	0.02	0.04	0.05	0.05	0.06	0.09	0.11	0.15	0.19	0.26	0.34	0.41
	0.46	0.43	0.33	0.21	0.09	-0.01	-0.09	-0.14	-0.17	-0.17	-0.12	-0.06
	0.02	0.08	0.10	0.11	0.10	0.12	0.14	0.17	0.21	0.28	0.35	0.43
	0.50	0.50	0.46	0.37	0.23	0.13	0.02	-0.07	-0.13	-0.17	-0.20	-0.21
19	-0.18	-0.15	-0.11	-0.11	-0.12	-0.13	-0.13	-0.12	-0.07	-0.02	0.04	0.11
	0.18	0.24	0.29	0.29	0.23	0.17	0.09	0.01	-0.05	-0.11	-0.14	-0.15
	-0.13	-0.09	-0.04	-0.01	0.02	0.02	0.02	0.03	0.06	0.11	0.16	0.20
	0.24	0.29	0.32	0.31	0.29	0.24	0.18	0.09	0.01	-0.08	-0.13	-0.17
20	-0.20	-0.21	-0.21	-0.20	-0.16	-0.13	-0.14	-0.12	-0.09	-0.06	0.00	0.06
	0.14	0.20	0.29	0.36	0.43	0.47	0.49	0.41	0.34	0.24	0.16	0.08
	0.02	-0.03	-0.04	-0.03	0.01	0.05	0.10	0.11	0.11	0.12	0.13	0.14
	0.17	0.21	0.23	0.26	0.28	0.28	0.28	0.24	0.20	0.13	0.05	-0.05
21	-0.13	-0.18	-0.22	-0.26	-0.27	-0.25	-0.20	-0.14	-0.08	-0.03	0.02	0.05
	0.09	0.13	0.17	0.23	0.29	0.35	0.40	0.43	0.46	0.43	0.35	0.23
	0.15	0.05	-0.03	-0.09	-0.12	-0.08	0.00	0.09	0.15	0.22	0.28	0.33
	0.37	0.40	0.43	0.46	0.48	0.52	0.52	0.55	0.52	0.52	0.49	0.40
22	0.26	0.12	0.01	-0.07	-0.13	-0.15	-0.11	-0.04	0.05	0.15	0.25	0.31
	0.38	0.43	0.47	0.52	0.53	0.56	0.58	0.61	0.64	0.66	0.64	0.58
	0.42	0.28	0.15	0.05	-0.03	-0.07	-0.08	-0.04	0.04	0.16	0.28	0.40
	0.46	0.51	0.54	0.58	0.58	0.58	0.59	0.57	0.55	0.53	0.56	0.50
23	0.40	0.23	0.10	-0.01	-0.09	-0.15	-0.21	-0.20	-0.08	0.01	0.10	0.22
	0.32	0.42	0.50	0.55	0.62	0.64	0.62	0.60	0.61	0.62	0.66	0.67
	0.59	0.44	0.26	0.05	0.00	-0.09	-0.15	-0.23	-0.11	-0.03	0.06	0.18
	0.31	0.38	0.47	0.49	0.54	0.55	0.53	0.45	0.37	0.31	0.28	0.26
24	0.23	0.09	0.02	-0.09	-0.16	-0.23	-0.29	-0.35	-0.39	-0.38	-0.26	-0.14
	-0.05	0.04	0.14	0.20	0.32	0.40	0.46	0.46	0.43	0.40	0.43	0.47
	0.52	0.53	0.41	0.22	0.08	-0.03	-0.11	-0.18	-0.24	-0.24	-0.11	0.01
	0.14	0.29	0.43	0.53	0.61	0.64	0.64	0.58	0.52	0.41	0.33	0.33
25	0.35	0.37	0.28	0.12	0.00	-0.09	-0.17	-0.25	-0.30	-0.37	-0.39	-0.24
	-0.11	-0.01	0.10	0.22	0.34	0.43	0.50	0.52	0.47	0.40	0.32	0.31
	0.35	0.43	0.46	0.35	0.16	0.04	-0.06	-0.14	-0.21	-0.27	-0.32	-0.17
	-0.04	0.09	0.22	0.37	0.52	0.61	0.68	0.68	0.61	0.52	0.40	0.29
26	0.26	0.28	0.31	0.24	0.09	-0.03	-0.12	-0.19	-0.26	-0.32	-0.39	-0.43
	-0.27	-0.13	-0.02	0.10	0.22	0.34	0.46	0.53	0.55	0.49	0.40	0.30
	0.26	0.30	0.40	0.44	0.34	0.16	0.02	-0.08	-0.15	-0.23	-0.29	-0.34
	-0.23	-0.08	0.05	0.20	0.37	0.52	0.64	0.72	0.73	0.66	0.53	0.40
27	0.28	0.23	0.26	0.29	0.24	0.09	-0.03	-0.13	-0.20	-0.26	-0.32	-0.39
	-0.43	-0.27	-0.12	-0.02	0.10	0.23	0.35	0.47	0.56	0.57	0.51	0.40
	0.29	0.23	0.28	0.35	0.42	0.34	0.16	0.03	-0.08	-0.15	-0.22	-0.28
	-0.34	-0.25	-0.08	0.05	0.20	0.35	0.51	0.64	0.72	0.76	0.67	0.56
28	0.41	0.29	0.25	0.28	0.34	0.29	0.14	0.00	-0.09	-0.17	-0.24	-0.30
	-0.37	-0.42	-0.28	-0.13	-0.02	0.10	0.22	0.36	0.49	0.56	0.58	0.49
	0.40	0.28	0.21	0.23	0.31	0.40	0.33	0.22	0.02	-0.07	-0.14	-0.21

	-0.28	-0.33	-0.29	-0.11	0.02	0.14	0.28	0.44	0.58	0.67	0.70	0.64
29	0.52	0.36	0.23	0.17	0.21	0.23	0.22	0.10	-0.03	-0.13	-0.20	-0.27
	-0.33	-0.40	-0.45	-0.31	-0.14	-0.04	0.06	0.18	0.29	0.43	0.53	0.56
	0.51	0.40	0.28	0.23	0.28	0.35	0.43	0.39	0.21	0.05	-0.04	-0.13
	-0.20	-0.27	-0.33	-0.33	-0.15	-0.03	0.09	0.21	0.35	0.47	0.56	0.61
30	0.56	0.47	0.35	0.23	0.21	0.23	0.28	0.29	0.17	0.03	-0.08	-0.16
	-0.23	-0.30	-0.37	-0.41	-0.31	-0.15	-0.05	0.05	0.17	0.28	0.47	0.50
	0.52	0.47	0.40	0.34	0.28	0.31	0.40	0.50	0.49	0.31	0.12	0.00
	-0.08	-0.15	-0.23	-0.29	-0.29	-0.15	-0.03	0.08	0.20	0.31	0.43	0.50
31	0.55	0.52	0.46	0.37	0.29	0.27	0.29	0.35	0.40	0.31	0.15	0.00
	-0.09	-0.18	-0.25	-0.32	-0.33	-0.26	-0.11	-0.01	0.10	0.22	0.32	0.43
	0.49	0.52	0.51	0.50	0.46	0.42	0.44	0.54	0.61	0.58	0.46	0.23
	0.09	-0.02	-0.09	-0.18	-0.23	-0.26	-0.15	-0.06	0.04	0.14	0.24	0.34
September 1991												
1	0.40	0.44	0.46	0.46	0.41	0.40	0.40	0.41	0.46	0.50	0.46	0.29
	0.11	-0.01	-0.09	-0.15	-0.21	-0.26	-0.26	-0.14	-0.03	0.05	0.16	0.24
	0.31	0.37	0.41	0.44	0.45	0.46	0.46	0.52	0.58	0.65	0.67	0.59
	0.41	0.22	0.09	-0.02	-0.09	-0.16	-0.20	-0.21	-0.14	-0.06	0.03	0.09
2	0.15	0.17	0.22	0.24	0.28	0.32	0.35	0.40	0.45	0.50	0.55	0.54
	0.47	0.34	0.19	0.06	-0.03	-0.11	-0.15	-0.19	-0.15	-0.08	0.03	0.07
	0.18	0.22	0.27	0.28	0.29	0.34	0.38	0.41	0.47	0.53	0.60	0.64
	0.63	0.55	0.40	0.23	0.10	-0.01	-0.08	-0.14	-0.20	-0.21	-0.20	-0.13
3	-0.08	-0.03	0.00	0.03	0.05	0.09	0.14	0.18	0.25	0.31	0.38	0.45
	0.49	0.51	0.49	0.40	0.25	0.14	0.03	-0.07	-0.12	-0.16	-0.19	-0.14
	-0.08	-0.02	0.04	0.10	0.13	0.12	0.09	0.17	0.23	0.29	0.34	0.40
	0.46	0.52	0.52	0.47	0.40	0.28	0.15	0.03	-0.07	-0.14	-0.20	-0.24
4	-0.26	-0.26	-0.17	-0.14	-0.09	-0.03	0.01	0.05	0.09	0.14	0.20	0.27
	0.32	0.39	0.44	0.49	0.50	0.46	0.38	0.26	0.15	0.03	-0.06	-0.13
	-0.18	-0.20	-0.20	-0.12	-0.03	0.04	0.10	0.16	0.21	0.25	0.30	0.36
	0.43	0.46	0.49	0.52	0.52	0.53	0.52	0.43	0.29	0.16	0.03	-0.07
5	-0.13	-0.20	-0.26	-0.29	-0.28	-0.19	-0.09	-0.03	0.04	0.10	0.18	0.24
	0.31	0.35	0.40	0.40	0.40	0.43	0.46	0.46	0.44	0.35	0.21	0.08
	-0.02	-0.11	-0.17	-0.23	-0.26	-0.20	-0.08	0.01	0.10	0.20	0.29	0.38
	0.46	0.50	0.52	0.52	0.50	0.48	0.49	0.52	0.52	0.46	0.34	0.17
6	0.05	-0.03	-0.12	-0.19	-0.26	-0.31	-0.32	-0.17	-0.03	0.06	0.16	0.28
	0.40	0.50	0.56	0.61	0.61	0.56	0.52	0.49	0.52	0.55	0.52	0.43
	0.23	0.10	-0.01	-0.09	-0.15	-0.22	-0.27	-0.24	-0.08	0.04	0.15	0.28
	0.42	0.55	0.64	0.70	0.70	0.64	0.56	0.47	0.41	0.44	0.46	0.41
7	0.28	0.11	0.03	-0.08	-0.14	-0.20	-0.26	-0.32	-0.36	-0.17	-0.02	0.07
	0.17	0.29	0.46	0.58	0.68	0.72	0.66	0.58	0.49	0.46	0.49	0.56
	0.58	0.43	0.22	0.11	0.01	-0.08	-0.14	-0.21	-0.26	-0.14	0.02	0.13
	0.27	0.43	0.58	0.71	0.82	0.88	0.82	0.71	0.59	0.52	0.53	0.58
10	-	-	-	-	-	-	0.89	1.01	1.07	0.96	0.72	0.52
	0.43	0.47	0.53	0.58	0.43	0.19	0.05	-0.05	-0.15	-0.24	-0.32	-0.40
	-0.27	-0.08	0.06	0.27	0.55	-	-	-	-	-	-	-
11	-	-	-	-	-	0.66	0.70	0.53	0.34	0.24	0.18	0.13
	0.03	-0.13	-0.18	-0.01	0.13	0.23	0.40	0.55	0.66	0.81	0.88	0.90
	0.79	0.64	0.50	0.46	0.50	0.61	0.67	0.53	0.23	0.05	-0.05	-0.14
	-0.20	-0.26	-0.13	0.02	0.17	0.35	0.54	0.71	0.84	0.93	0.95	0.88
12	0.76	0.58	0.43	0.37	0.43	0.50	0.48	0.31	0.12	0.03	-0.08	-0.15

	-0.21	-0.28	-0.33	-0.20	-0.04	0.08	0.20	0.34	0.49	0.63	0.72	0.75
	0.67	0.58	0.46	0.37	0.40	0.49	0.57	0.53	0.34	0.15	0.04	-0.04
	-0.13	-0.20	-0.26	-0.26	-0.08	0.05	0.17	0.31	0.45	0.58	0.66	0.71
13	0.68	0.61	0.50	0.40	0.34	0.39	0.48	0.53	0.41	0.22	0.08	-0.02
	-0.10	-0.17	-0.25	-0.29	-0.20	-0.05	0.06	0.18	0.30	0.41	0.51	0.59
	0.60	0.60	0.53	0.46	0.41	0.43	0.52	0.61	0.59	0.44	0.21	0.09
	-0.02	-0.09	-0.16	-0.22	-0.23	-0.11	0.01	0.10	0.21	0.31	0.40	0.46
14	0.49	0.47	0.44	0.39	0.34	0.32	0.38	0.46	0.51	0.44	0.26	0.10
	0.01	-0.10	-0.16	-0.22	-0.23	-0.18	-0.05	0.03	0.09	0.21	0.32	0.40
	0.45	0.47	0.49	0.47	0.46	0.44	0.49	0.56	0.62	0.62	0.51	0.32
	0.15	0.04	-0.05	-0.12	-0.17	-0.19	-0.13	-0.05	0.04	0.10	0.16	0.20
15	0.24	0.26	0.28	0.29	0.29	0.33	0.37	0.44	0.53	0.60	0.61	0.48
	0.31	0.16	0.06	-0.04	-0.10	-0.12	-0.07	0.01	0.09	0.19	0.27	0.33
	0.34	0.35	0.37	0.41	0.43	0.46	0.51	0.58	0.67	0.73	0.74	0.67
	0.49	0.33	0.19	0.06	-0.03	-0.08	-0.10	-0.08	-0.01	0.05	0.13	0.17
16	0.17	0.17	0.17	0.17	0.18	0.22	0.26	0.31	0.41	0.49	0.57	0.58
	0.54	0.44	0.30	0.19	0.11	0.03	-0.01	-0.04	0.00	0.05	0.11	0.16
	0.17	0.17	0.20	0.20	0.20	0.23	0.28	0.33	0.39	0.41	0.42	0.40
	0.35	0.24	0.17	0.07	0.01	-0.08	-0.13	-0.17	-0.18	-0.19	-0.18	-0.17
17	-0.14	-0.13	-0.12	-0.10	-0.07	-0.01	0.04	0.08	0.17	0.26	0.37	0.46
	0.51	0.54	0.53	0.48	0.40	0.32	0.25	0.19	0.15	0.14	0.16	0.17
	0.22	0.23	0.22	0.22	0.22	0.22	0.22	0.25	0.29	0.34	0.38	0.42
	0.46	0.47	0.46	0.41	0.37	0.29	0.20	0.11	0.04	-0.01	-0.04	-0.06
18	-0.08	-0.05	-0.02	0.02	0.02	0.02	0.02	0.04	0.08	0.10	0.16	0.22
	0.28	0.35	0.40	0.44	0.46	0.42	0.38	0.29	0.19	0.11	0.04	-0.02
	-0.06	-0.08	-0.10	-0.08	-0.07	-0.07	-0.07	-0.04	-0.04	-0.03	0.00	0.04
	0.08	0.12	0.14	0.15	0.18	0.20	0.20	0.17	0.14	0.08	0.01	-0.04
19	-0.09	-0.11	-0.11	-0.08	-0.02	0.05	0.14	0.20	0.25	0.28	0.32	0.34
	0.38	0.43	0.46	0.50	0.55	0.58	0.59	0.57	0.51	0.44	0.31	0.19
	0.07	-0.02	-0.10	-0.13	-0.13	-0.10	-0.04	0.03	0.09	0.14	0.17	0.19
	0.20	0.25	0.26	0.25	0.24	0.26	0.27	0.30	0.27	0.24	0.15	0.05
20	-0.05	-0.13	-0.19	-0.23	-0.28	-0.29	-0.22	-0.12	-0.05	0.02	0.10	0.17
	0.23	0.29	0.34	0.38	0.43	0.44	0.49	0.53	0.56	0.56	0.50	0.38
	0.23	0.09	0.00	-0.09	-0.14	-0.18	-0.14	-0.06	0.02	0.13	0.22	0.30
	0.36	0.39	0.39	0.41	0.40	0.39	0.38	0.37	0.36	0.37	0.34	0.18
21	0.12	-0.01	-0.10	-0.17	-0.23	-0.28	-0.30	-0.25	-0.12	-0.02	0.07	0.17
	0.27	0.36	0.43	0.48	0.50	0.51	0.49	0.49	0.53	0.57	0.59	0.54
	0.43	0.24	0.10	-0.01	-0.08	-0.16	-0.20	-0.22	-0.10	0.01	0.12	0.25
	0.38	0.48	0.54	0.60	0.60	0.60	0.57	0.51	0.46	0.44	0.44	0.41
22	0.35	0.20	0.06	-0.05	-0.13	-0.19	-0.25	-0.29	-0.29	-0.19	-0.07	0.02
	0.12	0.23	0.34	0.44	0.52	0.59	0.63	0.58	0.57	0.60	0.68	0.70
	0.67	0.53	0.32	0.14	0.03	-0.07	-0.13	-0.20	-0.20	-0.05	0.05	0.19
	0.39	0.53	0.65	0.74	0.77	0.82	0.72	0.72	0.60	0.52	0.53	0.56
23	0.56	0.39	0.27	0.09	-0.02	-0.09	-0.17	-0.25	-0.31	-0.33	-0.19	-0.04
	0.05	0.16	0.33	0.46	0.59	0.67	0.72	0.71	0.62	0.57	0.55	0.61
	0.67	0.70	0.56	0.34	0.15	0.04	-0.05	-0.14	-0.20	-0.23	-0.10	0.03
	0.18	0.35	0.50	0.65	0.77	0.84	0.87	0.81	0.72	0.58	0.46	0.44
24	0.45	0.46	0.40	0.21	0.06	-0.05	-0.11	-0.20	-0.26	-0.33	-0.32	-0.15
	0.01	0.12	0.24	0.38	0.50	0.62	0.75	0.83	0.77	0.66	0.51	0.44
	0.43	0.47	0.47	0.35	0.15	0.03	-0.05	-0.15	-0.21	-0.28	-0.30	-0.16

	0.00	0.12	0.29	0.47	0.60	0.78	0.93	1.01	0.98	0.86	0.74	0.60
25	0.63	0.67	0.72	0.69	0.43	0.21	0.09	0.00	-0.10	-0.17	-0.22	-0.22
	-0.04	0.09	0.25	0.44	0.65	0.80	0.92	1.02	1.06	0.99	0.87	0.77
	0.71	0.75	0.86	0.92	0.79	0.50	0.26	0.13	0.03	-0.06	-0.12	-0.19
	-0.09	0.06	0.16	0.36	0.53	0.72	0.85	0.97	1.03	0.98	0.86	0.72
26	0.52	0.46	0.50	0.56	0.55	0.38	0.15	0.03	-0.05	-0.13	-0.20	-0.27
	-0.29	-0.09	0.03	0.18	0.36	0.54	0.71	0.83	0.92	0.97	0.91	0.77
	0.63	0.55	0.60	0.69	0.75	0.66	0.41	0.18	0.06	-0.02	-0.12	-0.18
	-0.24	-0.13	0.01	0.12	0.33	0.53	0.71	0.83	0.95	1.01	1.00	0.91
27	0.72	0.59	0.53	0.57	0.65	0.64	0.47	0.22	0.07	-0.01	-0.09	-0.18
	-0.24	-0.28	-0.12	0.01	0.12	0.32	0.50	0.66	0.77	0.88	0.95	0.89
	0.79	0.66	0.58	0.61	0.70	0.77	0.70	0.46	0.23	0.10	0.00	-0.09
	-0.17	-0.23	-0.21	-0.03	0.10	0.24	0.42	0.56	0.71	0.85	0.95	0.98
28	0.95	0.82	0.71	0.66	0.69	0.77	0.85	0.78	0.54	0.29	0.15	0.05
	-0.04	-0.10	-0.03	0.10	0.22	0.43	0.62	0.83	0.99	1.08	1.13	1.16
	1.18	1.16	1.10	0.98	1.02	1.03	1.04	1.02	0.82	0.54	0.34	0.18
	0.08	-0.01	-0.08	-0.02	0.09	0.21	0.40	0.59	0.74	0.86	0.93	0.97
29	1.00	0.98	0.94	0.86	0.80	0.86	0.93	0.91	0.86	0.63	0.40	0.24
	0.12	0.04	-0.01	-0.06	0.00	0.10	0.24	0.39	0.53	0.61	0.67	0.72
	0.71	0.78	0.77	0.69	0.66	0.69	0.75	0.83	0.79	0.66	0.45	0.25
	0.10	0.02	-0.04	-0.12	-0.16	-0.15	-0.03	0.08	0.17	0.28	0.38	0.44
30	0.50	0.56	0.60	0.59	0.59	0.57	0.62	0.69	0.77	0.76	0.66	0.50
	0.31	0.14	0.06	-0.01	-0.05	-0.05	0.04	0.14	0.30	0.45	0.56	0.61
	0.64	0.68	0.70	0.74	0.74	0.77	0.80	0.85	0.92	0.95	0.91	0.74
	0.52	0.32	0.19	0.08	0.00	-0.06	-0.09	-0.02	0.06	0.17	0.29	0.36
October 1991												
1	0.37	0.43	0.47	0.53	0.58	0.63	0.65	0.69	0.72	0.76	0.72	0.68
	0.58	0.40	0.25	0.12	0.02	-0.04	-0.07	-0.10	-0.05	0.03	0.11	0.16
	0.18	0.21	0.24	0.27	0.31	0.36	0.43	0.48	0.53	0.59	0.62	0.63
	0.61	0.53	0.37	0.23	0.11	0.01	-0.05	-0.11	-0.14	-0.07	-0.01	0.03
2	0.03	0.06	0.09	0.12	0.16	0.24	0.31	0.41	0.51	0.60	0.70	0.78
	0.82	0.81	0.77	0.67	0.54	0.42	0.29	0.18	0.11	0.11	0.12	0.18
	0.28	0.36	0.41	0.41	0.39	0.37	0.36	0.36	0.41	0.43	0.46	0.48
	0.50	0.53	0.54	0.48	0.39	0.25	0.11	0.00	-0.07	-0.14	-0.20	-0.25
3	-0.27	-0.29	-0.26	-0.20	-0.14	-0.11	-0.03	0.03	0.10	0.19	0.27	0.36
	0.42	0.48	0.52	0.54	0.52	0.49	0.40	0.29	0.16	0.05	-0.03	-0.08
	-0.13	-0.15	-0.16	-0.13	-0.08	-0.02	0.03	0.04	0.07	0.10	0.14	0.19
	0.25	0.28	0.31	0.34	0.35	0.34	0.34	0.27	0.17	0.05	-0.03	-0.10
4	-0.16	-0.22	-0.24	-0.22	-0.12	0.01	0.11	0.23	0.34	0.44	0.53	0.61
	0.67	0.73	0.73	0.72	0.72	0.76	0.79	0.78	0.69	0.54	0.34	0.19
	0.08	-0.02	-0.09	-0.15	-0.19	-0.15	-0.04	0.09	0.13	0.21	0.31	0.39
	0.45	0.50	0.52	0.50	0.47	0.45	0.45	0.46	0.47	0.40	0.27	0.11
5	0.02	-0.05	-0.12	-0.18	-0.25	-0.29	-0.24	-0.09	0.02	0.11	0.22	0.34
	0.47	0.61	0.68	0.74	0.73	0.69	0.66	0.67	0.72	0.73	0.68	0.49
	0.25	0.14	0.03	-0.04	-0.11	-0.17	-0.21	-0.10	0.03	0.14	0.26	0.37
	0.47	0.59	0.65	0.67	0.65	0.56	0.49	0.43	0.45	0.49	0.46	0.35
6	0.19	0.06	-0.04	-0.10	-0.16	-0.23	-0.29	-0.32	-0.17	-0.02	0.09	0.21
	0.34	0.49	0.62	0.72	0.75	0.70	0.60	0.49	0.45	0.49	0.56	0.59
	0.48	0.28	0.13	0.04	-0.04	-0.11	-0.18	-0.24	-0.21	-0.02	0.11	0.22
	0.37	0.54	0.69	0.82	0.89	0.85	0.78	0.62	0.49	0.43	0.48	0.51

7	0.45	0.31	0.13	0.03	-0.04	-0.11	-0.18	-0.24	-0.30	-0.17	0.01	0.12
	0.26	0.41	0.58	0.71	0.84	0.98	1.00	0.90	0.77	0.66	0.68	0.71
	0.78	0.72	0.52	0.28	0.15	0.05	-0.02	-0.10	-0.15	-0.07	0.08	0.20
	0.37	0.56	0.72	0.89	1.05	1.12	1.15	1.08	0.97	0.83	0.74	0.77
8	0.79	0.77	0.63	0.37	0.22	0.11	0.02	-0.06	-0.12	-0.17	-0.09	0.05
	0.18	0.36	0.55	0.72	0.86	0.98	1.09	1.10	0.99	0.85	0.71	0.68
	0.74	0.82	0.77	0.59	0.34	0.19	0.10	0.01	-0.07	-0.13	-0.17	0.00
	0.14	0.29	0.49	0.67	0.84	0.97	1.10	1.13	1.08	0.94	0.79	0.62
9	0.66	0.71	0.76	0.66	0.46	0.23	0.14	0.04	-0.04	-0.10	-0.18	-0.13
	0.04	0.15	0.34	0.53	0.73	0.86	0.98	1.07	1.06	0.97	0.83	0.68
	0.60	0.71	0.75	0.78	0.60	0.34	0.21	0.10	0.02	-0.06	-0.10	-0.16
	-0.06	0.09	0.21	0.37	0.56	0.72	0.87	0.97	1.04	0.96	0.87	0.71
10	0.58	0.51	0.56	0.63	0.62	0.45	0.22	0.13	0.03	-0.04	-0.10	-0.17
	-0.21	-0.04	0.11	0.23	0.41	0.63	0.72	0.85	0.96	0.99	0.92	0.82
	0.67	0.56	0.59	0.65	0.73	0.62	0.45	0.22	0.13	0.04	-0.04	-0.10
	-0.15	-0.06	0.15	0.22	0.36	0.53	0.66	0.82	0.93	0.95	0.87	0.85
11	0.66	0.56	0.56	0.58	0.65	0.73	0.51	0.31	0.19	0.08	0.01	-0.05
	-0.12	-0.14	0.02	0.16	0.29	0.48	0.64	0.79	0.89	0.94	0.97	0.89
	0.83	0.68	0.61	0.63	0.70	0.82	0.76	0.50	0.30	0.18	0.08	0.01
	-0.06	-0.11	-0.01	0.13	0.27	0.46	0.61	0.72	0.83	0.91	0.95	0.91
12	0.88	0.82	0.74	0.76	0.82	0.91	0.93	0.80	0.60	0.36	0.23	0.13
	0.05	-0.01	0.02	0.14	0.27	0.42	0.58	0.72	0.81	0.87	0.91	0.91
	0.87	0.82	0.75	0.70	0.73	0.80	0.83	0.79	0.59	0.36	0.23	0.13
	0.06	0.00	-0.05	-0.01	0.11	0.23	0.39	0.51	0.61	0.69	0.73	0.75
13	0.76	0.75	0.70	0.65	0.66	0.74	0.83	0.86	0.77	0.59	0.41	0.23
	0.13	0.05	-0.01	0.00	0.10	0.20	0.34	0.49	0.59	0.66	0.70	0.75
	0.75	0.74	0.74	0.71	0.71	0.74	0.80	0.84	0.78	0.64	0.46	0.28
	0.16	0.07	-0.01	-0.03	-0.02	0.06	0.16	0.26	0.37	0.43	0.48	0.50
14	0.52	0.53	0.53	0.54	0.56	0.60	0.67	0.76	0.81	0.76	0.64	0.47
	0.33	0.22	0.13	0.08	0.07	0.12	0.20	0.30	0.42	0.49	0.52	0.52
	0.55	0.54	0.57	0.58	0.59	0.62	0.66	0.70	0.72	0.70	0.59	0.43
	0.27	0.16	0.08	0.02	-0.04	-0.07	-0.04	0.04	0.11	0.19	0.22	0.24
15	0.26	0.26	0.27	0.31	0.35	0.40	0.46	0.55	0.64	0.73	0.75	0.67
	0.58	0.42	0.31	0.20	0.14	0.09	0.12	0.17	0.25	0.32	0.37	0.39
	0.39	0.38	0.38	0.41	0.43	0.46	0.50	0.53	0.58	0.63	0.65	0.58
	0.50	0.39	0.30	0.19	0.11	0.07	0.03	0.02	0.07	0.13	0.19	0.20
16	0.24	0.26	0.26	0.29	0.32	0.37	0.44	0.52	0.62	0.72	0.79	0.84
	0.81	0.76	0.66	0.57	0.48	0.41	0.35	0.34	0.33	0.33	0.34	0.39
	0.37	0.39	0.37	0.35	0.37	0.39	0.42	0.44	0.43	0.40	0.39	0.32
	0.23	0.22	0.20	0.18	0.11	0.09	0.07	0.01	0.00	-0.02	0.01	0.05
17	0.10	0.16	0.22	0.29	0.35	0.45	0.54	0.64	0.76	0.89	1.01	1.07
	1.10	1.07	1.06	0.98	0.90	0.78	0.64	0.51	0.39	0.31	0.27	0.24
	0.24	0.22	0.25	0.26	0.28	0.30	0.32	0.38	0.43	0.49	0.53	0.50
	0.54	0.55	0.57	0.49	0.50	0.48	0.39	0.30	0.23	0.13	0.07	0.01
18	0.02	-0.01	0.05	0.08	0.12	0.17	0.20	0.23	0.29	0.37	0.44	0.55
	0.64	0.73	0.82	0.93	1.00	1.03	1.02	0.97	0.88	0.76	0.68	0.57
	0.53	0.50	0.54	0.60	0.66	0.71	0.72	0.71	0.69	0.69	0.67	0.66
	0.67	0.63	0.63	0.62	0.61	0.62	0.57	0.52	0.42	0.29	0.17	0.09
19	0.01	-0.04	-0.08	-0.09	-0.02	0.06	0.15	0.23	0.31	0.39	0.43	0.48
	0.52	0.54	0.58	0.60	0.65	0.70	0.76	0.79	0.75	0.66	0.51	0.35

	0.21	0.11	0.04	-0.01	-0.01	0.08	0.16	0.25	0.38	0.45	0.49	0.50
	0.52	0.54	0.52	0.52	0.49	0.49	0.52	0.57	0.59	0.52	0.41	0.26
20	0.15	0.06	-0.02	-0.08	-0.13	-0.14	-0.02	0.08	0.17	0.28	0.39	0.45
	0.51	0.51	0.51	0.52	0.50	0.48	0.50	0.53	0.59	0.61	0.53	0.40
	0.24	0.12	0.03	-0.03	-0.10	-0.14	-0.13	-0.01	0.09	0.19	0.28	0.39
	0.45	0.51	0.52	0.51	0.49	0.44	0.42	0.43	0.45	0.46	0.41	0.32
21	0.19	0.09	0.00	-0.06	-0.13	-0.17	-0.22	-0.17	-0.01	0.08	0.17	0.28
	0.39	0.46	0.55	0.59	0.61	0.56	0.52	0.50	0.53	0.61	0.67	0.62
	0.46	0.29	0.14	0.07	-0.02	-0.08	-0.14	-0.16	-0.04	0.08	0.19	0.30
	0.43	0.52	0.60	0.64	0.61	0.56	0.49	0.41	0.36	0.37	0.39	0.40
22	0.32	0.18	0.07	-0.01	-0.08	-0.16	-0.20	-0.25	-0.25	-0.06	0.07	0.15
	0.27	0.39	0.51	0.63	0.68	0.70	0.65	0.57	0.49	0.49	0.53	0.59
	0.58	0.43	0.24	0.12	0.03	-0.05	-0.11	-0.17	-0.23	-0.13	0.03	0.13
	0.25	0.39	0.53	0.63	0.71	0.72	0.66	0.57	0.47	0.36	0.35	0.38
23	0.42	0.35	0.19	0.07	0.00	-0.07	-0.14	-0.20	-0.25	-0.27	-0.09	0.06
	0.16	0.27	0.42	0.57	0.67	0.75	0.78	0.69	0.59	0.48	0.43	0.47
	0.54	0.58	0.43	0.23	0.11	0.03	-0.06	-0.12	-0.18	-0.23	-0.20	0.01
	0.11	0.22	0.36	0.52	0.65	0.68	0.77	0.72	0.60	0.48	0.34	0.29
24	0.34	0.40	0.36	0.22	0.09	0.01	-0.07	-0.14	-0.19	-0.25	-0.29	-0.13
	0.04	0.15	0.25	0.40	0.56	0.71	0.82	0.84	0.73	0.61	0.48	0.40
	0.44	0.51	0.57	0.46	0.23	0.11	0.03	-0.04	-0.12	-0.18	-0.23	-0.26
	-0.03	0.09	0.20	0.34	0.50	0.65	0.77	0.91	0.82	0.71	0.58	0.44
25	0.37	0.40	0.46	0.46	0.34	0.15	0.05	-0.02	-0.09	-0.15	-0.22	-0.26
	-0.15	0.03	0.13	0.24	0.40	0.56	0.71	0.81	0.86	0.81	0.68	0.55
	0.42	0.45	0.49	0.57	0.50	0.32	0.15	0.08	-0.02	-0.09	-0.16	-0.22
	-0.26	-0.09	0.04	0.15	0.29	0.45	0.61	0.73	0.82	0.84	0.76	0.63
26	0.50	0.39	0.43	0.48	0.54	0.44	0.25	0.11	0.03	-0.05	-0.12	-0.20
	-0.25	-0.16	0.01	0.12	0.27	0.42	0.60	0.74	0.85	0.91	0.88	0.80
	0.67	0.55	0.51	0.55	0.65	0.62	0.44	0.25	0.12	0.03	-0.05	-0.11
	-0.18	-0.23	-0.16	0.00	0.11	0.22	0.36	0.48	0.64	0.74	0.80	0.77
27	0.68	0.57	0.48	0.48	0.54	0.61	0.58	0.40	0.20	0.08	0.01	-0.06
	-0.13	-0.18	-0.20	0.00	0.10	0.21	0.37	0.52	0.65	0.76	0.83	0.83
	0.78	0.68	0.61	0.55	0.59	0.67	0.70	0.58	0.35	0.19	0.08	0.00
	-0.07	-0.13	-0.20	-0.23	-0.06	0.06	0.13	0.24	0.37	0.50	0.60	0.67
28	0.70	0.67	0.61	0.54	0.55	0.60	0.69	0.72	0.61	0.39	0.20	0.09
	0.01	-0.06	-0.12	-0.16	-0.06	0.06	0.15	0.30	0.43	0.55	0.65	0.71
	0.75	0.73	0.69	0.65	0.60	0.62	0.68	0.71	0.66	0.49	0.29	0.14
	0.05	-0.03	-0.11	-0.18	-0.23	-0.23	-0.08	0.01	0.09	0.17	0.26	0.35
29	0.41	0.47	0.50	0.50	0.49	0.49	0.54	0.62	0.68	0.68	0.56	0.36
	0.19	0.08	-0.01	-0.07	-0.13	-0.14	-0.06	0.04	0.15	0.26	0.36	0.44
	0.50	0.54	0.56	0.57	0.57	0.56	0.56	0.59	0.64	0.65	0.62	0.48
	0.31	0.17	0.05	-0.03	-0.09	-0.14	-0.14	-0.08	0.01	0.10	0.19	0.23
30	0.25	0.29	0.35	0.41	0.47	0.51	0.56	0.60	0.63	0.69	0.69	0.66
	0.56	0.41	0.26	0.14	0.04	-0.02	-0.06	-0.08	-0.03	0.04	0.12	0.21
	0.24	0.29	0.32	0.34	0.38	0.43	0.47	0.48	0.49	0.48	0.46	0.45
	0.43	0.34	0.20	0.08	0.00	-0.06	-0.14	-0.17	-0.21	-0.20	-0.14	-0.05
31	0.02	0.10	0.19	0.25	0.34	0.42	0.52	0.61	0.72	0.78	0.86	0.94
	0.97	1.02	0.96	0.84	0.66	0.51	0.36	0.24	0.20	0.20	0.24	0.30
	0.37	0.44	0.52	0.55	0.55	0.58	0.62	0.74	0.76	0.77	0.74	0.71
	0.65	0.64	0.55	0.48	0.38	0.32	0.16	0.07	-0.01	-0.06	-0.10	-0.13

November 1991

1	-0.13	-0.10	-0.02	0.04	0.10	0.18	0.25	0.33	0.40	0.48	0.54	0.58
	0.60	0.61	0.60	0.58	0.58	0.53	0.43	0.34	0.25	0.14	0.10	0.08
	0.11	0.17	0.28	0.42	0.46	0.55	0.61	0.59	0.65	0.73	0.76	0.79
	0.81	0.85	0.82	0.76	0.72	0.72	0.61	0.45	0.28	0.16	0.06	0.00
2	-0.06	-0.11	-0.12	-0.08	0.02	0.11	0.20	0.26	0.33	0.41	0.51	0.60
	0.68	0.71	0.69	0.66	0.63	0.60	0.58	0.57	0.42	0.27	0.12	0.05
	-0.02	-0.07	-0.12	-0.08	-0.01	0.10	0.21	0.32	0.39	0.50	0.51	0.59
	0.68	0.75	0.79	0.78	0.83	0.81	0.81	0.81	0.75	0.65	0.46	0.21
3	0.15	0.05	0.01	-0.04	-0.02	0.12	0.20	0.33	0.47	0.56	0.63	0.70
	0.80	0.87	0.89	0.88	0.86	0.81	0.80	0.72	0.70	0.58	0.51	0.27
	0.14	0.05	-0.01	-0.08	-0.12	-0.03	0.06	0.20	0.33	0.49	0.56	0.62
	0.73	0.80	0.86	0.88	0.88	0.85	0.82	0.78	0.81	0.80	0.71	0.55
4	0.32	0.16	0.08	0.02	-0.04	-0.07	0.06	0.17	0.32	0.50	0.62	0.73
	0.86	0.94	1.00	1.04	1.03	1.00	0.96	0.87	0.85	0.87	0.89	0.72
	0.46	0.23	0.11	0.04	-0.03	-0.10	-0.15	-0.15	-0.02	0.10	0.21	0.34
	0.45	0.55	0.61	0.69	0.70	0.65	0.54	0.48	0.43	0.46	0.49	0.49
5	0.37	0.18	0.05	-0.03	-0.09	-0.15	-0.20	-0.22	-0.11	0.01	0.18	0.36
	0.56	0.71	0.82	0.96	0.97	0.95	0.83	0.73	0.65	0.69	0.75	0.83
	0.74	0.55	0.26	0.13	0.03	-0.03	-0.09	-0.15	-0.20	-0.04	0.01	0.13
	0.30	0.44	0.55	0.61	0.68	0.67	0.62	0.54	0.42	0.34	0.37	0.45
6	0.52	0.43	0.25	0.07	-0.02	-0.08	-0.15	-0.20	-0.24	-0.27	-0.12	-0.01
	0.24	0.29	0.44	0.57	0.70	0.76	0.73	0.67	0.54	0.47	0.41	0.47
	0.56	0.56	0.43	0.19	0.05	-0.04	-0.11	-0.17	-0.23	-0.27	-0.27	-0.11
	0.00	0.11	0.25	0.36	0.49	0.58	0.64	0.60	0.52	0.40	0.29	0.22
7	0.27	0.28	0.26	0.13	-0.02	-0.11	-0.17	-0.23	-0.29	-0.33	-0.33	-0.17
	-0.05	0.06	0.22	0.39	0.53	0.68	0.80	0.91	0.86	0.74	0.69	0.64
	0.69	0.79	0.80	0.63	0.37	0.15	0.05	-0.06	-0.12	-0.18	-0.24	-0.18
	-0.04	0.09	0.24	0.35	0.46	0.56	0.65	0.75	0.76	0.69	0.50	0.45
8	0.39	0.42	0.50	0.51	0.39	0.15	0.02	-0.07	-0.15	-0.22	-0.27	-0.29
	-0.14	-0.03	0.09	0.26	0.43	0.54	0.66	0.76	0.82	0.80	0.69	0.62
	0.59	0.62	0.68	0.73	0.64	0.44	0.17	0.04	-0.05	-0.13	-0.19	-0.25
	-0.24	-0.10	0.02	0.14	0.28	0.40	0.49	0.56	0.61	0.61	0.58	0.51
9	0.40	0.36	0.41	0.48	0.51	0.40	0.18	0.04	-0.07	-0.15	-0.21	-0.27
	-0.32	-0.21	-0.09	0.02	0.16	0.32	0.45	0.54	0.62	0.64	0.60	0.57
	0.49	0.44	0.46	0.53	0.60	0.56	0.40	0.21	0.04	-0.06	-0.13	-0.20
	-0.26	-0.30	-0.20	-0.07	0.03	0.16	0.28	0.37	0.46	0.50	0.49	0.46
10	0.38	0.30	0.29	0.34	0.44	0.52	0.47	0.30	0.11	0.00	-0.09	-0.16
	-0.22	-0.27	-0.22	-0.09	0.00	0.12	0.26	0.39	0.48	0.53	0.54	0.52
	0.46	0.38	0.32	0.30	0.35	0.42	0.43	0.28	0.11	-0.01	-0.10	-0.17
	-0.23	-0.28	-0.32	-0.25	-0.13	-0.01	0.06	0.14	0.24	0.32	0.43	0.47
11	0.49	0.47	0.42	0.41	0.41	0.42	0.42	0.42	0.28	0.14	0.02	-0.08
	-0.16	-0.22	-0.22	-0.16	-0.10	-0.02	0.07	0.17	0.23	0.29	0.38	0.42
	0.42	0.47	0.47	0.51	0.60	0.71	0.76	0.71	0.62	0.43	0.22	0.07
	-0.01	-0.08	-0.11	-0.11	-0.04	0.06	0.18	0.34	0.41	0.43	0.45	0.47
12	0.47	0.49	0.45	0.45	0.47	0.52	0.61	0.67	0.68	0.58	0.40	0.23
	0.08	-0.01	-0.09	-0.14	-0.14	-0.04	0.05	0.16	0.27	0.37	0.46	0.50
	0.57	0.59	0.63	0.64	0.64	0.65	0.70	0.70	0.76	0.77	0.67	0.53
	0.41	0.16	0.05	-0.04	-0.08	-0.07	-0.03	0.03	0.12	0.19	0.24	0.22
13	0.23	0.27	0.31	0.33	0.36	0.40	0.46	0.39	0.39	0.30	0.30	0.19

	0.18	0.16	0.09	0.04	0.08	0.11	0.19	0.27	0.36	0.32	0.43	0.46
	0.57	0.57	0.63	0.63	0.58	0.64	0.73	0.65	0.65	0.56	0.52	0.44
	0.38	0.22	0.13	0.06	0.05	0.01	0.10	0.14	0.21	0.28	0.32	0.29
14	0.35	0.33	0.40	0.49	0.56	0.60	0.65	0.72	0.80	0.81	0.80	0.80
	0.73	0.68	0.53	0.42	0.31	0.25	0.19	0.19	0.21	0.25	0.28	0.25
	0.21	0.22	0.25	0.25	0.26	0.30	0.37	0.38	0.38	0.37	0.33	0.35
	0.29	0.23	0.13	0.07	-0.02	-0.08	-0.12	-0.14	-0.14	-0.13	-0.10	-0.07
15	-0.02	-0.01	0.02	0.06	0.11	0.16	0.24	0.31	0.38	0.44	0.49	0.55
	0.59	0.59	0.55	0.48	0.36	0.27	0.19	0.13	0.10	0.12	0.14	0.19
	0.22	0.24	0.26	0.25	0.27	0.30	0.34	0.39	0.43	0.45	0.48	0.47
	0.46	0.45	0.42	0.39	0.32	0.20	0.12	0.10	0.00	-0.04	-0.03	-0.01
16	0.02	0.08	0.13	0.14	0.17	0.20	0.26	0.31	0.38	0.43	0.49	0.54
	0.58	0.62	0.65	0.65	0.58	0.50	0.38	0.26	0.14	0.07	0.02	-0.03
	-0.03	0.02	0.08	0.12	0.14	0.15	0.15	0.19	0.21	0.26	0.30	0.32
	0.34	0.37	0.34	0.33	0.31	0.28	0.20	0.08	-0.02	-0.08	-0.14	-0.18
17	-0.21	-0.21	-0.16	-0.10	-0.04	0.05	0.10	0.13	0.17	0.22	0.29	0.38
	0.41	0.46	0.52	0.55	0.56	0.55	0.50	0.41	0.25	0.12	0.04	-0.05
	-0.11	-0.14	-0.13	-0.08	-0.02	0.07	0.14	0.20	0.24	0.29	0.35	0.41
	0.47	0.52	0.49	0.50	0.50	0.52	0.49	0.45	0.33	0.18	0.06	-0.04
18	-0.11	-0.16	-0.17	-0.14	-0.08	0.01	0.12	0.21	0.29	0.34	0.40	0.48
	0.57	0.63	0.64	0.69	0.69	0.69	0.69	0.66	0.60	0.44	0.27	0.12
	0.01	-0.07	-0.12	-0.15	-0.10	-0.04	0.04	0.15	0.25	0.28	0.28	0.32
	0.38	0.44	0.45	0.43	0.37	0.31	0.25	0.23	0.19	0.12	0.00	-0.11
19	-0.20	-0.26	-0.31	-0.35	-0.35	-0.28	-0.20	-0.10	0.03	0.16	0.23	0.30
	0.38	0.43	0.49	0.52	0.52	0.49	0.50	0.53	0.52	0.49	0.34	0.13
	-0.03	-0.12	-0.24	-0.28	-0.35	-0.40	-0.41	-0.35	-0.26	-0.19	-0.13	-0.07
	0.00	0.07	0.12	0.15	0.14	0.09	0.02	0.00	0.03	0.08	0.04	-0.06
20	-0.18	-0.25	-0.32	-0.37	-0.41	-0.43	-0.47	-0.46	-0.31	-0.18	-0.08	0.06
	0.13	0.21	0.24	0.23	0.20	0.14	0.05	-0.01	-0.04	0.03	0.10	0.07
	-0.04	-0.16	-0.24	-0.30	-0.35	-0.38	-0.43	-0.44	-0.44	-0.31	-0.19	-0.08
	0.03	0.14	0.21	0.24	0.21	0.17	0.10	0.00	-0.07	-0.05	0.02	0.05
21	-0.01	-0.13	-0.20	-0.26	-0.32	-0.35	-0.38	-0.41	-0.43	-0.37	-0.23	-0.11
	0.01	0.12	0.22	0.31	0.34	0.34	0.30	0.22	0.10	0.07	0.13	0.19
	0.19	0.10	-0.06	-0.15	-0.21	-0.27	-0.29	-0.31	-0.32	-0.34	-0.26	-0.14
	-0.03	0.07	0.19	0.29	0.39	0.44	0.43	0.39	0.28	0.19	0.15	0.21
22	0.26	0.22	0.11	-0.03	-0.11	-0.18	-0.23	-0.28	-0.32	-0.36	-0.23	-0.11
	0.02	0.19	0.35	0.47	0.59	0.67	0.69	0.64	0.57	0.46	0.39	0.40
	0.46	0.53	0.41	0.19	0.03	-0.08	-0.15	-0.22	-0.27	-0.33	-0.37	-0.30
	-0.15	-0.02	0.10	0.23	0.37	0.46	0.55	0.57	0.52	0.41	0.28	0.19
23	0.22	0.28	0.34	0.25	0.05	-0.07	-0.15	-0.22	-0.28	-0.33	-0.39	-0.38
	-0.18	-0.08	0.06	0.25	0.43	0.56	0.64	0.70	0.70	0.63	0.50	0.40
	0.37	0.41	0.49	0.46	0.28	0.06	-0.05	-0.14	-0.21	-0.27	-0.34	-0.39
	-0.39	-0.20	-0.08	0.05	0.19	0.32	0.45	0.56	0.64	0.64	0.56	0.43
24	0.33	0.29	0.36	0.45	0.45	0.27	0.04	-0.06	-0.15	-0.22	-0.28	-0.34
	-0.39	-0.21	-0.07	0.06	0.24	0.40	0.54	0.66	0.74	0.79	0.76	0.66
	0.54	0.43	0.46	0.51	0.56	0.45	0.21	0.02	-0.08	-0.16	-0.24	-0.30
	-0.36	-0.40	-0.24	-0.12	0.01	0.16	0.31	0.43	0.57	0.68	0.72	0.72
25	0.66	0.59	0.53	0.58	0.66	0.71	0.65	0.43	0.16	0.03	-0.08	-0.16
	-0.23	-0.27	-0.13	-0.03	0.12	0.31	0.49	0.63	0.71	0.78	0.80	0.80
	0.73	0.65	0.51	0.45	0.47	0.47	0.42	0.26	0.06	-0.08	-0.16	-0.23

	-0.30	-0.37	-0.43	-0.46	-0.34	-0.21	-0.12	0.00	0.12	0.24	0.36	0.45
26	0.52	0.48	0.43	0.36	0.37	0.42	0.48	0.50	0.36	0.15	-0.03	-0.12
	-0.21	-0.27	-0.34	-0.39	-0.26	-0.16	-0.06	0.10	0.24	0.33	0.42	0.47
	0.51	0.48	0.43	0.37	0.33	0.30	0.36	0.39	0.36	0.18	-0.02	-0.13
	-0.21	-0.28	-0.34	-0.40	-0.45	-0.47	-0.33	-0.20	-0.12	0.00	0.11	0.22
27	0.30	0.39	0.42	0.41	0.40	0.40	0.45	0.56	0.66	0.64	0.48	0.26
	0.07	-0.04	-0.15	-0.22	-0.28	-0.31	-0.21	-0.10	0.02	0.15	0.27	0.35
	0.39	0.41	0.41	0.39	0.34	0.28	0.24	0.26	0.29	0.32	0.25	0.14
	-0.08	-0.17	-0.24	-0.32	-0.38	-0.44	-0.48	-0.49	-0.38	-0.26	-0.17	-0.10
28	-0.02	0.08	0.15	0.21	0.26	0.27	0.27	0.30	0.36	0.45	0.50	0.46
	0.35	0.14	-0.01	-0.11	-0.21	-0.28	-0.33	-0.34	-0.25	-0.16	-0.07	0.04
	0.11	0.17	0.21	0.25	0.27	0.29	0.30	0.30	0.27	0.29	0.32	0.33
	0.26	0.11	-0.04	-0.16	-0.22	-0.29	-0.36	-0.42	-0.46	-0.41	-0.27	-0.18
29	-0.10	0.01	0.10	0.19	0.26	0.35	0.41	0.47	0.53	0.58	0.64	0.71
	0.74	0.73	0.63	0.43	0.23	0.08	-0.05	-0.13	-0.19	-0.23	-0.19	-0.10
	-0.01	0.08	0.14	0.17	0.20	0.20	0.23	0.25	0.29	0.29	0.28	0.28
	0.30	0.34	0.29	0.20	0.04	-0.09	-0.20	-0.27	-0.34	-0.40	-0.41	-0.41
30	-0.31	-0.23	-0.14	-0.07	0.01	0.09	0.16	0.23	0.29	0.36	0.40	0.44
	0.47	0.53	0.58	0.54	0.44	0.29	0.13	-0.02	-0.11	-0.18	-0.24	-0.28
	-0.27	-0.19	-0.11	0.00	0.06	0.09	0.12	0.16	0.21	0.24	0.29	0.34
	0.35	0.40	0.43	0.45	0.42	0.34	0.16	0.02	-0.10	-0.19	-0.27	-0.33
December 1991												
1	-0.37	-0.37	-0.29	-0.18	-0.10	0.01	0.08	0.16	0.21	0.26	0.31	0.37
	0.40	0.42	0.43	0.48	0.54	0.51	0.43	0.29	0.13	-0.03	-0.15	-0.22
	-0.29	-0.35	-0.38	-0.32	-0.23	-0.16	-0.13	-0.04	-0.01	0.02	0.06	0.09
	0.13	0.14	0.14	0.14	0.17	0.20	0.20	0.14	0.08	-0.09	-0.19	-0.27
2	-0.35	-0.41	-0.46	-0.48	-0.43	-0.29	-0.17	-0.10	-0.01	0.07	0.14	0.18
	0.23	0.27	0.28	0.27	0.28	0.38	0.36	0.35	0.31	0.17	0.00	-0.12
	-0.23	-0.29	-0.36	-0.42	-0.45	-0.40	-0.28	-0.19	-0.11	-0.05	0.02	0.08
	0.14	0.18	0.19	0.17	0.13	0.13	0.16	0.19	0.21	0.16	0.01	-0.12
3	-0.22	-0.29	-0.36	-0.42	-0.46	-0.48	-0.37	-0.24	-0.16	-0.05	0.04	0.14
	0.22	0.29	0.34	0.34	0.31	0.29	0.28	0.32	0.38	0.40	0.31	0.15
	-0.02	-0.13	-0.21	-0.29	-0.36	-0.41	-0.42	-0.35	-0.23	-0.15	-0.07	0.03
	0.09	0.15	0.22	0.22	0.22	0.18	0.15	0.15	0.20	0.25	0.28	0.18
4	0.03	-0.11	-0.20	-0.29	-0.35	-0.41	-0.45	-0.39	-0.24	-0.14	-0.03	0.10
	0.22	0.33	0.41	0.46	0.46	0.42	0.38	0.33	0.33	0.36	0.39	0.36
	0.23	0.06	-0.09	-0.19	-0.26	-0.31	-0.39	-0.43	-0.39	-0.24	-0.14	-0.04
	0.07	0.16	0.25	0.33	0.38	0.38	0.33	0.27	0.24	0.24	0.28	0.33
5	0.28	0.17	-0.01	-0.13	-0.22	-0.30	-0.36	-0.42	-0.45	-0.35	-0.19	-0.09
	0.03	0.14	0.24	0.33	0.38	0.37	0.34	0.26	0.21	0.15	0.18	0.23
	0.28	0.19	0.03	-0.12	-0.21	-0.29	-0.36	-0.42	-0.46	-0.48	-0.39	-0.26
	-0.17	-0.09	0.01	0.10	0.20	0.26	0.25	0.23	0.18	0.12	0.09	0.12
6	0.21	0.21	0.12	-0.04	-0.16	-0.24	-0.31	-0.38	-0.44	-0.48	-0.40	-0.24
	-0.14	-0.03	0.09	0.22	0.33	0.40	0.43	0.40	0.36	0.26	0.19	0.19
	0.21	0.26	0.21	0.07	-0.10	-0.19	-0.26	-0.34	-0.40	-0.44	-0.48	-0.45
	-0.31	-0.20	-0.12	-0.03	0.14	0.16	0.24	0.27	0.26	0.21	0.15	0.12
7	0.15	0.21	0.28	0.26	0.11	-0.05	-0.16	-0.24	-0.31	-0.37	-0.42	-0.34
	-0.21	-0.09	0.02	0.17	0.30	0.40	0.47	0.48	0.46	0.41	0.33	0.25
	0.20	0.26	0.30	0.29	0.14	-0.04	-0.13	-0.22	-0.30	-0.36	-0.42	-0.48
	-0.44	-0.30	-0.18	-0.10	0.00	0.09	0.21	0.29	0.35	0.33	0.29	0.23

8	0.17	0.20	0.26	0.34	0.34	0.19	0.00	-0.12	-0.21	-0.26	-0.33	-0.33
	-0.38	-0.24	-0.13	-0.02	0.12	0.25	0.37	0.44	0.46	0.44	0.40	0.32
	0.22	0.18	0.21	0.26	0.25	0.15	-0.02	-0.15	-0.24	-0.32	-0.39	-0.47
	-0.50	-0.49	-0.34	-0.23	-0.13	-0.03	0.09	0.17	0.24	0.28	0.26	0.20
9	0.14	0.10	0.11	0.17	0.26	0.31	0.19	0.00	-0.13	-0.20	-0.29	-0.36
	-0.42	-0.44	-0.31	-0.18	-0.07	0.06	0.20	0.29	0.37	0.42	0.43	0.37
	0.31	0.20	0.13	0.14	0.17	0.22	0.14	-0.01	-0.13	-0.23	-0.31	-0.37
	-0.44	-0.48	-0.51	-0.44	-0.30	-0.22	-0.13	-0.05	0.03	0.10	0.14	0.11
10	0.10	0.07	0.02	0.02	0.09	0.18	0.24	0.18	0.05	-0.11	-0.20	-0.28
	-0.36	-0.42	-0.43	-0.31	-0.20	-0.10	0.01	0.15	0.24	0.33	0.36	0.34
	0.27	0.22	0.16	0.10	0.11	0.14	0.15	0.09	-0.05	-0.17	-0.26	-0.33
	-0.40	-0.45	-0.49	-0.54	-0.49	-0.36	-0.28	-0.21	-0.14	-0.06	0.02	0.07
11	0.09	0.09	0.07	0.06	0.09	0.13	0.21	0.27	0.20	0.09	-0.06	-0.17
	-0.25	-0.31	-0.37	-0.41	-0.35	-0.24	-0.14	-0.06	0.03	0.12	0.16	0.21
	0.21	0.21	0.19	0.16	0.14	0.15	0.19	0.20	0.16	0.05	-0.11	-0.20
	-0.27	-0.35	-0.41	-0.45	-0.48	-0.43	-0.30	-0.24	-0.18	-0.12	-0.06	-0.01
12	0.03	0.06	0.06	0.06	0.08	0.12	0.18	0.25	0.33	0.28	0.15	0.00
	-0.12	-0.21	-0.27	-0.35	-0.38	-0.35	-0.24	-0.18	-0.09	0.00	0.06	0.10
	0.12	0.12	0.12	0.12	0.11	0.09	0.10	0.12	0.13	0.08	0.03	-0.10
	-0.20	-0.27	-0.35	-0.40	-0.45	-0.48	-0.48	-0.36	-0.30	-0.24	-0.18	-0.12
13	-0.07	-0.05	0.00	0.05	0.08	0.13	0.18	0.24	0.35	0.41	0.39	0.30
	0.14	0.00	-0.11	-0.20	-0.26	-0.30	-0.31	-0.24	-0.18	-0.11	-0.03	0.02
	0.09	0.11	0.11	0.11	0.11	0.11	0.11	0.12	0.15	0.17	0.17	0.11
	0.03	-0.09	-0.19	-0.26	-0.32	-0.37	-0.40	-0.40	-0.31	-0.22	-0.17	-0.11
14	-0.05	0.00	0.05	0.08	0.13	0.18	0.22	0.28	0.37	0.47	0.53	0.56
	0.52	0.41	0.30	0.11	-0.02	-0.09	-0.15	-0.17	-0.13	-0.07	0.00	0.09
	0.15	0.16	0.17	0.18	0.20	0.22	0.26	0.26	0.29	0.32	0.38	0.41
	0.36	0.29	0.15	0.05	-0.08	-0.15	-0.21	-0.26	-0.27	-0.23	-0.17	-0.11
15	-0.04	0.02	0.05	0.07	0.09	0.12	0.17	0.20	0.26	0.32	0.38	0.44
	0.48	0.47	0.43	0.29	0.17	0.05	-0.06	-0.13	-0.18	-0.19	-0.15	-0.11
	-0.05	0.02	0.07	0.08	0.08	0.12	0.14	0.18	0.20	0.23	0.26	0.29
	0.31	0.30	0.29	0.23	0.11	-0.01	-0.08	-0.17	-0.21	-0.24	-0.24	-0.20
16	-0.14	-0.07	0.00	0.07	0.13	0.18	0.24	0.26	0.30	0.38	0.43	0.50
	0.56	0.62	0.61	0.59	0.52	0.39	0.23	0.11	-0.02	-0.09	-0.15	-0.19
	-0.17	-0.13	-0.08	-0.01	0.02	0.04	0.06	0.08	0.12	0.17	0.20	0.23
	0.26	0.28	0.27	0.27	0.25	0.22	0.11	0.00	-0.08	-0.15	-0.21	-0.26
17	-0.27	-0.23	-0.15	-0.07	0.02	0.11	0.17	0.21	0.26	0.30	0.36	0.42
	0.45	0.49	0.53	0.56	0.55	0.52	0.46	0.31	0.17	0.02	-0.09	-0.19
	-0.25	-0.27	-0.27	-0.23	-0.15	-0.07	0.00	0.03	0.09	0.14	0.18	0.26
	0.32	0.33	0.32	0.32	0.32	0.29	0.21	0.18	0.11	0.00	-0.11	-0.21
18	-0.27	-0.34	-0.37	-0.37	-0.34	-0.23	-0.14	-0.06	0.05	0.11	0.23	0.34
	0.44	0.52	0.61	0.69	0.73	0.77	0.77	0.72	0.71	0.56	0.41	0.20
	0.08	-0.03	-0.11	-0.17	-0.14	-0.07	0.02	0.14	0.26	0.33	0.38	0.44
	0.49	0.50	0.51	0.50	0.50	0.50	0.50	0.56	0.53	0.50	0.35	0.16
19	0.01	-0.10	-0.19	-0.25	-0.27	-0.23	-0.15	-0.03	0.11	0.28	0.39	0.50
	0.57	0.65	0.71	0.74	0.72	0.62	0.59	0.61	0.62	0.59	0.53	0.33
	0.14	-0.02	-0.11	-0.19	-0.25	-0.28	-0.27	-0.18	-0.08	0.05	0.17	0.26
	0.32	0.38	0.46	0.50	0.53	0.50	0.52	0.47	0.46	0.49	0.50	0.46
20	0.33	0.10	-0.02	-0.11	-0.17	-0.23	-0.24	-0.11	0.02	0.17	0.35	0.49
	0.65	0.74	0.80	0.81	0.84	0.87	0.83	0.81	0.80	0.81	0.82	0.73

	0.62	0.35	0.15	0.03	-0.07	-0.15	-0.21	-0.27	-0.32	-0.23	-0.14	-0.02
	0.11	0.23	0.35	0.47	0.57	0.63	0.62	0.60	0.51	0.50	0.56	0.61
21	0.62	0.50	0.31	0.09	-0.02	-0.11	-0.18	-0.24	-0.29	-0.20	-0.04	0.14
	0.32	0.50	0.63	0.74	0.80	0.83	0.81	0.80	0.73	0.63	0.58	0.58
	0.58	0.49	0.32	0.11	-0.02	-0.12	-0.18	-0.24	-0.27	-0.32	-0.26	-0.11
	0.02	0.20	0.33	0.45	0.60	0.69	0.77	0.80	0.74	0.67	0.56	0.53
22	0.56	0.58	0.53	0.35	0.11	-0.02	-0.09	-0.18	-0.24	-0.28	-0.26	-0.11
	0.08	0.23	0.43	0.55	0.65	0.74	0.80	0.83	0.80	0.74	0.70	0.53
	0.52	0.50	0.50	0.38	0.16	-0.02	-0.11	-0.18	-0.24	-0.30	-0.34	-0.38
	-0.31	-0.13	0.02	0.16	0.32	0.44	0.58	0.69	0.75	0.77	0.67	0.50
23	0.42	0.43	0.46	0.50	0.46	0.26	0.04	-0.08	-0.14	-0.21	-0.29	-0.34
	-0.27	-0.08	0.08	0.23	0.40	0.57	0.73	0.80	0.81	0.82	0.81	0.78
	0.68	0.59	0.59	0.60	0.50	0.34	0.12	-0.02	-0.12	-0.19	-0.26	-0.33
	-0.38	-0.43	-0.23	-0.10	0.03	0.14	0.22	0.32	0.46	0.58	0.68	0.66
24	0.50	0.40	0.38	0.44	0.50	0.53	0.40	0.14	0.00	-0.09	-0.18	-0.26
	-0.32	-0.38	-0.30	-0.13	-0.01	0.18	0.35	0.50	0.65	0.75	0.77	0.73
	0.62	0.47	0.32	0.30	0.38	0.47	0.41	0.23	0.02	-0.09	-0.18	-0.26
	-0.30	-0.37	-0.43	-0.47	-0.38	-0.20	-0.11	-0.02	0.11	0.21	0.32	0.42
25	0.41	0.32	0.18	0.09	0.06	0.14	0.24	0.29	0.16	-0.03	-0.14	-0.22
	-0.29	-0.36	-0.43	-0.47	-0.38	-0.21	-0.08	0.02	0.17	0.31	0.43	0.50
	0.50	0.44	0.32	0.18	0.05	0.04	0.09	0.12	0.06	-0.09	-0.20	-0.29
	-0.36	-0.42	-0.47	-0.51	-0.56	-0.59	-0.43	-0.30	-0.21	-0.12	-0.02	0.08
26	0.18	0.26	0.26	0.18	0.11	0.04	0.08	0.15	0.20	0.16	0.00	-0.13
	-0.21	-0.30	-0.37	-0.43	-0.49	-0.47	-0.29	-0.15	-0.05	0.08	0.18	0.31
	0.41	0.48	0.51	0.49	0.44	0.40	0.37	0.43	0.52	0.56	0.41	0.14
	-0.02	-0.12	-0.20	-0.27	-0.37	-0.43	-0.44	-0.32	-0.18	-0.08	0.02	0.12
27	0.22	0.31	0.39	0.41	0.41	0.36	0.35	0.40	0.48	0.60	0.68	0.51
	0.30	0.09	-0.05	-0.14	-0.21	-0.30	-0.36	-0.36	-0.20	-0.11	-0.02	0.11
	0.17	0.23	0.27	0.26	0.22	0.17	0.11	0.03	-0.01	0.05	0.11	0.12
	0.03	-0.11	-0.20	-0.29	-0.37	-0.43	-0.49	-0.55	-0.57	-0.50	-0.38	-0.29
28	-0.23	-0.17	-0.10	-0.03	0.02	0.06	0.08	0.08	0.11	0.14	0.23	0.33
	0.38	0.27	0.11	-0.05	-0.14	-0.24	-0.30	-0.37	-0.41	-0.38	-0.26	-0.17
	-0.09	-0.03	0.01	0.06	0.09	0.11	0.11	0.11	0.09	0.09	0.11	0.17
	0.22	0.20	0.06	-0.08	-0.18	-0.25	-0.32	-0.39	-0.45	-0.50	-0.50	-0.41
29	-0.31	-0.25	-0.19	-0.13	-0.08	-0.02	0.05	0.11	0.15	0.18	0.23	0.31
	0.41	0.47	0.46	0.33	0.16	0.00	-0.12	-0.20	-0.26	-0.32	-0.37	-0.37
	-0.28	-0.20	-0.17	-0.14	-0.12	-0.11	-0.08	-0.08	-0.03	-0.02	0.02	0.05
	0.11	0.17	0.21	0.17	0.11	-0.05	-0.14	-0.23	-0.31	-0.38	-0.44	-0.48
30	-0.45	-0.37	-0.26	-0.20	-0.14	-0.09	-0.05	-0.03	-0.01	0.05	0.09	0.12
	0.17	0.23	0.29	0.34	0.30	0.21	0.08	-0.07	-0.15	-0.25	-0.32	-0.38
	-0.43	-0.44	-0.43	-0.36	-0.30	-0.27	-0.26	-0.24	-0.21	-0.18	-0.14	-0.09
	-0.05	-0.02	0.02	0.05	0.06	0.05	0.01	-0.08	-0.19	-0.26	-0.33	-0.41
31	-0.47	-0.50	-0.50	-0.41	-0.31	-0.25	-0.19	-0.14	-0.08	-0.02	0.05	0.11
	0.17	0.23	0.27	0.32	0.36	0.38	0.35	0.29	0.18	0.02	-0.09	-0.18
	-0.26	-0.32	-0.38	-0.42	-0.39	-0.32	-0.29	-0.27	-0.26	-0.24	-0.19	-0.15
	-0.08	-0.04	0.00	0.04	0.05	0.08	0.11	0.11	0.11	-0.02	-0.11	-0.20

January 1992

1	-0.27	-0.35	-0.41	-0.44	-0.44	-0.35	-0.26	-0.17	-0.09	-0.02	0.05	0.11
	0.18	0.25	0.32	0.37	0.38	0.40	0.43	0.46	0.41	0.31	0.17	-0.01
	-0.12	-0.20	-0.29	-0.36	-0.43	-0.47	-0.49	-0.44	-0.41	-0.38	-0.37	-0.32

	-0.26	-0.19	-0.10	-0.01	0.10	0.21	0.36	0.48	0.61	0.69	0.66	0.53
2	0.38	0.20	0.05	-0.06	-0.13	-0.12	-0.08	0.00	0.13	0.23	0.31	0.30
	0.29	0.30	0.31	0.30	0.27	0.23	0.18	0.14	0.09	0.08	0.02	-0.08
	-0.15	-0.25	-0.32	-0.40	-0.47	-0.55	-0.57	-0.53	-0.43	-0.32	-0.23	-0.16
	-0.08	0.01	0.10	0.17	0.26	0.31	0.33	0.38	0.41	0.47	0.50	0.47
3	0.41	0.25	0.09	-0.05	-0.14	-0.20	-0.26	-0.26	-0.18	-0.09	0.02	0.13
	0.21	0.27	0.33	0.38	0.45	0.50	0.50	0.47	0.44	0.44	0.44	0.43
	0.38	0.27	0.11	-0.03	-0.14	-0.21	-0.30	-0.36	-0.38	-0.32	-0.21	-0.11
	-0.05	0.08	0.14	0.20	0.27	0.37	0.43	0.44	0.44	0.44	0.47	0.50
4	0.53	0.50	0.37	0.18	0.02	-0.08	-0.17	-0.23	-0.26	-0.22	-0.13	-0.03
	0.10	0.23	0.32	0.41	0.45	0.52	0.56	0.56	0.55	0.54	0.55	0.56
	0.61	0.61	0.47	0.26	0.05	-0.06	-0.14	-0.25	-0.31	-0.35	-0.27	-0.15
	-0.05	0.08	0.20	0.31	0.38	0.43	0.47	0.49	0.46	0.41	0.38	0.37
5	0.41	0.47	0.48	0.37	0.16	-0.02	-0.12	-0.20	-0.28	-0.33	-0.32	-0.18
	-0.05	0.07	0.22	0.37	0.46	0.55	0.62	0.62	0.62	0.56	0.49	0.42
	0.43	0.50	0.50	0.41	0.23	0.02	-0.08	-0.19	-0.27	-0.35	-0.41	-0.43
	-0.29	-0.17	-0.08	0.01	0.11	0.17	0.25	0.30	0.32	0.32	0.24	0.17
6	0.14	0.16	0.20	0.25	0.18	0.00	-0.12	-0.20	-0.28	-0.37	-0.43	-0.42
	-0.26	-0.14	-0.02	0.12	0.26	0.38	0.47	0.53	0.56	0.55	0.47	0.40
	0.31	0.29	0.32	0.35	0.29	0.14	-0.04	-0.14	-0.21	-0.30	-0.37	-0.43
	-0.45	-0.32	-0.19	-0.09	0.00	0.11	0.18	0.28	0.37	0.41	0.41	0.35
7	0.26	0.24	0.27	0.33	0.39	0.33	0.17	-0.02	-0.11	-0.19	-0.26	-0.32
	-0.32	-0.19	-0.07	0.04	0.19	0.36	0.48	0.60	0.68	0.72	0.72	0.67
	0.59	0.53	0.56	0.62	0.63	0.56	0.41	0.17	0.01	-0.08	-0.17	-0.25
	-0.31	-0.33	-0.19	-0.09	0.02	0.14	0.26	0.38	0.45	0.52	0.60	0.63
8	0.55	0.55	0.57	0.62	0.72	0.74	0.69	0.56	0.31	0.12	-	-

Table C-2. Time-series of calculated cross-sectional mean current speeds (in m s^{-1}), at 30 minute intervals (starting at 0.15 GMT, daily).

January 1991

3	-	-	0.44	0.69	0.13	-3.25	-1.54	-1.08	-0.95	-0.82	-0.90	-0.80
	-0.70	0.37	0.23	1.28	0.04	0.18	0.25	0.25	0.00	0.07	-0.73	-1.06
	-1.40	-0.92	-0.08	0.12	-0.07	-1.35	-2.04	-1.39	-1.04	-0.74	-0.82	-0.91
	-0.74	-0.80	0.09	0.24	0.21	0.51	0.12	0.44	0.37	0.50	-0.18	-0.35
4	-0.86	-1.20	-0.70	0.13	0.33	-0.11	-1.33	-1.63	-1.67	-0.90	-0.76	-0.72
	-0.77	-0.46	0.29	0.41	0.52	0.99	0.52	0.07	0.08	0.20	0.14	-0.29
	-0.91	-1.63	-1.29	-0.33	-0.20	-0.46	-0.71	-1.19	-1.33	-0.84	-0.80	-0.73
	-0.75	-0.65	-0.58	-0.54	0.33	0.33	0.07	0.03	0.23	0.03	0.33	0.32
5	0.07	-0.64	-0.58	-0.59	0.13	-0.06	0.71	0.26	-1.24	-2.20	-1.44	-1.06
	-0.81	-0.68	-0.25	0.14	0.26	0.56	0.41	0.26	0.52	0.32	0.33	-0.29
	-0.54	-0.04	-1.17	-1.20	-1.03	-0.46	-0.46	-1.06	-0.89	-1.27	-0.89	-0.84
	-0.81	-0.75	-0.49	-0.74	-0.04	0.23	0.24	0.19	-0.13	0.15	0.23	0.24
6	0.04	-0.34	-0.28	-0.73	-1.08	-0.53	-0.31	-0.58	-0.76	-0.63	-1.17	-1.11
	-0.87	-0.77	-0.67	-0.78	-0.36	-0.19	0.25	0.13	0.10	0.02	0.02	0.26
	0.21	0.17	0.24	-0.46	-0.40	-0.40	-0.21	0.37	0.18	-0.38	-1.72	-1.65
	-1.62	-0.98	-0.83	-0.70	-0.67	-0.44	0.12	0.22	0.38	0.37	-0.18	0.08
7	0.08	0.08	0.15	-0.04	-0.10	-0.54	-0.23	0.34	0.22	-0.03	-0.27	-1.33
	-1.89	-1.65	-1.14	-0.89	-0.82	-0.51	-0.19	-0.01	0.21	0.29	0.15	-0.49
	-0.28	-0.22	-0.27	0.35	0.14	-0.50	-0.44	-1.19	-1.66	-	-	-
11	-1.16	-0.99	-0.99	-0.87	-0.92	-0.75	-0.78	-0.73	-0.99	-0.73	-0.76	-0.66
	-0.74	-0.63	-0.45	-0.80	-0.85	-0.75	-0.46	-1.11	-0.85	-1.26	-0.97	-0.86
12	-0.73	-0.78	-0.62	-0.58	-0.32	-0.34	-0.28	-0.25	-0.33	-0.27	-0.30	-0.18
	-0.13	-0.16	-0.48	-0.28	-0.47	-0.15	-0.27	-0.79	-0.67	-0.94	-1.28	-1.13
	-0.96	-0.86	-0.82	-0.74	-0.70	-0.75	-0.56	-0.51	-0.51	-0.50	-0.58	-0.58
	-0.46	-0.45	-0.27	-0.42	-0.41	-0.35	-0.18	-0.27	-0.24	-0.40	-0.88	-0.88
13	-0.89	-0.70	-0.70	-0.58	-0.66	-0.51	-0.32	0.18	0.07	-0.01	-0.38	-0.28
	-0.38	-0.38	-0.43	-0.38	-0.38	-0.43	-0.38	-0.38	-0.33	-0.23	-0.58	-0.76
	-0.87	-0.78	-0.70	-0.75	-0.52	-0.65	-0.58	-0.59	-0.26	-0.06	-0.16	-0.19
	-0.26	-0.21	-0.28	-0.36	-0.27	-0.40	-0.35	-0.39	-0.17	0.15	-0.27	-0.46
14	-0.60	-0.86	-0.79	-0.58	-0.70	-0.52	-0.52	-0.45	-0.13	0.27	0.20	0.08
	-0.13	-0.12	-0.21	-0.15	-0.30	-0.40	-0.36	-0.51	-0.41	-0.21	-0.21	-0.36
	-0.64	-0.84	-0.78	-0.78	-0.56	-0.61	-0.58	-0.46	-0.51	-0.22	0.15	0.11
	-0.03	-0.13	-0.12	-0.10	-0.27	-0.32	-0.32	-0.32	-0.36	-0.27	-0.18	0.15
15	-0.12	-0.73	-0.87	-0.79	-0.63	-0.67	-0.57	-0.58	-0.43	0.10	0.26	0.21
	0.18	0.29	-0.07	0.21	-0.10	-0.21	-0.32	-0.58	-0.65	-0.43	-0.12	-0.05
	0.05	-0.75	-1.10	-0.81	-0.75	-0.79	-0.49	-0.58	-0.51	-0.43	-0.06	0.26
	0.19	0.11	-0.03	-0.11	0.15	-0.12	-0.22	-0.17	-0.42	-0.38	-0.43	-0.01
16	-0.21	0.22	-0.97	-1.02	-0.83	-0.57	-0.77	-0.47	-0.64	-0.41	-0.04	0.31
	0.26	0.37	0.26	0.04	0.22	-0.07	-0.06	-0.44	-0.58	-0.57	-0.72	-0.32
	-0.22	-0.01	-0.62	-0.95	-0.78	-0.61	-0.66	-0.59	-0.57	-0.50	-0.42	0.29
	0.31	0.14	0.37	0.37	0.28	0.15	0.22	0.09	-0.24	-0.43	-0.24	-0.24
17	-0.05	0.66	0.09	-0.54	-1.72	-1.58	-0.92	-0.58	-0.70	-0.54	-0.82	0.74
	0.36	0.52	0.74	0.95	0.15	0.15	-0.10	-0.10	-0.60	-0.61	-1.13	-0.90
	-0.56	-0.25	-0.25	-0.79	-1.07	-0.89	-0.70	-0.70	-0.71	-0.95	-0.62	-0.60
	-0.12	0.31	0.15	0.00	0.09	-0.01	0.06	-0.01	0.01	-0.42	-0.60	-0.56

18	-0.56	-0.18	0.06	0.10	-0.62	-1.13	-1.00	-0.73	-0.67	-0.73	-0.63	-0.56
	0.27	0.20	0.27	0.44	0.59	0.38	0.22	0.29	-0.09	-0.54	-0.67	-1.21
	-0.42	-0.42	0.25	0.16	-0.49	-1.25	-1.49	-1.07	-0.76	-0.69	-0.62	-0.72
	-0.49	0.00	0.44	0.36	0.54	-0.21	-0.21	-0.10	-0.09	-0.25	-0.48	-0.83
19	-0.92	-0.85	-0.44	-0.11	-0.23	-0.86	-1.09	-1.03	-0.80	-0.74	-0.76	-0.74
	-0.71	-0.54	-0.11	0.00	0.06	0.07	-0.04	-0.10	-0.22	-0.16	-0.41	-0.67
	-0.82	-0.89	-0.53	-0.18	-0.11	-0.43	-0.98	-1.15	-0.87	-0.73	-0.79	-0.69
	-0.74	-0.63	-0.37	0.16	-0.06	0.35	0.06	-0.23	-0.06	-0.09	-0.30	-0.50
20	-0.72	-0.92	-0.66	-0.19	0.20	0.08	-0.61	-1.52	-1.21	-0.86	-0.75	-0.72
	-0.70	-0.71	-0.60	-0.19	0.02	0.21	-0.06	-0.21	-0.14	-0.01	-0.41	-0.51
	-0.71	-0.84	-0.83	-0.65	-0.45	-0.29	-0.40	-0.82	-0.90	-0.80	-0.70	-0.67
	-0.68	-0.61	-0.66	-0.58	-0.18	0.01	0.07	-0.10	-0.24	-0.13	-0.15	-0.23
21	-0.42	-0.46	-0.60	-0.46	-0.12	0.14	0.29	-0.36	-1.07	-1.19	-0.79	-0.68
	-0.65	-0.63	-0.61	-0.49	0.02	0.21	0.27	0.26	0.05	0.04	-0.08	-0.25
	-0.36	-0.48	-0.62	-0.70	-0.37	-0.09	0.18	-0.21	-0.82	-1.13	-0.95	-0.68
	-0.61	-0.66	-0.69	-0.58	-0.50	-0.10	0.18	0.13	0.00	-0.14	-0.26	-0.13
22	-0.30	-0.34	-0.47	-0.51	-0.43	-0.35	0.01	0.27	-0.01	-0.93	-0.92	-0.75
	-0.65	-0.67	-0.56	-0.63	-0.51	-0.42	0.13	0.14	0.10	-0.05	-0.08	-0.14
	-0.18	-0.34	-0.39	-0.47	-0.55	-0.55	-0.40	-0.09	-0.12	-0.43	-0.63	-0.72
	-0.67	-0.56	-0.58	-0.65	-0.52	-0.53	-0.44	0.07	0.08	-0.06	-0.18	-0.08
23	-0.07	-0.30	-0.22	-0.18	-0.33	-0.26	-0.22	0.11	0.15	0.10	-0.41	-0.84
	-0.89	-0.69	-0.63	-0.61	-0.59	-0.52	-0.43	-0.02	0.09	0.12	-0.07	-0.14
	-0.18	-0.13	-0.25	-0.29	-0.29	-0.29	-0.29	-0.29	-0.08	-0.07	-0.28	-0.53
	-0.85	-0.65	-0.63	-0.61	-0.59	-0.56	-0.53	-0.45	-0.10	0.15	0.00	-0.18
24	-0.18	-0.21	-0.06	-0.21	-0.08	-0.12	-0.15	-0.06	-0.05	0.15	0.19	-0.24
	-0.59	-0.97	-0.87	-0.67	-0.61	-0.55	-0.61	-0.59	-0.23	-0.01	0.06	0.02
	-0.13	-0.21	-0.25	-0.28	-0.28	-0.13	-0.20	-0.20	-0.16	-0.07	-0.14	-0.27
	-0.27	-0.51	-0.71	-0.68	-0.61	-0.60	-0.53	-0.60	-0.47	-0.28	-0.04	0.05
25	-0.04	-0.13	-0.16	-0.16	-0.16	-0.16	-0.03	0.02	-0.01	0.14	0.18	0.17
	-0.01	-0.28	-0.64	-0.94	-0.87	-0.70	-0.63	-0.61	-0.54	-0.47	-0.39	-0.17
	0.00	-0.09	-0.21	-0.24	-0.28	-0.16	-0.16	-0.08	-0.08	-0.03	-0.06	-0.13
	-0.08	-0.12	-0.29	-0.46	-0.58	-0.70	-0.59	-0.60	-0.54	-0.56	-0.49	-0.35
26	-0.21	0.06	0.00	-0.04	-0.12	-0.23	-0.11	-0.15	-0.07	0.06	-0.09	0.01
	0.03	0.00	-0.18	-0.23	-0.38	-0.65	-0.83	-0.73	-0.70	-0.52	-0.63	-0.57
	-0.44	-0.45	-0.16	0.11	-0.04	-0.16	-0.12	-0.16	-0.12	-0.04	0.01	0.06
	-0.04	-0.12	-0.07	-0.01	-0.14	-0.28	-0.42	-0.59	-0.82	-0.73	-0.63	-0.56
27	-0.54	-0.52	-0.34	-0.12	-0.10	-0.09	-0.11	-0.12	-0.13	-0.09	-0.04	-0.07
	0.02	-0.05	-0.14	-0.13	-0.13	-0.13	-0.32	-0.42	-0.77	-0.85	-0.72	-0.62
	-0.56	-0.63	-0.57	-0.50	-0.41	-0.05	0.21	0.01	-0.03	-0.03	-0.03	-0.02
	0.03	0.00	-0.07	-0.19	-0.24	-0.10	-0.05	-0.09	-0.28	-0.55	-0.87	-0.76
28	-0.61	-0.63	-0.53	-0.51	-0.47	-0.10	0.28	0.29	-0.10	0.43	0.10	0.09
	0.11	0.09	-0.16	-0.26	-0.32	-0.37	-0.42	-0.07	-0.27	-0.37	-0.77	-0.89
	-0.72	-0.61	-0.60	-0.54	-0.61	-0.54	-0.45	0.06	0.43	0.17	0.09	0.14
	0.13	0.25	0.06	0.08	-0.17	-0.32	-0.42	-0.27	-0.22	0.03	-0.17	-0.56
29	-1.02	-0.84	-0.64	-0.58	-0.60	-0.54	-0.52	-0.10	0.48	0.25	0.27	0.44
	0.30	0.34	0.28	0.06	-0.07	-0.53	-0.70	-0.59	-0.52	-0.07	-0.22	-0.47
	-0.86	-0.93	-0.68	-0.53	-0.63	-0.58	-0.61	-0.59	-0.40	0.44	0.39	0.21
	0.22	0.26	0.32	0.39	0.32	0.10	-0.33	-0.70	-0.65	-0.42	0.04	0.12
30	-0.15	-0.87	-1.16	-0.84	-0.60	-0.57	-0.59	-0.58	-0.61	0.22	0.46	0.26
	0.41	0.22	0.70	0.39	0.33	0.13	-0.52	-0.92	-1.00	-0.80	-0.45	-0.14

	-0.18	-0.53	-0.84	-0.79	-0.61	-0.51	-0.62	-0.56	-0.54	-0.62	-0.42	0.68
	0.48	0.17	0.23	0.26	0.36	0.40	0.32	-0.14	-0.74	-0.87	-0.77	-0.36
31	0.03	0.14	-0.41	-0.71	-1.00	-0.64	-0.58	-0.56	-0.59	-0.62	-0.39	0.71
	0.37	0.34	0.54	0.69	0.63	0.65	0.39	-0.25	-0.70	-1.24	-1.05	-0.90
	-0.27	0.06	-0.22	-0.72	-0.97	-0.71	-0.57	-0.59	-0.62	-0.56	-0.59	-0.62
	0.57	0.60	0.25	0.45	0.59	0.67	0.55	0.58	0.13	-0.64	-1.10	-0.97
February 1991												
1	-0.82	0.04	0.15	0.22	-0.95	-1.15	-0.88	-0.67	-0.57	-0.58	-0.57	-0.55
	0.08	0.54	0.34	0.52	0.82	0.69	0.78	0.45	0.14	-0.49	-0.95	-1.36
	-1.15	-0.74	-0.08	-0.07	-0.26	-0.93	-0.91	-0.60	-0.57	-0.59	-0.57	-0.61
	-0.54	-0.18	0.82	0.33	0.31	0.46	0.53	0.54	0.59	0.20	-0.32	-0.97
2	-1.07	-0.82	-0.45	0.07	0.30	-0.15	-1.15	-1.02	-0.67	-0.56	-0.61	-0.56
	-0.58	-0.42	0.56	0.41	0.36	0.42	0.58	0.43	0.59	0.27	-0.51	-0.84
	-1.01	-1.06	-0.78	-0.18	0.03	-0.13	-0.65	-0.91	-0.63	-0.57	-0.56	-0.54
	-0.61	-0.54	-0.51	0.66	0.40	0.22	0.27	0.27	0.63	0.10	0.28	-0.42
3	-0.79	-0.79	-0.66	-0.47	0.11	0.18	0.17	-0.82	-1.01	-0.66	-0.60	-0.54
	-0.56	-0.58	-0.57	0.29	0.52	0.26	0.25	0.39	0.48	0.38	0.22	-0.26
	-0.65	-0.85	-0.83	-0.73	-0.39	-0.02	0.03	-0.43	-0.79	-0.74	-0.57	-0.59
	-0.58	-0.56	-0.59	-0.51	0.34	0.48	0.22	0.19	0.25	0.25	0.20	0.20
4	-0.16	-0.41	-0.56	-0.67	-0.39	0.08	0.11	0.13	-0.74	-0.99	-0.79	-0.60
	-0.58	-0.56	-0.58	-0.57	0.24	0.12	0.22	0.18	0.20	0.20	0.10	0.07
	-0.16	-0.41	-0.49	-0.53	-0.52	-0.35	0.02	0.03	-0.35	-0.76	-0.82	-0.61
	-0.55	-0.62	-0.61	-0.54	-0.56	-0.12	0.54	0.28	0.06	0.03	0.07	0.01
5	-0.11	-0.14	-0.31	-0.35	-0.35	-0.27	-0.03	0.11	0.12	-0.40	-0.78	-0.87
	-0.68	-0.58	-0.60	-0.55	-0.57	-0.23	0.37	0.23	0.14	0.11	0.00	0.02
	-0.06	-0.22	-0.35	-0.35	-0.39	-0.47	-0.28	-0.08	-0.03	-0.19	-0.55	-0.71
	-0.68	-0.59	-0.58	-0.56	-0.59	-0.45	-0.07	0.21	0.12	0.11	0.02	-0.01
6	-0.08	-0.12	-0.16	-0.19	-0.19	-0.19	-0.15	0.02	0.12	0.15	-0.21	-0.63
	-0.81	-0.79	-0.64	-0.58	-0.56	-0.49	-0.32	0.09	0.11	0.18	0.03	-0.04
	-0.11	-0.07	-0.23	-0.39	-0.31	-0.23	-0.35	-0.20	0.00	0.02	-0.06	-0.44
	-0.67	-0.63	-0.64	-0.58	-0.66	-0.51	-0.48	-0.39	-0.08	0.19	0.03	-0.13
7	-0.09	-0.21	-0.25	-0.17	-0.13	-0.17	-0.05	0.00	0.09	0.06	0.04	-0.17
	-0.39	-0.64	-0.67	-0.63	-0.61	-0.50	-0.43	-0.35	-0.22	-0.13	-0.01	-0.01
	-0.17	-0.25	-0.17	-0.21	-0.21	-0.05	-0.08	-0.04	0.01	0.02	0.13	0.06
	-0.12	-0.49	-0.57	-0.68	-0.66	-0.51	-0.48	-0.37	-0.25	-0.09	-0.01	0.00
8	0.00	-0.27	-0.19	-0.19	-0.11	-0.10	-0.02	0.04	0.05	0.07	0.09	0.00
	-0.30	-0.30	-0.50	-0.84	-0.67	-0.62	-0.51	-0.52	-0.45	-0.33	-0.30	-0.21
	-0.21	-0.25	-0.29	-0.30	-0.25	-0.21	-0.17	-0.01	0.07	0.12	0.05	0.11
	0.04	-0.17	-0.34	-0.43	-0.30	-0.59	-0.46	-0.47	-0.40	-0.36	-0.28	-0.24
9	-0.20	-0.08	-0.20	-0.12	-0.23	-0.11	-0.11	-0.07	-0.06	0.03	0.00	0.10
	0.03	-0.11	-0.20	-0.30	-0.39	-0.43	-0.42	-0.50	-0.46	-0.50	-0.39	-0.31
	-0.27	-0.28	-0.16	-0.12	-0.15	-0.19	-0.15	-0.15	-0.15	-0.02	0.03	0.04
	0.15	0.03	-0.15	-0.10	-0.05	-0.20	-0.30	-0.40	-0.53	-0.64	-0.54	-0.53
10	-0.46	-0.35	-0.23	-0.23	-0.04	-0.03	-0.14	-0.22	-0.22	-0.18	-0.10	-0.10
	-0.01	0.00	-0.16	-0.16	-0.25	-0.21	-0.16	-0.29	-0.42	-0.50	-0.65	-0.46
	-0.55	-0.44	-0.46	-0.29	-0.25	-0.04	0.08	0.00	-0.07	-0.15	-0.15	-0.07
	-0.06	-0.02	-0.09	-0.13	-0.04	-0.07	-0.07	-0.16	-0.20	-0.34	-0.59	-0.65
11	-0.61	-0.58	-0.47	-0.45	-0.33	-0.07	0.09	0.16	0.05	-0.06	-0.09	-0.05
	-0.17	-0.12	-0.08	-0.20	-0.20	-0.12	-0.12	-0.16	-0.25	-0.25	-0.50	-0.65
	-0.65	-0.58	-0.56	-0.54	-0.57	-0.30	-0.11	0.20	0.21	0.05	0.13	0.02

	0.03	0.00	0.01	-0.02	-0.11	0.04	0.06	0.12	0.03	-0.08	-0.45	-0.65
12	-0.89	-0.79	-0.69	-0.66	-0.52	-0.45	-0.33	0.05	0.24	0.12	0.18	0.08
	0.05	0.02	-0.15	-0.06	-0.20	-0.34	-0.29	-0.29	-0.11	-0.20	-0.16	-0.42
	-0.59	-0.81	-0.65	-0.55	-0.54	-0.61	-0.55	-0.21	0.35	0.29	0.20	0.17
	0.19	0.05	0.07	0.04	-0.20	-0.20	-0.20	-0.20	-0.20	0.05	0.01	-0.02
13	-0.75	-0.84	-0.90	-0.69	-0.59	-0.57	-0.60	-0.44	0.07	0.42	0.24	0.17
	0.19	0.05	-0.07	-0.25	-0.25	-0.29	-0.34	-0.50	-0.38	-0.34	-0.10	-0.13
	-0.38	-0.61	-0.66	-0.60	-0.64	-0.54	-0.57	-0.60	-0.51	0.19	0.56	0.34
	0.08	0.20	0.14	0.08	0.10	-0.11	-0.25	-0.47	-0.38	-0.33	-0.09	0.09
14	0.07	-0.39	-0.76	-0.85	-0.70	-0.48	-0.63	-0.62	-0.56	-0.11	0.63	0.31
	0.24	0.35	0.42	0.20	0.24	-0.08	-0.29	-0.57	-0.70	-0.66	-0.47	-0.17
	-0.04	-0.25	-0.63	-0.85	-0.63	-0.61	-0.55	-0.59	-0.62	-0.55	0.01	0.64
	0.40	0.16	0.29	0.21	0.30	0.26	0.03	-0.19	-0.47	-0.55	-0.48	-0.07
15	0.19	0.15	-0.25	-1.05	-0.98	-0.74	-0.63	-0.57	-0.55	-0.48	0.26	0.31
	0.35	0.49	0.66	0.72	0.40	0.40	-0.05	-0.50	-0.63	-1.11	-0.83	-0.66
	-0.40	-0.21	-0.35	-0.65	-0.94	-0.55	-0.68	-0.55	-0.53	-0.60	-0.48	0.58
	0.43	0.27	0.42	0.61	0.72	0.53	0.59	0.33	-0.30	-0.56	-0.83	-0.66
16	-0.01	0.19	0.38	-0.45	-1.64	-1.54	-0.91	-0.68	-0.61	-0.62	-0.57	-0.24
	0.48	0.29	0.61	0.84	0.61	0.58	0.32	0.06	-0.44	-0.70	-1.37	-0.80
	-0.73	-0.12	0.14	-0.06	-1.03	-1.15	-0.80	-0.53	-0.67	-0.57	-0.60	-0.53
	-0.40	0.60	0.32	0.25	0.33	0.31	0.39	0.10	-0.21	-0.48	-0.62	-0.80
17	-0.71	-0.45	0.09	0.16	-0.04	-0.85	-0.93	-0.65	-0.62	-0.61	-0.55	-0.57
	-0.45	0.61	0.36	0.33	0.43	0.59	0.58	0.52	0.06	-0.39	-0.86	-0.92
	-0.88	-0.99	-0.07	-0.02	-0.10	-0.59	-0.97	-0.68	-0.62	-0.61	-0.59	-0.57
	-0.55	-0.30	0.50	0.57	0.21	0.33	0.36	0.44	0.38	0.05	-0.34	-0.44
18	-1.17	-0.73	-0.40	0.10	0.43	0.12	-1.12	-1.12	-0.71	-0.63	-0.57	-0.56
	-0.58	-0.42	0.27	0.66	0.36	0.51	0.59	0.44	0.53	0.07	-0.38	-0.58
	-1.02	-0.97	-0.76	-0.31	0.00	-0.13	-0.70	-0.83	-0.67	-0.61	-0.59	-0.58
	-0.56	-0.54	-0.39	0.67	0.35	0.18	0.24	0.28	0.29	0.25	0.12	-0.29
19	-0.52	-0.59	-0.65	-0.33	0.11	0.28	0.06	-0.69	-1.11	-0.77	-0.57	-0.55
	-0.53	-0.56	-0.49	0.38	0.41	0.32	0.40	0.44	0.42	0.47	0.22	-0.24
	-0.50	-0.58	-0.90	-0.76	-0.33	0.02	0.09	-0.48	-0.81	-0.85	-0.65	-0.51
	-0.53	-0.56	-0.59	-0.31	0.53	0.41	0.24	0.31	0.32	0.34	0.22	0.19
20	0.00	-0.51	-0.50	-0.49	-0.18	0.17	0.47	0.16	-0.74	-1.40	-1.05	-0.64
	-0.57	-0.54	-0.56	-0.45	0.19	0.37	0.30	0.42	0.36	0.42	0.30	0.27
	-0.04	-0.37	-0.43	-0.66	-0.56	-0.13	0.15	0.20	-0.23	-0.98	-1.16	-0.81
	-0.68	-0.50	-0.51	-0.53	-0.37	0.24	0.29	0.21	0.27	0.27	0.13	0.14
21	-0.04	-0.09	-0.25	-0.35	-0.40	-0.20	0.11	0.34	0.16	-0.36	-1.16	-1.07
	-0.82	-0.62	-0.55	-0.53	-0.50	-0.25	0.21	0.27	0.24	0.28	0.19	0.13
	0.16	0.13	0.02	-0.13	-0.19	-0.01	0.07	-0.05	0.14	0.27	-0.63	-1.67
	-1.19	-0.71	-0.70	-0.54	-0.44	-0.36	0.04	0.12	0.17	0.06	0.17	-0.07
22	-0.15	-0.20	-0.29	-0.24	-0.14	-0.03	-0.28	-0.28	0.00	-0.06	-0.16	-0.64
	-1.45	-0.85	-0.79	-0.65	-0.70	-0.61	-0.49	-0.28	-0.15	-0.07	0.01	-0.06
	-0.13	-0.16	-0.07	0.04	-0.02	0.15	0.07	0.15	0.16	0.26	0.00	0.01
	-0.57	-1.24	-1.07	-0.97	-0.87	-0.72	-0.52	-0.44	-0.17	-0.09	-0.03	-0.22
23	-0.42	-0.42	-0.47	-0.38	-0.34	-0.20	-0.18	-0.21	-0.30	-0.30	-0.40	-0.55
	-0.55	-0.60	-0.95	-0.68	-0.80	-0.77	-0.70	-0.64	-0.69	-0.49	-0.45	-0.37
	-0.40	-0.24	-0.39	-0.35	-0.34	-0.38	-0.05	-0.10	-0.16	-0.23	-0.17	-0.25
	-0.45	-0.45	-0.50	-0.69	-0.73	-0.64	-0.76	-0.80	-0.54	-0.66	-0.43	-0.27
24	-0.23	-0.14	-0.17	-0.28	-0.28	-0.28	-0.23	-0.04	0.03	0.08	-0.10	-0.06

-0.15 -0.31 -0.37 -0.42 -0.48 -1.04 -0.94 -0.81 -0.81 -0.66 -0.59 -0.60
-0.57 -0.50 -0.33 -0.29 -0.29 -0.32 -0.24 -0.24 -0.19 -0.18 -0.17 -
March 1991
4 - - - - - - - - - - - -0.62
-1.15 -1.07 -0.79 -0.26 0.15 0.33 -0.31 -1.24 -1.23 -0.67 -0.59 -0.56
-0.50 -0.51 -0.09 0.42 0.23 0.34 0.56 0.63 0.60 0.33 0.14 -0.52
5 -0.59 -0.80 -1.01 -0.17 -0.11 0.26 -0.10 -0.44 -1.81 -0.86 -0.61 -0.58
-0.35 -0.73 -0.46 0.05 0.28 0.12 0.27 0.37 0.26 0.22 0.10 -0.10
-0.60 -0.60 -0.73 -0.56 -0.24 -0.01 -0.04 -0.28 -0.91 -0.94 -0.61 -0.59
-0.52 -0.54 -0.56 -0.16 0.22 0.31 0.25 0.21 0.35 0.23 0.26 -0.11
6 -0.27 -0.27 -0.54 -0.33 -0.12 0.19 0.32 -0.06 -1.11 -1.28 -1.30 -0.84
-0.68 -0.61 -0.63 -0.35 0.05 0.17 0.34 0.44 0.17 0.04 -0.22 -0.11
-0.33 -0.38 -0.59 -0.28 -0.44 0.04 0.35 0.52 -0.65 -1.36 -1.10 -1.13
-0.76 -0.64 -0.57 -0.50 0.05 0.10 0.17 0.46 0.32 0.15 0.03 -0.14
7 -0.40 -0.40 -0.27 -0.40 -0.33 0.00 0.13 0.13 -0.19 -0.89 -1.51 -1.53
-1.13 -0.84 -0.68 -0.65 -0.46 -0.23 -0.10 0.13 0.10 -0.28 -0.27 -0.42
-0.37 -0.37 -0.37 -0.32 -0.17 -0.11 0.19 -0.01 0.07 -0.20 -0.86 -1.24
-1.08 -0.85 -0.80 -0.61 -0.49 -0.38 -0.06 0.01 0.15 -0.03 -0.21 -0.58
8 -0.38 -0.27 -0.16 -0.88 -0.38 -0.07 0.06 -0.29 -0.40 -0.09 -0.39 -0.92
-1.33 -1.07 -0.75 -0.55 -0.55 -0.47 -0.18 -0.25 -0.14 -0.01 -0.12 -0.19
-0.41 -0.36 -0.30 0.10 -0.40 -0.40 0.13 0.33 0.21 -0.49 -0.36 -0.43
-1.21 -1.24 -0.84 -0.85 -0.83 -0.67 -0.39 -0.34 -0.19 -0.27 -0.27 -0.69
9 -0.75 -0.80 -0.65 -0.50 -0.44 -0.31 -0.41 -0.19 -0.34 -0.46 -0.59 -0.79
-1.06 -0.89 -1.22 -1.10 -0.90 -0.95 -0.69 -0.78 -0.74 -0.70 -0.61 -0.65
-0.65 -0.69 -0.69 -0.69 -0.64 -0.41 -0.43 -0.51 -0.34 -0.31 -0.41 -0.62
-0.73 -0.89 -0.89 -0.95 -0.90 -0.81 -0.95 -0.87 -0.79 -0.71 -0.66 -0.82
10 -0.82 -0.86 -0.82 -0.90 -0.74 -0.73 -0.59 -0.48 -0.54 -0.57 -0.60 -0.64
-0.74 -0.85 -0.80 -0.75 -0.91 -0.86 -0.81 -1.01 -0.87 -0.92 -1.02 -0.90
-0.73 -0.81 -0.90 -0.81 -0.81 -0.77 -0.72 -0.72 -0.53 -0.45 -0.51 -0.70
-0.49 -0.52 -0.78 -0.73 -0.89 -0.91 -0.90 -1.01 -1.10 -1.01 -0.93 -0.67
11 -0.63 -0.55 -0.55 -0.59 -0.51 -0.55 -0.46 -0.54 -0.50 -0.41 -0.45 -0.40
-0.48 -0.43 -0.52 -0.52 -0.61 -0.52 -0.66 -0.71 -0.71 -0.84 -0.76 -0.77
-0.66 -0.70 -0.63 -0.51 -0.47 -0.42 -0.45 -0.40 -0.52 -0.35 -0.38 -0.41
-0.26 -0.33 -0.27 -0.35 -0.29 -0.33 -0.33 -0.54 -0.59 -1.16 -0.89 -0.87
12 -0.70 -0.62 -0.59 -0.48 -0.32 -0.07 -0.17 -0.33 -0.28 -0.27 -0.26 -0.35
-0.30 -0.20 -0.34 -0.28 -0.38 -0.48 -0.43 -0.39 -0.48 -0.76 -0.79 -0.82
-0.75 -0.68 -0.65 -0.50 -0.58 -0.34 -0.10 -0.05 -0.15 -0.21 -0.24 -0.27
-0.22 -0.16 -0.14 -0.28 -0.22 -0.27 -0.26 -0.21 -0.37 -0.42 -0.78 -0.95
13 -0.86 -0.84 -0.69 -0.54 -0.55 -0.44 -0.04 0.09 0.04 0.04 -0.16 -0.15
-0.24 -0.23 -0.23 -0.28 -0.38 -0.43 -0.43 -0.43 -0.38 -0.43 -0.52 -0.86
-0.88 -0.69 -0.66 -0.60 -0.53 -0.54 -0.46 -0.04 0.04 0.13 0.05 -0.05
-0.12 -0.20 -0.09 -0.23 -0.17 -0.48 -0.48 -0.28 -0.07 -0.27 -0.21 -0.60
14 -1.11 -0.91 -0.73 -0.66 -0.60 -0.62 -0.46 -0.09 0.07 0.24 0.21 0.19
-0.11 0.05 -0.03 -0.18 -0.45 -0.56 -0.50 -0.60 -0.45 -0.22 -0.26 -0.59
-0.84 -0.86 -0.70 -0.63 -0.61 -0.58 -0.51 -0.52 -0.04 0.19 0.23 0.11
0.16 0.07 0.05 -0.03 -0.13 -0.34 -0.56 -0.55 -0.51 -0.15 0.01 -0.11
15 -0.60 -1.15 -0.97 -0.71 -0.60 -0.61 -0.59 -0.52 -0.19 0.25 0.30 0.37
0.43 0.37 0.27 0.26 -0.25 -0.25 -0.65 -0.89 -0.80 -0.64 -0.13 -0.13
-0.38 -0.87 -1.07 -0.79 -0.64 -0.58 -0.59 -0.56 -0.49 0.02 0.25 0.30
0.33 0.43 0.42 0.36 0.26 -0.19 -0.32 -0.78 -0.94 -0.32 -0.64 -0.05

16	0.07	-0.54	-1.29	-1.18	-0.85	-0.73	-0.63	-0.68	-0.62	-0.37	0.27	0.25
	0.45	0.63	0.54	0.55	0.35	-0.03	-0.34	-0.73	-1.13	-1.22	-0.79	-0.27
	-0.21	-0.43	-0.94	-1.19	-0.89	-0.73	-0.63	-0.64	-0.61	-0.59	-0.04	0.31
	0.31	0.46	0.49	0.46	0.42	0.35	0.10	-0.47	-0.86	-1.20	-0.76	-0.31
17	0.03	-0.03	-0.68	-1.68	-1.66	-1.09	-0.88	-0.81	-0.79	-0.72	-0.57	0.07
	0.24	0.59	0.57	0.61	0.42	0.11	-0.07	-0.57	-1.01	-1.36	-1.40	-1.11
	-0.45	-0.24	-0.56	-1.12	-1.44	-1.04	-0.85	-0.74	-0.80	-0.73	-0.70	-0.63
	0.10	0.17	0.14	0.31	0.23	0.16	0.16	-0.29	-0.54	-1.07	-1.29	-1.27
18	-0.62	-0.17	-0.07	-0.66	-1.32	-1.32	-0.94	-0.83	-0.80	-0.82	-0.75	-0.76
	-0.31	0.10	0.27	0.30	0.42	0.24	0.18	-0.07	-0.51	-0.89	-1.30	-1.53
	-1.22	-0.57	0.04	-0.34	-0.83	-1.43	-1.19	-0.86	-0.79	-0.84	-0.82	-0.75
	-0.55	0.17	0.30	0.57	0.42	0.18	0.25	0.06	-0.18	-0.62	-0.94	-1.69
19	-1.40	-0.89	-0.20	-0.11	-0.74	-1.15	-1.58	-1.04	-0.88	-0.85	-0.86	-0.80
	-0.73	-0.53	0.03	0.15	0.14	0.08	0.11	0.10	-0.03	-0.41	-0.80	-1.27
	-1.33	-1.25	-0.60	-0.36	-0.44	-0.79	-1.23	-1.16	-0.85	-0.91	-0.84	-0.78
	-0.75	-0.67	-0.06	0.01	0.19	0.20	-0.10	-0.11	0.09	-0.09	-0.54	-0.70
20	-1.17	-1.01	-0.75	0.16	0.11	-0.58	-1.15	-1.65	-1.08	-0.91	-0.83	-0.73
	-0.70	-0.79	-0.56	0.12	0.20	0.34	0.16	0.01	0.27	0.08	-0.17	-0.62
	-0.82	-1.36	-0.98	-0.68	0.13	0.20	-0.64	-1.33	-1.65	-1.13	-0.91	-0.79
	-0.80	-0.70	-0.67	-0.11	0.09	0.29	0.22	-0.04	0.00	-0.19	-0.25	-0.44
21	-0.64	-0.91	-0.88	-0.91	-0.26	0.02	-0.12	-0.88	-1.41	-1.12	-0.78	-0.75
	-0.68	-0.70	-0.67	-0.60	-0.23	0.09	0.14	0.08	-0.14	-0.06	0.03	-0.02
	-0.21	-0.63	-0.61	-0.72	-0.41	0.08	0.04	-0.25	-0.79	-1.58	-1.28	-0.86
	-0.79	-0.72	-0.69	-0.62	-0.26	-0.02	0.23	0.24	-0.01	-0.13	-0.19	-0.18
22	-0.35	-0.40	-0.51	-0.46	-0.51	-0.14	0.21	0.12	-0.66	-1.18	-1.40	-1.02
	-0.73	-0.69	-0.62	-0.68	-0.61	-0.49	-0.17	0.00	0.02	-0.16	-0.18	-0.12
	-0.29	-0.24	-0.23	-0.32	-0.42	-0.37	-0.17	0.25	0.09	-0.40	-0.78	-1.38
	-1.03	-0.84	-0.65	-0.70	-0.60	-0.52	-0.28	0.00	0.10	-0.02	-0.34	-0.17
23	-0.30	-0.29	-0.34	-0.29	-0.24	-0.24	-0.19	0.03	0.06	-0.15	-0.58	-1.03
	-1.10	-0.84	-0.69	-0.62	-0.63	-0.60	-0.57	-0.46	-0.20	-0.16	-0.16	-0.31
	-0.27	-0.34	-0.26	-0.22	-0.13	-0.15	-0.23	-0.04	0.03	0.02	-0.07	-0.49
	-0.58	-1.03	-0.93	-0.72	-0.65	-0.62	-0.60	-0.49	-0.45	-0.16	-0.16	-0.20
24	-0.24	-0.35	-0.31	-0.31	-0.23	-0.15	-0.14	-0.17	-0.11	-0.01	-0.08	-0.31
	-0.41	-0.64	-0.88	-0.74	-0.66	-0.68	-0.62	-0.55	-0.51	-0.52	-0.35	-0.26
	-0.17	-0.34	-0.34	-0.30	-0.25	-0.17	-0.09	-0.16	-0.07	0.04	0.03	0.01
	-0.06	-0.41	-0.41	-0.55	-0.85	-0.70	-0.78	-0.63	-0.60	-0.58	-0.50	-0.41
25	-0.24	-0.11	-0.27	-0.39	-0.35	-0.35	-0.31	-0.27	-0.23	-0.19	-0.26	-0.18
	-0.21	-0.21	-0.24	-0.32	-0.52	-0.68	-0.65	-0.67	-0.53	-0.63	-0.56	-0.57
	-0.49	-0.34	-0.24	-0.10	-0.15	-0.24	-0.24	-0.15	-0.15	-0.19	-0.06	-0.05
	-0.08	-0.27	-0.27	-0.05	-0.08	-0.30	-0.35	-0.82	-0.80	-0.68	-0.66	-0.54
26	-0.55	-0.48	-0.36	-0.10	0.06	-0.02	-0.21	-0.24	-0.28	-0.24	-0.23	-0.19
	-0.23	-0.31	-0.26	-0.30	-0.26	-0.26	-0.30	-0.47	-0.67	-0.71	-0.61	-0.59
	-0.56	-0.58	-0.50	-0.56	-0.23	0.13	0.06	0.02	-0.05	-0.12	-0.11	-0.10
	-0.09	-0.12	-0.25	-0.29	-0.24	-0.29	-0.15	-0.14	-0.47	-0.69	-0.96	-0.67
27	-0.68	-0.58	-0.55	-0.52	-0.44	-0.18	0.15	0.10	0.12	-0.06	-0.09	-0.12
	-0.11	-0.10	-0.24	-0.33	-0.38	-0.42	-0.38	-0.33	-0.33	-0.51	-0.87	-0.75
	-0.56	-0.62	-0.56	-0.57	-0.50	-0.55	-0.27	0.26	0.22	0.11	0.05	0.03
	0.06	0.00	-0.03	-0.22	-0.81	-0.51	-0.15	-0.29	-0.05	-0.14	-0.42	-0.94
28	-0.85	-0.69	-0.59	-0.56	-0.58	-0.51	-0.48	-0.03	0.25	0.16	0.22	0.01
	0.03	-0.04	-0.17	-0.31	-0.50	-0.54	-0.62	-0.57	-0.33	-0.17	-0.25	-0.53

	-0.81	-0.63	-0.57	-0.50	-0.56	-0.48	-0.54	-0.56	-0.05	0.49	0.16	0.13
	0.19	0.11	0.10	0.09	-0.26	-0.61	-0.59	-0.75	-0.53	-0.13	0.01	-0.13
29	-0.65	-0.91	-0.60	-0.61	-0.59	-0.49	-0.54	-0.51	-0.38	0.31	0.30	0.14
	0.20	0.20	0.06	0.04	-0.15	-0.55	-0.67	-0.73	-0.71	-0.52	-0.25	-0.13
	-0.44	-0.68	-0.62	-0.56	-0.58	-0.46	-0.47	-0.58	-0.44	-0.29	0.60	0.30
	0.14	0.20	0.20	0.21	0.26	-0.13	-0.55	-0.83	-0.74	-0.68	-0.40	-0.03
30	-0.02	-0.43	-0.83	-0.64	-0.61	-0.55	-0.57	-0.50	-0.56	-0.43	0.37	0.31
	0.22	0.25	0.25	0.27	0.32	0.14	-0.45	-0.89	-0.91	-0.73	-0.67	-0.16
	0.01	-0.27	-0.75	-0.71	-0.57	-0.58	-0.56	-0.54	-0.56	-0.48	-0.28	0.57
	0.41	0.19	0.32	0.35	0.32	0.31	-0.17	-0.57	-0.88	-0.83	-0.86	-0.39
31	0.11	0.05	-0.48	-0.85	-0.75	-0.72	-0.54	-0.56	-0.58	-0.56	-0.42	0.27
	0.38	0.22	0.25	0.40	0.36	0.24	0.17	-0.41	-0.77	-0.95	-0.84	-0.80
	-0.27	0.01	-0.18	-0.55	-0.79	-0.68	-0.54	-0.56	-0.58	-0.56	-0.48	-0.33
	0.53	0.30	0.38	0.15	0.33	0.36	0.13	0.05	-0.57	-0.72	-0.93	-0.78

April 1991

1	-0.39	-0.01	0.10	-0.30	-0.85	-0.86	-0.56	-0.65	-0.59	-0.53	-0.50	-0.51
	0.31	0.38	0.27	0.35	0.39	0.32	0.25	0.22	-0.16	-0.74	-0.87	-1.07
	-0.73	-0.26	0.08	-0.07	-0.52	-0.96	-0.78	-0.53	-0.54	-0.55	-0.58	-0.50
	-0.23	0.50	0.22	0.32	0.25	0.36	0.22	0.30	0.16	-0.42	-0.69	-0.90
2	-0.83	-0.36	-0.04	0.08	-0.05	-0.94	-1.07	-0.76	-0.57	-0.63	-0.56	-0.54
	-0.42	0.39	0.32	0.32	0.44	0.46	0.23	0.43	0.29	-0.03	-0.48	-0.75
	-0.93	-0.61	-0.04	0.27	0.22	-0.63	-1.20	-1.34	-0.77	-0.68	-0.57	-0.54
	-0.52	0.17	0.29	0.34	0.43	0.46	0.21	0.09	0.16	-0.03	-0.42	-0.60
3	-0.93	-0.77	-0.36	-0.03	0.21	-0.47	-1.15	-1.28	-0.87	-0.70	-0.59	-0.65
	-0.67	-0.52	0.11	0.18	0.25	0.32	0.07	0.00	-0.03	0.03	-0.23	-0.35
	-0.46	-0.72	-0.51	-0.05	0.28	0.09	-0.54	-1.04	-	-	-	-
8	-	-	-	-	-	-	-	-0.58	-0.63	-0.51	-0.47	-0.39
	-0.35	-0.43	-0.42	-0.38	-0.38	-0.42	-0.22	-0.16	-0.14	-0.07	-0.27	-0.12
	-0.20	-0.34	-0.39	-0.59	-0.73	-0.81	-0.80	-0.68	-0.72	-0.61	-0.58	-0.51
9	-0.36	-0.32	-0.36	-0.35	-0.39	-0.35	-0.31	-0.31	-0.31	-0.22	-0.26	-0.25
	-0.16	-0.28	-0.40	-0.36	-0.40	-0.57	-0.69	-0.62	-0.63	-0.56	-0.61	-0.49
	-0.50	-0.42	-0.33	-0.33	-0.25	-0.36	-0.32	-0.36	-0.32	-0.24	-0.19	-0.14
	-0.33	-0.21	-0.16	-0.23	-0.36	-0.31	-0.44	-0.57	-0.69	-0.69	-0.58	-0.56
10	-0.53	-0.46	-0.34	-0.21	-0.17	-0.21	-0.24	-0.31	-0.27	-0.27	-0.19	-0.22
	-0.17	-0.25	-0.20	-0.28	-0.24	-0.32	-0.37	-0.54	-0.70	-0.70	-0.63	-0.56
	-0.57	-0.55	-0.43	-0.34	-0.13	-0.05	-0.09	-0.08	-0.14	-0.22	-0.17	-0.16
	-0.06	-0.18	-0.22	-0.17	-0.16	-0.10	-0.25	-0.30	-0.81	-0.68	-0.92	-0.72
11	-0.61	-0.58	-0.51	-0.52	-0.40	-0.08	-0.08	0.05	-0.21	-0.17	-0.16	-0.28
	-0.19	-0.23	-0.18	-0.35	-0.40	-0.48	-0.36	-0.32	-0.44	-0.60	-0.65	-0.66
	-0.63	-0.53	-0.54	-0.50	-0.51	-0.24	0.01	0.08	0.01	0.06	-0.08	-0.10
	-0.09	-0.12	-0.11	-0.25	-0.30	-0.34	-0.25	-0.10	-0.24	-0.44	-0.68	-0.94
12	-0.74	-0.63	-0.56	-0.53	-0.54	-0.43	0.03	0.14	0.16	0.11	0.11	-0.05
	0.02	-0.07	-0.05	-0.21	-0.43	-0.57	-0.27	-0.27	-0.17	-0.27	-0.58	-0.97
	-0.91	-0.66	-0.55	-0.56	-0.58	-0.55	-0.30	0.11	0.22	0.29	0.31	0.25
	0.09	0.16	-0.08	-0.19	-0.49	-0.42	-0.42	-0.43	0.11	0.08	-0.26	-0.80
13	-1.32	-1.00	-0.65	-0.61	-0.63	-0.56	-0.49	-0.33	0.24	0.20	0.23	0.29
	0.11	0.20	0.06	-0.20	-0.46	-0.70	-0.75	-0.72	-0.49	-0.24	-0.16	-0.41
	-0.73	-0.81	-0.55	-0.60	-0.49	-0.51	-0.56	-0.44	-0.16	0.34	0.19	0.17
	0.26	0.23	0.19	0.07	-0.09	-0.57	-0.51	-0.61	-0.60	-0.14	0.07	0.20
14	-0.81	-1.07	-0.80	-0.64	-0.61	-0.55	-0.52	-0.45	-0.55	0.23	0.28	0.22

	0.35	0.29	0.26	0.07	-0.19	-0.45	-0.75	-0.83	-0.79	-0.68	-0.25	0.00
	-0.19	-0.72	-0.80	-0.58	-0.55	-0.53	-0.59	-0.47	-0.48	-0.39	0.47	0.29
	0.17	0.29	0.37	0.36	0.23	-0.18	-0.57	-0.86	-0.83	-0.78	-0.28	-0.12
15	0.11	-0.18	-0.37	-	-	-	-	-	-	-	-	-
30	-	-	-	-	-	-	-	-0.72	-0.65	-0.63	-0.61	-0.50
	-0.11	0.25	0.29	0.44	0.42	0.21	-0.17	-0.17	-0.38	-0.54	-0.56	-0.84
May 1991												
1	-0.95	-0.42	0.13	0.11	-0.69	-1.05	-1.16	-0.88	-0.78	-0.68	-0.69	-0.62
	-0.68	-0.55	0.02	0.00	0.01	-0.16	-0.22	-0.17	-0.28	-0.36	-0.54	-0.67
	-0.67	-0.67	-0.20	-0.01	0.13	-0.49	-1.03	-1.11	-0.77	-0.70	-0.72	-0.65
	-0.62	-0.59	-0.11	0.12	0.14	0.07	0.04	-0.11	-0.29	-0.39	-0.69	-0.59
2	-0.66	-0.56	-0.44	-0.08	0.14	-0.09	-0.70	-0.96	-0.61	-0.62	-0.60	-0.54
	-0.51	-0.57	-0.39	-0.01	0.19	0.17	-0.06	0.06	0.04	-0.11	-0.36	-0.36
	-0.40	-0.56	-0.45	-0.17	0.16	0.24	-0.22	-0.70	-0.96	-0.68	-0.62	-0.60
	-0.58	-0.56	-0.43	0.12	0.26	0.13	0.30	0.10	0.00	-0.12	-0.26	-0.45
3	-0.32	-0.53	-0.32	-0.32	0.01	0.07	-0.18	-0.62	-0.80	-0.76	-0.54	-0.60
	-0.54	-0.51	-0.53	-0.34	0.14	0.24	0.21	0.10	-0.01	-0.08	-0.03	-0.24
	-0.19	-0.36	-0.28	-0.24	0.01	0.16	0.35	-0.06	-0.72	-1.02	-0.84	-0.60
	-0.58	-0.56	-0.49	-0.42	0.11	0.29	0.17	0.23	-0.03	-0.15	-0.19	-0.26
4	-0.34	-0.34	-0.26	-0.34	-0.22	-0.02	-0.01	-0.13	-0.47	-0.71	-0.74	-0.56
	-0.53	-0.51	-0.49	-0.56	-0.32	-0.07	0.23	0.16	0.07	-0.08	-0.16	0.00
	-0.19	-0.23	-0.23	-0.15	0.02	0.03	0.23	0.32	-0.15	-0.55	-0.88	-0.87
	-0.66	-0.56	-0.49	-0.51	-0.39	-0.08	0.12	0.19	0.15	0.01	-0.22	-0.21
5	-0.13	-0.29	-0.21	-0.17	-0.25	-0.13	0.04	0.01	-0.16	-0.33	-0.62	-0.76
	-0.58	-0.51	-0.53	-0.51	-0.49	-0.36	-0.16	0.16	0.10	0.05	-0.15	-0.19
	-0.15	-0.19	-0.23	-0.07	-0.07	-0.02	0.19	0.18	0.31	0.27	-0.24	-0.65
	-0.83	-0.70	-0.69	-0.50	-0.51	-0.36	-0.24	0.05	0.16	0.13	0.07	-0.20
6	-0.16	-0.28	-0.20	-0.20	-0.16	-0.07	-0.07	0.02	0.03	-0.19	-0.32	-0.49
	-0.72	-0.63	-0.57	-0.46	-0.48	-0.45	-0.47	-0.24	0.00	0.08	0.06	-0.14
	-0.06	-0.18	-0.18	-0.14	-0.10	-0.01	0.11	0.08	0.10	0.31	0.22	-0.18
	-0.38	-0.65	-0.41	-0.89	-0.60	-0.53	-0.42	-0.30	-0.22	0.02	-0.02	-0.06
7	-0.21	-0.21	-0.21	-0.25	-0.18	-0.14	-0.10	-0.01	-0.01	0.04	-0.16	-0.28
	-0.20	-0.44	-0.60	-0.52	-0.46	-0.47	-0.48	-0.37	-0.33	-0.24	-0.02	-0.06
	-0.02	-0.06	-0.14	-0.10	-0.14	-0.06	0.02	0.07	0.09	0.15	0.22	0.16
	0.07	-0.29	-0.49	-0.62	-0.72	-0.69	-0.60	-0.49	-0.42	-0.39	-0.31	-0.23
8	-0.10	-0.10	-0.18	-0.22	-0.18	-0.22	-0.14	-0.06	-0.06	-0.10	0.02	-0.05
	-0.16	-0.24	-0.28	-0.25	-0.48	-0.49	-0.46	-0.47	-0.44	-0.45	-0.33	-0.33
	-0.15	0.07	0.06	-0.02	-0.06	-0.14	-0.10	-0.10	0.06	0.03	0.05	0.06
	0.22	0.10	-0.08	-0.13	-0.33	-0.38	-0.69	-0.70	-0.64	-0.56	-0.46	-0.47
9	-0.31	-0.23	-0.10	-0.02	-0.10	-0.18	-0.18	-0.18	-0.06	-0.13	-0.17	-0.21
	-0.13	-0.13	-0.25	-0.21	-0.25	-0.29	-0.37	-0.53	-0.50	-0.44	-0.50	-0.47
	-0.44	-0.30	-0.19	0.19	0.16	0.10	0.06	0.02	0.03	-0.05	-0.04	0.01
	0.02	0.03	0.00	0.00	0.07	-0.08	-0.38	-0.47	-0.81	-0.65	-0.67	-0.68
10	-0.38	-0.43	-0.26	-0.22	0.03	0.27	-0.05	0.11	-0.12	-0.08	-0.07	-0.07
	-0.23	-0.19	-0.23	-0.15	-0.19	-0.23	-0.27	-0.59	-0.55	-0.56	-0.50	-0.53
	-0.46	-0.38	-0.39	0.12	0.35	0.15	0.22	0.03	0.08	0.01	-0.10	-0.02
	-0.10	-0.18	0.00	-0.13	0.01	-0.03	-0.18	-0.46	-0.79	-0.79	-0.55	-0.52
11	-0.45	-0.47	-0.49	-0.32	0.10	0.25	0.19	0.08	0.04	0.05	0.02	-0.10
	-0.14	-0.14	-0.35	-0.18	-0.26	-0.14	-0.14	-0.26	-0.34	-0.74	-0.55	-0.49
	-0.46	-0.48	-0.56	-0.43	-0.17	0.40	0.33	0.15	0.27	0.21	0.16	0.09

	0.11	-0.02	-0.17	-0.27	-0.22	-0.12	0.08	-0.01	-0.32	-0.74	-0.94	-0.73
12	-0.46	-0.51	-0.49	-0.47	-0.49	-0.17	0.37	0.29	0.20	0.21	0.10	0.12
	0.01	-0.03	-0.12	-0.21	-0.35	-0.47	-0.42	-0.26	-0.02	-0.14	-0.38	-0.69
	-0.58	-0.48	-0.45	-0.47	-0.54	-0.47	-0.38	0.29	0.54	0.24	0.28	0.30
	0.25	0.25	0.19	-0.01	-0.36	-0.51	-0.49	-0.39	0.00	0.06	-0.12	-0.61
13	-0.86	-0.65	-0.46	-0.44	-0.49	-0.47	-0.50	-0.42	0.33	0.40	0.24	0.24
	0.26	0.21	0.29	0.19	-0.16	-0.41	-0.53	-0.51	-0.34	-0.09	0.09	-0.12
	-0.67	-0.77	-0.50	-0.51	-0.49	-0.42	-0.58	-0.42	-0.06	0.64	0.32	0.28
	0.39	0.41	0.38	0.38	0.01	-0.26	-0.52	-0.71	-0.67	-0.30	-0.04	0.06
14	-0.25	-0.72	-0.80	-0.53	-0.46	-0.48	-0.46	-0.48	-0.45	-0.16	0.74	0.29
	0.25	0.39	0.50	0.56	0.49	0.32	-0.14	-0.73	-0.83	-0.75	-0.25	0.08
	0.20	-0.45	-0.96	-0.81	-0.53	-0.46	-0.43	-0.49	-0.42	-0.49	0.35	0.38
	0.40	0.42	0.49	0.49	0.49	0.29	-0.01	-0.66	-0.94	-0.69	-0.65	-0.03
15	0.11	0.13	-0.65	-0.86	-0.60	-0.53	-0.42	-0.48	-0.41	-0.48	-0.50	0.30
	0.58	0.21	0.26	0.36	0.42	0.50	0.33	-0.19	-0.46	-0.76	-0.78	-0.53
	0.00	0.09	-0.03	-0.58	-0.80	-0.52	-0.54	-0.39	-0.50	-0.48	-0.50	-0.05
	0.75	0.33	0.30	0.49	0.48	0.61	0.48	0.26	-0.33	-0.81	-0.84	-0.68
16	-0.24	0.17	0.31	-0.30	-0.94	-0.93	-0.56	-0.49	-0.46	-0.44	-0.45	-0.48
	-0.35	0.76	0.30	0.30	0.36	0.36	0.43	0.51	0.20	-0.31	-0.61	-0.80
	-0.94	0.01	0.15	0.27	-0.10	-0.88	-0.85	-0.60	-0.45	-0.42	-0.44	-0.50
	-0.48	0.23	0.52	0.29	0.43	0.49	0.43	0.51	0.20	-0.07	-0.53	-0.73
17	-0.73	-0.50	-0.11	0.16	0.14	-0.52	-0.91	-0.63	-0.56	-0.46	-0.47	-0.50
	-0.48	-0.45	-0.20	0.67	0.35	0.18	0.30	0.29	0.38	0.34	0.16	-0.31
	-0.55	-0.61	-0.50	0.10	0.16	0.29	-0.39	-0.95	-0.80	-0.52	-0.49	-0.47
	-0.44	-0.51	-0.24	0.48	0.38	0.30	0.40	0.37	0.38	0.26	0.07	-0.24
18	-0.52	-0.60	-0.65	-0.37	0.06	0.07	-0.10	-0.67	-0.84	-0.59	-0.45	-0.47
	-0.49	-0.47	-0.50	-0.47	0.02	0.58	0.28	0.14	0.18	0.27	0.21	0.20
	0.18	-0.38	-0.42	-0.32	-0.15	0.11	0.27	0.15	-0.63	-0.96	-0.63	-0.48
	-0.53	-0.47	-0.44	-0.42	-0.14	0.43	0.30	0.22	0.27	0.22	0.11	0.18
19	-0.10	-0.14	-0.43	-0.37	-0.41	-0.19	0.02	-0.02	-0.19	-0.73	-0.71	-0.52
	-0.46	-0.43	-0.45	-0.52	-0.51	-0.42	0.19	0.48	0.20	0.07	0.14	0.15
	0.20	0.13	0.11	-0.10	-0.19	-0.19	0.07	0.28	0.32	-0.14	-0.70	-0.95
	-0.76	-0.55	-0.44	-0.42	-0.43	-0.40	-0.18	0.29	0.23	0.14	0.15	0.08
20	0.05	-0.07	-0.11	-0.06	-0.23	-0.23	-0.23	-0.11	-0.03	-0.02	-0.36	-0.64
	-0.63	-0.48	-0.50	-0.43	-0.45	-0.48	-0.45	-0.42	0.24	0.38	0.16	-0.39
26	-	-	-	-	-0.12	-0.28	-0.33	-0.21	0.05	0.52	0.16	-0.15
	0.09	0.06	-0.02	-0.14	-0.22	-0.30	-0.26	-0.26	-0.34	-0.07	-0.07	-0.11
	-0.54	-0.50	-0.44	-0.50	-0.39	-0.46	-0.33	0.13	0.50	0.36	0.24	0.29
	0.23	0.22	0.15	-0.13	-0.13	-0.41	-0.22	-0.40	-0.14	0.04	0.00	-0.35
27	-0.76	-0.57	-0.54	-0.44	-0.41	-0.43	-0.50	-0.43	-0.12	0.50	0.34	0.16
	0.12	0.17	0.22	0.03	-0.01	-0.18	-0.35	-0.34	-0.30	0.02	0.11	0.08
	-0.39	-0.66	-0.57	-0.43	-0.48	-0.37	-0.48	-0.46	-0.07	0.43	0.41	0.24
	0.37	0.32	0.32	0.26	0.03	-0.58	0.02	-0.46	-0.45	-0.13	0.09	0.15
28	-0.13	-0.72	-0.79	-0.61	-0.51	-0.36	-0.41	-0.43	-0.46	-0.22	0.34	0.30
	0.20	0.12	0.20	0.18	0.11	-0.05	-0.18	-0.35	-0.35	-0.30	-0.10	0.10
	0.16	-0.14	-0.60	-0.69	-0.54	-0.44	-0.41	-0.43	-0.40	-0.22	0.46	0.36
	0.28	0.41	0.37	0.38	0.23	0.04	-0.35	-0.43	-0.56	-0.44	-0.35	-0.01
29	0.08	-0.04	-0.56	-0.74	-0.53	-0.51	-0.40	-0.46	-0.49	-0.42	-0.22	0.28
	0.45	0.17	0.16	0.24	0.26	0.16	0.00	-0.22	-0.26	-0.34	-0.34	-0.10
	0.11	0.30	0.10	-0.58	-0.79	-0.57	-0.50	-0.44	-0.41	-0.43	-0.26	0.41

	0.36	0.32	0.38	0.43	0.40	0.28	-0.02	-0.33	-0.43	-0.42	-0.50	-0.39
30	-0.04	0.09	0.15	-0.58	-0.47	-0.88	-0.49	-0.43	-0.44	-0.42	-0.44	-0.31
	0.18	0.46	0.25	0.17	0.21	0.27	0.12	0.05	-0.21	-0.17	-0.38	-0.21
	-0.13	0.08	0.32	0.21	-0.50	-0.77	-0.77	-0.41	-0.50	-0.40	-0.41	-0.29
	0.24	0.45	0.29	0.38	0.43	0.35	0.29	0.04	-0.28	-0.37	-0.42	-0.49
31	-0.30	-0.04	0.06	0.11	-0.36	-0.89	-0.61	-0.45	-0.50	-0.39	-0.41	-0.43
	-0.30	0.17	0.36	0.29	0.13	0.22	0.23	0.17	0.01	-0.08	-0.21	-0.30
	-0.30	-0.04	0.13	0.29	0.23	-0.42	-0.84	-0.70	-0.60	-0.38	-0.47	-0.40
	-0.02	-0.07	0.37	0.33	0.35	0.43	0.30	0.19	0.05	-0.12	-0.37	-0.37
June 1991												
1	-0.36	-0.35	-0.03	0.16	0.03	-0.41	-0.74	-0.73	-0.53	-0.46	-0.39	-0.41
	-0.47	-0.30	0.03	0.45	0.29	0.13	0.34	0.16	0.17	0.05	-0.08	-0.21
	-0.30	-0.13	0.01	0.15	0.32	0.38	-0.44	-0.86	-0.89	-0.61	-0.45	-0.42
	-0.39	-0.36	-0.02	0.38	0.25	0.34	0.37	0.28	0.17	-0.02	-0.27	-0.27
2	-0.31	-0.44	-0.26	-0.17	0.04	0.01	-0.17	-0.55	-0.65	-0.53	-0.46	-0.39
	-0.41	-0.47	-0.30	-0.11	0.43	0.26	0.09	0.21	0.14	0.11	-0.01	-0.04
	0.00	-0.21	-0.04	-0.08	0.14	0.36	0.24	-0.12	-0.73	-0.88	-0.42	-0.72
	-0.41	-0.38	-0.27	0.02	0.25	0.25	0.35	0.21	0.14	0.11	-0.07	-0.12
3	-0.17	-0.12	-0.17	-0.31	-0.12	-0.08	-0.03	-0.35	-0.51	-0.69	-0.52	-0.45
	-0.38	-0.40	-0.41	-0.29	0.03	0.32	0.25	0.17	0.22	0.15	0.12	0.05
	0.10	0.11	0.03	0.03	0.19	0.26	0.36	0.28	-0.50	-0.63	-1.03	-0.84
	-0.61	-0.48	-0.45	-0.30	-0.14	0.09	0.25	0.26	0.29	0.05	0.01	-0.03
4	-0.07	-0.12	-0.07	-0.16	-0.21	-0.03	0.02	0.03	-0.26	-0.40	-0.64	-0.65
	-0.52	-0.41	-0.42	-0.35	-0.37	-0.19	0.12	0.31	0.14	0.14	0.10	0.11
	0.04	0.00	0.05	0.01	0.06	0.12	0.23	0.38	0.39	0.02	-0.41	-0.90
	-0.88	-0.71	-0.48	-0.48	-0.37	-0.22	-0.06	0.18	0.18	0.23	0.16	-0.01
5	-0.09	-0.09	-0.13	-0.09	-0.04	-0.13	-0.09	-0.04	0.01	-0.08	-0.32	-0.45
	-0.64	-0.54	-0.50	-0.43	-0.40	-0.37	-0.20	-0.08	0.17	0.20	0.08	0.17
	0.14	0.03	-0.01	0.08	0.14	0.16	0.18	0.25	0.63	0.15	0.27	0.02
	-0.63	-1.07	-0.77	-0.92	-0.56	-0.50	-0.38	-0.15	-0.07	0.13	0.18	0.07
6	-0.10	-0.10	-0.14	-0.09	-0.05	-0.05	0.05	0.01	-0.08	-0.08	-0.23	-0.13
	-0.41	-0.53	-0.55	-0.58	-0.42	-0.43	-0.36	-0.33	-0.25	0.00	0.16	0.12
	0.08	0.08	0.01	-0.02	-0.02	0.07	0.12	0.14	0.15	0.23	0.25	0.26
	0.07	-0.25	-0.67	-0.84	-0.68	-0.60	-0.50	-0.50	-0.27	-0.19	-0.08	0.12
7	0.17	0.18	-0.06	-0.14	0.30	-0.22	0.00	0.05	0.01	0.07	-0.03	-0.02
	-0.13	-0.13	-0.28	-0.66	-0.61	-0.55	-0.54	-0.38	-0.43	-0.52	-0.16	0.29
	0.20	0.20	0.26	0.16	0.09	0.00	0.06	0.17	0.18	0.19	0.04	0.12
	0.28	0.27	0.02	-0.31	-0.84	-0.92	-0.96	-0.73	-0.54	-0.50	-0.39	-0.23
8	-0.11	0.16	0.17	0.14	0.11	-0.14	0.08	0.00	0.05	-0.08	-0.04	-0.13
	-0.03	-0.13	-0.08	-0.08	-0.27	-0.49	-0.68	-0.50	-0.53	-0.42	-0.35	-0.36
	-0.24	-0.12	0.22	0.28	0.20	0.22	0.15	0.17	0.19	0.12	0.08	0.16
	0.09	0.10	0.06	0.14	0.28	-0.31	-0.38	-1.03	-1.00	-0.81	-0.53	-0.46
9	-0.43	-0.32	-0.20	0.20	0.16	0.16	0.14	0.11	0.12	0.00	0.05	0.01
	-0.08	-0.18	-0.13	-0.23	-0.18	-0.32	-0.22	-0.31	-0.63	-0.58	-0.42	-0.47
	-0.40	-0.33	-0.16	0.09	0.32	0.28	0.25	0.28	0.27	0.36	0.37	0.20
	0.25	0.27	-0.05	-0.05	0.01	0.14	-0.18	-0.31	-0.96	-1.12	-1.05	-0.66
10	-0.49	-0.41	-0.46	-0.31	0.01	0.25	0.17	0.26	0.24	0.18	0.10	0.17
	0.23	0.25	0.05	-0.44	-0.39	-0.37	-0.17	-0.12	-0.27	-0.50	-0.73	-0.69
	-0.45	-0.42	-0.35	-0.41	-0.33	0.02	0.30	0.28	0.25	0.31	0.30	0.29
	0.34	0.31	0.16	0.14	-0.36	-0.23	-0.06	0.00	0.01	-0.41	-0.92	-1.05

11	-0.75	-0.50	-0.46	-0.43	-0.45	-0.38	-0.21	0.35	0.32	0.16	0.29	0.32
	0.27	0.31	0.38	0.04	-0.17	-0.50	-0.43	-0.18	0.02	0.18	-0.12	-0.68
	-0.98	-0.70	-0.54	-0.43	-0.40	-0.41	-0.16	-0.12	0.45	0.28	0.45	0.56
	0.52	0.51	0.47	0.40	-0.05	-0.37	-0.64	-0.49	-0.18	0.12	-0.12	-0.41
12	-1.19	-0.98	-0.67	-0.58	-0.39	-0.44	-0.42	-0.39	0.01	0.45	0.27	0.28
	0.44	0.36	0.37	0.40	0.29	0.07	-0.52	-0.67	-0.64	-0.13	0.12	-0.08
	-0.33	-0.75	-0.94	-0.58	-0.51	-0.44	-0.37	-0.47	-0.17	0.46	0.47	0.36
	0.45	0.64	0.56	0.79	0.59	0.27	-0.24	-0.75	-1.03	-0.49	-0.13	-0.06
13	-0.17	-0.70	-1.17	-0.87	-0.49	-0.50	-0.39	-0.40	-0.38	-0.44	0.25	0.46
	0.36	0.25	0.36	0.56	0.39	0.91	0.21	0.08	-0.63	-0.86	-0.65	-0.02
	0.15	0.15	-0.54	-1.16	-0.96	-0.49	-0.46	-0.47	-0.40	-0.42	-0.20	0.56
	0.36	0.37	0.50	0.64	0.57	0.69	0.41	0.15	-0.43	-0.89	-0.80	-0.49
14	-0.07	0.15	-0.12	-0.88	-1.00	-0.77	-0.41	-0.46	-0.39	-0.41	-0.48	-0.31
	0.31	0.47	0.32	0.41	0.42	0.49	0.49	0.71	0.28	-0.43	-0.76	-0.80
	-0.47	0.18	0.32	0.15	-0.81	-1.14	-0.74	-0.57	-0.42	-0.43	-0.36	-0.42
	0.07	0.50	0.36	0.43	0.58	0.74	0.69	0.54	0.47	0.15	-0.68	-1.08
15	-0.80	-0.50	0.20	0.09	-0.12	-1.08	-1.13	-0.61	-0.46	-0.51	-0.40	-0.42
	-0.44	-0.26	0.63	0.44	0.29	0.43	0.50	0.64	0.49	0.54	0.28	-0.50
	-0.90	-0.76	-0.23	0.25	0.33	-0.29	-0.97	-1.26	-0.66	-0.53	-0.42	-0.39
	-0.45	-0.34	0.27	0.41	0.28	0.55	0.55	0.54	0.42	0.48	0.15	-0.18
16	-0.84	-0.77	-0.64	-0.28	0.11	0.12	-0.33	-1.10	-0.79	-0.58	-0.43	-0.41
	-0.42	-0.44	-0.51	-0.18	0.68	0.35	0.19	0.41	0.37	0.48	0.52	0.21
	-0.12	-0.51	-0.73	-0.48	0.01	0.32	0.40	-0.24	-1.04	-1.10	-0.86	-0.27
	-0.43	-0.41	-0.42	-0.30	0.34	0.35	0.32	0.47	0.75	0.12	0.24	0.16
17	-0.18	-0.45	-0.73	-0.66	-0.44	-0.14	0.04	0.00	-0.53	-0.83	-0.58	-0.51
	-0.40	-0.42	-0.39	-0.51	-0.44	-0.07	0.63	0.25	0.12	0.32	0.21	0.28
	0.22	0.15	-0.13	-0.41	-0.40	-0.18	0.04	0.33	0.28	-0.33	-0.97	-0.91
	-0.58	-0.39	-0.44	-0.46	-0.39	-0.21	0.40	0.32	0.24	0.33	0.28	0.18
18	0.21	-0.02	-0.17	-0.27	-0.50	-0.44	-0.26	-0.05	0.00	-0.13	-0.47	-0.77
	-0.57	-0.43	-0.41	-0.42	-0.44	-0.47	-0.33	0.30	0.43	0.25	0.13	0.17
	0.17	0.23	0.08	0.14	-0.08	-0.31	-0.13	0.01	0.25	0.38	0.04	-0.62
	-1.01	-0.83	-0.53	-0.46	-0.39	-0.45	-0.34	-0.07	0.35	0.28	0.25	0.30
19	0.16	0.00	0.00	-0.09	-0.04	-0.27	-0.35	-0.31	-0.14	-0.05	-0.09	-0.18
	-0.59	-0.65	-0.54	-0.43	-0.45	-0.43	-0.40	-0.42	-0.22	0.42	0.35	0.13
	0.16	0.17	0.14	0.15	0.16	0.09	0.10	-0.13	0.17	0.23	0.36	0.26
	-0.12	-0.76	-1.14	-0.75	-0.70	-0.53	-0.42	-0.40	-0.20	0.13	0.20	0.25
20	0.27	0.04	0.00	-0.13	-0.04	-0.12	-0.04	-0.03	-0.08	-0.08	0.07	-0.12
	0.03	-0.27	-0.62	-0.71	-0.60	-0.53	-0.43	-0.40	-0.42	-0.20	-0.02	0.27
	0.29	0.13	0.22	0.11	0.16	0.00	0.10	0.16	0.03	0.08	0.19	0.36
	0.41	-0.11	-0.31	-0.63	-1.03	-0.88	-0.65	-0.52	-0.45	-0.39	-0.19	-0.06
21	0.14	0.21	0.14	0.07	-0.09	-0.01	0.00	-0.04	0.05	-0.03	0.01	0.02
	0.02	0.03	-0.07	-0.12	-0.59	-0.68	-0.64	-0.48	-0.41	-0.38	-0.40	-0.19
	-0.02	0.31	0.18	0.18	0.19	0.12	0.09	-0.04	0.10	0.16	0.03	0.09
	0.14	0.21	0.05	-0.11	-0.27	-0.59	-0.85	-0.72	-0.61	-0.52	-0.37	-0.37
22	-0.26	-0.09	0.15	0.14	0.11	-0.01	-0.01	-0.12	0.00	0.00	0.08	0.09
	-0.03	0.02	-0.02	0.02	-0.02	-0.16	-0.34	-0.71	-0.52	-0.51	-0.40	-0.42
	-0.35	-0.23	0.12	0.19	0.14	0.18	0.23	0.12	0.14	0.10	0.12	0.18
	0.09	0.20	0.05	0.16	-0.10	-0.05	-0.43	-0.60	-0.78	-0.83	-0.55	-0.52
23	-0.53	-0.42	-0.39	-0.27	0.07	0.02	0.02	0.02	-0.09	-0.12	-0.12	-0.04
	0.01	-0.15	-0.11	-0.06	-0.06	0.04	-0.05	-0.14	-0.32	-0.71	-0.68	-0.59

	-0.56	-0.34	-0.26	-0.06	0.14	0.18	0.20	0.24	0.23	0.02	0.08	-0.07
	0.04	0.04	-0.17	-0.22	-0.17	-0.01	-0.17	-0.28	-0.38	-0.94	-0.94	-0.75
24	-0.63	-0.52	-0.49	-0.47	-0.39	-0.40	-0.01	0.15	-0.01	-0.01	-0.24	0.04
	-0.03	0.06	-0.01	0.00	-0.12	-0.17	0.02	-0.06	-0.05	-0.26	-0.51	-0.93
	-0.75	-0.55	-0.48	-0.49	-0.50	-0.30	0.03	0.14	0.27	0.22	0.13	-0.03
	-0.07	-0.11	-0.06	-0.16	-0.21	-0.26	-0.36	-0.26	-0.11	-0.16	-0.36	-0.78
25	-0.82	-0.72	-0.49	-0.58	-0.43	-0.53	-0.46	-0.15	0.14	0.13	0.17	0.07
	-0.04	0.02	-0.06	-0.09	-0.09	-0.27	-0.27	-0.27	-0.04	-0.08	-0.07	-0.47
	-0.73	-0.78	-0.72	-0.57	-0.54	-0.43	-0.49	-0.07	0.17	0.21	0.27	0.24
	0.09	0.12	0.04	-0.05	-0.16	-0.37	-0.21	-0.47	-0.27	-0.27	-0.32	-0.25
26	-0.63	-0.89	-0.74	-0.51	-0.48	-0.49	-0.47	-0.53	-0.27	0.25	0.23	0.07
	0.16	0.06	0.08	0.06	0.03	-0.01	-0.15	-0.36	-0.21	-0.10	0.05	0.07
	-0.25	-0.66	-1.04	-0.84	-0.58	-0.51	-0.52	-0.41	-0.25	0.11	0.23	0.33
	0.34	0.26	0.25	0.07	0.02	-0.14	-0.13	-0.47	-0.46	-0.25	-0.04	-0.27
27	-0.83	-0.13	-0.73	-0.85	-0.59	-0.52	-0.49	-0.46	-0.35	-0.36	0.20	0.22
	0.22	0.28	0.19	-0.01	0.05	0.16	0.13	-0.17	-0.53	-0.32	-0.08	0.28
	0.25	-0.22	-0.70	-1.04	-0.86	-0.63	-0.48	-0.45	-0.50	-0.39	0.07	0.30
	0.31	0.38	0.36	0.33	0.21	0.05	0.00	-0.39	-0.38	-0.50	-0.58	-0.21
28	-0.01	-0.01	-0.41	-0.75	-0.86	-0.57	-0.50	-0.43	-0.44	-0.42	-0.34	-0.02
	0.38	0.28	0.17	0.27	0.27	0.16	0.14	0.00	-0.26	-0.31	-0.35	-0.25
	-0.02	0.20	0.23	-0.42	-0.94	-0.89	-0.65	-0.49	-0.42	-0.43	-0.41	-0.16
	0.45	0.21	0.38	0.44	0.37	0.35	0.17	-0.26	-0.36	-0.48	-0.61	-0.48
29	-0.33	-0.02	-0.02	-0.20	-0.63	-0.73	-0.60	-0.45	-0.43	-0.44	-0.46	-0.43
	0.09	0.11	0.38	0.17	0.30	0.21	0.24	0.13	0.00	-0.30	-0.29	-0.34
	-0.25	-0.02	0.27	0.26	-0.20	-0.89	-0.93	-0.68	-0.45	-0.42	-0.43	-0.44
	-0.19	0.35	0.29	0.30	0.38	0.35	0.20	0.16	-0.04	-0.30	-0.45	-0.49
30	-0.60	-0.28	-0.07	-0.06	-0.11	-0.54	-0.76	-0.55	-0.41	-0.42	-0.43	-0.45
	-0.43	-0.19	0.48	0.31	0.14	0.19	0.24	0.10	0.16	0.09	-0.10	-0.34
	-0.47	-0.24	-0.11	0.12	0.33	-0.09	-0.77	-0.91	-0.63	-0.48	-0.45	-0.43
	-0.40	-0.27	0.33	0.30	0.30	0.33	0.33	0.28	0.16	0.03	-0.14	-0.39
July 1991												
1	-0.49	-0.47	-0.37	-0.10	0.12	-0.14	-0.50	-0.80	-0.59	-0.48	-0.41	-0.42
	-0.44	-0.46	-0.14	0.23	0.44	0.15	0.19	0.29	0.15	0.17	0.09	-0.14
	-0.38	-0.28	-0.32	-0.06	0.22	0.25	0.12	-0.70	-0.90	-0.75	-0.51	-0.48
	-0.41	-0.38	-0.31	0.21	0.35	0.19	0.36	0.32	0.23	0.16	0.01	-0.28
2	-0.38	-0.33	-0.37	-0.49	-0.06	-0.01	-0.14	-0.40	-0.71	-0.58	-0.43	-0.41
	-0.42	-0.44	-0.46	-0.38	0.36	0.34	0.20	0.15	0.20	0.21	0.11	0.03
	-0.09	-0.18	-0.27	-0.23	-0.06	0.13	0.29	0.12	-0.53	-0.85	-0.67	-0.58
	-0.47	-0.40	-0.42	-0.26	0.13	0.24	0.23	0.32	0.31	0.17	0.15	0.12
3	-0.13	-0.28	-0.38	-0.37	-0.36	-0.14	-0.05	-0.01	-0.32	-0.64	-0.70	-0.55
	-0.44	-0.42	-0.44	-0.46	-0.28	0.11	0.39	0.16	0.15	0.20	0.13	0.06
	0.07	-0.14	-0.10	-0.23	-0.14	-0.06	0.13	0.19	0.27	-0.34	-0.88	-0.72
	-0.62	-0.47	-0.40	-0.41	-0.34	-0.17	0.25	0.23	0.23	0.25	0.15	0.08
4	0.05	-0.13	-0.18	-0.18	-0.35	-0.31	-0.18	0.03	-0.13	-0.26	-0.42	-0.65
	-0.58	-0.39	-0.45	-0.43	-0.45	-0.42	-0.02	0.39	0.26	0.16	0.12	0.13
	0.14	0.07	-0.01	-0.05	-0.05	-0.09	0.05	0.20	0.17	0.32	0.04	-0.72
	-0.80	-0.85	-0.61	-0.46	-0.39	-0.36	-0.28	0.09	0.24	0.20	0.21	0.13
5	0.06	-0.06	-0.01	-0.14	-0.14	-0.23	-0.23	-0.15	-0.01	-0.05	-0.19	-0.32
	-0.65	-0.67	-0.43	-0.56	-0.42	-0.44	-0.27	-0.18	0.13	0.28	0.19	0.15
	0.16	0.13	0.11	-0.01	-0.01	0.09	0.16	-0.14	0.01	0.34	0.39	0.26

	-0.72	-0.62	-1.05	-0.80	-0.60	-0.55	-0.36	-0.32	-0.25	0.15	0.19	0.19
6	0.34	-0.20	0.02	-0.19	0.03	-0.10	-0.15	-0.01	-0.19	0.00	-0.10	-0.14
	-0.14	-0.52	-0.63	-0.64	-0.48	-0.56	-0.38	-0.34	-0.31	-0.05	0.15	0.14
	0.18	0.11	0.09	-0.03	-0.03	0.02	-0.02	0.08	0.05	0.16	0.24	0.13
	0.23	-0.13	-0.44	-0.93	-0.86	-0.66	-0.64	-0.52	-0.41	-0.29	-0.22	0.11
7	0.11	0.11	0.04	-0.04	-0.03	-0.11	-0.03	-0.02	-0.02	-0.01	-0.01	0.00
	-0.14	-0.14	-0.33	-0.33	-0.54	-0.64	-0.51	-0.36	-0.49	-0.34	-0.30	-0.14
	0.11	0.14	0.18	0.20	0.13	0.15	0.03	0.04	0.00	0.32	0.18	0.02
	0.15	0.27	0.07	-	-	-	-	-	-	-	-	-
26	-	-	-	-	-	-	-	-	-0.31	0.11	-0.27	0.21
	0.18	-0.27	-0.71	-0.82	-0.69	-0.46	-0.47	-0.40	-0.33	-0.16	0.46	0.28
	0.37	0.50	0.44	0.44	0.20	0.06	-0.18	-0.39	-0.54	-0.48	-0.46	-0.08
27	0.02	-0.17	-0.49	-0.76	-0.65	-0.41	-0.46	-0.40	-0.41	-0.43	-0.11	0.41
	0.37	0.21	0.30	0.33	0.32	0.32	0.19	0.04	-0.33	-0.42	-0.37	-0.12
	0.18	0.27	-0.17	-0.68	-0.89	-0.70	-0.53	-0.42	-0.43	-0.40	-0.24	0.38
	0.32	0.33	0.54	0.44	0.44	0.32	0.07	-0.18	-0.40	-0.59	-0.63	-0.49
28	-0.17	-0.08	-0.03	-0.43	-0.74	-0.60	-0.49	-0.38	-0.44	-0.42	-0.44	-0.16
	0.44	0.46	0.25	0.30	0.37	0.37	0.38	0.11	-0.11	-0.34	-0.52	-0.40
	-0.12	0.11	0.34	-0.06	-0.72	-0.91	-0.65	-0.49	-0.46	-0.43	-0.41	-0.29
	0.49	0.41	0.38	0.59	0.55	0.63	0.54	0.22	-0.30	-0.50	-0.63	-0.71
29	-0.52	-0.17	0.02	0.02	-0.22	-1.14	-0.65	-0.49	-0.50	-0.40	-0.51	-0.39
	-0.21	0.59	0.37	0.24	0.42	0.48	0.36	0.43	0.21	-0.17	-0.44	-0.56
	-0.47	-0.12	0.02	0.39	0.04	-0.73	-0.99	-0.70	-0.53	-0.42	-0.43	-0.40
	-0.24	0.46	0.36	0.46	0.62	0.69	0.68	0.54	0.28	-0.30	-0.43	-0.89
30	-0.61	-0.77	0.03	-0.02	0.04	-0.63	-0.88	-0.69	-0.53	-0.22	-0.66	-0.40
	-0.42	-0.25	0.46	0.37	0.29	0.35	0.43	0.35	0.34	0.31	-0.11	-0.28
	-0.38	-0.42	-0.47	0.18	0.39	0.10	-0.65	-1.07	-0.71	-0.60	-0.41	-0.46
	-0.39	-0.28	0.33	0.38	0.42	0.56	0.62	0.52	0.48	0.22	-0.11	-0.43
31	-0.85	-0.48	-0.52	-0.16	0.04	-0.11	-0.41	-0.83	-0.65	-0.56	-0.45	-0.42
	-0.40	-0.41	-0.24	0.46	0.38	0.29	0.35	0.39	0.40	0.34	0.31	0.07
	-0.39	-0.43	-0.47	-0.16	0.09	0.21	0.38	-0.50	-1.18	-0.81	-0.60	-0.44
	-0.41	-0.42	-0.57	0.44	0.33	0.34	0.45	0.57	0.50	0.32	0.28	-0.10
August 1991												
1	-0.30	-0.40	-0.63	-0.52	-0.21	0.04	0.14	-0.41	-0.72	-0.82	-0.59	-0.40
	-0.41	-0.43	-0.41	-0.28	0.34	0.43	0.26	0.31	0.38	0.39	0.29	0.28
	0.11	-0.16	-0.42	-0.41	-0.16	0.25	0.42	0.20	-0.41	-1.13	-0.89	-0.69
	-0.48	-0.48	-0.37	-0.34	-0.06	0.38	0.26	0.31	0.43	0.30	0.30	0.11
2	-0.11	-0.16	-0.36	-0.31	-0.44	-0.25	-0.07	0.07	-0.11	-0.48	-0.82	-0.51
	-0.48	-0.41	-0.38	-0.45	-0.38	0.09	0.46	0.26	0.26	0.31	0.26	0.20
	0.12	0.04	-0.11	-0.21	-0.16	-0.11	0.04	0.30	0.32	-0.16	-0.88	-0.98
	-0.65	-0.47	-0.48	-0.37	-0.38	-0.18	0.19	0.26	0.26	0.24	0.26	0.15
3	0.12	0.03	-0.16	-0.11	-0.25	-0.20	-0.20	0.03	0.08	0.04	-0.44	-0.64
	-0.64	-0.51	-0.40	-0.41	-0.43	-0.31	-0.14	0.21	0.27	0.18	0.19	0.16
	0.17	0.10	0.06	-0.02	-0.06	-0.02	-0.01	0.09	0.20	0.32	0.01	-0.58
	-0.90	-0.76	-0.60	-0.43	-0.44	-0.37	-0.30	-0.18	0.11	0.19	0.11	0.15
4	0.04	0.08	0.01	-0.07	-0.03	-0.03	-0.20	0.01	0.02	0.07	-0.02	-0.11
	-0.47	-0.49	-0.63	-0.43	-0.36	-0.37	-0.39	-0.22	-0.05	0.20	0.27	0.11
	0.15	0.16	0.09	0.01	0.01	0.02	0.02	0.03	0.23	0.15	0.27	0.22
	-0.16	-0.58	-0.91	-0.68	-0.56	-0.51	-0.40	-0.41	-0.30	-0.22	-0.01	0.11
5	0.11	0.07	0.07	-0.04	-0.04	0.04	0.04	0.09	0.01	0.02	0.07	0.12

	-0.06	-0.16	-0.25	-0.51	-0.53	-0.59	-0.40	-0.40	-0.33	-0.30	-0.09	0.03
	0.19	0.22	0.15	0.00	0.00	0.00	0.05	0.10	0.11	0.17	0.19	0.20
	0.11	0.06	-0.16	-0.31	-0.82	-0.70	-0.61	-0.47	-0.43	-0.36	-0.37	-0.30
6	-0.13	0.15	0.11	0.11	0.15	0.04	0.08	0.13	0.14	0.16	0.27	0.25
	0.17	0.11	0.18	0.09	-0.29	-0.38	-0.99	-0.71	-0.54	-0.60	-0.43	-0.32
	-0.29	-0.05	0.11	0.26	0.16	0.17	0.01	0.10	0.02	0.08	0.13	0.10
	0.15	0.06	0.06	-0.05	-0.05	-0.21	-0.42	-0.77	-0.74	-0.64	-0.43	-0.40
7	-0.36	-0.37	-0.26	-0.09	0.19	0.19	0.15	0.23	0.17	0.10	0.11	0.26
	0.19	0.05	0.12	0.16	0.06	-0.37	0.00	-0.10	-0.47	-0.99	-0.63	-0.64
	-0.43	-0.36	-0.37	-0.21	0.11	0.23	0.31	0.33	0.41	0.32	0.20	0.11
	0.11	0.12	0.08	-0.22	-0.38	-0.05	-0.05	-0.15	-0.47	-0.76	-0.78	-0.64
8	-0.51	-0.40	-0.41	-0.34	-0.44	-0.27	0.09	0.45	0.19	0.19	0.24	0.26
	0.28	0.27	0.25	0.00	-0.31	-0.26	-0.25	0.09	0.10	0.07	-0.56	-0.84
	-0.69	-0.51	-0.43	-0.40	-0.38	-0.39	-0.22	0.46	0.42	0.23	0.45	0.47
	0.39	0.43	0.12	0.02	-0.33	-0.52	-0.56	-0.44	-0.15	0.03	-0.20	-0.51
9	-0.76	-0.47	-0.43	-0.40	-0.38	-0.44	-0.42	-0.39	0.11	0.58	0.31	0.23
	0.31	0.38	0.48	0.40	0.32	-0.26	-0.60	-0.54	-0.33	-0.11	0.12	0.04
	-0.56	-0.70	-0.59	-0.39	-0.44	-0.42	-0.44	-0.41	-0.14	0.61	0.47	0.27
	0.37	0.55	0.66	0.55	0.30	-0.03	-0.62	-0.74	-0.76	-0.38	-0.11	-0.02
10	-0.15	-0.67	-0.63	-0.51	-0.40	-0.37	-0.38	-0.40	-0.47	-0.35	0.71	0.56
	0.27	0.32	0.48	0.61	0.74	0.56	0.30	-0.61	-0.89	-0.75	-0.30	0.10
	0.25	0.01	-0.86	-0.95	-0.59	-0.43	-0.43	-0.37	-0.46	-0.40	0.39	0.54
	0.39	0.51	0.65	0.85	0.75	0.68	0.23	-0.53	-1.12	-1.13	-0.91	-0.29
11	-0.02	-0.01	-0.47	-0.77	-0.51	-0.39	-0.44	-0.37	-0.43	-0.41	-0.44	0.11
	0.82	0.38	0.35	0.43	0.63	0.82	0.82	0.55	-0.09	-1.00	-1.04	-0.71
	-0.05	0.15	0.28	-0.31	-1.12	-0.78	-0.55	-0.39	-0.44	-0.41	-0.43	-0.09
	0.61	0.50	0.53	0.82	0.90	1.01	0.74	0.42	-0.15	-0.78	-1.38	-1.17
12	-0.66	-0.05	0.10	0.40	-1.25	-0.82	-0.55	-0.39	-0.36	-0.37	-0.38	-0.49
	-0.33	0.71	0.54	0.31	0.47	0.73	0.80	0.76	0.74	0.23	-0.85	-1.20
	-0.79	-0.40	0.20	0.38	0.27	-0.91	-1.30	-0.60	-0.51	-0.43	-0.40	-0.41
	-0.39	-0.31	1.05	0.67	0.69	0.81	1.11	0.68	0.61	0.04	-0.53	-1.24
13	-1.47	-1.01	-0.20	0.13	0.09	-0.44	-0.88	-0.59	-0.43	-0.40	-0.41	-0.43
	-0.40	-0.43	0.39	0.65	0.31	0.36	0.53	0.67	0.69	0.69	0.30	-0.35
	-1.01	-0.94	-0.50	0.04	0.36	0.27	-0.47	-1.12	-0.74	-0.51	-0.43	-0.40
	-0.41	-0.43	0.09	0.59	0.39	0.46	0.63	0.88	0.71	0.62	0.29	-0.47
14	-0.86	-0.97	-0.96	-0.38	0.08	0.14	0.05	-0.90	-0.77	-0.54	-0.35	-0.44
	-0.41	-0.39	-0.45	0.10	0.63	0.35	0.32	0.39	0.53	0.51	0.49	0.31
	-0.29	-0.62	-0.81	-0.58	0.08	0.24	0.45	0.06	-1.06	-0.94	-0.59	-0.50
	-0.39	-0.40	-0.38	-0.22	0.53	0.39	0.36	0.48	0.56	0.60	0.38	0.24
15	-0.16	-0.49	-0.79	-0.66	-0.43	0.03	0.19	0.20	-0.20	-0.95	-0.85	-0.50
	-0.43	-0.36	-0.42	-0.44	-0.13	0.47	0.39	0.27	0.33	0.41	0.37	0.36
	0.17	-0.04	-0.36	-0.45	-0.35	-0.10	0.20	0.39	0.17	-0.78	-1.04	-0.65
	-0.54	-0.39	-0.40	-0.41	-0.30	0.17	0.43	0.27	0.25	0.31	0.26	0.24
16	0.16	-0.05	-0.25	-0.25	-0.34	-0.29	0.04	0.29	0.21	-0.15	-0.89	-0.83
	-0.55	-0.46	-0.39	-0.41	-0.34	-0.13	0.29	0.35	0.28	0.25	0.27	0.26
	0.19	0.10	-0.05	-0.05	-0.20	-0.10	0.16	0.38	0.48	0.24	-0.74	-1.10
	-0.98	-0.60	-0.54	-0.39	-0.35	-0.28	-0.04	0.27	0.27	0.21	0.14	0.11
17	0.03	-0.01	-0.15	-0.15	-0.01	-0.15	-0.15	0.08	0.18	0.15	-0.05	-0.54
	-0.68	-0.67	-0.42	-0.47	-0.36	-0.33	-0.12	0.08	0.16	0.20	0.20	0.09
	0.10	0.06	0.02	-0.02	0.03	0.04	0.14	0.20	0.50	0.30	0.24	-0.42

	-0.64	-1.06	-0.67	-0.59	-0.42	-0.35	-0.31	-0.12	0.08	0.12	0.12	0.09
18	-0.03	-0.07	-0.11	-0.07	0.02	-0.02	0.07	0.07	0.22	0.29	0.26	0.17
	-0.25	-0.66	-0.67	-0.62	-0.51	-0.42	-0.31	-0.23	-0.12	0.08	0.12	0.20
	0.14	-0.02	-0.06	-0.15	-0.02	-0.02	0.03	0.08	0.23	0.25	0.35	0.28
	-0.09	-0.31	-0.57	-0.78	-0.54	-0.55	-0.46	-0.34	-0.27	-0.23	-0.16	0.01
19	0.01	0.04	-0.11	-0.15	-0.15	-0.11	-0.07	0.08	0.09	0.13	0.18	0.20
	0.17	0.14	-0.09	-0.38	-0.37	-0.44	-0.43	-0.34	-0.34	-0.23	-0.15	-0.03
	0.05	0.09	0.01	0.01	-0.10	-0.10	-0.06	0.02	0.10	0.11	0.08	0.08
	0.14	0.05	-0.14	-0.19	-0.33	-0.37	-0.48	-0.43	-0.46	-0.30	-0.27	-0.23
20	-0.15	-0.11	-0.07	0.04	0.01	-0.15	-0.03	0.01	0.01	0.13	0.14	0.23
	0.16	0.32	0.26	0.29	0.12	0.02	-0.51	-0.45	-0.58	-0.45	-0.44	-0.34
	-0.30	-0.15	-0.07	0.05	0.06	0.10	-0.06	-0.10	-0.06	-0.06	-0.06	0.03
	0.08	-0.01	0.04	0.00	-0.10	-0.10	-0.28	-0.28	-0.40	-0.43	-0.50	-0.42
21	-0.31	-0.28	-0.28	-0.16	-0.04	0.08	0.12	0.12	0.08	0.09	0.01	0.06
	0.06	0.07	0.17	0.18	0.20	0.16	0.07	0.06	-0.25	-0.54	-0.68	-0.46
	-0.52	-0.43	-0.35	-0.23	0.04	0.20	0.25	0.15	0.21	0.18	0.15	0.11
	0.07	0.07	0.06	0.02	0.14	-0.09	0.10	-0.28	-0.09	-0.27	-0.57	-0.81
22	-0.72	-0.56	-0.43	-0.35	-0.20	0.04	0.16	0.24	0.31	0.34	0.19	0.26
	0.17	0.12	0.19	-0.03	0.10	0.04	0.10	0.10	0.04	-0.22	-0.48	-1.01
	-0.81	-0.69	-0.52	-0.43	-0.27	-0.15	0.04	0.20	0.39	0.44	0.51	0.22
	0.18	0.09	0.17	-0.09	-0.09	-0.03	-0.22	-0.22	-0.22	0.10	-0.47	-0.63
23	-0.95	-0.68	-0.56	-0.43	-0.36	-0.36	-0.09	0.34	0.23	0.25	0.40	0.37
	0.40	0.32	0.21	0.36	0.03	-0.23	-0.23	-0.03	-0.03	0.16	-0.03	-0.62
	-0.99	-1.02	-1.02	-0.32	-0.47	-0.36	-0.44	0.34	0.19	0.24	0.39	0.49
	0.25	0.37	0.01	0.20	-0.03	-0.23	-0.55	-0.53	-0.41	-0.25	-0.20	-0.24
24	-0.71	-0.39	-0.54	-0.39	-0.40	-0.37	-0.38	-0.31	-0.09	0.39	0.35	0.23
	0.24	0.30	0.16	0.46	0.31	0.22	-0.10	-0.25	-0.26	0.06	0.12	0.19
	-0.03	-0.74	-1.05	-0.71	-0.55	-0.43	-0.39	-0.36	-0.12	0.39	0.35	0.42
	0.57	0.61	0.45	0.43	0.10	-0.09	-0.48	-0.49	-0.69	-0.50	-0.10	0.00
25	0.00	-0.55	-0.82	-0.59	-0.46	-0.43	-0.44	-0.33	-0.43	-0.22	0.51	0.39
	0.28	0.33	0.41	0.48	0.41	0.28	0.03	-0.37	-0.46	-0.50	-0.15	0.11
	0.35	0.06	-0.69	-0.99	-0.60	-0.50	-0.42	-0.39	-0.36	-0.33	0.49	0.39
	0.41	0.46	0.63	0.70	0.50	0.37	-0.09	-0.54	-0.68	-0.73	-0.66	-0.24
26	0.00	0.05	-0.43	-0.75	-0.58	-0.46	-0.38	-0.40	-0.37	-0.43	-0.31	0.58
	0.44	0.32	0.38	0.42	0.48	0.56	0.31	0.04	-0.45	-0.56	-0.60	-0.29
	0.10	0.41	0.12	-0.64	-0.93	-0.68	-0.50	-0.38	-0.43	-0.36	-0.33	0.34
	0.47	0.40	0.53	0.72	0.70	0.70	0.43	-0.02	-0.53	-0.93	-0.79	-0.70
27	-0.33	0.04	0.05	-0.33	-0.75	-0.58	-0.50	-0.39	-0.36	-0.37	-0.43	-0.31
	0.58	0.48	0.28	0.38	0.46	0.49	0.55	0.45	-0.02	-0.47	-0.67	-0.65
	-0.38	0.14	0.26	0.30	-0.50	-0.93	-0.64	-0.54	-0.38	-0.39	-0.36	-0.37
	0.26	0.55	0.40	0.53	0.62	0.75	0.76	0.43	0.17	-0.66	-0.80	-0.92
28	-0.70	-0.29	0.05	0.20	-0.34	-0.78	-0.67	-0.46	-0.42	-0.39	-0.36	-0.42
	-0.35	0.49	0.48	0.32	0.38	0.42	0.58	0.60	0.34	0.04	-0.66	-0.57
	-0.70	-0.42	-0.01	0.28	0.36	-0.45	-0.62	-0.94	-0.46	-0.38	-0.39	-0.40
	-0.33	0.05	0.60	0.40	0.39	0.53	0.72	0.73	0.50	0.11	-0.47	-0.87
29	-0.93	-0.72	-0.36	0.08	0.00	-0.14	-0.61	-0.62	-0.49	-0.38	-0.39	-0.37
	-0.43	-0.36	0.52	0.57	0.28	0.29	0.41	0.41	0.62	0.46	0.11	-0.40
	-0.67	-0.70	-0.33	0.14	0.26	0.35	-0.30	-0.97	-0.77	-0.46	-0.45	-0.38
	-0.39	-0.37	-0.12	0.61	0.36	0.38	0.42	0.58	0.55	0.45	0.24	-0.41
30	-0.62	-0.73	-0.67	-0.18	0.00	0.14	-0.04	-0.64	-0.68	-0.53	-0.42	-0.38

	-0.40	-0.42	-0.30	0.33	0.53	0.28	0.29	0.40	0.41	0.87	0.08	0.03
	-0.37	-0.45	-0.39	-0.39	0.06	0.37	0.44	-0.14	-1.06	-0.95	-0.58	-0.41
	-0.38	-0.42	-0.36	-0.11	0.45	0.36	0.34	0.42	0.42	0.52	0.29	0.23
31	-0.27	-0.42	-0.56	-0.49	-0.18	0.01	0.21	0.17	-0.54	-0.82	-0.71	-0.45
	-0.45	-0.39	-0.40	-0.15	0.18	0.49	0.29	0.35	0.43	0.39	0.47	0.24
	0.09	-0.14	-0.14	-0.30	-0.29	0.02	0.48	0.38	-0.28	-0.81	-1.25	-0.70
	-0.54	-0.37	-0.45	-0.30	-0.23	0.33	0.25	0.29	0.32	0.35	0.40	0.23

September 1991

1	0.14	0.04	-0.07	-0.33	-0.12	-0.07	-0.02	0.19	0.15	-0.29	-0.93	-0.88
	-0.56	-0.39	-0.32	-0.32	-0.29	-0.09	0.39	0.34	0.24	0.38	0.28	0.26
	0.23	0.15	0.09	-0.02	-0.02	-0.07	0.27	0.33	0.39	0.06	-0.58	-1.10
	-1.02	-0.64	-0.52	-0.35	-0.36	-0.24	-0.13	0.19	0.23	0.27	0.16	0.18
2	0.01	0.15	0.02	0.12	0.12	0.08	0.18	0.20	0.20	0.24	-0.13	-0.47
	-0.77	-0.78	-0.62	-0.44	-0.39	-0.24	-0.24	0.07	0.19	0.35	0.08	0.39
	0.10	0.16	-0.02	-0.02	0.18	0.13	0.09	0.25	0.28	0.39	0.20	-0.13
	-0.59	-0.88	-0.92	-0.64	-0.52	-0.35	-0.32	-0.32	-0.13	-0.05	0.19	0.11
3	0.11	0.04	0.04	0.00	0.09	0.13	0.10	0.24	0.22	0.29	0.30	0.15
	0.05	-0.18	-0.54	-0.83	-0.56	-0.53	-0.47	-0.28	-0.24	-0.20	0.11	0.15
	0.15	0.16	0.17	0.05	-0.12	-0.20	0.26	0.19	0.21	0.18	0.23	0.25
	0.27	-0.07	-0.35	-0.44	-0.68	-0.66	-0.57	-0.47	-0.35	-0.32	-0.25	-0.17
4	-0.09	0.27	0.03	0.11	0.15	0.08	0.08	0.09	0.13	0.19	0.25	0.17
	0.28	0.20	0.20	-0.01	-0.29	-0.49	-0.67	-0.57	-0.57	-0.43	-0.35	-0.28
	-0.16	-0.09	0.23	0.27	0.20	0.17	0.18	0.15	0.11	0.17	0.23	0.31
	0.09	0.10	0.11	-0.07	0.00	-0.13	-0.56	-0.78	-0.67	-0.61	-0.47	-0.31
5	-0.36	-0.33	-0.21	-0.05	0.28	0.31	0.15	0.20	0.17	0.27	0.20	0.26
	0.13	0.18	-0.07	-0.07	0.09	0.09	-0.07	-0.17	-0.56	-0.74	-0.63	-0.48
	-0.43	-0.32	-0.32	-0.21	0.16	0.38	0.27	0.29	0.35	0.35	0.39	0.36
	0.15	0.05	-0.07	-0.18	-0.18	-0.01	0.11	-0.07	-0.40	-0.72	-0.87	-0.58
6	-0.39	-0.43	-0.36	-0.37	-0.29	-0.13	0.52	0.46	0.28	0.34	0.47	0.54
	0.46	0.31	0.26	-0.06	-0.39	-0.32	-0.24	0.11	0.13	-0.25	-0.55	-1.08
	-0.64	-0.52	-0.39	-0.31	-0.36	-0.29	0.04	0.54	0.39	0.38	0.51	0.64
	0.65	0.52	0.33	-0.06	-0.45	-0.58	-0.60	-0.38	0.09	0.04	-0.33	-0.73
7	-0.83	-0.40	-0.51	-0.31	-0.32	-0.33	-0.34	-0.26	0.69	0.50	0.28	0.34
	0.48	0.79	0.66	0.59	0.20	-0.45	-0.58	-0.63	-0.23	0.10	0.36	0.07
	-0.93	-1.13	-0.55	-0.48	-0.43	-0.31	-0.36	-0.29	0.39	0.54	0.37	0.55
	0.74	0.80	0.78	0.64	0.32	-0.44	-0.76	-0.84	-0.52	0.00	0.26	0.35
11	-	-	-	-	-	0.20	-1.17	-1.07	-0.55	-0.34	-0.29	-0.48
	-0.70	-0.28	0.58	0.49	0.37	0.78	0.75	0.65	0.90	0.38	0.07	-0.75
	-1.02	-0.98	-0.28	0.15	0.66	0.33	-0.97	-1.59	-0.84	-0.47	-0.43	-0.32
	-0.32	0.43	0.51	0.55	0.78	0.94	1.04	0.77	0.51	0.07	-0.49	-0.82
12	-1.22	-0.93	-0.39	0.26	0.31	-0.18	-1.00	-0.93	-0.44	-0.51	-0.35	-0.32
	-0.37	-0.30	0.45	0.54	0.40	0.44	0.59	0.73	0.85	0.52	0.13	-0.57
	-0.65	-0.79	-0.55	0.10	0.41	0.43	-0.33	-1.07	-0.95	-0.53	-0.39	-0.43
	-0.36	-0.32	-0.08	0.62	0.43	0.43	0.58	0.64	0.71	0.46	0.26	-0.25
13	-0.52	-0.79	-0.59	-0.37	0.19	0.41	0.22	-0.71	-1.02	-0.67	-0.48	-0.39
	-0.35	-0.40	-0.25	0.28	0.50	0.36	0.43	0.48	0.49	0.47	0.47	0.00
	-0.06	-0.52	-0.46	-0.33	0.04	0.42	0.53	-0.19	-0.96	-1.23	-0.59	-0.52
	-0.35	-0.35	-0.32	-0.12	0.39	0.39	0.29	0.40	0.40	0.39	0.25	0.10
14	-0.18	-0.23	-0.33	-0.32	-0.17	0.24	0.36	0.21	-0.45	-0.98	-0.77	-0.44
	-0.51	-0.31	-0.32	-0.12	0.11	0.42	0.24	0.17	0.44	0.45	0.34	0.20

	0.04	0.04	-0.18	-0.12	-0.17	0.20	0.36	0.33	-0.06	-0.78	-1.08	-0.85
	-0.53	-0.43	-0.35	-0.28	-0.16	0.15	0.23	0.28	0.17	0.18	0.10	0.11
15	0.02	0.02	-0.02	-0.07	0.13	0.13	0.31	0.43	0.39	0.00	-0.92	-1.00
	-0.76	-0.49	-0.47	-0.31	-0.16	0.11	0.23	0.25	0.35	0.29	0.22	-0.02
	-0.02	0.03	0.15	0.04	0.09	0.21	0.39	0.52	0.32	0.00	-0.51	-1.24
	-0.92	-0.73	-0.62	-0.43	-0.27	-0.16	0.00	0.19	0.16	0.25	0.10	-0.07
16	-0.07	-0.07	-0.07	-0.03	0.11	0.11	0.17	0.44	0.36	0.43	0.00	-0.33
	-0.62	-0.78	-0.58	-0.42	-0.40	-0.24	-0.20	0.08	0.12	0.17	0.14	-0.03
	-0.07	0.06	-0.07	-0.07	0.06	0.16	0.18	0.24	0.04	-0.01	-0.17	-0.32
	-0.60	-0.39	-0.49	-0.32	-0.43	-0.27	-0.24	-0.12	-0.12	-0.04	-0.04	0.04
17	-0.04	-0.04	0.00	0.04	0.16	0.12	0.09	0.31	0.34	0.48	0.41	0.21
	0.12	-0.13	-0.35	-0.49	-0.47	-0.41	-0.34	-0.25	-0.12	0.01	-0.03	0.15
	-0.03	-0.12	-0.07	-0.07	-0.07	-0.07	0.07	0.12	0.18	0.13	0.15	0.14
	-0.01	-0.12	-0.33	-0.29	-0.47	-0.49	-0.46	-0.36	-0.27	-0.20	-0.16	-0.16
18	0.04	0.04	0.08	-0.08	-0.08	-0.08	0.00	0.09	0.01	0.18	0.19	0.21
	0.28	0.19	0.15	0.04	-0.28	-0.28	-0.53	-0.53	-0.42	-0.36	-0.31	-0.23
	-0.16	-0.16	0.00	-0.04	-0.08	-0.08	0.04	-0.08	-0.04	0.04	0.08	0.09
	0.09	0.01	-0.03	0.06	0.02	-0.07	-0.20	-0.20	-0.32	-0.36	-0.27	-0.27
19	-0.16	-0.08	0.04	0.15	0.20	0.30	0.19	0.16	0.07	0.13	0.03	0.13
	0.20	0.09	0.15	0.24	0.13	0.00	-0.19	-0.45	-0.45	-0.73	-0.63	-0.58
	-0.44	-0.39	-0.20	-0.08	0.04	0.15	0.20	0.17	0.13	0.06	0.01	-0.03
	0.16	-0.02	-0.12	-0.12	0.02	-0.02	0.07	-0.21	-0.21	-0.47	-0.49	-0.47
20	-0.39	-0.32	-0.24	-0.29	-0.13	0.20	0.31	0.19	0.20	0.25	0.22	0.20
	0.21	0.18	0.13	0.20	-0.01	0.20	0.17	0.13	-0.06	-0.44	-0.70	-0.81
	-0.68	-0.44	-0.43	-0.27	-0.24	0.07	0.23	0.24	0.37	0.32	0.31	0.24
	0.08	-0.07	0.04	-0.12	-0.12	-0.12	-0.12	-0.12	-0.02	-0.22	-0.82	-0.33
21	-0.60	-0.43	-0.35	-0.32	-0.29	-0.17	0.12	0.43	0.31	0.28	0.35	0.38
	0.38	0.32	0.20	0.05	-0.01	-0.18	-0.07	0.17	0.20	0.07	-0.39	-0.67
	-1.03	-0.68	-0.52	-0.35	-0.39	-0.24	-0.16	0.39	0.35	0.37	0.50	0.58
	0.46	0.29	0.33	-0.06	-0.06	-0.26	-0.45	-0.34	-0.17	-0.07	-0.23	-0.37
22	-0.79	-0.67	-0.52	-0.39	-0.32	-0.33	-0.25	-0.09	0.32	0.38	0.27	0.33
	0.40	0.46	0.48	0.37	0.39	0.20	-0.39	-0.13	0.13	0.45	0.07	-0.26
	-0.98	-1.18	-0.90	-0.53	-0.47	-0.32	-0.36	-0.09	0.50	0.31	0.51	0.89
	0.68	0.72	0.52	0.13	0.26	-0.70	-0.06	-0.84	-0.59	-0.01	0.13	-0.07
23	-0.99	-0.68	-0.86	-0.52	-0.35	-0.39	-0.40	-0.34	-0.18	0.48	0.50	0.28
	0.38	0.71	0.64	0.73	0.45	0.26	-0.13	-0.64	-0.39	-0.20	0.33	0.32
	0.13	-0.97	-1.23	-0.95	-0.53	-0.43	-0.43	-0.32	-0.21	0.42	0.43	0.55
	0.73	0.72	0.92	0.71	0.38	0.13	-0.44	-0.63	-0.97	-0.79	-0.17	-0.02
24	-0.02	-0.39	-1.01	-0.71	-0.52	-0.32	-0.44	-0.33	-0.38	-0.05	0.60	0.54
	0.37	0.45	0.62	0.56	0.72	0.77	0.45	-0.44	-0.77	-1.05	-0.45	-0.12
	0.14	-0.07	-0.71	-1.01	-0.57	-0.40	-0.47	-0.32	-0.37	-0.17	0.47	0.54
	0.41	0.69	0.84	0.76	1.09	0.88	0.44	-0.24	-0.81	-0.82	-0.97	0.13
25	0.19	0.26	-0.26	-1.77	-1.18	-0.59	-0.44	-0.47	-0.36	-0.29	-0.09	0.61
	0.44	0.62	0.89	1.31	0.90	0.69	0.56	0.19	-0.49	-0.81	-0.69	-0.45
	0.19	0.63	0.31	-0.88	-1.94	-1.29	-0.65	-0.49	-0.44	-0.32	-0.36	0.30
	0.51	0.34	0.87	0.83	1.17	0.76	0.69	0.31	-0.37	-0.81	-0.95	-1.37
26	-0.40	0.15	0.31	-0.13	-0.98	-1.16	-0.57	-0.40	-0.40	-0.36	-0.37	-0.17
	0.70	0.39	0.54	0.78	0.88	1.04	0.70	0.50	0.25	-0.43	-0.94	-0.96
	-0.59	0.26	0.52	0.32	-0.64	-1.65	-1.19	-0.58	-0.40	-0.47	-0.32	-0.33
	0.34	0.46	0.37	0.88	0.98	1.10	0.70	0.69	0.31	-0.12	-0.62	-1.26

27	-0.91	-0.46	0.20	0.45	-0.13	-1.18	-1.34	-0.72	-0.40	-0.40	-0.44	-0.33
	-0.26	0.54	0.42	0.37	0.83	0.89	0.98	0.64	0.63	0.38	-0.43	-0.69
	-0.90	-0.59	0.13	0.52	0.38	-0.51	-1.64	-1.24	-0.64	-0.48	-0.44	-0.40
	-0.33	-0.01	0.61	0.44	0.53	0.84	0.71	0.91	0.83	0.56	0.13	-0.28
28	-0.91	-0.80	-0.43	0.09	0.41	0.41	-0.54	-1.66	-1.45	-0.76	-0.54	-0.49
	-0.37	0.14	0.39	0.39	0.94	1.05	1.24	0,90	0.46	0.21	0.09	0.03
	-0.21	-0.45	-0.83	0.15	-0.03	-0.03	-0.22	-1.34	-1.91	-1.17	-0.87	-0.55
	-0.49	-0.41	0.10	0.31	0.39	0.82	0.96	0.86	0.66	0.34	0.15	0.06
29	-0.24	-0.37	-0.62	-0.51	0.25	0.31	-0.25	-0.44	-1.60	-1.51	-0.95	-0.68
	-0.49	-0.37	-0.37	0.06	0.24	0.45	0.60	0.60	0.39	0.25	0.19	-0.20
	0.32	-0.19	-0.64	-0.33	0.06	0.25	0.38	-0.38	-0.96	-1.52	-1.16	-0.81
	-0.49	-0.40	-0.48	-0.33	-0.14	0.29	0.27	0.22	0.35	0.36	0.18	0.17
30	0.22	0.11	-0.21	-0.15	-0.28	0.18	0.31	0.37	-0.20	-0.78	-1.19	-1.18
	-0.94	-0.51	-0.46	-0.34	-0.18	0.17	0.24	0.56	0.60	0.49	0.18	0.05
	0.11	-0.01	0.12	-0.14	0.05	0.05	0.18	0.30	0.05	-0.38	-1.21	-1.57
	-1.22	-0.77	-0.64	-0.50	-0.42	-0.30	0.09	0.14	0.29	0.38	0.19	-0.10
October 1991												
1	0.18	0.07	0.20	0.19	0.19	-0.01	0.12	0.06	0.12	-0.39	-0.39	-0.78
	-1.15	-0.91	-0.73	-0.57	-0.41	-0.29	-0.29	0.02	0.14	0.16	0.05	-0.07
	-0.02	-0.02	-0.01	0.04	0.10	0.24	0.12	0.15	0.25	0.06	-0.07	-0.27
	-0.66	-0.99	-0.84	-0.68	-0.57	-0.41	-0.41	-0.29	0.10	0.06	-0.01	-0.13
2	-0.01	0.00	0.00	0.05	0.24	0.22	0.39	0.42	0.48	0.54	0.41	0.15
	-0.16	-0.35	-0.74	-0.95	-0.77	-0.77	-0.62	-0.42	-0.12	-0.08	0.13	0.34
	0.29	0.17	-0.11	-0.22	-0.21	-0.16	-0.11	0.17	-0.01	0.05	0.00	0.00
	0.07	-0.04	-0.46	-0.59	-0.82	-0.74	-0.57	-0.40	-0.41	-0.37	-0.34	-0.20
3	-0.20	0.00	0.12	0.12	0.00	0.20	0.13	0.18	0.28	0.27	0.35	0.24
	0.22	0.14	0.03	-0.22	-0.27	-0.57	-0.65	-0.69	-0.56	-0.43	-0.31	-0.31
	-0.19	-0.16	0.00	0.08	0.12	0.09	-0.07	0.01	0.02	0.06	0.11	0.17
	0.04	0.05	0.05	-0.05	-0.15	-0.10	-0.44	-0.55	-0.61	-0.43	-0.38	-0.34
4	-0.34	-0.19	-0.03	0.28	0.40	0.31	0.43	0.44	0.47	0.41	0.44	0.31
	0.31	-0.08	-0.14	-0.08	0.18	0.11	-0.14	-0.65	-1.06	-1.14	-0.80	-0.56
	-0.50	-0.37	-0.34	-0.26	0.05	0.32	0.42	0.07	0.25	0.38	0.32	0.23
	0.19	0.03	-0.20	-0.25	-0.19	-0.09	-0.03	-0.03	-0.45	-0.75	-0.80	-0.47
5	-0.38	-0.38	-0.34	-0.39	-0.28	0.09	0.48	0.32	0.26	0.38	0.48	0.61
	0.82	0.37	0.30	-0.15	-0.34	-0.28	-0.02	0.24	-0.02	-0.40	-1.33	-1.31
	-0.59	-0.55	-0.38	-0.38	-0.34	-0.27	0.32	0.40	0.35	0.44	0.45	0.44
	0.66	0.31	0.05	-0.21	-0.67	-0.52	-0.41	0.02	0.13	-0.25	-0.68	-0.85
6	-0.65	-0.50	-0.34	-0.34	-0.39	-0.36	-0.24	0.49	0.48	0.34	0.42	0.53
	0.71	0.77	0.56	0.11	-0.40	-0.73	-0.81	-0.30	0.13	0.34	0.11	-0.78
	-1.10	-0.77	-0.47	-0.42	-0.38	-0.38	-0.35	0.01	0.63	0.42	0.38	0.64
	0.81	0.89	0.75	0.36	-0.33	-0.52	-1.11	-0.94	-0.41	0.18	0.08	-0.41
7	-0.79	-0.91	-0.50	-0.37	-0.37	-0.38	-0.34	-0.35	0.42	0.60	0.35	0.53
	0.67	0.88	0.76	0.75	0.80	0.05	-0.69	-0.89	-0.78	0.05	0.12	0.37
	-0.46	-1.38	-1.39	-0.68	-0.51	-0.37	-0.41	-0.30	0.21	0.50	0.42	0.73
	0.94	0.96	1.00	0.92	0.36	0.11	-0.49	-0.74	-0.95	-0.65	0.12	0.05
8	-0.20	-0.98	-1.57	-0.82	-0.57	-0.46	-0.41	-0.34	-0.30	0.21	0.45	0.45
	0.76	0.92	1.02	0.81	0.67	0.60	-0.01	-0.74	-0.94	-0.97	-0.27	0.31
	0.43	-0.39	-1.24	-1.42	-0.80	-0.48	-0.46	-0.41	-0.34	-0.26	0.56	0.47
	0.59	1.02	1.10	1.01	0.74	0.73	0.11	-0.37	-0.93	-1.02	-1.17	0.17
9	0.23	0.23	-0.73	-1.40	-1.26	-0.50	-0.52	-0.43	-0.35	-0.43	0.08	0.55

	0.35	0.78	0.91	1.21	0.74	0.67	0.47	-0.14	-0.63	-0.96	-1.04	-0.61
	0.62	0.17	0.11	-1.25	-1.50	-0.72	-0.58	-0.43	-0.43	-0.27	-0.35	0.27
	0.48	0.41	0.67	0.92	0.95	0.87	0.54	0.35	-0.57	-0.64	-1.10	-0.95
10	-0.57	0.21	0.35	-0.17	-1.19	-1.28	-0.52	-0.54	-0.41	-0.37	-0.41	-0.30
	0.52	0.47	0.40	0.79	1.22	0.48	0.72	0.59	0.09	-0.53	-0.72	-1.06
	-0.82	0.09	0.28	0.41	-0.81	-1.19	-1.28	-0.52	-0.50	-0.45	-0.37	-0.33
	0.21	0.71	0.19	0.56	0.78	0.74	0.92	0.59	0.03	-0.60	-0.22	-1.34
11	-0.79	-0.14	-0.01	0.32	0.38	-1.56	-1.21	-0.71	-0.62	-0.44	-0.40	-0.44
	-0.25	0.45	0.42	0.44	0.92	0.91	0.83	0.50	0.19	0.07	-0.62	-0.50
	-1.08	-0.59	0.00	0.32	0.64	-0.51	-1.82	-1.23	-0.71	-0.58	-0.44	-0.44
	-0.37	0.22	0.40	0.47	0.82	0.81	0.58	0.57	0.38	0.13	-0.37	-0.30
12	-0.49	-0.63	0.01	0.26	0.45	0.01	-0.93	-1.41	-1.45	-0.77	-0.58	-0.48
	-0.39	-0.04	0.34	0.44	0.62	0.78	0.78	0.45	0.26	0.14	-0.11	-0.36
	-0.43	-0.56	-0.44	0.07	0.33	0.07	-0.37	-1.41	-1.38	-0.77	-0.58	-0.44
	-0.39	-0.35	0.00	0.33	0.38	0.65	0.50	0.53	0.39	0.14	0.01	-0.04
13	-0.17	-0.43	-0.43	-0.04	0.41	0.47	0.09	-0.67	-1.27	-1.14	-1.02	-0.57
	-0.46	-0.37	-0.10	0.27	0.30	0.54	0.68	0.53	0.34	0.15	0.21	-0.11
	-0.17	-0.11	-0.30	-0.11	0.09	0.28	0.15	-0.48	-1.00	-1.31	-1.03	-0.67
	-0.51	-0.45	-0.22	-0.10	0.18	0.29	0.32	0.43	0.21	0.15	0.00	0.01
14	-0.04	-0.11	-0.04	0.03	0.16	0.35	0.48	0.22	-0.41	-0.87	-1.22	-0.87
	-0.64	-0.51	-0.33	-0.16	0.08	0.23	0.35	0.50	0.26	0.07	-0.11	0.08
	-0.17	0.09	-0.04	-0.04	0.09	0.16	0.16	0.03	-0.23	-0.81	-1.05	-0.92
	-0.61	-0.46	-0.37	-0.36	-0.25	-0.01	0.19	0.16	0.22	0.02	-0.03	-0.02
15	-0.11	-0.06	0.08	0.10	0.15	0.21	0.42	0.49	0.48	0.03	-0.61	-0.68
	-1.02	-0.66	-0.62	-0.37	-0.32	0.01	0.10	0.25	0.23	0.15	0.00	-0.11
	-0.16	-0.11	0.06	0.00	0.06	0.12	0.08	0.23	0.23	0.03	-0.55	-0.62
	-0.68	-0.56	-0.62	-0.46	-0.28	-0.28	-0.16	0.08	0.13	0.15	-0.07	0.08
16	-0.01	-0.10	0.04	0.05	0.15	0.28	0.34	0.56	0.55	0.36	0.23	-0.28
	-0.40	-0.73	-0.68	-0.65	-0.47	-0.40	-0.15	-0.15	-0.10	-0.05	0.15	-0.20
	0.00	-0.20	-0.20	0.00	0.00	0.06	0.01	-0.15	-0.26	-0.15	-0.46	-0.53
	-0.15	-0.20	-0.19	-0.41	-0.19	-0.19	-0.35	-0.15	-0.19	0.00	0.05	0.09
17	0.14	0.16	0.22	0.20	0.44	0.41	0.56	0.68	0.73	0.66	0.29	0.10
	-0.26	-0.14	-0.57	-0.58	-0.84	-0.99	-0.94	-0.73	-0.51	-0.30	-0.25	-0.11
	-0.20	0.03	-0.06	-0.01	-0.01	0.00	0.20	0.17	0.22	0.14	-0.27	0.15
	-0.03	0.04	-0.59	-0.04	-0.21	-0.57	-0.56	-0.43	-0.55	-0.36	-0.35	-0.07
18	-0.23	0.13	0.01	0.06	0.11	0.03	0.03	0.18	0.31	0.28	0.53	0.50
	0.49	0.49	0.61	0.35	0.11	-0.14	-0.39	-0.64	-0.84	-0.60	-0.80	-0.36
	-0.27	0.15	0.30	0.30	0.23	-0.02	-0.15	-0.22	-0.09	-0.22	-0.15	-0.02
	-0.35	-0.09	-0.15	-0.15	-0.02	-0.42	-0.42	-0.63	-0.76	-0.65	-0.44	-0.43
19	-0.31	-0.27	-0.15	0.16	0.21	0.27	0.25	0.28	0.31	0.12	0.17	0.14
	0.03	0.17	0.04	0.24	0.24	0.30	0.11	-0.34	-0.66	-1.07	-0.94	-0.77
	-0.53	-0.39	-0.31	-0.11	0.25	0.23	0.30	0.55	0.28	0.12	-0.03	0.03
	0.03	-0.21	-0.09	-0.26	-0.09	0.08	0.24	0.04	-0.55	-0.68	-0.86	-0.59
20	-0.48	-0.43	-0.34	-0.31	-0.15	0.35	0.29	0.28	0.40	0.46	0.22	0.24
	-0.09	-0.09	-0.03	-0.21	-0.20	0.02	0.09	0.30	0.04	-0.61	-0.79	-0.90
	-0.63	-0.47	-0.35	-0.38	-0.27	-0.08	0.35	0.29	0.32	0.31	0.46	0.22
	0.24	-0.03	-0.15	-0.21	-0.36	-0.20	-0.04	0.01	-0.04	-0.36	-0.55	-0.70
21	-0.52	-0.46	-0.34	-0.38	-0.27	-0.31	0.09	0.51	0.26	0.28	0.41	0.47
	0.28	0.43	0.18	0.05	-0.41	-0.34	-0.20	0.09	0.44	0.31	-0.41	-1.12
	-0.95	-0.77	-0.39	-0.46	-0.34	-0.34	-0.19	0.36	0.37	0.37	0.42	0.57

	0.40	0.44	0.18	-0.28	-0.41	-0.52	-0.51	-0.37	-0.04	0.01	-0.04	-0.49
22	-0.74	-0.56	-0.42	-0.37	-0.42	-0.26	-0.31	-0.11	0.63	0.41	0.24	0.45
	0.52	0.55	0.70	0.24	0.05	-0.40	-0.60	-0.58	-0.08	0.15	0.31	-0.15
	-0.95	-1.05	-0.62	-0.46	-0.42	-0.34	-0.34	-0.35	0.29	0.52	0.31	0.44
	0.61	0.66	0.57	0.44	-0.01	-0.47	-0.67	-0.69	-0.67	-0.14	0.06	0.13
23	-0.48	-0.85	-0.60	-0.38	-0.38	-0.38	-0.34	-0.31	-0.19	0.60	0.49	0.32
	0.40	0.67	0.76	0.57	0.43	0.11	-0.65	-0.73	-0.78	-0.35	0.13	0.32
	0.18	-0.95	-1.10	-0.62	-0.42	-0.45	-0.34	-0.34	-0.31	0.01	0.71	0.31
	0.38	0.59	0.76	0.77	0.11	0.50	-0.40	-0.86	-0.86	-0.84	-0.34	0.16
24	0.22	-0.31	-0.77	-0.65	-0.42	-0.41	-0.37	-0.30	-0.35	-0.27	0.53	0.56
	0.36	0.35	0.67	0.79	0.89	0.62	0.05	-0.77	-0.85	-0.93	-0.51	0.13
	0.30	0.31	-0.74	-1.25	-0.61	-0.42	-0.37	-0.41	-0.34	-0.30	-0.23	0.79
	0.38	0.38	0.57	0.76	0.90	0.69	0.81	-0.64	-0.78	-0.92	-0.90	-0.46
25	0.08	0.23	-0.08	-0.74	-0.97	-0.51	-0.37	-0.37	-0.33	-0.38	-0.27	0.33
	0.60	0.32	0.39	0.72	0.79	0.89	0.56	0.24	-0.39	-0.90	-0.92	-0.80
	0.08	0.13	0.42	-0.52	-1.05	-0.87	-0.39	-0.49	-0.37	-0.37	-0.34	-0.27
	0.56	0.41	0.36	0.55	0.73	0.92	0.70	0.50	0.05	-0.58	-0.91	-0.93
26	-0.66	0.13	0.18	0.27	-0.64	-1.05	-0.71	-0.42	-0.41	-0.37	-0.42	-0.31
	0.25	0.56	0.35	0.58	0.67	0.97	0.83	0.62	0.30	-0.26	-0.58	-0.91
	-0.86	-0.33	0.17	0.57	-0.27	-1.20	-1.04	-0.70	-0.46	-0.41	-0.33	-0.38
	-0.30	0.17	0.52	0.35	0.39	0.59	0.55	0.97	0.57	0.31	-0.26	-0.65
27	-0.79	-0.63	-0.08	0.27	0.38	-0.27	-1.09	-1.07	-0.60	-0.38	-0.37	-0.37
	-0.30	-0.18	0.67	0.31	0.38	0.69	0.71	0.77	0.63	0.37	-0.07	-0.39
	-0.71	-0.53	-0.47	0.18	0.44	0.12	-0.86	-1.31	-0.85	-0.56	-0.42	-0.37
	-0.33	-0.38	-0.22	0.56	0.38	0.20	0.39	0.55	0.60	0.59	0.38	0.12
28	-0.27	-0.47	-0.54	-0.02	0.25	0.50	0.12	-0.79	-1.34	-1.01	-0.56	-0.42
	-0.37	-0.33	-0.26	0.29	0.38	0.28	0.59	0.57	0.59	0.57	0.31	0.18
	-0.20	-0.33	-0.34	-0.40	0.05	0.31	0.12	-0.40	-1.19	-1.19	-0.77	-0.47
	-0.41	-0.41	-0.38	-0.30	-0.11	0.48	0.25	0.23	0.24	0.32	0.36	0.21
29	0.22	0.07	-0.09	-0.15	-0.09	0.20	0.43	0.30	-0.09	-0.87	-1.16	-0.91
	-0.57	-0.47	-0.35	-0.35	-0.16	0.19	0.28	0.35	0.39	0.40	0.34	0.23
	0.15	0.04	-0.03	-0.09	-0.16	-0.09	0.10	0.23	-0.02	-0.28	-1.03	-1.03
	-0.75	-0.61	-0.43	-0.35	-0.31	-0.12	0.12	0.24	0.25	0.28	0.08	-0.05
30	0.05	0.16	0.17	0.18	0.09	0.19	0.14	0.07	0.27	-0.12	-0.32	-0.78
	-0.96	-0.90	-0.68	-0.56	-0.39	-0.31	-0.24	0.04	0.12	0.18	0.25	-0.01
	0.10	0.01	-0.04	0.07	0.14	0.08	-0.08	-0.07	-0.18	-0.24	-0.18	-0.24
	-0.64	-0.80	-0.66	-0.47	-0.39	-0.47	-0.28	-0.32	-0.13	0.07	0.19	0.11
31	0.16	0.23	0.12	0.29	0.26	0.40	0.45	0.58	0.25	0.38	0.38	0.06
	0.19	-0.49	-0.87	-1.28	-1.12	-0.93	-0.74	-0.34	-0.16	0.03	0.13	0.21
	0.23	0.30	0.05	-0.14	0.06	0.13	0.64	0.00	-0.06	-0.32	-0.32	-0.52
	-0.20	-0.72	-0.56	-0.67	-0.45	-0.89	-0.54	-0.48	-0.36	-0.33	-0.29	-0.27

November 1991

1	-0.15	0.05	-0.02	-0.01	0.10	0.08	0.16	0.13	0.20	0.14	0.05	-0.08
	-0.14	-0.27	-0.34	-0.21	-0.54	-0.76	-0.73	-0.67	-0.73	-0.41	-0.33	-0.12
	0.01	0.26	0.48	-0.01	0.31	0.18	-0.34	0.18	0.31	-0.01	-0.01	-0.07
	0.06	-0.38	-0.58	-0.45	-0.20	-0.91	-1.21	-1.09	-0.78	-0.66	-0.49	-0.53
2	-0.50	-0.35	-0.15	0.09	0.08	0.11	0.00	0.08	0.15	0.28	0.35	0.28
	-0.04	-0.36	-0.43	-0.43	-0.43	-0.37	-0.31	-1.09	-1.02	-0.94	-0.57	-0.57
	-0.49	-0.50	-0.15	-0.03	0.15	0.20	0.25	0.10	0.33	-0.19	0.29	0.35
	0.22	0.03	-0.29	0.09	-0.35	-0.22	-0.22	-0.61	-0.87	-1.49	-1.53	-0.48

3	-0.64	-0.39	-0.43	-0.16	0.33	0.12	0.40	0.56	0.34	0.27	0.27	0.46
	0.26	-0.05	-0.24	-0.30	-0.49	-0.24	-0.69	-0.31	-0.97	-0.65	-1.53	-0.80
	-0.60	-0.47	-0.51	-0.40	0.11	0.12	0.37	0.40	0.65	0.23	0.20	0.52
	0.26	0.20	-0.05	-0.17	-0.36	-0.37	-0.43	0.01	-0.24	-0.75	-1.23	-1.42
4	-0.96	-0.57	-0.48	-0.48	-0.36	0.27	0.23	0.48	0.76	0.59	0.52	0.64
	0.32	0.20	0.07	-0.23	-0.36	-0.42	-0.74	-0.31	-0.05	-0.05	-1.26	-1.89
	-1.38	-0.75	-0.52	-0.52	-0.52	-0.45	-0.25	0.26	0.24	0.25	0.40	0.39
	0.37	0.20	0.33	-0.12	-0.51	-0.91	-0.55	-0.47	-0.05	-0.04	-0.20	-0.82
5	-1.10	-0.75	-0.53	-0.45	-0.46	-0.43	-0.31	0.20	0.25	0.49	0.66	0.88
	0.80	0.53	0.72	-0.09	-0.28	-0.91	-0.80	-0.68	0.09	0.22	0.34	-0.74
	-1.40	-1.75	-0.78	-0.62	-0.45	-0.45	-0.46	-0.43	0.39	-0.02	0.28	0.57
	0.52	0.44	0.22	0.28	-0.24	-0.50	-0.70	-0.84	-0.59	-0.04	0.24	0.24
6	-0.64	-1.07	-0.94	-0.53	-0.41	-0.45	-0.38	-0.35	-0.31	0.41	0.25	0.88
	0.08	0.61	0.61	0.70	0.25	-0.33	-0.52	-0.99	-0.55	-0.46	0.17	0.39
	-0.14	-0.88	-1.34	-0.75	-0.53	-0.45	-0.42	-0.42	-0.35	-0.19	0.44	0.25
	0.27	0.45	0.39	0.54	0.43	0.25	-0.40	-0.67	-0.79	-0.71	-0.49	0.10
7	-0.08	-0.23	-0.71	-0.75	-0.50	-0.39	-0.40	-0.41	-0.33	-0.17	0.49	0.31
	0.29	0.54	0.71	0.62	0.86	0.65	0.58	-0.42	-0.87	-0.44	-0.44	0.21
	0.53	-0.05	-1.20	-1.61	-1.17	-0.56	-0.58	-0.38	-0.39	-0.40	0.08	0.39
	0.37	0.51	0.40	0.47	0.46	0.47	0.53	-0.05	-0.56	-1.36	-0.40	-0.44
8	0.04	0.31	-0.06	-0.76	-1.27	-0.67	-0.50	-0.46	-0.43	-0.36	-0.24	0.44
	0.28	0.34	0.61	0.74	0.49	0.67	0.53	0.27	-0.23	-0.81	-0.57	-0.31
	0.08	0.27	0.21	-0.69	-1.41	-1.46	-0.68	-0.50	-0.46	-0.39	-0.39	-0.12
	0.40	0.32	0.35	0.50	0.48	0.35	0.31	0.21	-0.11	-0.31	-0.58	-0.70
9	-0.34	0.16	0.25	0.06	-0.70	-1.18	-0.71	-0.57	-0.45	-0.38	-0.39	-0.36
	0.30	0.33	0.29	0.45	0.62	0.61	0.40	0.41	0.02	-0.37	-0.31	-0.61
	-0.38	-0.01	0.28	0.35	-0.37	-0.99	-1.06	-0.84	-0.53	-0.41	-0.42	-0.39
	-0.32	0.26	0.36	0.26	0.41	0.42	0.33	0.36	0.11	-0.17	-0.28	-0.54
10	-0.53	-0.17	0.13	0.43	0.32	-0.40	-1.07	-0.98	-0.58	-0.49	-0.41	-0.38
	-0.35	0.05	0.36	0.21	0.35	0.49	0.53	0.36	0.18	-0.05	-0.24	-0.45
	-0.54	-0.42	-0.22	0.13	0.27	-0.06	-0.88	-0.88	-0.62	-0.49	-0.42	-0.38
	-0.35	-0.32	0.14	0.33	0.33	0.14	0.20	0.32	0.26	0.44	0.10	-0.02
11	-0.24	-0.39	-0.19	-0.13	-0.08	-0.13	-0.13	-0.84	-0.77	-0.64	-0.55	-0.47
	-0.40	-0.17	0.07	0.07	0.15	0.21	0.27	0.13	0.14	0.32	0.08	-0.13
	0.13	-0.13	0.09	0.46	0.59	0.20	-0.44	-0.70	-1.29	-1.20	-0.79	-0.47
	-0.43	-0.27	-0.16	0.11	0.24	0.36	0.61	0.22	-0.03	-0.03	-0.02	-0.13
12	-0.02	-0.35	-0.13	-0.03	0.15	0.46	0.26	-0.06	-0.77	-1.14	-0.99	-0.79
	-0.51	-0.47	-0.36	-0.16	0.23	0.20	0.31	0.35	0.36	0.34	0.09	0.31
	0.00	0.13	-0.06	-0.13	-0.06	0.20	-0.12	0.26	-0.06	-0.76	-1.04	-0.78
	-1.34	-0.61	-0.51	-0.32	-0.12	0.00	0.08	0.22	0.15	0.08	-0.24	-0.14
13	0.00	0.01	-0.08	-0.03	0.05	0.14	-0.55	-0.18	-0.64	-0.18	-0.70	-0.24
	-0.28	-0.49	-0.40	-0.04	-0.07	0.15	0.18	0.27	-0.38	0.38	-0.02	0.48
	-0.17	0.22	-0.16	-0.49	0.22	0.42	-0.68	-0.16	-0.75	-0.43	-0.61	-0.50
	-0.97	-0.59	-0.49	-0.24	-0.36	0.16	-0.03	0.11	0.14	0.01	-0.33	0.10
14	-0.31	0.15	0.28	0.24	0.07	0.14	0.27	0.33	-0.11	-0.24	-0.18	-0.62
	-0.50	-1.16	-0.79	-0.76	-0.50	-0.48	-0.21	-0.12	-0.03	-0.07	-0.35	-0.39
	-0.17	-0.07	-0.21	-0.16	-0.02	0.15	-0.15	-0.20	-0.25	-0.41	-0.10	-0.51
	-0.49	-0.65	-0.47	-0.59	-0.47	-0.39	-0.32	-0.24	-0.20	-0.12	-0.12	-0.02
15	-0.17	-0.09	-0.04	0.00	0.02	0.16	0.15	0.17	0.14	0.09	0.19	0.09
	-0.17	-0.43	-0.59	-0.81	-0.63	-0.56	-0.45	-0.32	-0.12	-0.11	0.02	-0.06

	-0.10	-0.10	-0.24	-0.09	-0.04	0.02	0.07	0.04	-0.07	-0.01	-0.23	-0.23
	-0.23	-0.34	-0.34	-0.54	-0.75	-0.54	-0.28	-0.61	-0.36	-0.17	-0.13	-0.07
16	0.05	0.02	-0.14	-0.05	-0.05	0.10	0.07	0.19	0.10	0.16	0.14	0.11
	0.11	0.04	-0.15	-0.61	-0.67	-0.80	-0.77	-0.71	-0.47	-0.39	-0.39	-0.19
	0.01	0.05	-0.02	-0.10	-0.14	-0.18	0.00	-0.09	0.06	0.02	-0.07	-0.07
	-0.02	-0.32	-0.22	-0.27	-0.32	-0.54	-0.69	-0.59	-0.43	-0.43	-0.36	-0.30
17	-0.18	0.01	0.05	0.06	0.19	0.04	-0.04	0.01	0.06	0.17	0.31	0.02
	0.12	0.19	0.05	-0.07	-0.21	-0.45	-0.62	-0.96	-0.73	-0.49	-0.52	-0.41
	-0.29	-0.14	0.02	0.06	0.19	0.13	0.10	0.02	0.08	0.15	0.16	0.17
	0.14	-0.32	-0.09	-0.14	-0.02	-0.32	-0.36	-0.81	-0.86	-0.67	-0.57	-0.44
18	-0.37	-0.21	-0.05	0.06	0.19	0.29	0.24	0.22	0.10	0.16	0.28	0.42
	0.26	-0.07	0.19	-0.13	-0.13	-0.13	-0.32	-0.52	-1.10	-1.00	-0.82	-0.60
	-0.48	-0.36	-0.29	0.02	0.07	0.15	0.30	0.29	-0.01	-0.15	0.05	0.16
	0.18	-0.09	-0.24	-0.47	-0.45	-0.43	-0.24	-0.33	-0.45	-0.64	-0.59	-0.58
19	-0.48	-0.45	-0.42	-0.25	0.06	0.09	0.16	0.29	0.33	0.11	0.14	0.22
	0.08	0.14	-0.01	-0.18	-0.35	-0.12	0.00	-0.24	-0.35	-0.98	-1.16	-0.86
	-0.57	-0.70	-0.40	-0.54	-0.47	-0.30	0.02	0.14	0.05	0.01	0.01	0.06
	0.07	0.00	-0.08	-0.25	-0.41	-0.49	-0.29	-0.09	-0.01	-0.37	-0.61	-0.83
20	-0.65	-0.68	-0.61	-0.59	-0.50	-0.61	-0.37	0.28	0.15	0.02	0.20	-0.05
	0.02	-0.18	-0.36	-0.46	-0.59	-0.71	-0.58	-0.47	-0.07	-0.05	-0.46	-0.78
	-0.82	-0.69	-0.63	-0.61	-0.53	-0.64	-0.46	-0.41	0.19	0.11	0.06	0.08
	0.12	-0.02	-0.18	-0.46	-0.50	-0.63	-0.74	-0.62	-0.28	-0.07	-0.22	-0.53
21	-0.77	-0.59	-0.56	-0.58	-0.47	-0.48	-0.48	-0.44	-0.07	0.26	0.15	0.17
	0.16	0.16	0.16	-0.11	-0.26	-0.46	-0.65	-0.80	-0.41	-0.04	-0.02	-0.28
	-0.67	-0.93	-0.66	-0.55	-0.57	-0.41	-0.42	-0.38	-0.42	0.00	0.16	0.12
	0.10	0.22	0.19	0.24	0.01	-0.31	-0.47	-0.82	-0.69	-0.45	-0.01	0.03
22	-0.38	-0.68	-0.77	-0.53	-0.50	-0.43	-0.44	-0.41	-0.42	0.30	0.24	0.29
	0.50	0.56	0.46	0.57	0.35	-0.04	-0.49	-0.63	-0.83	-0.56	-0.13	0.13
	0.21	-0.83	-1.27	-0.87	-0.65	-0.50	-0.51	-0.44	-0.49	-0.42	0.06	0.37
	0.28	0.27	0.36	0.49	0.29	0.34	-0.05	-0.51	-0.77	-0.85	-0.61	-0.04
23	0.11	0.13	-0.61	-1.04	-0.66	-0.51	-0.48	-0.45	-0.42	-0.49	-0.18	0.62
	0.19	0.36	0.64	0.74	0.57	0.37	0.24	-0.15	-0.60	-1.01	-0.69	-0.33
	0.06	0.26	-0.32	-1.08	-1.14	-0.62	-0.55	-0.48	-0.45	-0.51	-0.44	-0.22
	0.58	0.27	0.32	0.41	0.43	0.56	0.48	0.37	-0.15	-0.68	-0.89	-0.72
24	-0.35	0.20	0.33	-0.15	-1.07	-1.16	-0.57	-0.53	-0.46	-0.44	-0.45	-0.43
	0.56	0.36	0.34	0.61	0.65	0.61	0.64	0.38	0.18	-0.33	-0.78	-0.92
	-0.76	0.01	0.13	0.17	-0.78	-1.37	-0.96	-0.57	-0.49	-0.51	-0.44	-0.46
	-0.38	0.49	0.28	0.33	0.45	0.53	0.45	0.65	0.57	0.12	-0.14	-0.52
25	-0.59	-0.53	0.19	0.38	0.19	-0.52	-1.56	-1.46	-0.70	-0.60	-0.49	-0.46
	-0.35	0.37	0.22	0.44	0.70	0.83	0.78	0.38	0.32	0.00	-0.13	-0.57
	-0.65	-1.05	-0.47	-0.04	-0.14	-0.41	-0.96	-1.02	-0.72	-0.49	-0.46	-0.47
	-0.49	-0.47	-0.35	0.36	0.35	0.17	0.30	0.32	0.37	0.44	0.34	0.25
26	-0.37	-0.41	-0.53	-0.10	0.13	0.18	-0.03	-0.88	-1.13	-0.89	-0.52	-0.53
	-0.42	-0.48	-0.41	0.37	0.22	0.21	0.47	0.45	0.28	0.31	0.12	0.08
	-0.31	-0.41	-0.47	-0.35	-0.30	0.16	0.01	-0.30	-1.00	-0.98	-0.60	-0.49
	-0.47	-0.44	-0.46	-0.44	-0.30	0.46	0.35	0.14	0.30	0.28	0.32	0.22
27	0.31	0.02	-0.20	-0.20	-0.14	0.12	0.50	0.52	-0.26	-1.19	-1.26	-0.98
	-0.60	-0.60	-0.45	-0.43	-0.31	0.22	0.25	0.30	0.37	0.39	0.25	0.06
	-0.04	-0.14	-0.25	-0.40	-0.45	-0.34	-0.06	-0.01	0.00	-0.49	-0.64	-1.04
	-0.52	-0.46	-0.52	-0.45	-0.48	-0.40	-0.25	0.34	0.33	0.18	0.10	0.15

28 0.24 0.14 0.11 0.08 -0.10 -0.14 0.00 0.16 0.35 0.14 -0.35 -0.73
-1.12 -0.76 -0.55 -0.56 -0.46 -0.39 -0.22 0.20 0.19 0.18 0.27 0.13
0.10 0.03 0.04 -0.05 -0.05 -0.09 -0.14 -0.29 -0.05 0.01 -0.09 -0.48
-0.81 -0.76 -0.63 -0.41 -0.46 -0.48 -0.46 -0.38 0.05 0.43 0.19 0.15
29 0.27 0.21 0.24 0.18 0.31 0.17 0.18 0.21 0.20 0.27 0.33 0.07
-0.18 -0.77 -1.37 -1.15 -0.79 -0.67 -0.47 -0.40 -0.33 -0.01 0.19 0.19
0.21 0.10 -0.02 -0.01 -0.14 -0.01 -0.05 0.05 -0.14 -0.19 -0.14 -0.04
0.06 -0.39 -0.56 -0.82 -0.66 -0.59 -0.45 -0.47 -0.45 -0.23 -0.18 0.27
30 0.16 0.19 0.12 0.16 0.18 0.15 0.17 0.15 0.22 0.09 0.08 0.03
0.22 0.20 -0.39 -0.68 -0.89 -0.86 -0.75 -0.50 -0.43 -0.40 -0.33 -0.13
0.16 0.15 0.27 0.09 -0.02 -0.02 0.03 0.08 0.00 0.10 0.12 -0.08
0.12 0.03 -0.02 -0.29 -0.54 -0.98 -0.72 -0.62 -0.51 -0.48 -0.42 -0.34
December 1991
1 -0.17 0.18 0.28 0.16 0.28 0.14 0.20 0.08 0.10 0.11 0.17 0.04
-0.02 -0.07 0.14 0.23 -0.31 -0.56 -0.84 -0.86 -0.79 -0.62 -0.43 -0.45
-0.42 -0.30 0.10 0.21 0.12 -0.04 0.20 -0.03 -0.03 0.02 -0.02 0.03
-0.10 -0.14 -0.14 -0.01 -0.01 -0.14 -0.40 -0.39 -0.82 -0.54 -0.48 -0.50
2 -0.44 -0.41 -0.27 0.08 0.46 0.33 0.12 0.20 0.18 0.15 0.04 0.09
0.06 -0.08 -0.18 -0.08 0.38 -0.23 -0.18 -0.33 -0.78 -0.84 -0.61 -0.58
-0.40 -0.46 -0.44 -0.31 0.07 0.36 0.21 0.16 0.09 0.13 0.10 0.11
0.04 -0.09 -0.22 -0.31 -0.14 -0.01 0.00 -0.04 -0.35 -0.75 -0.65 -0.54
3 -0.44 -0.46 -0.44 -0.36 -0.27 0.36 0.39 0.17 0.28 0.21 0.28 0.22
0.20 0.12 -0.12 -0.28 -0.22 -0.17 0.07 0.18 -0.01 -0.58 -0.86 -0.83
-0.57 -0.46 -0.48 -0.46 -0.39 -0.21 0.16 0.34 0.16 0.16 0.25 0.11
0.12 0.18 -0.13 -0.13 -0.31 -0.26 -0.13 0.09 0.10 0.01 -0.59 -0.76
4 -0.69 -0.50 -0.52 -0.41 -0.43 -0.35 0.12 0.48 0.25 0.28 0.38 0.39
0.40 0.28 0.15 -0.12 -0.33 -0.34 -0.37 -0.12 0.03 0.03 -0.27 -0.76
-0.86 -0.73 -0.53 -0.43 -0.36 -0.51 -0.35 0.03 0.48 0.25 0.25 0.30
0.24 0.28 0.26 0.13 -0.12 -0.37 -0.42 -0.27 -0.13 0.06 0.12 -0.37
5 -0.63 -0.87 -0.61 -0.50 -0.48 -0.41 -0.43 -0.31 0.30 0.51 0.25 0.33
0.32 0.31 0.31 0.13 -0.17 -0.27 -0.51 -0.36 -0.39 0.00 0.10 0.11
-0.54 -0.80 -0.72 -0.50 -0.47 -0.46 -0.43 -0.36 -0.27 0.27 0.40 0.21
0.17 0.25 0.23 0.30 0.15 -0.17 -0.22 -0.35 -0.39 -0.26 -0.01 0.26
6 -0.12 -0.52 -0.77 -0.61 -0.46 -0.44 -0.46 -0.44 -0.36 0.23 0.53 0.25
0.29 0.35 0.43 0.40 0.24 0.04 -0.28 -0.34 -0.62 -0.44 -0.13 -0.04
0.11 -0.35 -0.72 -0.80 -0.49 -0.43 -0.49 -0.42 -0.35 -0.36 -0.01 0.48
0.30 0.17 0.21 0.55 -0.04 0.23 0.02 -0.17 -0.35 -0.39 -0.26 0.00
7 0.14 0.20 -0.21 -0.78 -0.77 -0.56 -0.46 -0.44 -0.41 -0.38 0.21 0.39
0.33 0.30 0.49 0.48 0.39 0.26 -0.06 -0.22 -0.38 -0.52 -0.51 -0.35
0.15 0.07 -0.17 -0.80 -0.85 -0.48 -0.49 -0.47 -0.41 -0.43 -0.45 0.04
0.48 0.34 0.17 0.26 0.23 0.39 0.25 0.18 -0.22 -0.32 -0.40 -0.39
8 0.01 0.15 0.27 -0.12 -0.83 -0.91 -0.60 -0.49 -0.35 -0.44 -0.15 -0.37
0.45 0.29 0.29 0.43 0.45 0.48 0.26 -0.01 -0.22 -0.33 -0.52 -0.59
-0.30 0.01 0.11 -0.17 -0.57 -0.82 -0.64 -0.50 -0.48 -0.46 -0.54 -0.31
-0.11 0.55 0.31 0.25 0.25 0.35 0.21 0.19 0.07 -0.21 -0.40 -0.39
9 -0.29 -0.09 0.13 0.28 0.12 -0.68 -0.91 -0.64 -0.42 -0.51 -0.45 -0.43
-0.25 0.43 0.38 0.29 0.38 0.46 0.30 0.29 0.16 -0.06 -0.44 -0.42
-0.64 -0.43 -0.08 0.00 0.10 -0.48 -0.74 -0.60 -0.53 -0.48 -0.41 -0.48
-0.36 -0.32 0.20 0.48 0.18 0.21 0.17 0.18 0.15 0.04 -0.25 -0.17
10 -0.25 -0.33 -0.13 0.15 0.26 0.15 -0.39 -0.67 -0.76 -0.49 -0.47 -0.49

	-0.43	-0.20	0.39	0.30	0.25	0.29	0.44	0.28	0.31	0.03	-0.22	-0.46
	-0.35	-0.39	-0.38	-0.09	0.00	-0.08	-0.38	-0.69	-0.60	-0.50	-0.44	-0.47
	-0.40	-0.36	-0.43	0.11	0.46	0.19	0.14	0.13	0.17	0.18	0.07	-0.05
11	-0.13	-0.21	-0.17	-0.01	0.04	0.22	0.16	-0.44	-0.59	-0.73	-0.56	-0.46
	-0.39	-0.41	-0.34	0.12	0.31	0.25	0.17	0.22	0.24	0.05	0.10	-0.12
	-0.12	-0.21	-0.25	-0.21	-0.08	0.05	-0.08	-0.30	-0.58	-0.76	-0.49	-0.43
	-0.49	-0.42	-0.35	-0.31	0.09	0.43	0.10	0.10	0.09	0.10	0.06	0.03
12	-0.01	-0.13	-0.13	-0.05	0.04	0.13	0.20	0.27	-0.36	-0.71	-0.74	-0.60
	-0.49	-0.38	-0.49	-0.28	-0.02	0.32	0.10	0.21	0.22	0.11	0.04	-0.04
	-0.12	-0.12	-0.12	-0.17	-0.21	-0.08	-0.04	-0.08	-0.33	-0.33	-0.64	-0.53
	-0.42	-0.49	-0.38	-0.39	-0.31	-0.16	0.42	0.11	0.10	0.10	0.10	0.06
13	-0.05	0.07	0.07	0.00	0.09	0.10	0.15	0.42	0.19	-0.22	-0.57	-0.84
	-0.69	-0.56	-0.49	-0.38	-0.31	-0.18	0.15	0.10	0.14	0.18	0.07	0.16
	-0.04	-0.12	-0.12	-0.12	-0.12	-0.12	-0.08	0.01	-0.03	-0.12	-0.38	-0.45
	-0.60	-0.52	-0.42	-0.39	-0.36	-0.28	-0.15	0.25	0.23	0.06	0.10	0.10
14	0.07	0.07	0.00	0.09	0.10	0.06	0.16	0.34	0.42	0.24	0.09	-0.36
	-0.70	-0.67	-0.97	-0.65	-0.40	-0.36	-0.21	0.02	0.10	0.15	0.24	0.13
	-0.08	-0.08	-0.07	-0.03	-0.03	0.07	-0.11	0.03	0.03	0.19	0.05	-0.39
	-0.47	-0.75	-0.54	-0.64	-0.40	-0.37	-0.34	-0.18	0.02	0.10	0.10	0.14
15	0.10	-0.01	-0.05	-0.05	0.00	0.09	0.01	0.15	0.17	0.19	0.21	0.10
	-0.16	-0.32	-0.82	-0.67	-0.63	-0.56	-0.41	-0.33	-0.18	0.02	0.02	0.10
	0.14	0.07	-0.09	-0.13	0.04	-0.04	0.05	-0.03	0.01	0.02	0.02	-0.02
	-0.17	-0.17	-0.40	-0.65	-0.61	-0.41	-0.49	-0.30	-0.26	-0.14	0.02	0.08
16	0.12	0.12	0.13	0.11	0.07	0.13	-0.04	0.06	0.27	0.14	0.25	0.25
	0.27	-0.18	-0.25	-0.58	-0.82	-0.93	-0.66	-0.67	-0.42	-0.39	-0.31	-0.08
	0.00	0.04	0.12	-0.03	-0.07	-0.07	-0.06	0.02	0.07	-0.01	0.00	0.00
	-0.04	-0.18	-0.13	-0.23	-0.27	-0.62	-0.59	-0.46	-0.43	-0.39	-0.36	-0.22
17	-0.02	0.14	0.14	0.19	0.21	0.10	0.02	0.08	0.04	0.16	0.19	0.02
	0.08	0.10	0.06	-0.20	-0.33	-0.47	-0.98	-0.80	-0.78	-0.60	-0.56	-0.42
	-0.26	-0.18	-0.02	0.14	0.14	0.11	-0.04	0.08	0.05	0.02	0.21	0.14
	-0.10	-0.20	-0.15	-0.15	-0.29	-0.52	-0.29	-0.45	-0.60	-0.59	-0.56	-0.46
18	-0.52	-0.36	-0.23	-0.10	0.23	0.14	0.10	0.23	0.05	0.33	0.35	0.38
	0.27	0.42	0.36	0.10	0.10	-0.16	-0.48	-0.22	-1.13	-1.00	-1.21	-0.70
	-0.64	-0.52	-0.45	-0.10	0.06	0.15	0.29	0.35	0.16	0.08	0.15	0.10
	-0.11	-0.11	-0.23	-0.17	-0.17	-0.17	0.21	-0.36	-0.35	-0.97	-1.07	-0.86
19	-0.68	-0.61	-0.51	-0.35	-0.11	0.05	0.21	0.32	0.52	0.34	0.37	0.24
	0.32	0.19	0.00	-0.32	-0.84	-0.40	-0.07	-0.13	-0.40	-0.60	-1.27	-1.10
	-0.89	-0.60	-0.57	-0.51	-0.40	-0.23	0.09	0.13	0.26	0.26	0.18	0.07
	0.09	0.21	0.01	-0.03	-0.38	-0.09	-0.49	-0.26	-0.05	-0.15	-0.43	-0.95
20	-1.29	-0.75	-0.63	-0.52	-0.53	-0.34	0.22	0.23	0.35	0.60	0.51	0.82
	0.36	0.17	-0.14	-0.02	-0.02	-0.46	-0.33	-0.27	-0.14	-0.14	-0.78	-0.93
	-1.72	-1.18	-0.76	-0.67	-0.60	-0.53	-0.54	-0.52	0.07	0.06	0.18	0.25
	0.26	0.33	0.41	0.38	0.17	-0.29	-0.35	-0.82	-0.29	0.15	0.10	-0.22
21	-1.07	-1.32	-1.30	-0.78	-0.71	-0.64	-0.62	-0.59	-0.02	0.26	0.38	0.50
	0.66	0.57	0.43	0.11	-0.07	-0.39	-0.33	-0.71	-0.92	-0.61	-0.28	-0.28
	-0.86	-1.22	-1.27	-0.86	-0.75	-0.60	-0.62	-0.51	-0.60	-0.14	0.22	0.15
	0.42	0.30	0.36	0.63	0.30	0.24	-0.08	-0.65	-0.72	-1.00	-0.48	-0.05
22	-0.11	-0.57	-1.20	-1.37	-0.81	-0.58	-0.66	-0.56	-0.49	-0.25	0.27	0.45
	0.36	0.75	0.42	0.41	0.34	0.15	-0.04	-0.41	-0.61	-0.49	-1.35	-0.31
	-0.37	-0.25	-0.89	-1.31	-1.02	-0.65	-0.59	-0.56	-0.58	-0.51	-0.52	-0.03

	0.40	0.28	0.29	0.47	0.35	0.57	0.47	0.15	-0.10	-0.87	-1.35	-0.63
23	-0.16	-0.05	0.01	-0.43	-1.23	-1.17	-0.72	-0.49	-0.54	-0.59	-0.49	0.02
	0.48	0.39	0.41	0.63	0.73	0.84	0.26	-0.12	-0.12	-0.25	-0.38	-0.83
	-0.78	-0.20	-0.13	-0.87	-1.06	-1.23	-0.80	-0.64	-0.53	-0.55	-0.57	-0.50
	-0.52	0.59	0.25	0.26	0.22	0.12	0.25	0.56	0.52	0.45	-0.32	-1.21
24	-0.70	-0.28	0.15	0.15	0.01	-0.87	-1.41	-0.76	-0.55	-0.56	-0.54	-0.47
	-0.49	0.12	0.46	0.26	0.59	0.62	0.62	0.82	0.49	-0.03	-0.41	-0.87
	-1.15	-0.99	-0.28	0.23	0.30	-0.49	-1.08	-1.07	-0.63	-0.56	-0.54	-0.39
	-0.53	-0.51	-0.43	0.20	0.53	0.14	0.15	0.33	0.24	0.34	0.33	-0.20
25	-0.61	-0.81	-0.55	-0.29	0.16	0.28	0.08	-0.75	-0.94	-0.61	-0.50	-0.48
	-0.50	-0.53	-0.41	0.22	0.52	0.32	0.21	0.45	0.49	0.45	0.23	-0.15
	-0.47	-0.76	-0.81	-0.71	-0.21	0.03	-0.04	-0.42	-0.76	-0.61	-0.56	-0.52
	-0.48	-0.45	-0.42	-0.49	-0.40	0.64	0.38	0.17	0.17	0.21	0.23	0.27
26	0.21	-0.15	-0.51	-0.45	-0.44	0.00	0.14	0.07	-0.33	-0.81	-0.67	-0.49
	-0.55	-0.49	-0.47	-0.49	-0.09	0.63	0.38	0.22	0.35	0.27	0.45	0.36
	0.23	0.03	-0.25	-0.41	-0.35	-0.31	0.18	0.35	0.12	-0.97	-1.43	-0.81
	-0.55	-0.48	-0.46	-0.61	-0.47	-0.24	0.36	0.39	0.22	0.23	0.25	0.28
27	0.28	0.26	-0.03	-0.14	-0.42	-0.19	0.11	0.28	0.64	0.39	-1.24	-1.27
	-1.08	-0.71	-0.51	-0.45	-0.54	-0.44	-0.18	0.48	0.18	0.19	0.37	0.10
	0.12	0.04	-0.19	-0.33	-0.37	-0.41	-0.48	-0.32	0.08	0.09	-0.11	-0.52
	-0.71	-0.52	-0.54	-0.53	-0.47	-0.49	-0.52	-0.32	0.19	0.39	0.21	0.07
28	0.07	0.10	0.11	0.04	0.00	-0.07	-0.15	-0.03	-0.03	0.25	0.33	0.11
	-0.70	-0.86	-0.80	-0.51	-0.57	-0.42	-0.48	-0.37	-0.05	0.33	0.19	0.14
	0.07	0.00	0.04	-0.03	-0.07	-0.15	-0.15	-0.24	-0.15	-0.07	0.10	0.07
	-0.24	-0.74	-0.71	-0.56	-0.45	-0.47	-0.49	-0.47	-0.45	-0.19	0.26	0.27
29	0.08	0.08	0.07	0.04	0.08	0.13	0.10	0.02	-0.01	0.08	0.24	0.37
	0.19	-0.18	-0.84	-0.93	-0.80	-0.62	-0.47	-0.41	-0.42	-0.39	-0.17	0.22
	0.16	-0.04	-0.04	-0.08	-0.12	-0.04	-0.16	0.04	-0.11	0.01	-0.03	0.10
	0.11	0.04	-0.32	-0.40	-0.79	-0.51	-0.52	-0.50	-0.48	-0.46	-0.38	-0.03
30	0.20	0.30	0.08	0.08	0.04	0.00	-0.07	-0.07	0.09	0.02	-0.02	0.07
	0.13	0.15	0.12	-0.33	-0.56	-0.70	-0.74	-0.46	-0.56	-0.46	-0.43	-0.41
	-0.22	-0.13	0.15	0.09	-0.04	-0.12	-0.08	-0.04	-0.04	0.00	0.04	0.00
	-0.03	0.01	-0.03	-0.11	-0.19	-0.31	-0.50	-0.58	-0.44	-0.46	-0.53	-0.46
31	-0.33	-0.18	0.27	0.28	0.09	0.08	0.04	0.08	0.09	0.13	0.10	0.12
	0.13	0.05	0.11	0.07	-0.03	-0.28	-0.43	-0.64	-0.80	-0.58	-0.50	-0.48
	-0.41	-0.43	-0.36	-0.03	0.14	-0.04	-0.08	-0.12	-0.08	0.04	0.00	0.12
	0.01	0.01	0.01	-0.10	-0.02	-0.02	-0.14	-0.14	-0.67	-0.50	-0.51	-0.44
January 1992												
1	-0.50	-0.44	-0.31	-0.17	0.25	0.22	0.20	0.16	0.13	0.13	0.11	0.16
	0.18	0.21	0.13	-0.08	-0.01	0.04	0.04	-0.39	-0.63	-0.78	-0.88	-0.57
	-0.47	-0.52	-0.46	-0.49	-0.37	-0.28	0.08	-0.03	-0.03	-0.12	0.05	0.09
	0.12	0.20	0.20	0.30	0.34	0.59	0.51	0.73	0.40	-0.31	-0.96	-0.92
2	-1.00	-0.77	-0.58	-0.42	-0.12	0.00	0.16	0.38	0.30	0.25	-0.18	-0.18
	-0.08	-0.08	-0.18	-0.28	-0.32	-0.36	-0.31	-0.35	-0.18	-0.39	-0.54	-0.43
	-0.56	-0.46	-0.53	-0.51	-0.61	-0.30	0.04	0.34	0.33	0.21	0.12	0.16
	0.20	0.22	0.16	0.27	0.11	-0.03	0.12	0.04	0.19	0.04	-0.29	-0.45
3	-0.95	-0.84	-0.71	-0.51	-0.40	-0.41	-0.17	0.15	0.19	0.28	0.30	0.21
	0.14	0.16	0.12	0.24	0.14	-0.13	-0.29	-0.29	-0.13	-0.13	-0.18	-0.40
	-0.69	-0.85	-0.71	-0.58	-0.44	-0.53	-0.43	-0.26	0.09	0.28	0.23	0.08
	0.36	0.10	0.12	0.18	0.37	0.19	-0.08	-0.13	-0.13	0.03	0.04	0.05

4	-0.31	-0.82	-1.05	-0.81	-0.55	-0.51	-0.41	-0.29	-0.01	0.19	0.23	0.37
	0.42	0.29	0.32	0.08	0.26	0.13	-0.13	-0.19	-0.19	-0.06	-0.06	0.20
	-0.13	-1.03	-1.20	-1.05	-0.59	-0.47	-0.60	-0.42	-0.35	0.16	0.31	0.23
	0.36	0.36	0.37	0.22	0.13	0.08	-0.02	-0.29	-0.40	-0.30	-0.19	0.08
5	0.18	-0.08	-0.72	-1.13	-0.89	-0.55	-0.48	-0.50	-0.39	-0.14	0.40	0.34
	0.32	0.49	0.59	0.34	0.39	0.33	-0.13	-0.13	-0.52	-0.56	-0.51	-0.08
	0.24	-0.13	-0.61	-1.04	-1.03	-0.55	-0.59	-0.49	-0.52	-0.45	-0.28	0.44
	0.31	0.18	0.19	0.25	0.11	0.21	0.10	-0.04	-0.14	-0.53	-0.46	-0.28
6	-0.07	0.03	0.08	-0.46	-0.90	-0.63	-0.48	-0.50	-0.57	-0.46	-0.14	0.52
	0.30	0.30	0.41	0.47	0.46	0.34	0.21	0.06	-0.20	-0.60	-0.51	-0.60
	-0.24	0.00	0.01	-0.44	-0.82	-0.88	-0.55	-0.45	-0.54	-0.48	-0.46	-0.29
	0.41	0.35	0.22	0.19	0.29	0.15	0.31	0.31	0.08	-0.14	-0.44	-0.59
7	-0.24	-0.01	0.15	0.16	-0.45	-0.89	-0.93	-0.52	-0.48	-0.46	-0.43	-0.18
	0.35	0.29	0.27	0.47	0.66	0.50	0.64	0.39	0.13	-0.13	-0.45	-0.65
	-0.53	0.06	0.26	-0.07	-0.59	-0.97	-1.31	-0.82	-0.52	-0.52	-0.50	-0.43
	-0.27	0.39	0.22	0.26	0.33	0.38	0.46	0.23	0.25	0.39	0.06	-0.66
8	-0.14	-0.01	0.19	0.51	-0.01	-0.45	-0.98	-1.46	-1.02	-	-	-

Table C-3. Time-series of suspended sediment concentrations (in mg l^{-1}), at 1 hour intervals (starting at 0.00 GMT, daily).

January, 1991												
17	-	-	-	-	-	6.6	8.7	7.5	9.0	7.5	7.2	7.5
18	6.6	6.6	9.9	7.2	6.9	7.2	8.1	8.7	8.7	-	-	-
	-	-	-	-	-	-	-	9.6	7.8	7.5	6.9	6.9
19	6.9	7.2	7.2	6.9	7.8	7.5	8.1	9.3	9.3	-	-	-
	-	-	-	-	-	-	8.7	7.5	9.9	10.2	9.6	9.6
20	7.8	7.8	7.2	10.8	8.1	7.8	8.4	8.7	-	-	-	-
	-	-	-	-	-	9.0	9.0	9.0	10.5	9.9	10.5	9.0
21	9.0	8.7	8.7	11.1	8.7	8.7	8.7	8.7	8.7	-	-	-
	-	-	-	-	-	8.4	8.4	8.7	10.8	9.9	10.8	8.7
22	8.4	8.4	8.4	8.4	9.3	8.4	8.4	8.7	-	-	-	-
	-	-	-	-	-	8.4	8.4	8.4	8.7	8.7	9.0	8.4
23	8.4	8.1	7.8	7.8	8.4	8.4	8.1	7.8	7.8	-	-	-
	-	-	-	-	-	7.5	7.8	7.8	7.8	7.8	8.1	8.1
24	8.1	7.8	7.5	7.5	7.5	8.4	7.8	7.8	-	-	-	-
	-	-	-	-	-	7.5	7.5	7.8	8.1	9.0	8.7	8.1
25	7.8	8.1	7.8	8.1	8.1	8.4	8.1	8.1	7.5	-	-	-
	-	-	-	-	-	7.8	7.8	7.8	7.8	7.8	8.1	8.1
26	8.1	8.1	9.0	8.4	8.4	8.1	8.1	8.4	8.4	-	-	-
	-	-	-	-	-	8.1	8.7	8.4	8.1	8.1	7.8	7.8
27	7.8	8.4	8.4	8.7	8.4	8.1	8.1	7.8	7.8	-	-	-
	-	-	-	-	-	8.1	7.8	7.8	7.8	7.8	7.8	8.1
28	8.1	8.4	8.4	8.7	8.4	8.4	7.8	7.8	7.8	-	-	-
	-	-	-	-	-	8.1	8.1	8.1	7.8	7.8	7.5	7.8
29	7.2	7.8	7.8	7.8	8.4	9.0	8.1	7.8	7.8	-	-	-
	-	-	-	-	-	8.4	8.4	8.4	8.4	8.1	8.1	7.8
30	8.4	8.1	8.1	8.1	8.4	8.7	9.0	9.0	-	-	-	-
	-	-	-	-	-	9.0	8.7	9.0	9.0	9.0	8.7	8.4
31	6.9	8.7	7.8	8.1	8.4	9.3	9.3	9.0	8.4	-	-	-
	-	-	-	-	-	8.4	10.8	10.8	9.0	8.7	8.7	8.7
February, 1991												
1	8.4	8.4	13.7	10.5	11.6	14.6	9.9	11.4	-	-	-	-
	-	-	-	-	-	-	11.9	11.4	10.8	9.9	9.3	8.7
2	9.0	8.7	10.2	10.8	9.0	9.0	9.0	11.1	-	-	-	-
	-	-	-	-	-	-	9.3	10.8	9.6	10.5	10.2	10.2
3	9.0	8.4	8.4	11.6	9.6	8.7	9.0	9.9	-	-	-	-
	-	-	-	-	-	-	8.7	11.1	10.8	10.5	9.6	8.7
4	8.7	8.7	8.7	8.7	10.8	8.7	8.7	9.0	-	-	-	-
	-	-	-	-	-	-	8.4	8.4	9.3	10.2	9.3	9.0
5	9.0	9.0	8.7	8.4	9.3	8.7	8.7	8.7	-	-	-	-
	-	-	-	-	-	9.0	9.0	9.0	10.8	9.6	9.3	9.6
6	9.0	9.0	9.0	8.7	9.9	11.1	8.7	8.7	-	-	-	-
	-	-	-	-	-	10.2	9.3	11.4	11.4	11.4	9.9	9.6
7	10.2	9.0	9.0	9.0	9.6	14.9	14.0	9.3	-	-	-	-
	-	-	-	-	-	12.5	11.6	9.6	8.4	8.4	8.7	8.7
8	11.6	9.6	10.2	9.3	10.8	11.4	10.8	-	-	-	-	-

	-	-	-	-	-	9.6	9.3	9.3	8.7	8.4	8.4	8.4
9	8.4	8.4	8.7	9.0	8.7	9.0	9.0	9.0	-	-	-	-
	-	-	-	-	-	8.4	8.4	8.4	8.4	8.4	8.4	8.4
10	8.4	8.4	8.4	9.0	8.7	8.7	8.7	9.0	-	-	-	-
	-	-	-	-	-	8.7	9.0	10.2	9.6	9.3	9.3	8.7
11	8.4	8.4	8.4	8.4	9.9	9.3	9.3	9.0	-	-	-	-
	-	-	-	-	-	10.8	9.6	9.6	9.3	9.3	9.3	9.3
12	8.4	8.7	8.4	8.7	8.7	9.3	9.3	9.3	-	-	-	-
	-	-	-	-	-	11.1	10.2	9.6	9.3	9.3	8.7	9.6
13	9.6	8.7	8.7	9.3	11.6	10.8	9.6	9.0	-	-	-	-
	-	-	-	-	-	10.5	11.9	10.8	10.8	10.2	9.3	8.7
14	10.5	9.6	8.7	8.7	9.0	9.6	11.1	9.6	-	-	-	-
	-	-	-	-	-	11.6	12.2	10.5	9.6	9.3	9.0	8.7
15	8.4	9.6	9.6	9.6	14.6	12.5	11.6	0.0	-	-	-	-
	-	-	-	-	-	14.6	10.5	15.2	14.0	11.9	10.5	10.2
16	9.0	10.2	10.2	9.0	8.7	9.0	9.0	11.1	9.6	-	-	-
	-	-	-	-	-	-	-	10.2	9.6	8.7	11.1	8.7
17	8.7	8.4	10.5	10.3	10.2	10.0	10.0	9.9	-	-	-	-
	-	-	-	-	-	11.6	11.9	12.2	12.2	11.1	10.8	9.6
18	8.7	8.1	10.5	9.6	9.3	9.3	9.3	9.6	9.6	-	-	-
	-	-	-	-	-	-	-	-	9.0	10.8	10.8	8.4
19	9.0	9.9	11.1	11.4	8.7	8.4	8.4	8.7	-	-	-	-
	-	-	-	-	-	-	8.4	8.7	9.6	10.8	9.9	9.3
20	9.3	9.0	8.7	9.3	9.3	9.3	9.3	-	-	-	-	-
	-	-	-	-	-	9.0	9.0	9.0	9.3	9.3	11.6	10.2
21	9.3	9.3	9.3	9.3	10.5	9.3	9.3	-	-	-	-	-
	-	-	-	-	-	-	9.6	9.6	10.2	10.8	10.2	10.2
22	9.3	9.0	9.3	9.3	9.0	10.5	10.2	-	-	-	-	-
	-	-	-	-	9.0	9.3	10.2	11.9	11.6	11.6	11.6	11.4
23	11.6	13.7	12.2	11.4	11.6	14.6	13.1	-	-	-	-	-
	-	-	-	-	9.0	9.0	9.3	9.9	9.6	8.7	8.1	7.5
24	7.2	7.2	5.3	5.9	8.7	8.7	-	-	-	-	-	-
March, 1991												
4	-	-	-	11.6	9.6	11.4	11.4	11.4	12.2	12.2	10.5	9.9
5	9.6	9.0	8.4	12.5	10.5	9.3	9.3	9.3	4.7	10.2	9.6	-
	-	-	-	-	7.5	8.1	9.0	9.3	10.5	9.3	9.6	9.6
6	9.0	9.0	8.4	9.3	9.3	8.7	8.7	7.8	-	-	-	-
	-	-	-	-	9.6	7.8	8.4	8.7	9.3	9.6	8.7	8.7
7	8.7	8.7	8.7	8.7	10.5	8.7	8.7	8.1	-	-	-	-
	-	-	-	-	7.2	9.0	8.7	8.7	9.0	9.3	9.3	9.3
8	9.3	9.6	9.3	9.3	9.3	9.6	9.3	9.3	13.1	14.3	13.1	12.2
	10.5	10.5	10.5	10.5	12.8	11.4	11.4	11.1	10.2	10.2	10.2	10.2
9	9.9	10.8	10.2	10.5	10.2	10.2	10.5	10.8	10.2	10.2	10.2	8.1
	7.2	6.6	8.7	8.4	-	-	-	-	-	11.6	12.2	12.2
10	12.2	12.2	12.5	12.5	12.5	12.5	12.8	13.1	13.1	13.1	13.1	12.8
	13.1	13.1	13.4	14.0	14.3	14.3	14.3	-	-	-	-	-
11	12.2	11.9	11.9	11.6	11.4	11.1	-	-	-	-	-	-
	11.4	11.4	10.5	9.9	9.0	9.3	10.2	9.9	8.7	8.7	8.7	10.2
12	10.2	9.6	9.6	8.7	11.6	8.7	8.7	8.7	8.7	11.1	8.4	-
	-	-	-	-	9.0	8.7	8.4	8.4	8.4	8.4	8.4	9.3

13	9.6	9.9	10.2	9.9	10.5	8.7	8.7	8.4	5.9	8.7	-	-
	-	-	-	5.6	7.5	9.0	9.3	9.3	9.3	9.3	9.0	8.7
14	9.3	9.3	9.3	9.3	9.3	10.8	10.8	9.9	9.6	-	-	-
	-	-	8.1	8.5	8.7	12.8	10.8	10.2	10.2	10.2	10.2	9.6
15	10.8	10.8	9.9	10.5	11.1	11.6	11.1	9.6	9.0	-	-	-
	-	-	-	6.2	7.5	11.9	10.5	10.2	10.2	10.2	10.8	10.2
16	11.1	10.5	10.5	10.8	11.4	11.9	11.1	10.2	8.4	-	-	-
	-	-	-	-	-	-	-	11.1	9.9	9.9	9.6	9.6
17	9.6	11.6	10.5	9.3	9.6	10.5	11.1	10.8	-	-	-	-
	-	-	-	-	-	-	-	12.5	11.1	9.9	9.6	8.4
18	8.1	8.1	7.8	8.4	8.7	9.3	11.1	14.6	-	-	-	-
	-	-	-	-	-	-	20.7	20.7	10.2	9.3	9.9	10.2
19	10.5	9.3	10.2	10.8	11.6	11.1	13.1	13.1	-	-	-	-
	-	-	-	-	-	-	-	12.2	15.2	13.4	11.6	11.1
20	9.3	9.0	8.1	8.7	9.3	9.3	9.3	9.3	11.1	12.2	11.6	11.1
	8.7	9.3	8.4	11.6	9.0	9.6	10.5	12.2	18.9	11.6	11.4	11.4
21	9.3	10.2	10.5	9.6	9.6	10.8	10.8	10.8	11.9	14.6	12.2	10.2
	8.7	8.7	8.1	8.4	8.4	8.1	8.7	9.0	9.0	9.6	9.6	9.6
22	9.0	8.1	8.7	8.7	9.6	8.7	8.7	8.7	-	-	-	-
	-	-	-	-	-	-	-	-	-	-	8.1	7.8
23	7.5	7.2	7.2	7.2	7.2	7.5	7.8	-	-	-	-	-
	-	-	-	-	-	-	-	-	8.1	8.7	8.4	8.4
24	8.7	7.5	7.5	7.2	7.2	7.2	7.5	7.5	-	-	-	-
	-	-	-	-	-	-	-	8.1	8.1	7.8	8.1	8.7
25	8.7	8.7	8.7	8.4	8.7	7.8	7.5	-	-	-	-	-
	-	-	-	-	-	-	-	8.8	8.1	8.7	10.2	9.3
26	9.9	9.9	9.9	8.7	7.8	7.8	7.2	7.5	-	-	-	-
	-	-	-	-	-	-	-	7.5	7.5	7.2	7.5	8.7
27	7.8	8.7	8.4	8.7	8.1	7.5	7.5	-	-	-	-	-
	-	-	-	-	-	-	-	7.8	7.5	8.1	8.7	7.8
28	7.8	9.3	9.6	9.6	9.9	9.3	8.7	-	-	-	-	-
	-	-	-	-	-	-	-	7.8	7.8	8.7	8.4	8.7
29	9.6	9.0	9.9	10.2	10.2	10.2	10.2	-	-	-	-	-
	-	-	-	-	-	-	-	8.1	7.5	7.5	8.7	8.1
30	7.8	8.7	9.0	9.6	10.2	10.8	11.4	-	-	-	-	-
	-	-	-	-	-	-	-	8.7	7.8	7.5	9.0	8.7
31	9.0	9.0	8.7	9.3	9.9	10.8	11.6	-	-	-	-	-
	-	-	-	-	-	-	-	8.4	7.2	7.2	8.4	8.7
April, 1991												
1	8.7	8.7	8.7	9.0	9.9	10.2	11.6	-	-	-	-	-
	-	-	-	-	-	-	-	10.5	10.8	8.7	8.7	9.3
2	9.3	9.3	11.4	10.2	9.9	9.6	10.5	-	-	-	-	-
	-	-	-	-	-	-	-	10.8	8.4	7.8	7.5	7.5
3	9.3	9.3	8.4	9.3	9.9	10.2	10.2	-	-	-	8.7	6.6
8	8.7	8.7	4.7	8.4	7.2	8.7	10.8	11.4	8.7	8.7	10.2	10.2
9	10.2	10.2	10.8	10.5	10.5	10.2	8.7	8.7	8.7	8.7	8.7	8.7
	8.1	8.1	8.1	8.1	7.8	8.7	8.7	9.0	9.3	9.3	9.3	10.5
10	9.6	10.2	10.5	10.8	10.5	10.2	9.9	9.6	9.0	-	-	-
	-	-	-	-	7.5	8.7	10.2	10.5	10.2	10.2	8.7	8.7
11	8.7	8.7	8.7	8.7	9.0	8.7	8.7	8.7	8.1	8.1	8.1	8.1

	7.8	8.1	7.5	7.8	7.8	8.7	9.9	10.2	10.5	11.4	10.8	9.9
12	9.0	9.3	9.3	9.3	9.3	10.5	9.6	7.8	7.2	-	-	-
	-	-	-	-	-	-	6.2	8.4	9.3	9.3	9.0	8.7
13	9.3	9.3	9.3	9.3	9.3	9.6	11.1	9.3	-	-	-	-
	-	-	-	-	8.1	11.1	9.3	8.4	8.1	8.1	8.1	8.1
14	8.1	8.1	8.1	8.1	8.7	9.6	9.3	9.3	8.1	8.1	8.1	7.8
	8.1	8.1	7.2	7.2	7.8	8.4	9.0	9.0	8.1	8.1	8.1	8.1
15	8.1	7.8	9.6	6.5	4.4	5.9	5.9	7.2	7.2	6.2	6.2	6.2
May, 1991												
1	6.6	6.6	10.2	6.9	6.9	6.9	8.4	8.4	7.5	8.7	8.7	5.6
	7.2	0.6	8.7	6.9	6.9	7.5	8.4	8.1	9.3	8.4	8.4	8.1
2	7.8	7.8	7.8	8.7	7.5	7.5	8.4	8.4	8.7	9.3	7.2	8.1
	7.5	7.2	7.2	8.7	6.9	7.5	7.8	8.7	8.7	8.4	7.5	7.2
3	7.8	8.1	7.8	8.4	8.4	8.1	8.1	8.4	9.0	8.7	8.1	8.7
	5.6	4.1	3.8	7.2	8.7	6.9	7.8	8.1	8.4	7.8	6.9	7.5
4	7.2	7.5	7.5	6.9	6.9	8.1	7.8	8.1	8.1	8.7	8.4	7.8
	5.6	5.3	5.6	6.2	7.5	6.2	6.2	6.2	7.8	8.7	7.8	7.5
5	7.8	7.2	7.2	7.2	7.2	7.5	7.5	7.8	8.4	9.0	8.7	7.2
	8.1	4.1	5.3	5.6	7.2	7.2	5.6	6.2	6.9	8.1	7.8	8.1
6	8.1	8.1	6.9	8.1	7.8	8.4	8.4	7.5	8.4	10.2	9.9	7.5
	7.2	4.1	4.4	5.9	7.2	8.7	8.7	8.7	8.1	8.4	9.0	8.7
7	8.7	8.7	8.7	8.7	8.4	8.1	8.4	8.7	8.7	8.7	8.4	8.7
	8.7	8.4	8.4	8.4	8.1	7.2	8.7	8.7	8.7	8.7	9.3	9.3
8	9.3	9.3	9.3	9.3	9.0	9.0	9.3	9.3	9.3	9.3	9.3	9.3
	11.1	10.8	9.6	8.7	8.7	8.7	8.7	9.3	9.9	11.6	10.2	10.2
9	10.2	10.2	9.9	10.2	10.2	10.2	10.2	10.2	10.2	9.6	9.6	-
	-	-	-	10.2	8.7	9.3	11.1	9.3	11.6	11.6	10.8	10.2
10	9.9	10.2	10.2	11.1	11.1	10.8	10.8	10.8	11.1	10.8	10.5	10.2
	9.6	10.2	10.2	9.6	9.9	9.3	10.2	10.5	12.8	10.5	10.8	10.2
11	9.9	9.3	9.3	9.6	9.6	9.0	8.7	8.7	8.7	9.0	9.0	9.6
	9.6	9.6	9.6	9.6	9.6	9.6	9.6	9.9	10.2	10.2	10.2	9.3
12	6.9	6.2	6.9	6.6	7.8	7.2	7.2	8.1	7.2	5.6	6.6	6.9
	6.2	7.2	5.6	5.6	5.6	7.2	7.2	7.2	7.2	5.9	5.6	5.6
13	5.0	4.1	5.6	5.3	5.6	5.6	5.6	5.6	5.9	5.6	5.6	4.1
	-	-	-	-	8.7	8.1	8.4	8.4	8.7	8.7	8.7	8.7
14	7.8	8.7	8.7	8.7	8.7	8.7	8.7	8.7	-	-	-	-
	-	-	-	-	-	8.7	8.7	8.7	8.7	8.7	8.4	8.7
15	8.4	8.7	8.7	8.7	8.7	8.7	8.7	8.7	8.7	-	-	-
	-	8.7	8.7	8.7	8.7	8.7	8.7	8.7	8.1	8.4	8.1	8.7
16	8.7	8.7	8.7	8.7	8.7	8.7	8.7	8.7	-	-	-	-
	-	8.4	8.1	8.4	8.7	8.7	8.7	8.7	8.7	8.7	8.4	8.4
17	8.7	8.7	8.7	8.7	8.7	8.7	8.7	8.7	8.7	-	-	-
	-	8.7	8.4	7.5	8.4	8.7	9.3	9.3	9.3	9.3	9.0	8.7
18	9.0	9.0	9.3	8.7	9.0	9.3	9.3	9.3	9.3	11.6	7.2	8.7
	8.4	8.4	8.4	9.0	8.7	9.0	9.3	10.2	11.6	10.2	9.0	9.0
19	10.2	8.7	9.6	9.6	8.7	9.0	9.0	9.0	9.0	9.6	9.6	9.6
	9.0	8.7	8.7	8.7	8.7	8.1	8.4	9.0	9.6	9.9	9.9	9.9
20	9.0	8.4	8.1	8.4	8.4	8.4	8.4	8.4	9.0	9.3	9.6	9.6
June, 1991												
6	-	-	-	-	-	-	-	-	-	-	7.5	8.1

	11.4	11.4	11.4	10.8	11.6	11.6	11.6	11.6	11.4	11.4	10.8	11.1
7	11.1	11.4	11.4	11.4	11.1	10.5	10.5	9.6	9.0	8.1	8.1	8.4
	7.8	8.4	8.1	7.8	8.1	9.3	9.3	9.9	9.3	9.3	8.4	8.7
8	8.1	7.5	9.0	8.4	7.5	8.1	8.1	7.8	8.4	7.5	6.9	6.6
	6.6	6.6	9.0	8.7	9.6	8.7	9.3	9.0	9.3	9.0	8.4	9.6
9	9.0	9.9	10.8	11.9	13.1	12.8	12.2	11.9	11.6	9.9	9.3	11.4
	15.2	24.8	36.3	11.4	11.6	9.6	10.2	10.2	11.4	11.6	11.6	12.2
10	8.4	29.9	37.4	46.0	43.7	35.5	35.5	6.6	7.5	7.8	8.1	8.1
	9.0	7.8	7.5	7.5	12.2	10.5	10.5	10.5	10.8	8.4	9.0	10.2
11	7.2	6.9	6.9	6.9	6.9	8.4	9.0	8.4	10.2	8.1	6.9	8.4
	7.5	7.5	7.8	10.2	9.9	8.6	7.8	6.6	7.2	8.4	9.3	9.6
12	9.3	8.4	9.6	11.9	17.3	16.1	11.1	9.0	8.7	8.4	7.2	9.0
	6.9	7.5	9.0	11.1	19.2	20.1	11.9	8.7	8.7	9.0	10.2	10.5
13	17.0	8.7	8.4	8.7	9.3	9.3	12.8	10.2	7.8	6.2	7.8	17.6
	5.6	4.4	6.6	8.7	11.6	14.6	15.5	9.9	9.9	9.6	9.3	9.3
14	6.6	12.2	6.6	7.8	8.7	10.2	10.2	11.6	10.2	8.1	8.7	8.4
	5.0	5.0	6.6	6.9	6.9	8.7	11.9	17.6	11.1	7.5	7.2	8.4
15	2.2	2.9	3.5	5.0	16.1	20.7	14.6	13.1	17.6	10.2	8.7	8.7
	3.2	5.0	7.2	12.2	6.9	6.2	8.1	10.2	12.2	11.4	11.6	11.6
16	8.7	8.4	8.4	11.1	9.6	38.2	13.1	14.6	20.7	12.5	13.1	13.7
	5.0	1.3	6.2	6.6	8.7	8.4	7.2	8.4	11.1	13.1	13.1	13.1
17	8.1	8.7	8.4	8.4	10.5	9.6	7.8	8.1	9.3	12.8	12.8	8.7
	7.5	7.2	6.9	8.1	9.9	8.7	10.2	5.3	7.8	9.6	13.1	11.6
18	12.8	11.1	11.6	11.9	11.1	12.2	11.1	9.0	9.3	9.9	8.4	15.5
	11.6	2.5	10.5	10.2	8.7	14.6	13.4	8.7	8.1	10.8	12.5	12.5
19	11.6	12.5	11.4	11.6	10.8	13.1	13.1	10.2	10.2	8.7	8.1	10.2
	14.6	15.2	11.9	8.7	13.4	16.4	16.4	14.3	14.6	11.9	11.6	14.0
20	12.8	12.8	10.8	11.6	12.2	9.6	11.1	11.1	9.3	6.6	3.8	5.0
	8.7	8.7	8.4	9.6	8.7	10.2	10.2	11.6	12.5	11.6	10.5	11.1
21	12.2	14.0	13.1	13.4	14.3	14.0	14.6	14.6	14.0	10.8	11.6	11.6
	10.9	8.7	10.2	8.7	5.6	11.9	12.8	14.0	14.0	14.6	10.2	9.3
22	15.5	13.7	16.7	15.2	15.8	16.4	16.1	15.2	14.6	14.6	14.6	15.8
	14.6	16.1	16.1	14.6	14.6	16.4	16.4	15.5	17.6	17.6	17.0	17.3
23	14.0	17.0	17.6	18.5	20.7	22.0	21.0	18.9	18.9	18.9	15.8	15.8
	12.8	14.6	16.1	11.6	14.6	13.1	14.0	15.5	16.1	16.1	16.1	14.6
24	10.8	11.1	12.2	13.7	15.2	21.0	22.6	22.0	18.9	18.9	20.7	17.6
	8.7	8.1	9.6	11.4	13.1	14.6	14.0	14.6	15.2	15.2	16.1	14.3
25	13.7	10.8	11.6	13.7	15.2	15.8	16.7	15.2	14.6	14.0	15.2	15.2
	11.6	11.9	12.2	13.7	14.9	15.2	14.0	14.0	14.9	15.5	14.6	13.7
26	12.8	11.1	11.1	11.6	12.5	12.8	14.3	14.3	12.8	14.3	10.5	11.6
	8.1	10.8	10.8	11.9	14.6	16.7	16.7	13.7	15.5	15.2	15.2	14.6
27	14.9	14.0	13.4	14.0	14.9	15.8	15.2	14.6	13.7	15.2	13.4	10.8
	12.2	13.4	12.2	9.3	8.7	10.8	12.2	13.7	13.7	13.7	13.7	12.8
28	12.5	13.7	11.9	11.4	10.8	11.4	10.8	11.1	8.4	12.2	10.2	9.9
	9.3	9.3	9.3	9.0	7.5	11.6	10.5	12.8	12.2	12.2	12.2	12.5
29	11.9	12.2	12.2	12.2	11.1	11.1	10.8	11.1	10.5	11.9	10.8	9.0
	3.5	12.5	11.4	9.6	11.9	11.9	12.8	12.2	12.8	13.4	13.4	13.4
30	13.7	13.4	14.9	14.0	13.4	14.0	14.0	14.0	16.4	14.9	13.4	13.4
	9.9	11.1	10.5	12.5	13.4	17.9	17.9	15.5	15.8	15.2	14.9	14.6

July, 1991

1	14.9	13.1	13.7	14.0	14.9	14.0	14.0	13.7	13.1	14.0	14.0	12.8
	15.2	14.6	11.6	11.6	11.9	12.5	13.4	13.7	13.7	13.1	13.1	12.8
2	13.4	14.3	13.7	14.0	13.1	11.9	8.7	7.8	6.6	9.6	9.9	9.9
	9.9	8.0	5.0	7.2	8.7	12.5	12.8	11.1	11.6	14.6	11.9	11.6
3	11.6	11.6	12.2	12.2	12.2	11.6	11.1	7.8	7.5	4.1	8.7	9.3
	8.1	8.4	6.6	6.6	6.6	7.5	10.2	10.2	10.5	11.1	11.6	11.6
4	11.1	11.1	11.1	11.1	11.6	11.1	10.8	8.7	8.7	5.6	13.1	11.6
	11.6	11.1	9.9	11.6	11.6	11.4	10.2	10.5	11.6	12.5	12.8	13.7
5	13.7	13.1	13.1	13.1	13.1	13.1	12.8	12.8	11.1	10.5	14.0	-
26	-	-	-	-	-	7.8	8.4	8.4	8.7	8.7	9.0	10.8
27	11.9	9.3	13.7	11.6	11.6	14.6	16.4	11.6	9.9	9.0	8.7	10.2
	8.7	8.7	5.6	9.3	18.5	12.8	11.6	10.8	9.6	9.3	9.3	10.2
28	10.2	9.9	9.6	10.2	10.5	14.3	14.9	15.2	16.1	15.8	16.4	14.0
	9.6	10.5	10.2	9.3	9.6	9.3	9.3	10.5	11.1	12.2	12.2	12.8
29	10.2	10.5	9.9	10.2	11.1	11.6	11.9	11.9	11.6	11.6	11.6	11.6
	9.6	9.9	10.2	9.6	10.5	11.9	13.4	13.4	11.1	10.8	10.8	10.8
30	9.9	10.2	10.2	10.2	10.8	10.8	11.4	11.9	11.9	11.1	10.8	10.5
	8.1	7.5	9.0	8.7	8.1	8.4	9.0	9.6	9.9	9.6	12.5	13.1
31	9.9	9.6	9.6	10.5	9.9	9.9	9.6	9.3	9.6	10.2	10.2	10.2
	8.4	8.1	8.1	9.0	8.7	8.7	9.3	11.6	11.6	11.6	10.8	11.1
August, 1991												
1	11.1	11.1	11.6	11.9	11.6	12.2	11.6	11.4	11.9	14.0	14.6	14.3
	-	-	-	-	-	5.6	8.7	11.9	11.6	16.1	15.2	15.2
2	11.4	11.4	11.1	10.8	11.4	11.4	9.0	8.7	9.6	11.4	14.9	17.6
	13.4	15.2	15.2	13.4	17.6	18.9	8.5	3.2	4.7	24.5	8.7	5.6
3	4.1	5.9	6.9	8.1	8.7	9.0	9.6	9.9	11.6	11.9	12.2	16.7
	9.0	10.8	11.6	11.6	12.5	14.0	7.2	9.0	9.0	11.6	14.3	15.5
4	15.2	12.8	13.1	12.5	12.8	13.7	14.6	15.2	11.0	12.3	12.9	12.9
	10.9	12.5	10.0	10.0	10.0	10.9	12.2	12.9	15.6	18.7	18.7	22.2
5	19.6	15.9	14.3	8.5	8.2	7.9	7.5	7.2	7.2	7.2	8.1	8.1
	7.1	6.1	8.2	8.6	8.9	10.4	10.7	10.1	10.7	12.2	13.1	13.4
6	12.2	13.7	12.5	11.9	6.2	5.6	5.9	5.9	5.6	5.0	5.9	7.8
	7.8	11.4	9.6	10.2	7.5	9.6	10.2	9.6	10.5	9.9	10.5	13.1
7	13.7	13.7	13.1	14.3	13.1	11.9	11.6	16.7	11.6	11.6	11.6	10.8
	7.8	6.9	6.2	11.6	10.8	11.1	11.6	11.6	11.9	19.5	11.6	5.3
8	10.2	12.5	13.7	15.5	17.9	7.8	7.2	6.9	7.8	4.1	5.0	7.2
	5.6	7.2	11.1	8.7	10.8	10.2	10.2	11.1	11.6	11.6	11.6	12.5
9	11.6	11.4	11.6	12.2	13.7	14.9	13.7	11.6	11.6	12.2	7.5	8.7
	7.2	7.5	7.2	9.0	10.2	11.6	11.9	12.2	11.9	12.2	11.4	11.4
10	11.9	11.1	10.2	10.5	11.1	12.5	12.2	10.2	10.2	10.2	10.2	9.6
	6.6	8.4	9.6	13.1	11.4	13.1	13.1	10.2	10.8	10.5	10.5	11.1
11	11.1	10.8	11.4	11.6	12.2	13.1	13.1	13.1	10.2	11.1	11.1	11.9
	11.6	11.9	9.9	9.3	11.4	11.4	14.9	14.6	13.7	13.4	13.1	14.0
12	12.2	12.2	12.2	12.5	12.2	12.2	10.5	8.4	9.9	11.9	9.9	9.9
	10.2	10.2	10.5	9.6	9.6	9.6	11.4	12.2	12.5	12.2	11.9	11.9
13	12.2	12.5	11.9	11.9	12.2	12.2	9.6	10.5	11.1	10.2	9.6	9.6
	9.9	9.0	9.0	11.4	9.3	16.1	21.3	16.7	19.8	13.4	13.7	12.5
14	12.5	12.2	12.5	12.5	12.5	12.2	12.2	12.2	12.5	12.5	11.1	10.8
	10.8	9.0	9.0	9.0	9.6	9.0	9.0	11.9	13.4	14.0	13.1	12.5
15	12.2	12.2	12.2	12.5	12.2	12.2	12.2	12.2	12.2	12.5	12.2	11.9

	11.6	11.6	11.6	11.6	11.6	11.6	13.1	16.1	16.1	16.4	16.1	15.2
November, 1991												
9	9.7	9.6	10.8	10.2	10.5	10.8	10.8	10.8	11.1	11.1	11.1	11.4
10	10.8	10.5	10.8	10.5	9.9	10.2	10.2	10.5	13.7	10.5	11.6	12.2
	9.3	8.1	8.4	9.0	9.3	10.8	11.9	11.9	12.2	16.1	18.5	18.5
11	12.8	11.6	12.5	12.5	11.9	14.0	12.8	14.0	13.7	12.5	13.4	16.4
	13.1	14.0	14.0	12.8	9.9	9.9	10.5	10.8	10.8	12.5	17.0	17.3
12	16.7	16.7	15.8	15.8	13.7	12.8	13.4	14.6	14.3	10.5	9.6	7.5
	7.8	8.7	9.0	9.3	9.3	9.0	8.4	7.5	8.1	8.4	13.4	9.9
13	8.1	16.7	9.3	12.2	13.1	12.2	13.1	13.1	12.8	14.6	13.1	12.8
	14.0	13.7	11.1	12.5	12.8	12.8	7.2	7.2	7.2	7.5	10.8	9.6
14	7.2	7.2	7.8	7.8	6.9	7.2	13.7	13.1	13.1	12.8	12.5	11.4
	21.0	21.3	21.6	21.0	20.7	21.3	19.8	19.2	20.4	16.7	16.7	16.7
15	16.7	17.0	18.5	19.2	19.2	19.2	19.2	19.8	21.6	20.1	20.1	16.1
	13.1	14.0	14.0	14.3	14.6	14.6	16.4	13.1	12.8	13.1	13.7	13.7
16	14.0	13.1	13.7	14.0	14.0	8.7	8.7	8.7	8.7	7.8	5.3	5.6
	4.1	6.2	9.3	9.3	7.5	9.3	10.2	9.0	10.5	6.2	6.9	6.2
17	5.9	5.9	8.4	9.0	8.1	8.1	8.4	8.1	8.4	8.1	9.0	10.5
	10.5	9.9	5.9	5.9	6.6	6.9	6.6	6.9	13.1	9.6	5.3	10.5
18	10.5	10.8	11.6	12.2	10.2	12.5	11.1	10.5	11.6	12.2	10.5	7.2
	9.3	9.3	9.6	10.2	9.3	9.3	9.9	10.2	10.8	10.5	10.5	11.1
19	7.2	7.8	7.8	9.9	9.6	9.3	9.0	9.0	8.7	8.1	8.1	8.1
	6.9	8.4	9.3	14.3	13.7	11.1	10.5	10.2	9.3	11.4	11.1	10.8
20	10.2	13.1	16.7	17.6	14.6	11.9	9.9	9.9	9.3	9.3	9.0	10.2
	9.3	10.2	11.6	14.3	13.7	12.2	9.6	9.9	9.6	9.6	9.3	9.6
21	9.6	9.9	10.5	12.5	14.9	16.1	11.1	10.2	9.3	9.3	8.7	9.6
	9.3	9.3	10.5	11.4	14.3	17.3	12.2	9.9	9.6	9.3	11.4	11.1
22	9.3	10.8	11.1	11.9	12.5	14.0	10.2	9.3	9.3	8.7	9.0	10.5
	9.3	10.2	9.6	10.8	11.4	11.4	10.2	9.0	9.0	9.0	8.7	10.2
23	9.3	9.3	9.9	10.8	11.1	11.4	11.1	9.9	9.3	9.3	8.7	9.3
	9.0	9.3	9.3	9.3	10.2	10.2	10.8	9.6	9.3	9.3	8.7	9.3
24	9.3	9.0	9.3	9.3	9.6	10.8	11.1	9.9	9.3	8.7	9.0	9.0
	6.6	8.7	8.4	8.7	9.6	10.8	13.1	17.3	10.8	9.0	9.0	9.0
25	10.8	9.3	10.2	9.9	9.3	10.5	10.8	11.6	11.1	9.9	9.6	9.3
	9.0	9.0	9.3	8.7	9.0	9.6	9.9	11.1	11.1	9.3	8.7	8.7
26	8.7	9.0	9.0	9.6	9.6	9.3	9.6	9.6	9.6	8.7	9.9	8.7
	7.5	8.1	8.4	8.4	8.4	9.0	9.0	9.3	9.6	9.9	11.1	11.1
27	10.8	10.2	11.4	10.5	11.6	10.8	10.5	10.5	9.3	9.6	10.2	10.5
	9.6	9.9	9.6	9.6	9.9	9.9	9.9	9.9	9.9	10.2	10.8	10.2
28	10.2	10.2	10.2	9.9	9.9	9.9	9.9	9.6	9.9	9.9	9.0	9.3
	8.1	8.4	9.3	9.3	9.3	9.3	9.3	9.6	9.6	9.9	10.2	10.5
29	9.6	10.2	10.2	9.6	9.6	10.2	10.5	10.5	10.2	10.2	10.2	9.6
	9.6	9.3	9.3	9.6	10.2	10.2	10.2	10.2	10.2	10.5	11.6	14.3
30	12.8	11.4	10.8	11.1	10.8	10.8	10.5	11.6	11.4	11.4	10.8	10.8
	10.5	11.1	10.8	10.8	11.1	11.1	11.6	11.4	10.2	10.2	10.2	10.5
December, 1991												
1	10.2	10.5	11.4	11.1	11.1	10.8	11.1	11.1	12.2	11.1	9.6	6.6
	9.0	9.0	9.9	9.9	10.2	10.2	10.2	10.2	10.2	9.9	9.9	9.6
2	9.6	10.8	11.6	10.5	9.6	9.3	9.3	9.3	9.3	9.6	9.6	9.6
	8.7	9.0	9.9	10.2	9.0	9.0	9.0	9.3	11.1	9.0	9.6	11.1

3	9.3	10.2	11.4	10.5	9.9	9.3	9.3	9.3	12.2	10.5	9.6	12.5
	8.1	8.4	9.6	11.1	10.5	9.6	9.3	9.6	9.6	9.6	9.6	9.9
4	15.5	14.0	12.5	14.6	12.2	9.6	9.3	9.3	10.2	11.6	9.9	10.5
	10.8	10.2	8.7	10.5	12.8	9.6	7.8	8.1	7.8	8.7	9.6	8.7
5	9.3	9.3	15.2	16.7	22.9	32.1	19.8	-	-	-	-	-
	-	-	5.3	6.6	8.1	9.9	9.0	9.0	8.7	9.9	10.5	11.4
6	9.6	10.8	9.3	9.3	10.8	11.6	10.5	8.4	7.5	9.3	10.8	10.8
	8.7	9.9	7.8	7.2	8.7	9.9	11.6	11.6	11.4	9.9	12.8	12.5
7	5.9	8.4	5.9	5.9	5.9	7.8	9.0	7.5	6.2	5.9	6.2	7.8
	6.6	5.6	8.1	7.2	7.8	7.8	8.1	9.0	7.8	8.1	8.1	11.1
8	10.5	9.0	10.2	7.2	9.9	10.2	10.2	10.5	8.7	8.7	9.3	9.9
	11.1	11.1	11.1	11.1	11.4	11.6	13.1	14.0	11.1	11.4	11.1	11.1
9	10.8	10.8	11.9	11.4	11.4	11.4	11.9	11.6	11.4	11.1	10.8	10.5
	10.8	10.8	10.5	11.1	11.4	11.4	11.6	11.6	11.4	11.6	11.1	11.1
10	10.8	10.8	11.1	11.4	10.8	10.8	10.8	11.4	11.4	10.8	9.3	8.4
	8.1	10.5	10.2	10.5	11.1	11.1	11.1	11.4	11.4	11.4	10.8	10.8
11	10.8	10.5	10.5	10.8	10.8	11.1	11.1	11.1	10.8	10.8	10.2	9.3
	8.1	6.6	8.4	10.2	10.5	10.8	11.1	11.1	11.1	11.1	11.4	11.4
12	10.8	10.8	10.8	11.1	11.1	10.8	10.8	10.8	10.8	10.8	10.8	10.2
	-	-	8.1	10.2	10.5	10.8	11.1	11.1	11.1	11.1	11.4	11.4
13	11.1	10.8	10.8	11.1	11.4	11.4	11.1	11.1	11.1	11.1	9.9	7.8
	7.8	7.8	10.2	10.5	10.8	11.4	11.4	11.4	11.4	11.4	11.4	11.4
14	11.1	10.8	10.5	10.8	10.8	11.1	10.8	10.8	10.8	10.5	9.0	11.1
	10.8	10.5	10.8	11.1	11.1	11.1	11.1	11.1	11.1	11.4	11.4	11.4
15	10.8	10.8	10.8	10.8	10.8	10.8	10.8	10.8	10.8	10.8	10.8	10.5
	10.5	10.5	10.2	10.5	10.8	10.8	10.8	10.8	10.8	11.1	11.1	11.1
16	10.8	10.8	10.5	10.5	10.5	10.2	10.2	10.2	10.2	10.5	10.5	10.5
	10.2	10.2	10.2	10.2	10.2	10.2	10.2	10.2	10.2	11.1	11.1	11.6
17	11.4	11.6	11.1	10.5	10.5	10.5	10.2	10.2	10.5	10.2	9.9	9.9
	9.9	10.8	11.1	10.5	9.9	9.6	9.6	9.9	9.9	11.6	12.5	16.7
18	17.6	16.1	11.6	10.2	10.8	10.8	10.5	11.1	13.1	13.1	10.2	-
	-	-	-	10.5	10.5	10.5	10.5	9.9	9.9	9.9	10.8	11.4
19	11.4	11.1	11.4	11.4	10.5	10.2	10.5	10.2	10.2	10.5	10.5	11.6
	11.9	12.8	12.2	12.2	10.2	9.6	9.6	9.9	9.9	10.2	10.2	10.2
20	10.2	10.5	10.8	11.4	11.9	11.1	11.1	11.1	10.5	10.8	10.2	10.2
	9.9	10.2	10.8	13.1	12.5	12.5	11.9	11.6	11.1	10.5	10.2	10.2
21	12.5	10.8	11.6	12.8	13.4	13.4	10.5	10.5	10.5	10.5	10.8	10.5
	10.2	10.2	10.5	12.5	15.8	22.0	10.2	9.6	9.6	9.6	11.4	11.6
22	4.4	5.9	6.9	11.9	11.4	8.7	8.1	7.8	6.9	9.0	8.7	8.4
	10.8	10.5	11.1	11.4	11.4	13.4	16.1	12.2	10.5	10.2	10.2	10.5
23	9.9	9.9	10.8	12.2	13.7	15.2	17.6	11.6	11.4	11.1	11.1	12.2
	13.7	13.7	14.0	17.9	18.9	15.8	14.0	14.3	10.8	10.8	10.8	10.2
24	10.2	9.6	10.5	10.2	10.2	10.2	10.5	10.5	11.6	10.8	10.8	10.2
	9.9	7.8	11.4	10.2	10.2	9.9	9.9	10.2	11.4	10.2	10.2	10.2
25	9.6	9.6	9.6	9.3	9.3	9.6	9.6	9.9	11.1	10.8	9.6	9.6
	8.4	8.1	8.1	8.7	9.0	9.6	9.6	9.6	11.4	10.8	9.6	9.6
26	9.3	9.3	9.3	9.3	9.9	10.2	10.2	10.2	10.2	10.5	10.5	10.5
	10.2	9.6	9.0	9.3	11.1	8.7	8.4	8.1	9.0	9.9	9.9	9.9
27	8.7	8.4	8.1	7.8	8.4	7.8	7.8	8.1	8.7	8.7	8.4	8.7
	8.1	7.8	7.5	8.4	8.4	9.3	8.4	8.7	9.0	9.6	12.5	12.5

28	9.6	9.9	9.9	9.9	10.2	10.5	7.5	9.3	9.3	9.6	9.6	9.6
	8.7	8.7	9.0	9.3	10.5	10.8	11.1	11.1	11.1	11.4	11.9	13.7
29	12.2	11.9	11.6	11.6	11.6	11.6	11.6	11.1	8.4	8.7	8.7	9.0
	8.7	8.4	8.4	9.3	9.6	9.6	10.2	10.5	10.5	10.8	10.8	11.4
30	11.1	11.1	10.8	10.8	10.8	10.8	10.8	10.8	10.8	10.2	10.2	10.8
	8.1	8.4	8.7	9.0	9.0	9.3	9.3	9.3	9.9	10.8	11.1	11.6
31	9.6	11.4	11.6	10.2	10.5	11.6	11.6	11.6	12.2	12.5	10.5	11.6
	4.4	6.9	7.8	7.8	8.1	9.0	10.5	11.1	10.2	10.5	10.8	10.8

APPENDIX D. FRESHWATER DISCHARGE DATA

Table D. Mean daily freshwater discharges for the rivers Stour, Avon and Moors, 1991 (in m^3s^{-1}).

Date	Stour	Avon	Moors	Total	Date	Stour	Avon	Moors	Total
January									
1	20.400	16.165	1.888	38.453	2	27.300	24.350	4.360	56.010
3	26.100	35.767	3.132	64.999	4	21.800	27.459	2.326	51.585
5	25.000	23.687	3.473	52.160	6	22.600	29.531	3.005	55.136
7	22.300	24.960	2.356	49.616	8	26.400	25.432	3.545	55.377
9	34.100	42.519	6.231	82.850	10	44.300	60.932	9.169	114.401
11	39.000	71.595	6.217	116.812	12	30.900	40.674	4.310	75.884
13	25.200	25.784	3.172	54.156	14	22.600	19.131	2.358	44.089
15	21.500	16.413	2.061	39.974	16	21.400	14.769	1.925	38.094
17	22.000	14.844	1.909	38.753	18	23.600	21.154	2.222	46.976
19	28.600	28.741	3.513	60.854	20	26.300	30.671	2.597	59.568
21	23.600	19.907	2.118	45.625	22	22.000	16.707	1.860	40.567
23	21.100	14.676	1.712	37.488	24	20.500	13.415	1.601	35.516
25	19.900	12.389	1.525	33.814	26	19.800	11.870	1.487	33.157
27	19.500	11.342	1.446	32.288	28	19.200	10.830	1.427	31.457
29	19.300	10.722	1.276	31.298	30	19.200	10.415	1.254	30.869
31	19.600	10.198	1.263	31.061					
February									
1	19.160	10.136	1.284	30.580	2	18.890	10.039	1.235	30.164
3	18.880	9.818	1.142	29.840	4	19.500	9.600	1.132	30.232
5	19.860	9.322	1.095	30.277	6	19.980	9.154	1.079	30.213
7	19.860	8.893	1.060	29.813	8	19.360	8.835	1.059	29.254
9	18.840	8.720	1.044	28.604	10	18.780	8.411	1.012	28.203
11	18.450	8.172	0.997	27.619	12	18.550	8.252	1.009	27.811
13	18.810	8.185	1.037	28.032	14	19.020	8.366	1.008	28.394
15	18.930	9.116	1.245	29.291	16	18.890	11.956	1.239	32.085
17	18.860	12.079	1.105	32.044	18	18.780	10.305	1.068	30.153
19	17.220	9.324	1.016	27.560	20	16.860	8.827	1.023	26.710
21	18.000	9.416	1.259	28.675	22	21.610	17.569	1.993	41.172
23	25.260	29.452	2.740	57.452	24	20.260	25.640	1.893	47.793
25	22.780	15.621	1.615	40.016	26	19.070	14.143	1.517	34.730
27	18.810	12.349	1.440	32.599	28	18.870	11.377	1.388	31.635
March									
1	17.600	11.062	1.320	29.982	2	17.390	10.501	1.273	29.164
3	17.340	9.791	1.372	28.503	4	17.750	10.559	1.659	29.968
5	18.360	12.746	1.877	32.983	6	21.030	17.828	2.586	41.444
7	26.910	21.178	3.908	51.996	8	29.620	26.863	4.829	61.312
9	33.180	54.331	6.307	93.818	10	34.730	68.285	5.887	108.902
11	29.650	38.148	4.764	72.562	12	25.330	26.175	3.248	54.753
13	24.140	20.726	2.527	47.393	14	23.190	18.394	2.159	43.743
15	22.700	16.050	2.004	40.754	16	25.710	18.840	3.058	47.608

17	28.200	35.874	3.737	67.811	18	29.370	42.481	3.177	75.028
19	34.870	38.498	4.270	77.638	20	31.910	35.848	3.278	71.036
21	29.790	27.180	3.099	60.069	22	27.790	22.404	2.550	52.744
23	26.000	19.079	2.151	47.230	24	24.790	17.377	1.909	44.076
25	24.100	15.952	1.804	41.856	26	23.340	15.175	1.691	40.206
27	23.340	14.769	1.609	39.718	28	22.070	14.154	1.527	37.751
29	20.870	13.338	1.477	35.685	30	20.970	12.848	1.454	35.272
31	20.800	13.170	1.467	35.437					
April									
1	20.240	13.255	1.464	34.959	2	20.950	14.203	1.723	36.876
3	27.080	15.668	1.708	44.456	4	26.610	19.644	2.248	48.502
5	28.710	33.239	2.179	64.128	6	28.710	25.460	2.055	56.225
7	29.720	27.910	2.174	59.804	8	30.550	24.192	1.834	56.576
9	28.680	17.690	1.628	47.998	10	26.360	16.239	1.588	44.187
11	25.520	15.155	1.482	42.157	12	23.940	14.127	1.435	39.502
13	23.800	12.839	1.346	37.985	14	22.960	12.418	1.279	36.657
15	25.010	11.888	1.367	38.265	16	21.760	11.472	1.232	34.464
17	21.870	11.127	1.125	34.122	18	21.260	10.995	1.097	33.352
19	21.370	10.715	1.157	33.242	20	22.050	10.475	1.095	33.620
21	20.620	10.233	1.080	31.933	22	20.620	9.917	1.153	31.690
23	19.780	9.628	1.069	30.477	24	19.270	9.458	1.072	29.800
25	19.010	9.666	1.111	29.787	26	19.360	10.034	1.072	30.466
27	18.940	9.624	1.024	29.588	28	18.880	9.002	0.988	28.870
29	18.290	10.983	1.385	30.658	30	19.820	19.342	2.280	41.442
May									
1	31.146	23.713	1.533	56.392	2	21.131	14.265	1.305	36.701
3	18.493	11.776	1.197	31.466	4	17.307	10.658	1.132	29.097
5	16.615	10.005	1.042	27.662	6	15.776	9.213	1.009	25.998
7	15.919	9.348	1.190	26.457	8	15.951	9.378	1.090	26.419
9	15.839	9.273	1.050	26.162	10	15.254	8.721	0.985	24.960
11	14.807	8.299	0.950	24.056	12	14.479	7.990	0.895	23.364
13	14.191	7.718	0.865	22.774	14	13.861	7.407	0.815	22.083
15	13.476	7.043	0.791	21.310	16	13.322	6.898	0.821	21.041
17	13.175	6.759	0.805	20.739	18	13.139	6.725	0.795	20.659
19	13.032	6.625	0.788	20.445	20	12.916	6.515	0.780	20.211
21	12.734	6.343	0.747	19.824	22	12.572	6.191	0.718	19.481
23	12.444	6.070	0.708	19.222	24	12.256	5.892	0.684	18.832
25	12.265	5.901	0.674	18.840	26	12.136	5.779	0.659	18.574
27	11.996	5.647	0.658	18.301	28	12.155	5.797	0.649	18.601
29	11.916	5.572	0.649	18.137	30	11.512	5.191	0.645	17.348
31	11.399	5.084	0.632	17.115					
June									
1	11.680	4.931	0.619	17.230	2	11.680	4.934	0.593	17.207
3	11.480	4.860	0.607	16.947	4	11.210	4.703	0.614	16.527
5	11.660	5.821	0.765	18.246	6	12.570	5.329	0.908	18.807
7	12.440	5.197	0.740	18.377	8	11.980	5.368	0.700	18.048
9	12.420	5.314	0.733	18.467	10	11.830	5.098	0.657	17.585
11	12.120	5.540	0.646	18.306	12	12.580	5.664	0.906	19.150
13	11.990	5.015	0.734	17.739	14	11.520	5.095	0.717	17.332
15	11.930	5.208	0.740	17.878	16	13.110	5.185	0.833	19.128

17	12.480	5.050	0.956	18.486	18	12.140	4.973	0.769	17.882
19	12.580	4.934	0.687	18.201	20	11.670	4.774	0.661	17.105
21	11.460	4.542	0.634	16.636	22	10.630	4.404	0.613	15.647
23	15.680	8.350	1.589	25.619	24	21.280	7.607	1.087	29.974
25	19.280	9.737	2.775	31.792	26	16.890	10.493	2.065	29.448
27	14.790	8.905	1.487	25.182	28	13.310	8.104	1.144	22.558
29	12.680	7.907	0.952	21.539	30	12.820	6.998	0.869	20.687
July									
1	12.764	6.372	0.869	20.005	2	12.355	5.986	0.868	19.209
3	12.612	5.804	0.865	19.281	4	11.873	5.531	0.828	18.232
5	12.118	5.762	2.152	20.032	6	11.748	5.413	3.504	20.665
7	11.594	5.268	3.504	20.366	8	11.892	5.549	1.420	18.861
9	11.561	5.237	1.120	17.918	10	11.361	5.048	0.945	17.354
11	11.524	5.202	0.848	17.574	12	11.318	5.008	0.859	17.185
13	11.362	5.049	0.849	17.260	14	11.262	4.955	0.869	17.086
15	11.219	4.914	0.833	16.966	16	11.158	4.857	0.802	16.817
17	11.461	5.142	0.748	17.351	18	13.656	7.213	1.732	22.601
19	12.425	6.052	2.444	20.921	20	13.978	7.517	1.485	22.980
21	14.984	8.466	1.061	24.511	22	13.309	6.886	0.897	21.092
23	13.023	6.616	0.854	20.493	24	12.237	5.875	0.919	19.031
25	11.838	5.498	1.121	18.457	26	11.578	5.253	1.098	17.929
27	11.382	5.068	0.961	17.411	28	11.202	4.898	0.853	16.953
29	11.614	5.287	0.835	17.736	30	11.316	5.006	0.808	17.130
31	11.012	4.719	0.759	16.490					
August									
1	10.740	4.462	0.761	15.963	2	10.609	4.339	0.736	15.684
3	10.519	4.254	0.708	15.481	4	10.463	4.201	0.699	15.363
5	10.465	4.203	0.700	15.368	6	10.458	4.196	0.685	15.339
7	10.411	4.152	0.672	15.235	8	10.316	4.062	0.656	15.034
9	10.269	4.018	0.627	14.914	10	10.260	4.009	0.607	14.876
11	10.249	3.999	0.591	14.839	12	10.177	3.931	0.596	14.704
13	10.122	3.879	0.594	14.595	14	10.046	3.808	0.589	14.443
15	10.048	3.809	0.589	14.446	16	9.949	3.716	0.588	14.253
17	9.893	3.663	0.579	14.135	18	9.775	3.552	0.565	13.892
19	9.586	3.374	0.569	13.529	20	9.586	3.374	0.565	13.525
21	9.865	3.637	0.563	14.065	22	10.031	3.793	0.573	14.397
23	10.518	4.253	0.712	15.483	24	9.977	3.742	0.781	14.500
25	9.852	3.625	0.676	14.153	26	9.568	3.357	0.615	13.540
27	9.545	3.335	0.586	13.466	28	9.608	3.394	0.576	13.578
29	9.362	3.162	0.567	13.091	30	9.264	3.070	0.552	12.886
31	9.116	2.930	0.546	12.592					
September									
1	6.896	2.973	0.538	10.407	2	6.761	2.951	0.536	10.248
3	6.670	2.896	0.531	10.097	4	6.935	2.780	0.520	10.235
5	6.682	2.844	0.526	10.052	6	6.700	2.794	0.521	10.015
7	6.727	2.801	0.522	10.050	8	6.680	2.808	0.523	10.011
9	6.680	2.786	0.521	9.987	10	6.680	2.666	0.510	9.856
11	6.680	2.670	0.510	9.860	12	6.640	2.721	0.515	9.876
13	6.680	2.744	0.517	9.941	14	6.680	2.787	0.521	9.988
15	6.680	2.805	0.522	10.007	16	6.680	2.801	0.522	10.003

17	6.640	2.735	0.516	9.891	18	6.651	2.783	0.520	9.954
19	6.722	2.741	0.517	9.980	20	6.591	2.785	0.521	9.897
21	6.624	2.857	0.527	10.008	22	6.760	3.060	0.545	10.365
23	6.852	2.909	0.532	10.293	24	6.818	3.029	0.543	10.390
25	6.977	3.036	0.543	10.556	26	7.046	3.002	0.540	10.588
27	7.105	3.054	0.545	10.704	28	8.857	7.216	0.919	16.992
29	12.678	7.950	0.986	21.614	30	13.268	8.831	1.065	23.164

October

1	11.316	9.594	0.836	21.746	2	9.728	6.253	0.662	16.643
3	8.646	4.895	0.558	14.099	4	8.100	4.212	0.566	12.878
5	8.349	4.482	0.660	13.491	6	8.414	4.012	0.754	13.180
7	8.017	3.858	0.640	12.515	8	8.009	4.159	0.612	12.780
9	8.535	4.825	0.899	14.259	10	9.907	6.023	0.950	16.880
11	10.723	9.754	0.905	21.382	12	10.174	8.593	1.058	19.825
13	9.974	6.723	0.829	17.526	14	9.165	6.420	0.809	16.394
15	8.962	5.824	0.709	15.495	16	8.718	5.245	0.677	14.640
17	9.160	4.873	0.706	14.739	18	8.805	4.679	0.666	14.150
19	8.442	4.870	0.632	13.944	20	8.184	5.139	0.613	13.936
21	7.915	4.799	0.587	13.301	22	7.863	4.471	0.574	12.908
23	8.080	4.317	0.571	12.968	24	7.780	4.279	0.588	12.647
25	7.660	4.206	0.578	12.444	26	7.721	4.176	0.576	12.473
27	7.686	4.175	0.569	12.430	28	7.772	4.257	0.583	12.612
29	8.250	5.275	0.818	14.343	30	11.134	6.650	1.963	19.747
31	10.659	9.448	1.359	21.466					

November

1	16.340	13.592	3.035	32.967	2	15.467	19.558	2.689	37.714
3	13.742	14.629	1.771	30.142	4	12.371	17.021	1.466	30.858
5	11.743	14.884	1.123	27.750	6	10.685	10.629	0.992	22.306
7	9.933	7.898	0.981	18.812	8	9.895	7.450	0.890	18.235
9	9.196	7.196	0.848	17.240	10	9.015	7.635	0.822	17.472
11	10.467	8.093	1.090	19.650	12	10.122	8.703	1.271	20.096
13	11.436	13.290	1.572	26.298	14	11.161	16.978	1.394	29.533
15	11.065	14.291	1.192	26.548	16	10.544	12.822	1.071	24.437
17	10.195	10.591	1.051	21.837	18	10.330	9.428	1.084	20.842
19	13.537	11.791	2.249	27.577	20	15.388	26.815	2.295	44.498
21	15.094	21.552	1.452	38.098	22	13.155	13.285	1.238	27.678
23	12.380	10.931	1.126	24.437	24	11.210	10.229	1.075	22.514
25	10.960	9.446	1.097	21.503	26	10.889	9.397	1.070	21.356
27	10.746	9.600	1.018	21.364	28	10.385	8.968	0.991	20.344
29	10.233	8.582	0.949	19.764	30	10.011	8.309	0.923	19.243

December

1	9.932	8.018	0.893	18.843	2	9.787	7.745	0.867	18.399
3	9.603	7.542	0.848	17.993	4	9.426	7.368	0.846	17.640
5	9.480	7.231	0.831	17.542	6	9.440	7.059	0.821	17.320
7	9.362	6.756	0.812	16.930	8	9.320	6.811	0.809	16.940
9	9.327	6.913	0.808	17.048	10	9.295	6.950	0.820	17.065
11	9.230	6.840	0.803	16.873	12	9.152	6.769	0.795	16.716
13	9.171	6.300	0.791	16.262	14	9.159	6.264	0.789	16.212
15	9.522	6.465	0.798	16.785	16	10.894	7.132	1.032	19.058
17	11.806	7.696	1.504	21.006	18	13.033	11.216	1.703	25.952

19	13.750	16.550	1.482	31.782	20	14.280	18.853	2.050	35.183
21	14.711	28.022	1.955	44.688	22	13.699	22.866	1.635	38.200
23	13.254	16.726	1.338	31.318	24	11.954	12.541	1.104	25.599
25	11.104	10.323	1.036	22.463	26	10.734	9.102	1.016	20.852
27	10.561	8.993	0.982	20.536	28	10.967	8.563	0.931	20.461
29	10.334	8.192	0.917	19.443	30	10.223	7.947	0.904	19.074
31	10.024	7.765	0.884	18.673					

APPENDIX E. PUBLICATIONS

(1) **Gao, S. and Collins, M.** 1991 A critique of the "McLaren Method" for defining sediment transport paths. *Journal of Sedimentary Petrology*, 61, 143-146. (Note: this research was initiated jointly by SG and MC, the analysis was undertaken by SG, and the paper was written jointly by SG and MC).

(2) **Gao, S. and Collins, M.** 1992 Modelling exchange of natural trace sediments between an estuary and adjacent continental shelf. *Journal of Sedimentary Petrology*, 62, 35-40.
(Note: this research was initiated by SG, the analysis was mainly undertaken by SG and partly by MC, and the paper was written jointly by SG and MC).

DISCUSSION

A CRITIQUE OF THE "McLAREN METHOD" FOR DEFINING SEDIMENT TRANSPORT PATHS–DISCUSSION[1]

SHU GAO AND MICHAEL COLLINS
Department of Oceanography
The University
Southampton, S09 5NH, U.K.

INTRODUCTION

On the basis of the particle size distributions of natural sedimentary material, sedimentologists can 1) identify the environments of deposition of sediments (e.g., Folk 1951; Passega 1957, 1964; Friedman 1961); 2) through the analysis of a single curve, isolate various modes of transport, or identify the dominant mechanisms controlling sediment movement (e.g., Visher 1969); or 3) compare specific characteristics of the distributions, for the delineation of sediment transport paths (e.g., Plumley 1948; Yeakel 1962; Mothersill 1969; Pettijohn et al. 1972).

In early analyses, complete particle size distributions were determined on the basis of sieving or use of the pipette method (e.g., BS 1377 (1975)). More recently, "modern" techniques such as the SediGraph (Stein 1985; Singer et al. 1988), the (Malvern) laser particle sizer (McCave et al. 1986; Singer et al. 1988), and the sedimentation tower (Rigler et al. 1981) have been applied (for a summary, see Buller and McManus 1979). These latter techniques have enhanced our ability to generate a large number of data sets; there is a parallel need, however, to undertake a more rigorous and quantitative analysis of the trends in the distribution curves.

A recent development in this research area has been an attempt to relate net sediment transport directions to spatial changes in grain size parameters. Three cases of such changes have been defined (McLaren 1981) and have been related to transport paths (McLaren and Bowles 1985). The approach (referred to as the "McLaren Method" in the following text) has now been applied widely for engineering and dredging schemes (e.g., McLaren and Powys 1989), an understanding of pollutant transport (McLaren and Little 1987), and examining sediment transport patterns and stability (McLaren and Collins 1989).

Validation for some of the interpretations outlined above has been obtained through the use of alternative approaches to the identification of transport paths in the various studies. Nonetheless, some criticism of the application of the method remains, and it is the intention of this paper to 1) promote constructive discussion of the application of this technique, through the use of published scientific literature; and 2) propose some modifications to the original approach, to improve the "two-dimensional" character of the analysis.

[1] Manuscript received 10 May 1990.

PROBLEMS ASSOCIATED WITH THE McLAREN METHOD

The model established by McLaren and Bowles (1985) relates net sediment transport paths to spatial changes in the mean grain size, μ, the sorting coefficient, σ^2, and the skewness, Sk, of the distribution. As shown on Figure 1, for sampling sites d_1 and d_2, $d_1(s)$ is the grain size distribution of d_1 and $d_2(s)$ is that of d_2 (where s represents the grain size in ϕ units). If the net transport is from d_1 to d_2, the sediment at d_2 will be better sorted than that at d_1. Furthermore, $d_2(s)$ can be related to $d_1(s)$ by means of a "transfer function" X(s), given by:

$$d_2(s) = k\, d_1(s)\, X(s)$$

where k is a coefficient. McLaren and Bowles (1985) have argued that if X(s) is positively skewed, sediments at d_2 will become coarser and more positively-skewed than the sediments at d_1; on the other hand, if X(s) is negatively-skewed, the sediments will become finer and more negatively skewed. Consequently, there are two cases associated with net transport from d_1 to d_2, defined as Case B and Case C:

$$\text{Case B: } \sigma_2^2 < \sigma_1^2,\ \mu_2 > \mu_1 \text{ and } Sk_2 < Sk_1$$
$$\text{Case C: } \sigma_2^2 < \sigma_1^2,\ \mu_2 < \mu_1 \text{ and } Sk_2 > Sk_1$$

where the subscripts 1 and 2 represent sampling sites d_1 and d_2, respectively. Certainly, both Case B and Case C may occur even if there is no net transport (in the sense that the deposition sites involved have no relationship of material exchange with each other). In this situation, however, there are another six cases (in addition to Case B and Case C) which may also occur; the probability of Case B or Case C is assumed, therefore, to be ⅛. Thus, if there is transport along a line, the probability of a Case B or Case C condition, for one of the two directions associated with the line, will be considerably larger than ⅛.

To determine if the probability is high enough for such transport, McLaren and Bowles (1985) have suggested a "significance test" method to determine a preferred transport direction with a certain level of confidence. Their procedure is to take n samples along the survey line to form $(n^2 - n)/2$ possible sample pairs, then to apply a Z-score technique (Spiegel 1961) to determine the most probable transport directions.

Despite the several successful applications of the McLaren Method described previously, there are certain points in its theoretical foundation and technical procedure which need further analysis and discussion.

JOURNAL OF SEDIMENTARY PETROLOGY, VOL. 61, NO. 1, JANUARY, 1991, P. 143–146

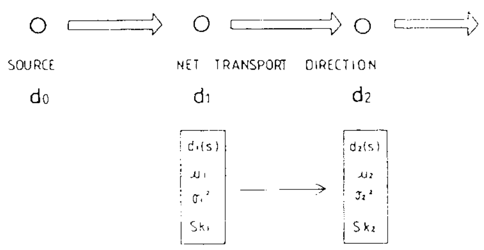

FIG. 1.—Definition sketch of sampling sites and related grain size parameters.

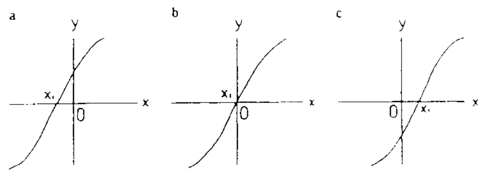

FIG. 2.—Three possible patterns of differences in mean (x) differences in skewness (y) (where $x = \mu_2 - \mu_1$, $y = Sk_1 - Sk_2$). a: $x_1 < 0$; b: $x_1 = 0$; c: $x_1 > 0$. (See text for explanation.)

Firstly, McLaren and Bowles have argued that either Case B or Case C will occur along a transport path. This pattern implies that $\mu_2 - \mu_1$ and $Sk_1 - Sk_2$ will always have the same signs. The relationship between them appears to be more complicated than this, however, as demonstrated by the following analysis.

Let $\mu_2 - \mu_1 = x$ and $Sk_1 - Sk_2 = y$. Because

$$\sigma_2^2 = \int_{-\infty}^{\infty} (s - \mu_2)^2 \cdot d_2(s) \cdot ds$$
$$= \int_{-\infty}^{\infty} s^2 \cdot d_2(s) \cdot ds - \mu_2^2$$

we have

$$y = Sk_1 - Sk_2$$
$$= Sk_1 - (\sigma_2^2)^{-3/2} \int_{-\infty}^{\infty} (s - \mu_2)^3 \, d_2(s) \, ds$$
$$= Sk_1 - (\sigma_2^2)^{-3/2}$$
$$\left[\int_{-\infty}^{\infty} s^3 \, d_2(s) \, ds - 3\sigma_2^2(x + \mu_1) - (x + \mu_1)^3\right]$$
$$= Ax^3 + Bx^2 + Cx + D \qquad [1]$$

where

$$A = (\sigma_2^2)^{-3/2};\ B = 3\mu_1 A;\ C = 3(\sigma_2^2 + \mu_1^2)A;$$

and

$$D = Sk_1 - A\left(\int_{-\infty}^{\infty} s^3 \, d_2(s) \, ds - 3\sigma_2^2\mu_1 - \mu_1^3\right).$$

Equation 1 has only one real root, because

$$B^2 - 3AC = 9\mu_1^2A^2 - 3A \cdot 3(\sigma_2^2 + \mu_1^2)A$$
$$= -9\sigma_2^2A^2 < 0$$

Let the root be x_1. Corresponding to three possibilities of $x_1 > 0$, $x_1 = 0$ and $x_1 < 0$ there are three patterns of the x-y curves (Fig. 2). For the situations that $x_1 \neq 0$, there exists a gap with a width of $|x_1|$, in which x and y have opposite signs. Because of this gap, whether x and y will always have the same sign remains a problem.

Secondly, the McLaren Method assumes that the probabilities of both Case B and Case C under "no transport" conditions are ⅛. The equations concerning the probabilities of Case B (P_b) and Case C (P_c) can be written as

$$P_b = P(\sigma_2 < \sigma_1^2)$$
$$\cdot P(\mu_2 > \mu_1 | \sigma_2^2 < \sigma_1^2) \cdot P(Sk_1 > Sk_2 | \mu_2 > \mu_1)$$
$$= P_1 \cdot P_2 \cdot P_4 \qquad [2]$$

and

$$P_c = P(\sigma_2^2 < \sigma_1^2)$$
$$\cdot P(\mu_2 < \mu_1 | \sigma_2^2 < \sigma_1^2) \cdot P(Sk_1 < Sk_2 | \mu_2 < \mu_1)$$
$$= P_1 \cdot P_3 \cdot P_5 \qquad [3]$$

In the situation of "no transport," it can be proved that $P_1 = ½$. However, it is questionable that P_2, P_3, P_4 and P_5 are also ½; they may be not completely independent of P_1. There are certain inherent relationships between mean grain size and sorting (Inman 1949; Griffiths 1967) and between the mean and the skewness (see Eq. 1) for a particular sedimentary environment. It may not be appropriate, therefore, to assume simply that the background value of both P_b and P_c are ⅛. These two parameters are so important in the significance test that they should be determined accurately.

Finally, the McLaren Method considers all possible $n(n - 1)/2$ pairs, from n samples, along the survey line. However, the space-scale is "confused" in this approach. It does not mean the same to compare two neighboring samples and two samples which are some distance apart. As a result of such a space-scale confusion, the "noise" caused by samples with extreme grain size parameters, or by additional sediment sources along the survey line, would be intensified.

SUGGESTED MODIFICATIONS

The theoretical foundation of the McLaren Method, in our opinion, is that the spatial distribution pattern of grain size parameters in "transport" conditions differs

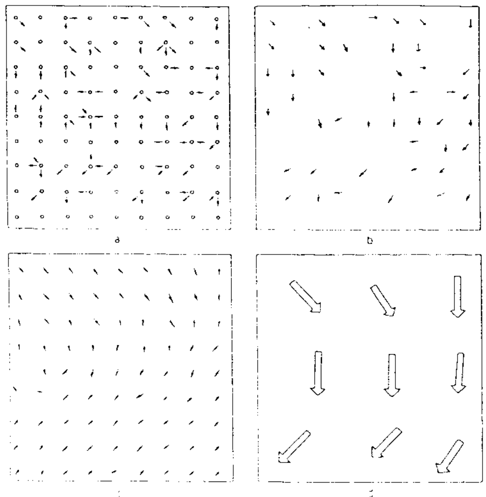

FIG. 3.—Schematic procedure of suggested 2-D data treatment (sampling sites o). a: "transport" vectors obtained from statistical counting; b: summing of the vectors; c: filtering (smoothing) operation; and d: the defined net transport direction.

markedly from that in "no transport" situations. For an environment where net transport is taking place, let P_1 and P_2 in Eq. 2 and 3 be α and β, respectively. According to Eq. 2 and 3, we have

$$P_b = \alpha \cdot \beta \cdot P_4 \qquad [4]$$

and

$$P_c = \alpha \cdot (1 - \beta) \cdot P_5 \qquad [5]$$

Many studies have shown that sorting improves in the direction of transport (e.g., Plumley 1948; Folk 1951). Consequently, α is expected to be larger than ½. Studies show also that the mean grain size can either increase (McLaren and Bowles 1985) or decrease (Pettijohn and Ridge 1932; Pettijohn et al. 1972) in the direction of transport, depending on the specific environments of deposition. Either β or $1 - \beta$ therefore, should be larger than ½. Furthermore, although the x-y relationship presented in Eq. 1 is valid (whether there is net transport or not), P_4 and P_5 in "transport" situations might still be larger than those under "no transport" situations. The reason for this is that when transport occurs, the gap $|x_1|$ is probably smaller, and the probability of the x-y data point falling into the gap may be lower. Therefore, either P_b or P_c in transport is expected to be considerably larger than that in "no transport" situations. If this serves as the basis for the significance test, the concept of the "transfer function" becomes unnecessary as far as the problem of net transport direction is concerned.

As stated above, the probabilities of Case B and Case C for "no transport" situations are two crucial parameters in the significance test. Because the grain size distribution is influenced by the depositional environment, these two parameters might vary from one environment to another. One of the possible methods for determining them is to consider samples taken over an area of investigation. Instead of maintaining the spatial distribution pattern, randomly selected samples can be compared and the probabilities of Case B and Case C patterns calculated. In this way, any instantaneous spatial relationship between samples are destroyed. The probabilities obtained should represent, therefore, the background values.

Basically, the McLaren Method is one-dimensional in character, although the procedure can be repeated over several sampling lines so as to incorporate a "two-dimensional" area. A two-dimensional treatment of data, however, could produce, more meaningful results (and reduce implied "bias" in the selection of the sampling lines). A procedure for the treatment of two-dimensional data is suggested in Figure 3 (in this figure, a series of "transport vectors" (a) is assumed, from which (b) and (c) are qualitatively derived). The first step is to compare each sample with its neighboring samples, drawing in vectors (with unit length) for each Case B situation—with the direction of the vector lying from a higher to a lower sorting coefficient (Fig. 3a). Such vectors are then summed, so that only a single vector is left for each sampling site (Fig. 3b). Finally, "noise" in the data is filtered, by a smoothing operation (here, it has been done by averaging the vectors of the central point and its neighboring points), in order to obtain the "residual" distribution of the vectors; this defines the most probable net sediment transport pattern (Fig. 3c and d). The same procedure can be followed for Case C patterns, between samples. The significance test can be applied between the first and the second steps of the analysis, or after the third step of the analysis outlined above. In both cases, the background P_b and P_c should be determined carefully.

The modifications outlined above are based upon the principle that grain size distributions show some ordered patterns, due to the energy input and related transport processes. There are still some uncertainties, however, concerning the explanation of the results. One of these is the time scale in the result obtained. The result is influenced, to some extent, by the sampling procedures, local hydrodynamics, and the rates of sediment deposition.

Another uncertainty is that concerning the spatial resolution associated with the technique. Theoretically, the net transport pattern can be examined at various space-scales, by collecting samples at various distance intervals. If the sampling intervals are small and the gradient in the grain size parameters is low, however, errors introduced by the analysis procedure could destroy any ordered pattern in the grain size parameters. For this reason, even if the significance test rejects the hypothesis that there is a preferred transport direction, this does not necessarily mean that no net transport is taking place in that particular environment.

SUMMARY

The McLaren Method and the modifications proposed in this contribution are based upon the general principles of spatial changes in grain size parameters resulting from sediment transport. Such changes are statistical in character. The proposed modification could provide an objective procedure to determine net sediment transport patterns. The time- and space-scales involved in the explanation of the result cannot be determined, however, by using the method itself; these should be considered as separate problems.

REFERENCES

BRITISH STANDARDS, 1975, Methods of the Test for Soils for Civil Engineering Purposes, BS 1377: 1975: British Standards Institute, London.

BULLER, A. T., AND MCMANUS, J., 1979, Sediment sampling and analysis, *in* Dyer, K. R., ed., Estuarine Hydrography and Sedimentation: Cambridge Univ. Press, p. 87–130.

FOLK, R. L., 1951, Stages of textural maturity in sedimentary rocks: Jour. Sed. Petrology, v. 21, p. 127–130.

FRIEDMAN, G. M., 1961, Distinction between dune, beach and river sands from their textural characteristics: Jour. Sed. Petrology, v. 31, p. 514–529.

GRIFFITHS, J. C., 1967, Scientific Method in Analysis of Sediments: New York, McGraw-Hill, p. 308–309.

INMAN, D. L., 1949, Sorting of sediments in the light of fluid mechanics: Jour. Sed. Petrology, v. 19, p. 51–70.

MCCAVE, I. N., BRYANT, J. R., COOK, H. F., AND COUGHANOWR, C. A., 1986, Evaluation of a laser-diffraction-size analyzer for use with natural sediments: Jour. Sed. Petrology, v. 56, p. 561–564.

MCLAREN, P., 1981, An interpretation of trends in grain-size measurements: Jour. Sed. Petrology, v. 51, p. 611–624.

MCLAREN, P., AND BOWLES, D., 1985, The effects of sediment transport on grain-size distributions: Jour. Sed. Petrology, v. 55, p. 457–470.

MCLAREN, P., AND COLLINS, M. B., 1989, Sediment transport pathways in the Severn Estuary and Bristol Channel: Severn Barrage Devel Proj., Working Document Ref., STPG/GEOSEA/3.1 (m)f, 54 p.

MCLAREN, P., AND LITTLE, D. I., 1987, The effects of sediment transport on contaminant disposal: an example from Milford Haven: Marine Pollution Bull., v. 18, p. 586–594.

MCLAREN, P., AND POWYS, R. I. L., 1989, The use of sediment trends to assess the fate of dredged material: Proceedings of WODCON XII, World Dredging Congress, p. 223–233.

MOTHERSILL, J., 1969, A grain size analysis of longshore-bars and troughs, Lake Superior, Ontario: Jour. Sed. Petrology, v. 39, p. 1317–1324

PASSEGA, R., 1957, Texture as characteristic of clastic deposition: A.A.P.G. Bull., v. 41, p. 1952–1984.

———, 1964, Grain size representation by CM patterns as a geological tool: Jour. Sed. Petrology, v. 34, p. 830–847

PETTIJOHN, F.G., AND J. D. RIDGE, 1932, A textural variation series of beach sands from Cedar Point, Ohio: Jour. Sed. Petrology, v. 2, p. 76–88.

PETTIJOHN, F. G., POTTER, P. D., AND SEIVER, R., 1972, Sand and Sandstone: New York, Springer-Verlag, p. 77–81.

PLUMLEY, W. J., 1948, Black Hills terrace gravels: a study in sediment transport: Jour. Geology, v. 55, p. 526–577

RIGLER, J. K., COLLINS, M. B., AND WILLIAMS, S. J., 1981, A high precision, digital-recording sedimentation tower for sands: Jour. Sed Petrology, v. 51, p. 642–644.

SINGER, J. K., ANDERSON, J. B., LEDBETTER, M. T., MCCAVE, I. N., JONES, K. P. N., AND WRIGHT, R., 1988, An assessment of analytical techniques for the size analysis of fine grained sediments: Jour. Sed Petrology, v. 58, p. 534–543.

SPIEGEL, M. R., 1961, Theory and Problems of Statistics: New York, McGraw Hill, Shaum's Outline Series, 359 p.

STEIN, R., 1985, Rapid grain-size analyses of clay and silt fraction by SediGraph 5000D: comparison with Coulter Counter and Atterberg methods: Jour. Sed. Petrology, v. 55, p. 590–615.

VISHER, G. S., 1969, Grain size distributions and depositional processes: Jour. Sed. Petrology, v. 39, p. 1074–1106

YEAKEL, L. S., JR., 1962, Tuscarora, Juniata and Bald Eagle paleocurrents and paleogeography in the central Appalachians: G.S.A. Bull., v. 73, p. 1515–1540.

MODELLING EXCHANGE OF NATURAL TRACE SEDIMENTS BETWEEN AN ESTUARY AND ADJACENT CONTINENTAL SHELF[1]

SHU GAO AND MICHAEL COLLINS
Department of Oceanography
The University
Southhampton SO9 5NH, U.K.

ABSTRACT: A mathematical model is developed to investigate the exchange of natural trace sediments between an estuary and an adjacent continental shelf, assuming that the tracer originates from the shelf. The model is run for four cases representing various landward-seaward sediment transport patterns at the entrance to the estuary.

The results show that landward flux of the tracer takes place independent of net sediment transport direction. This observation implies that there is some transport from the source but that the mere presence of the tracer in the estuary is not necessarily indicative of net landward sediment transport.

The model also suggests that the magnitude of the tracer concentration in any estuarine stratigraphic record is controlled by 1) sediment discharge associated with the river input, 2) tracer concentration at the source, 3) processes of dispersion, 4) patterns of landward-seaward net sediment transport, and 5) the amount of time required for equilibrium to occur. Hence, net transport pathways can be defined on the basis of the magnitude of the tracer concentration in estuarine sediments, when compared against a critical level.

INTRODUCTION

Estuaries are sinks for sediments until basin infilling is completed. But two questions arise: 1) what is the source of the deposited sediments; and 2) is there a *net* sediment transport to landward, crossing the entrance to the estuarine system.

There have been many attempts to answer these questions, relating the source of sediment supply and the patterns of net sediment transport to tracer dynamics. Natural tracers have been used as indicators of sediment supply and net transport. These tracers often include benthic foraminiferal tests (Murray 1987), marine diatoms (Gessner and Simonsen 1967), trace metals (Merefield 1981; Brown 1987; Salomons and Mook 1987), and heavy and clay mineral suites (Trask 1952; Byrne and Kulm 1967; Eisma et al. 1978). Although studies of sediment supply based upon tracer technique appear to have been successful, some doubts exist as to whether or not, and under what conditions, *net* transport pathways can be inferred from the flux of the trace material.

We present here results of a mathematical model of the exchange of natural trace sediments between an estuary and the open sea, under various sediment transport regimes (i.e., net transport to landward or seaward). Based upon the model results, the possibility of using natural trace sediments as indicators of net sediment transport is discussed. The notations used in the text are listed in Table 1.

MODEL FORMULATION

We model here the exchange of trace sediments between an estuary and the adjacent continental shelf. The model is based upon an analysis of the balance of the tracers within the estuarine system. The major components of sediment input and output over a unit time, for a tidal estuary (Fig. 1), are 1) input from the sea through the entrance, q_s; 2) output toward the sea, q_o; and 3) input from the river, q_r. The sediment budget will then be

$$q_n = q_s + q_r - q_o \quad [1]$$

where q_n is the amount of sediment stored within the estuarine system, over unit time. In any sedimentary environment, there is mixing between the sediments in transit and the bed material, due to either the physical processes of exchange (Einstein 1950) or bioturbation at the bed (Clifton and Hunter 1973; Ludtke and Bender 1979). As a result, q_o cannot consist of sediments from q_s and q_r alone; rather, it contains some material from the deposit itself. Therefore, q_o can be written as

$$q_o = (1 - a_s)q_s + (1 - a_r)q_r + q_m \quad [2]$$

where a_s and a_r are the fractions of the material from q_s and q_r, respectively, that remain in the basin due to mixing between the input material and the bay sediments. q_m is the part of q_o which is derived from the moving layer (or the depth of disturbance, i.e., the surficial layer which is subject to transport processes). Combining Equations 1 and 2 yields, for the amount stored,

$$q_n = a_s q_s + a_r q_r - q_m. \quad [3]$$

Assuming that the trace sediments under consideration are present only in the marine sediments (i.e., they are absent in the river sediments), the budget of the tracers over the unit time can be expressed as

$$T_n = C_1 q_s - C_2 q_o \quad [4]$$

where T_n is the amount of the tracers stored per unit time within the estuarine system, and C_1 and C_2 are the concentrations of the trace material in q_s and q_o, respectively. In a similar manner to Equation 2, $C_2 q_o$ can be written as

$$C_2 q_o = (1 - a_s)C_1 q_s + C_m q_m \quad [5]$$

where C_m is the concentration of the tracer within the moving layer. From Equations 4 and 5 we have

$$T_n = a_s C_1 q_s - C_m q_m. \quad [6]$$

[1] Manuscript received 19 March 1991; accepted 12 June 1991.

JOURNAL OF SEDIMENTARY PETROLOGY, VOL. 62, NO. 1, JANUARY, 1992, P. 35–40

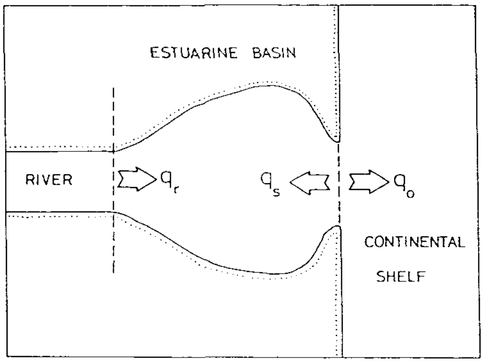

FIG. 1.—Major components of the sediment balance for an estuarine system.

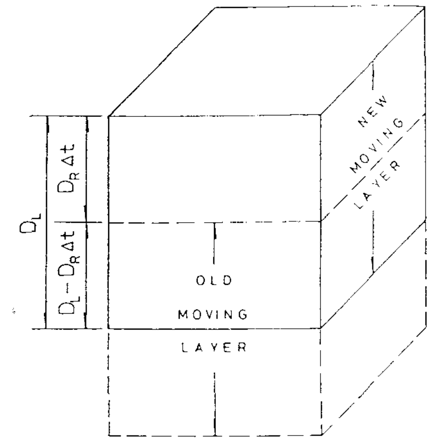

FIG. 2.—Schematic diagram showing the change in the moving layer, between t and t + Δt. The moving layer at t is shown by the dashed box and that at t + Δt is shown by the solid box.

Further, the average tracer concentration of the loosely-consolidated sediments within the estuarine system can be defined as

$$C_b = V_m/V \qquad [7]$$

where V is the total volume of the loosely-consolidated sediments within the estuary and V_m is the volume of the tracer in V. The time change rate of C_b will be

$$\frac{dC_b}{dt} = \frac{d(V_m/V)}{dt} = \frac{1}{V}\frac{dV_m}{dt} - \frac{C_b}{V}\frac{dV}{dt} = \frac{1}{V}T_n - \frac{C_b}{V}q_n. \qquad [8]$$

Inserting Equations 3 and 6 into Equation 8,

$$\frac{dC_b}{dt} = \frac{1}{V}[a_s C_1 q_s - C_m q_m - (a_s q_s + a_r q_r - q_m) C_b]. \qquad [9]$$

In a finite differential form, Equation 9 can be rewritten as

$$C_{b,t+\Delta t} - C_{b,t} = \frac{1}{V_t}[a_s c_1 q_s - C_{m,t} q_m - (a_s q_s + a_r q_r - q_m) C_{b,t}]\,\Delta t. \qquad [10]$$

In Equation 10, V_t and $C_{m,t}$ also vary with time (with other parameters assumed to be constant). The total volume of the bay sediments (V) will change according to:

$$V_{t+\Delta t} = V_t + q_n\,\Delta t = V_t + (a_s q_s + a_r q_r - q_m)\,\Delta t \qquad [11]$$

The concentration of the tracer within the moving layer is controlled by accretionary processes within the estuary. If the thickness of the moving layer remains constant, after a time (Δt) the newly-deposited sediments and the upper part of the original moving layer will form a "new" moving layer (Fig. 2). At the same time, the lower part of the original moving layer will become immobile. Let $C_{m,t}$ be the tracer concentration in the original moving layer. After a unit time, the quantity of the tracer per unit area consists of two parts which combine together to form a "new" moving layer. One part is the amount of tracer contained in the influx, over the time Δt:

$$V_1 = \frac{T_n}{q_n} D_R\,\Delta t \qquad [12]$$

where D_R is the deposition rate ($D_R = q_n/A_b$, where A_b is the area of the embayment). The other part is the contribution made by the original moving layer:

$$V_2 = C_{m,t}(D_L - D_R\,\Delta t) \qquad [13]$$

where D_L is the thickness of the moving layer. Thus, the concentration within the "new" moving layer becomes

$$C_{m,t+\Delta t} = \frac{V_1 + V_2}{D_L} = \frac{1}{D_L}\left[\frac{T_n\,\Delta t}{A_b} + C_{m,t}(D_L - D_R\,\Delta t)\right] = \frac{\Delta t}{D_L}\left[\frac{a_s C_1 q_s}{A_b} + \left(\frac{D_L}{\Delta t} - D_R - \frac{q_m}{A_b}\right) C_{m,t}\right]$$

(assuming $D_L > D_R$). [14]

Equations 10, 11 and 14 model changes in the concentration of the tracer, in the total estuarine sediments and within the moving layer. The assumptions for the model include: 1) the tracers in consideration are derived from marine sediments; 2) the components of the sediment budgets, the budgets of the total sediments and the tracers, and the tracer concentration of the marine sediments are constant (although these are represented as variables in the controlling equation); 3) the concentrations of the tracers in the total estuarine sediments and the moving layer are space-averaged (i.e., they are functions of time only); 4) the thickness of the moving layer is much greater than the thickness of the layer deposited over unit time; and 5) the deposition rate and thickness of the moving layer are uniform over all the basin area.

PARAMETERS FOR MODEL INPUT

To run the model numerically, the unit time and initial conditions need to be specified. For convenience, the unit is taken as one year. For the initial conditions, because the trace material is assumed to be absent in the river sediments, it is assumed that

$$C_{b(init)} = C_{m(init)} = 0. \qquad [15]$$

For the total volume of bay sediments, the initial value is defined as the volume of the moving layer:

$$V_{(init)} = D_L A_b. \qquad [16]$$

The input parameters required by the model include A_b (the area of the estuarine basin), D_R (thickness of the deposit in unit time), C_1 (tracer concentration in the marine sediments), D_L (the thickness of the moving layer), q_s (sediment input from the sea), q_r (sediment input from the river), q_m (part of sediment output derived from the estuarine sediments), a_s (fraction of the marine sediments remaining within the estuary), and a_r (fraction of the river sediments remaining within the estuary). Values for these parameters are derived below on the basis of published information.

Generally, the area of estuarine systems is of the order of $1–10^3$ km^2. For the present study, A_b has been assumed to be 20 km^2. In modern estuaries, the average rates of sediment accumulation are 2×10^{-3} m a^{-1} for humid estuaries and 1×10^{-3} m a^{-1} for arid and semi-arid estuaries (Rusnak 1967). Thus, D_R in the model input has been taken to be within the same order of magnitude, except for the case of no net accumulation or erosion in the estuarine basin.

The concentration of the trace material varies with location, depending upon the type of tracer being considered. Some information is available in the literature, however, concerning the order of magnitude of such tracer concentrations. On continental shelves, concentrations of heavy minerals can be as much as 10–30% (Barrie et al. 1988), and those of foraminiferal tests can be as high as 40% (Milliman 1976). A value of C_1 for the model input has been assumed, therefore, to be 10%.

The depth of disturbance on coastal beaches is dependent upon the wave height and type, together with grain

TABLE 1.—*List of notations used in the text*

A_b:	Area of the estuarine basin, km^2
A_D:	Dispersion coefficient, m^2 s^{-1}
a_r:	Fraction of the material from the river sediment which remains in the estuary
a_s:	Fraction of the material from the marine sediment which remains in the estuary
C:	Volume concentration of trace sediments, m^3 m^{-3}
C_b:	Average volume concentration of tracer in the estuarine deposits
C_m:	Volume concentration of tracer in the moving layer
C_1:	Volume concentration of tracer in the marine sediments
C_2:	Volume concentration of tracer in the output from the estuary, to the adjacent continental shelf
D_L:	Thickness of the moving layer, m
D_R:	Average deposition rate within the estuarine system, m a^{-1}
M_0:	Transport of tracer due to advection, m^3 a^{-1}
q_m:	Part of sediments in the total output from the estuary to the open sea, which is from the estuarine deposit, m^3 a^{-1}
q_n:	Amount of sediments stored within the estuarine system over a unit time, m^3 a^{-1}
q_o:	Sediment output toward the open sea, over unit time, m^3 a^{-1}
q_r:	Sediment input from the river, over unit time, m^3 a^{-1}
q_s:	Sediment input from the sea, over unit time, m^3 a^{-1}
T_{eq}:	Amount of time for equilibrium of the concentration of tracer within the moving layer to occur, a
T_n:	Amount of trace sediments stored with the estuarine system, over unit time, m^3 a^{-1}
V:	Total volume of the loosely-consolidated sediments in the estuarine system, m^3
V_m:	Volume of tracer in V, m^3
V_1:	Volume of tracer in sediments, per unit area, accumulated during unit time, m^3 m^{-2}
V_2:	Volume of the tracer in sediments, per unit area, within part of the moving layer, m^3 m^{-2}

size characteristics of the beach material. Under breaking wave heights of around 100 cm, the depth of disturbance has been reported to be of the order of 3 cm (King 1951) or 20–40 cm (Otvos 1965; Williams 1971). The thickness is assumed here, therefore, to be 10 cm.

For the determination of q_s, q_o and q_r, four transport cases at the entrance are considered: 1) landward net sediment transport ($q_s > q_o$); 2) no net transport ($q_s = q_o$); 3) seaward net transport, with sediment accumulation within the estuarine basin ($q_s < q_o$ and $q_r > q_o - q_s$); and 4) seaward net transport, with no accretion in the basin ($q_o = q_s + q_r$). Sediment discharge (q_r) from the river system is assumed to be 4×10^4 m^3 a^{-1}. Further, q_s, q_o, q_r, a_s and a_r are selected to satisfy each of the four possible transport cases. D_R and q_m are then calculated from these parameters. The model for changes in the concentrations of trace sediments of the total estuarine sediments and the moving layer is run under these four different cases. Input parameters for the four cases are shown in Table 2.

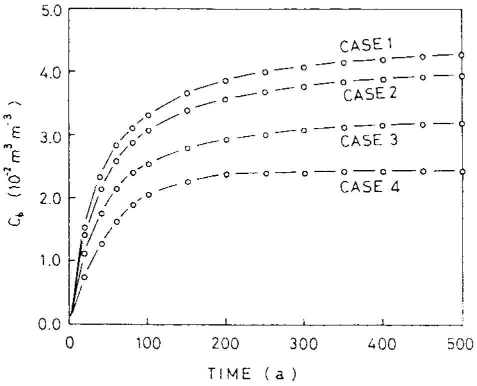

FIG. 3.—Time series of C_b for the four cases, in years.

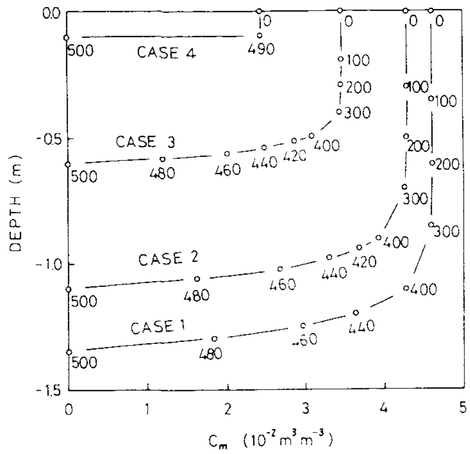

FIG. 4.—C_m in the stratigraphic records, for the four cases under investigation. The numbers at the data points represent the age of the deposit (in years).

RESULTS

The model for the changes in the tracer concentrations has been run for 500 unit time spans (i.e., over 500 years). For each case, a time series of C_b is obtained (Fig. 3). A significant feature is that C_b increases progressively with time, no matter what the net sediment transport patterns are. In other words, there is some transport from the source, independent of the landward or seaward net transport at the entrance. Because net sediment transport consists of two components, advection and dispersion, the influx of the tracer must be influenced strongly by dispersion. This influence is particularly significant in cases 3 and 4, in which the advection component is directed seaward. The dispersion component is not small compared with the advention component; this is also true for beach environments (Murray 1967; Price 1969) and in shallow marine areas (Pizzuto 1987).

According to Fischer et al. (1979), the flux due to dispersion is $-A_D\, \partial C/\partial x$. This, together with the flux due to advection (M_0), forms the total budget of the tracer:

$$T_n = -A_D \frac{\partial C}{\partial x} + M_0 \qquad [17]$$

where C is the tracer concentration and A_D is the dispersion coefficient. From Equations 6 and 17 we have

$$A_D \frac{\partial C}{\partial x} = M_0 - a_s c_1 q_s + c_m q_m. \qquad [18]$$

On the basis of the parameters of the present experiments for each of the cases, A_D is estimated from Equation 18 to be on the order of 0.1–10 $cm^2\, s^{-1}$, which is equivalent to that found in high energy environments.

Figure 4 shows the distribution of the tracer concentration in the stratigraphic records, for the four cases. It reveals two characteristics.

First, after the period of sediment exchange, an equilibrium state is attained eventually. At such a time, the concentration becomes stable throughout the record. The length of time for C_m to reach equilibrium (T_{eq}) is considerable (Table 3). For all cases, the amount of time for equilibrium to occur lies between 300 and 360 years. Thus, T_{eq} is another factor which influences the observed tracer concentration.

Second, the equilibrium tracer concentrations ($C_{m,eq}$), or the dimensionless ratio $C_{m,eq}/C_1$, for the four cases vary considerably (Table 3). This equilibrium level should be controlled by 4 factors which form the basis of the model: 1) sediment discharge from the river, 2) the concentration in the source area, 3) landward-seaward net transport patterns, and 4) the processes of dispersion. Because for the four cases only q_s among the input parameters is an

TABLE 2.—*Input parameters for the trace sediment exchange model, as defined by Equations 10, 11 and 14*

Case	A_b, km^2	q_s $m^3 a^{-1}$	q_o $m^3 a^{-1}$	q_r $m^3 a^{-1}$	q_m* $m^3 a^{-1}$	D_r cm	D_R** cm	a_s	a_r	C_s %
1	20	80,000	70,000	40,000	2,000	10	0.25	0.3	0.7	10
2	20	70,000	70,000	40,000	9,000	10	0.20	0.3	0.7	10
3	20	50,000	70,000	40,000	23,000	10	0.10	0.3	0.7	10
4	20	30,000	70,000	40,000	37,000	10	0.00	0.3	0.7	10

* On the basis of Equation 2.
** Based upon $D_R = q_n/A_b = (q_s + q_r - q_o)/A_b$.

TABLE 3.—*Time for equilibrium of the tracer concentration within the moving layer (T_{eq}) to be reached, together with the related equilibrium tracer concentrations ($C_{m,eq}$), for the four cases*

Case	T_{eq} a	$C_{m,eq}$ $m^3\ m^{-3}$	$C_{m,eq}/C_i$
1	357	0.0462	0.462
2	351	0.0429	0.429
3	320	0.0349	0.349
4	311	0.0243	0.243

independent variable, the derived equilibrium levels should represent the influence of net transport patterns.

As an example of this exchange process, Wang and Murray (1983) noticed differences in the percentage of exotic benthic foraminiferal tests in estuaries with a variety of tidal ranges. They interpreted those differences in terms of the magnitude of tidal energy: the higher the tidal energy level, the larger the percentage of exotic benthic foraminiferal tests. According to the results described above, however, the differences could have been due also to *net* sediment transport patterns.

DISCUSSION AND CONCLUSIONS

Although some negative examples of using the mere presence of natural tracers within the estuarine system as an indicator of net sediment transport have been presented (Figs. 3 and 4), it is still possible to use the tracers to infer sediment transport pathways. This is because the magnitude of the tracer concentration is controlled by, among other factors, the patterns of net landward-seaward sediment transport. In such an analysis, the concentration under "neutral" conditions (i.e., net transport through the entrance is zero, $q_s = q_o$, case 2 in Table 2) can be considered as a critical value which represents the concentration controlled by the dispersion only. If any observed tracer concentration (due to both advection and dispersion) within an estuarine system exceeds this critical level, this should imply net landward sediment transport. Likewise, any observed concentration less than the critical value will define net seaward transport. For the values of Table 2, the critical level is $C_{m,eq} = 0.0429$, or $C_{m,eq}/C_i = 0.429$ (Table 3). Thus, case 1 ($C_{m,eq} > 0.0429$) defines a net landward transport and cases 3 and 4 ($C_{m,eq} < 0.0429$) represent a net seaward transport.

The identification of the critical level for practical applications is associated with an understanding of dispersive processes, which needs, however, further investigation. Once the dispersion coefficient A_D in Equation 18 is known, the model developed here can be used to define the critical concentration.

Our conclusions are:

1) the presence of an exotic tracer within an estuarine system indicates some sediment transport from the source, due to exchange processes;
2) the mere presence of the tracer is *not* indicative, however, of a net transport direction; and
3) to interpret the net sediment transport direction, information on the "critical" concentration of the tracer within the estuarine system (due to dispersion only) and the "actual" concentration (due to both advection and dispersion) must be known.

ACKNOWLEDGMENTS

The authors are grateful to Professor J.W. Murray (Department of Geology, Southampton University) for his comments. Dr G. Voulgaris (Department of Oceanography, Southampton University) is thanked for his critical check of the mathematics. Professors A. Monaco (University of Perpignan) and E. Merino (Indiana University) reviewed the manuscript and suggested improvements. We would like to thank them warmly for their comments.

REFERENCES

BARRIE, J.V., EMORY-MOORE, M., LUTERNAUER, J.L., AND BORNHOLD, B.D., 1988, Origin of modern heavy mineral deposits, north British Columbia continental shelf: Marine Geology, v. 84, p. 43–51.

BROWN, L., 1987, ^{10}Be as a tracer of erosion and sediment transport: Chemical Geology, v. 65, p. 189–196.

BYRNE, J.V., AND KULM, L.D., 1967, Natural indicators of estuarine sediment movement: Journal of the Waterways and Harbors Division, American Society of Civil Engineers, v. 93(WW2), p. 181–194.

CLIFTON, H.E., AND HUNTER, R.E., 1973, Bioturbational rates and effects in carbonate sand, St. John, U.S. Virgin Islands: Journal of Geology, v. 81, p. 253–268.

EINSTEIN, H.A., 1950, The bed-load function for sediment transportation in open channel flows: Technical Bulletin No. 1026, United States Department of Agriculture, Soil Conservation Service, Washington, D.C., 78 p.

EISMA, D., GAAST, VAN DER S.T., MARTIN, J.M., AND THOMAS, A.T., 1978, Suspended matter and bottom deposits of the Orinoco delta: turbidity, mineralogy and elementary composition: Netherlands Journal of Sea Research, v. 12, p. 224–251.

FISCHER, H.B., LIST, E.J., KOH, R.C.Y., IMBERGER, J., AND BROOKS, N.Y., 1979, Mixing in Inland and Coastal Waters: New York, Academic Press, 483 p.

GESSNER, F., AND SIMONSEN, R., 1967, Marine diatoms in the Amazon? Liminology and Oceanography, v. 12, p. 709–711.

KING, C.A.M., 1951, Depth of disturbance of sand on sea beaches by waves: Journal of Sedimentary Petrology, v. 21, p. 131–140.

LUDTKE, N.A., AND BENDER, M.L., 1979, Tracer study of sediment-water interactions in estuaries: Estuarine and Coastal Marine Science, v. 9, p. 643–651.

MEREFIELD, J.R., 1981, Caesium in the up-estuary transport of sediments: Marine Geology, v. 39, p. M45–M55.

MILLIMAN, J.D., 1976, *Miniacina minacea:* modern foraminiferal sands on the outer Moroccan shelf: Sedimentology, v. 23, p. 415–419.

MURRAY, J.W., 1987, Biogenetic indicators of suspended sediment transport in marginal marine environments: quantitative examples from SW Britain: Journal of the Geological Society of London, v. 144, p. 127–133.

MURRAY, S.P., 1967, Control of grain dispersion by particle size and wave state: Journal of Geology, v. 75, p. 612–634.

OTVOS, E.G., 1965, Sedimentation-erosion cycles of single tidal period on Long Island Sound beaches: Journal of Sedimentary Petrology, v. 35, p. 604–609.

PIZZUTO, J.E., 1987, Dispersion of dyed sand tracers in an oscillatory flow field: Journal of Geophysical Research, v. 92(C2), p. 1923–1933.

PRICE, W.A., 1969, Variable dispersion and its effects on the movements of tracers on beaches: Proceedings of 11th Conference on Coastal Engineering, p. 329–334.

RUSNAK, G.A., 1967, Rates of sediment accumulation in modern estuaries, *in* Lauff, G.H., ed., Estuaries: American Association for the Advancement of Science, Washington, D.C., p. 180–184.

SALOMONS, W., AND MOOK, W.G., 1987, Natural tracers for sediment transport studies: Continental Shelf Research, v. 7, p. 1333–1343.

TRASK, P.D., 1952, Source of beach sand at Santa Barbara, California, as indicated by mineral grain studies: U.S. Army Corps of Engineers, Beach Erosion Board Technical Memorandum no. 28, 24 p.
WANG, P., AND MURRAY, J.W., 1983, The use of foraminifera as indicators of tidal effects in estuarine deposits: Marine Geology, v. 51, p. 239–250.
WILLIAMS, A.T., 1971, An analysis of some factors involved in the depth of disturbance of beach sand by waves: Marine Geology, v. 11, p. 145–158.